



This work is protected by copyright and other intellectual property rights and duplication or sale of all or part is not permitted, except that material may be duplicated by you for research, private study, criticism/review or educational purposes. Electronic or print copies are for your own personal, non-commercial use and shall not be passed to any other individual. No quotation may be published without proper acknowledgement. For any other use, or to quote extensively from the work, permission must be obtained from the copyright holder/s.

Molecular characterisation of human atopic  
asthma and house dust mite induced  
pulmonary inflammation in a murine  
experimental model

Emma Louise Whittle

A thesis submitted for the degree of  
Doctor of Philosophy

March 2020

Keele University

## Acknowledgements

Firstly, I'd like to say a huge thanks to my supervisor Dr Dan Tonge for giving me the opportunity to complete a PhD in such an interesting and novel field of research. His patience and guidance, particularly with regards to the bioinformatic aspects of my project, were invaluable and much appreciated.

I'd next like to thank Dr Martin Leonard and Professor Debbie Jarvis for their provision of the murine and human samples that made my research possible. I'd also further like to extend my gratitude to Martin for giving me the opportunity to visit him at his lab in Public Health England, and for his insight in experimental models of asthma.

I'd next like to thank all my friends at Huxley for all the support they've provided over the last four years. We've been there for each other through the highs and lows of completing a PhD, and without them my time at Keele wouldn't have been half as fun.

Lastly, I would like to thank my parents, without whom I would not be the person I am today. They've supported me throughout the 22 years of education it has taken to get to this point, and I will always be grateful for their encouragement over the years.

## Abstract

Asthma is one of the most common chronic diseases of the 21<sup>st</sup> century, affecting over 300 million people worldwide <sup>1</sup>. It is an inflammatory disorder of the airways that is a major public concern globally due to increasing prevalence and rates of mortality <sup>2-5</sup>, and each year the disease is estimated to cause 250,000 premature deaths <sup>1</sup>.

There is an unmet need for the identification of phenotype-specific markers and accompanying molecular tools that facilitate the classification of asthma phenotypes/endotypes. This study utilised a range of molecular techniques to characterise a well-defined group of female adults with poorly controlled atopic asthma associated with a house dust mite (HDM) sensitivity and non-asthmatic subjects.

Quantification and differential expression analysis of circulating messenger RNA (mRNA) and microRNA (miRNA) revealed significant alterations to circulating RNA expression in the asthmatic subjects compared to the control subjects that may influence systemic immune activity. Quantification of circulatory inflammatory proteins (IL-4, 5, 10, 13, 17A, eotaxin, GM-CSF, IFN $\gamma$ , MCP-1, RANTES, TARC, TNF $\alpha$ , total IgE) found an overall trend of increased inflammatory protein in the asthmatic subjects, although no individual protein was identified as being significantly increased in the asthmatic subjects. Quantification of the bacterial protein, endotoxin, was observed to be decreased in the asthmatic subjects.

Comparison of the circulatory microbiome in atopic and non-atopic subjects revealed that atopic disease was associated with significant changes to the circulatory microbiome composition and function potential. Moreover, characterisation of the murine gut and airway microbiome in an experimental model of atopic asthma found that HDM-induced pulmonary inflammation significantly altered the composition and function potential of the

airway and gut microbiomes, thus demonstrating that atopic disease can actively induce changes to the microbiome.

In conclusion, this study provides a valuable insight into the systemic changes that occur in HDM-associated asthma. A number of circulatory molecules were identified that were condition-specific and have biomarker potential, and clear changes in the atopic microbiome were detected.

# Table of Contents

Acknowledgements .....	i
Abstract .....	ii
Table of Contents .....	iv
Table of Figures .....	1
Table of Tables .....	8
List of Abbreviations .....	13
<b>Chapter 1: Introduction to Molecular Characterisation of Atopic Asthma.....</b>	<b>18</b>
<b>1.1. Introduction to Asthma .....</b>	<b>18</b>
<b>1.2. The Causes of Asthma .....</b>	<b>18</b>
<b>1.3. Clinical Presentation of Asthma .....</b>	<b>19</b>
<b>1.4. Asthma Phenotypes and Endotypes .....</b>	<b>20</b>
<b>1.5. The Atopic March.....</b>	<b>23</b>
<b>1.6. Atopic Asthma Pathogenic Mechanisms.....</b>	<b>24</b>
<b>1.7. The Allergen Sensitisation Phase.....</b>	<b>24</b>
<b>1.7.1. Activation of the Epithelial Cells.....</b>	<b>25</b>
<b>1.7.2. Activation of the Innate Immune Cells.....</b>	<b>27</b>
<b>1.7.3. T Helper 2 Priming and IgE Production .....</b>	<b>28</b>
<b>1.7.4. The Role of the Innate Cytokines in Airway inflammation.....</b>	<b>34</b>
<b>1.8. The Effector Phase of IgE-mediated Hypersensitivity .....</b>	<b>35</b>
<b>1.8.1. The Early Phase of Allergic Inflammation in Atopic Asthma .....</b>	<b>36</b>

<b>1.8.2.</b>	The Late Phase of Allergic Inflammation in Atopic Asthma .....	<b>39</b>
<b>1.8.3.</b>	The Role of the T Helper 2 Cells in the Late Phase Reactions.....	<b>41</b>
<b>1.9.</b>	Immune Mechanisms Associated with Chronic Airway Inflammation in Atopic Asthma .....	<b>42</b>
<b>1.10.</b>	Diagnosis of Atopic Asthma and its Endotypes .....	<b>44</b>
<b>1.11.</b>	Identification of Peripheral Biomarkers in Asthma.....	<b>47</b>
<b>1.11.1.</b>	Transcriptomic Biomarkers of Asthma .....	<b>47</b>
<b>1.11.2.</b>	Protein Biomarkers of Asthma .....	<b>49</b>
<b>1.12.</b>	Atopic Asthma and Sex Differences .....	<b>50</b>
<b>1.13.</b>	Atopic Asthma Prevalence .....	<b>50</b>
<b>1.14.</b>	Introduction to the Hygiene Hypothesis.....	<b>51</b>
<b>1.15.</b>	The Human Microbiota .....	<b>53</b>
<b>1.15.1.</b>	The Evolution of the Human Microbiota.....	<b>55</b>
<b>1.15.2.</b>	Establishment of the Human Microbiota .....	<b>55</b>
<b>1.15.3.</b>	Maturation of the Human Microbiota .....	<b>56</b>
<b>1.15.4.</b>	The Role of the Human Microbiota in Immune development .....	<b>57</b>
<b>1.15.5.</b>	Changes to the Microbiota Composition.....	<b>58</b>
<b>1.16.</b>	The Human Microbiota and Atopic Asthma.....	<b>60</b>
<b>1.16.1.</b>	The Gut Microbiota and Asthma .....	<b>60</b>
<b>1.16.2.</b>	The Airway Microbiota and Asthma .....	<b>65</b>
<b>1.16.3.</b>	The Microbiota and Asthma Pathogenesis.....	<b>69</b>

<b>1.17.</b>	<b>Introduction to the Circulatory Microbiome.....</b>	<b>74</b>
<b>1.17.1.</b>	<b>Detection Techniques used to Characterise the Circulatory Microbiome....</b>	<b>76</b>
<b>1.17.2.</b>	<b>Origins of the Circulatory Microbiome.....</b>	<b>78</b>
<b>1.17.3.</b>	<b>The Circulatory Microbiome and Human Disease.....</b>	<b>80</b>
<b>1.17.4.</b>	<b>Asthma and the Circulatory Microbiome .....</b>	<b>82</b>
<b>1.17.5.</b>	<b>Potential Use of the Circulatory Microbiome in Clinical Diagnostics .....</b>	<b>82</b>
<b>1.17.6.</b>	<b>The Importance of the Experimental Negative Control.....</b>	<b>82</b>
<b>1.18.</b>	<b>Experimental Models of Asthma.....</b>	<b>84</b>
<b>1.19.</b>	<b>The HDM Allergen and the Microbiome.....</b>	<b>86</b>
<b>1.20.</b>	<b>Aims and Objectives .....</b>	<b>87</b>
<b>Chapter 2: General Methodology .....</b>	<b>.....</b>	<b>89</b>
<b>2.1.</b>	<b>Maintenance of Sterile Conditions during PCR set-up .....</b>	<b>89</b>
<b>2.2.</b>	<b>Visualisation of PCR Products using Gel Electrophoresis.....</b>	<b>90</b>
<b>2.3.</b>	<b>Amplicon Purification .....</b>	<b>91</b>
<b>2.3.1.</b>	<b>MinElute DNA Purification Protocol .....</b>	<b>92</b>
<b>2.3.2.</b>	<b>AMPure XP PCR Purification Protocol .....</b>	<b>92</b>
<b>2.4.</b>	<b>Analysis of the Microbiome .....</b>	<b>94</b>
<b>2.4.1.</b>	<b>Assignment of Sequenced Reads to Bacterial Operational Taxonomic Units .....</b>	<b>94</b>
<b>2.4.2.</b>	<b>Generation of a Rarefaction Curve .....</b>	<b>95</b>
<b>2.4.3.</b>	<b>Comparison of Species Richness.....</b>	<b>95</b>



2.4.4.	Assignment of the Bacterial Operational Taxonomic Units to Bacterial Taxa	95
2.4.5.	Comparison of Alpha Diversity in the Microbiome of Atopic and Non-Atopic Control Subjects	96
2.4.6.	Comparison of Beta Diversity in the Microbiome of Atopic and Non-Atopic Control Subjects	97
2.4.7.	Metagenomic Functional Analysis	97
2.5.	Statistical Analysis	98
<b>Chapter 3: Characterisation of Atopic Asthma at the Molecular level</b>		<b>100</b>
3.1.	Introduction	100
3.1.1.	Aims of the Chapter	101
3.2.	Methods	102
3.2.1.	Sample Collection	102
3.2.2.	Asthma Control Questionnaire	103
3.2.3.	Total RNA Extraction, Library Preparation, and Next Generation Sequencing	104
3.2.4.	Alignment of mRNA to the Human Genome and Differential Expression Analysis	104
3.2.5.	Alignment of miRNA to the Human Genome and Differential Expression Analysis	106
3.2.6.	RNA Functional Analysis	107

<b>3.2.7.</b>	Analysis of the Biological Significance of Differentially Expressed Genes in the Asthmatic Population .....	<b>107</b>
<b>3.2.8.</b>	Analysis of the Biological Significance of Differentially Expressed miRNA in the Asthmatic Population .....	<b>108</b>
<b>3.2.9.</b>	Analysis of the Combined Effect of Differentially Expressed mRNA and miRNA in the Asthmatic Population .....	<b>108</b>
<b>3.2.10.</b>	Qualitative Analysis of Circulatory Inflammatory Protein Levels.....	<b>109</b>
<b>3.2.11.</b>	Quantitative Analysis of Circulatory Total IgE Concentrations.....	<b>109</b>
<b>3.2.12.</b>	Quantitative Analysis of Circulatory Endotoxin Concentrations.....	<b>110</b>
<b>3.3.</b>	Results.....	<b>111</b>
<b>3.3.1.</b>	Characterisation of the Atopic Asthmatic Subjects .....	<b>111</b>
<b>3.3.2.</b>	mRNA detected in the Plasma Samples .....	<b>114</b>
<b>3.3.3.</b>	Differential Gene Expression detected in the Asthmatic Subjects compared to the Control Subjects .....	<b>115</b>
<b>3.3.4.</b>	Diversity of Gene Expression detected in the Asthmatic Subjects compared to the Control Subjects .....	<b>119</b>
<b>3.3.5.</b>	miRNA detected in the Plasma Samples .....	<b>122</b>
<b>3.3.6.</b>	Differential miRNA Expression detected in the Asthmatic Subjects compared to the Control Subjects .....	<b>123</b>
<b>3.3.7.</b>	Diversity of miRNA detected in the Asthmatic Subjects compared to the Control Subjects.....	<b>127</b>
<b>3.3.8.</b>	RNA Functional Analysis .....	<b>129</b>

3.3.9.	Biological Significance of Differential Gene Expression in the Asthmatic Subjects .....	129
3.3.10.	Biological Significance of Differentially Expressed miRNA in the Asthmatic Subjects .....	131
3.3.11.	Combined Effect of Differential Gene Expression and miRNA Expression in the Asthmatic Subjects .....	134
3.3.12.	Characterisation of Circulatory Inflammatory Protein Levels .....	139
3.3.13.	Quantification of Circulatory Total IgE Concentrations .....	141
3.3.14.	Quantification of Circulatory Endotoxin Concentrations .....	142
3.4.	Discussion.....	144
3.4.1.	Transcriptomic Characterisation of the Asthma Phenotype .....	144
3.4.2.	Biological Significance of the Asthmatic RNA Profiles .....	146
3.4.3.	Protein Characterisation of the Asthma Phenotype.....	149
3.4.4.	Identification of Peripheral Biomarkers .....	152
3.4.5.	Chapter Summary .....	154
<b>Chapter 4: Characterisation of the Circulatory Microbiome in Atopic Asthma .....</b>		<b>155</b>
4.1.	Introduction .....	155
4.1.1.	Aims of the Chapter .....	157
4.2.	Methods.....	158
4.2.1.	Sample Collection.....	158
4.2.2.	Extraction of bacterial DNA from the Human Plasma Samples .....	158

<b>4.2.3.</b>	Development of a Protocol for PCR amplification of the V3-V4 region of the bacterial 16S rRNA gene in Human Plasma Samples.....	<b>160</b>
<b>4.2.4.</b>	Nested PCR Amplification of the V3-V4 region of the bacterial 16S rRNA gene in Human Plasma Samples.....	<b>163</b>
<b>4.2.5.</b>	Amplification of the V4 region of the 16S rRNA gene .....	<b>165</b>
<b>4.2.6.</b>	Preparation of the V4 amplicons for Ion Torrent Sequencing.....	<b>166</b>
<b>4.2.7.</b>	Preparation of the V4 amplicons for Illumina Sequencing.....	<b>168</b>
<b>4.2.8.</b>	Sequencing of the V3-V4 amplicons and the V4 16S rRNA amplicons using Ion Torrent Sequencing Technology .....	<b>170</b>
<b>4.2.9.</b>	Quantification of amplicon concentration using Qubit dsDNA High-Sensitivity Assay.....	<b>170</b>
<b>4.2.10.</b>	Generation of Template Positive Ion Sphere Particles .....	<b>171</b>
<b>4.2.11.</b>	Enrichment of the Template-Positive Ion Sphere Particles.....	<b>172</b>
<b>4.2.12.</b>	Quality Control Testing of the Template Positive Ion Sphere Particles.....	<b>173</b>
<b>4.2.13.</b>	Sequencing of the Ion Sphere Particle Templates.....	<b>174</b>
<b>4.2.14.</b>	Sequencing of the V4 16S amplicons using Illumina Sequencing Technology .....	<b>175</b>
<b>4.2.15.</b>	Alignment of the Sequenced V4 reads to known Bacterial Genomes.....	<b>176</b>
<b>4.2.16.</b>	Comparison of the Asthmatic Microbiome to the Control Microbiome ....	<b>176</b>
<b>4.2.17.</b>	Prediction of Metagenome Function Content .....	<b>178</b>
<b>4.2.18.</b>	Culturing of Plasma Samples on Selective Growth Media .....	<b>178</b>
<b>4.2.19.</b>	Amplification of the 16S rRNA gene from the Bacterial Colonies.....	<b>180</b>

4.2.20.	Sanger Sequencing of total 16S rRNA amplicons amplified from Human Plasma Samples .....	182
4.3.	Results.....	183
4.3.1.	Development of a Protocol for Amplifying Regions of the Bacterial 16S rRNA Gene from Human Blood Samples.....	183
4.3.2.	Amplification of the V3-V4 region of the 16S rRNA gene using Nested PCR .....	184
4.3.3.	Quantification of the Ion Torrent V3-V4 amplicons .....	185
4.3.4.	Sequencing of the V3-V4 amplicons using Ion Torrent Sequencing Technology .....	186
4.3.5.	Amplification of the V4 region of the 16S rRNA gene from Human Plasma Samples using Nested PCR .....	187
4.3.6.	Quantification of the Ion torrent V4 amplicons .....	190
4.3.7.	Quantification of the Illumina V4 amplicons .....	192
4.3.8.	Sequencing of the V4 amplicons using Ion Torrent Sequencing Technology .....	193
4.3.9.	Taxonomic Classification of the OTUs detected in the Human Plasma Samples using Ion Torrent Sequencing Technology .....	196
4.3.10.	Sequencing of the V4 amplicons using Illumina Sequencing Technology ..	198
4.3.11.	Taxonomic Classification of the OTUs detected in the Human Plasma Samples using Illumina Sequencing Technology .....	201

4.3.12.	Bacterial Alpha Diversity in the Asthmatic Circulatory Microbiome compared to the Control Microbiome .....	204
4.3.13.	Bacterial Beta Diversity in the Asthmatic Circulatory Microbiome compared to the Control Microbiome .....	206
4.3.14.	Differential Bacterial Abundance in the Asthmatic Circulatory Microbiome compared to the Control Microbiome .....	208
4.3.14.	Prediction of the Plasma Metagenome Function Content.....	210
4.3.15.	Bacterial Growth Cultures and Identification of Viable Bacteria .....	213
4.3.16.	Likely Origins of the Circulatory Microbiome .....	220
4.4.	Discussion.....	223
4.4.1.	Development of Research Techniques.....	223
4.4.2.	Detection of a Human Circulatory Microbiome .....	224
4.4.3.	Comparison of Bacterial diversity in the Asthmatic Circulatory Microbiome compared to the Healthy Controls .....	225
4.4.4.	Differential Relative Abundance of Bacterial Populations detected in the Circulatory Microbiome .....	227
4.4.5.	Predicted Functional Activity of the Circulatory Microbiome .....	230
4.4.6.	The Detection of Viable Bacteria in Human Plasma Samples.....	232
4.4.7.	Likely Origins of the Circulatory Microbiome .....	233
4.4.8.	Chapter Summary .....	235
<b>Chapter 5: Characterisation of the Circulatory Microbiome in Different Atopic Populations.....</b>		<b>236</b>

<b>5.1.</b>	<b>Introduction .....</b>	<b>236</b>
<b>5.1.1.</b>	<b>Aims of the Chapter .....</b>	<b>237</b>
<b>5.2.</b>	<b>Methods.....</b>	<b>238</b>
<b>5.2.1.</b>	<b>Sample Collection.....</b>	<b>238</b>
<b>5.2.2.</b>	<b>Extraction and Amplification of the V4 region of the Bacterial 16S rRNA Gene .....</b>	<b>238</b>
<b>5.2.3.</b>	<b>Sequencing of the XT-V4 amplicons.....</b>	<b>240</b>
<b>5.2.4.</b>	<b>Alignment of the V4 Amplicons to known Bacterial Genomes.....</b>	<b>241</b>
<b>5.2.5.</b>	<b>Comparison of the Atopic Microbiome compared to the Control Microbiome .....</b>	<b>241</b>
<b>5.2.6.</b>	<b>Prediction of the Serum Metagenome Functional Content .....</b>	<b>242</b>
<b>5.2.7.</b>	<b>Culturing of Serum Samples on Selective Growth Media .....</b>	<b>243</b>
<b>5.3.</b>	<b>Results.....</b>	<b>244</b>
<b>5.3.1.</b>	<b>Amplification of the V4 region of the 16S rRNA gene from Bacterial DNA present in Human Serum Samples.....</b>	<b>244</b>
<b>5.3.2.</b>	<b>Sequencing of the V4 16S rRNA reads generated from Human Serum Samples .....</b>	<b>245</b>
<b>5.3.3.</b>	<b>Taxonomic Classification of the detected OTUs.....</b>	<b>249</b>
<b>5.3.4.</b>	<b>Alpha Diversity of the Circulatory Microbiome in Atopic Populations.....</b>	<b>251</b>
<b>5.3.5.</b>	<b>Beta Diversity of the Circulatory microbiome in Atopic Populations.....</b>	<b>255</b>
<b>5.3.6.</b>	<b>Differential Bacterial Abundance in the Atopic Subjects compared to the Control Subjects.....</b>	<b>258</b>

5.3.7.	Prediction of the Serum Metagenome Functional Content .....	269
5.3.8.	Analysis of Viable Bacterial Cells in the Serum Samples .....	273
5.4.	Discussion.....	274
5.4.1.	Characterisation of the Serum Circulatory Microbiome .....	274
5.4.2.	Comparison of the Serum Circulatory Microbiome compared to the Plasma Circulatory Microbiome.....	275
5.4.3.	Comparison of the Significant Changes in Different Atopic Diseases .....	276
5.4.4.	Microbial dysbiosis associated with Atopic Disease.....	277
5.4.5.	Microbial dysbiosis Associated with Disease Phenotype.....	279
5.4.6.	Microbial dysbiosis associated with Atopic Disease Severity.....	280
5.4.7.	Loss of Beneficial Bacteria and Atopic Pathogenesis.....	282
5.4.8.	Expansion of Harmful Bacteria and Atopic Pathogenesis .....	284
5.4.9.	Microbial dysbiosis and Treatment Responsivity.....	286
5.4.10.	Microbial Dysbiosis a consequence of Atopic Pathogenesis .....	286
5.4.11.	Changes in Microbial Activity in the Atopic Circulatory Microbiome.....	290
5.4.12.	Chapter Summary .....	294
<b>Chapter 6: Characterisation of the Murine Microbiome following exposure to the House</b>		
<b>Dust Mite allergen .....</b>		
6.1.	Introduction .....	296
6.1.1.	Chapter Aims .....	298
6.2.	Methods.....	299



<b>6.2.1.</b>	<b>Murine HDM Exposure Model.....</b>	<b>299</b>
<b>6.2.2.</b>	<b>Sample Collection.....</b>	<b>300</b>
<b>6.2.3.</b>	<b>Extraction of Microbial DNA from the Murine BAL and Faecal Samples....</b>	<b>300</b>
<b>6.2.4.</b>	<b>Direct amplification of the V4 region of the 16S rRNA gene from Murine Plasma Samples .....</b>	<b>301</b>
<b>6.2.5.</b>	<b>Amplification of the V4 region of the 16S rRNA gene from Microbial DNA isolated from the Murine BAL and Faecal Samples .....</b>	<b>304</b>
<b>6.2.6.</b>	<b>Sequencing of the V4 amplicons using Illumina Sequencing Technology ..</b>	<b>305</b>
<b>6.2.7.</b>	<b>Alignment of the V4 amplicons to known Bacterial Genomes .....</b>	<b>306</b>
<b>6.2.8.</b>	<b>Comparison of the HDM-exposed Microbiome to the HDM-naïve Microbiome .....</b>	<b>306</b>
<b>6.2.9.</b>	<b>Prediction of the Murine Microbiome Metagenome Function Content ....</b>	<b>307</b>
<b>6.3.</b>	<b>Results.....</b>	<b>309</b>
<b>6.3.1.</b>	<b>Amplification of the V4 region of the 16S rRNA gene from Microbial DNA present in Murine Plasma Samples.....</b>	<b>309</b>
<b>6.3.2.</b>	<b>Amplification of the V4 region of the 16S rRNA gene from Microbial DNA isolated from Murine BAL Samples.....</b>	<b>309</b>
<b>6.3.3.</b>	<b>Amplification of the V4 region of the 16S rRNA gene from Microbial DNA isolated from Murine Faecal Samples.....</b>	<b>310</b>
<b>6.3.4.</b>	<b>Sequencing of the V4 16S rRNA reads generated from Murine BAL Samples .....</b>	<b>312</b>

6.3.5.	Sequencing of the V4 16S rRNA reads generated from Murine Faecal Samples .....	314
6.3.6.	Taxonomic Classification of the OTUs detected in the Murine BAL Samples .....	317
6.3.7.	Taxonomic Classification of the OTUs detected in the Murine Faecal Samples .....	320
6.3.8.	Changes in Bacterial Diversity in the Microbiome of mice exposed to the HDM allergen compared to HDM-naïve mice.....	323
6.3.9.	Significant changes to Bacterial Relative Abundance in the Murine Airway Microbiome .....	328
6.3.10.	Significant Changes to Bacterial Relative Abundance in the Murine Gut Microbiome .....	330
6.3.11.	Prediction of Microbial Activity of the Murine Airway Microbiome .....	333
6.3.12.	Prediction of Microbial Activity of the Murine Gut Microbiome .....	334
6.4.	Discussion.....	338
6.4.1.	Atopic HDM Sensitisation and Composition of the Murine Microbiome ...	338
6.4.2.	Characterisation of the Murine Circulatory Microbiome.....	339
6.4.3.	Characterisation of the Murine Airway and Gut Microbiomes .....	340
6.4.4.	HDM-induced changes to the Bacterial Composition of the Murine Microbiome .....	341
6.4.5.	Loss of beneficial bacterial Taxa as a result of HDM Exposure.....	342

6.4.6.	Expansion of Bacterial Taxa Protective against Atopy in the HDM-exposed Gut Microbiome.....	346
6.4.7.	HDM-induced Changes to the Microbial Activity of the Murine Microbiome .....	347
6.4.8.	The Lung-Gut Axis influences changes to the Murine Microbiome .....	348
6.4.9.	Suitability of the Experimental Murine Model in studying Atopic Asthma.	350
6.4.10.	Chapter Summary .....	351
<b>Chapter 7: Conclusions and Future Work .....</b>		<b>352</b>
7.1.	Summary of Research Findings.....	352
7.1.1.	Characterisation of Atopic Asthma at the Molecular Level.....	353
7.1.2.	Characterisation of the Circulatory Microbiome in Atopic Asthma.....	355
7.1.3.	Characterisation of the Circulatory Microbiome in different Atopic Disease States .....	357
7.1.4.	Characterisation of the Murine Microbiome following exposure to the HDM allergen .....	362
7.2.	Research Limitations associated with the Study.....	364
7.3.	Future Work .....	367
<b>Publications arising from Thesis .....</b>		<b>375</b>
<b>Supplementary Materials.....</b>		<b>376</b>
<b>References.....</b>		<b>430</b>

# Table of Figures

## Chapter 1

<b>Figure 1. 1:</b> Airway remodelling in asthma .....	<b>22</b>
<b>Figure 1.2:</b> The role of epithelial-secreted cytokines in allergen sensitisation .....	<b>26</b>
<b>Figure 1.3:</b> Receptors involved in allergen recognition and internalisation by airway dendritic cells .....	<b>30</b>
<b>Figure 1.4:</b> Maturation of the T naïve cells into effector T cell subsets.....	<b>31</b>
<b>Figure 1.5:</b> Priming of the allergic response by allergens.....	<b>33</b>
<b>Figure 1.6:</b> Mast cell mediated early phase reactions .....	<b>38</b>
<b>Figure 1.7:</b> The late phase reactions in the effector phase of atopic asthma .....	<b>40</b>
<b>Figure 1.8:</b> Chronic inflammation and the occurrence of airway remodelling.....	<b>43</b>
<b>Figure 1.9:</b> Established asthma biomarkers available for clinical practise and promising biomarkers under investigation.....	<b>46</b>
<b>Figure 1.10:</b> Functions of the microbiota beneficial to human health .....	<b>52</b>
<b>Figure 1.11:</b> The composition of the various microbial communities of the human microbiota.....	<b>54</b>
<b>Figure 1.12:</b> Variations in the gut microbiome of children and adults living in Malawi, the Amazonas, and the United States .....	<b>59</b>
<b>Figure 1.13:</b> Diversity of the gut microbiome detected in 1-year old infants whom asthma was and was not developing .....	<b>63</b>
<b>Figure 1.14:</b> Comparison of the neonatal homogeneous microbiome to the maternal microbiome.....	<b>66</b>
<b>Figure 1.15:</b> Changes in the composition of the airway microbiome in corticosteroid sensitive and corticosteroid resistant asthma compared to healthy control subjects .....	<b>68</b>

<b>Figure 1.16:</b> Histological examination of the airways in germ free mice and specific pathogen free mice before and after OVA allergen challenge .....	<b>70</b>
<b>Figure 1.17:</b> Sequencing of the bacterial 16S rRNA gene.....	<b>78</b>
<b>Figure 1.18:</b> Human disease that have been associated with changes in the circulatory microbiome.....	<b>81</b>

## Chapter 2

<b>Figure 2.1:</b> Schematic diagram of the AMPure XP PCR purification protocol .....	<b>93</b>
---	-----------

## Chapter 3

<b>Figure 3.1:</b> Identification significant differential gene expression in the asthmatic subjects compared to non-asthmatic subjects using the Galaxy Tuxedo Protocol .....	<b>106</b>
<b>Figure 3.2:</b> Total number of mRNA reads isolated and sequenced from the human plasma samples.....	<b>114</b>
<b>Figure 3.3:</b> Heatmap showing highly expressed genes in asthmatic subjects compared to control subjects.....	<b>118</b>
<b>Figure 3.4:</b> Principal component analysis of circulatory gene expression profiles detected in asthmatic and control subjects .....	<b>120</b>
<b>Figure 3.5:</b> Principal component analysis of circulatory gene expression profiles detected in the asthmatic and control subjects on the basis of age and BMI.....	<b>121</b>
<b>Figure 3.6:</b> Total number of miRNA reads isolated and sequenced from the human plasma samples.....	<b>122</b>
<b>Figure 3.7:</b> A Heatmap showing expression levels of circulatory miRNA in asthmatic subjects compared to control subjects.....	<b>124</b>

<b>Figure 3.8:</b> Differential levels of circulatory miRNA in asthmatic subjects compared to control subjects.....	<b>126</b>
<b>Figure 3.9:</b> Principal component analysis of circulatory miRNA profiles detected in asthmatic and control subjects.....	<b>128</b>
<b>Figure 3.10:</b> Levels of circulatory inflammatory proteins in asthmatic and control subjects .....	<b>140</b>
<b>Figure 3.11:</b> Circulatory total IgE concentration detected in asthmatic subjects compared to control subjects.....	<b>141</b>
<b>Figure 3.12:</b> Circulatory endotoxin concentrations detected in asthmatic subjects compared to control subjects.....	<b>143</b>
 Chapter 4	
<b>Figure 4.1:</b> Attachment of a barcode and adapter to the V3-V4 amplicons during end-point PCR amplification of the V3-V4 region of the bacterial 16S rRNA gene.....	<b>162</b>
<b>Figure 4.2:</b> A schematic diagram showing the order and volume of OneTouch™ 2 ES reagents loaded into the OneTouch™ ES following reagent preparation.....	<b>173</b>
<b>Figure 4.3:</b> Generation of V3-V4 amplicons containing the ion torrent sequencing motifs from human plasma samples using nested PCR.....	<b>185</b>
<b>Figure 4.4:</b> Generation of V4 amplicons containing the ion torrent sequencing motifs from human plasma samples from asthmatic subjects and non-asthmatic control subjects using nested PCR.....	<b>189</b>
<b>Figure 4.5:</b> Generation of V4 amplicons containing the Illumina sequencing motifs from human plasma samples from asthmatic subjects and non-asthmatic control subjects using nested PCR.....	<b>190</b>

<b>Figure 4.6:</b> Quantification of bacterial V4 reads sequenced from human plasma samples using ion torrent sequencing.....	<b>195</b>
<b>Figure 4.7:</b> Relative abundance of bacteria detected in the human circulatory microbiome using Ion torrent sequencing.....	<b>197</b>
<b>Figure 4.8:</b> Quantification of bacterial V4 reads sequenced from human plasma samples using Illumina sequencing .....	<b>200</b>
<b>Figure 4.9:</b> Relative abundance of bacteria detected in the human circulatory microbiome .....	<b>203</b>
<b>Figure 4.10:</b> Comparison of alpha diversity in the asthmatic circulatory microbiome compared to the control microbiome .....	<b>205</b>
<b>Figure 4.11:</b> Comparison of beta diversity in the asthmatic circulatory microbiome compared to the control microbiome .....	<b>207</b>
<b>Figure 4.12:</b> Significant changes in bacterial taxa relative abundance in the circulatory microbiome of atopic asthmatic subjects compared to control subjects .....	<b>209</b>
<b>Figure 4.13:</b> Functional analysis of the plasma circulatory microbiome .....	<b>211</b>
<b>Figure 4.14:</b> Comparison of energy metabolism abundance in the asthma circulatory microbiome compared to the control microbiome .....	<b>212</b>
<b>Figure 4.15:</b> Bacterial growth on selective media streaked with nutrient broth inoculated with human plasma samples .....	<b>214</b>
<b>Figure 4.16:</b> Amplification of total 16S rRNA gene from DNA extracted from bacterial colonies cultured from human plasma .....	<b>217</b>
<b>Figure 4.17:</b> Principal coordinate analysis of weighted unifrac distances between the V4 16S rRNA data generated from human plasma samples and the Human Microbiome Project Gut, Oral Cavity, and Skin data.....	<b>222</b>

## Chapter 5

<b>Figure 5.1:</b> Direct amplification of the V4 region of the bacterial 16S rRNA gene from human serum samples .	<b>245</b>
<b>Figure 5.2:</b> Quantification of bacterial V4 reads sequenced from human serum samples using Illumina sequencing.	<b>248</b>
<b>Figure 5.3:</b> Composition of the bacterial circulatory microbiome in control and atopic subjects.....	<b>250</b>
<b>Figure 5.4:</b> Comparison of Shannon diversity detected in the circulatory microbiome of atopic subjects compared to control subjects .....	<b>253</b>
<b>Figure 5.5:</b> Comparison of Chao1 diversity detected in the circulatory microbiome of atopic subjects compared to control subjects .....	<b>254</b>
<b>Figure 5.6:</b> Comparison of beta diversity of the bacterial populations detected in the circulatory microbiome of atopic subjects compared to a control subjects .....	<b>256</b>
<b>Figure 5.7:</b> Significant changes in bacterial taxa relative abundance in the circulatory microbiome of atopic subjects compared to control subjects .....	<b>261</b>
<b>Figure 5.8:</b> Significant changes in bacterial taxa relative abundance in the circulatory microbiome of asthmatic subjects compared to control subjects.....	<b>264</b>
<b>Figure 5.9:</b> Significant changes in bacterial taxa relative abundance in the circulatory microbiome of allergic rhinitis subjects compared to control subjects.....	<b>267</b>
<b>Figure 5.10:</b> Significant changes in bacterial taxa relative abundance in the circulatory microbiome of hyper-allergic subjects compared to control subjects .....	<b>269</b>
<b>Figure 5.11:</b> Functional analysis of the serum circulatory microbiome.....	<b>270</b>
<b>Figure 5.12:</b> Comparison of microbial activity in hyper-allergic subjects compared to heathy controls .....	<b>273</b>



<b>Figure 6.1:</b> Experimental protocol for intranasal administration of HDM .....	<b>299</b>
<b>Figure 6.2:</b> Amplification of the V4 region of the bacterial 16S rRNA gene from microbial DNA extracted from murine BAL samples .....	<b>310</b>
<b>Figure 6.3:</b> Amplification of the V4 region of the bacterial 16S rRNA gene from microbial DNA extracted from murine faecal samples .....	<b>312</b>
<b>Figure 6.4:</b> Quantification of bacterial V4 reads sequenced murine BAL samples using Illumina sequencing.....	<b>314</b>
<b>Figure 6.5:</b> Quantification of bacterial V4 reads sequenced from murine faecal samples using Illumina sequencing .....	<b>317</b>
<b>Figure 6.6:</b> Composition of the bacterial gut microbiome in mice exposed to the HDM allergen compared to HDM-naïve mice .....	<b>319</b>
<b>Figure 6.7:</b> Composition of the bacterial gut microbiome in mice exposed to the HDM allergen compared to HDM-naïve mice .....	<b>322</b>
<b>Figure 6.8:</b> Comparison of alpha diversity in the airway microbiome of HDM-exposed mice compared to HDM-naïve mice.....	<b>324</b>
<b>Figure 6.9:</b> Comparison of alpha diversity in the gut microbiome of HDM-exposed mice compared to HDM-naïve mice.....	<b>325</b>
<b>Figure 6.10:</b> Comparison of beta diversity of the bacterial populations detected in the murine airway and gut microbiomes .....	<b>327</b>
<b>Figure 6.11:</b> Significant changes in bacterial taxa relative abundance in the murine airway microbiome of mice exposed to the HDM allergen compared to HDM naïve mice .....	<b>329</b>
<b>Figure 6.12:</b> Significant changes in bacterial taxa relative abundance in the gut microbiome of mice exposed to the HDM allergen compared to HDM naïve mice .....	<b>331</b>

<b>Figure 6.13:</b> Microbial functions of the murine airway microbiome.....	<b>333</b>
<b>Figure 6.14:</b> Microbial functions of the murine gut microbiome.....	<b>335</b>
<b>Figure 6.15:</b> Comparison of microbial activity in the gut microbiome of mice exposed to the HDM allergen compared to HDM naïve mice.....	<b>337</b>
Supplementary Materials	
<b>Figure S1:</b> Plate layout of the multi-analyte sandwich ELISAs used to analysis the inflammatory protein levels present in plasma samples from asthmatic subjects (n = 5) and non-asthmatic subjects (n = 5). (A) = plate 1, (B) = plate 2 .....	<b>387</b>
<b>Figure S2:</b> Gradient PCR amplification of the V3-V4 region of the 16S rRNA gene using <i>Escherichia coli</i> DNA .....	<b>412</b>
<b>Figure S3:</b> Amplification of the V3-V4 region of the bacterial 16S rRNA gene from microbial DNA extracted from the human plasma samples.....	<b>413</b>
<b>Figure S4:</b> End-point PCR amplification of the V3-V4 region of the bacterial 16S rRNA gene performed directly on human plasma samples.....	<b>414</b>
<b>Figure S5:</b> Generation of V3-V4 16S rRNA amplicons containing the ion torrent sequencing motifs from human plasma samples using end-point PCR .....	<b>415</b>
<b>Figure S6:</b> Nested PCR amplification of the V3-V4 region of the bacterial 16S rRNA gene using <i>Escherichia coli</i> DNA at varying concentrations .....	<b>416</b>
<b>Figure S7:</b> Generation of V3-V4 amplicons containing the ion torrent sequencing motifs from human plasma samples from asthmatic subjects and non-asthmatic control subjects using nested PCR . .....	<b>417</b>
<b>Figure S8:</b> Gradient PCR amplification of the V4 region of the 16S rRNA gene using <i>Escherichia coli</i> DNA .....	<b>418</b>

<b>Figure S9:</b> Direct PCR amplification of the V4 region of the 16S rRNA gene from microbial DNA present in murine plasma samples.....	<b>425</b>
---	------------

## Table of Tables

### Chapter 1

<b>Table 1.1:</b> Bacteria detected in the human microbiome that have been found to have beneficial or harmful functional properties that are associated with atopic disease pathology.....	<b>73</b>
---	-----------

### Chapter 3

<b>Table 3. 1:</b> A full list of the donor population characteristics required for the human atopic asthma study .....	<b>103</b>
<b>Table 3. 2:</b> Asthma presentation and disease characterisation in the asthmatic cohort at the time of sample collection .....	<b>112</b>
<b>Table 3.3:</b> Characterisation of the asthmatic and non-asthmatic subjects at the time of sample collection.....	<b>113</b>
<b>Table 3.4:</b> A list of genes that displayed the highest degree of differential expression in the asthmatic subjects compared to the control subjects .....	<b>116</b>
<b>Table 3.5:</b> Genes with significant differential expression in the asthmatic subjects compared to control subjects that are associated with asthma pathology.....	<b>130</b>
<b>Table 3 6:</b> Genes targeted by the differentially expressed miRNAs that displayed significant differential expression in the asthmatic subjects compared to the control subjects.....	<b>132</b>

<b>Table 3.7:</b> The top 15 biological pathways that were predicted to be altered in the asthmatic subjects as a result of differential miRNA expression .....	<b>133</b>
<b>Table 3.8:</b> Upstream gene regulators with predicted significantly altered activity in the asthmatic subjects compared to the control subjects .....	<b>135</b>
<b>Table 3.9:</b> Canonical pathways predicted to have significantly altered activity in the asthmatic subjects.....	<b>137</b>
<b>Table 3.10:</b> Biological functions predicted to have significantly altered activity in the asthmatic subjects compared to control subjects .....	<b>138</b>

#### Chapter 4

<b>Table 4.1:</b> Molecular properties of the primers used to amplify the V3-V4 region of the bacterial 16S rRNA gene.....	<b>160</b>
<b>Table 4.2:</b> First stage of Nested PCR amplification of the V3-V4 region of the bacterial 16S rRNA gene human plasma samples.....	<b>163</b>
<b>Table 4.3:</b> Second stage nested PCR protocol used to attach the Ion torrent sequencing barcode and adaptors to purified V3-V4 amplicons generated from human plasma samples.....	<b>164</b>
<b>Table 4.4:</b> Molecular properties of the primers used to amplify the V4 region of the 16S rRNA gene .....	<b>165</b>
<b>Table 4.5:</b> Second stage nested PCR protocol used to attach the Ion torrent sequencing barcode and adaptors to purified V4 amplicons generated from human plasma samples .....	<b>167</b>
<b>Table 4.6:</b> Molecular properties of the 515F/806R oligonucleotide primers used to incorporate the Illumina Nextera transposase adaptors.....	<b>168</b>

<b>Table 4.7:</b> Second stage nested PCR protocol used to attach Illumina sequencing motifs to purified V4 amplicons generated from human plasma samples.....	<b>169</b>
<b>Table 4.8:</b> Molecular properties of the primers used to amplify the total 16S rRNA gene .....	<b>181</b>
<b>Table 4.9:</b> PCR cycling parameters used when amplifying the total 16S rRNA gene using the GoTaq Green master mix protocol.....	<b>181</b>
<b>Table 4. 10:</b> PCR cycling parameters used when amplifying the total 16S rRNA gene using the Phusion Blood Direct protocol.....	<b>182</b>
<b>Table 4.11:</b> Quantification of V3-V4 reads containing the ion torrent sequencing motif generated from human plasma samples .....	<b>186</b>
<b>Table 4.12:</b> Quantification of the number of enriched V3-V4-positive Ion Sphere™ Particles generated from the V3-V4 amplicon library.....	<b>187</b>
<b>Table 4. 13:</b> Quantification of V4 amplicons containing the Ion torrent sequencing motifs generated from human plasma samples .....	<b>191</b>
<b>Table 4.14:</b> Quantification of V4 amplicons containing the Illumina sequencing motifs generated from human plasma samples .....	<b>193</b>
<b>Table 4.15:</b> Identification of bacterial colonies grown on selective media streaked with nutrient broth inoculated with human plasma samples .....	<b>218</b>

## Chapter 5

<b>Table 5.1:</b> PCR Amplification of the V4 region of the 16S rRNA gene in historic serum samples.....	<b>239</b>
<b>Table 5.2:</b> Attachment of Illumina sequencing motifs onto V4 16S rRNA amplicons generated from historic serum samples using PCR .....	<b>240</b>

## Chapter 6

<b>Table 6.1:</b> Amplification of the V4 region of the 16S rRNA gene from microbial DNA present in murine plasma samples using an optimised Phusion blood direct protocol...	<b>302</b>
<b>Table 6.2:</b> Amplification of the V4 region of the 16S rRNA gene from microbial DNA present in murine plasma samples using a SureDirect Blood PCR protocol .....	<b>303</b>
<b>Table 6.3:</b> PCR Amplification of the V4 region of the 16S rRNA gene from microbial DNA extracted from murine BAL and faecal samples.....	<b>305</b>

## Supplementary Materials

<b>Table S1:</b> Asthma Quality Questionnaire (ACQ) completed by the asthmatic subjects following sample collection.....	<b>384</b>
<b>Table S2:</b> Characterisation of the Atopic Asthma cohort at the time of sample collection .....	<b>388</b>
<b>Table S3:</b> Results of the ACQ taken at the time of sample collection by the asthmatic subjects.....	<b>389</b>
<b>Table S4:</b> Genes with significant differential expression in asthmatic subjects compared to control subjects.....	<b>390</b>
<b>Table S5:</b> Levels of circulatory inflammatory proteins in asthmatic and control subjects .....	<b>404</b>
<b>Table S6:</b> Total circulatory IgE concentrations in asthmatic and control subjects .....	<b>405</b>
<b>Table S7:</b> Circulatory endotoxin concentrations present in asthmatic and control subjects .....	<b>406</b>
<b>Table S8:</b> Molecular properties of the V3-V4 16S Amp oligonucleotide primers with the Ion torrent sequencing motifs incorporated.....	<b>407</b>

<b>Table S9:</b> Molecular properties of the V4 16S Amp oligonucleotide primers with the Ion torrent sequencing motifs incorporated .....	<b>409</b>
<b>Table S10:</b> The number of V4 reads generated from human plasma samples following amplification of the V4 region of the 16S rRNA bacterial gene and Illumina sequencing of the V4 amplicons .....	<b>419</b>
<b>Table S11:</b> Alpha diversity of the blood microbiome detected in plasma samples from asthma subjects compared to plasma samples from control subjects.....	<b>420</b>
<b>Table S12.</b> End-point PCR amplification of the 16S rRNA gene from bacterial DNA extracted from cultured bacterial colonies generated from human plasma samples .....	<b>421</b>
<b>Table S13:</b> The number of V4 reads generated from human serum samples following amplification of the V4 region of the 16S rRNA bacterial gene and Illumina sequencing of the V4 amplicons .....	<b>423</b>
<b>Table S14:</b> Microbial functions predicted to be significantly altered in the circulatory microbiome of hyper-allergic subjects compared to the circulatory microbiome of non-atopic subjects .....	<b>424</b>
<b>Table S15:</b> The number of V4 reads generated from murine BAL samples following amplification of the V4 region of the 16S rRNA bacterial gene and Illumina sequencing of the V4 amplicons.....	<b>426</b>
<b>Table S16:</b> The number of V4 reads generated from murine faecal samples following amplification of the V4 region of the 16S rRNA bacterial gene and Illumina sequencing of the V4 amplicons.....	<b>427</b>
<b>Table S17:</b> Microbial functions predicted to be significantly altered in the gut microbiome of mice exposed to the HDM allergen compared to HDM-naïve mice .....	<b>428</b>

## List of Abbreviations

A.R.I.A	Anaerobe recovery and isolation agar
ACQ	Asthma Control Questionnaire
BAL	Bronchoalveolar lavage
BC	Barcode
bp	Base pairs
CCL	C-C motif ligand
CD	Cluster of differentiation
CLED	Cystine lactose electrolyte deficient
COPD	Chronic obstructive pulmonary disorder
CPM	Counts per million
CR	Corticosteroid resistant
CS	Corticosteroid sensitive
CXCL	C-X-C motif ligand
Cys-LTs	Cysteinyl leukotrienes
DAMP	Danger-associated molecule patterns molecule
DC-SIGN	Dendritic cell-specific intracellular adhesion molecule 3-bragging non-integrin
dH <sub>2</sub> O	Distilled water
dsDNA	Double stranded DNA
Dyna beads	Dynabeads® MyOne Streptavidin C1 beads
EDTA	Ethylenediaminetetraacetic acid
ELISA	Enzyme-linked immunosorbent assay
ES	Enrichment system
FCER	Fc fragment of IgE receptor



FcεRI	High-affinity IgE receptor
FcεRII	Low-affinity IgE receptor
FDR	False rate of discovery
FN1	Fibronectin 1
FPKM	Fragments per kilobase of transcript per million mapped
GF	Germ free
GM-CSF	Granulocyte-macrophage colony-stimulating factor
GO	Gene ontology
GSTA1	Glutathione S-transferase alpha 1
HDM	House dust mite
HLA	Human leukocyte antigen
HMP	Human microbiome project
HS	High sensitivity
i5	Illumina index 2
i7	Illumina index 1
ICAM-1	Intracellular adhesion molecule 1
IFNγ	Interferon gamma
Ig	Immunoglobulin
IL	Interleukin
IL7R	Interleukin 7 receptor
ILC2	Type 2 innate lymphoid cells
IPA	Ingenuity pathway analysis
ISPs	Ion sphere particles
KEGG	Kyoto Encyclopaedia of Genes and Genomes

LAL	Limulus ameocyte lysate
LDA	Linear discriminant analysis
LEfSe	Linear discriminant analysis effect size
LGALS3	Galectin 3
LPS	Lipopolysaccharide
LT	Leukotriene
MCP	Monocyte chemoattractant protein
MDC	Macrophage derived protein
MHC	Major histocompatibility complex
MIP-1 $\alpha$	Macrophage inflammatory protein 1-alpha
MiRNA	MicroRNA
MPO	Myeloperoxidase
MR	Mannose receptor
mRNA	Messenger RNA
mV3-V4	Modified V3-V4
mV4	Modified V4
NKT	Natural killer T
NTS	Neurotensin
OTU	Operational taxonomic unit
OVA	Ovalbumin
PAMPs	Pathogen-associated molecular patterns
PAR	Protease activated receptor
PBS	Phosphate buffered saline
PCA	Principal component analysis

PCoA	Principal coordinate analysis
PCR	Polymerase chain reaction
PDE4A	Phosphodiesterase 4A
PG	Prostaglandins
PGM	Personal genome machine
PICRUSt	Phylogenetic investigation of communities by reconstruction of unobserved states
PPAR	Peroxisome proliferator-activated receptor
PRR	Pathogen recognition receptor
qPCR	Quantitative polymerase chain reaction
RIG	Retinoic acid-inducible gene 1
rRNA	Ribosomal RNA
S.D	Standard deviation
SCFA	Short chain fatty acid
SPF	Specific pathogen free
SPRI	Solid-phase reversible immobilisation
TAE	Tris-acetate EDTA
TARC	Thymus and activation regulated chemokine
T <sub>FH</sub>	T follicular helper
TGF- $\beta$	Transforming growth factor beta
Th	T helper
Th0	Naïve T helper
TLR	Toll-like receptor
TNF	Tumour necrosis factor

Treg	T regulatory
TrP1	Truncated P1 adaptor
TSLP	Thymic stromal lymphopoietin
UV	Ultraviolet
V3-V4	Hypervariable regions 3-4 of the 16S rRNA gene
V4	Hypervariable region 4 of the 16S rRNA gene
VCAM-1	Vascular adhesion molecule 1
VDR	Vitamin D receptor
VEGF	Vascular endothelial growth factor
XT	Nextera transposase
GFP	Green fluorescent protein

# Chapter 1: Introduction to Molecular Characterisation of Atopic Asthma

## 1.1. Introduction to Asthma

Asthma is an ancient disease that has been affecting humans for thousands of years. Current estimates by the World Health Organisation predict that over 300 million people worldwide are living with the disease <sup>1</sup>, making it one of the most common chronic diseases globally. It is an inflammatory disorder of the airways that is a major public health concern due to increasing prevalence and rates of mortality <sup>2-5</sup>, and causing a global estimate of 250,000 premature deaths each year <sup>1</sup>.

The disease can develop during childhood (early-onset) or in adulthood (late-onset) and is characterised by variable and recurrent symptoms of wheezing, coughing, and shortness of breath. Symptoms arise as a result of intermittent episodes of reversible airway obstruction due to airway hyperresponsiveness and structural changes to the airways, such as airway fibrosis, goblet cell hyperplasia, increased smooth muscle mass, and increased angiogenesis <sup>6,7</sup>.

## 1.2. The Causes of Asthma

The causes of asthma are multi-factorial and development of the disease is thought to be consequence of a complex array of contributing influences, including genetic susceptibility, environmental factors, and immune status <sup>6,8-12</sup>.

Traditionally, asthma has been defined as being either atopic or non-atopic on the basis of the presumed causative factor, whereby atopic asthma is induced by an environmental antigen, whilst non-atopic asthma is due to an internal stimulus.

Following development, asthma is typically characterised by periods of disease stability interspersed with periods of exacerbation. Asthma exacerbation is defined as acute or subacute episodes of progressively worsening airway narrowing and lung function that present as shortness of breath, wheezing, and chest tightness <sup>13</sup>. Airway narrowing associated with asthma exacerbations has been demonstrated to be the result of smooth muscle contraction, airway wall oedema, and excessive mucous production <sup>13-15</sup>. Causative factors of acute asthma exacerbations, similar to asthma development, are multifactorial, and include viral infections, exposure to allergens (house dust mite, pollen, animal dander), occupational exposures (grains, cleaning agents, irritants, metals, woods), hormones (menstrual asthma), exercise, stress, and air pollutants<sup>13</sup>.

### 1.3. Clinical Presentation of Asthma

The first clinical descriptions of asthma appeared in medical literature around 2600 BCE <sup>16-18</sup>. Today asthma is a clinical term to describe a group of patients with broad general respiratory symptoms that are associated with reversible airway obstruction and airway hyperresponsiveness <sup>19</sup>, and clinical presentation is highly heterogeneous <sup>20</sup>. The disease can vary greatly in terms of onset (i.e. early-onset and late-onset) and response to current asthma treatments. It can present as a stable, chronic disease, but also present as acute asthma exacerbations that can be fatal <sup>21</sup>. Symptoms may be mild or severe, and arise as a consequence of a range of pathogenic mechanisms and causative factors, such as immunoglobulin (Ig)E-mediated allergic responses, exposure to pollutants, exercise, stress, or airway infections <sup>21</sup>.

The variation in asthma presentation and cause has resulted in speculation into whether asthma is a single disease or a spectrum of related diseases with subtle but distinct

differences in aetiology and pathophysiology<sup>22,23</sup>. This has led to asthma being separated into a number of phenotypes, which are then further subdivided into several endotypes<sup>20,22–25</sup>.

The asthma phenotypes and endotypes differ with regards to disease presentation in terms of cause, development, severity, and response to medication. Individuals with eosinophilic asthma, for example, have been reported to have a good therapeutic response to inhaled or oral corticosteroid therapy, whereas individuals with neutrophilic asthma have been found to respond poorly to this therapeutic approach.

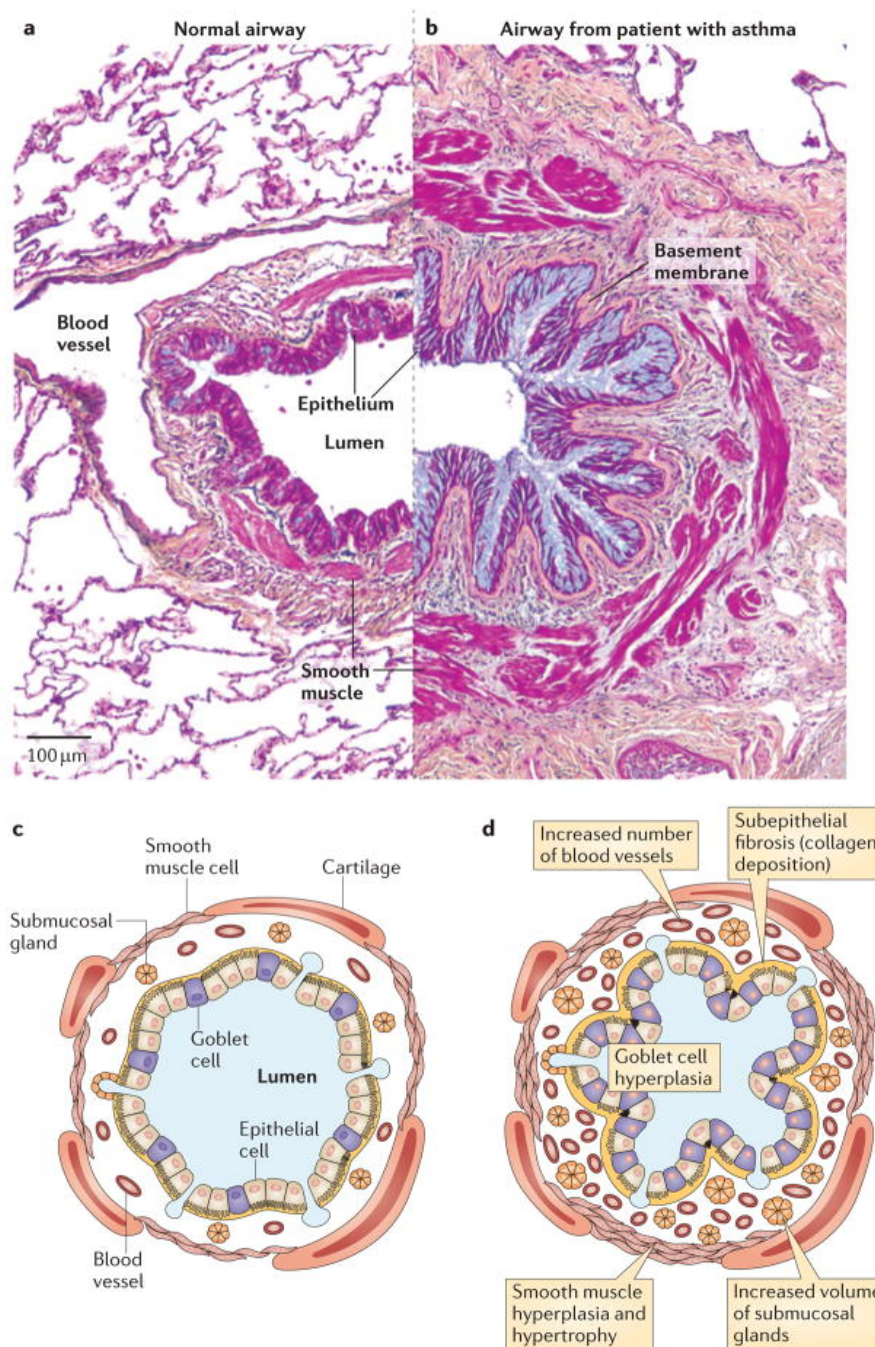
#### 1.4. Asthma Phenotypes and Endotypes

Currently asthma diagnostics involves assigning asthma cases to either the atopic phenotype or the non-atopic phenotype. First proposed over 70 years ago by Rackemann, the phenotypes are based on age of onset and presence or absence of an environmental trigger<sup>26</sup>. Atopic asthma typically develops during early childhood and is associated with sensitisation to one or more airborne allergen, such as animal dander, pollen, mould, or house dust mite (HDM). In contrast non-atopic asthma is typically late-onset, shows no association with allergen sensitisation, and is thought to occur as a result of a yet unidentified intrinsic asthma trigger<sup>27</sup>. Current theories regarding the intrinsic asthma trigger include the suggestion that non-atopic asthma is triggered by a microbial agent, as respiratory influenza-like illness has often been observed to precede the development of non-atopic asthma<sup>27</sup>. Another theory is that non-atopic asthmatics are sensitive to an as yet unidentified allergen, and thus elude skin prick tests designed to detect sensitisation to known allergens<sup>27</sup>.

An estimated 70-90% of asthmatic patients are estimated to suffer from atopic asthma<sup>27,30</sup>, making it the most commonly diagnosed asthma phenotype. The disease belongs to a group of diseases known as the atopic diseases, which are all clinical manifestations of allergen sensitisation, and include atopic asthma, allergic rhinitis (hay fever), atopic dermatitis (eczema), and some food allergies<sup>31</sup>.

Allergen sensitisation occurs due to a failure to develop immune tolerance to one or more allergens present ubiquitously in the environment. Over time exposure to the allergen results in chronic localised allergic inflammation, and subsequent long-term changes to the structure and function of the organs affected. In atopic asthma, chronic allergic inflammation occurs in the airways as a consequence of inhalation of airborne allergens, such as pollen, animal dander, and HDM, and results in chronic airway inflammation, structural changes to the airways, known as airway remodelling, and intermittent episodes of reversible airway obstruction as a result of airway narrowing (Figure 1.1).





**Figure 1. 1: Airway remodelling in asthma.** Histological examination of airway vessels from asthmatic subjects (compared to control subjects have revealed significant remodelling in the asthmatic airways compared to control subjects (A – D). This is due to several structural changes in the airway vessels, including goblet cell hyperplasia, subepithelial fibrosis, smooth muscle hyperplasia and hypertrophy, and increased airway vascularity (angiogenesis). Images **A** and **B** depict cross-sections of the large airways stained with Movat’s pentachrome stain from a control subjects (**A**) and a subject with severe asthma (**B**). The epithelium in the asthmatic airway cross-section is observed to exhibit mucous hyperplasia and hypersecretion (blue staining). Additionally, the asthmatic cross-section exhibits significant basement membrane thickening and increased smooth muscle volume. Diagrams **C** and **D** are schematic representations of the structure of the large airways in control subjects (**C**) and asthmatic subjects (**D**). [Taken from Fahy, 2015 <sup>32</sup>]

As understanding of asthma has progressed, new atopic asthma endotypes have been proposed and characterised on the basis of associated immunological responses. Simpson *et al* (2006), for instance, identified four additional endotypes that are characterised by the degree of granulocytic populations present; these comprise of eosinophilic asthma, neutrophilic asthma, mixed granulocytic asthma, and paucigranulocytic (non-inflammatory) asthma <sup>28</sup>. Furthermore, subsequent work carried out by Woodruff *et al* (2009), has revealed two more endotypes, known as T helper (Th)2-high, in which asthmatic patients displayed high levels of Th2 lymphocytes and Th2-low, in which the Th2 lymphocyte population size was indistinguishable to the healthy control subjects <sup>29</sup>.

### 1.5. The Atopic March

Allergen sensitisation typically occurs during the first two years of life in genetically predisposed infants and can persist through a lifetime, with disease commonly first presenting as atopic dermatitis (0 – 2 years), followed by the development of asthma (> 5 years) in approximately half of atopic dermatitis patients, and allergic rhinitis (> 8 years) in approximately two thirds of atopic dermatitis patients <sup>33,34</sup>. The pattern of clinical manifestations presenting in atopic individuals is referred to as the atopic march.

This results in atopic individuals frequently presenting with more than one clinical manifestation of atopic disease. A study carried out by Kapoor *et al* (2008), for instance, found that by the age of 3 years 66% of infants diagnosed with atopic dermatitis had developed one or more additional forms of atopic disease <sup>35</sup>.

## 1.6. Atopic Asthma Pathogenic Mechanisms

In the general population, inhalation of aeroallergens is relatively harmless, resulting in low grade immune responses that are characterised by the production of allergen-specific IgG1 and IgG4, and the differentiation and proliferation of interferon gamma (IFN $\gamma$ ) producing Th1 cells due to interleukin (IL)-12 secreting macrophages<sup>36,37</sup>. In individuals genetically predisposed toward atopy, however, an exaggerated immune response may occur following exposure to one or more aeroallergen. The immune response that occurs is characterised by the production of allergen-specific IgE and a Th2-driven immune response involving the production of IL-4, IL-5, and IL-13 in the airways<sup>38,39</sup>.

The inflammatory responses associated with airborne allergens in atopic asthmatics are generally classified into four temporal phases; allergen sensitisation, which occurs in genetically predisposed individuals upon first exposure to the allergen, early-phase inflammation, which occurs within seconds to minutes of allergen exposure, late-phase inflammation, which occurs within several hours of allergen exposure, and chronic allergic inflammation, which persists in the asthmatic airways as a result of repeated exposure to the allergen.

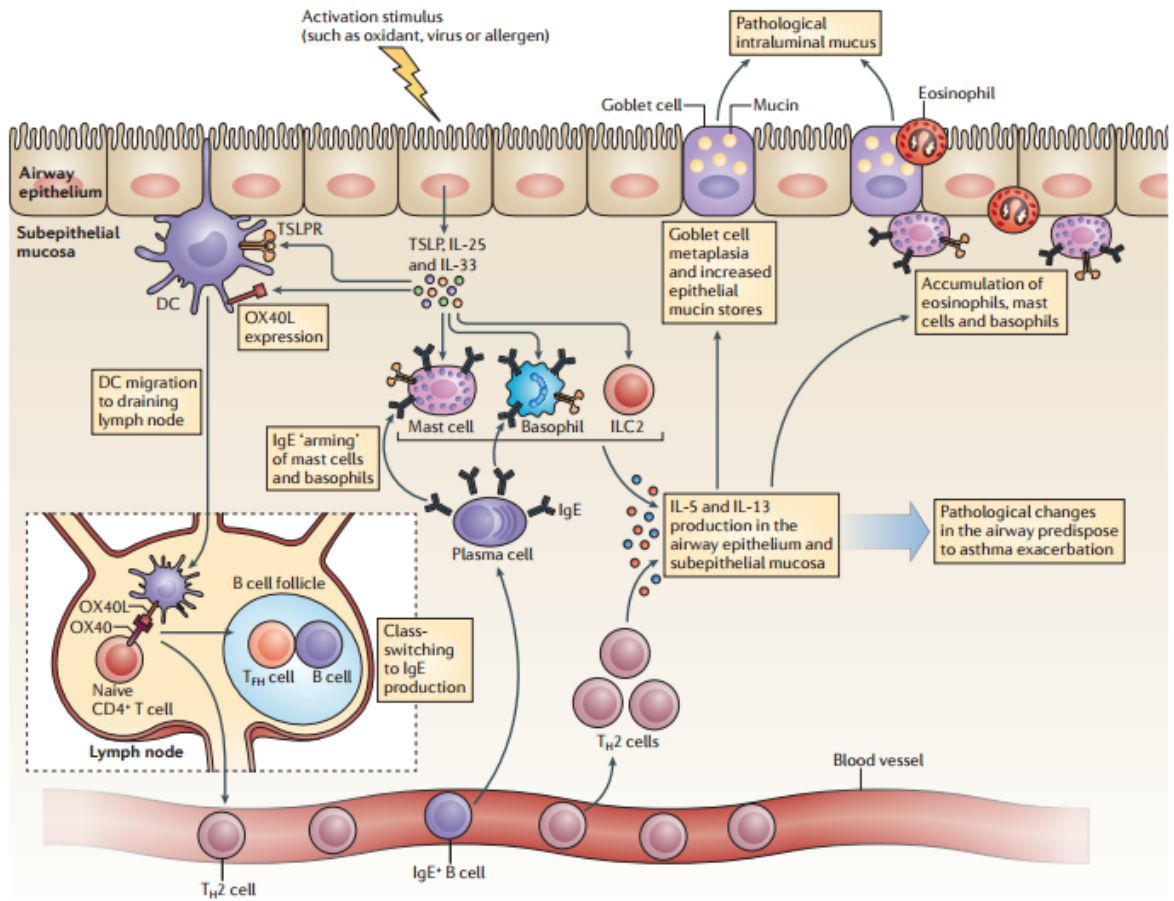
## 1.7. The Allergen Sensitisation Phase

The sensitisation phase of IgE-mediated hypersensitivity is initiated upon first exposure to an airborne allergen, and generally occurs within minutes of allergen inhalation<sup>31</sup>. During this phase the immune system is primed against the allergen as a result of the generation of plasma and memory cells that produce allergen specific IgE and the induction of a Th2 mediated immune response.

Allergen sensitisation typically occurs during early childhood following first exposure to the allergen. Upon entry into the airways the allergen induces an immune response as a consequence of interactions with the subepithelial mucosal layer. These interactions result in the activation of the epithelial and myeloid cells, the migration of dendritic cells to the draining lymph node and subsequent Th2 differentiation, and the recruitment of a range of immune cells to the airways.

#### 1.7.1. Activation of the Epithelial Cells

Aeroallergens are recognised by the epithelial cells through pathogen recognition receptors (PRR's), such as toll-like receptors (TLRs), C-type lectin receptors, and protease activated receptors (PARs) expressed on the epithelial cell surface <sup>40</sup>. Recognition of the allergen results in the secretion of alarmins (also known as danger-associated molecular patterns molecules, DAMPs). Examples include uric acid and adenosine triphosphate; cytokines, such as IL-1 $\alpha$ , IL-25, IL-33, granulocyte-macrophage colony-stimulating factor (GM-CSF), and thymic stromal lymphopoietin (TSLP); and chemokines, such as chemokine C-C motif ligand (CCL)2 (also referred to as monocyte chemoattractant protein 1, MCP-1), CCL3 (previously known as macrophage inflammatory protein 1-alpha, MIP-1 $\alpha$ ), and CCL20 <sup>41</sup>. These proteins are designed to activate innate immune cells, such macrophages, type 2 innate lymphoid (ILC2) cells, and pulmonary dendritic cells, and recruit immune cells to the airways. These functions have been demonstrated to an important role in allergen sensitisation and airway inflammation (Figure 1.2).



**Figure 1.2: The role of epithelial-secreted cytokines in allergen sensitisation.** The production of alarmins following epithelial activation have been demonstrated to play a number of important roles in allergen sensitisation. The secretion of TSLP, for example, has been demonstrated to activate immature dendritic cells present in the airways, causing the cells to migrate to the lymph nodes where they induce Th2 differentiation and expansion. The Th2 cells then enter the systemic circulatory system where they are recruited to the inflamed airways or they induce B cell recombinant class switching, resulting in the production of IgE. TSLP, along with IL-25 and IL-33, has also been demonstrated to induce migration of the allergen-specific IgE presenting mast cells and basophils, subsequently causing accumulation of allergen-primed cells within the airways that results in the rapid induction of an immune response following later re-exposure to the allergen. Additionally, IL-25 and IL-33 have also been found to induce production of IL-5 and IL-13 by the mast cells, basophils, and ILC2 cells, subsequently causing increased mucous production, accumulation of eosinophils, mast cells and basophils, and airway remodelling.

[Taken from Fahy, 2015 <sup>32</sup>]

### 1.7.2. Activation of the Innate Immune Cells

In addition to activating the epithelium cells, the HDM allergen also activates innate myeloid cells present in the subepithelial mucosal layer due to its ability to increase epithelium permeability and enter the subepithelial mucosal layer.

Activation of airway myeloid cells (dendritic cells, macrophages, mast cells, eosinophils, basophils, and neutrophils) works similarly to allergen-induced activation of the epithelial cells, whereby allergen binding to PRRs, such as TLRs, retinoic acid-inducible gene 1 (RIG) receptors, Nod-like receptors, C-type lectin receptors, and mannose receptors upregulated on the cell surface of the lung myeloid cells.

These germ-line encoded receptors have evolved to recognise components of microbial cells, known as pathogen-associated molecular patterns (PAMPs) <sup>42</sup>. It is therefore speculated that allergens induce innate immune responses through mimicry of PAMPs, the presence of microbial structures within the allergen itself, and through the allergen's ability to directly engage with the PRRs <sup>43</sup>.

Following activation of the myeloid cells, the cells produce a number of pro-inflammatory chemokines and cytokines that contribute towards airway inflammation. HDM-induced activation of alveolar macrophages, for example, has been demonstrated to increase production of IL-6, TNFA, and nitric oxide <sup>44</sup>, whilst HDM-induced activation of mast cells has been found to induce the expression of IL-1 $\beta$ , IL-4, IL-6, IL-9, IL-13, and TNFA <sup>45</sup>.

It has also been speculated that HDM indirectly activates invariant natural killer T (iNKT) cells. Akbari *et al* (2003), for example, found that inhibition of iNKT cell activity led to the complete ablation of airway hyperreactivity in mice sensitised and challenged with the common laboratory allergen Ovalbumin (OVA) <sup>46</sup>. This was associated with reduced levels

of OVA-specific IgE, IL-4 and IL-13, and a significant reduction in airway eosinophilia, a key factor in the effector phases of atopic asthma <sup>46</sup>. Moreover, the iNKT cells were found to play an essential role in Th2 priming against the OVA allergen <sup>46</sup>.

In response to these findings, Akbari and colleagues (2003) have proposed an intriguing novel mechanism of allergen sensitisation. In this proposed mechanism, the presence of aeroallergens in the mucosal layer results in exposure of self-glycolipids that are typically inaccessible to the airway immune cells. NKT cells present in the airways are thought to bind to the newly exposed glycolipids, resulting in activation of the cells and subsequent generation of IL-4 and IL-13 prior to dendritic cell-mediated Th0 priming in the draining lymph nodes. The NKT cells, therefore, are thought to be an important source of the exogenous IL-4 and IL-13 required to induce Th2 differentiation in the draining lymph nodes, and thus is essential for Th2 accumulation within the airways <sup>46</sup>.

### 1.7.3. T Helper 2 Priming and IgE Production

Following initiation of the innate immune responses, HDM exposure in individuals genetically predisposed towards atopy also triggers a Th2-driven immune response. This is mediated by the dendritic cells <sup>47-49</sup>, which possess cellular structures, called processes, that enable them to detect allergens present in the bronchial lumen in addition to the subepithelial mucosal layer.

The airway dendritic cells are present in the basolateral layer of the epithelium, and constantly sample from the airway lumen by extending their processes between the epithelial cells and into the airway lumen. Inhaled allergens may be detected by the dendritic cell processes in the airway lumen, or the allergen may translocate across the

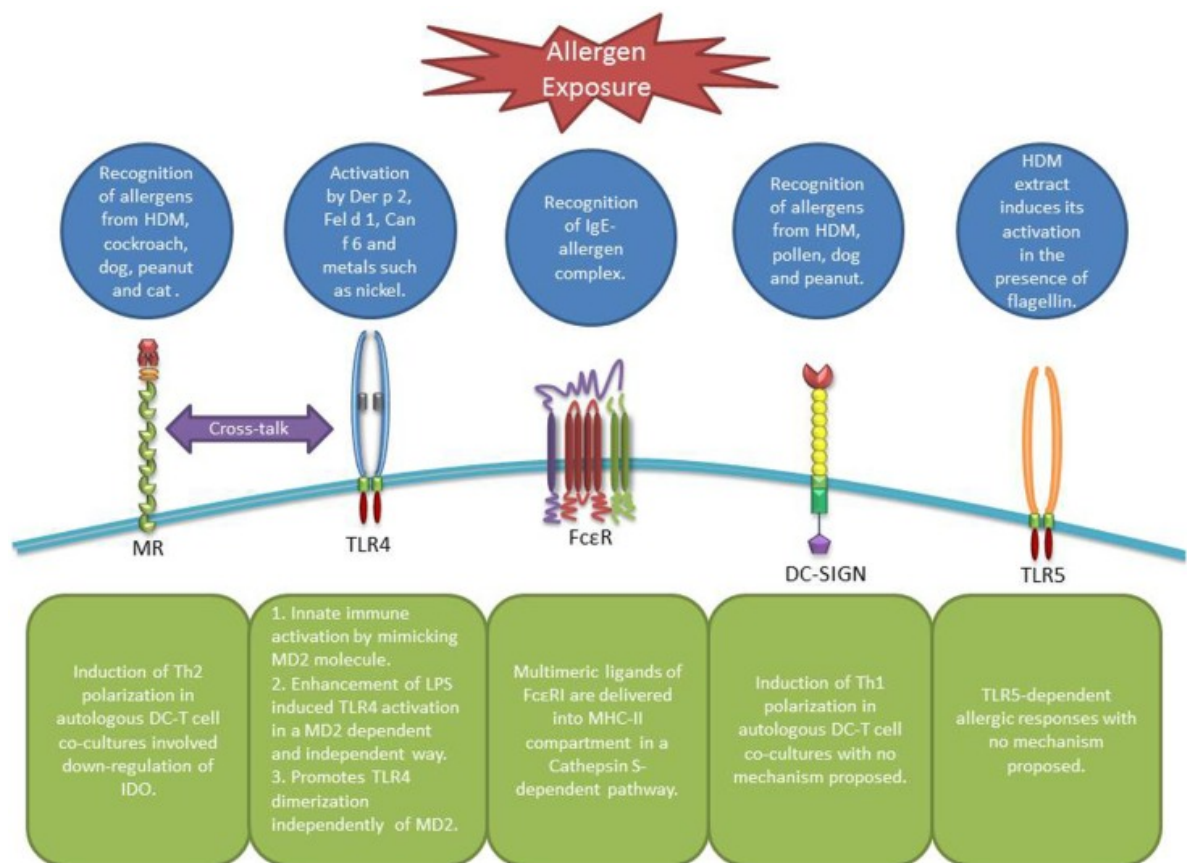
epithelial layer and interact with dendritic cells present in the underlying submucosal layer

50.

Following detection of the allergen, dendritic cells internalise the allergen through one of three mechanisms; macropinocytosis, phagocytosis, and receptor-mediated endocytosis<sup>51-53</sup>. Macropinocytosis involves passive allergen internalisation whereby internalisation occurs as a result of non-specific uptake of large amounts of fluid and solutes from the dendritic cell's immediate environment. In contrast phagocytosis and receptor-mediated endocytosis involves active internalisation that occurs as a result of the allergen binding to dendritic cell surface receptors, resulting in activation of the cell and internalisation of the allergen (Figure 1.3)<sup>51-53</sup>.

Once internalised, the allergen is delivered to late endosomes and degraded into small peptides using cathepsin proteases<sup>51</sup>. The allergen peptides are then processed and presented on the dendritic cell surface by major histocompatibility complex II (MHC II) molecules<sup>47, 52, 54</sup>.



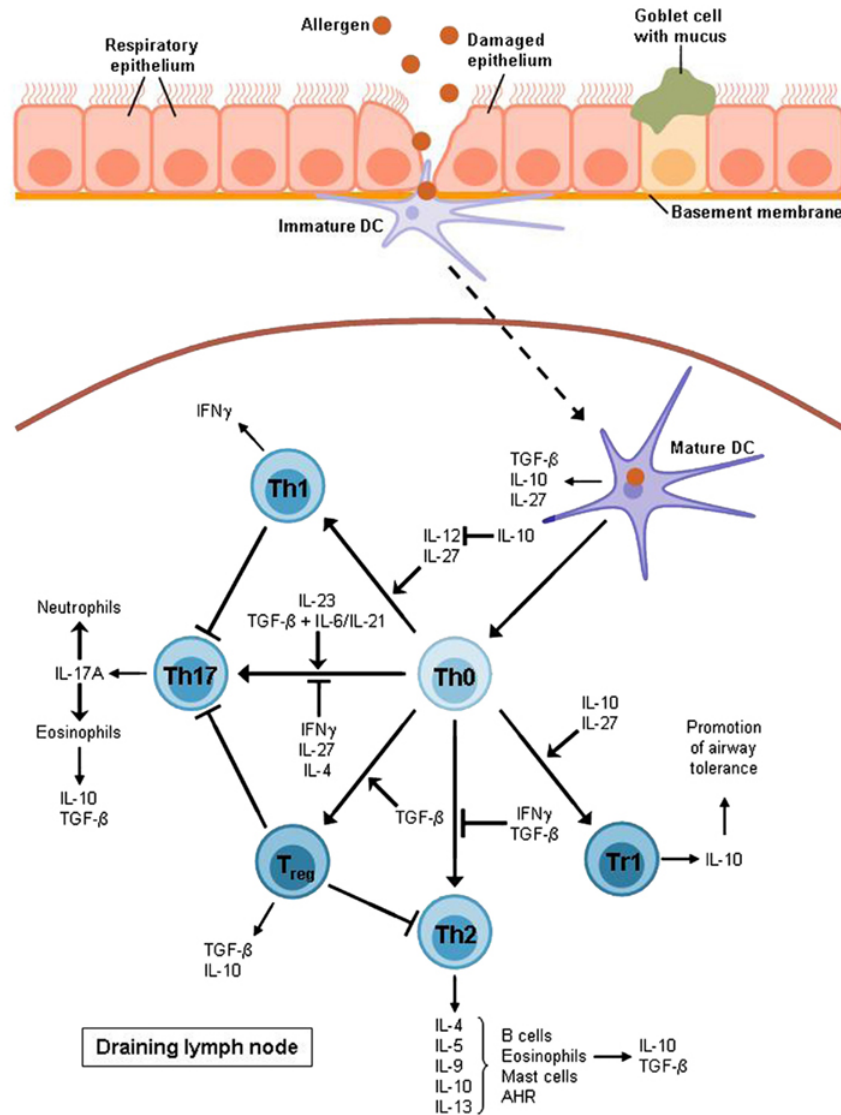


**Figure 1.3: Receptors involved in allergen recognition and internalisation by airway dendritic cells.** The C-Type lectin receptors, such as mannose receptor (MR) and dendritic cell-specific intracellular adhesion molecule 3-bragging non-integrin (DC-SIGN) are primarily involved in recognition of glycol-allergens, such as pollen. The TLRs primarily recognise the HDM allergen Der p 2 and flagellin, a contaminate of HDM extracts. TLR4 is also capable of recognising the feline allergen Fel d1, the canine allergen Can f 6, and nickel. The high affinity IgE receptor (FcεRI) recognises IgE-allergen complex and plays an important role in IgE-dependent allergen presentation.

[Taken from Salazar & Ghaemmaghami, 2013 <sup>40</sup>]

The activated dendritic cells then upregulate co-stimulatory molecules on the cell surface and migrate to the draining lymph nodes where they present the MHC II-bound allergen peptides to naïve T helper (Th0) cells <sup>47,55</sup>. This stimulates the Th0 cells to become IL-4 competent <sup>32,47</sup>, and is dependent on the presence of exogenous IL-4 within the Th0 microenvironment <sup>56</sup>.

Following priming the IL-4 competent cells migrate from the paracortical area, which is primarily composed of T cells, into the secondary lymphoid follicle, which is predominately populated by B cells<sup>57</sup>. In the secondary lymphoid follicle the IL-4 competent T cells either differentiate into T follicular helper (T<sub>FH</sub>) cells or they exit the draining lymph node to enter the blood circulation where they complete maturation (Figure 1.4)<sup>32,58,59</sup>.



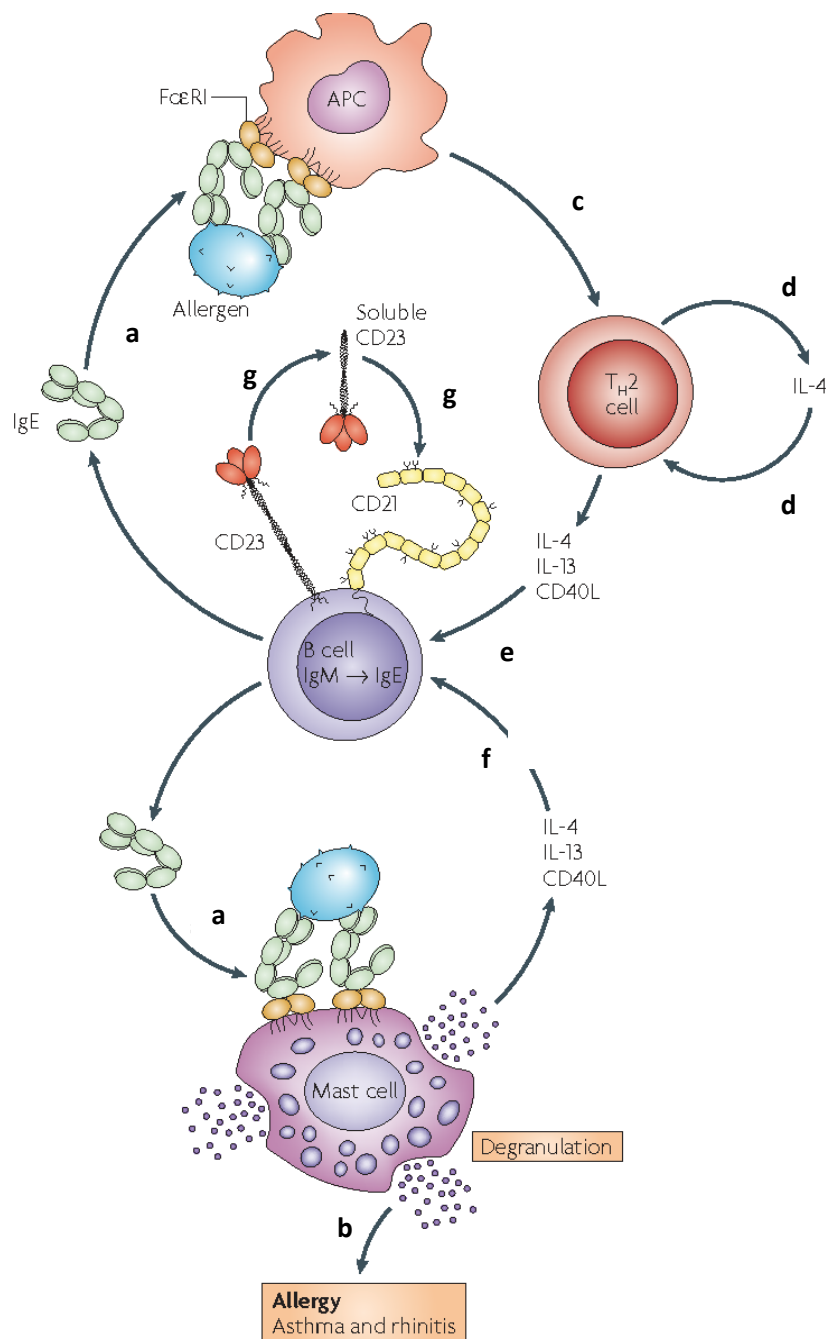
**Figure 1.4: Maturation of the T naïve cells into effector T cell subsets.** Differentiation of T naïve cells into effector T cells subsets is dependent on cytokine stimulation. Th1 differentiation requires IL-12 or IL-27 stimulation, Th2 differentiation is dependent on IL-2 and IL-4, TGF- $\beta$  triggers Treg differentiation, and Th17 differentiation is stimulated by IL-23, TGF- $\beta$  + IL-6, and IL-21. Following differentiation, the effector T cells produce cytokines that activate immune cells and inhibit differentiation of naïve T cells into other effector

subjects. The cytokines produced by the Th2 cells, for example, activate B cells, eosinophils, and mast cells, whilst the cytokines produced by the Treg cells (TGF- $\beta$ , IL-10) inhibit Th1, Th2, and Th17 differentiation. Asthma is characterised by expansion of the Th2 subset and decreased differentiation of Tregs.

[Taken from Andreev *et al.*, 2012 <sup>60</sup>]

The Th2 cells in conjunction with an exogenous source of IL-4 mediate isotype switching of the B cells present in the germinal centre of the lymphoid follicle <sup>32, 56, 58,61</sup>, resulting in the production of allergen-specific IgE that exits the draining lymph node to enter the bloodstream <sup>62</sup> (Figure 1.5). Once in circulation the IgE antibodies bind to either the high affinity IgE receptor (Fc $\epsilon$ RI) or the low affinity IgE receptor (Fc $\epsilon$ RII) (Figure 1.5). The Fc $\epsilon$ RI receptor is expressed on the cell surface of mast cells and basophils <sup>63,64</sup>, and to a lesser extent, on the cell surface of antigen presenting cells, such as Langerhan cells <sup>65</sup> and monocytes <sup>66</sup>. The Fc $\epsilon$ RII receptor, however, is expressed on a range of innate and adaptive immune cells, including T lymphocytes, B cells, monocytes and macrophages, and eosinophils, and platelets <sup>64</sup>.

In atopic asthma, the migration and expansion of the mast cells within the airways results in localised accumulation of allergen-specific IgE within the submucosal layer as a consequence of allergen-specific IgE binding to the high affinity Fc $\epsilon$ RI receptors upregulated on the lung mast cells (Figure 1.5). This induces allergen hypersensitivity within the airways, thus priming the immune system against future allergen exposure.



**Figure 1.5: Priming of the allergic response by allergens.** Following allergen exposure IgE is produced and secreted by B cells. IgE binds to the FcεRI receptor expressed on the cell surface of mast cells and antigen presenting cells (a). Allergen binding to IgE triggers mast cell degranulation, causing an allergic response (b). Allergen binding to antigen presenting cells causes the cells to present allergen peptides to Th2 cells (c). The allergen-activated Th2 cells secrete IL-4 (d), resulting in maintenance of the Th2 lineage and increased differentiation of Th0 cells into Th2 effector cells. The Th2 cells also secrete IL-13 and express the CD40 ligand, which together with IL-4 stimulate B cell class switching to IgE (e). The allergen activated mast cells further contribute to IgE class switching by secreting IL-4 and IL-13 (f). IL-4, IL-13, and CD40 also increase the release of soluble CD23 (g). CD23 further increases IgE synthesis and secretion by interacting with CD21.

[Adapted from Gould and Sutton, 2008 <sup>67</sup>]

#### 1.7.4. The Role of the Innate Cytokines in Airway inflammation

The production of the innate cytokines by allergen stimulated epithelial cells (e.g. GM-CSF, TSLP, IL-25, and IL-33) and NKT cells (e.g. IL-4 and IL-13) are key mediators in Th2 differentiation, and thus have essential roles in the pathogenic mechanisms of allergen sensitisation.

The production of GM-CSF, TSLP, IL-25, and IL-33 by the epithelial cells, for instance, has been found by various authors to induce migration of monocytes, dendritic cells, mast cells, eosinophils, basophils, and Th2 cells, into the asthmatic airways <sup>68-71</sup>. Moreover, these cytokines have also been found to enhance the proinflammatory potential of the recruited cells. GM-CSF, for example, has been shown to increase the survival, proliferation, and activation of various immune cells, including monocytes and macrophages <sup>72</sup>, neutrophils <sup>73</sup>, eosinophils <sup>74</sup>, and dendritic cells <sup>75</sup>, whilst TSLP appears to be an important mediator of dendritic cell activation <sup>76</sup>.

Soumelis *et al* (2002), for example, demonstrated that the addition of TSLP to cultured dendritic cells resulted in cellular activation that was characterised by increased upregulation of human leukocyte antigen (HLA)-DR and the co-stimulatory molecules, cluster of differentiation (CD) 40, CD80, CD83, and CD86, compared to dendritic cells that were activated by the CD40 ligand, bacterial lipopolysaccharide (LPS), and the IL-7 cytokine, and thus resulted in elevated dendritic cell antigen presenting potential <sup>76</sup>. Moreover, TSLP was observed to enhance dendritic cell survival and alter cellular activity, whereby the cells released the chemokines thymus and activation regulated chemokine (TARC) and macrophage derived protein (MDC), and induced Th0 cells to produce high levels of IL-5, IL-13, and tumour necrosis factor (TNF), moderate levels of IL-4, and decreased concentrations of the anti-inflammatory cytokine IL-10 and the Th1 cytokine IFN $\gamma$  <sup>76</sup>. This,

therefore, suggests that *in vivo* TSLP activated dendritic cells would drive a Th2 biased immune response following exposure to allergen, and thus are a critical component in the development of atopic asthma.

In contrast to GM-CSF and TSLP, IL-33 has been revealed to be essential for granulocyte activity, in particular the mast cells and basophils. Kondo *et al* (2008), for example, found that exposure of cultured basophils to IL-33 resulted in increased generation of a number of cytokines (IL-4, IL-6, IL-9, IL-13, GM-CSF) and chemokines (RANTES/CCL5, MIP-1 $\alpha$ /CCL3, MIP-1 $\beta$ /CCL4, and CCL2) that are associated with increased survival, activation, and migration of number of inflammatory cells and the occurrence of Th2 inflammation <sup>77</sup>. Similarly, Allakhverdi and colleagues (2007) demonstrated that exposure of cultured mast cells to IL-33 led to a dose-dependent increase in the production and release of a range of proinflammatory cytokines and chemokines, such as IL-5, IL-6, IL-8, IL-10, IL-13, TNF, GM-CSF, and CCL1 <sup>78</sup>.

IL-33 has also been found to increase mast cell differentiation. Allakhverdi *et al* (2007), for instance, found that exposure of immature CD34<sup>+</sup> to IL-33 resulted in elevated rates of cellular maturation of the progenitor cells into tryptase-producing mast cells <sup>78</sup>. Moreover, IL-33 is likely to increase mast cell survival in the lungs as a consequence of the cytokines ability to increase mast cell expression of the anti-apoptotic factor BCLXL <sup>79</sup>.

## 1.8. The Effector Phase of IgE-mediated Hypersensitivity

Following the generation of allergen specific IgE and the recruitment of inflammatory cells into the airways, the atopic individual becomes sensitised to the allergen. Upon subsequent exposure to the allergen, atopic disease will occur as a consequence of the initiation of the effector phase of hypersensitivity. This phase is composed of two stages; the early phase

reactions, which occur within minutes of allergen challenge and generally last around 30-60 minutes, and the late phase reactions late-phase reaction, which generally develops 2-6 hours later, and typically resolves within 1 to 2 days <sup>31</sup>.

#### 1.8.1. The Early Phase of Allergic Inflammation in Atopic Asthma

The early phase reactions occur almost immediately upon secondary allergen challenge following the development of allergen sensitivity and are the result of allergen binding to the allergen specific IgE that is generated during the previous sensitisation reactions.

In atopic asthmatics, the majority of allergen specific IgE is localised within the airway epithelial layer as a result of IgE antibodies binding to FcεRI upregulated on mast cells localised within the airways. Upon adhesion to IgE, bivalent or multivalent allergens can bind to adjacent allergen-specific IgE receptors present on the cell surface, subsequently causing FcεRI aggregation as a result of IgE crosslinking <sup>31</sup>.

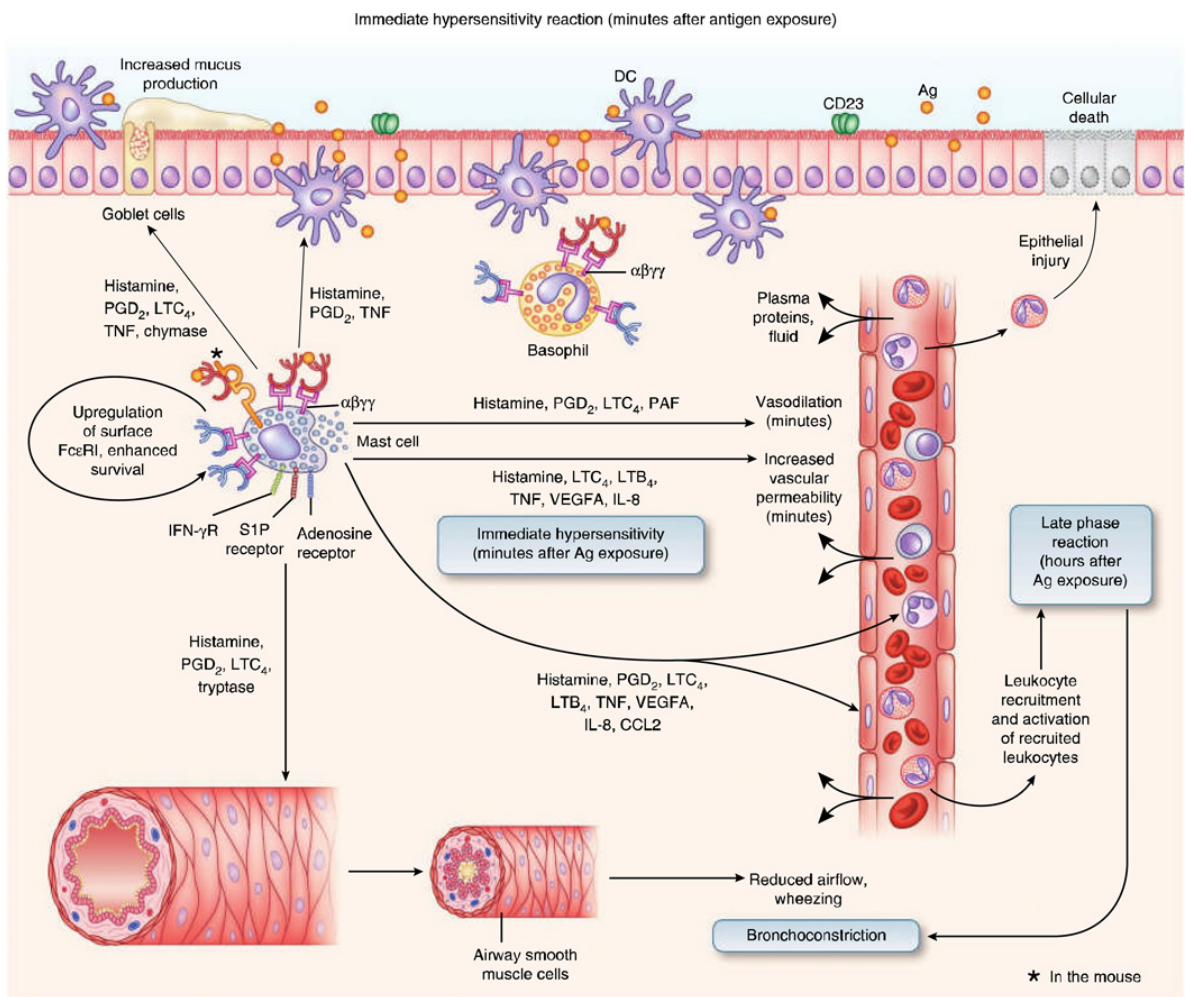
This triggers a complex sequence of intracellular signalling events that activates the mast cell and induces the release of a range of preformed mediators, including biogenic amines (histamine), serglycin proteoglycans (heparin and chondroitin sulphate), serine proteases (tryptases, chymases, and carboxypeptidases), and a number of other growth factors and cytokines that may be associated with the granule, such as TNFα and vascular endothelial growth factor A (VEGF), into the airway lumen (known as mast cell degranulation) <sup>31</sup>.

Activation of the mast cells also induces the release of a number of lipid-derived mediators into the mast cell microenvironment (Figure 1.6). These mediators induce the breakdown of arachidonic acid by stimulating the cyclooxygenase and lipoxygenase pathways, resulting

in the release of a number of prostaglandins (PG), including PGD<sub>2</sub>, leukotriene (LT) B<sub>4</sub>, and cysteinyl leukotrienes, such as LTC<sub>4</sub> <sup>31</sup>.

The release of the preformed mast cell mediators results in the stimulation of the early phase reactions within minutes of mast cell degranulation <sup>80</sup>. These reactions induce rapid airway obstruction and subsequent wheezing as a consequence of increased vascular permeability, bronchoconstriction, vasodilation, and mucous production, and are mediated by a range of mast cell products <sup>80,81</sup> (Figure 1.6). Moreover, they also contribute towards the late phase reactions by inducing the migration of inflammatory leukocytes into the airways. This is mediated by the secretion of TNF, which interacts with the endothelial cells to stimulate upregulation of adhesion molecules such as E-selectin, intracellular adhesion molecule 1 (ICAM-1), and vascular cell adhesion molecule 1 (VCAM-1), on the cell surface <sup>80-82</sup>. This causes the release of a number of chemotactic mediators, such as, PGD<sub>2</sub>, IL-8, IL-16, lymphotaxin /XCL1, CCL2, CCL3, CCL4, CCL5, MIP-3 $\alpha$  /CCL20, and C-X-C motif ligand (CXCL) 10 <sup>80-82</sup>.



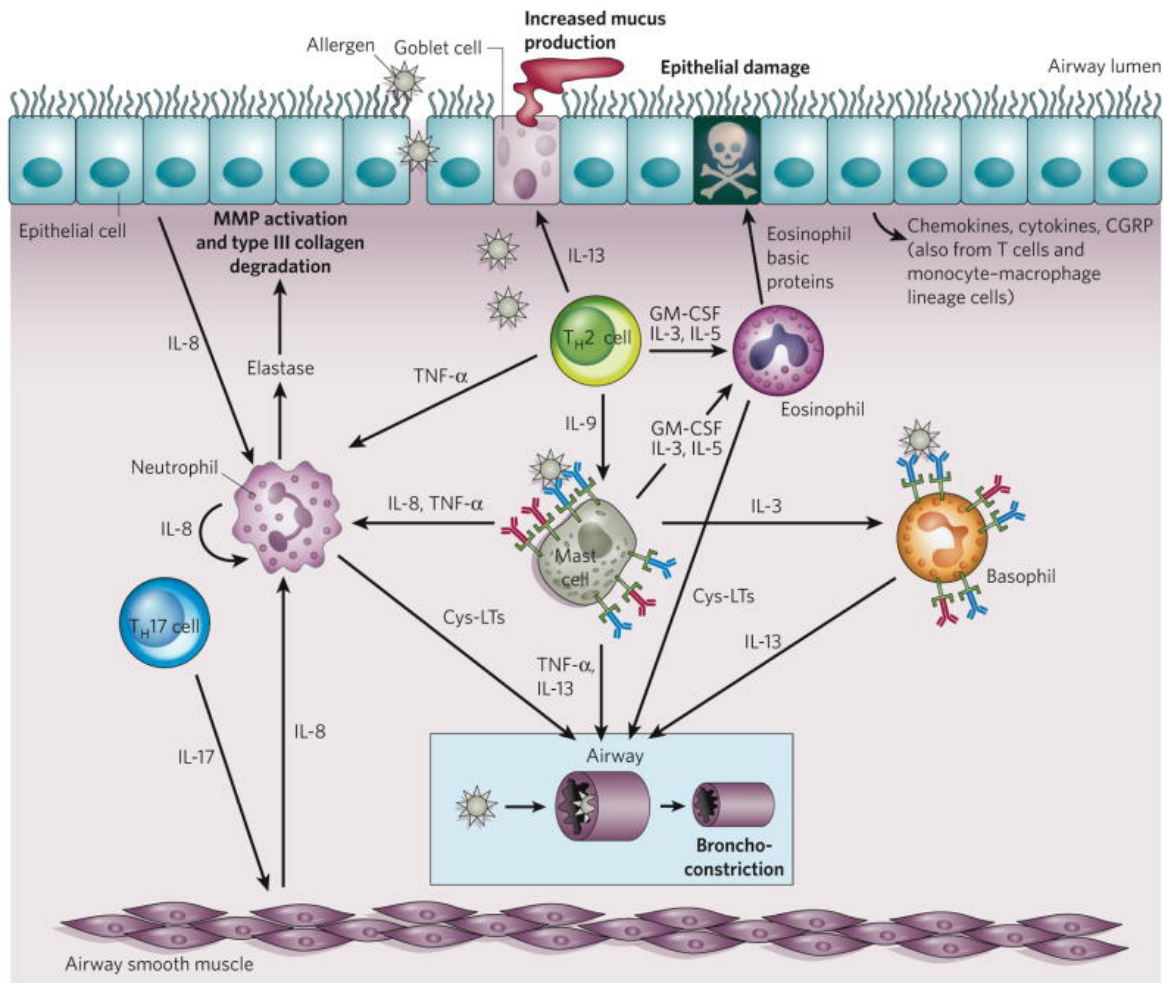


**Figure 1.6: Mast cell mediated early phase reactions.** Following re-exposure to the allergen, the mast cells present in the subepithelial layer of the airways are activated as a consequence of allergen-IgE cross-linking on the mast cell surface. This results in the release of a range of preformed mediators and the subsequent induction of the early phase reactions. These reactions are primarily mediated by the mast cell autocoids, proteases, cytokines, and chemokines. The autocoids (histamine, PGD<sub>2</sub>, LTC<sub>2</sub>) and proteases (chymase, tryptase) increase mucous production and contraction of the smooth muscle, resulting in airway obstruction and the occurrence of wheezing within minutes of mast cell degranulation. The autocoids also induce airway hyperreactivity in conjunction with the mast cell cytokines TNF and IL-8, the CCL2 chemokine, and VEGF, as a consequence of increased vasodilation, vascular permeability, and the influx of inflammatory cells. Moreover, the influx of leukocytes into the airways as a result of mast cell mediated leukocyte recruitment and activation leads to the development of the late phase reactions a number of hours following mast cell degranulation.

[Taken from Galli & Tsai, 2012 <sup>80</sup>]

### 1.8.2. The Late Phase of Allergic Inflammation in Atopic Asthma

In addition to the release of preformed products, allergen-induced IgE cross-linking also activates the mast cells to synthesise and secrete a number of chemokines (including; MCP-1, RANTES, eotaxin, TARC, MDC, CXCL2, and CXCL10), cytokines and growth factors [including; IL-3, IL-4, IL-5, IL-8, IL-9, IL-13, IL-25, TNF $\alpha$ , transforming growth factor beta (TGF $\beta$ ) 1, TSLP and GM-CSF], and free radicals (including; Nitric oxide, superoxide) <sup>82</sup>. The release of these products augments the influx of Th2 cells, granulocytes (mainly eosinophils with lower numbers of neutrophils and basophils), and monocytes, into the airway submucosal layer, and results in a second round of activity within the airways, referred to as the late phase reactions. The late phase reactions occur 2-6 hours after allergen exposure and is characterised by airway narrowing and excess mucous production as a consequence of mast cell products and the activities of the recruited inflammatory cells (Figure 1.7) <sup>31</sup>.



**Figure 1.7: The late phase reactions in the effector phase of atopic asthma.** The late phase reactions of the effector phase are mediated by granulocytes (mast cells, eosinophils, basophils, and neutrophils) that were recruited to the airways as a consequence of the early phase reactions. Upon entry into the airways the granulocytes undergo degranulation as a result of stimulation by pro-inflammatory cytokines release by the activated epithelial cells and the Th2 cells localised within the airways. The release of the granules into the airway environment induces a range of pathogenic mechanisms that contributes towards the occurrence of clinical disease. The eosinophils, for example, release eosinophilic basic proteins that induces epithelial apoptosis, subsequently resulting in increased epithelial permeability, and thus increasing the ability of the allergen to enter the submucosal layer. The cells also induce airway narrowing and bronchoconstriction. Neutrophils, release elastase, which causes epithelial fibrosis as a consequence of increased collagen deposition, whilst the release of cysteinyl leukotrienes (Cys-LTs), IL-13, and TNF, by the neutrophils, mast cells, eosinophils, basophils induces bronchoconstriction and subsequent airway hyperreactivity.

[Taken from Galli *et al.*, 2008<sup>31</sup>]

### 1.8.3. The Role of the T Helper 2 Cells in the Late Phase Reactions

Recruitment and activation of the Th2 cells is thought to be crucial for the development of the late phase reactions. This is primarily due to the functions of the Th2 cytokines IL-3, IL-5, IL-9, and IL-13.

The production of IL-13 by these cells, for instance, has been demonstrated to increase mucous production in the airways as a consequence of enhanced goblet cell metaplasia<sup>83-86</sup>, whilst IL-5 has been demonstrated to have a critical role in the occurrence of eosinophilia within the airways, with studies reporting that elevated IL-5 concentrations led to increased eosinophil survival<sup>87</sup>, differentiation<sup>88,89</sup>, proliferation<sup>88-90</sup>, activation<sup>88,91</sup>, chemotaxis<sup>87</sup>, and adhesion to the airway endothelial cells<sup>92</sup>.

Moreover, IL-9, has been found to induce mast cell migration to the airway epithelium, and function synergistically with stem cell factor to induce mast cell growth and differentiation<sup>93</sup>, and IL-3 has been demonstrated to function synergistically with other proteins to induce various pro-inflammatory activities. Grouard *et al* (1997)<sup>94</sup>, for example, found that IL-3 functions synergistically with the CD40 ligands to enhance survival and activation of a subset of plasmacytoid dendritic cells that were later demonstrated by Rissoan and colleagues to induce Th2 polarisation<sup>95</sup>. Furthermore, Ebner *et al* (2002) demonstrated that when co-cultured with IL-3 and IL-4 human monocytes differentiated into dendritic cells that secreted reduced levels of IL-12<sup>96</sup>, an important cytokine in promoting Th1 immune responses. Additionally, various authors have demonstrated that together with IL-5, IL-6, and GM-CSF, IL-3 increases proliferation of the granulocytes (eosinophils, neutrophils, basophils) and monocytes<sup>90,97-100</sup>.

## 1.9. Immune Mechanisms Associated with Chronic Airway Inflammation in Atopic Asthma

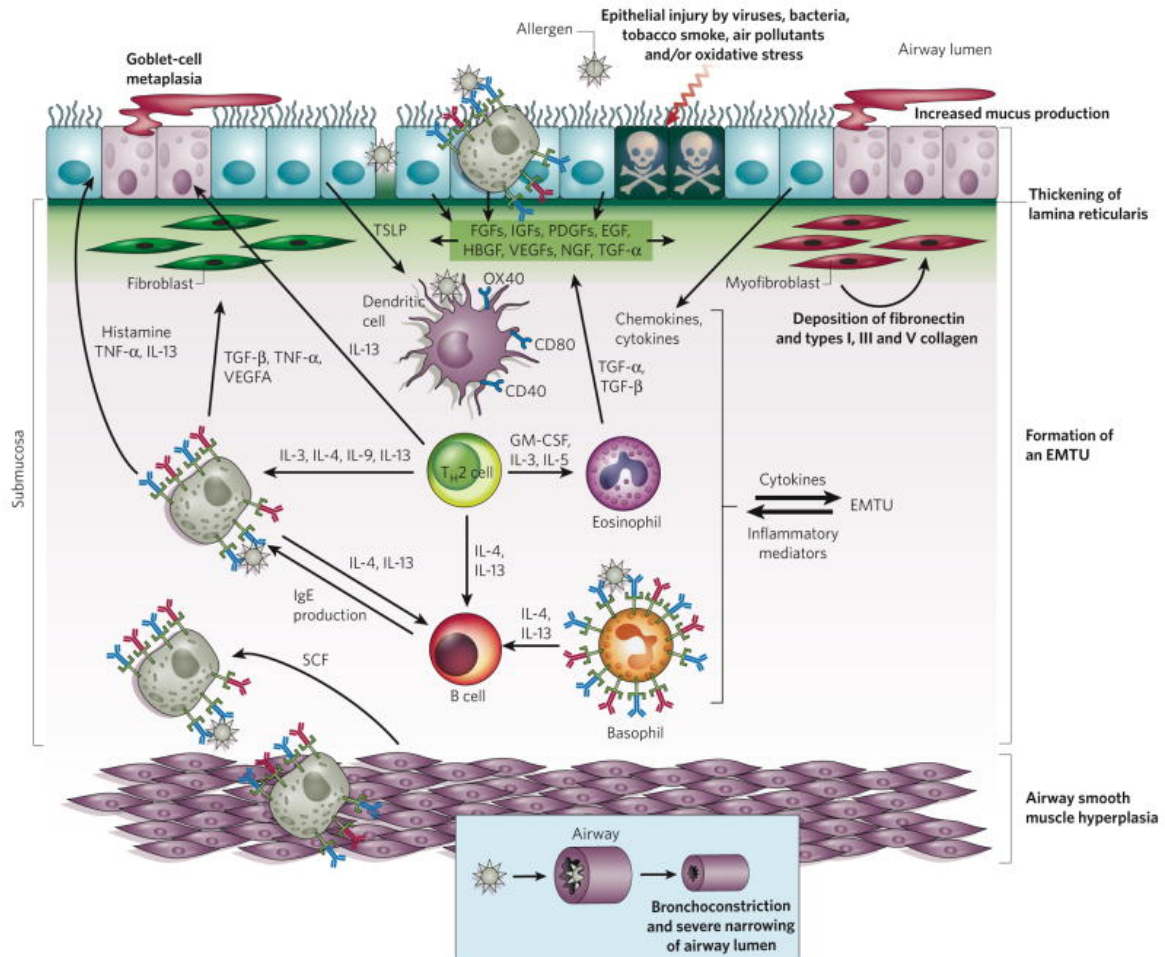
Allergens typically associated with atopic asthma (grass pollen, animal dander, HDM) are ubiquitous in the environment, and thus repetitive and persistent exposure to the allergen following initial sensitisation is inevitable.

Repetitive exposure to the allergen results in chronic inflammation within the airways. This leads to the permanent residence of innate immune cells (eosinophils, basophils, mast cells, and neutrophils) and adaptive immune cells (Th2 cells and B cells), and the occurrence of airway remodelling as a result of inflammatory cell activity on the structural cells (Figure 1.8).

Over time this results in changes to the epithelium, including increased cytokine and chemokine secretion by the epithelial cells, upregulation of cell surface receptors, areas of epithelial injury and repair, and extensive inflammation of the submucosa<sup>31</sup>. A number of structural changes (known as airway remodelling) also occur that lead to increased thickening of the mucosal, epithelial, and smooth muscle layers of the airways. Examples of these structural changes include loss of ciliated cells, goblet cell hyperplasia (increased numbers of goblet cells in the airway wall), airway fibrosis (increased deposition of extracellular matrix proteins in the lamina reticularis by fibrocytes), hypertrophy of airway smooth muscle cells (increased size of muscle cells), hyperplasia of airway smooth muscle cells (increased number of muscle cells), increased airway vascularity (angiogenesis), and reduced cartilage integrity<sup>31,101</sup>.

The structural changes cause lumen narrowing of the asthmatic airways and are responsible for many of the breathing symptoms associated with asthma, including coughing, shortness of breath, and difficulty breathing. It also alters the behaviour of the

airway epithelial cells, causing increased production of chemokines and cytokines which further contribute to airway inflammation by inducing migration and activation of immune cells.



**Figure 1.8: Chronic inflammation and the occurrence of airway remodelling.** Over time repetitive exposure to the aeroallergen results in permanent residence of a range of innate and adaptive immune cells, including basophils, eosinophils, mast cells, neutrophils, Th2 cell, and B cells. This results in localised accumulation of a variety of cytokines, chemokines, and other growth factors within the airways that influence the activity of the structural cells. Production of IL-4 and IL-13 by the Th2 cells, mast cells, and basophils, for instance, results in activation of B cells within the airways, which subsequently leads to persistent IgE elevations within the airways. This causes chronic degranulation of the granulocytic cells, which results in the accumulation of a range of proteins within the airways that induce airway remodelling. The release of TGF- $\beta$ , by the eosinophils and mast cells, for example, leads to increased deposition of collagen and fibronectin and subsequent epithelial fibrosis, whilst the production of IL-13 by various inflammatory cells has been found to induce goblet cell differentiation, subsequently resulting in goblet cell metaplasia and excess mucous production within the airways. [Taken from Galli et al., 2008 <sup>31</sup>]

## 1.10. Diagnosis of Atopic Asthma and its Endotypes

Standard diagnosis of atopic asthma relies on patient history of symptoms and confirmed expiratory airflow limitation to diagnosis the patient with asthma <sup>102</sup>. Skin prick tests are then used to identify allergen sensitisation and confirm an atopic disease state <sup>103</sup>. Asthma as a disease, however, is highly heterogeneous, and thus symptom presentation and lung function measurements may not always reflect the underlying airway inflammation <sup>102</sup>.

Furthermore, diagnostic tools for identifying the various asthma endotypes are limited, and currently rely on bronchoalveolar lavage (BAL) and bronchoscopy with bronchial biopsy as the optimum method for assessing airway inflammation and remodelling <sup>102</sup>. The invasiveness of these techniques limits their usefulness in daily clinical practice and makes them unsuitable in the diagnosis of young children <sup>102</sup>.

These limitations alongside an incomplete knowledge of the pathogenetic mechanisms behind the different asthma endotypes has restricted development and access to optimal asthma treatment protocols.

Overall, an estimated 5 -10% of asthmatics fail to respond to conventional medications <sup>104</sup>. Moreover, long-term use of conventional asthma treatments, such as inhaled  $\beta$ 2 adrenoreceptor 2 selective agonists (function as bronchodilators to reduce airway narrowing) and glucocorticoids (suppress airway inflammation), has been associated with a number of health concerns <sup>105</sup>, including the stunting of growth in children <sup>106</sup>, cataract development <sup>107,108</sup>, osteoporosis <sup>109,110</sup>, and cardiovascular events <sup>111</sup>.

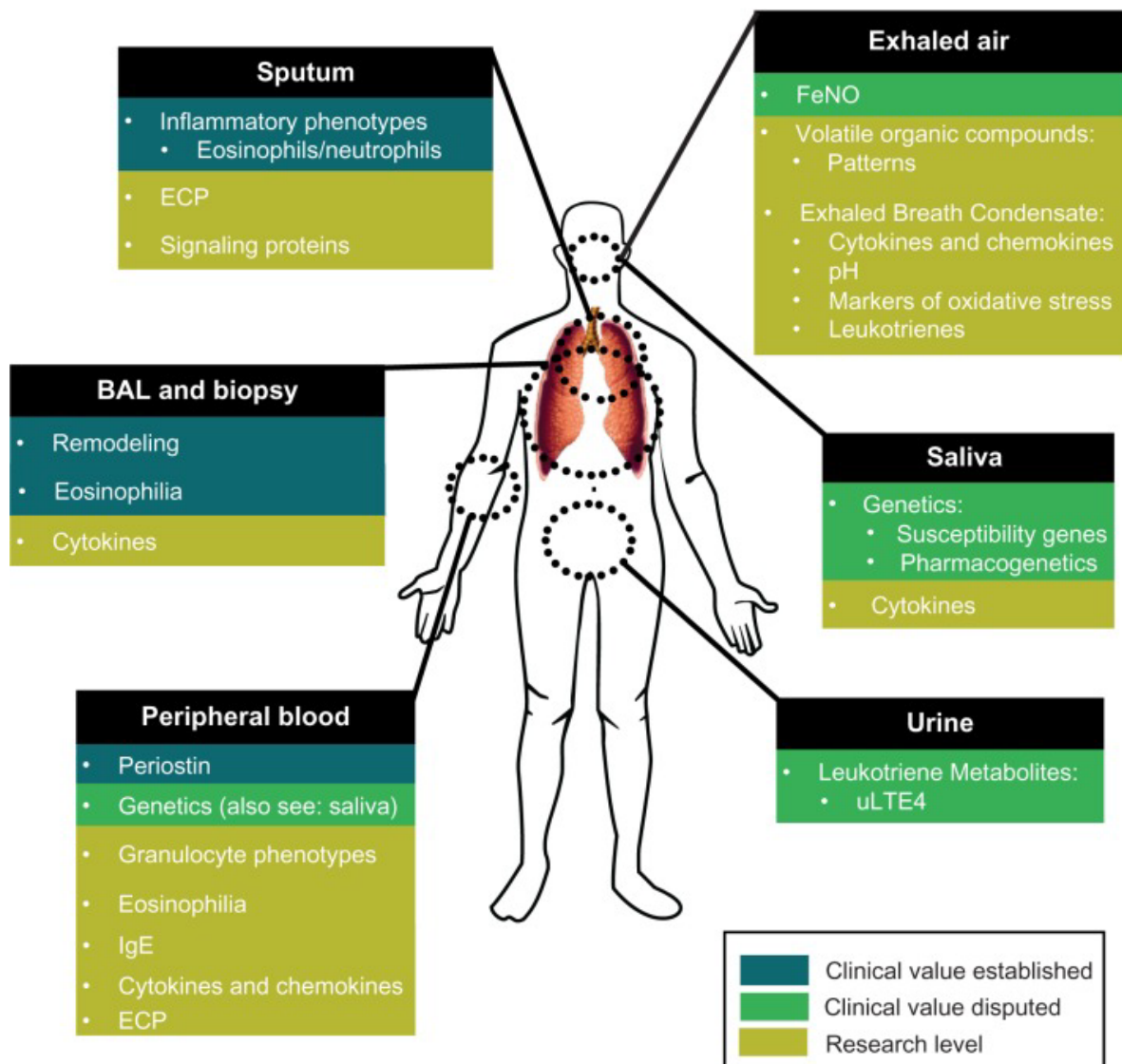
In order to improve diagnosis of the asthma phenotypes/ endotypes, an improved knowledge of the molecular mechanisms that underlie the various asthma phenotypes is required. Long-term, this may also reduce asthma mortality rates and improve quality of

life by facilitating the targeted use of conventional medications aligned to the individual asthmatic phenotypes, and development of new medications specifically designed to treat specific asthma phenotypes/ endotypes.

Biomarkers have been proposed as a means of performing risk assessment before clinical diagnosis, to determine the disease stage and severity following asthma diagnosis, and as a means of monitoring responsiveness to treatment <sup>112</sup>.

Biomarkers are characteristics or biomolecules that can be objectively measured and evaluated as an indicator of normal biological processes, pathogenic processes, or response to therapeutic treatment <sup>113</sup>. In asthma, there are increasing numbers of potential biomarkers being identified in various clinical samples, including BAL fluid, sputum, exhaled air, saliva, urine, and peripheral blood (Figure 1.9).





**Figure 1.9: Established asthma biomarkers available for clinical practise and promising biomarkers under investigation.** Investigations into asthma pathology have identified a number of possible asthma biomarkers from a range of clinical samples. Several of these biomarkers are available for use in the clinical setting (blue), and there are increasing numbers being investigated for potential use in asthma evaluation, diagnostics, and assessment of treatment response (green and yellow).

*Abbreviations: ECP, eosinophilic cationic protein; FeNO, fraction of exhaled nitric oxide; uLTE4, urinary leukotriene E4.*

[Taken from Vijverberg *et al.*, 2013<sup>114</sup>]

## 1.11. Identification of Peripheral Biomarkers in Asthma

The majority of studies have focussed on identifying biomarkers from clinical samples taken from the airways (sputum, BAL fluid, lung tissue) in order to better characterise airway inflammation and remodelling. However, collection of these samples is invasive and not suitable for daily clinical activity. This has led to an increasing interest in the identification of biomarkers from more accessible clinical samples, such as blood, urine, and saliva.

Thus far there have been three methods of identifying biomolecules that could function as biomarkers for asthma. These include genomic, epigenomic, and proteomic analysis.

### 1.11.1. Transcriptomic Biomarkers of Asthma

Transcriptomic analysis has typically been achieved using high and low-throughput sequencing techniques to enable quantification of messenger RNA (mRNA) present in clinical samples in order to identify genes that are up or down regulated in asthmatic subjects compared to non-asthmatic subjects. These studies have identified hundreds of potential genes that may function as biomarkers for asthma. These genes have typically been associated with biological pathways/ processes involved in airway remodelling, production of mucous, and shifting the immune response towards a Th2 biased phenotype<sup>112</sup>. In a study by Gemou-Engesaeth *et al* (1997), for example, increased levels of mRNA coding for Th2 cytokines (IL-2, IL-4, IL-5) and GM-CSF was observed in peripheral blood samples from asthmatic subjects compared to control subjects<sup>115</sup>.

Transcriptomic analysis has also been used to characterise the different asthma phenotypes and endotypes. A study by Kuo *et al* (2017), for example, identified three transcriptome-associated clusters (TACs) in a patient cohort of moderate-to-severe

asthmatics that defined one Th2-high eosinophilic asthma phenotype (TAC1) and two Th2-low asthma phenotypes (TAC2, TAC3) <sup>116</sup>. TAC1 was characterised by increased gene signatures for TH2 and ILC2 cells, and was identified in patients with severe asthma, high levels of sputum eosinophilia, severe airflow obstruction, and an oral corticosteroid dependency. In contrast TAC2 was characterised by IFN, TNFA, and inflammasome-associated genes, and was identified in asthmatic patients with high sputum neutrophilia, serum C-reactive protein levels, and atopic dermatitis; and TAC3 was characterised by genes of metabolic pathways, ubiquitination, and mitochondrial function, and was detected in asthmatic subjects with moderate to high sputum eosinophilia.

Moreover, IL-5 and IL-17 expression in the blood has been found to positively correlate with disease severity <sup>117,118</sup>.

In addition to changes in gene expression, changes in gene coding sequences have also been identified as useful biomarkers of asthma. A single nucleotide polymorphism in the gene coding for the low-affinity IgE-receptor, *FCER2*, for example, has been associated with increased risk of asthma-related hospital visits, failure to respond to treatment, and the need for higher daily steroid dosages <sup>119,120</sup>. Similarly, studies have identified variations in the stress induced phosphoprotein 1 (*STIP1*) and the T-box transcription factor 21 (*TBX21*) coding regions that are associated with improved lung function following treatment with corticosteroids <sup>121,122</sup>.

More recently, changes in micro RNA (miRNA) expression have also been detected in asthmatic subjects. <sup>123–125</sup>. miRNA-181, for example, has been detected in decreased concentrations in asthmatic plasma samples <sup>126</sup>, and decreased concentrations of the miRNA has been associated with increased sputum and bronchial submucosal eosinophilia <sup>126</sup>. In contrast, miRNA-1248 has been observed at increased levels in serum samples from

asthmatic subjects, and has been demonstrated to bind to the 3' untranslated region of the IL-5 transcript, resulting in increased IL-5 expression <sup>127</sup>. miRNA levels have also been shown to reflect immune state. miRNA-192, for example, has been shown to be present at significantly decreased levels in the blood of asthmatic subjects following allergen inhalation challenge compared to pre-challenge, suggesting that the immune responses associated with allergen sensitivity negatively influenced expression of the miRNA <sup>128</sup>.

#### 1.11.2. Protein Biomarkers of Asthma

Proteomic approaches involve quantification and/ or characterisation of proteins in order to identify changes in protein expression and modification in asthmatic subjects compared to non-asthmatic subjects. Previous studies have identified a number of potential blood protein biomarkers that are associated with asthma. Increased sputum and circulatory levels of eosinophilic cationic protein, for instance, has been associated with asthma severity <sup>129,130</sup>, whilst CCL-17 (also known as TARC), a chemokine involved in recruitment of Th2 cells, has been demonstrated to be increased in the blood of asthmatic children <sup>131</sup>.

Another protein showing strong potential for use as an asthma biomarker is periostin, a matricellular protein produced by bronchial epithelial cells activated by IL-13. In asthmatic subjects increased blood periostin concentrations have been observed in asthmatics with eosinophilic airway inflammation compared to asthmatics subjects with minimal eosinophilic airway inflammation <sup>132</sup>, therefore suggesting that the protein could be used as an indicator of airway eosinophilia. Blood biomarkers could also be used to predict treatment response. Increased blood concentrations of the chitinase-like protein YKL-40, for example, have been observed to be increased in children with severe, therapy-resistant asthma compared to non-asthmatic children and children with well-controlled asthma <sup>133</sup>.

The protein was also found to be positively correlated to blood neutrophil levels and degree of bronchial wall thickening <sup>133</sup>, suggesting that it could also function as a biomarker of systemic inflammation and airway remodelling in asthmatic patients.

### 1.12. Atopic Asthma and Sex Differences

Atopic asthma prevalence during childhood is typically higher in males compared to females <sup>134–137</sup>. However, when the disease does develop in females it is more likely to persist into adulthood <sup>138,139</sup>, be associated with additional atopic diseases, such as allergic rhinitis and atopic dermatitis <sup>140,141</sup>, and increased susceptibility to asthma exacerbations <sup>140,142–144</sup>. Females are also more prone to developing severe asthma <sup>139,145</sup>, suffer asthma control problems <sup>140</sup>, and reduced quality of life <sup>140</sup> that is associated with higher asthma mortality rates <sup>145,146</sup>.

There is, therefore, a great need to identify biomarkers in the female asthmatic population suffering from poorly controlled asthma, in order to better diagnose, monitor, and treat this group of asthmatic patients.

### 1.13. Atopic Asthma Prevalence

Epidemiological studies have revealed that over the past 50 years asthma prevalence has been increasing at a rapid rate, particularly in regards to early onset, atopic asthma, occurring in westernised societies <sup>147–151</sup>. More recent studies have suggested that asthma rates are now beginning to plateau out <sup>149,152–154</sup>. However, an explanation for why rates of asthma have risen in the human population is still required in order to better understand the disease and develop mechanisms to reduce asthma prevalence in future generations.

The strongest explanation proposed thus far for the increasing incidence rates of atopic asthma is the 'Hygiene hypothesis', which proposes that reduced exposure to environmental microbes due to changes in human behaviour and lifestyle is altering the natural development of the human immune system during early childhood.

#### 1.14. Introduction to the Hygiene Hypothesis

The hygiene hypothesis was first proposed by Strachan in 1989, who noted an inverse correlation between exposure to infectious agents and hay fever incidence in 17,000 British children born in 1958 <sup>155</sup>. Strachan suggested that changes in human behaviour, such as declining family size, increased standards of personal hygiene, and better living standards, was resulting in decreased transmission of infection during early childhood, and that this loss of early childhood exposure to infectious agents was increasing the risk of developing atopic disease <sup>155</sup>.

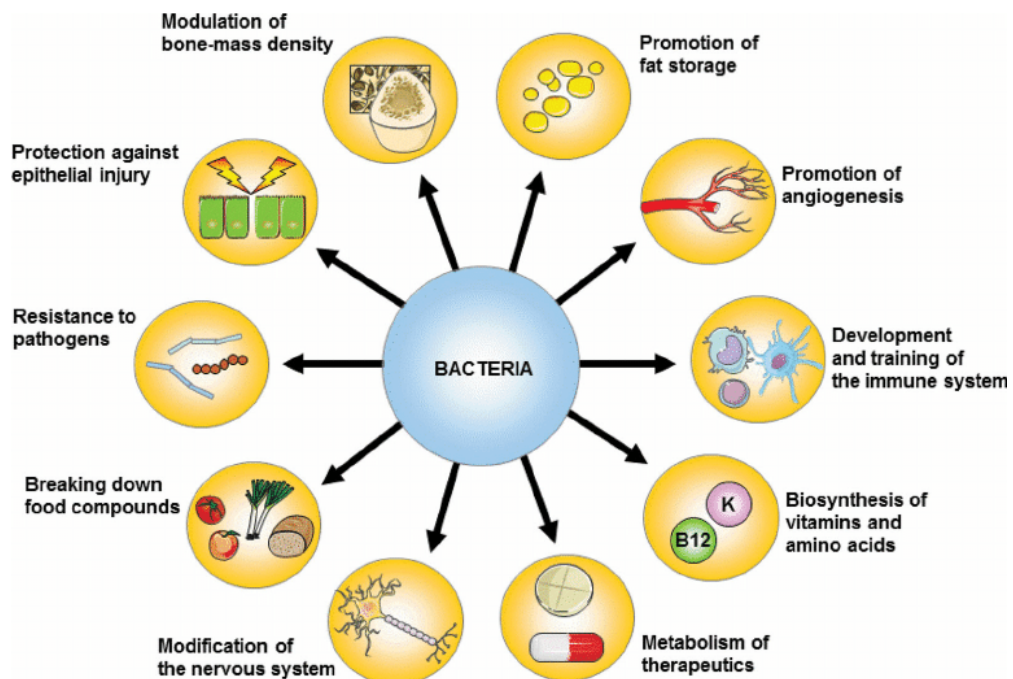
The theory was further supported by observations that prior infection with the hepatitis A virus <sup>156,157</sup>, the *Toxoplasma gondii* protozoan parasite <sup>157</sup>, the *Helicobacter pylori* bacterium <sup>157</sup>, or the *Mycobacterium tuberculosis* bacterium <sup>158</sup>, appeared to be protective against developing atopic asthma.

The protective role of childhood infection against atopy was thought to be due to the important role microbial infections have in the natural development of the immune system and immune tolerance.

As technology has advanced this hypothesis has evolved into the 'Old friends' and 'Biodiversity' hypotheses, whereby reduced exposure to environmental microbes alters the

bacterial populations inhabiting the human body, making the individual more susceptible to atopic disease <sup>159,160</sup>.

These microbial populations, known as the human microbiota, are predominately composed of non-pathogenic bacterial species that have formed synergistic relationships over the course of evolution. These relationships play an essential role in good health, and the bacterial members of the human microbiome, particularly those residing in the gut, have been demonstrated to perform various functions important to human health (Figure 1.10).



**Figure 1.10: Functions of the microbiota beneficial to human health.** The human microbiota, in particular the gut microbiota, has been demonstrated to carry out functional activities beneficial to human health. These include the breakdown of food compounds <sup>161,162</sup>, the synthesis of essential vitamins <sup>162,163</sup>, the development and training of the immune system <sup>164–170</sup>, protection against pathogens through competitive colonisation <sup>169,171,172</sup>, protection against epithelial injury <sup>173</sup>, and promotion of angiogenesis <sup>174,175</sup> and fat storage <sup>176</sup>. The microbiota has also been found to modify the nervous system <sup>177</sup>,

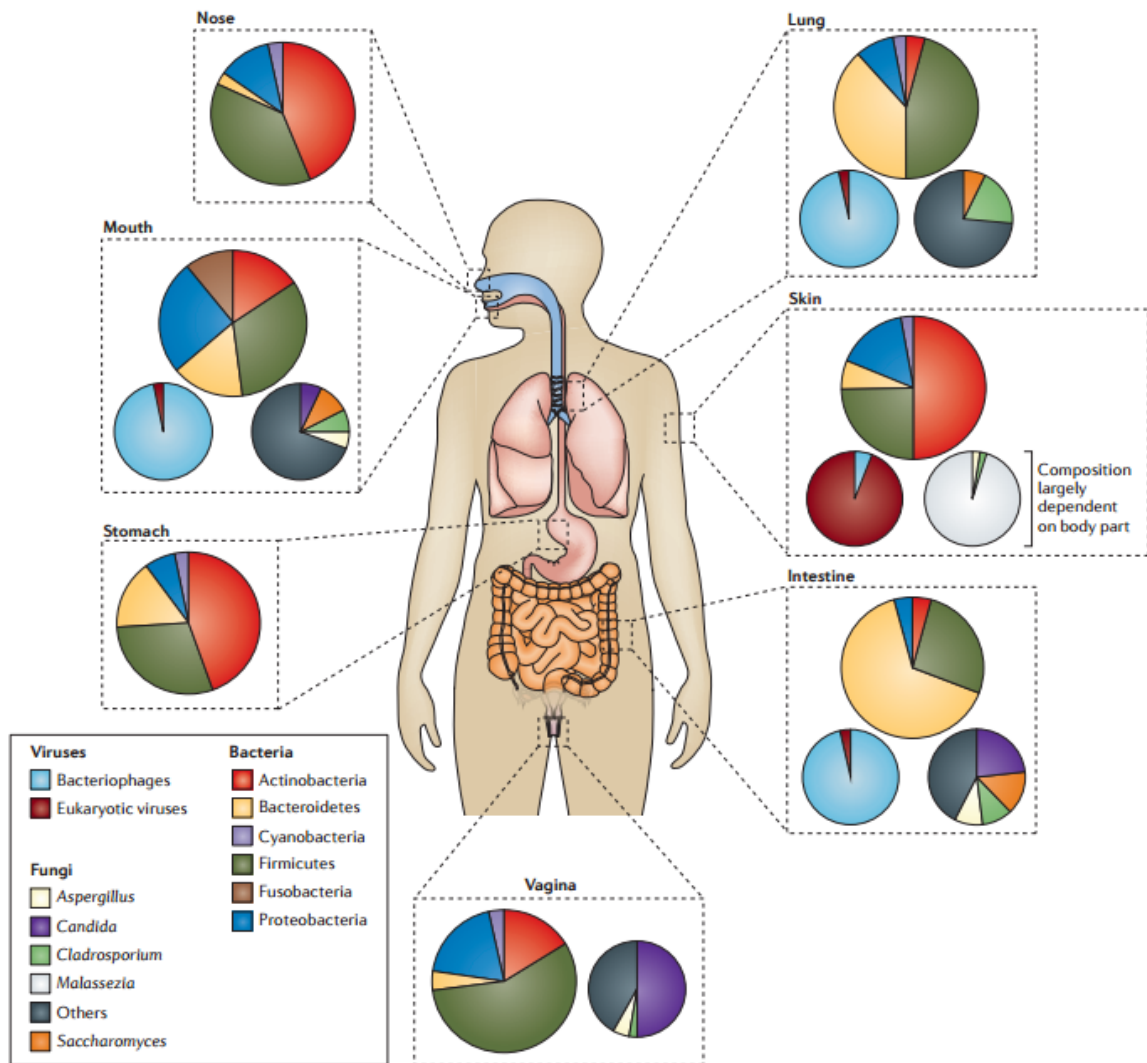
modulate bone-mass density <sup>178-180</sup>, and metabolise therapeutic agents into their active compounds <sup>181,182</sup>.

[Taken from Laukens *et al.*, 2016 <sup>183</sup>]

### 1.15. The Human Microbiota

The human microbiota is the collective term to describe the endogenous microbial populations that colonise almost every available epithelial surface present in the human body. These populations are composed of bacterial, viral, fungal, and protozoan species that form complex microbial communities that differ significantly between anatomical sites and display intraspecific and interspecific variation at the species and genus level, respectively <sup>184,185</sup> (Figure 1.11). Collectively the microbial cells making up the human microbiota are equivalent to the number of human cells, with current estimates predicting a 1:1 ratio of microbial to human cells in the human body <sup>186,187</sup>.





**Figure 1.11: The composition of the various microbial communities of the human microbiota.** The composition of the human microbiota differs across the various habitats of the human body. These microbial populations are composed of bacterial, viral, and fungal species, and are dominated by the bacterial species. Intriguingly, despite studies demonstrating a high degree of variability at the species level, at the phylum level there is a low degree of variability across the body habitats, with the majority of the identified bacterial species belonging to just four phyla; the Actinobacteria, Bacteroidetes, Firmicutes, and Proteobacteria.

[Taken from Marsland & Gollwitzer, 2014 <sup>188</sup>]

### 1.15.1.The Evolution of the Human Microbiota

Vertebrates have been colonised with microbes for millions of years, and thus humans have always had a microbiota that has co-evolved with the human race. The human microbiota is predominately composed of bacterial species that have formed synergistic relationships with humans.

The evolution of the microbiota appears to have been controlled by strong selective pressures, as shown by observations that whilst the mammalian microbiota displays a high degree of interspecies diversity (microbial diversity between different mammalian species) this is restricted to the lower taxonomic clades, with the majority of bacteria detected belonging to just four phyla – Actinobacteria, Bacteroidetes, Firmicutes, and Proteobacteria <sup>189–194</sup>.

Moreover, the microbial communities of free-living microbial communities have been found to differ significantly from the microbial communities observed in the vertebrate microbiota <sup>184</sup>. This suggests that the microbiota has evolved to be specifically adapted to the vertebrate host. This is further supported by the observations that the human gut microbiota more closely resembles the gut microbiota of other primates compared to non-primates <sup>184</sup>, thus supporting the presence of shared evolutionary pathways resulting in similar microbial communities.

### 1.15.2.Establishment of the Human Microbiota

It is currently thought that the microbial communities making up the human microbiota are established upon birth whereupon the sterile neonate is exposed to a variety of microbes present in the immediate environment, such as the maternal vaginal and faecal microbiota

if it's a vaginal birth or the skin microbiota of those present at the birth if it's a caesarean delivery<sup>195</sup>. However, it should be noted that there is emerging evidence suggesting that the foetus may be exposed to microbes *in utero*, as evidenced by detection of bacteria in the meconium (the neonates earliest faeces)<sup>196–198</sup>, the amniotic fluid<sup>199–202</sup>, umbilical cord blood<sup>202–204</sup>, and placental<sup>205–207</sup> and foetal membranes<sup>208</sup>

The initial communities making up the infant microbiota are relatively simple in composition and are homogeneously distributed across the various body habitats. The pioneer species are initially dominated by facultative anaerobes, such as *Staphylococci*, *Streptococci*, *Enterobacteria*, and *Enterococci* species<sup>190,209,210</sup>, as a consequence of oxygen availability in the neonatal habitats. Over time the metabolic activity of the pioneer species results in a reduction of oxygen, subsequently creating an environment that favours the growth of obligate anaerobic bacteria, such as *Bifidobacteria*, *Bacteroides*, and *Clostridium spp.*<sup>209,211,212</sup>, which the infant is exposed to through breast milk or formula milk<sup>210,213–216</sup>.

### 1.15.3. Maturation of the Human Microbiota

During the first few years of life the microbiota is highly dynamic and composed of a series of temporary colonisers. As the infant develops its microbiota develops with it, evolving from a relatively simple and undifferentiated ecosystem to complex, differentiated microbial communities that possess a high degree of diversity<sup>217,218</sup>.

The successive colonisation pathways during infant development results in the formation of a stable microbiota by age three that closely resembles the composition of the adult microbiota<sup>190,219–221</sup>. A number of early life factors have been found to influence the successive pathways and subsequent composition of the adult microbiota, including method and location of delivery<sup>195,221</sup>, diet<sup>191,221–224</sup>, the presence of older siblings and/

or pets in the household <sup>155,225</sup>, and maternal prenatal and infant postnatal antibiotic usage <sup>226,227</sup>.

#### 1.15.4. The Role of the Human Microbiota in Immune development

The foetal mucosal and systemic immune functions are significantly different compared to the adult immune system <sup>228–231</sup>. The foetal immune system has evolved to promote intrauterine foetal-maternal coexistence rather than process potential pathogens <sup>229,231,232</sup>. This phenotype is characterised by a naïve, Th2 bias, and following birth the neonatal immune system undergoes extensive postnatal development, switching from a Th2 biased system to a Th1 or Th17 phenotype capable of protecting the infant against potential pathogens <sup>231</sup>.

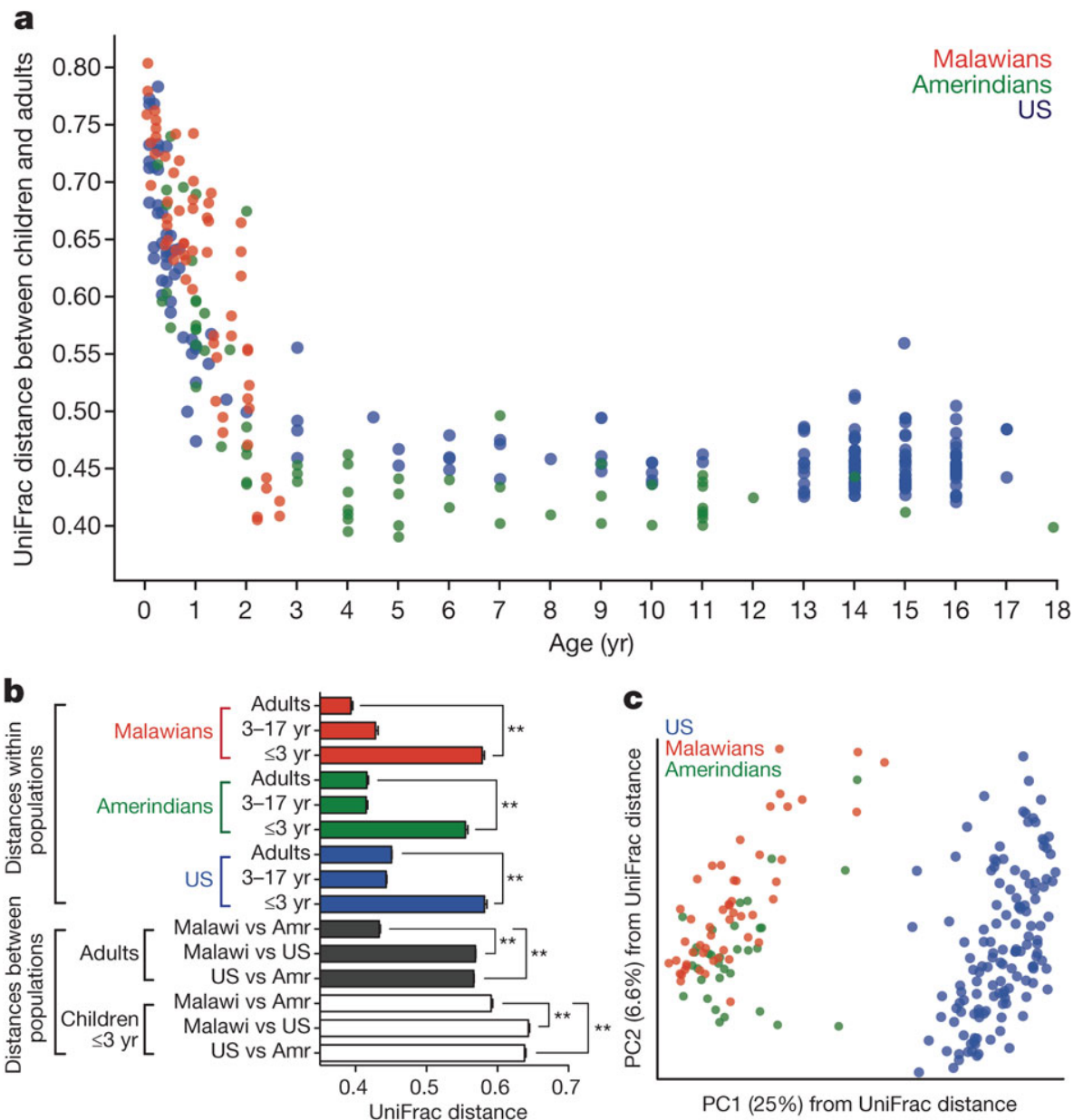
The human microbiota is thought to play an essential role in maturation of the infant immune system. This is evidenced in observations that early-life antibiotic usage, for instance in pre-term infants, is associated with immune impairment <sup>233</sup> and the occurrence of asthma, atopic dermatitis, multiple sclerosis, and irritable bowel disease <sup>234–238</sup>.

Furthermore, in experimental investigations using germ-free (GF) mice or mice colonised with a defined microbiota (gnotobiotic mice), loss of commensal microbiota has been demonstrated to be associated with significant immune defects, including decreased IgA, decreased intraepithelial lymphocytes, defects in lymphoid tissue development in the spleen, thymus, lymph node, and mucosal interface (gut-associated lymphoid tissue, GALT), and increased susceptibility to pathogens <sup>164, 170, 231,239–241</sup>.

The postnatal period of development, therefore, represents a critical window of time whereby early-life microbial exposure has significant influence over morphological and functional development of the immune system <sup>170</sup>.

#### 1.15.5.Changes to the Microbiota Composition

In the past century, changes in human lifestyle, particularly in developed countries, are thought to be altering the natural development of the infant microbiota, and subsequent composition of the adult microbiota. In a study carried out by Yatsunenکو *et al* (2012), for example, comparison of the gut microbiome (the combined genetic material of the gut microbiota) of individuals from three distinct populations [rural Malawi, the Amazonas of Venezuela (Amerindians), and US metropolitan areas] found that the gut microbiome of individuals from US metropolitan areas was markedly different from those from rural Venezuela and Malawi (Figure 1.12) <sup>220</sup>. As all three populations differed significantly with regards to geographical location and environment, the observed disparity of the American gut microbiome is likely the result of differences in the American lifestyle rather than environment and/ or genetic variations.



**Figure 1.12: Variations in the gut microbiome of children and adults living in Malawi, the Amazonas, and the United States.** Examination of the similarity of microbial populations in the gut microbiome of Malawian, Amerindian, and American children and adults revealed that in all three populations the gut microbiome of children under the age of three was highly divergent from the adult microbiome (**A** and **B**). After the age of three, however, the gut microbiome of the children closely resembled that of the adult one, as demonstrated by significantly lower UniFrac scores. Intriguingly, the gut microbiota of American children and adults were persistently different to the Malawian and Amerindian microbiome (**A – C**). In contrast the gut microbiome of Malawian and Amerindian were more similar to one another, particularly in the adults (**B & C**), thus indicating differences in American culture rather than environment was responsible for the divergent gut microbiome observed in American subjects. [Taken from Yatsunenکو et al (2012)<sup>220</sup>]

In Westernised societies, there are numerous factors that have arisen in the past century that have reduced exposure to microbes and explain the observed changes in the microbiome. These include reduced family sizes <sup>155,164</sup>, increased use of caesarean sections <sup>193, 221,242,243</sup> and formula milk <sup>222,223</sup>, increased sanitisation <sup>155,244</sup> and urbanisation <sup>159,245</sup>, increased consumption of processed foods <sup>191,224</sup>, and antibiotic usage <sup>226,227</sup>.

Alterations in the natural maturation of the microbiota during early childhood is thought to be altering how the immune system matures in both developed and developing countries, and it is thought that changes in the human microbiota are responsible for the current asthma epidemic. In particular numerous studies have associated mode of delivery <sup>242,246</sup>, increased urbanisation <sup>245,247–250</sup>, and the use of antibiotics <sup>235,251–253</sup> with increased risk of atopic sensitisation and asthma development.

## 1.16. The Human Microbiota and Atopic Asthma

It has been firmly established that there are significant changes in the gut and airway microbiomes of asthmatic individuals compared to non-asthmatics <sup>242, 254, 263,255–262</sup>. These changes have typically been detected during early childhood, and it is thought that reduced exposure to environmental microorganisms during these critical developmental years is having an adverse impact on the development of the immune system, thus increasing the risk of childhood asthma.

### 1.16.1. The Gut Microbiota and Asthma

The composition of the gut microbiota matures during the first year of life, during which the maturing microbiota is thought to play a significant role in the maturation of the infant

immune system. Studies investigating whether dysbiosis of the gut microbiota contributes towards asthma development and pathology, therefore, typically investigate the gut microbiota during this vital developmental stage.

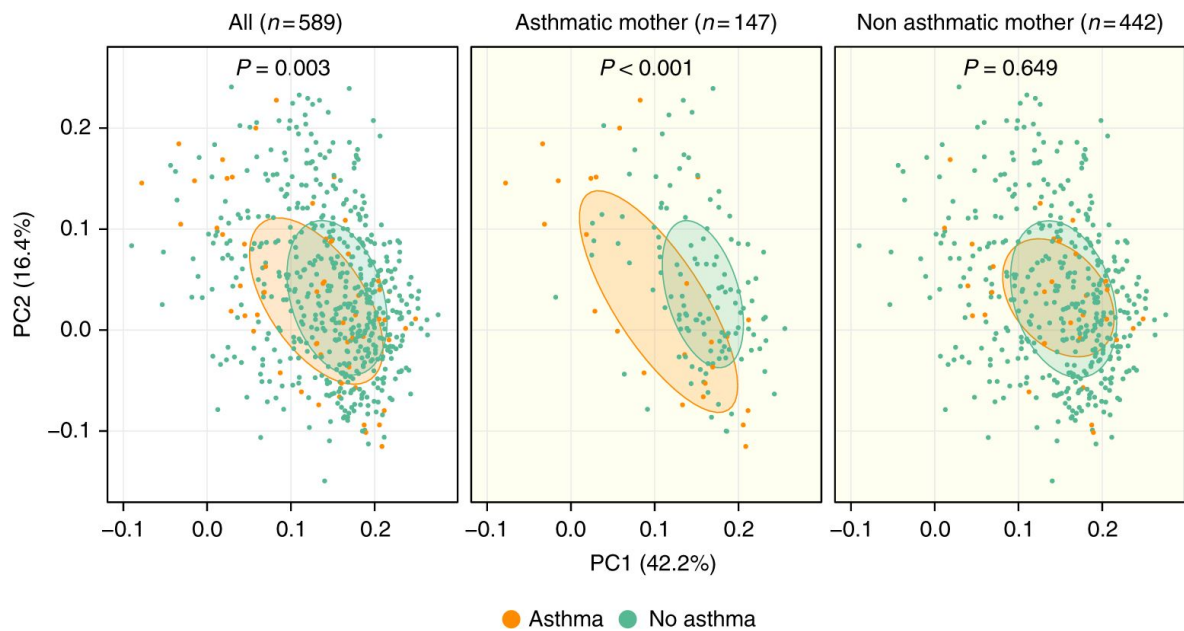
During the neonatal stage of development (defined as the first 28 days of life) characterisation of the neonatal gut microbiome has provided strong evidence of a positive association between development of atopic disease during early childhood (before the age of 5 years) and dysbiosis of the gut microbiota <sup>218, 242, 254,264–268</sup>. Overall, these studies have demonstrated that neonates that later develop atopic disease typically present with increased colonisation by Clostridia species <sup>242, 264,269</sup> and decreased colonisation by Bifidobacteria species <sup>254, 264,268</sup>. Kalliomaki and colleagues (2001), for example, demonstrated that at 3 weeks of age, neonates who went on to develop atopy displayed reduced Bifidobacteria dominance and subsequent expansion of Lactobacillus, Enterococci, Clostridia, and *Bacteroides* <sup>264</sup>. Additionally, work by Abrahamsson and colleagues (2012) has revealed that the diversity of bacteria residing in the neonate is reduced in infants who go on to develop atopic disease <sup>267</sup>.

Early colonisers, referred to as pioneer species, determine the ecosystem conditions of the various body habitats and thus influence the composition of the subsequent colonisers of the human microbiota following initial colonisation. Microbial dysbiosis during the neonatal developmental period, therefore, is likely to adversely affect maturation of the gut microbiota during the first year of life. Arrieta et al (2015), for example, characterised the gut microbiome in infants aged 3 months and again at 1 year of age <sup>258</sup>. Changes in the gut microbiome of infants at risk of developing asthma at 3 months (decreased abundance of *Lachnospira*, *Veillonella*, *Faecalibacterium*, and *Rothia*) were found to persist up to the age of 1 year, whereby *Lachnospira* and *Veillonella* remained significantly decreased in the



atopic infants<sup>258</sup>. Moreover, this was found to significantly alter the functional activity of the gut microbiota, as evidenced by significantly decreased levels of the short chain fatty acid (SCFA) acetate (a major product of the microbiota in the infant gut) in the atopic infants<sup>258</sup>.

The findings of Arrieta and colleagues are further supported by work carried out by Durack *et al* (2018) and Stokholm *et al* (2018), who independently demonstrated delayed microbiota maturation in infants at risk of developing asthma<sup>217,270</sup>. Durack *et al* (2018) reported a reduced rate of gut bacterial diversification during the first year of life, as evidenced by decreased gains in both community richness and evenness, whilst Stokholm *et al* (2018) reported significant differences in beta diversity and decreased abundance of bacterial genera thought to be determinants of a healthy gut microbiota (*Faecalibacterium*, *Bifidobacterium*, *Roseburia*, *Alistipes*, *Lachnospira incertae sedis*, *Rumminococcus*, and *Dialister*) in at risk infants. Intriguingly the observed changes by Stokholm *et al* (2018) were only apparent in infants born to asthmatic mothers (Figure 1.13), thus suggesting that microbial dysbiosis is a trigger for asthma development in genetically susceptible infants.



**Figure 1.13: Diversity of the gut microbiome detected in 1-year old infants whom asthma was and was not developing.** Analysis of microbial diversity in the gut microbiome of 1-year old infants in whom asthma was and was not developing was performed using PCoA plots of weighted UniFrac distances. Comparison of the microbial diversity detected in the gut microbiome revealed that maternal asthmatic state significantly influenced microbial diversity, whereby only asthmatic infants with an asthmatic mother differed significantly compared to the non-asthmatic infants. This suggested that microbial dysbiosis was only associated with increased asthma risk in infants genetically predisposed towards the disease.

[Taken from Stokholm *et al.*, 2018 <sup>217</sup>]

The observations of gut microbial dysbiosis during the first year of life is likely to result in the development of a microbiota lacking key commensal organisms required for optimal physiological and immune development, and subsequent maintenance of immune homeostasis. West *et al* (2015), for instance, demonstrated that at 1 week and 1 month old, neonates who later developed atopic disease displayed significantly reduced levels of *Ruminococcaceae* colonisation, and colonisation by *Ruminococcaceae* was found to be inversely associated with TLR2 induced IL-6 and TNF $\alpha$  levels <sup>218</sup>. The neonates were also observed to exhibit a pattern of lower Proteobacteria colonisation (in particular

*Enterobacteriaceae* and *Escherichia-Shigella*), and that colonisation with these bacteria was inversely associated with TLR4-induced TNF $\alpha$  and IL-6 levels <sup>218</sup>.

Changes in immune maturation in the infants is likely to increase susceptibility to developing atopic diseases, thus providing a mechanism whereby gut microbiota dysbiosis contributes towards disease development. Furthermore, variations in immune maturation are likely to alter microbial tolerance and colonisation following introduction of solid foods to the diet at around 6 months, subsequently increasing the risk of persistent microbial dysbiosis in the gut.

In support of this interpretation are a significant number of studies that have demonstrated atopic disease is associated with changes in the gut microbiome in both children and adults suffering from atopic disease <sup>253,270–276</sup>.

Candela *et al* (2012), for example, observed variations in the gut microbiome of children aged 2 – 14 years with clinical diagnoses of various atopic diseases (allergic rhinitis, atopic asthma, atopic dermatitis, and cow's milk allergy) compared to non-atopic children <sup>271</sup>. These observations were only detected at the lower taxonomic levels, as both atopic and non-atopic children display similar degrees of phylum diversity <sup>271</sup>. Using a phylogenetic microarray platform, the authors determined that atopic children displayed a tendency towards reduced numbers of *Akkermansia muciniphila*, *Faecalibacterium prausnitzii*, *Ruminococcus bromii et rel*, and *Clostridium* cluster XIVa species, and expansion of *Enterobacteriaceae*, *Veillonella parvula*, and Fusobacteria species <sup>271</sup>.

Interestingly the gut microbiome did not differ significantly between the different atopic disease states, thus suggesting that microbial dysbiosis simply increases the risk of developing atopic disease and that other factors are responsible for determining the specific disease outcome. Following disease development, it is likely that changes in

microbiota contribute towards disease severity and/ or function as biomarkers for atopic disease.

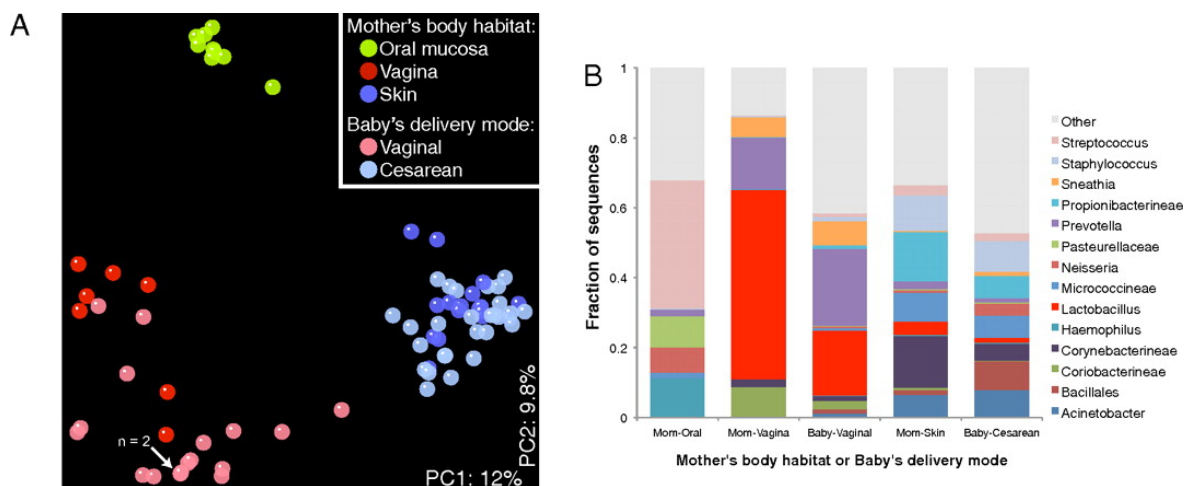
#### 1.16.2. The Airway Microbiota and Asthma

In addition to changes in the gut microbiota, recent studies have suggested that atopic disease is also associated with altered airway microbiota composition. These investigations are relatively recent compared to those carried out on the gut microbiota as it wasn't until the development of next Generation sequencing that the airways have been shown to possess a microbiota<sup>256,277-279</sup>.

Investigations into the airway microbiota have found that there is greater bacterial colonisation and diversity in the airways of asthmatic individuals compared to the airways of non-asthmatic, healthy controls<sup>256, 277,280</sup>. This is characterised by expansion of the Proteobacteria (in particular pathogenic organisms, such as *Haemophilus*, *Neisseria*, *Bordetella*, *Moraxella*, and *Shigella*) and increased Streptococci<sup>256, 277,280,281</sup>.

Moreover, the association between atopic asthma and the airway microbiota appears to be dependent upon age of colonisation. Bisgaard and colleagues (2007), for instance, found that neonates that were highly colonised by *Haemophilus influenzae*, *Moraxella catarrhalis*, and *Streptococcus pneumoniae* during the first month of life displayed a greater incidence of recurrent wheeze that was associated with the development of asthma in later life<sup>280</sup>. In contrast, infants who were colonised by the bacterial species at 12 months of age did not display an increased risk of asthma development<sup>280</sup>, thus suggesting that colonisation must occur early in life to influence atopic sensitisation and subsequent asthma pathology.

Furthermore, neonatal colonisation of *Haemophilus*, *Neisseria*, and *Streptococci* was found by Dominguez-Bello *et al* (2010) to be associated with method of birth delivery, whereby increased abundance of *Haemophilus*, *Neisseria*, and *Streptococci* was associated with caesarean delivery, and increased *Prevotella* colonisation was associated with vaginal delivery <sup>195</sup> (Figure 1.14). This, therefore, suggests that the positive association between caesarean sections and atopic asthma may be the consequence of increased Proteobacteria species within the airways in infants born by caesarean section.

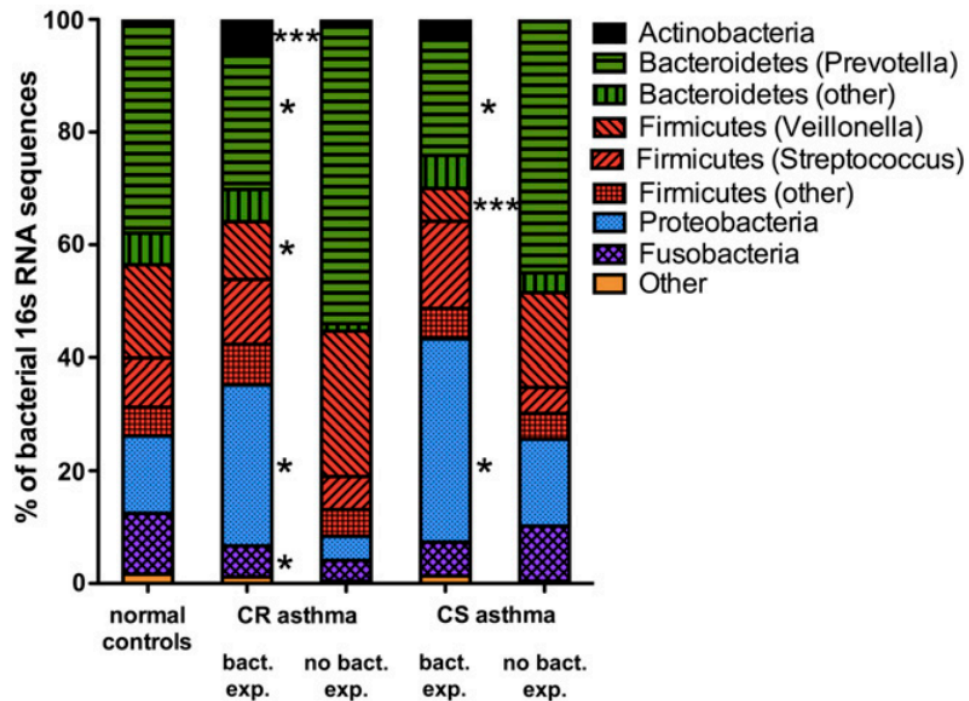


**Figure 1.14: Comparison of the neonatal homogeneous microbiome to the maternal microbiome.** Characterisation of the homogenous neonatal microbiome and the maternal microbiome at various habitats (oral, skin, vaginal) revealed that the method of delivery had a significant impact on the diversity (A) and composition (B) of the neonate microbiome. Infants delivered vaginally had a similar microbiome to the maternal vaginal microbiome, whilst infants delivered by caesarean section displayed a similar microbiome to the maternal skin microbiome (A & B). Furthermore, a number of bacterial genera positively associated with the development of atopic disease in infants (*Streptococcus*, *Haemophilus*, *Neisseria*) were observed to be increased in the microbiome of infants delivered by caesarean section, thus suggesting a mechanism by which birth by caesarean section increases the risk of developing atopy.

[Adapted from Dominguez-Bello *et al* (2010)<sup>195</sup> ]

In addition to the association of asthma development, the airway microbiota composition has also been found to influence the severity of asthma disease<sup>256,281</sup>. Huang *et al* (2011), for example, determined that there was a strong relationship between increased airway microbiota diversity and airway hyperresponsiveness, and that there were approximately 100 different bacterial taxa that displayed a positive correlation between abundance and airway hyperresponsiveness<sup>281</sup>. The taxa were predominately Proteobacteria, thus supporting the earlier findings by Bisgaard (2007)<sup>280</sup> regarding the importance of Proteobacteria in asthma pathology.

Furthermore, subsequent research carried out by Goleva and colleagues (2013) has suggested that the composition of the airway microbiota may also influence disease severity and treatment responses<sup>255</sup>. In this study the authors characterised the airway microbiome using BAL samples from asthmatic subjects who were corticosteroid resistant (CR) and asthmatic subjects who were corticosteroid sensitive (CS). In comparison to the airway microbiome of non-asthmatics, the asthmatic subjects were found to display bacterial expansion at the phylum level, and that composition of these expansions varied between the CR and CS samples (Figure 1.15). In the CR subjects, increased expansion of the Actinobacteria and Proteobacteria phyla was observed, whilst in the CS samples only Proteobacteria expansion was detected (Figure 1.15). Moreover, the CR samples also displayed significant reduction in the Fusobacteria phylum, and the *Prevotella* and *Veillonella* genera, whilst the CS subjects were found to have reduced levels of *Prevotella* and *Veillonella* (Figure 1.15).



**Figure 1.15: Changes in the composition of the airway microbiome in corticosteroid sensitive and corticosteroid resistant asthma compared to healthy control subjects.** Characterisation of the airway microbiome revealed that asthma is associated with bacterial expansion at the phylum level. Corticosteroid sensitive (CS) asthma was associated with a significant expansion of the Proteobacteria phylum and decreased levels of Bacteroidetes (Prevotella) and Firmicutes (Veillonella) compared to the control subjects. In contrast, corticosteroid resistant (CR) asthma was associated with expansion of the Actinobacteria and Proteobacteria phyla and a significant decrease in bacteria belonging to the Bacteroidetes (Prevotella genera) Firmicutes (Veillonella) and Fusobacteria phyla compared to the control subjects.

\* =  $P < 0.05$  and \*\*\* =  $P < 0.001$  compared to normal controls.

[Taken from Goleva *et al.*, 2011<sup>255</sup>]

The distinct microbial profiles of the CR and CS asthmatic subjects suggest that different asthma phenotypes have distinct airway microbiomes to one another, which could be useful in the diagnosis of the asthma phenotypes. These distinct microbial profiles may reflect different asthma pathogenic mechanisms present in the two groups that indirectly alter composition of the airway microbiota, or it may be that composition of the airway

microbiota influences susceptibility towards corticosteroid treatment. Additionally, it should also be noted that a study carried out by Huang *et al* (2014) found that corticosteroid treatment following an acute exacerbation in individuals with chronic obstructive pulmonary disease (COPD) resulted in Proteobacteria expansion in the airway microbiota <sup>282</sup>, thus suggesting that treatment with corticosteroids can influence the asthmatic airway microbiota composition.

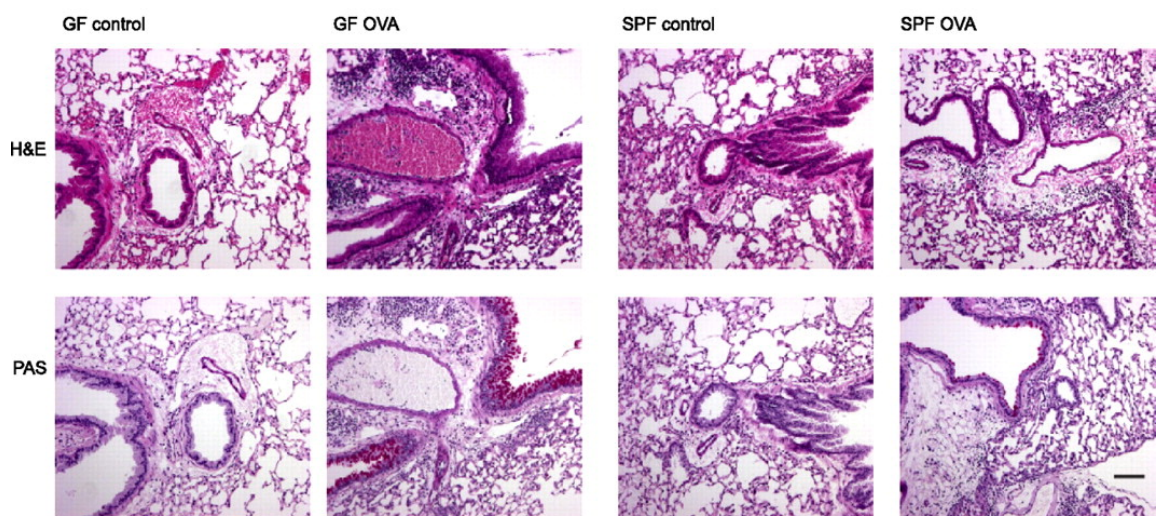
### 1.16.3. The Microbiota and Asthma Pathogenesis

The gut microbiota, particularly during the neonatal period, has been demonstrated to have an important role in allergen sensitisation and subsequent atopic disease development. The role of the gut microbiota in atopy has typically been investigated using GF murine studies, whereby mice are reared in sterile conditions and allergen sensitisation is induced through intranasal or subcutaneous exposure <sup>165,283–286</sup>.

In the absence of microbial colonisation, the immune system fails to mature properly and is characterised by altered levels of immune cells (T cells, B cells) and increased total IgE concentrations <sup>286–289</sup>, thus suggesting that the absence of a microbiota results in a predisposition towards atopic sensitisation. In support of this theory, Herbst and colleagues (2011) reported that there was elevated Th2 responses towards the OVA allergen in GF mice compared to specific pathogen free (SPF) mice and GF mice that were recolonised prior to allergen exposure <sup>284</sup>. This was characterised by increased airway hyperresponsiveness, basophilia, goblet cell hyperplasia, perivascular and peribronchial inflammatory cell infiltration, IL-4 and IL-5 production, and elevated IgE serum levels (Figure 1.16) <sup>284</sup>. Moreover, in the GF mice prior to allergen exposure there was reduced alveolar macrophages, IgA, and conventional dendritic cells present in the lungs compared



to SPF mice <sup>284</sup>. Following allergen exposure, the GF mice were found to have fewer plasmacytoid and conventional dendritic cells in the lungs compared to the SPF mice, and the conventional dendritic cells that were detected were observed to have reduced activity and display a different phenotype compared to those observed in the SPF mice <sup>284</sup>. This suggested that the immune system in the GF mice had not fully matured, and thus had maintained the neonatal Th2 bias.



**Figure 1.16: Histological examination of the airways in germ free mice and specific pathogen free mice before and after OVA allergen challenge.** Examination of lung tissue in germ free (GF) and specific pathogen free (SPF) mice found that following allergen (OVA) sensitisation and challenge, GF mice exhibited increased inflammatory cell infiltration (perivascular and peribronchial) and increased goblet cell hyperplasia compared to SPF mice. The exaggerated inflammatory response in the GF mice suggested that the absence/presence of commensal bacteria has a functional impact on allergen-induced inflammation.

[Adapted from Herbst *et al.*, 2011 <sup>284</sup>]

Subsequent work carried out by Olszak and colleagues (2012) found that GF mice displayed significantly greater allergic responses to the OVA allergen compared to SPF mice <sup>285</sup>. This was associated with an increased accumulation of invariant natural killer cells (iNKT) cells

in the lungs that was observed to induce enhanced eosinophilia, IgE production, and airway hyperreactivity<sup>285</sup>. Moreover, the increase in iNKT cell accumulation within the lungs was found to be due to increased epithelial expression of the iNKT cell chemokine, CXCL16, as a consequence of hypermethylation of *cxcl16*. This, therefore, suggested that microbial colonisation modulates allergen-induced inflammation by influencing cellular activity as a result of epigenetic-mediated mechanisms.

However, the ability of the endogenous microbes to suppress hypermethylation of *cxcl16* appeared to be restricted to the neonatal period of development. This was determined by the observation that when the GF mice were exposed to conventional SPF microbiota during the first 6 weeks of life, iNKT cell abundance and subsequent allergic asthma susceptibility significantly decreased, whilst when the GF mice were exposed to microbes as adults there was no change in iNKT cell abundance<sup>285</sup>. Moreover, the absence of the microbiota during the neonatal period appeared to have long-term consequences, whereby the levels of iNKT cells remained consistently high throughout life.

This, therefore, supported the theory of a 'critical window of opportunity' whereby colonisation of microbes must occur to ensure proper development of the immune system.

The importance of the microbiota during the neonatal period of development is likely due to microbial signals that are required for lymphoid development and maintenance of the gut, and thus changes in the microbiota could result in altered epithelial cell signalling cascades and subsequent dysregulation of the innate and adaptive immune response<sup>290</sup>. This may result in the persistence of the neonatal Th2 bias, and consequently increased susceptibility towards allergic asthma.

The mechanisms whereby the composition of the microbiota may influence asthma susceptibility have typically been examined through the inoculation of murine models with

specific bacteria, and examination of the consequences of inoculation. Through the use of such experimental models, a number of bacterial species have been identified that either protect against allergen sensitisation or increase the risk of sensitisation occurring (Table 1.1). In humans these bacterial species have been detected at altered levels in asthmatic subjects compared to non-asthmatic subjects, thus suggesting that the immunological mechanisms detected in experimental models of asthma also apply to clinical disease. Bacteria associated with protection against atopic sensitisation and disease include the *Bifidobacteria* spp. and the *Lactobacillus* spp., and bacteria associated with increased risk of atopic sensitisation and disease development include *Sphingomonadaceae*, *Clostridium difficile*, and *Chlamydiae pneumoniae* (Table 1.1).

**Table 1.1: Bacteria detected in the human microbiome that have been found to have beneficial or harmful functional properties that are associated with atopic disease pathology**

Organism	Beneficial effects on the host	References
<i>Bifidobacteria spp.</i>	- Increase T regulatory cells	291,292
	- Increase IL-10 production	292
	- Decrease IL-2, IL-4, IL-6, IFN $\gamma$ , and TNF $\alpha$ production	291,292
	- Decrease serum IgE levels	291
	- Increase Th1 differentiation	292
	- Reduce inflammatory cell infiltration	291,292
	- Reduce mast cell degranulation	292
	- Reduce airway remodelling	292
	- Reduce T cell activity	292
<i>Lactobacillus spp.</i>	- Decrease airway hyperresponsiveness	292,293
	- Decrease lung resistance	292
	- Suppress airway remodelling	292
	- Decrease airway immune cell infiltration	292,293
	- Decrease peripheral eosinophil populations	293
	- Decrease IL-2, IL-4, IL-5, IL-6, IL-13, IL-17A, MCP-1, and TNF	292–294
	- Increase IL-10, IL-12, and IL-18 production	294,295
	- Increase IgA production	294
	- Suppress mucosal mast cell degranulation	292
	- Suppress T cell activation	292
- Decrease expression of TLR4	292	
	- Increase Th1 differentiation	295
Organism	Harmful effects on the host	References
<i>Sphingomonadaceae spp.</i>	- Activate natural killer cells	296–298
<i>Clostridium difficile</i>	- Increase permeability of the epithelial layer	299,300
	- Macrophage activation	301
	- IL-8 production	301
<i>Chlamydia pneumoniae</i>	- Increase epithelial cell adhesion molecules	302
	- Increase production of IL-6 and IL-8	303–305
	- Promote smooth muscle proliferation	306
	- Increase IL-4 expression	307
	- Increase MUC5AC expression	308
	- Induce airway remodelling	302,306
	- Induce airway hyperresponsiveness	306,308

## 1.17. Introduction to the Circulatory Microbiome

Whilst colonisation of the specific body sites that are in contact with the external environment (such as the gastrointestinal tract, skin, and respiratory tract) by microorganisms is both well-described and universally accepted, the existence of microbial populations in other “classically sterile” locations, including the blood, is a relatively new concept<sup>309</sup>.

Traditionally, the blood was thought to be a sterile environment during good health, and the presence of microbes within circulation was thought to only occur in cases of sepsis<sup>310</sup>. The presence of bacteriostatic and bactericidal components within the blood creates a hostile environment unfavourable for bacterial growth and survival<sup>309</sup>, and the majority of literature available has demonstrated that bacteraemia is typically short-lived and transient<sup>311</sup>. However, over the past few decades there has been mounting evidence to support the existence of a circulatory microbiota/ microbiome in mammals composed of transient and/ or permanent microbial colonisers and/ or microbial DNA translocated from other body sites.

The possibility of a blood microbiota was first reported in an early study by Tedeshi *et al* (1969), who detected the presence of intraerythrocytic bacteria in clinically healthy human subjects<sup>312</sup>. These early observations were followed by a number of studies that demonstrated the presence of bacteria or bacterial-like structures within the circulation in the absence of overt disease<sup>313–319</sup>. Domingue and Schlegel (1977), for example, surveyed the blood from 60 healthy control subjects and observed bacteria resembling streptococcal, staphylococcal, and Gram positive filamentous forms in 7% of blood samples analysed<sup>315</sup>.

Following the advent of culture-independent techniques for bacterial detection, in particular 16S ribosomal RNA (rRNA) sequencing techniques, interest in the circulatory microbiota/ microbiome has increased. Important research carried out by Nikkari *et al* (2001)<sup>320</sup> and McLaughlin *et al* (2002)<sup>319</sup>, who independently used qPCR to identify bacterial DNA in the blood of healthy donors, has led the way in providing the first in-depth characterisation of the circulatory microbiome.

Since the early investigations there have been increasing reports demonstrating the presence of bacteria-specific DNA in human whole blood, plasma, buffy coat, and serum samples from healthy human subjects<sup>310, 321, 330–339,322–329</sup>, and various other mammalian species, including arthropods (fleas, tarsaloes)<sup>340</sup>, rodents<sup>341</sup>, Pikas<sup>340</sup>, cats<sup>342</sup>, chickens<sup>343</sup>, and cows<sup>344</sup>. These investigations have primarily characterised the circulatory microbiome through the use of amplification and sequencing of the bacterial 16S rRNA gene or whole genome sequencing. This, therefore, means that whilst they provide evidence of bacteria-derived genetic material within the circulation, they do not provide evidence for the presence of a blood microbiota composed of viable organisms.

Critical work carried out by Damgaard *et al* (2015), however, has demonstrated the possibility that the observed bacterial structures are viable organisms<sup>345</sup>. The authors found culturable bacteria in 62% of blood samples from human donors with no overt disease<sup>345</sup>. These findings are further supported by the work of Panaiotov *et al* (2018) who demonstrated the presence culturable Actinobacteria, Bacteroidetes, Cyanobacteria, Firmicutes, Fusobacteria, and Proteobacteria in the blood of healthy individuals<sup>333</sup>, and Schierwagen and colleagues (2019), who demonstrated the presence of culturable *Staphylococcus* and *Acinetobacter* in blood samples taken from patients with liver cirrhosis

<sup>346</sup>.

### 1.17.1. Detection Techniques used to Characterise the Circulatory Microbiome

Early characterisation of the blood microbiota utilised a range of classic microbiology techniques, including microbial culture, Gram staining, microscopy, sera reactivity, and metabolic assays<sup>313, 315, 319,347</sup>. These techniques were reliant on the presence of viable bacteria, and typically required the bacteria to be cultured in growth media prior to analysis.

However, the majority of bacteria that make up the human microbiota cannot be cultured. The Human Microbiome Consortium (2012), for example, sampled 242 healthy adults from 18 different anatomical sites, and demonstrated the presence of 5,177 microbial taxa using 16S rRNA sequencing techniques. When culture techniques were applied, however, only 800 of the microbial taxa could be detected<sup>348</sup>.

The majority of investigations into the blood microbiota, therefore, rely on non-culture techniques in order to characterise the microbial populations present in the human circulatory system. These studies have been primarily facilitated by the invention of PCR and DNA sequencing techniques, and the discovery that ribosomal RNA sequences can be used for phylogeny<sup>349</sup>.

Since the first use of 16S rRNA pyrosequencing to successfully identify and characterise the bacterial populations present in environmental samples<sup>350</sup>, 16S rRNA sequencing has been the technique of choice when investigating the circulatory microbiome.

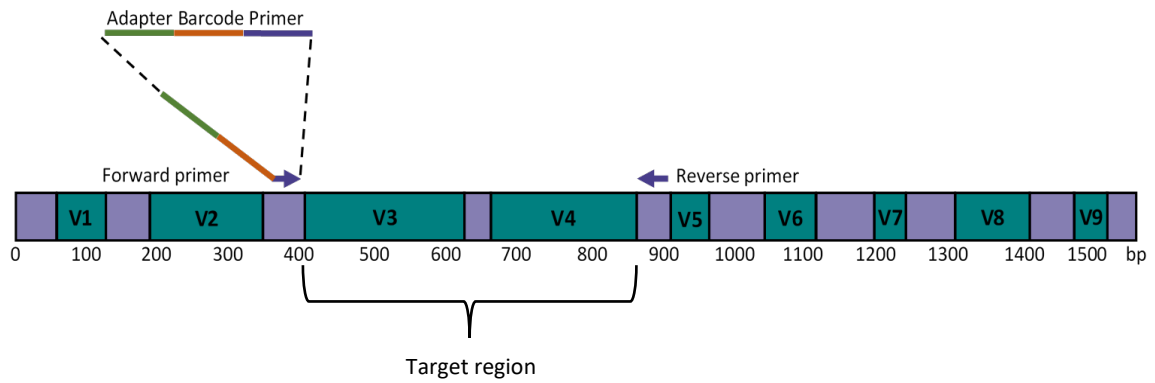
This technique makes use of the bacterial 16S rRNA gene as a housekeeping genetic marker due to its expression in almost all known bacterial species, its absence in the human genome, the highly conserved nature of the gene, and its optimum size (1,500bp)<sup>351</sup>. The gene encodes a component of the 30S small subunit of the bacterial ribosome and is

composed of 10 highly conserved regions and 9 hypervariable regions (Figure 1.17). The conserved regions provide primer binding sites, whilst the hypervariable regions provide species-specific nucleotide sequence signatures that can be used to identify the bacterial taxa/ species (Figure 1.17). In 16S rRNA sequencing, PCR is used to amplify one or more hypervariable regions of the 16S rRNA gene using primers designed to bind to the conserved regions adjacent to the hypervariable region of interest (Figure 1.17). Next generation sequencing (e.g. Illumina sequencing, Ion torrent sequencing) is then typically performed to sequence the amplified hypervariable region. The sequenced DNA reads are then compared to known bacterial 16S rRNA sequences in order to identify operational taxonomic units (OTUs) that correspond to bacterial species/ bacterial group (taxa) <sup>350</sup>.

Sequencing of the 16S rRNA genes or fragments of the 16S rRNA gene has been proven to be an effective method of characterising the human microbiome without bias or need for cultivation <sup>352</sup>, and thus is currently the method of choice for the detection of bacteria within the circulatory system.

Evidence of blood microbiota/ microbiome has also been provided indirectly through quantification of bacterial endotoxins and gut uremic toxins present in the blood <sup>336,353–357</sup>.





**Figure 1.17: Sequencing of the bacterial 16S rRNA gene.** The bacterial 16S rRNA gene is a 1,500 base pair long gene encoding the 30S small subunit of the bacterial ribosome. It is composed of 10 highly conserved regions (purple) and 9 hypervariable regions (teal) that contain species-specific nucleotide sequences. In microbiome investigations, primers are designed to bind to the conserved regions adjacent to the hypervariable region of interest (the target region). The forward primer typically contains an adapter and barcode to enable incorporation of the adapter and barcode to the end of the amplified target region nucleotide sequence. The target region is amplified using PCR and then sequenced using Next generation sequencing techniques.

### 1.17.2. Origins of the Circulatory Microbiome

Unlike previously characterised microbiota environments, where the environment is exposed to external bacteria, the circulatory system is an internal environment that in the absence of injury or surgical intervention, does not come into contact with the external environment.

The blood does, however, circulate the body, where it functions as a medium that samples from virtually all body sites<sup>358</sup>. The general consensus regarding the origins of the bacterial structures and DNA detected in the blood is that it is likely the result of atropobiosis; a process whereby microbial DNA and/ or viable microorganisms translocate into the blood vessels from other microbial niches, such as the gut, oral cavities and airways, and enter the circulation<sup>311,325</sup>.

Atopobiosis may occur due to trauma (dental, surgical, or injury) or as a consequence of bacterial virulence attributes that enables the bacteria to invade the vascular system <sup>311</sup>.

In support of this explanation, characterisation of the microbial populations in the coronary artery tissues by Lehtiniemi *et al* (2005) identified known members of the oral microbiota present in the blood tissues <sup>321</sup>. This suggested that bacteria had translocated from the oral cavities into the bloodstream, potentially as a result of damage caused by tooth brushing or by leakage across the mucosal surfaces <sup>321</sup>. Furthermore, a number of studies have demonstrated a correlation between changes in the gut environment and altered microbial populations detected in the blood <sup>359-361</sup>. Additionally, in HIV/ AIDS patients, many of the bacteria detected in the circulation are known members of the gut microbiota, suggesting that a compromised immune system as a result of CD4+ lymphocytopenia enabled increased translocation of bacteria from the gut into the vascular system <sup>362</sup>.

These findings are supported by recent work carried out by Loohuis *et al* (2018), who found that when the circulatory microbiome was compared to the Human Microbiome datasets, the circulatory microbiome most closely resembled the gut and oral microbiomes <sup>332</sup>. Similarly, when Li *et al* (2018) compared 16S rRNA reads amplified and sequenced from the blood of acute pancreatitis patients and healthy controls to the 16S rRNA gene dataset from the National Center for Biotechnology and Information (NCBI), an average of 87.0% of the circulatory microbiome taxa were identified as known commensal or pathogenic members of the gut microbiota <sup>331</sup>.

Another proposed explanation for the circulatory microbiome/ microbiota is that microbial contamination of the blood samples occurred during collection of the samples and/ or downstream experimental procedures.

However, when taking into account the increasing numbers of studies demonstrating significant changes in the composition of the circulatory microbiome in diseased states compared to healthy control subjects this argument seems unlikely. Moreover, examination of the bacterial taxa reported in circulatory microbiome studies reveal similar bacterial populations across the different studies, whereby Proteobacteria dominate, displaying relative abundance values typically ranging from 85% - 90%, and Firmicutes, Actinobacteria, and Bacteroidetes detected at a lesser extent, with relative abundance scores typically less than 10%<sup>327, 331–333, 336, 338, 339, 360, 361</sup>. This suggests the existence of a core circulatory microbiome profile.

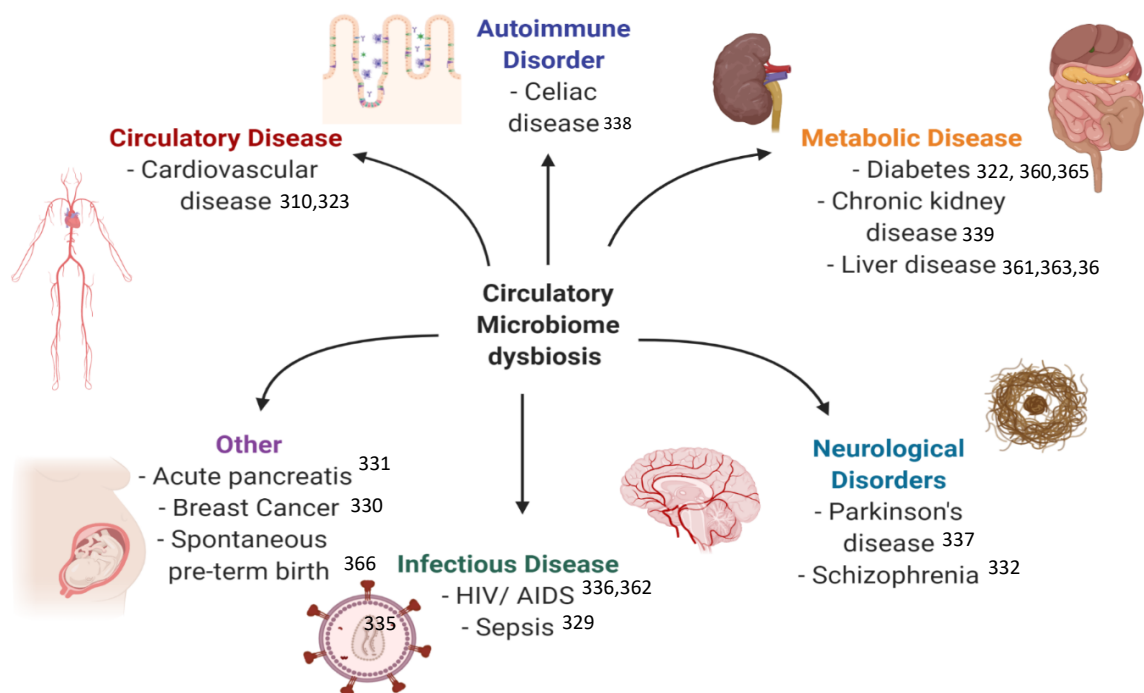
### 1.17.3. The Circulatory Microbiome and Human Disease

Comparison of the circulatory microbiota/ microbiome in healthy and diseased states have detected significant differences in the blood. Scanning electron microscope analysis of whole blood, for example, has revealed that blood microbes lurk intracellularly and that different disease states are associated with different morphological types of microbes. Alzheimer's disease, for example, has been associated with the detection of mostly coccus microbes, whilst Parkinson's disease has been associated with both coccus and bacillus bacteria<sup>326</sup>.

Furthermore, more recent studies that have utilised 16S rRNA sequencing techniques to characterise the circulatory microbiome, have identified a number of diseased states that display altered microbial populations in circulation compared to healthy control subjects<sup>310, 322, 360–365, 323, 329–332, 337–339</sup> (Figure 1.18). The majority of identified diseases directly alter the circulatory environment (cardiovascular disease, HIV, Type 2 diabetes mellitus, kidney disease, liver disease, sepsis) (Figure 1.18), and thus it is unsurprising that they have been

linked to changes in the circulatory microbiome. Moreover, a number of the diseases identified are metabolic diseases (Type 2 diabetes mellitus, kidney disease, liver disease). This suggests that changes to the gut environment as a consequence of disease results in increased bacterial translocation into the circulatory vessels.

Additionally, significant difference in the circulatory microbiome have been detected in the midtrimester serum of pregnant women who go on to have a spontaneous preterm birth compared to women who had a term birth <sup>335</sup>. This has raised the possibility that changes in the circulatory microbiome could be used as a method of identifying women at risk for a spontaneous pre-term birth.



**Figure 1.18: Human disease that have been associated with changes in the circulatory microbiome.** A literature search utilising Google scholar, PubMed, and ResearchGate was utilised to identify all published research demonstrating significant changes in the circulatory microbiome in diseased states compared to healthy control subjects.

#### 1.17.4. Asthma and the Circulatory Microbiome

To date there have been no publications regarding atopic disease and changes to the blood microbiome barring the published work generated from this thesis <sup>367,368</sup>. However, as microbial dysbiosis in both the airways and the gut have been well described in atopic disease, and the circulatory microbiome is predicted to be derived from microbial translocation from other body habitats, such as the airways and gut, it is highly likely that the development of asthma would have a significant impact on the composition of the circulatory microbiome given that microbial dysbiosis is a well described feature of this disease.

#### 1.17.5. Potential Use of the Circulatory Microbiome in Clinical Diagnostics

The association of various diseased states with changes in the circulatory microbiome/ microbiota are likely to reflect microbial dysbiosis at distant body sites. Characterisation of the circulatory microbiome/ microbiota, therefore, offers potential opportunities for novel biomarker and therapeutic developments.

#### 1.17.6. The Importance of the Experimental Negative Control

One of the biggest concerns with regards to microbiome research is that the highly sensitive techniques used to characterise the microbial populations present in environmental and clinical samples are susceptible to microbial contamination. Contaminating microbial DNA can compromise the integrity of the microbiome data generated from environmental/ clinical samples, distort the taxonomic distributions and frequencies of the detected microbes, and potentially contribute towards erroneous interpretations <sup>369,370</sup>.

Samples with a low biomass (such as blood and mucosal samples) have been demonstrated to be particularly susceptible to the risk of contaminating microbial DNA <sup>371</sup>, presumably as a result of the contaminating DNA dominating the low level of microbial DNA present in the samples. Investigations into the origins of the contaminating microbial DNA have identified the DNA extraction kits and laboratory reagents/ equipment as the predominant source of contaminating DNA <sup>369,371–375</sup>. Efforts have been made to remove and/ or reduce contaminating microbial DNA from entering the microbiome pipeline during the DNA extraction and amplification steps. These include performing DNA extraction and amplification in sterile UV cabinets in order to reduce the risk of the samples/ reagents coming into contact with environmental microbes, using UV irradiation to mutate the contaminating DNA, and using restriction endonucleases to digest microbial DNA present in the laboratory reagents <sup>370,371,376</sup>.

These methods, however, have thus far not been proven to effectively eradicate contaminating microbial DNA from the microbiome pipeline <sup>369,376</sup>. Furthermore, a number of the methods developed are technically complicated, and thus unsuitable for high-throughput work that frequently involves large sample numbers <sup>370</sup>. Moreover, the methods have been demonstrated to reduce PCR sensitivity, thus making them unsuitable for microbiome pipelines designed to characterise samples with low-biomass <sup>370</sup>.

Characterising experimental negative controls, consisting of 'blank' DNA extractions and subsequent PCR amplifications, whereby molecular biology grade water replaces the clinical sample during the DNA extraction process, is therefore essential as it enables identification of potential contaminating microbes <sup>369, 371,377,378</sup>. Furthermore, comparison of the level of microbial DNA present in the negative controls compared to the clinical samples is important in determining the level of microbial DNA detected in the clinical

samples that can be attributed to contaminating microbial DNA<sup>369, 371,377,378</sup>. This is particularly important when using low-biomass samples, where low level microbial contamination may be mistaken for a microbiome<sup>369, 371,377</sup>.

### 1.18. Experimental Models of Asthma

Asthma is a disease that specifically affects humans and, with the exception of cats and horses who present diseased states similar to asthma (eosinophilic bronchitis and heaves, respectively), there is no known animal that naturally exhibits an asthma-like disease similar to the human disease<sup>379</sup>.

Experimental models of asthma, however, have been developed using a number of animal species, including *Drosophila*, mice, rats, guinea pigs, cats, dogs, pigs, primates, and horses<sup>380</sup>. Of the experimental animal models available for studying asthma, none thus far have been able to reproduce all the pathophysiological mechanisms and symptoms of the uniquely human disease.

Of the animal models available, the murine experimental model is currently the most commonly used. This is in part due to the ease in which mice can be bred, maintained, and handled. Moreover, mice are easily sensitised to a number of antigens including OVA, HDM, cockroach antigens, *Aspergillus fumigatus*, and ragweed, and there are a wide array of specific reagents available for analysis of the cellular and humoral responses in allergen-exposed mice<sup>380,381</sup>. Furthermore, a comprehensive understanding of the murine genome has enabled the development of transgenic and/ or gene-knockout mice to better understand the pathophysiological mechanisms behind allergen-induced airway inflammation<sup>380</sup>.

The induction of experimental asthma involves two phases; allergen sensitisation and allergen challenge. The sensitisation phase has traditionally involved sensitising the mice systemically to OVA in conjunction with an adjuvant, usually aluminium hydroxide, to prime the immune system to respond to the allergen in the desired way <sup>381</sup>. Peripheral sensitisation is performed using the intraperitoneal, subcutaneous, or dermal routes, and then followed by OVA challenge 1-2 weeks later using aerosol, intranasal, or intratracheal instillation routes <sup>381</sup>.

More recently, however, efforts have been made to have the animal model more closely mimic the human disease. This has involved replacing the OVA allergen, with known human allergens, such as the HDM allergen, and using intranasal methods of allergen exposure to reflect the allergen entry route observed in human disease, inhalation.

The HDMs are one of the most common allergens worldwide, with an estimated 50-85% of asthmatics diagnosed with a HDM allergy. *Dermatophagoides pteronyssinus* (European HDM) and *Dermatophagoides farinae* (American HDM) have both been demonstrated to produce allergenic proteins and contain bacterial and fungal proteins, such as LPS and  $\beta$ -glucan <sup>382</sup>.

In mice repeated administration of HDM results in a number of hallmark features of asthma, Th2-driven inflammation in the airways, eosinophilia, increased infiltration of neutrophils and lymphocytes, increased mucin production, increased muscle cell proliferation, and increased respiratory system resistance and elastance of the airway tissues <sup>383</sup>.



## 1.19. The HDM Allergen and the Microbiome

With regards to the effect asthma has on the microbiome, there is increasing evidence supporting the theory that the development of asthma can directly alter composition of the microbiome. This has been shown by a number of studies independently demonstrating that OVA- and HDM-induced experimental asthma results in significant changes to the murine gut microbiome <sup>384–386</sup> and lung microbiome <sup>384,387,388</sup>.

The observation that HDM sensitisation resulted in significant changes to the microbiome suggests that possibility that HDM sensitisation may influence the composition of the human microbiome. This may make the individual more susceptible to immune dysregulation and the development of atopic diseases.

Remot *et al* (2017), for example, demonstrated that CNCM I 4970, a member of the *Staphylococcus* genus, was increased in the murine lung following HDM sensitisation, and induced secretion of a number of pro-inflammatory cytokines, including TSLP, IL-10, IL-17A, and IL-12p70 <sup>388</sup>.

These investigations, however, have typically looked at microbial composition in either the murine gut microbiome or the murine lung microbiome. This, therefore, has prevented analysis on whether HDM-induced inflammatory responses in the lungs can simultaneously affect the microbiome at multiple body sites.

## 1.20. Aims and Objectives

Asthma has been present in the human population for thousands of years. However, prevalence of the disease has rapidly increased in the last 50 years, and the disease is now one of the most common chronic diseases of the 21<sup>st</sup> century.

As understanding of asthma increases the importance of being able to clearly distinguish between the different asthma phenotypes and endotypes is becoming more apparent. Increased understanding of the different aetiologies and pathologies will enable better diagnosis of the disease and offer novel therapeutic targets.

Investigations into causative factors that explain the increased incidence rates observed worldwide have found that changes in human lifestyle is a major contributing factor. It is now widely accepted that the changes in human behaviour and environment that have occurred during the past century are having an adverse effect on the development, composition, and function of the human microbiota, and this in turn is making the human race more susceptible to atopic disease. Changes in the atopic microbiome have been described in depth with regards to the airway and gut environments. However, there is limited knowledge of how atopic disease affects novel human microbiomes, such as the circulatory microbiome.

This thesis, therefore, aims to address the unmet need for the identification of phenotype-specific markers of atopic asthma, to explore how atopic disease affects the circulatory microbiome, and to determine whether allergen-induced airway inflammation adversely alters the microbiome composition. To achieve this the following will be performed;

- Quantification and characterisation of messenger and micro RNA detected in human plasma samples from healthy control subjects and atopic asthmatic subjects with a HDM allergy. Differential expression analysis will be performed to identify significant changes in the asthmatic subjects compared to the control subjects, and functional analysis will be carried out to determine which biological processes are likely to be affected by the observed changes in messenger and micro RNA expression.
- Quantification of inflammatory proteins in human plasma samples from healthy control subjects and atopic asthmatic subjects with a HDM allergy. This will include pro-inflammatory proteins with known functions in asthma pathogenesis (IL-4, 5, 10, 13, 17A, eotaxin, GM-CSF, INF $\gamma$ , MCP-1, TARC, TNF $\alpha$ ), total IgE (important in allergen sensitisation and reactivity), and endotoxin (a protein marker for Gram negative bacteria).
- Development of a protocol for characterising the circulatory microbiome in healthy control subjects and atopic subjects. Following successful development, the protocol will be used to identify significant changes in bacterial diversity, abundance, and function potential in the atopic circulatory microbiome compared to the non-atopic, control circulatory microbiome.
- Characterisation of the airway, gut, and circulatory microbiomes of mice sensitised and challenged to HDM allergen compared to HDM naïve mice. This will be achieved using murine BAL, faecal, and plasma samples, and statistical analyses will be applied to identify significant changes in the bacterial diversity, abundance, and function potential in the microbiomes of HDM-exposed mice compared to HDM-naïve mice.

## Chapter 2: General Methodology

Much of the experimental methods utilised were specific to a given results chapter, and so will be described within the experimental chapters. Chapters 3-5 did, however, share several experimental protocols and statistical analysis techniques, and thus are presented below.

### 2.1. Maintenance of Sterile Conditions during PCR set-up

Preparation of the PCR reactions was performed in a sterile environment using an ultraviolet (UV) bench-top hood to reduce the risk of the PCR reagents and reaction tubes being exposed to microorganisms present in the immediate environment. UV germicidal irradiation was also performed by exposing the PCR workspace, pipettes, molecular biology grade water, PCR tubes, and PCR master mix to short-wavelength UV for 30 minutes prior to use.

In addition to maintaining sterile conditions and using UV germicidal irradiation, negative controls were utilised at every experimental procedure to monitor microbial contamination. This involved using UV-treated molecular grade biology water in replacement of human plasma, murine faeces, and murine BAL samples during DNA extraction using the QIAamp UCP mini pathogen kit (*Qiagen*), and in replacement of human and murine blood samples (plasma and serum) during the first PCR stage of the nested PCR protocol using the Phusion blood direct kit (*Thermo Fisher Scientific*). Once generated, the experimental negative control underwent all the downstream applications that the human and murine samples underwent. This included DNA purification using the MinElute purification protocol and bead-based purification, PCR, agarose gel electrophoresis,

amplicon purification and quantification, library preparation, and sequencing of the 16S rRNA reads.

## 2.2. Visualisation of PCR Products using Gel Electrophoresis

Analysis of the size and quantity of PCR product generated from end-point PCR amplification was assessed using agarose gel electrophoresis. This involved preparing a 1X Tris-acetate Ethylenediaminetetraacetic acid (EDTA) (TAE) buffer (40mM Tris, 20mM acetic acid, 1mM EDTA) from 50X TAE buffer by mixing 90ml of 50X TAE electrophoresis buffer (*Thermo Fisher Scientific*) with 410ml of distilled H<sub>2</sub>O (dH<sub>2</sub>O). A 2% agarose gel was then prepared by dissolving two 0.5g TopVision agarose tablets (*Thermo Fisher Scientific*) in 50ml of 1X TAE buffer. Once the tablets were fully dissolved in the buffer the agarose-buffer mixture was poured into the gel electrophoresis mould and the gel was left to set at room temperature for 20 minutes.

Once the 2% agarose gel was fully set it was loaded into a gel electrophoresis tank containing the appropriate amount of 1X TAE buffer. 5µl of PCR products generated from Phusion blood direct PCR and Accuprime *Pfx* SuperMix PCR were then mixed with 1µl of purple 6x Gel loading dye (*New England Biolabs*). PCR products generated using the GoTaq Green master mix did not undergo the loading dye preparation step as the PCR reaction mixture contained a reaction buffer that increased sample density and provided both yellow and blue loading dyes. 6µl of each PCR product was then loaded into the gel along with 6µl of a 100 base pair (bp) DNA ladder (*New England BioLabs*), and the gel was run for approximately 1 hour at 85V using a Pharmacia LKB Multidrive XL power supply (*A N Pharmacia Laboratories Pvt Ltd*). The gel was post-stained in an ethidium bromide solution containing 60µl ethidium bromide (*VWR Life Science*) and 300ml 1X TAE buffer for 20

minutes. Excess staining solution was washed off using distilled water (dH<sub>2</sub>O) and the stained gel was viewed under UV light.

### 2.3. Amplicon Purification

Extracted and amplified microbial DNA was purified using either the MinElute Protocol or the AMPure XP PCR purification protocol. The MinElute protocol was applied following DNA extraction from the murine faecal and BAL samples, and after the first stage of end-point PCR during the nested PCR protocol. AMPure XP PCR purification was applied after the second stage of end-point PCR during the nested PCR protocol. The protocol was used to remove any DNA products below the predicted amplicon size, purify the DNA samples by removing any unused PCR reagents, and to concentrate the 16S rRNA amplicons by using a low elution buffer volume.

DNA purification was also performed on the experimental negative controls in order to concentrate and purify any microbial DNA amplified from the negative control as a result of microbial contamination. This step was essential as it enabled successful sequencing of contaminating microbial DNA introduced during the DNA extraction and amplification steps. The generated sequencing data was then used to determine the level of contaminating microbial DNA that was likely introduced during the DNA extraction and amplification steps, and to identify any bacterial taxa that were likely detected as a result of contaminating microbial DNA.

### 2.3.1. MinElute DNA Purification Protocol

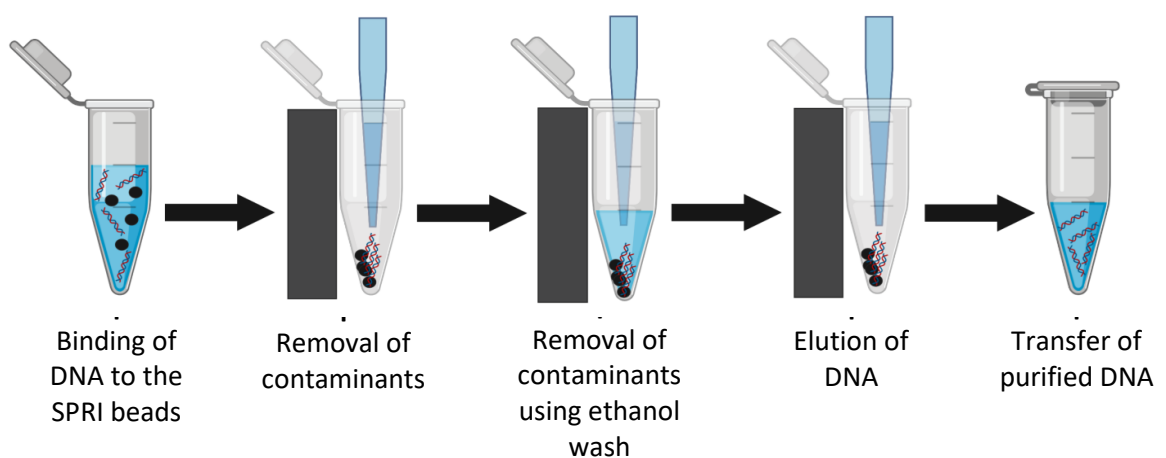
Buffer PB was mixed with the PCR product at a 5:1 ratio, to enable binding of the double stranded PCR products to the MinElute membrane and removal of unused oligonucleotide primer. The PCR-PB mixture was mixed thoroughly by vortexing and then transferred to a sterile MinElute column and centrifuged for 1 minute at 13,000xg. The flow-through was discarded and the MinElute column was washed with buffer PE (750µl) and centrifuged for 1 minute at 13,000xg to remove unused oligonucleotide primers and impurities (such as salts, unused polymerase, unincorporated nucleotides). The flow-through was discarded and the washing procedure was repeated twice more to ensure residual ethanol from the PE buffer was completely removed from the tubes. Following removal of flow-through from the third wash the columns were centrifuged at 13,000xg for 1 minute. The columns were then transferred to sterile 1.5ml Eppendorf tubes and 10µl of elution buffer (10mM Tris.Cl, pH 8.5) was applied to the centre of the column membrane. The columns were left to stand at room temperature for 1 minute and then centrifuged for 1 minute at 13,000xg to enable elution of the microbial DNA. The eluted DNA (approximately 8-9µl) was then placed in storage at -20°C.

### 2.3.2. AMPure XP PCR Purification Protocol

During the AMPure XP PCR purification protocol, the PCR amplicons were purified using solid-phase reversible immobilisation (SPRI) paramagnetic beads, and non-specific PCR products (such as primer dimers) were removed using left-side size selection (Figure 2.1).

The PCR product was mixed with SPRI beads at a 0.8X ratio (i.e. for 15µl of PCR product used, 12µl of SPRI beads) to remove DNA fragments less than 200bp long. The PCR-SPRI

reaction mixture was thoroughly mixed by pipetting 10 times and then incubated at room temperature for 1 minute. The reaction tubes were then placed on a magnetic stand and the beads were allowed to settle to the magnet. Once the beads had fully settled to the magnet the supernatant was carefully removed so as not to disturb the bead pellet. With the reaction tubes still attached to the magnetic stand, ethanol (180µl, 85% non-denatured ethanol) was added to the reaction tubes, and the reaction tubes were incubated at room temperature for 30 seconds to remove impurities. The ethanol supernatant was then carefully removed, and the reaction tubes were removed from the magnetic stand. 20µl of UV-treated molecular biology grade water was then added to the reaction tubes and mixed with the beads by pipetting 10 times to resuspend the beads. The reaction tubes were incubated at room temperature for 1 minute to elute the purified PCR amplicons from the SPRI beads. Following the final incubation step the reaction tubes were placed on the magnetic stand and the SPRI beads were allowed to settle against the magnet. The supernatant containing the eluted amplicons was transferred to sterile 1.5ml Eppendorf tubes, and then placed in storage at -20°C.



**Figure 2.1: Schematic diagram of the AMPure XP PCR purification protocol**



## 2.4. Analysis of the Microbiome

### 2.4.1. Assignment of Sequenced Reads to Bacterial Operational Taxonomic Units

To analyse the sequenced V4 16S rRNA data, Quantitative Insights Into Microbial Ecology (QIIME) software was applied using the *Nephele* 2.0 online platform [public web access: <https://nephele.niaid.nih.gov/#cloud>].

Low-quality V4 reads (defined as having a Phred quality score less than 19.0) and chimeric sequences were removed from the Ion Torrent sequencing data using the *Nephele* 2.0 QIIME 16S FASTQ single-end open reference pipeline (*Nephele* 2.0 software, Public web access: <https://nephele.niaid.nih.gov/#cloud>). The high-quality reads were then clustered in operational taxonomic units (OTUs) at a 99% similarity threshold using an open reference OTU picking strategy. This involved first running an initial closed-reference step, whereby the high-quality reads were clustered against the Silva 16S rRNA reference database (SILVA 99 v132) <sup>389,390</sup>. Sequences that failed to be assigned to an OTU using the Silva reference database were then clustered as *de novo* OTU on the basis of pairwise similarity among all V4 sequences present in the dataset <sup>390</sup>. The procedure was repeated for the V4 reads generated from Illumina sequencing using the *Nephele* 2.0 QIIME 16S FASTQ paired-end open reference pipeline [Public web access: <https://nephele.niaid.nih.gov/#cloud>].

The *Nephele* 2.0 open reference pipelines were also used to assign the bacterial OTUs to bacterial taxa, to determine the metagenomic functional content of the detected microbiota using Phylogenetic Investigation of Communities by Reconstruction of Unobserved States (PICRUSt), and to perform the appropriate statistical analysis as described below

#### 2.4.2. Generation of a Rarefaction Curve

Rarefaction curves were generated for each of the samples that underwent 16S rRNA sequencing in order to demonstrate the species richness of bacterial OTUs sequenced from the sample<sup>391,392</sup>. Rarefaction was used in order to correct for OTU diversity bias due to unequal sample sequencing depths (differences in read numbers generated from the samples) by standardising the number of OTUs expected in the sample if the sample had the same number of reads as the sample with the smallest number of reads<sup>391,392</sup>. Generation of rarefaction curves was performed using *R* software (see Supplementary Materials S1 for the R code used) and involved repeated random sub-sampling of the complete set of OTU reads and calculation of mean diversity.

#### 2.4.3. Comparison of Species Richness

The overall species richness was determined by measuring the total number of observed OTUs detected in the samples using *Nephele* 2.0 QIIME 16S FASTQ paired-end open reference pipeline [Public web access: <https://nephele.niaid.nih.gov/#cloud>].

The appropriate statistical tests were then performed using *R* software (see Supplementary Materials S2 for R codes used) to determine if there was a statistically significant difference in species richness in the atopic samples compared to the non-atopic samples.

#### 2.4.4. Assignment of the Bacterial Operational Taxonomic Units to Bacterial Taxa

The bacterial OTUs were assigned to bacterial taxa using the *Nephele* 2.0 open reference pipelines (single-end for the Ion torrent sequencing data, paired-end for the Illumina sequencing data). *R* software was then utilised to measure relative abundance of the

detected bacterial taxa (see Supplementary Materials S3 for R codes used), and highly abundant taxa (taxa with a total relative abundance  $\geq 1.0\%$ ) were plotted as a relative abundance bar graph using *R* software (see Supplementary Materials S3 for R code used).

#### 2.4.5. Comparison of Alpha Diversity in the Microbiome of Atopic and Non-Atopic Control Subjects

The *Nephele* 2.0 QIIME 16S FASTQ paired-end open reference pipeline was used to generate Shannon and Chao1 diversity indices from the 16S rRNA sequencing data [public web access: <https://nephele.niaid.nih.gov/#cloud>]. The diversity index scores were uploaded onto *R* and *R* software was used to generate alpha diversity boxplots and perform statistical analysis (See Supplementary materials S4 and S2 respectively for R codes used). With regards to statistical analysis, the Shapiro-Wilk test was performed first to determine if the alpha diversity dataset displayed gaussian distribution. If the dataset did not display gaussian distribution ( $P$  value  $< 0.05$ ) a Wilcoxon rank sum test was performed to determine if the sample groups differed significantly with regards to alpha diversity. If the samples were found to exhibit a gaussian distribution ( $P$  value  $> 0.05$ ) an F test was performed to determine if variances in the two sample groups was equal. If the two sample groups were found to have equal variance ( $P$  value  $> 0.05$ ) an Unpaired T test was performed. If the two samples were found to have significantly different variance ( $P$  value  $< 0.05$ ) a Welch's two sample T test was carried out

#### 2.4.6. Comparison of Beta Diversity in the Microbiome of Atopic and Non-Atopic Control Subjects

Comparison of the bacterial OTU profiles between pairs of individual samples was carried out by measuring beta diversity of the detected bacterial communities. This involved uploading the OTU table generated from the *Nephele* 2.0 QIIME 16S FASTQ paired-end open reference pipeline [Public web access: <https://nephele.niaid.nih.gov/#cloud>] onto *R* and calculating Bray-Curtis dissimilarity using the *Vegan R* package (See Supplementary Materials S9 for R codes used). The Bray-Curtis dissimilarity scores were then plotted using Principal coordinate analysis (PCoA) and the *ggplots R* package (See Supplementary Materials S5 for R codes used).

#### 2.4.7. Metagenomic Functional Analysis

To determine metagenomic functional analysis of the detected microbiota the *Nephele* 2.0 QIIME 16S FASTQ paired-end pipeline was utilised to generate OTU tables from the Illumina V4 16S rRNA sequencing using a closed reference OTU picking strategy and the GreenGenes 99 database.

PICRUSt software was then used to predict functional composition of the metagenome (the genetic material present in the samples, in this incidence the microbial 16S rRNA reads) using the OTU tables.

PICRUSt analysis was performed using the online *Galaxy* version of PICRUSt developed by the Langille lab [Public web access: <http://galaxy.morganlangille.com/>]. The closed reference OTU tables generated using the GreenGene 99 reference genome database were uploaded onto *Galaxy* and first underwent normalisation by dividing the abundance of each

detected OTU by its predicted 16S copy number<sup>393</sup>. This was performed to account for 16S rRNA copy numbers varying greatly amongst the different known bacterial genomes<sup>393</sup>.

Gene family abundances were calculated for each bacterial taxon present in the GreenGene 99 annotated reference genome database. The normalised OTU abundances were then multiplied by the generated family abundances to determine the total gene family abundance present in each sample<sup>393</sup>. The predicted gene family counts were then used to measure abundance of Kyoto Encyclopaedia of Genes and Genomes (KEGG) pathways in the sample meta-genomes, thus enabling microbial activity of the detected microbiota to be inferred.

## 2.5. Statistical Analysis

Comparison of the atopic subjects compared to the non-atopic subjects was achieved using a variety of statistical analysis tests. With regards to total RNA counts (mRNA, miRNA, V4 16S rRNA reads), protein levels (absorbance values, ng/ml, EU/ml), OTU counts, and alpha diversity index scores (Shannon, Chao1), a Shapiro-Wilk test was performed to determine whether the dataset exhibited a gaussian distribution. If the dataset did not display gaussian distribution ( $P$  value  $< 0.05$ ) a Wilcoxon rank sum test was performed. For datasets that did exhibit a gaussian distribution ( $P$  value  $> 0.05$ ) an F test was performed to determine if variances in the two sample groups was equal. If the two sample groups were found to have equal variance ( $P$  value  $> 0.05$ ) an Unpaired T test was performed. If the two sample groups were found to have significantly different variance ( $P$  value  $< 0.05$ ) a Welch's two sample T test was carried out (See Supplementary Materials S2).

PERMANOVA analysis based on 999 permutations was also performed to determine if there was a significant association between atopic state and beta diversity of the bacterial

communities detected. This involved using the *Adonis* *R* function and the *Vegan* *R* package (See Supplementary Materials S5 for R codes used).

To determine statistically significant differences in bacterial taxa and predicted microbiome function, linear discriminant analysis effect size (LEfSe) analysis was applied to the relative abundance tables generated from *R* software. This involved uploading the relative abundance tables to the online *Galaxy* workflow framework developed by the Huttenhower group<sup>394</sup> [public web access: <http://huttenhower.sph.harvard.edu/galaxy/>]. The default settings were applied (the  $\alpha$  value for the factorial Kruskal-Wallis sum-rank test was 0.05 and the threshold value used on the logarithmic discriminate analysis score for discriminate features was 2.0) and analysis involved the following steps .

The non-parametric factorial Kruskal-Wallis sum-rank test was applied to the relative abundance data in order to detect features with significant differential abundance in the two sample groups. A set of pairwise tests among subclasses using the unpaired Wilcoxon rank-sum test were then carried out to assess whether the detected differences in relative abundance were consistent with respect to biological behaviour. Linear discriminant analysis (LDA) was then performed to predict the effect of each differentially abundant bacterial taxa identified. The KEGG pathway abundance scores were then converted into abundance percentages and LEfSe analysis using the default settings was applied to determine differential microbial activity in the atopic state compared to the non-atopic control state.

## Chapter 3: Characterisation of Atopic Asthma at the Molecular level

### 3.1. Introduction

The complex nature of asthma pathogenesis and presentation has resulted in the disease being separated into a number of phenotypes, which are then further sub-divided into several endotypes<sup>20,22–25</sup>. The asthma phenotypes and endotypes differ with regards to disease presentation in terms of cause, development, severity, and response to medication.

Diagnostic tools for identifying the various asthma phenotypes and endotypes currently rely on bronchoalveolar lavage and bronchoscopy with bronchial biopsy as the optimum method for assessing airway inflammation and remodelling<sup>102</sup>. The invasiveness of these techniques limits their usefulness in daily clinical practice and makes them unsuitable in diagnosing young children<sup>102</sup>.

These limitations alongside an incomplete knowledge of the pathogenetic mechanisms behind the different asthma phenotypes/ endotypes has restricted development and access to optimal asthma treatment protocols.

Biomarkers have been proposed as a means of performing risk assessment before clinical diagnosis, to determine the disease stage and severity following diagnosis, and as a means of monitoring responsiveness to treatment<sup>112</sup>.

In asthma, there are increasing numbers of potential biomarkers being identified in various clinical samples, including BAL fluid, sputum, exhaled air, saliva, urine, and peripheral blood. The majority of studies have focussed on identifying biomarkers from clinical samples taken from the airways (sputum, BAL fluid, lung tissue). However, collection of these samples is invasive and not suitable for daily clinical activity. This had led to an

increasing interest in the identification of biomarkers from more accessible samples, such as blood and urine.

The identification of peripheral blood biomarkers is of particular interest. In asthma the inflamed airway tissue releases chemoattractants and cytokines into the bloodstream in order to recruit activated immune cells from the peripheral blood vessels. Analysis of the blood, therefore, can be used as an indirect indicator of disease state by assessing the dynamic process of immune cells entering and leaving the circulatory system <sup>114</sup>.

### 3.1.1. Aims of the Chapter

The focus of this investigation was to analyse blood samples from a small, but well-defined cohort of female subjects with poorly controlled atopic asthma associated with a HDM allergy, in order to identify potential biomarkers present in the blood.

This was achieved by performing a comprehensive molecular characterisation of circulating mRNA, miRNA and protein-based biomarkers of the immune response, using a range of molecular tools.

Circulating mRNA and miRNA were sequenced and quantified, and differential expression analysis was performed on the two RNA populations to determine how gene expression and regulation varied in the asthmatic subjects compared to the non-asthmatic control subjects. Additionally a number of inflammatory proteins (IL-4, IL-5, IL-10, IL-13, IL-17A, eotaxin, GM-CSF, IFN $\gamma$ , MCP-1, RANTES, TARC, TNF $\alpha$ , total IgE, and endotoxin) were quantified to determine whether the protein profiles differed significantly in the asthmatic subjects compared to the control subjects.



## 3.2. Methods

### 3.2.1. Sample Collection

Female atopic asthmatic individuals (n = 5) with physician diagnosed HDM allergy were recruited to the study through *Sera Laboratories Limited*. The asthma subjects were from Florida, US, and were selected on the basis that they had developed atopic asthma during early childhood and that their condition had persisted into adulthood and remained “poorly controlled”. A full list of recruitment criteria is presented in (Table 3.1). An additional five non-asthmatic healthy subjects that were age and gender matched to the asthmatic subjects were recruited as control subjects.

Whole blood was drawn, following alcohol cleansing of the skin surface, into EDTA containing tubes and stored on ice prior to centrifugation at 1000×g to obtain the plasma component. All samples were analysed anonymously and written informed consent to utilise the samples for the research was obtained.

The Independent Investigational Review Board Inc. ethically approved sample collection by *Sera Laboratories Limited* from human donors giving informed written consent. Furthermore, ethical approval from Keele University Ethical Review Panel 3 for the study was obtained. All methods were performed in accordance with relevant guidelines and regulations.

**Table 3. 1: A full list of the donor population characteristics required for the human atopic asthma study**

<b>Patient Criteria</b>
• Have a BMI < 30
• Be a non-smoker
• Diagnosed with atopic asthma during childhood
• Have severe/ poorly controlled asthma
• Must not be on any oral steroid treatment
• Allergic to house dust mite

### 3.2.2. Asthma Control Questionnaire

Following sample collection, the asthmatic subjects were asked to complete an Asthma Control Questionnaire (ACQ). The ACQ is a standardised asthma control questionnaire devised by Juniper and colleagues (1999) to determine how well controlled the asthmatics condition was at the time of sample collection<sup>395</sup>. The questionnaire involves six questions that are designed to assess how well-controlled the disease is by assessing the asthmatic subject's quality of life (i.e. how the disease affected the subjects sleep patterns and ability to carry out everyday activities), how often the subject experiences respiratory symptoms (i.e. shortness of breath, wheezing), and how often the subject uses short-acting bronchodilator's during the course of the week. A copy of the ACQ can be located in the Supplementary Materials (Supplementary materials, Table S1).

For each question the asthmatic subjects were requested to give a score between 0 – 6, and subjects that scored a total value greater than 10.0 were classified as having poorly controlled asthma<sup>396</sup> and were deemed suitable for the study.

### 3.2.3. Total RNA Extraction, Library Preparation, and Next Generation Sequencing

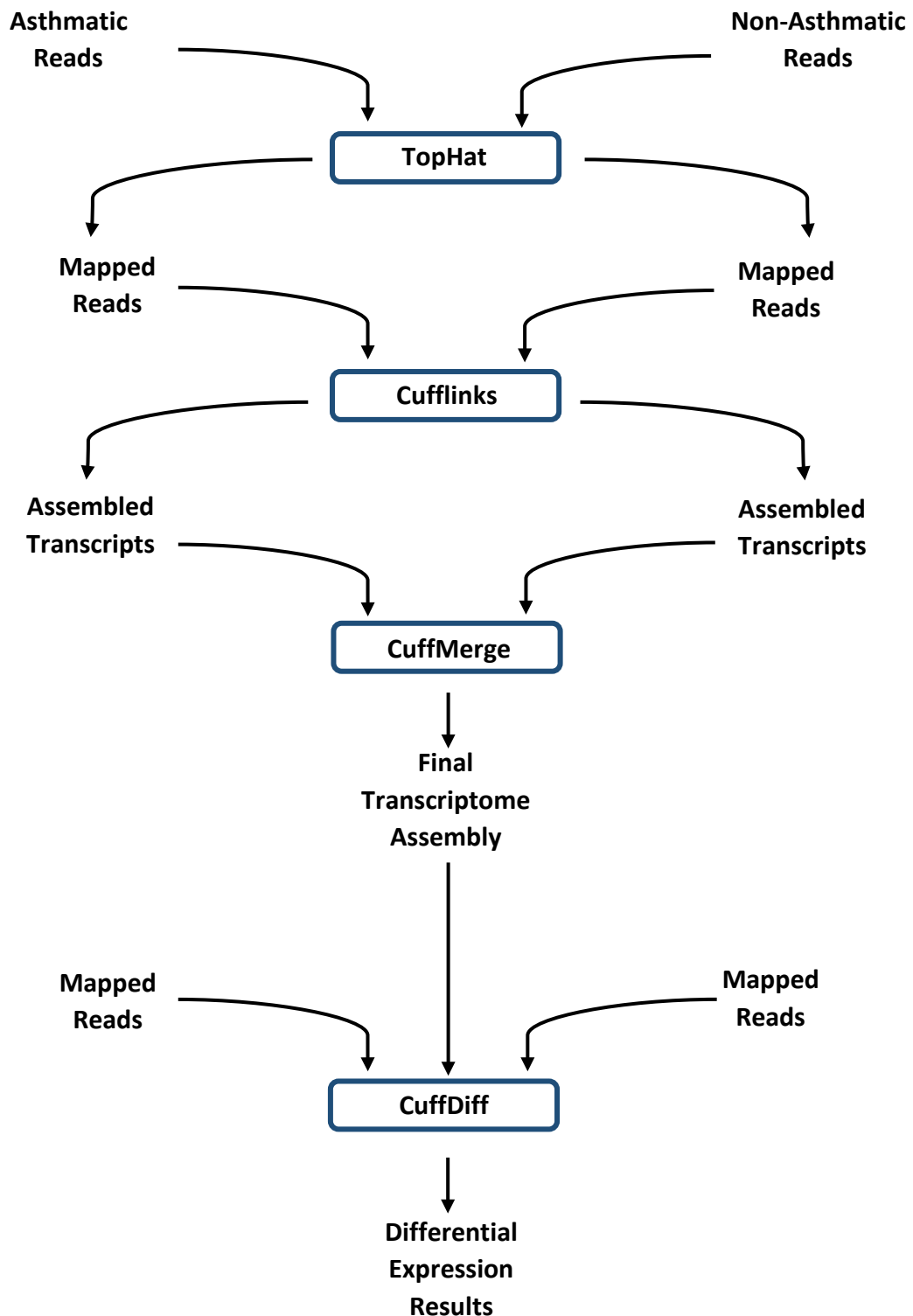
1.5ml of the human plasma samples were submitted to the *Beijing Genomics Institute* where the samples underwent total RNA extraction and sequencing. The following steps were performed by the *Beijing Genomics Institute*; total RNA was extracted from 500µl of human plasma using a miRNeasy Serum/ Plasma kit (*Qiagen*). The quantity and quality of the RNA extracts was determined using the QuBit fluorimeter (*Invitrogen*) and BioAnalyzer (*Agilent*). mRNA sequencing libraries were generated from the human plasma samples using the SMARTer Universal Low Input RNA kit (*Takara Bio*). The libraries were then sequenced using Illumina HiSeq 2000 with a paired-end 90 nucleotide read metric. miRNA sequencing libraries were prepared using the TruSeq small RNA library kit (*Illumina*), and sequencing was performed using the Illumina HiSeq 2000 platform.

### 3.2.4. Alignment of mRNA to the Human Genome and Differential Expression Analysis

The mRNA FASTQ files were analysed using the online data analysis platform *Galaxy* [public web access: <http://usegalaxy.org>]. The FASTQ files were uploaded onto *Galaxy* and the FASTQ Groomer package was applied to convert the data to the Sanger encoding format (Sanger and Illumina 1.8). A quality control step was then performed using FastQC to confirm the sequencing data from each plasma sample was of sufficient quality to allow for valid analysis of mRNA present in the samples.

Trimming was then performed on the sequencing data to remove the sequencing adapters and low-quality reads using the Trim Galore package. Reads with a Phred-like quality score greater than 30 were retained for further downstream analysis.

The Tuxedo protocol <sup>397</sup> was applied to the trimmed reads to map the reads to the Human Genome build hg19 reference genome, to assemble and quantify individual transcripts, and to conduct statistical analysis to determine differential gene expression between the control and asthma samples at the time point at which the sample was taken (Figure 3.1).



**Figure 3.1: Identification significant differential gene expression in the asthmatic subjects compared to non-asthmatic subjects using the *Galaxy Tuxedo Protocol*.** Sequenced RNA data generated from plasma samples from asthmatic subjects (n = 5) and non-asthmatic control subjects (n = 5) was uploaded onto *Galaxy*. Following adaptor trimming and quality control assessment, the Tuxedo protocol was performed to determine the presence of significant differential gene expression (as determined by a *Q* value < 0.05, and a log fold change > 2.0) in the asthmatic subjects compared to the control subjects. The RNA reads were first mapped to the human hg19 reference genome using TopHat. Cufflinks was then used to generate a transcriptome assembly from the alignment files generated by TopHat. The transcriptome assemblies were then merged together using the CuffMerge package, and gene expression levels and statistical significance was determined using the CuffDiff package.

[Adapted from Trapnell *et al.*, 2012<sup>397</sup>]

Highly expressed genes, as determined by a mean LOG2 Fragments Per Kilobase of transcript per Million mapped (FPKM) score  $\geq 7.0$ , were then plotted as a heatmap using *R* software (See Supplementary Materials S6 for *R* codes used). Similarity of gene expression profiles was determined using Euclidean distance (See Supplementary Materials S6 for *R* codes used), PCA, and PERMANOVA (See Supplementary Materials S5 for *R* codes used).

### 3.2.5. Alignment of miRNA to the Human Genome and Differential Expression Analysis

The *sRNAtoolbox*<sup>398</sup> was utilised to map the sequenced miRNA reads to the miRbase Version 21; a public repository of miRNA hairpin precursor (mir's) and mature miRNA (miR's) sequences and annotations<sup>399</sup> [public web access: <http://mirbase.org/>]. Following assignment of the miRNA reads to known human miRNA sequences, differential miRNA expression analysis was performed using edgeR for *R*<sup>400</sup>.

Total miRNA expression was then plotted as a heatmap using *R* software (See Supplementary Materials S6 for *R* codes used). Similarity of sample miRNA expression

profiles was determined using Euclidean distance cluster analysis (See Supplementary Materials S6 for R codes used), PCA, and PERMANOVA (See Supplementary Materials S5 for R codes used).

### 3.2.6. RNA Functional Analysis

Following identification of differential mRNA and miRNA levels in the plasma samples from the asthmatic subjects compared to the control subjects, RNA functional analysis was performed. This involved using a number of software programmes to determine the biological significance of altered mRNA and miRNA expression in the asthmatic subjects. This included determining which upstream regulators are likely responsible for the observed changes in gene expression in the asthmatic subjects, which downstream pathways are likely to be affected by changes in gene expression, which genes are likely to be effected by changes in miRNA expression, and which biological functions are likely to be affected by changes in mRNA and miRNA expression.

### 3.2.7. Analysis of the Biological Significance of Differentially Expressed Genes in the Asthmatic Population

The likely impact of individual differentially expressed genes on asthma pathogenesis was analysed by comparing the differentially expressed genes to a recently released database of genes associated with asthma pathology (AllerGAtlas, 2018 <sup>401</sup>)[public web access: <http://biokb.ncpsb.org/AlleRGAtlas/>]. A literature search was then utilised to determine the effects of the identified genes on asthma pathology and immune function.

### 3.2.8. Analysis of the Biological Significance of Differentially Expressed miRNA in the Asthmatic Population

Functional analysis was performed on the differentially expressed miRNA using the online software suite DIANA-miRPath v3.0<sup>402</sup> to determine the key regulatory roles of the differentially expressed miRNA [public web access: <http://snf-515788.vm.oceanos.grnet.gr/>]. Biological pathways likely to be affected by the altered miRNA levels were then identified using *in silico* predicted targets from TargetScan v6.2, a prediction tool that utilises miRNA seed sequences to determine target genes of the miRNA.

### 3.2.9. Analysis of the Combined Effect of Differentially Expressed mRNA and miRNA in the Asthmatic Population

The combined effects of differential gene and miRNA expression on known biological processes was explored using Ingenuity Pathway analysis (IPA) software<sup>403</sup>. Causal inference analysis was applied to determine upstream regulator activity that may explain the pattern of differential expression observed in the asthmatic subjects. This involved the generation of an enrichment score (Fisher's exact test *P* value) and a *Z* score to determine the possible upstream biological causes of the differential gene expression<sup>403</sup>. The enrichment score measured the overlap of observed and predicted regulated gene sets, whilst the *Z* score assessed the match of observed and predicted up/ downstream patterns<sup>403</sup>. Putative regulators that scored an overlap *P* value < 0.05 were deemed statistically significant, and the *Z* scores were used to determine the activity of the putative regulators (an upstream regulator with a *Z* score greater than 2.0 was considered activated in the asthmatic subjects, whilst an upstream regulator with a *Z* score less than -2.0 was considered deactivated).

Causal inference analysis was also used to predict the downstream effects of the differentially expressed genes and miRNA could have on biological processes and functions in the asthmatic subjects.

### 3.2.10. Qualitative Analysis of Circulatory Inflammatory Protein Levels

Plasma levels of interleukin IL-4, IL-5, IL-10, IL-13, IL-17A, IFN $\gamma$ , TARC, Eotaxin, GM-CSF, MCP-1, RANTES, and TNF $\alpha$ , was determined using two qualitative enzyme-linked immunosorbent assays (ELISA) custom designed for this study. Two multi-analyte sandwich ELISAs (*Qiagen*) were used, and analysis of the inflammatory proteins was achieved using the recommended Multi-Analyte ELISArray kit protocol (*Qiagen*). Statistical analysis was performed by carrying out a Shapiro-Wilk normality test and a Wilcoxon rank sum test using *R* software Version 3.5.0.

The layout of each plate is shown in the Supplementary materials (Supplementary materials, Figure S1).

### 3.2.11. Quantitative Analysis of Circulatory Total IgE Concentrations

The concentration of total IgE was determined using sandwich ELISA (*Genesis Diagnostics Ltd*). The ELISA was performed in duplicate using the recommended protocol, and absorbance was measured at 450nm using an ELX800 absorbance reader (*BioTek*). The absorbance scores were log<sub>10</sub> transformed and the standard curve was interpolated using the Sigmoidal 4PL (4 parameter logistic) curve to determine total IgE concentration in International units per millilitre (IU/ml) using GraphPad Prism. Total IgE concentration in IU/ml in the plasma samples was determined using the standard curve and the values were



multiplied by 5 to account for the 1:5 dilution factor used. The IU/ml values were then converted into nano gram per ml (ng/ ml) values by multiplying each IU/ml value by 2.4. Statistical analysis was then performed using a Shapiro-Wilk normality test and an Unpaired T test using *R* software Version 3.5.0.

### 3.2.12. Quantitative Analysis of Circulatory Endotoxin Concentrations

Circulating bacterial endotoxin concentration was measured using a Pierce™ Limulus Amebocyte Lysate (LAL) Chromogenic Endotoxin quantitative kit (*Thermo Fisher Scientific*). The assay was performed in triplicate using the recommended protocol, and absorbance was measured at 450nm using an ELX800 Absorbance reader (*BioTek*). The absorbance scores were log<sub>10</sub> transformed and the standard curve was interpolated using the Sigmoidal 4PL (4 parameter logistic) curve to determine endotoxin concentration in endotoxin units per millilitre (EU/ml) using GraphPad Prism. Endotoxin concentration in EU/ml in the plasma samples was determined using the standard curve and the values were multiplied by 50 to account for the 1:50 dilution factor used. Statistical analysis was performed by carrying out a Shapiro-Wilk normality test and an unpaired T test using *R* software Version 3.5.0.

### 3.3. Results

#### 3.3.1. Characterisation of the Atopic Asthmatic Subjects

Five female asthmatic subjects were recruited in accordance with the inclusion criteria detailed in Table 3.1. The mean age of the asthmatic subjects was  $39.6 \pm 11.7$  years, and all had been clinically diagnosed with a HDM allergy and atopic asthma during early childhood (mean age of asthma onset =  $6.2 \pm 3.2$  years) (Table 3.2)(See also Supplementary Materials Table S2). At the time of sample collection, the asthmatic subjects were on prophylactic therapy to minimise the occurrence of disease symptoms (Table 3.2). These treatments included one or more bronchodilator medication (Dulera, Albuterol, Symbicort), that were prescribed to all asthmatic subjects, and one or more anti-inflammatory drugs (Qvar, Zyrtec,), that were prescribed to two of the asthmatic subjects (Table 3.2)(See also Supplementary Materials Table S2).

Asthma severity was determined using the internationally recognised ACQ questionnaire<sup>395,404</sup>, and all five asthmatic subjects scored a total  $\geq 10.0$  (mean total score =  $10.8 \pm 0.75$ ) (Table 3.2, see also Supplemental Materials Table S3 for greater detail). Additionally, three of the asthmatic subjects were clinically diagnosed with other atopic diseases, including allergic rhinitis, allergic dermatitis, and nasal polyps (Table 3.2). Overall, however, the individuals were regarded as healthy, as defined by a BMI below 30, and were non (never) smokers (Table 3.3).

Five non-asthmatic females with a mean BMI of  $24.3 \pm 2.1$  were recruited to the study as healthy controls. The control subjects had never smoked and had a mean age of  $39.4 \pm 10.3$  years (Table 3.3). Two of the controls, Control\_2 and Control\_3, reported self-diagnosed

dermatitis, although neither had received diagnosis by a physician for this condition (Table 3.3).

**Table 3. 2: Asthma presentation and disease characterisation in the asthmatic cohort at the time of sample collection.** Five asthmatic subjects with HDM sensitisation and a clinical diagnosis of atopic asthma made during early childhood were recruited through *Sera Laboratories Limited*. At the time of sample collection, the asthmatic subjects completed an ACQ to determine asthma severity and control at the time of sample collection.

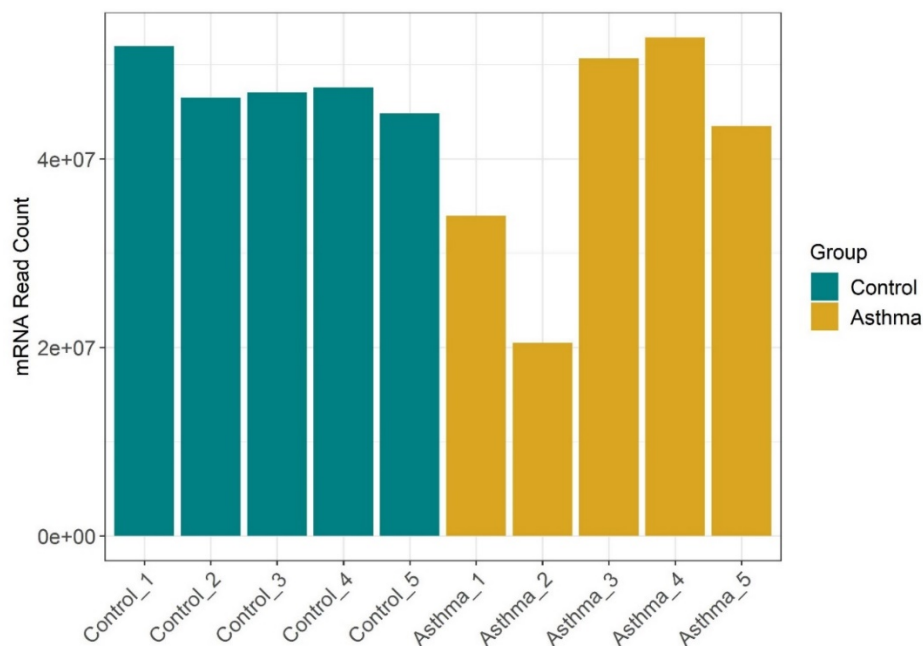
Patient	Diagnosis	Allergy	Age of Diagnosis (years)	ACQ Total score	Medications
Asthma_1	Atopic Asthma	Dust mite	7	12	Dulera, Albuterol
Asthma_2	Atopic Asthma	Dust mite	4	11	Dulera, Albuterol
Asthma_3	Atopic Asthma	Dust mite	12	11	Symbicort, Zyrtec, Albuterol
Asthma_4	Atopic Asthma	Dust mite	5	10	Albuterol, Qvar
Asthma_5	Atopic Asthma	Dust mite	3	10	Albuterol

**Table 3.3: Characterisation of the asthmatic and non-asthmatic subjects at the time of sample collection.** Five asthmatic subjects and five non-asthmatic control subjects were recruited from Florida, USA, through *Sera Laboratories Limited*. All subjects were female and classed as healthy (BMI < 30.0).

Sample	Age (years)	Sex	BMI (kg/m <sup>2</sup> )	Smoking History	Other chronic conditions
<b>Asthmatic subjects</b>					
Asthma_1	52	F	27.8	Never smoked	Allergic rhinitis, nasal polyps
Asthma_2	36	F	27.3	Never smoked	Allergic rhinitis, polycystic ovary
Asthma_3	42	F	23.3	Never smoked	None
Asthma_4	19	F	21.5	Never smoked	Allergic rhinitis, allergic dermatitis
Asthma_5	49	F	22.3	Never smoked	None
<b>Non-Asthmatic subjects</b>					
Control_1	49	F	26.4	Never smoked	None
Control_2	23	F	21	Never smoked	Allergic dermatitis
Control_3	44	F	26.4	Never smoked	Allergic dermatitis
Control_4	49	F	24.9	Never smoked	None
Control_5	32	F	22.7	Never smoked	None

### 3.3.2. mRNA detected in the Plasma Samples

A total of 439,448,931 high-quality mRNA reads were isolated and sequenced from the human plasma samples. This included 237,918,933 mRNA reads from the non-asthmatic control samples (average number of reads per sample = 47,583,786.60; range = 44,833,552 – 51,955,898) and 201,529,998 mRNA reads from the asthma samples (average number of reads per sample = 40,305,999.60; range = 20,495,443 – 52,900,114)(Figure 3.2). Statistical analysis of the read counts found that there was no significant difference in the number of mRNA reads detected in the asthmatic subjects compared to the control subjects ( $P$  value = 0.5476, *Wilcoxon rank sum test*).



**Figure 3.2: Total number of mRNA reads isolated and sequenced from the human plasma samples.** Total RNA was extracted from 500 $\mu$ l of human plasma from non-asthmatic control subjects (n = 5) and asthmatic subjects (n = 5) using the Qiagen serum and plasma miRNeasy kit. mRNA sequencing libraries were prepared using the SMARTer Universal Low Input RNA kit and sequenced using Illumina HiSeq 2000.

### 3.3.3. Differential Gene Expression detected in the Asthmatic Subjects compared to the Control Subjects

Expression of a total of 14,226 genes was detected through assessment of the circulating transcriptome. mRNA reads generated from Asthma\_2 failed to map satisfactorily to the hg19 reference genome and subsequently the sample was excluded from further mRNA downstream analysis due to concerns it would induce bias.

Statistical analysis revealed that 287 genes were differentially expressed in the asthmatic subjects compared to the control subjects (as defined by a  $Q \leq 0.05$  and a Log fold change  $> 2.0$ ). Within the asthmatic subjects, 90 genes showed significantly increased expression, and 197 genes displayed significantly decreased expression compared to the control subjects. Genes that displayed the highest degree of differential expression are listed in Table 3.4. A full list of the differentially expressed genes can be viewed in the Supplementary Materials (Supplementary Materials, Table S4).

**Table 3.4: A list of genes that displayed the highest degree of differential expression in the asthmatic subjects compared to the control subjects.** The Tuxedo protocol was used to determine differential gene expression in asthmatic subjects (n = 4) compared to control subjects (n = 5). A total of 287 genes were found to be differentially expressed in the asthmatic subjects compared to the control subjects. Genes with the highest degree of differential expression are shown below. Where genes are expressed in a condition-specific manner, Log2 fold change is replaced with “Control Only” or “Asthma Only” as appropriate. Quantity of the gene is shown as FPKM reads.

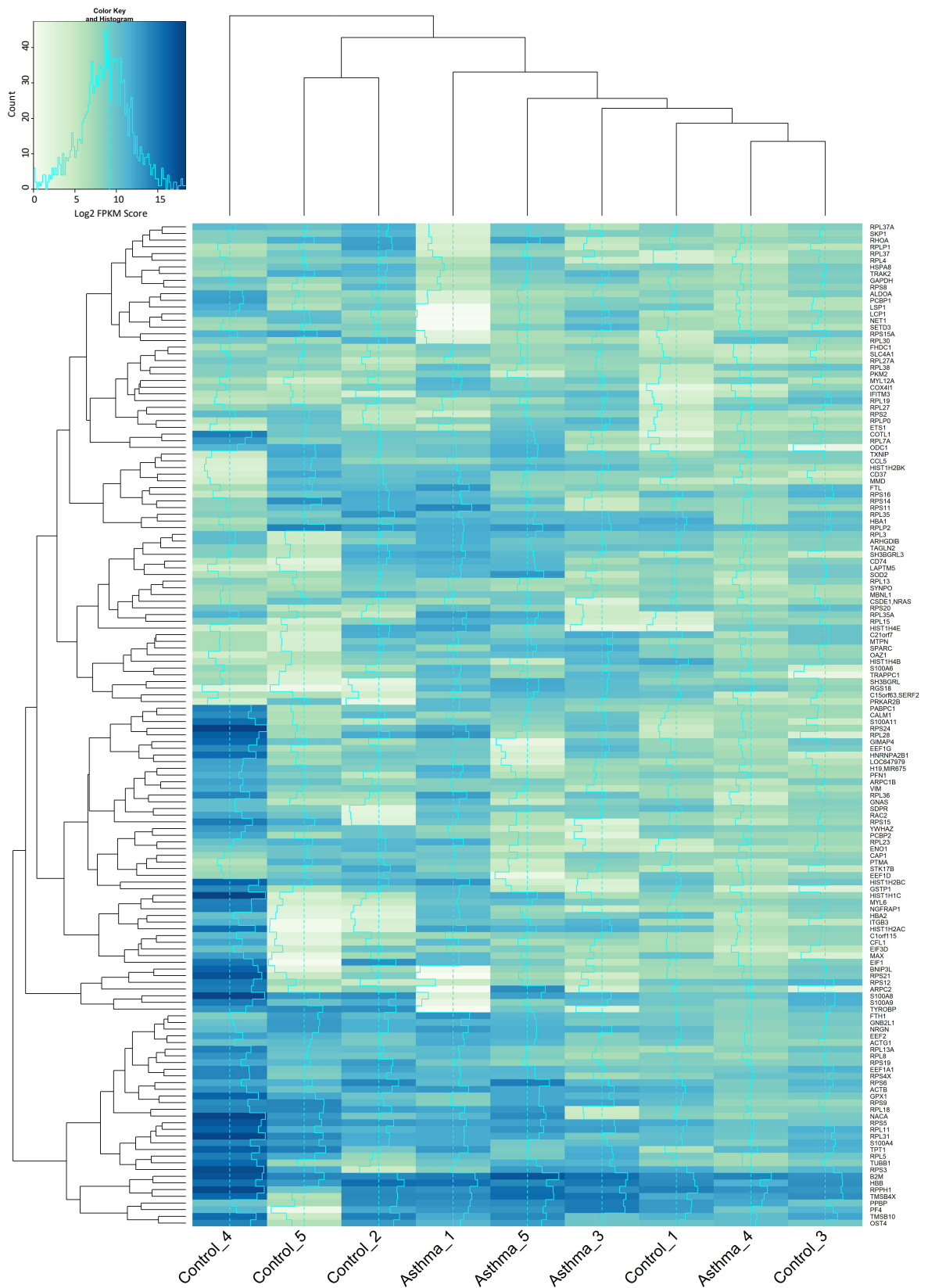
Gene	Control Mean	Asthma Mean	Fold Change (log2)	Q Value
<b>Downregulated Genes</b>				
DOHH	972.908	0.000	Control Only	0.0030
PTRH2	87.791	0.000	Control Only	0.0030
C15orf41	79.198	0.000	Control Only	0.0030
HIST1H3I	30.233	0.000	Control Only	0.0030
HOXC10	26.492	0.000	Control Only	0.0030
TSPYL5	18.952	0.000	Control Only	0.0030
NFXL1	17.842	0.000	Control Only	0.0030
RAB3IL1	15.123	0.000	Control Only	0.0030
LINC00085	15.023	0.000	Control Only	0.0030
ARV1	14.064	0.000	Control Only	0.0030
<b>Upregulated Genes</b>				
HIST1H3C	0.000	90.578	Asthma Only	0.0030
HDAC9	0.732	52.163	6.156	0.0052
PRAM1	0.000	3.057	Asthma Only	0.0052
PML	0.948	178.238	7.554	0.0072
RAB6B	0.000	8.903	Asthma Only	0.0072
NRP1	0.924	18.895	4.354	0.0108
CD93	0.000	14.337	Asthma Only	0.0108
GPR56	1.870	98.538	5.720	0.0126
MR1	1.076	17.892	4.055	0.0180
TOP1MT	0.345	59.034	7.421	0.0180

To determine whether the asthmatic subjects had a distinct gene expression profile compared to the control subjects, genes that displayed robust levels of expression (the top 150 most highly expressed genes as determined by a mean Log2 FPKM score  $\geq 7.0$ ) were

plotted as a heatmap and unsupervised cluster analysis was performed using Euclidean distance (Figure 3.3).

Cluster analysis revealed that Control\_4 had a relatively unique mRNA profile compared to the other subjects under investigation. For the remaining subjects, two clusters formed. Cluster one contained the control subjects Control\_5 and Control\_2; and Cluster two was made up of Asthma\_1, Asthma\_5, Asthma\_3, Control\_1, Asthma\_4, and Control\_3. Of note was Asthma\_4, whose RNA profile more closely resembled the control subjects than the asthmatic subjects in Cluster two.





**Figure 3. 3: Heatmap showing highly expressed genes in asthmatic subjects compared to control subjects.** Analysis was performed by sequencing mRNA isolated from plasma samples from asthmatic subjects (n = 4) and non-asthmatic control subjects (n = 5) , and mapping the sequenced mRNA reads the human hg19 genome reference using *Galaxy*.

Gene expression was determined by quantification of circulatory mRNA detected in the plasma samples and is expressed as log<sub>2</sub> normalised FPKM reads. Highly expressed genes (LOG<sub>2</sub> FPKM score  $\geq 7.0$ ) were plotted. Cluster analysis (Euclidean distance) informs the X and Y-axis dendrograms.

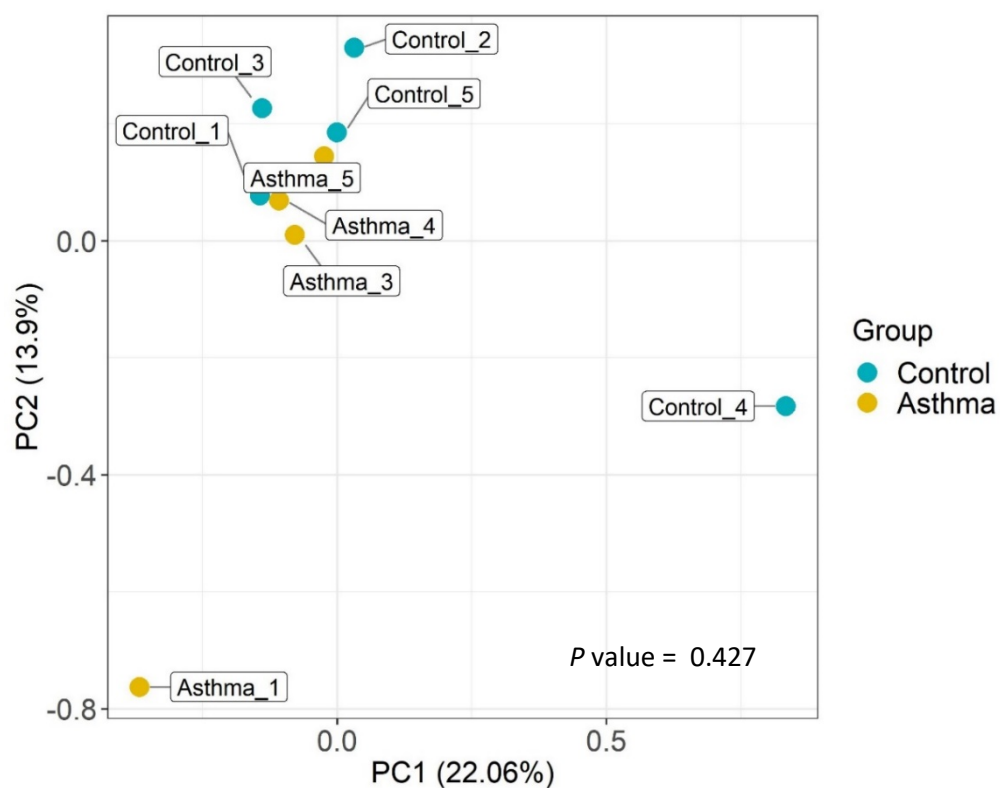
#### 3.3.4. Diversity of Gene Expression detected in the Asthmatic Subjects compared to the Control Subjects

The diversity of genes being expressed in the asthmatic subjects compared to the control subjects was assessed by performing PCA on the log<sub>2</sub> FPKM values of all 14,226 genes with detectable levels of expression (Figure 3.4). There was some degree of separation of the control and asthmatic subjects on the basis of PC2 scores. Of note was the observation that in the asthmatic subjects PC2 score was negatively correlated to asthma severity, Asthma\_1, for instance had the highest ACQ score and the lowest PC2 score, whereas Asthma\_5 and Asthma\_4 had the lowest ACQ scores and the highest PC2 scores that were most similar to the control subject PC2 scores.

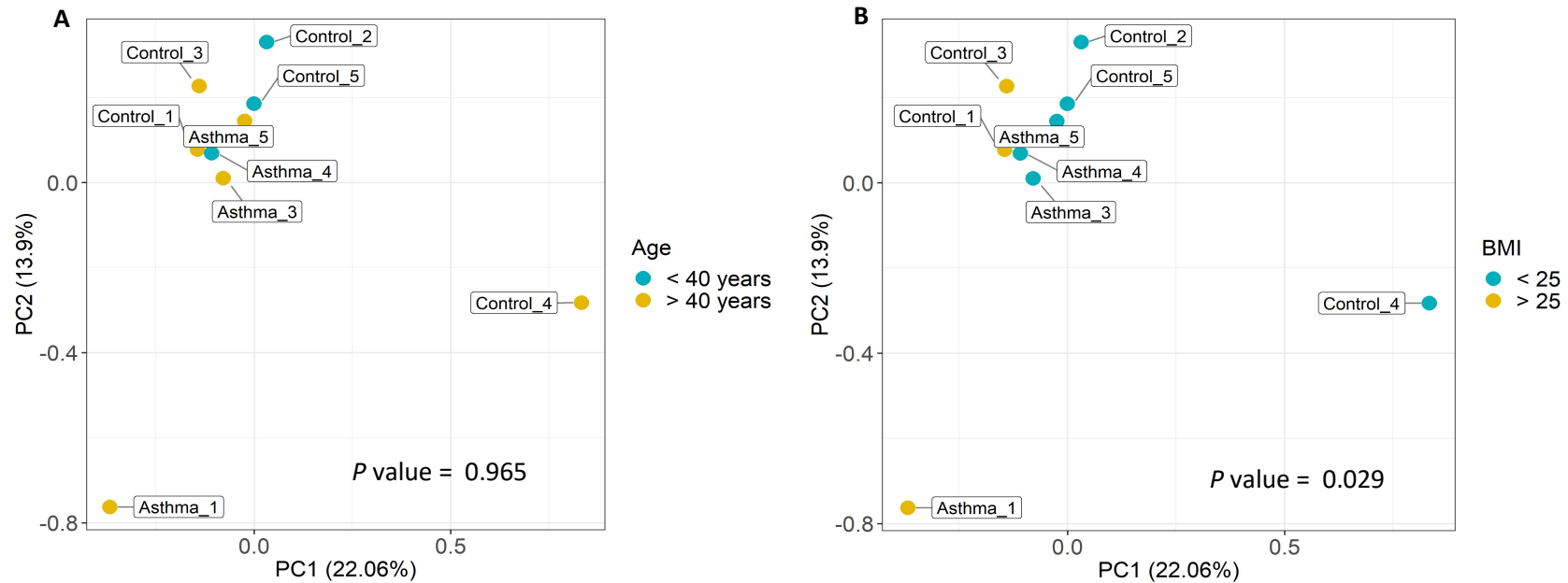
Statistical analysis of gene expression diversity in the control and asthma plasma samples, however, revealed that there was no significant difference in the diversity of genes being expressed in the asthmatic subjects compared to the control subjects ( $P$  value = 0.427, *PERMANOVA*).

Analysis of the effect of age and BMI on gene expression revealed that whilst age had no impact of gene expression diversity ( $P$  value = 0.965, *PERMANOVA*) (Figure 3.5.A), BMI had a significant impact on diversity of gene expression ( $P$  value = 0.0210, *PERMANOVA*) (Figure 3.5.B). BMI ranged from 21.0 to 27.8 across the experimental test subjects (Table 3.3). When the plasma samples were grouped into BMI < 25 and BMI > 25, samples from subjects with a BMI greater than 25 displayed significant separation from the samples from subjects

with a BMI less than 25 (Figure 3.5.B). However, since the purpose of this experiment was to assess the effects of asthma on RNA populations, there was not an even distribution of subjects with a BMI greater/ less than 25 as analysis of the effects of BMI was not the primary goal of this study. Further investigation, therefore, would be required to determine whether the observed effect of BMI on gene expression diversity is a significant finding.



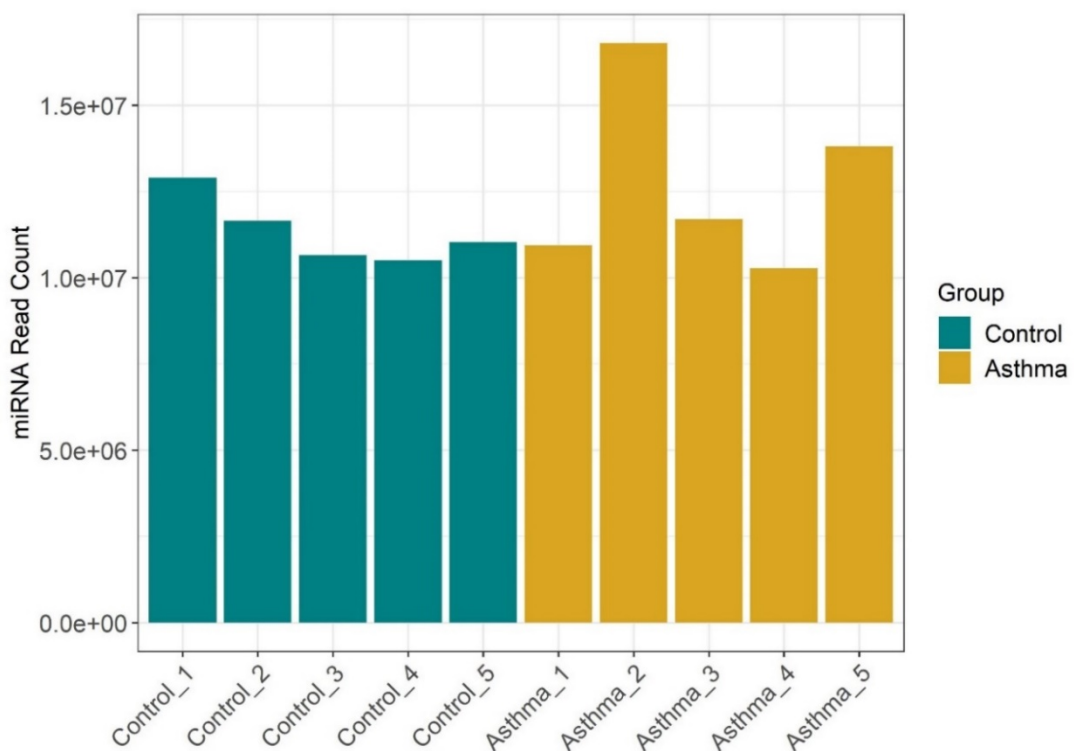
**Figure 3. 4: Principal component analysis of circulatory gene expression profiles detected in asthmatic and control subjects.** PCA was performed on the gene population dataset generated from the asthma (n = 4) and control (n = 5) plasma samples using quantitative mRNA FPKM reads that had been normalised using log2. The PCA was performed using Euclidean distance and R software. Each data point represents the gene expression profile of a plasma sample and the distance between two plotted points is proportional to the degree of similarity between the two expression profiles.



**Figure 3. 5: Principal component analysis of circulatory gene expression profiles detected in the asthmatic and control subjects on the basis of age and BMI.** PCA was performed on the gene population dataset generated from the asthma (n = 4) and control (n = 5) plasma samples using quantitative mRNA FPKM reads that had been normalised using log<sub>2</sub>. The PCA was performed using Euclidean distance and R software. Each data point represents the gene expression profile of a plasma sample and the distance between two plotted points is proportional to the degree of similarity between the two expression profiles. Comparison of gene expression profiles was assessed using age (A) and BMI (B) as the variable.

### 3.3.5. miRNA detected in the Plasma Samples

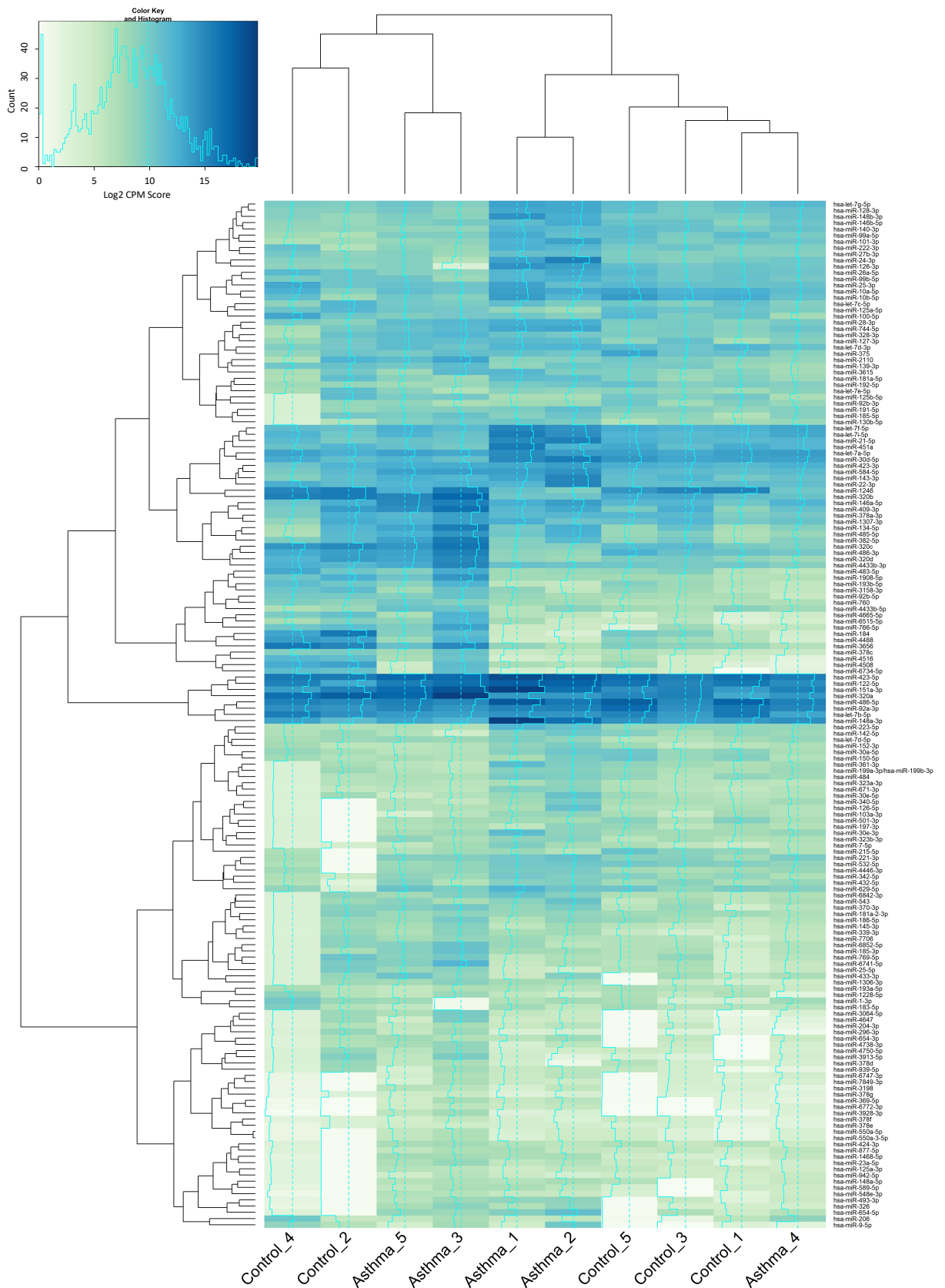
A total of 120,305,814 high-quality miRNA reads were isolated and sequenced from the plasma samples. This included 56,752,743 reads from the non-asthmatic control samples (average = 11,350,548.60; range = 10,506,135 – 12,905,879) and 63,553,071 reads (average = 12,710,614.20; range = 10,276,765 – 16,812,591) from the asthmatic samples (Figure 3.6). Statistical analysis of the read count values revealed there was no significant difference in total miRNA detected in the asthmatic subjects compared to the control subjects ( $P$  value = 0.5476, *Wilcoxon rank sum test*). Of interest was the high number of miRNAs detected in Asthma\_2. This sample displayed significantly lower mRNA counts, which may be explained by the high level of miRNAs observed.



**Figure 3. 6: Total number of miRNA reads isolated and sequenced from the human plasma samples.** Total RNA was extracted from 500 $\mu$ l of human plasma from non-asthmatic control subjects ( $n = 5$ ) and asthmatic subjects ( $n = 5$ ) using the Qiagen serum and plasma miRNeasy kit. miRNA sequencing libraries were prepared using the TruSeq small RNA library kit and sequenced using the Illumina HiSeq 2000 platform.

### 3.3.6. Differential miRNA Expression detected in the Asthmatic Subjects compared to the Control Subjects

Using miRanalyzer<sup>398</sup> and edgeR<sup>400</sup>, 165 known miRNAs were detected in the plasma samples (average number of miRNAs detected per sample = 163.80; range = 158 – 165), which was consistent with previously reported studies on circulatory miRNA populations<sup>405–409</sup>. To determine whether the asthmatic subjects had distinct miRNA profiles compared to the control subjects, total miRNA was plotted as a heatmap, and unsupervised clustering was performed using Euclidean distance (Figure 3.7). Cluster analysis revealed the presence of two clusters with regards to the circulatory miRNA populations. Cluster one was composed of Control\_4, Control\_2, Asthma\_5, and Asthma\_3; and Cluster two was made up of Asthma\_1, Asthma\_2, Control\_5, Control\_3, Control\_1, and Asthma\_4. Within each cluster two sub-clusters formed, and each sub-cluster was comprised of either control or asthmatic subjects. Of interest was the observation that the asthmatic subjects not diagnosed with additional atopic diseases (Asthma\_3 and Asthma\_5; see table 3.3) clustered together, and the asthmatic subjects diagnosed with additional atopic diseases (Asthma\_1 and Asthma\_2; see Table 3.3) clustered together (Figure 3.7). Furthermore, similar to the results obtained for mRNA population analysis, Asthma\_4 again clustered more closely with the control subjects rather than the remaining asthmatic subjects.

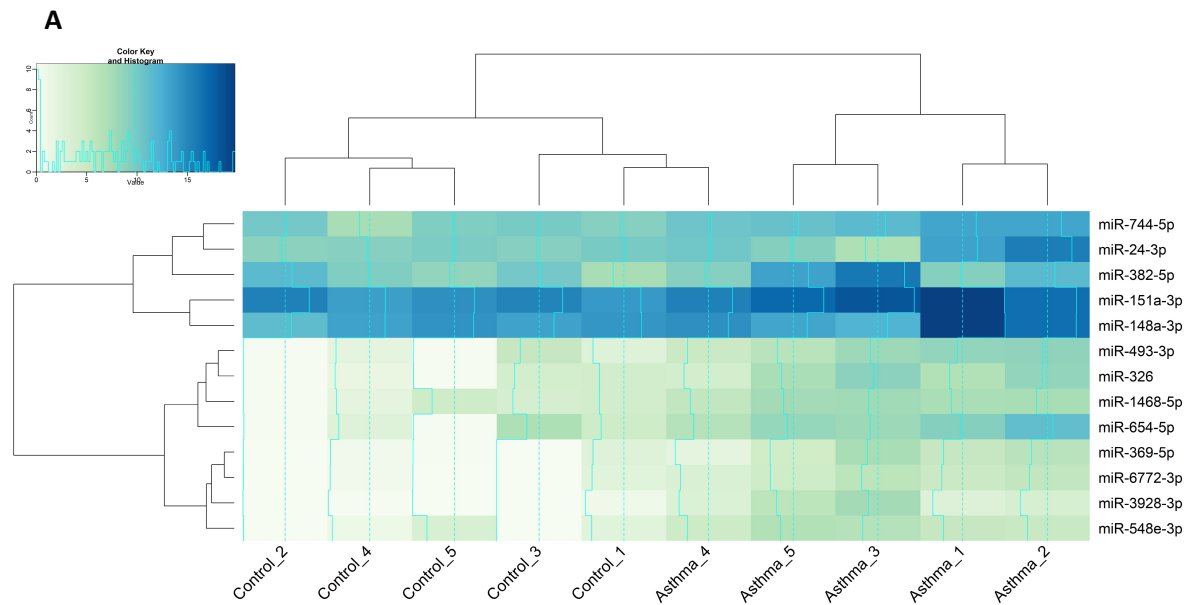


**Figure 3.7:** A Heatmap showing expression levels of circulatory miRNA in asthmatic subjects compared to control subjects. Analysis was performed by sequencing miRNA isolated from plasma samples from asthmatic subjects (n = 5) and non-asthmatic control

subjects (n = 5) , and mapping the sequenced miRNA reads the human miRbase Version 21 using sRNAtoolbox. miRNA expression was determined by quantification of circulatory miRNA detected in the plasma samples and is expressed as log<sub>2</sub> normalised Counts per Million mapped (CPM) reads. All miRNAs that were detected in the plasma samples are plotted, and cluster analysis (Euclidean distance) informs the X and Y-axis dendrograms.

Statistical analysis revealed that 13 miRNAs displayed significant increased expression [defined as having a false rate of discovery (FDR)-adjusted *P* value  $\leq 0.05$  and a log fold change  $\geq 2.0$ ] in the asthmatic subjects compared to the control subjects (Figure 3.8). Cluster analysis of the significantly expressed miRNAs using Euclidian distance revealed that with regards to expression of the significantly differentially expressed miRNAs, the control and asthma subjects formed two distinct clusters. Asthma\_4 was the exception, and clustered with the control subjects rather than the remaining asthmatic subjects.





**B**

miRNA	Control Log2 Mean	Asthma Log2 Mean	Log Fold Change	P Value	FDR P Value
hsa-miR-326	2.1264	7.1121	4.7496	0.0008	0.0337
hsa-miR-369-5p	0.7449	5.0816	5.1778	0.0007	0.0337
hsa-miR-6772-3p	0.2589	4.6294	7.1583	0.0002	0.0337
hsa-miR-3928-3p	0.6837	4.9272	4.6020	0.0005	0.0337
hsa-miR-148a-3p	2.9770	7.1062	3.5864	0.0021	0.0369
hsa-miR-151a-3p	13.2692	15.1776	4.0379	0.0022	0.0369
hsa-miR-24-3p	14.5123	17.3715	3.3452	0.0016	0.0369
hsa-miR-1468-5p	9.4299	11.0648	4.0795	0.0018	0.0369
hsa-miR-493-3p	2.1441	7.3314	4.3598	0.0022	0.0369
hsa-miR-548e-3p	1.4292	5.7366	4.1425	0.0019	0.0369
hsa-miR-382-5p	9.4403	11.9116	3.8968	0.0027	0.0375
hsa-miR-654-5p	2.9741	8.6871	4.4341	0.0026	0.0375
hsa-miR-744-5p	9.2020	11.8328	2.7522	0.0037	0.0470

**Figure 3.8: Differential levels of circulatory miRNA in asthmatic subjects compared to control subjects.** Analysis was performed by sequencing and mapping miRNA reads isolated from non-asthmatic control plasma samples (n = 5) and asthmatic plasma samples (n = 5) using sRNAtoolbox. (A) miRNA expression was determined by quantification of circulatory miRNA detected in the plasma samples and is expressed as log2 normalised CPM reads. Differential expression was determined using the edgeR program (Bioconductor software), and significant expression was defined as having a log fold change greater than 2.0 and an FDR-adjusted P value  $\leq 0.05$ . Cluster analysis (Euclidean distance) informs the X

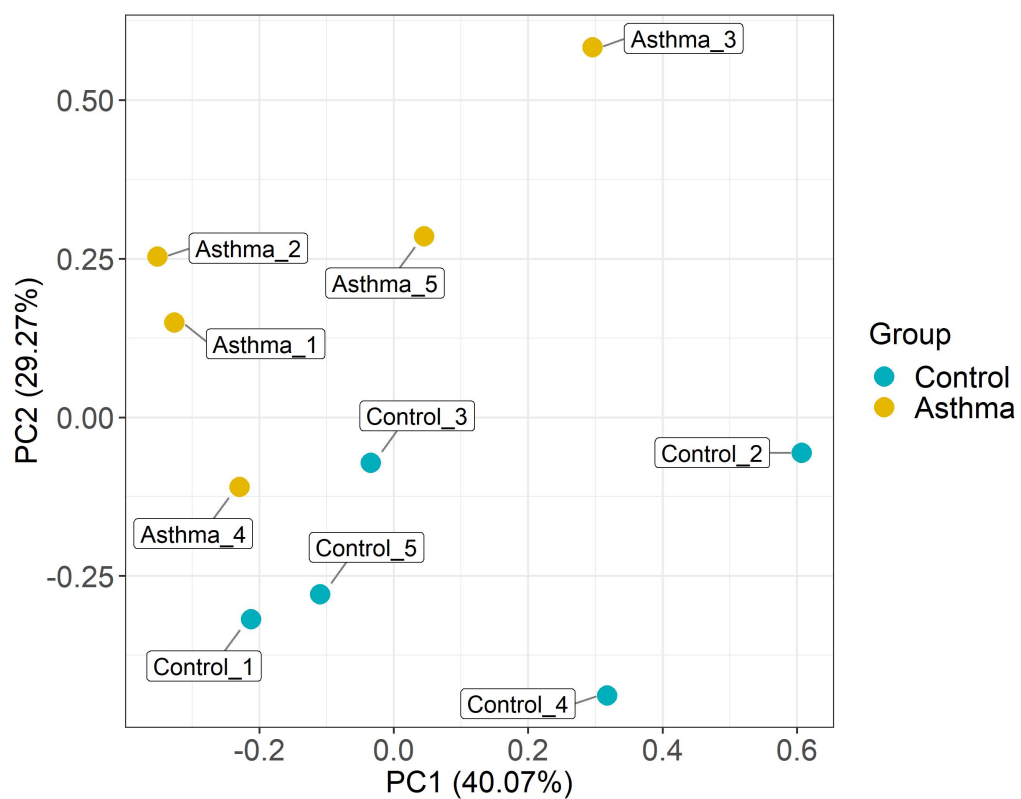
and Y-axis dendrograms. **(B)** Statistical analysis of the miRNA reads detected at significantly increased levels in the asthmatic subjects compared to the control subjects.

### 3.3.7. Diversity of miRNA detected in the Asthmatic Subjects compared to the Control Subjects

The diversity of circulatory miRNA populations in the asthmatic subjects was compared to the control subjects by carrying out PCA on the log<sub>2</sub> CPM values of all miRNAs with detectable levels of expression in the plasma samples (Figure 3.9). The PCA plot comprising of the first two principal components, which collectively explained the majority of total variance in the miRNA populations (69.34%), revealed that overall the asthmatic subjects clustered separately from the control subjects (Figure 3.9). Separation of the two subject groups was due to differences in PC2 scores, whereby the asthmatic subjects had positive PC2 scores and the control subjects had negative PC2 scores (Figure 3.9). Moreover, PC1 scores appeared to reflect the absence/ presence of additional atopic diseases in the asthmatic subjects, whereby subjects diagnosed with additional atopic diseases (Asthma\_1, Asthma\_2, and Asthma\_4) had negative PC1 values, and asthmatic subjects that did not suffer from additional atopic diseases (Asthma\_3 and Asthma\_5) scored positive PC1 values. However, as this study was a preliminary investigation with a small sample size, further investigation would be required to confirm this finding.

Additionally, the circulatory miRNA profile detected in the Asthma\_4 sample was observed to be more similar to the control subjects than the remaining asthmatic subjects. This was particularly apparent with regards to the PC2 scores, whereby Asthma\_4, like the control subjects, displayed a negative PC2 score, whilst the remaining asthmatic subjects displayed positive PC2 scores.

Statistical analysis of Euclidean distance detected in the plasma samples revealed that miRNA expression diversity was significantly altered in the asthmatic subjects compared to the control subjects ( $P$  value = 0.0440, *PERMANOVA*). *PERMANOVA* analysis was also applied to determine whether age or BMI had a significant impact on miRNA profile diversity and in both instances the variable had no impact on miRNA expression diversity ( $P$  value > 0.05, data not shown).



**Figure 3.9: Principal component analysis of circulatory miRNA profiles detected in asthmatic and control subjects.** PCA was performed on the miRNA population dataset generated from the asthma ( $n = 5$ ) and control ( $n = 5$ ) plasma samples. This was achieved by measuring Euclidean distance using log<sub>2</sub> normalised miRNA CPM read numbers that had been generated from the asthma and control samples. Each data point represents the gene expression profile of a plasma sample and the distance between two plotted points is proportional to the degree of similarity between the two expression profiles.

### 3.3.8. RNA Functional Analysis

### 3.3.9. Biological Significance of Differential Gene Expression in the Asthmatic Subjects

To determine whether the observed differential gene expression observed in the plasma samples of asthmatic subjects could be linked to asthma pathology, the differentially expressed genes identified were compared to a recently released database of genes associated with asthma pathology – AllerGAtlas 1.0 <sup>401</sup> [public web access: <http://biokb.ncpsb.org/AlleRGAtlas/index.php/Home/Browse/>].

Of the 287 genes that displayed significant differential expression in the asthmatic subjects, 10 genes were identified in the asthma database. These genes included *CD46*, fibronectin 1 (*FN1*), glutathione S-transferase alpha 1 (*GSTA1*), interleukin 7 receptor (*IL7R*), galectin 3 (*LGALS3*), myeloperoxidase (*MPO*), neurotensin (*NTS*), phosphodiesterase 4A (*PDE4A*), *TLR1*, and vitamin D receptor (*VDR*). 5 of the genes were upregulated in the asthmatic subjects (*GSTA1*, *MPO*, *NTS*, *TLR1*, and *VDR*) and 5 were downregulated in the asthmatic subjects (*CD46*, *FN1*, *IL7R*, *LGAL3*, and *PDE4A*) (Table 3.5). Moreover, gene expression was predominately condition specific. Of the upregulated genes, *NTS*, *TLR1*, and *MPO* mRNA was only detectable in the asthma samples, whilst in the downregulated genes, *IL7R* and *PDE4R* mRNA was only observed in the control samples (see Supplementary Materials, Table S4).

**Table 3.5: Genes with significant differential expression in the asthmatic subjects compared to control subjects that are associated with asthma pathology.** Differential gene expression was determined using the Tuxedo protocol (*Galaxy* software) on log<sub>2</sub> normalised mRNA FPKM reads sequenced from plasma samples from asthma subjects (n = 4) and control subjects (n = 5). Gene function with regards to asthma pathology was determined using the asthma database AllerGAtlas, 2018<sup>401</sup> and a general literature search using the relevant search engines.

Gene	Expression in Asthma subjects	Function	Reference
CD46	Downregulated	Differentiation of IL-10 producing regulatory T cell type 1 cells	410,411
		Differentiation of Th1 cells	412,413
		Inhibition of HDM allergenic activity	414
FN1	Downregulated	Development of pulmonary fibrosis	415,416
		Airway smooth muscle proliferation, survival, and contraction	417–419
GSTA1	Upregulated	Protection against oxidative stress	420,421
IL7R	Downregulated	Marker for Treg activation	422
		T cell development and survival	423–427
		B cell development	423,428
		Eosinophil survival	429
LGALS3	Downregulated	Inhibition of IL-5 expression	430
		Inhibition of eosinophil and T cell infiltration	430
		Negative regulation of Th17 polarization	431
MPO	Upregulated	Initiation of lipid peroxidation	432
NTS	Upregulated	Mast cell degranulation	433,434
		Production of CD4+ T cell cytokines (IL-2, IL-4, IL-5, IFN $\gamma$ )	435–437
PDE4A	Downregulated	Production of TNF $\alpha$	435
		Production of leukotriene B4	435
		Production of eotaxin	437
		Airway goblet cell hyperplasia	437
TLR1	Upregulated	Antimicrobial activity	438–440
		Development of airway inflammation and hyperresponsiveness	441
VDR	Upregulated	Eosinophilia	441
		Inhibits IgE production	441,442

### 3.3.10. Biological Significance of Differentially Expressed miRNA in the Asthmatic Subjects

miRNAs are known regulators of gene expression, typically with regards to gene silencing<sup>443-445</sup>. To determine how differential miRNA expression in the asthmatic subjects may have altered gene expression, Gene Ontology (GO) analysis was performed using DIANA-miRPath V3.0 to determine the genes and biological pathways likely to be affected by the differentially expressed miRNA.

In total, the differentially expressed miRNAs were found to target 1,831 genes, of which, 25 genes exhibited differential expression in the asthmatic subjects. (Table 3.6). As expected, the majority of these genes were significantly downregulated in the asthmatic subjects (21/28 genes), and 10 genes were found to show no expression at all in the asthmatic subjects (Table 3.6). With regards to the 7 genes significantly upregulated in the asthmatic subjects, 3 displayed unique expression to the asthmatic subjects (*SH2D1B*, *SYNDIG1L*, *UBXN10*), and expression of these genes were undetected in the control subjects (Table 3.6).

**Table 3 6: Genes targeted by the differentially expressed miRNAs that displayed significant differential expression in the asthmatic subjects compared to the control subjects.** mRNA expression was determined by quantification of circulatory mRNA detected in the plasma samples of asthmatic subjects (n = 4) and control subjects (n = 5) and is expressed as log2 normalised FPKM reads. Significant differential expression in the asthmatic subjects was defined as having a log fold change greater than 2.0 and an FDR-adjusted *P* value  $\leq 0.05$ . Identification of the gene as a target of differentially expressed miRNA was determined using TargetScan v6.2.

Gene	Control Mean	Asthma Mean	Fold Change (log2)	Expression State	<i>P</i> Value	<i>Q</i> Value
ADAMTS18	4.844	0.000	-inf	Downregulated	0.000	0.003
ANKRD11	20.860	0.481	-5.439	Downregulated	0.000	0.007
ASPH	15.551	2.130	-2.868	Downregulated	0.001	0.034
B4GALT5	11.155	0.320	-5.122	Downregulated	0.002	0.041
BRI3BP	5.777	0.000	-inf	Downregulated	0.000	0.003
CHMP1A	898.053	10.776	-6.381	Downregulated	0.000	0.013
CSF2RB	6.862	0.000	-inf	Downregulated	0.000	0.003
ELOF1	806.425	17.862	-5.497	Downregulated	0.000	0.018
GDF7	1.192	0.000	-inf	Downregulated	0.000	0.003
KIF26A	10.373	0.190	-5.772	Downregulated	0.001	0.038
MXRA7	9.572	152.388	3.993	Upregulated	0.001	0.020
NCAN	12.170	0.000	-inf	Downregulated	0.000	0.005
NRP1	0.924	18.895	4.354	Upregulated	0.000	0.011
PMM2	129.114	2.491	-5.696	Downregulated	0.002	0.041
PSMD9	192.358	1.203	-7.321	Downregulated	0.001	0.019
PTS	9.203	0.000	-inf	Downregulated	0.001	0.029
RAB3IL1	15.123	0.000	-inf	Downregulated	0.000	0.003
SH2D1B	0.000	2.288	inf	Upregulated	0.001	0.038
SSTR1	1.882	0.000	-inf	Downregulated	0.000	0.003
ST3GAL4	37.716	0.729	-5.693	Downregulated	0.001	0.020
SYNDIG1L	0.000	4.403	inf	Upregulated	0.000	0.003
TOP1MT	0.345	59.034	7.421	Upregulated	0.000	0.018
TRIOBP	182.005	1.406	-7.016	Downregulated	0.001	0.039
UBXN10	0.000	17.007	inf	Upregulated	0.000	0.003
VDR	1.116	24.331	4.447	Upregulated	0.002	0.043
WDR87	6.160	0.000	-inf	Downregulated	0.001	0.019
ZNF710	132.550	0.805	-7.363	Downregulated	0.002	0.046
ZNRF2	18.166	0.000	-inf	Downregulated	0.002	0.047

Analysis of biological pathways likely to be affected by significant differential expression of the miRNAs identified 50 pathways likely to be altered in the asthmatic subjects as a consequence of significantly altered miRNA levels. The top 15 biological pathways identified are shown in Table 3.7.

**Table 3.7: The top 15 biological pathways that were predicted to be altered in the asthmatic subjects as a result of differential miRNA expression.** Functional analysis was performed on the differentially expressed miRNA detected in the asthmatic subjects (n = 4) compared to the control subjects (n = 5) in order to identify biological pathways likely to be altered in the asthmatic subjects. Functional analysis was achieved using DIANA-miRPath v3.0 and the 15 biological pathways most likely to be altered in the asthmatic subjects are presented.

GO Category	P Value	# Genes	# miRNAs
Organelle (GO:0043226)	1.18E-33	936	13
Ion binding (GO:0043167)	2.90E-23	599	13
Cellular nitrogen compound metabolic process (GO:0034641)	3.20E-15	445	13
Biosynthetic process (GO:0009058)	3.13E-11	381	13
Small molecule metabolic process (GO:0044281)	1.84E-07	226	12
Neurotrophin TRK receptor signalling pathway (GO:0048011)	4.10E-07	35	8
Protein binding transcription factor activity (GO:0000988)	1.41E-06	62	11
Molecular function (GO:0003674)	1.52E-06	1554	13
Cytoskeletal protein binding (GO:0008092)	2.38E-06	92	12
Blood coagulation (GO:0007596)	2.74E-06	55	10
Gene expression (GO:0010467)	3.41E-06	61	10
Cellular protein modification process (GO:0006464)	1.19E-05	214	13
Synaptic transmission (GO:0007268)	4.93E-05	53	10
Fc-epsilon receptor signalling pathway (GO:0038095)	5.15E-05	22	8
Cellular component (GO:0005575)	5.40E-05	1562	13



### 3.3.11. Combined Effect of Differential Gene Expression and miRNA Expression in the Asthmatic Subjects

To determine the combined biological significance of differential gene expression and regulation in the asthmatic subjects, causal inference analysis using *IPA* software was carried out to identify the likely upstream regulators responsible for the differential mRNA and miRNA expression.

In total, 246 upstream gene regulators had a *P* value of overlap  $\leq 0.05$ ; indicating that the regulators had altered functional activity in the asthmatic subjects compared to the control subjects on the basis of differential mRNA and miRNA expression. Of these regulators, 7 had *Z* scores greater than 2.0, thus enabling their activity in the asthmatic subjects to be predicted. 2 upstream regulators were predicted to have significantly increased activity in the asthmatic subjects (*P* value overlap  $\leq 0.05$ ; *Z* score  $\geq 2.0$ ), and 5 regulators were predicted to have significantly decreased activity in the asthmatic subjects (*P* value of overlap  $\leq 0.05$ ; *Z* score  $\leq -2.0$ ) (Table 3.8).

**Table 3.8: Upstream gene regulators with predicted significantly altered activity in the asthmatic subjects compared to the control subjects.** Causal inference analysis was used to predict upstream regulators that have significantly altered activity in the asthmatic subjects (n = 4) compared to the control subjects (n = 5) (defined as having a *P* value of overlap  $\leq 0.05$  and a *Z* score greater than 2.0). Activated upstream regulators are defined as having a *Z* score  $\geq 2.0$ , and inhibited upstream regulators are defined as having a *Z* score  $\leq -2.0$ . Target molecules activated = genes present in the RNA dataset that are activated by the upstream regulator; target molecules inhibited = genes present in the RNA dataset that are inhibited by the upstream regulator; target molecules affected = genes present in the RNA dataset whose activity is known to be altered by the upstream regulator but there is insufficient evidence to prove this is activation or inhibition.

Upstream Regulator	Molecule type	Activity state	Z score	<i>P</i> value of overlap	# Target molecules activated	# Target molecules inhibited	# Target molecules affected
Sirolimus	Chemical drug	Activated	2.75	0.0107	12	1	0
GFI1	Transcription regulator	Activated	2.00	0.0077	4	0	1
EIF4E	Transcription regulator	Inhibited	-2.00	0.0074	0	4	2
Mycophenolic acid	Chemical drug	Inhibited	-2.00	0.0211	0	4	0
Streptozocin	Chemical drug	Inhibited	-2.16	0.0492	0	5	1
SOX4	Transcription regulator	Inhibited	-2.24	0.0770	0	5	0
SYVN1	Transporter	Inhibited	-2.45	0.0069	0	6	0

Causal inference analysis using *IPA* was also used to predict the downstream consequences of the observed differential mRNA and miRNA expression in the asthmatic subjects. The downstream effects of the differential expression were primarily assessed by examination of the predicted canonical pathways and biological functions impacted.

14 canonical pathways were predicted to have significantly altered biological activity ( $P$  value  $\leq 0.05$ ) within the asthmatic subjects compared to the control subjects (Table 3.9). Several of the canonical pathways predicted to have altered activity in the asthmatic subjects influence immune activity, including lymphocyte and B cell activity, phagosome maturation, signalling in rheumatoid arthritis, B cell development, and Nur77 signalling in lymphocytes.

**Table 3.9: Canonical pathways predicted to have significantly altered activity in the asthmatic subjects.** IPA software was used to predict downstream canonical signalling pathways likely to be affected by changes in gene expression and regulation in the asthmatic subjects (n = 4) compared to the control subjects (n = 5). Molecules with increased gene expression are genes that had significantly increased numbers of mRNA reads in the asthma plasma samples, and molecules with decreased gene expression are genes that had significantly decreased numbers of mRNA reads in the asthma plasma samples.

Canonical Pathway	P Value	Molecules with increased gene expression	Molecules with decreased gene expression
Altered T Cell and B Cell Signalling in Rheumatoid Arthritis	0.0053	SLAMF1,TLR1,HLA-DQA1,TNFRSF13C	HLA-DRB5
B Cell Development	0.0092	HLA-DQA1	IL7R, HLA-DRB5
Antigen Presentation Pathway	0.0116	HLA-DQA1, MR1	HLA-DRB5
Melatonin Degradation III	0.0124	MPO	-
TNFR1 Signalling	0.0241	-	TRADD, IKBKB, PAK4
Acute Myeloid Leukemia Signalling	0.0287	PML	CSF2RB, CEBPA, IDH3B
Tetrahydrobiopterin Biosynthesis I	0.0368	-	PTS
Hypusine Biosynthesis	0.0368	-	DOHH
Tetrahydrobiopterin Biosynthesis II	0.0368	-	PTS
Nur77 Signalling in T Lymphocytes	0.0369	HDAC9, HLA-DQA1	HLA-DRB5
Phagosome Maturation	0.0375	MPO, GOSR2	CTSL, CTSG, HLA-DRB5
Catecholamine Biosynthesis	0.0487	-	PNMT
Mitotic Roles of Polo-Like Kinase	0.0488	STAG2	ANAPC4, PPP2R5C
Type I Diabetes Mellitus Signalling	0.0496	HLA-DQA1	TRADD, IKBKB, HLA-DRB5

With regards to biological functions likely to be impacted by changes in the observed mRNA and miRNA expression patterns in the asthmatic subjects, a number of pathways were predicted to have altered activity within the asthmatic cohort (Table 3.10).

Significantly altered activity was defined as having a  $P$  value  $\leq 0.05$  and a  $Z$  score greater than 2.0, with negative  $Z$  scores representing predicted decreased activity, and positive  $Z$  scores representing predicted increased activity. In total 10 biological functions had predicted significantly altered activity within the asthmatic subjects, of which 2 were predicted to have increased activity, and 8 were predicted to have decreased activity (Table 3.10).

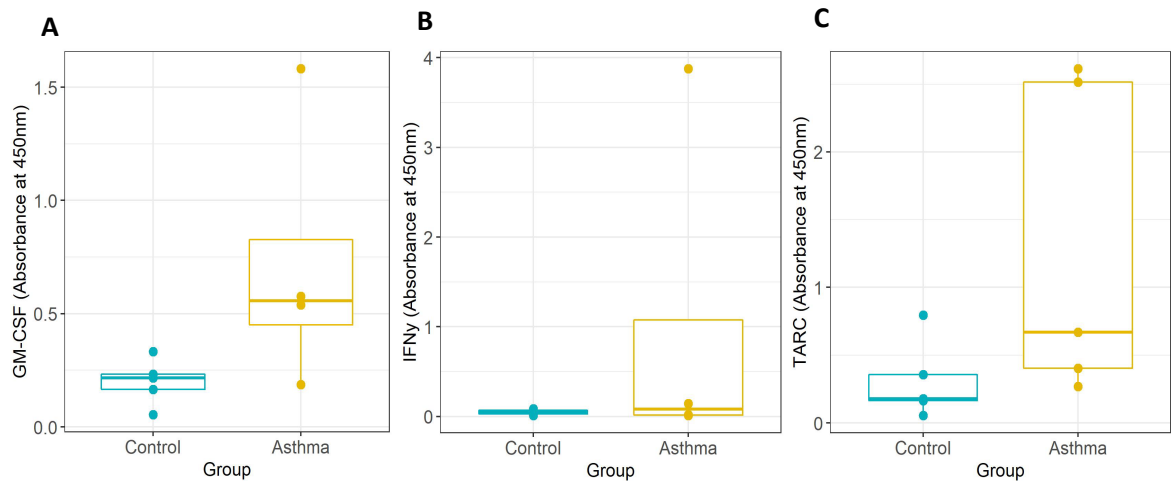
**Table 3.10: Biological functions predicted to have significantly altered activity in the asthmatic subjects compared to control subjects.** Causal inference using *IPA* software was used to predict biological functions likely to have altered activity in the asthmatic subjects ( $n = 4$ ) compared to the control subjects ( $n = 5$ ). This was determined through analysis of genes and miRNA that had altered expression in the asthmatic subjects, to predict which biological functions would likely be altered. Biological functions predicted to be significantly altered in the asthmatic subjects were defined as having a  $P$  value  $\leq 0.05$  and a  $Z$  score greater than 2.0. Biological functions with predicted increased activity were defined as having a  $Z$  score  $\geq 2.0$ , and biological functions with predicted decreased activity were defined as having a  $Z$  score  $\leq -2.0$ .

Biological Functions	$P$ Value	Activation State	$Z$ score
Binding of endothelial cells	9.75E-03	Decreased	-2.123
Binding of leukocytes	1.73E-03	Decreased	-2.062
Cell transformation	1.32E-03	Decreased	-3.228
Differentiation of fibroblast cell lines	4.44E-03	Decreased	-2.184
Immune response of leukocytes	6.79E-04	Decreased	-2.031
Interaction of endothelial cells	3.55E-03	Decreased	-2.346
Killing of natural killer cells	5.44E-03	Decreased	-2.63
Proliferation of hepatocytes	6.53E-03	Increased	2.177
Tumorigenesis of tissue	4.94E-04	Increased	2.215
Viral infection	1.34E-02	Decreased	-2.099

### 3.3.12.Characterisation of Circulatory Inflammatory Protein Levels

To determine the immune status of the asthmatic patients at the time of sample collection, characterisation of various chemokines and cytokines associated with asthma pathology was performed.

A total of 10 out of the 12 inflammatory proteins under investigation were detected in the plasma samples (see Supplementary Materials, Table S5). Overall the asthmatic subjects were found to have elevated levels of inflammatory proteins compared to the controls, as determined by increased absorbance scores for all inflammatory proteins examined (See Supplementary Materials, Table S5). This was particularly apparent for chemokines TARC ( $P$  value = 0.0952), GM-CSF ( $P$  value = 0.1111), and IFN $\gamma$  ( $P$  value = 0.1945) (Figure 3.10). However, it should be noted that no statistically significant increases were detected for any of the individual proteins. This was likely due to the asthmatic subjects having a greater level of diversity with regards to inflammatory protein levels compared to the control subjects (Figure 3.10; see also Supplementary Materials, Table S5).



**D**

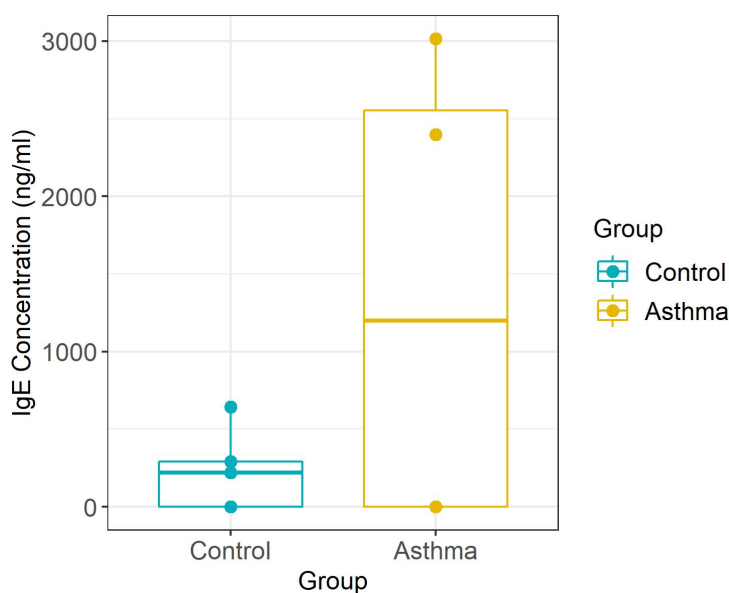
Protein	Control Mean (S.D)	Asthma Mean (S.D)	P Value
GM-CSF	0.200 (0.09)	0.721 (0.52)	0.1111
IFN $\gamma$	0.019 (0.03)	0.810 (1.53)	0.1945
TARC	0.310 (0.26)	1.294 (1.05)	0.0952

**Figure 3.10: Levels of circulatory inflammatory proteins in asthmatic and control subjects.** Qualitative ELISAs were performed on plasma samples from asthmatic subjects (n = 5) and control subjects (n = 5). Inflammatory protein levels were determined by measuring absorbance at 450nm, and statistical analysis using Wilcoxon rank sum test with continuity correction. **(A)** Levels of GM-CSF detected in plasma samples from asthmatic (n = 5) and control subjects (n = 5). **(B)**. Levels of IFN $\gamma$  detected in plasma samples from asthmatic (n = 5) and control subjects (n = 5). **(C)**. Levels of TARC detected in plasma samples from asthmatic (n = 5) and control subjects (n = 5).

*Abbreviations: S.D, standard deviation*

### 3.3.13. Quantification of Circulatory Total IgE Concentrations

Total IgE was detected in 50% of plasma samples under investigation (three control subjects and two asthmatic subjects) (Figure 3.11, see also Supplementary Materials, Table S6). For the purpose of statistical analysis, samples with undetectable levels of IgE were given an IgE concentration value of 0. Comparison between the asthmatic and control samples revealed no significant difference in IgE concentration ( $P$  value = 0.7012, *Wilcoxon rank sum test with continuity correction*).



Protein	Control Mean (S.D)	Asthma Mean (S.D)	$P$ Value
IgE	384.56 (185.13)	2707.04 (308.86)	0.7012

**Figure 3.11: Circulatory total IgE concentration detected in asthmatic subjects compared to control subjects.** Total IgE concentrations were measured in plasma samples from asthma subjects ( $n = 4$ ) and control subjects ( $n = 5$ ) using a sandwich ELISA. Absorbance was measured at 450nm and converted into protein concentration using a standard curve. (A). Concentration of total IgE protein detected in the asthmatic subjects ( $n = 4$ ) compared to the control subjects ( $n = 5$ ). (B). Statistical analysis of total IgE detected in the asthmatic subjects ( $n = 4$ ) compared to the control subjects ( $n = 5$ ) using a Wilcoxon rank sum test with continuity correction.

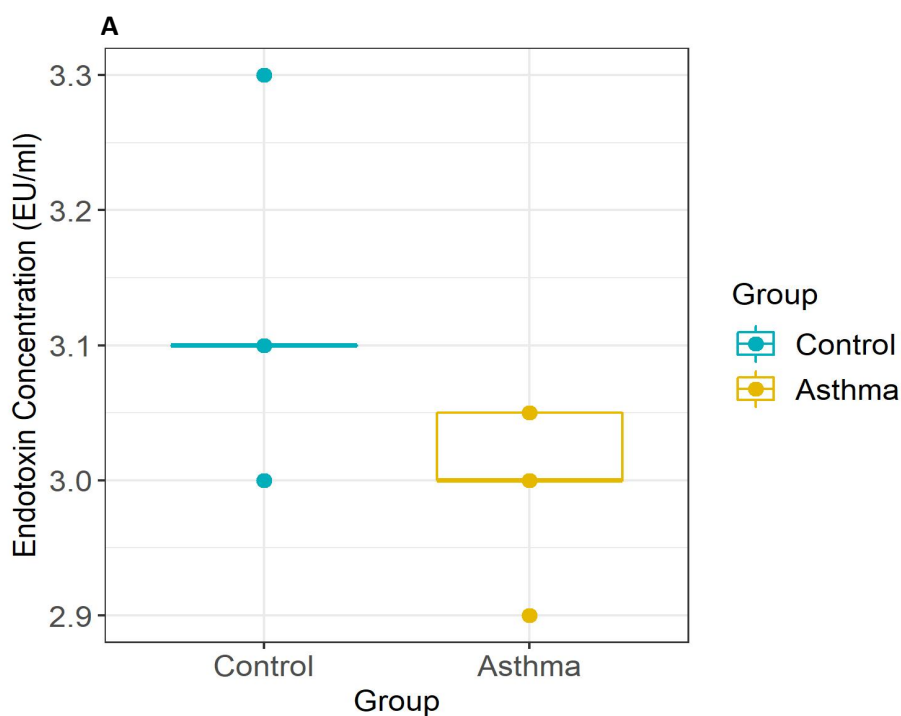


### 3.3.14. Quantification of Circulatory Endotoxin Concentrations

Endotoxin protein was detected in all plasma samples investigated, and overall the asthmatic subjects exhibited decreased levels of the protein in the blood ( $P$  value = 0.0650, *Unpaired t test*) (Figure 3.12, see also Supplementary Materials, Table S7).

Within the asthma cohort, subjects diagnosed with additional atopic diseases (i.e. allergic rhinitis, allergic dermatitis) displayed lower endotoxin concentrations compared to the asthmatic subjects that were not diagnosed with additional atopic diseases (see Supplementary Materials, Table S7). Within the control cohort, subjects with previously reported atopic dermatitis displayed circulatory endotoxin concentrations similar (i.e. lower than those subjects reporting no atopic conditions) to those observed in the asthma cohort (see Supplementary Materials, Table S7).

Whilst the observed decrease in circulatory endotoxin levels was non-significant, it was predicted that with a larger cohort of asthmatic subjects, endotoxin levels would be detected at significantly reduced levels.



**B**

Protein	Control Mean (S.D)	Asthma Mean (S.D)	P Value
Endotoxin	3.12 (0.10)	3.00 (0.05)	0.0650

**Figure 3.12: Circulatory endotoxin concentrations detected in asthmatic subjects compared to control subjects.** Circulatory endotoxin concentrations were measured in plasma samples from asthmatic subjects (n = 5) and non-asthmatic control subjects using a Pierce™ Limulus Amebocyte Lysate (LAL) assay. Absorbance was measured at 450nm and converted into protein concentration using a standard curve. **(A)** Concentration of endotoxin protein detected in the asthmatic subjects (n = 5) compared to the control subjects (n = 5). **(B)** Statistical analysis of endotoxin detected in the asthmatic subjects compared to the control subjects using a Wilcoxon rank sum test with continuity correction.

### 3.4. Discussion

This study aimed to characterise a small, yet specific, population of female adult asthma patients who had developed atopic asthma during childhood that was associated with a HDM allergy. A range of molecular techniques were applied to quantify circulating inflammatory proteins and determine gene expression, regulation, and predicted activity in an asthmatic cohort compared to a non-asthmatic control cohort. These investigations were carried out to increase understanding of a specific asthma phenotype, to begin to explore the molecular mechanisms responsible, and to identify potential biomarkers associated with the asthma phenotype.

#### 3.4.1. Transcriptomic Characterisation of the Asthma Phenotype

Analysis of the diversity of RNA expression in the asthmatic subjects revealed that the asthmatic subjects exhibited RNA profiles distinct from the control RNA profiles; this was particularly apparent in the miRNA analysis. When combined with differential expression analyses, asthma severity was found to influence gene expression, whilst miRNA expression appeared to be influenced by the presence of additional atopic diseases.

Investigation of differentially expressed mRNAs using the AllerGAtlas asthma gene database found that 10 genes had been previously found to influence asthma pathogenesis. These genes have been demonstrated to influence a number of key components of asthma pathology, including airway remodelling, eosinophil and T cell migration, production of Th2 cytokines (IL-4, IL-5, and IL-13), mast cell degranulation, IgE production, and airway hyperresponsiveness. Moreover, several of the downregulated genes (*CD46*, *IL7R*), have been found to have roles in T regulatory (Treg) cell differentiation

and activation. These cells are important regulators of T cell activity, and thus downregulation of *CD46* and *IL7R* suggests loss of control of T cell activity in the asthmatic subjects. It was further observed that several of the genes detected at altered levels in the asthmatic subjects have antimicrobial activity, thus suggesting that immune dysregulation was influencing how the asthmatic immune system responds to microbes.

It was intriguing to note that Asthma\_4 displayed similar mRNA and miRNA profiles to the control subjects. This asthmatic subject was the youngest member of the asthma cohort, with an age of 19 years, and the subject had been suffering from asthma for just 14 years compared to the mean length of 38 years that the other asthmatic subjects had been living with the disease. It is tempting to speculate that asthmatic mRNA profiles become more divergent from control profiles as the disease progresses, however the sample size of this study restricted further analysis of this. Moreover, at the time of sample collection Asthma\_4 was suffering from the highest number of atopic diseases from the atopic triad (atopic asthma, atopic dermatitis, and allergic rhinitis). It is possible that the presence of atopic dermatitis and allergic rhinitis would augment the observed changes in the RNA profile which could explain why this individual differed to the other asthmatic subjects. That said, it was surprising that the individual displayed increased similarity to the control subjects, and thus further study is warranted to determine whether age, the presence of additional atopic diseases, or variations in the medication taken were responsible for the variation observed.

Sequencing and differential expression analysis identified 13 miRNAs that displayed significant increased expression in the asthmatic subjects compared to the control subjects. Many of the identified miRNAs have been previously associated with elements of asthma pathology and other atopic conditions. miR-148, for example, has been identified as a

candidate biomarker for asthma and allergic rhinitis<sup>408</sup>, whilst miR-382 has been proposed as a biomarker of asthma and COPD<sup>446</sup>. Furthermore, miR-548 has been observed to be dysregulated in asthma bronchial epithelial cells<sup>447</sup> and miR-744 has been found to be elevated in a murine model of chronic asthma<sup>448</sup>. miR's 151a and 24 have been implicated in the pathogenesis of atopic dermatitis<sup>449</sup> and the regulation of allergic inflammation<sup>450</sup>, respectively. miR-326 has been reported to regulate the profibrotic functions of TGF- $\beta$  in pulmonary fibrosis<sup>451</sup>.

The upregulated miRNAs were found to regulate the expression of 1,831 genes. This finding was reflected in the mRNA data, whereby the asthmatic subjects displayed significant gene expression downregulation compared to the control subjects. With regards to asthma pathology, changes in miRNA expression was predicted to significantly affect IgE signalling (Fc-epsilon receptor signalling pathway). IgE is known to be crucial in allergen sensitisation and subsequent atopic disease, and thus it is predicted that the observed miRNA profiles in the asthmatic subjects would have an important role in the initial development of asthma and subsequent HDM-induced asthma exacerbations. It would, therefore, be interesting to determine if what was observed in miRNA profiles of adult asthmatics also occurs in asthmatic children and/ or children with an increased risk of developing asthma. Moreover, as there are distinct differences in asthma prevalence and severity between the two sexes, it would be beneficial to determine if similar miRNA profiles are present in male asthmatics.

#### 3.4.2. Biological Significance of the Asthmatic RNA Profiles

When functional analysis was performed to determine the combined effects of altered mRNA and miRNA expression in the asthmatic subjects, a number of immune functions

were predicted to have significantly altered activity. With regards to upstream regulators predicted to have altered activity in the asthmatic subjects, the activated state of *GFI1* was of interest. *GFI1* encodes a transcription factor that has been observed to have a role in the differentiation and maintenance of ILC2 cells<sup>452</sup>. These cells are potent producers of IL-5 and IL-13, and have been demonstrated to be activated by epithelial cells (IL-25, IL-33, TSLP) and mast cells (LTD<sub>4</sub>, PGD<sub>2</sub>, LXA<sub>4</sub>), and play a critical role in the pathogenic features of experimental asthma in mice<sup>453–459</sup> and clinical disease in humans<sup>460–464</sup>.

Furthermore, *GFI1* activity has also been shown to be induced by T cell activation and IL-4/Stat6 signalling<sup>465</sup>, and is known to enhance Th2 expansion<sup>465</sup>. Increased activity of the transcription regulator, therefore, suggests increased IL-4 signalling in the asthmatic subjects and the presence of a positive feedback loop whereby increased levels of IL-4 in asthmatic subjects results in activation of the *GFI1* transcription regulator, subsequently causing increased IL-4-producing Th2 populations, resulting in further activation of the *GFI1* regulator.

Evidence of increased Th2 expansion and activity in the asthmatic cohort was further supported by the prediction of significant inhibition of the upstream regulator *SOX4* in the asthmatic cohort. This transcription factor has been observed to suppress Th2 differentiation<sup>466</sup>, and thus its inhibition would likely result in increased expansion of the Th2 populations in the asthmatic subjects.

When the predicted downstream effects of altered mRNA and miRNA expression were analysed, similar findings of predicted immune dysregulation were observed. A number of canonical pathways involved in B and T cell activity, including signalling in rheumatoid arthritis, B cell development, and Nur77 signalling in T lymphocytes, were predicted to be significantly affected by the differential expression of mRNA and miRNA in the asthmatic

cohort. It is interesting to note that the canonical pathways involved in rheumatoid arthritis and Type 1 diabetes were identified, as both diseases have been found to display co-occurrence with asthma <sup>467,468</sup>. It is tempting to speculate that the presence of similar/shared underlying immune pathologies in the three diseases.

Unsurprisingly, a number of biological functions were predicted to be altered as a consequence of changed upstream activity and altered canonical signalling. Of relevance to asthma pathology was the observation of predicted decreased leukocyte binding, differentiation of fibroblast lines, and immune responses of leukocytes.

The predicted changes to leukocyte activity was of particular interest. However, at this level of analysis, the downstream effects on biological function of the different classes of leukocytes was not determined, and thus further study would be required to ascertain which class of leukocytes would likely have altered activity in the asthmatic subjects compared to the control subjects as a result of changes to mRNA and miRNA expression. Study of the specific leukocyte affected in the asthma subjects would be crucial, as inhibition of the Th1 or Treg lymphocytes would likely enhance asthma pathophysiology, whereas inhibition of the Th2 and Th17 lymphocyte classes would likely alleviate asthma pathophysiology.

It was also of interest to observe the predicted decrease in killing of natural killer cells. This cell population has been previously identified as having a critical role in immune defence against viruses and bacteria <sup>469-472</sup>. In particular, viral infections have been long characterised to exacerbate asthma <sup>473-476</sup>, and asthmatics have been observed to be deficient in type I IFN production <sup>477-479</sup>, which likely influences natural killer cell activity. Moreover, in a murine model, natural killer cell activity was found to be decreased during a Th2 response <sup>480</sup>. This suggests that in asthmatic subjects there is reduced natural killer

cell activity, resulting in the known associations with asthma and respiratory infections. Moreover, this may also partially explain the changes in the airway microbiome that are observed in asthmatic populations.

### 3.4.3. Protein Characterisation of the Asthma Phenotype

At the protein level there were no significant differences detected in the asthmatic subjects compared to the control subjects. However, there were several interesting observations, and it is predicted that with a larger cohort of subjects, observed differences in the asthmatic subjects compared to the control subjects would be more significant

Firstly, the range of inflammatory protein levels detected within the asthmatic cohort was noticeably higher than the range observed in the control subjects. This was explained by the presence of two distinct clusters in the asthmatic cohort; Cluster one was composed of subjects Asthma\_2 and Asthma\_4, and was characterised by high inflammatory protein levels; and Cluster two was made up of Asthma\_1, Asthma\_3, and Asthma\_5, and was characterised by lower levels of circulatory inflammatory proteins that were similar to those observed in the control subjects. This level of variability observed in the asthma cohort is reflective of the heterogenous nature of asthma pathology and suggests the possibility of asthma sub-phenotypes within the asthma cohort studied.

Of interest was the levels of IL-17A observed. This cytokine, whilst not significantly increased in the asthmatic subjects ( $P$  value = 0.4130, *Wilcoxon rank sum test*), was found to be present at higher levels in the asthmatic subjects who suffered additional atopic diseases (Asthma\_1, Asthma\_2, and Asthma\_4) and the two control subjects who had self-reported atopic dermatitis (Control\_2 and Control\_3). This finding is reflective of previous studies that have detected increased levels of IL-17 associated with asthma severity<sup>481–485</sup>,



the Th2 immune response<sup>486,487</sup>, and atopic dermatitis<sup>486–488</sup>. Moreover, increased levels of IL-17A in asthmatic subjects has been associated with treatment response<sup>484</sup>. The association of IL-17A with the various asthma phenotypes, therefore, warrants further investigation.

Measurement of circulatory total IgE concentrations revealed that IgE was only detectable in half the plasma samples investigated (3 control subjects and 2 asthmatic subjects). The low detection rate of IgE was not unexpected given its short half-life (approximately two days) and low concentration within the blood<sup>64</sup>. There was no significant difference in IgE levels in the asthmatic subjects compared to the control subjects. This was likely due to the small number of samples with detectable levels of IgE. However, it was observed that IgE was detected in the asthma subjects belonging to the proposed Cluster one (Asthma\_2 and Asthma\_4). This provides further support to the theory that within the asthmatic subjects there were two sub-phenotypes present with differing levels of circulatory inflammatory proteins.

Endotoxin protein was detected in all the plasma samples. The protein is a bacterial cell surface protein produced by Gram negative bacteria, and thus the detection of the protein provided evidence of translocation of bacterial cells and/ or bacterial protein into the circulatory vessels.

In contrast to the inflammatory protein and IgE results, measurement of bacterial endotoxin revealed decreased levels of the microbial protein present in the asthmatic subjects compared to the control subjects ( $P$  value = 0.0650, *Unpaired t test*). Moreover, there appeared to be an inverse correlation between circulatory endotoxin levels and the presence of additional atopic diseases. This was a particularly interesting finding as exposure to endotoxin during early childhood has been previously found to be protective

against the development of childhood asthma<sup>489–493</sup>. This association is thought to specifically affect the sensitisation stage of atopic asthma. In rats, for example, Tulic *et al* demonstrated that the protective effects of endotoxin only occurred when the rats were exposed to endotoxin prior to OVA sensitisation<sup>494</sup>.

As this study involved a cohort of adult asthmatics, the observed decrease in endotoxin levels in the asthmatic subjects suggests that the association between reduced endotoxin levels and asthma persists into adulthood and the chronic, life-long form of the disease.

In mice, exposure to endotoxin prior to HDM sensitisation and challenge has been demonstrated to be protective against development of experimental asthma as a result of reduced Th2 cytokine production (IL-5 and IL-13), reduced levels of GM-CSF and CCL20 in the lungs, reduced levels of IgE in the lungs, and reduced recruitment of inflammatory cells (dendritic cells, eosinophils, lymphocytes)<sup>250</sup>. Moreover, when the study was replicated in humans through the use of an *in vitro* model, whereby normal human bronchial endothelial cells were exposed to endotoxin prior to HDM exposure, endotoxin exposure suppressed HDM-induced production of IL-1 $\alpha$  and GM-CSF<sup>250</sup>.

Additionally, endotoxin has been demonstrated to be a potent inducer of IFN $\gamma$ <sup>489,495</sup> and IL-12<sup>496</sup>; two type 1 cytokines that have been demonstrated to promote Th1 differentiation whilst suppressing Th2 differentiation and activity<sup>497–499</sup>. It is, therefore, speculated that exposure to endotoxin during childhood is important in shifting the naïve, Th2-dominant, neonatal immune system towards a more balanced Th1-Th2 immune system; and that by regulating the Th1/Th2 balance endotoxin is protective against HDM sensitisation. In older children and adults, endotoxin is likely protective against HDM challenge by suppressing the endothelial cells reactivity towards the HDM allergen, and reduced levels of the protein is likely to result in increased bronchial reactivity towards the allergen.

In addition to reduced exposure to endotoxin in the environment, reduced levels of endotoxin in the asthmatic subjects may also be due to the constant state of increased immune activity in the asthmatic subjects. IL-17A, for example, was increased in the asthmatic subjects and has previously been demonstrated to be positively associated with expression of anti-microbial peptides<sup>500,501</sup>. Endotoxin is an inflammatory protein present in the outer membrane of Gram negative bacteria, and thus reduced levels of the protein may represent reduced microbial populations present in the asthmatic subjects due to increased concentrations of circulatory anti-microbial peptides as a result of increased IL-17A activity. This interpretation is further supported by genomic characterisation of the asthmatic subjects, which revealed increased expression of *MPO* and *TLR1* in the asthmatic subjects compared to the control subjects. Both genes encode proteins involved in antimicrobial activity (Myeloperoxidase and Toll-like receptor 1, respectively), and thus upregulation of these genes has the potential to influence microbiome composition.

#### 3.4.4. Identification of Peripheral Biomarkers

Asthma is increasingly being recognised as a clinical umbrella term to describe a chronic respiratory disorder caused by a variety of disease phenotypes and endotypes. The disease is highly heterogeneous and current diagnostic tools are increasingly being recognised as insufficient tools in the correct identification of the asthma phenotypes/ endotypes.

Biomarkers have been proposed as a means of performing risk assessment before clinical diagnosis, to determine the disease stage and severity following asthma diagnosis, and as a means of monitoring responsiveness to treatment<sup>112</sup>. The majority of studies investigating potential asthma biomarkers have focused on clinical samples taken from the airways. However, the techniques used to obtain these samples are invasive and not

suitable for daily clinical activity. The collection of blood samples, however, is significantly less invasive and easily obtained in the clinical setting.

This study aimed to identify potential asthma biomarkers present in blood samples. With regards to RNA biomarkers, there was a significant number of mRNAs and miRNAs that were present at significantly altered levels in the asthmatic subjects compared to the control subjects.

A total of 287 genes were found to exhibit significant differential expression in the asthmatic subjects compared to the control subjects. The high number of genes identified made it difficult to determine which genes would be useful blood biomarkers of asthma, and thus further study involving a larger asthma cohort would be required to determine if the identified genes would remain statistically significant in a larger asthmatic population.

Analysis of the identified genes did, however, detect a number of genes that showed promise as potential blood biomarkers of asthma. These genes included 10 genes listed on the AllerGAtlas database of genes associated with asthma pathogenesis (*CD46*, *FN1*, *GSTA1*, *IL7R*, *LGALS3*, *MPO*, *NTS*, *PDE4A*, *TLR1*, *VDR*) and a number of genes that were uniquely detected in the asthma blood samples (including *HIST1H3C*, *PRAM1*, *RAB6B* and *CD93*). *CD93* was of particular interest as elevated levels of soluble CD93 protein have been previously reported in the serum of asthmatics during acute asthma exacerbations<sup>502</sup> and in the serum of steroid-naïve asthmatic patients<sup>503 503</sup>.

With regards to miRNA profiles, the asthmatic subjects exhibited overall increased miRNA expression, with 13 miRNAs detected at significantly increased levels in the asthmatic subjects compared to the control subjects. Increased total miRNA levels may, therefore, function as a blood biomarker of asthma. With regards to specific miRNA biomarkers, several of the significantly increased miRNAs showed promise. miRNA-148<sup>408</sup> and miRNA-

382<sup>446</sup>, for example, have been previously identified as potential blood biomarkers for asthma, whilst miR-548<sup>448</sup>, miR-744<sup>448</sup>, and miR-24<sup>450</sup> have demonstrated to contribute towards asthma pathology .

As for potential protein blood biomarkers GM-CSF, IFN $\gamma$ , TARC, and endotoxin showed the most promise. However, as levels of these proteins were not quite present at significantly altered levels in the blood of asthmatics compared to the control subjects, further investigation would be required to determine their usefulness as biomarkers.

#### 3.4.5. Chapter Summary

In summary the occurrence of atopic asthma associated with HDM sensitisation in a cohort of adult females was found to have a significant impact on the levels of circulating mRNA and miRNA. RNA functional analysis revealed a number of biological pathways involved in immune activity are likely to be significantly altered in the asthmatic subjects. Further support of immune dysregulation in the asthmatic subjects was provided by inflammatory protein analysis, whereby the asthmatic subjects were found to exhibit of overall increased trend in levels of circulatory, pro-inflammatory proteins. RNA analysis also revealed that the asthmatic subjects likely have altered microbial defence activity compared to the control subjects, which likely explains the observed decreased levels of endotoxin detected in the asthmatic plasma samples.

With regard to blood biomarker identification a number of RNAs and proteins showed promise as potential use as asthma biomarkers. A larger study, however, would be required to determine the validity of the identified RNAs and proteins as potential biomarkers as this study was a preliminary investigation.

## Chapter 4: Characterisation of the Circulatory Microbiome in Atopic Asthma

### 4.1. Introduction

Changes in the asthma microbiome have been well described for both the airways and the gut <sup>242, 254, 263,255–262</sup>. Alterations to the asthma microbiomes have been detected both in early infancy and in later life, and microbial dysbiosis in the asthmatic microbiome has been associated with asthma development, severity, and treatment responsiveness. This suggests that characterisation of the microbiome could be used in asthma diagnosis, analysis of disease severity and treatment response, and identification of infants at risk of disease development.

However, collection of the samples typically used to characterise the airway and gut microbiome (BAL fluid and faecal samples, respectively) is not practical for daily clinical practice. Faecal sample collection, for example, has been linked to low patient compliance rates <sup>504</sup>, whilst the collection of BAL samples is invasive and associated with ethical concerns with regards to sample collection from young children <sup>102,505</sup>.

In contrast, blood samples are relatively simple to collect in the clinical setting. Characterisation of the circulatory microbiome in asthmatic subjects compared to control subjects would, therefore, be of benefit as it would enable the identification of circulatory microbial biomarkers that could be used in asthma diagnosis and assessment.

However, whilst colonisation of various body sites that are in contact with the external environment (such as the gastrointestinal tract, skin, and respiratory tract) by microorganisms is both well-described and universally accepted, the existence of microbial

populations in other “classically sterile” locations, such as the blood, is a relatively new concept<sup>309</sup>.

Traditionally, the blood was thought to be a sterile environment during good health, and the presence of microbes within circulation was thought to only occur during cases of sepsis<sup>310</sup>. However, over the past few decades there has been mounting evidence to support the existence of a circulatory microbiota/ microbiome in mammals.

Investigations into the circulatory microbiota/ microbiome have primarily focussed on characterising the circulatory microbiome using the culture-independent technique of amplifying and sequencing the bacterial 16S rRNA gene. These studies are increasingly demonstrating the presence of bacterial DNA in whole blood<sup>310, 323, 327–329, 331–334, 338</sup>, plasma<sup>324, 327, 330, 336, 358, 506</sup>, buffy coat<sup>327, 339</sup>, serum<sup>335, 363, 366, 507</sup>, red blood cells<sup>327</sup>, peripheral leukocytes<sup>322, 337</sup> and neutrophils<sup>331</sup>, and coronary tissue<sup>321</sup> samples from healthy human donors and various other mammalian species<sup>340–344</sup>.

The blood circulates the body, where it functions as a medium the samples from virtually all body sites<sup>358</sup>. The general consensus regarding the origins of the bacterial structures and DNA detected in the blood is that it is likely the result of atropobiosis, a process whereby microbial DNA and/ or viable microorganisms translocate from other microbial niches, such as the gastrointestinal tract, oral cavities, and airways, and enter the circulation<sup>311, 325</sup>.

Another proposed explanation for the microbial structures and DNA detected in blood samples is that microbial contamination occurs during sample collection and/ or during downstream experimental procedures. However, this explanation seems less likely given the increasing numbers of investigations successfully characterising a circulatory microbiota/ microbiome. Moreover, across the different studies similar bacterial

populations are being reported, and significant changes in the circulatory microbiota/microbiome are being reported in diseased states.

The association of the various diseased states with changes in the circulatory microbiota/microbiome is likely to reflect microbial dysbiosis at distant body sites. Characterisation of the circulatory microbiota/microbiome, therefore, offers the potential opportunities for novel biomarker and therapeutic development.

#### 4.1.1. Aims of the Chapter

The aim of this investigation was to continue the work described in Chapter 3 by investigating potential microbial biomarkers of atopic asthma.

This was achieved by developing a reliable and efficient 16S rRNA sequencing protocol that enabled successful characterisation of the circulatory microbiome in the previously described cohort of female asthmatic and control subjects. Statistical analysis was performed to compare differences in bacterial diversity, abundance, and function in the asthmatic circulatory microbiome, and bacterial culture techniques were applied to determine the presence of viable bacteria in the plasma samples.



## 4.2. Methods

### 4.2.1. Sample Collection

Characterisation of the circulatory microbiome was performed on plasma samples taken from the asthmatic and control subjects described in Chapter 3. In brief, 5 atopic asthmatic subjects with physician diagnosed HDM allergy were recruited to the study through *Sera Laboratories Limited*. Asthma subjects were selected on the basis that they had developed atopic asthma during early childhood and that their condition had continued into adulthood and was classed as “poorly controlled”. An additional 5 non-asthmatic healthy subjects that were age and gender matched to the asthmatic subjects were recruited as control subjects.

Whole blood was drawn, following alcohol cleansing of the skin surface, into EDTA containing tubes and stored on ice prior to centrifugation at 1000×g to obtain the plasma component.

### 4.2.2. Extraction of bacterial DNA from the Human Plasma Samples

Bacterial DNA was extracted from the human plasma samples using the QIAamp UCP Mini Pathogen kit (*Qiagen*). The bacterial cells present in the plasma samples were lysed by transferring 200µl of plasma sample and 100µl ATL lysis buffer into sterile pathogen lysis tubes. The tubes were vortexed horizontally at 13,000×g for 10 minutes and then centrifuged for 5 seconds at 8,000×g.

The supernatant (200µl) was transferred into sterile 2ml Eppendorf tubes and proteinase K (20µl) was added to denature any proteins present in the plasma samples. Following a 10-minute incubation at 56°C, buffer APL2 (100µl) was added and the lysate were vortexed

for 30 seconds. The tubes were then incubated at 70°C for 10 minutes. Ethanol (150µl) was added and the lysate mixture was mixed thoroughly by vortexing for 30 seconds. The lysate mixture was then transferred to QIAamp UCP Mini Columns and centrifuged for 1 minute at 8,000xg.

The filtrate was discarded and the QIAamp UCP Mini Columns were transferred to new 2ml collection tubes. The columns were then washed through the addition of APW1 (300µl) and centrifugation at 8,000xg for 1 minute. The columns were transferred to new collection tubes and washed with APW2 buffer (375µl). The tubes were centrifuged at full speed (13,000xg) for 3 minutes and transferred to new collection tubes and centrifuged at full speed for 1 minute. The collection tubes were then incubated at 56°C for 3 minutes to enable evaporation of any residual ethanol/ buffer solution present in the columns. The columns were transferred to sterile 1.5ml elution tubes and elution buffer (20µl) was added the centre of the QIAamp UCP mini column membranes and the tubes were incubated at room temperature for 1 minute. The tubes were then centrifuged at full-speed for 1 minute to elute then DNA, and the eluted DNA was placed in storage at -20°C.

An experimental negative control was generated, whereby human plasma was replaced with UV-treated molecular biology grade water. The negative control underwent all the same DNA extraction steps as the human plasma samples and was generated to test for bacterial DNA contamination that may occur due to bacteria/ bacterial DNA present in the immediate environment and/ or present in the laboratory reagents

#### 4.2.3. Development of a Protocol for PCR amplification of the V3-V4 region of the bacterial 16S rRNA gene in Human Plasma Samples

Amplification and sequencing of the bacterial 16S rRNA gene was initially performed using oligonucleotide primers that target the hypervariable regions 3 and 4 (V3-V4 region). Amplification of the V3-V4 region was performed on microbial DNA extracted from the human plasma samples using QIAamp UCP Mini Pathogen kit (*Qiagen*), followed by end-point PCR using oligonucleotide primers that target the V3-V4 region of the 16S rRNA gene (V3-V4 primers) (Table 4.1). These primers had previously been designed by Herlemann and colleagues (2011)<sup>508</sup> and confirmed as providing a good representation of bacterial diversity down to the genus level by Klindworth *et al* (2013)<sup>509</sup>.

**Table 4.1: Molecular properties of the primers used to amplify the V3-V4 region of the bacterial 16S rRNA gene.**

Primer	Sequence (5' -> 3')	Concentration [pmol/μl]	Melting temperature (°C)	GC Content (%)
V3-V4 Fwd	CCTACGGGNGGC WGCAG (17)	10.0	61.2	73.5
V3-V4 Rev	GACTACHVGGGT ATCTAATCC (21)	10.0	57.9	47.6

Gradient PCR using the GoTaq Green master mix (*Promega*) and *Escherichia coli* DNA (25ng/μl) was performed to determine the optimum V3-V4 annealing temperature. The PCR reactions were performed using the recommended protocol and the following annealing temperatures; 54°C, 55°C, 56°C, 57°C, 59°C, and 61°C.

End-point PCR using the optimum V3-V4 primer annealing temperature and the GoTaq Green master mix protocol was performed on microbial DNA extracted from the plasma samples. The protocol was unsuccessful and so V3-V4 amplification was performed directly

on the plasma samples using a Phusion blood direct PCR kit (*Thermo Fisher Scientific*) and the recommended protocol. The PCR reaction was performed using 5% plasma and 20% plasma to determine the optimum plasma concentration required. The protocol was successful at amplifying the V3-V4 region. However, when the protocol was performed using modified V3-V4 primers (mV3-V4) primers designed to generate V3-V4 amplicons containing the required ion torrent sequencing motifs, the protocol was unsuccessful. This led to the development of a nested PCR protocol. Different lengths of first and second stage nested PCR cycles were performed to determine the optimum number of PCR cycles required to successfully amplify the V3-V4 region and attach Ion torrent sequencing motifs to the V3-V4 amplicons.

Attachment of the Ion torrent sequencing motifs was essential as it enabled the sequenced V3-V4 reads to be demultiplexed (separated into individual sample sequencing files) on the basis of the barcode sequence. For instance, when amplifying the V3-V4 region in the plasma sample from Control\_1 a modified V3-V4 (mV3-V4) Fwd primer with a barcode (BC)1 was used, whilst for Control\_2 a mV3-V4 Fwd primer with a BC2 barcode attached was used (Figure 4.1). Following sequencing, sequenced reads with a BC1 nucleotide sequence were placed in one data file, whilst V3-V4 sequenced reads with a BC2 nucleotide sequence were placed in a second data file, thus enabling microbial profiling of the individual plasma samples (Figure 4.1).

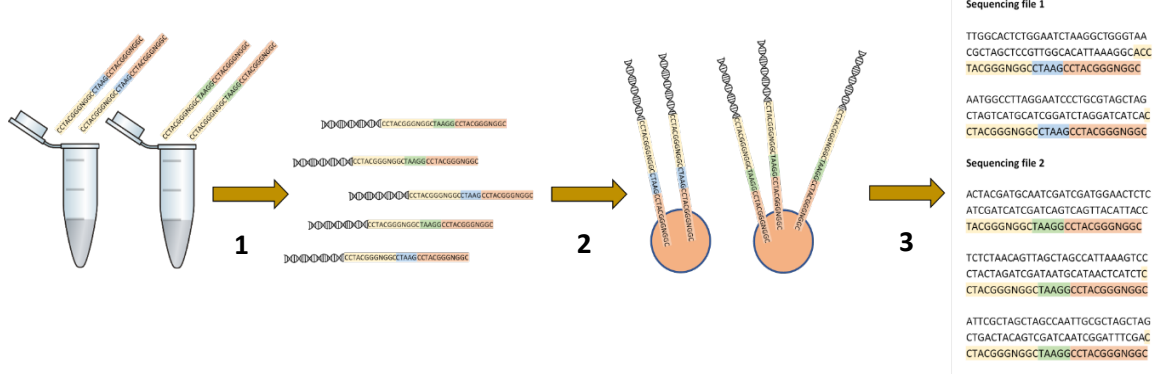
In addition to attaching a unique barcode sequence to the V3-V4 reads generated from the different plasma samples, an Ion A-adapter (5'-CCATCTCATCCCTGCGTGTCTCCGACTCAG-3') and key sequence (TCAG) were attached to the V3-V4 amplicons using the forward primer (Figure 4.1, see also Supplementary Materials, Table S8), and a truncated P1 adapter (TrP1; 5'-CCTCTCTATGGGCAGTCGGTGATGACTACHCGGGTATCTAATCC-3') was attached to the V3-

V4 amplicons using the reverse primer. This enabled generation of V3-V4 amplicons with the required motifs for the amplicons to be sequenced uni-directionally using an Ion torrent personal genome (PGM) system (*Thermo fisher Scientific*)<sup>510</sup>.

**A.**

Primer	Sequence (5' -> 3')	Concentration [pmol/μl]	Melting temperature (°C)	GC Content (%)
mV3-V4 Fwd BC1	CCATCTCATCCCTGCGT GTCTCCGACT <b>CAG</b> CTA AGGTAACCCTACGGG NGGCWGCAG(57)	10.0	82.7	60.6
mV3-V4 Fwd BC2	CCATCTCATCCCTGCGT GTCTCCGACT <b>CAG</b> TAA GGAGAACCCTACGGG NGGCWGCAG (57)	10.0	58.3	50.0

**B.**



**Figure 4.1: Attachment of a barcode and adaptor to the V3-V4 amplicons during end-point PCR amplification of the V3-V4 region of the bacterial 16S rRNA gene. (A)** Molecular properties of the V3-V4 forward primer containing the Ion-A adaptor, the sequencing key, and either barcode BC1 or BC2 attached. Yellow nucleotides = A-adaptor, Blue nucleotides = BC1, green nucleotides = BC2, orange nucleotides = V3-V4 forward primer sequence, and bold text indicates the location of the sequencing key. **(B)** A schematic diagram of the use of barcoded primers in the amplification and sequencing of the V3-V4 region of the 16S rRNA gene using two plasma samples. **(B1)** Amplification of the V3-V4 beads with sequencing barcode and adaptor added. **(B2)** Attachment of the V3-V4 amplicons to the sequencing bead using the sequencing adaptor. **(B3)** Generation of individual sample sequencing data.

#### 4.2.4. Nested PCR Amplification of the V3-V4 region of the bacterial 16S rRNA gene in Human Plasma Samples

Following successful development of a nested PCR protocol for amplifying the V3-V4 region of the bacterial 16S rRNA gene, the protocol was applied to the human plasma samples. This involved first amplifying the V3-V4 region in triplicate using the optimised Phusion blood direct PCR protocol and 5% human blood (Table 4.2).

**Table 4.2: First stage of Nested PCR amplification of the V3-V4 region of the bacterial 16S rRNA gene human plasma samples.** The first stage of nested PCR amplification of the V3-V4 region of the 16S rRNA gene from 5% human plasma involved amplifying the V3-V4 region using a Phusion blood direct PCR protocol. **(A)** The reagents used in the Phusion blood direct PCR protocol. **(B)** The cycling parameters used in the Phusion blood direct PCR protocol.

##### A.

Reagent	Volume (µl)
2X Phusion blood PCR buffer	10.0
Phusion blood II DNA polymerase	0.4
V3-V4 Fwd primer	1.5
V3-V4 Rev primer	1.5
UV-treated molecular biology grade water	5.6
Human Plasma	1.0

##### B

Cycle Step	Temperature (°C)	Time	Cycles
Initialisation	98	5 minutes	1
Denaturation	98	1 second	
Annealing	55	5 seconds	35
Extension	73	15 seconds	
Final Extension	73	1 minute	1

Following confirmation of successful amplification of the V3-V4 region using gel electrophoresis the V3-V4 amplicons underwent DNA purification using the MinElute protocol (see Chapter 2, sections 2.1-2.3 for protocols). A second stage of PCR was then performed on the purified V3-V4 amplicons using the mV3-V4 primers and the GoTaq Green master mix protocol (Table 4.3). This was carried out in order to attach the Ion torrent sequencing motifs (the Ion A and TrP1 adaptors, a sequencing key, and a unique barcode nucleotide sequence) onto the purified V3-V4 amplicons.

**Table 4.3: Second stage nested PCR protocol used to attach the Ion torrent sequencing barcode and adaptors to purified V3-V4 amplicons generated from human plasma samples.** Following purification of V3-V4 amplicons generated from plasma samples second stage nested PCR was performed to attach Ion torrent sequencing motifs onto the V3-V4 amplicons. This was performed using a Green master mix PCR protocol and V3-V4 primers modified to contain the Ion torrent sequencing motifs. **(A)** The reagents used in the Green master mix end-point PCR protocol, **(B)** The cycling parameters used in the Green master mix end-point PCR protocol.

**A.**

Reagent	Volume (µl)
GoTaq Green Master mix	12.5
mV3-V4 (BC1 – BC10) Fwd primer	2.0
mV3-V4 Rev (TrP1) primer	2.0
UV-treated molecular biology grade water	6.5
Purified V3-V4 amplicons	1.5

**B.**

Cycle Step	Temperature (°C)	Time	Cycles
Initial denaturation	95	2 minutes	1
Denaturation	95	30 seconds	
Annealing	55	30 seconds	7
Extension	68	45 seconds	
Final Extension	68	7 minutes	1

In order to monitor the possible introduction of contaminating microbial DNA an experimental negative control was generated during the first stage of nested PCR, whereby UV-treated molecular biology grade water replaced human plasma during the PCR set-up. PCR products generated from the experimental negative control then underwent all the same downstream procedures as the PCR products generated from the human plasma samples (gel electrophoresis, V3-V4 amplicon purification, second stage nested PCR, Ion torrent sequencing).

#### 4.2.5. Amplification of the V4 region of the 16S rRNA gene

In addition to sequencing the V3-V4 region of the bacterial 16S rRNA gene, the V4 region of the bacterial 16S rRNA gene was also amplified and sequenced using oligonucleotide primers that target the hypervariable V4 region of the 16S rRNA gene (V4 primers) (Table 4.4).

**Table 4.4: Molecular properties of the primers used to amplify the V4 region of the 16S rRNA gene.**

Primer	Sequence (5' -> 3')	Concentration [pmol/μl]	Melting temperature (°C)	GC Content (%)
V4_Fwd	GTGCCAGCMGCCGCGGT AA (19)	10.0	64.2	71.1
V4_Rev	GGACTACHVGGGTWTCT AAT (20)	10.0	55.2	45.0

Amplification of the V4 region of the 16S rRNA gene was performed on the human plasma samples using the nested PCR protocol initially developed for amplification and sequencing of the V3-V4 region of the bacterial 16S rRNA gene. Direct amplification of the V4 region



was first performed in triplicate on the human plasma samples using the optimised Phusion blood direct PCR protocol (Table 4.2) and the V4 primers.

Following confirmation of successful amplification of the V4 region using gel electrophoresis, the V4 amplicons generated from the triplicate PCR's were combined and purified using the MinElute PCR purification kit (see Chapter 2, sections 2.1 and 2.2.1 for a full description of the methods used). Second stage nested PCR was then performed on the purified V4 amplicons in order to attach the Ion torrent sequencing motifs and the Illumina sequencing motifs onto the amplicons, as described in the below sections.

An experimental negative control was generated to enable monitoring of possible bacterial DNA contamination during the experimental procedures. This involved replacing human plasma with UV-treated molecular biology grade water during the first stage of nested PCR amplification of the V4 region. PCR product generated from the negative controls then underwent all the downstream procedures as the V4 amplicons generated from the human plasma samples (gel electrophoresis, V4 amplicon purification, second stage nested PCR, Ion torrent sequencing).

#### 4.2.6. Preparation of the V4 amplicons for Ion Torrent Sequencing

To prepare the V4 amplicons for ion torrent sequencing, a second round of PCR was performed on the purified amplicons in order to attach the ion torrent sequencing motifs.

In order to attach the sequencing motifs, the V4 primers were modified to contain the ion torrent sequencing motifs. 10 different modified forward V4 16S Amp primers were developed that all contained the A1 adaptor, the ion sequencing key, and a unique barcode.

A modified reverse V4 primer was also developed to contain the TrP1 adaptor (Supplementary Materials, Table S9).

7 cycles of PCR were then performed on the purified V4 amplicons using the modified V4 (mV4) primers (a different modified forward primer was used for each sample) and an Accuprime *Pfx* SuperMix (*Thermo Fisher Scientific*) end-point PCR protocol (Table 4.5).

**Table 4.5: Second stage nested PCR protocol used to attach the Ion torrent sequencing barcode and adaptors to purified V4 amplicons generated from human plasma samples.** Following purification of V4 amplicons generated from plasma samples second stage nested PCR was performed to attach Ion torrent sequencing motifs onto the V4 amplicons. This was performed using an Accuprime PCR protocol and V4 primers modified to contain the Ion torrent sequencing motifs. **(A)** The reagents used in the Accuprime end-point PCR protocol, **(B)** The cycling parameters used in the Accuprime end-point PCR protocol.

**A.**

Reagent	Volume ( $\mu$ l)
Accuprime <i>Pfx</i> SuperMix	22.5
mV4 (BC1 – BC10) Fwd primer	0.5
mV4 Rev primer	0.5
Purified V4 amplicons	1.5

**B.**

Cycle Step	Temperature ( $^{\circ}$ C)	Time	Cycles
Initial denaturation	95	2 minutes	1
Denaturation	95	30 seconds	
Annealing	55	30 seconds	7
Extension	68	45 seconds	
Final Extension	68	7 minutes	1

#### 4.2.7. Preparation of the V4 amplicons for Illumina Sequencing

In addition to being sequenced using Ion torrent sequencing technology, the V4 amplicons also underwent Illumina MiSeq sequencing. This involved generating V4 amplicons from the human plasma samples that contained the Illumina Nextera Transposase (XT) adapters required for Illumina sequencing (Table 4.6).

**Table 4.6: Molecular properties of the 515F/806R oligonucleotide primers used to incorporate the Illumina Nextera transposase adapters.** Following successful amplification of the V4 region of the 16S rRNA gene the Illumina XT adapters were attached to the V4 amplicons using PCR and V4 16S Amp primers (blue) modified to contain the XT adapter (purple).

Primer	Sequence (5' -> 3')	Concentration [pmol/μl]	Melting temperature (°C)	GC Content (%)
515F	TCGTCGGCAGCGTCAGATG TGTATAAGAGACAGGTGCC AGCMGCCGCGGTAA (52)	10.0	64.2	71.1
806R	GTCTCGTGGGCTCGGAGAT GTGTATAAGAGACAGGGAC TACHVGGGTWTCTAAT (54)	10.0	55.2	45.0

In order to generate V4 amplicons containing the Illumina sequencing motifs the nested PCR protocol developed for amplification of the V3-V4 amplicons was utilised and adapted. The first stage of nested PCR was performed to amplify the V4 region the optimised Phusion blood direct protocol (see Table 4.2).

Successful amplification was determined using gel electrophoresis (see Chapter 2, section 2.1 for a full description), and amplicons from successful triplicate reactions were combined and purified using the MinElute PCR purification kit (*Qiagen*) (See Chapter 2, section 2.2.1 for a full description).

A further 7 cycles of PCR were performed on the amplicons to incorporate the Illumina XT adapters in preparation for Illumina sequencing. This involved using a AccuPrime *Pfx* SuperMix PCR protocol and the primer pair 515F and 806R V4 primers developed by Caporaso *et al* (2011)<sup>511</sup> and optimised by Parada *et al* (2016)<sup>512</sup> (Table 4.7).

**Table 4.7: Second stage nested PCR protocol used to attach Illumina sequencing motifs to purified V4 amplicons generated from human plasma samples.** Following purification of V4 amplicons generated from plasma samples, second stage nested PCR was performed to attach Illumina XT sequencing motifs onto the V4 amplicons. This was performed using an Accuprime PCR protocol and V4 primers modified to contain the Ion torrent sequencing motifs. **(A)** The reagents used in the Accuprime end-point PCR protocol. **(B)** The cycling parameters used in the Accuprime end-point PCR protocol.

**A.**

Reagent	Volume (µl)
Accuprime <i>Pfx</i> SuperMix	22.5
515F primer	0.5
806R primer	0.5
Purified V4 amplicons	1.5

**B.**

Cycle Step	Temperature (°C)	Time	Cycles
Initial denaturation	95	2 minutes	1
Denaturation	95	15 seconds	
Annealing	55	30 seconds	7
Extension	68	25 seconds	
Final Extension	68	10 minutes	1

#### 4.2.8. Sequencing of the V3-V4 amplicons and the V4 16S rRNA amplicons using Ion Torrent Sequencing Technology

Following successful generation of the V3-V4 amplicons and V4 amplicons containing the ion torrent sequencing motifs from human plasma, ion torrent sequencing was carried out. The amplicon concentrations were first quantified using a Qubit 3.0 double stranded DNA (dsDNA) high-sensitivity (HS) assay (*Thermo fisher Scientific*) and then diluted to a 100pM concentration. The diluted amplicons were then sequenced using the Ion PGM™ Hi-Q™ protocol.

#### 4.2.9. Quantification of amplicon concentration using Qubit dsDNA High-Sensitivity Assay

The Qubit® working solution was first prepared by diluting the Qubit® dsDNA HS Reagent 1:200 in Qubit® dsDNA HS buffer. Two DNA standards, S1 (0 ng/μl in TE buffer) and S2 (10ng/μl in TE buffer) were prepared by transferring 190μl of working solution to a sterile 500μl PCR tubes and adding 10μl of each Qubit® standard to the appropriate tube. The standards were then mixed with the working solution by vortexing 2-3 seconds. Individual sample tubes were then generated containing 1μl of the purified amplicons generated from each plasma sample and 199μl of working solution. The sample assay tubes were mixed by vortexing 2-3 seconds, and then left to incubate at room temperature for 2 minutes.

The S1 tube was then loaded into the Qubit® 3.0 Fluorometer sample chamber and the dsDNA HS assay type was selected. The assay was calibrated by first reading S1 and then loading and reading the S2 assay tube. Following calibration, the individual sample tubes were loaded into the sample chamber and the concentration of dsDNA was measured.

Following quantification of the purified amplicons, the amplicons were diluted to 100pM and sequenced using an ion torrent PGM machine following the recommended Ion PGM™ Hi-Q™ protocol (*Thermo fisher Scientific*).

#### 4.2.10.Generation of Template Positive Ion Sphere Particles

Enriched, template-positive Ion PGM™ Hi-Q Ion Sphere™ Particles (ISPs) with 400bp average insert libraries were generated from the diluted V3-V4/ V4 amplicon samples. This involved using the PGM: Ion PCM™ Hi-Q™ OT2 KIT- 400 kit (*Thermo fisher Scientific*) and the Ion OneTouch™ 2 instrument (*Thermo fisher Scientific*) to prepare template-positive ISPs containing the V3-V4/V4 amplicons.

An amplicon library was first generated by transferring 5µl of each 100pM amplicon sample into a fresh Eppendorf tube to generate a 100pM library containing amplicons generated from all the plasma samples. The library was then diluted by mixing 6.5µl of amplicon library with 18.5µl of nuclease free water. The Ion PGM™ Hi-Q ISPs were then prepared by vortexing at maximum speed for 1 minute, centrifuging for 2 seconds, and pipetting up and down 20 times to resuspend the particles.

An amplification solution containing nuclease free water (25µl), Ion PGM™ Hi-Q™ enzyme mix (50µl), diluted amplicon library (25µl), and Ion PGM™ Hi-Q™ ISPs (100µl), was prepared and vortexed at maximum speed for 5 seconds. The amplicon solution was then loaded immediately into the sample port of the Ion OneTouch™ reaction filter. 1.7ml of Ion OneTouch™ reaction oil was loaded into the filter and the OneTouch™ machine was run using the PGM™ Hi-Q™ OT2 kit – 400.

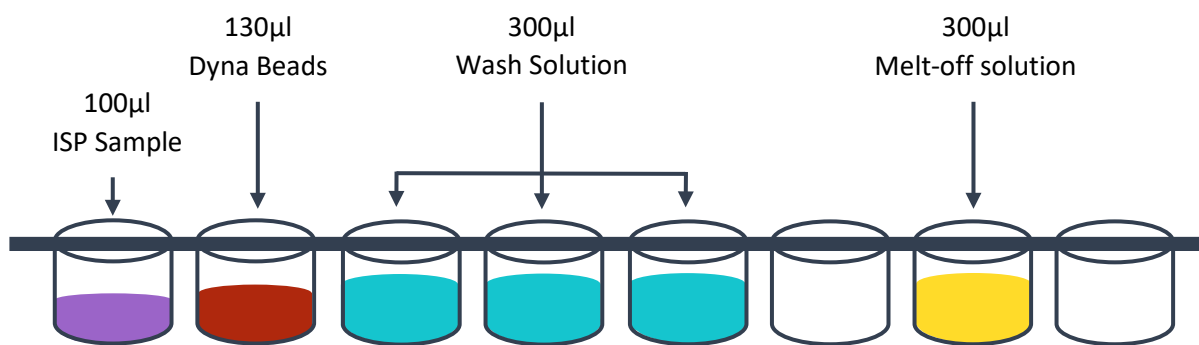
Following completion of the OneTouch 2 run, the Ion OneTouch™ recovery tubes were removed from the machine, and all but 100µl of recovery solution was removed from each tube. The ISP pellet present in each tube was resuspended in the remaining recovery solution, and 500µl of Ion OneTouch™ wash solution was added to each recovery tube. The recovery tube solution was then pipetted up and down to fully disperse the ISPs, and the solution from each recovery tube was transferred into a 1.5ml Eppendorf tube. The ISPs were then centrifuged for 2.5 minutes at 13,000xg, and then all but 100µl of wash solution was removed from the Eppendorf tube.

#### 4.2.11. Enrichment of the Template-Positive Ion Sphere Particles

The template-positive ISPs were then enriched using the Ion OneTouch™ Enrichment system (ES) (*Thermo fisher Scientific*) and the recommended protocol.

The Ion OneTouch™ ES melt-off solution was first prepared by mixing Tween® solution (280µl) with 1M NaOH (40µl). Dynabeads® MyOne™ Streptavidin C1 (Dyna) beads were then vortexed for 30 seconds to resuspend the beads. 13µl of Dyna beads were transferred to a fresh 1.5ml Eppendorf tube, and the Eppendorf tube was placed on a magnet for 2 minutes. The Dyna bead supernatant was removed, and the Dyna bead pellet was resuspended in 130µl of MyOne™ Beads wash solution.

Once the OneTouch 2™ ES reagents had been prepared, they were loaded into an 8-well strip in the below layout (Figure 4.2), and the strip of 8 wells was loaded onto the OneTouch™ 2 ES tray. 10µl of neutralisation solution was transferred into a fresh 0.2ml PCR tube, and the tube was loaded into the tube holder at the base of OneTouch™ tip loader. A new tip was attached to the tip loader and then the OneTouch™ 2 ES program was run.



**Figure 4.2: A schematic diagram showing the order and volume of OneTouch™ 2 ES reagents loaded into the OneTouch™ ES following reagent preparation.**

#### 4.2.12. Quality Control Testing of the Template Positive Ion Sphere Particles

Quality control testing was then performed to determine the percentage of templated ISPs generated from the amplicon samples. This was achieved using the Qubit 3.0 Ion sphere quality control protocol.

The Ion sphere quality control Alexa fluor 488 and Alexa fluor 647 calibration standards were thawed, vortexed for 1 minute, and then centrifuged for 30 seconds at 13,000xg. 200µl of each standard was transferred into individual Qubit assay tubes and then centrifuged briefly at 13,000xg. The Ion Sphere protocol was selected on the Qubit 3.0 fluorometer and the raw fluorescence values were measured for each of the standards.

19µl of annealing buffer and 1µl of ion probes (green-fluorescent Alexa Fluor 488 dye-labelled oligonucleotides and red-fluorescent Alexa Fluor 647 dye-labelled oligonucleotide) was then mixed with 2.0µl of the enriched, template-positive ISP library. The ISP library was then heated to 95°C for 3 minutes and 37°C for 2 minutes. Unbound ion probes were then removed by washing the ISP library 3 times using the following protocol. 200µl of Quality control wash buffer was added to the ISP library and the mixture was vortexed briefly and



then centrifuged for 1.5 minutes at 13,000xg. The supernatant was removed, and the washing procedure was repeated twice more.

After the final wash, 190µl of the Quality control wash buffer was added to the ISP library and mixed by pipetting up and down 5 times. The sample was then transferred to a fresh Qubit assay tube and sample fluorescence emission of each dye conjugate was measured.

All ISPs bind to the Alexa Fluor 488 oligonucleotide, and thus measurement of the Alexa Fluor 488 conjugate measured total ISPs present in the sample. In contrast, only template-positive ISPs bind to the Alexa Fluor 647 labelled oligonucleotides, and thus the percentage of template-positive ISPs could be determined from the ratio of the Alexa Fluor 647 dye signal to the Alexa Fluor 488 dye signal.

#### 4.2.13. Sequencing of the Ion Sphere Particle Templates

Following confirmation of successful attachment of the amplicons to the ISPs beads, the attached amplicon templates were sequenced using the recommended Ion PGM™ Hi-Q™ protocol and the Ion PGM system (*Thermo fisher Scientific*).

A sequencing plan was generated using the ion torrent browser. The Ion PGM™ Sequencer was then cleaned and initialised using the recommended protocol. Following successful initialisation of the sequencer, the enriched, template-positive ISPs were mixed with 5µl of control ISPs and centrifuged for 2 minutes at 13,000xg. The supernatant was removed, and the ISP pellet was mixed with 12µl of Sequencing Primer to a total volume of 27µl (Annealing buffer was added if required to ensure the total volume was 27µl). The pellet was then disrupted by pipetting up and down 20 times, and ISP-Sequencing Primer samples were heated to 95°C for 2 minutes and then 37°C for 2 minutes using a thermal cycler.

A Chip check was then performed on a new Ion 314™ Chip v2 following the recommended *Thermo fisher* protocol to ensure the sequencing chip was functioning correctly. The ISP-Sequencing primer samples were removed from the thermocycler and 3µl of Ion PGM™ Hi-Q™ Sequencing Polymerase was added to the samples. The samples were pipetted up and down 20 times to ensure thorough mixing, and then incubated for 5 minutes at room temperature.

Following Chip calibration, the chip was removed from the Ion PGM™ Sequencer and as much liquid as possible was removed from the chip's loading port. The chip was then centrifuged upside-down for 5 seconds to ensure the chip was completely emptied of liquid. 10µl of the prepared ISPs was then loaded into the chip, and the chip was centrifuged for 30 seconds whilst pointing in, and then centrifuged for a further 30 seconds whilst pointing out. The loaded ISPs were then slowly pipetted out and back into the chip. As much liquid as possible was then removed from the chip using a pipette and centrifuge. The chip was then loaded into the sequencer and the sequencing run was initiated.

#### 4.2.14. Sequencing of the V4 16S amplicons using Illumina Sequencing Technology

The XT-V4 amplicons were submitted to the *Earlham Institute* where they were purified and quantified. In brief, the Nextera DNA library kit was used to tagment the V4 amplicons (cleave the double stranded V4 DNA to generate universal single stranded DNA overhangs) and attach the Illumina index 1 (i7) and index 2 (i5) adapters to the V4 amplicons. The V4-adaptor amplicons were then purified, quantified, barcoded, multiplexed (the individual sample V4 libraries were pooled together), and sequenced using the Illumina MiSeq system with a 250 bp-end read metric.

#### 4.2.15. Alignment of the Sequenced V4 reads to known Bacterial Genomes

Following successful sequencing of the V4 amplicons using ion torrent sequencing technology, the sequenced data was uploaded to the web-based platform *Galaxy* [Public web access: <https://galaxyproject.org/>]. *Galaxy* software was used to demultiplex the sequencing data using the barcode splitter tool and remove the 5' adaptor and barcode sequence using the FASTQ Trimmer tool.

The FASTQ trimmed sequencing data was then uploaded to *Nephele* 2.0 to undergo microbiome analysis [Public web access: <https://nephele.niaid.nih.gov/#cloud>]. The *Nephele* 2.0 QIIME 16S FASTQ single-end open reference pipeline was used to remove low-quality reads (defined as having a Phred quality score less than 19.0) and chimeric sequences. The high-quality trimmed V4 reads were then aligned to bacterial OTUs with a 99% similarity threshold using the Silva database (see Chapter 2, section 2.4.1 for more detail).

With regards to the V4 reads generated using Illumina sequencing technology, the trimmed and demultiplexed sequencing data was uploaded to *Nephele* 2.0 [Public web access: <https://nephele.niaid.nih.gov/#cloud>]. The *Nephele* 2.0 QIIME 16S FASTQ paired-end open reference pipeline was used to remove low-quality V4 reads (defined as having a Phred quality score less than 19.0) and chimeric sequences. The high-quality V4 reads were then aligned to bacterial OTUs with a 99% similarity threshold using the Silva database (see Chapter 2, section 2.4.1 for more detail).

#### 4.2.16. Comparison of the Asthmatic Microbiome to the Control Microbiome

The species richness of the identified bacterial OTUs were first assessed by generating a rarefaction curve in order to compare species richness from the different blood samples

using *R* software (see Chapter 2, section 2.4.2 for additional detail). Statistical analysis was then performed on the total number of OTUs detected in the asthmatic samples compared to the control samples to determine whether species richness differed in the asthmatic circulatory microbiome compared to the control microbiome (see Chapter 2, section 2.4.3). The identified bacterial OTUs were then assigned to bacterial taxa and the relative abundance of the bacterial taxa present in the blood samples was calculated using *R* software (See Chapter 2, section 2.3.2 for additional detail). The relative abundance values of high-abundant bacterial taxa (taxa with a relative abundance greater than 1%) were then plotted (see Chapter 2, section 2.4.4).

Alpha diversity indices for the blood samples were measured using the *Nephele* 2.0 QIIME 16S FASTQ paired-end open reference pipeline to calculate Shannon and Chao1 diversity [Public web access: <https://nephele.niaid.nih.gov/#cloud>]. *R* software was then used to plot alpha diversity as a boxplot and perform the appropriate statistical tests to determine if the asthma samples differed significantly to the control samples with regards to alpha diversity of the circulatory microbiome (see Chapter 2, section 2.4.5).

Comparison of the bacterial OTU profiles between pairs of individual plasma samples was also carried out by measuring beta diversity of the detected bacterial communities. This involved calculating Bray-Curtis dissimilarity and plotting a PCoA graph using Bray-Curtis dissimilarity and *R* software (See Chapter 2, section 2.4.6 for additional information). PERMANOVA analysis was also performed to determine if there was a significant association between asthma and beta diversity of the circulatory microbiome (See Chapter 2, section 2.4.6 for additional information).

LEfSe analysis was then applied to the relative abundance data to determine bacterial taxa significantly associated with either the asthma or control microbiome. This was performed

using the relative abundance tables of all bacterial taxa detected in the plasma samples and the online *Galaxy* workflow framework<sup>394</sup> with the default settings applied [Public web access: <http://huttenhower.sph.harvard.edu/galaxy/>] (See Chapter 2, Section 2.4.3. for additional information).

#### 4.2.17. Prediction of Metagenome Function Content

To predict microbial activity of the detected microbiome PICRUSt analysis was performed using the online *Galaxy* platform. An OTU table was generated from the V4 16S rRNA sequencing data using *Nephele* 2.0 software with a closed reference OTU picking strategy and the GreenGenes 99 database. The OTU table was uploaded to *Galaxy*, normalised, and functional predictions were performed to determine KEGG ortholog abundances present in the plasma samples (See Chapter 2, section 2.4.5 for additional information).

The level 1, 2, and 3 KEGG ortholog counts were converted into abundance percentages, and *R* software was used to plot the abundance of highly abundant level 3 KEGG orthologs (defined as having a predicted total abundance greater than 1% in the plasma samples metagenome)(See Supplementary Materials S7 for *R* codes used). LEfSe analysis was then performed on the level 1,2, and 3 KEGG orthologs to determine differential KEGG ortholog abundance present in the asthma plasma samples compared to the control samples. Abundance of KEGG orthologs that displayed significant differential abundance were plotted as boxplots using *R* software (see Supplementary Materials S4 for *R* codes used).

#### 4.2.18. Culturing of Plasma Samples on Selective Growth Media

10 14ml falcon tubes containing 10ml of brain heart infusion broth was inoculated with human plasma (250µl). A negative experimental control and a positive experimental

control were generated by replacing human plasma with UV-treated molecular biology grade water for a negative control and *Pseudomonas* bacterial colonies for the positive control.

The inoculated nutrient broths were incubated at 37°C for 5 days. After 5 days of incubation the nutrient broths were removed from the incubator and immediately streaked onto Columbia Blood agar (*Biomerieux*), Cystine Lactose Electrolyte Deficient (CLED) medium (*Biomerieux*), and Anaerobe Recovery and Isolation agar (A.R.I.A) plates (*Biomerieux*) using sterile 20µl loops. Streaking of the agar plates involved placing the sterile loop at the bottom of the Eppendorf and slowly bringing the loop to the surface of the broth to ensure bacteria present in the different layers of the broth were collected onto the loop. The inoculated loop was then streaked onto the agar plates and then disposed in 1% Virkon. A negative control was generated for the Columbia Blood agar, CLED medium, and A.R.I.A plates using the UV-treated molecular biology grade water inoculated nutrient broth, and a positive control was generated using the *Pseudomonas* inoculated nutrient broth. For each sample/ control streaking of the agar plates was carried out in duplicate to ensure reliability of the experiment.

Inoculation of the nutrient broths and agar plates was carried out in a Category II UV hood to ensure sterile conditions. The pipette tips used to inoculate the nutrient broths were filter tips, and all equipment used in both stages of inoculation was exposed to UV for 30 minutes beforehand to ensure that any bacteria potential present on the equipment were killed.

Following inoculation, the Columbia Blood agar plates and CLED medium plates were incubated at 37°C for 72 hrs. At 24 hrs, 48 hrs, and 72 hrs the plates were assessed for bacterial growth. After 72 hrs individual colonies were selected from each of the plates

where bacterial growth had occurred and suspended in 50µl of UV-treated molecular biology grade water. The suspended colonies were then placed in storage at -20°C.

The A.R.I.A plates were placed in a 2.5L anaerobic chamber (*Sigma-Aldrich*) along with a AnaeroGen™ 2.5L chamber sachet (*Thermo fisher Scientific*). The anaerobic chamber was then incubated at 37°C for 120 hrs. After 120 hrs the anaerobic chamber was removed from the incubator, and the A.R.I.A. plates were removed from the anaerobic chamber. The plates were assessed for bacterial growth, and where growth had occurred three individual colonies were selected from each of the plates and suspended in 50µl of UV-treated molecular grade biology. The suspended colonies were then placed in storage at -20°C.

#### 4.2.19. Amplification of the 16S rRNA gene from the Bacterial Colonies

To identify the bacterial colonies cultured from the human plasma samples Sanger sequencing was performed on the suspended colonies.

This involved performing PCR on the suspended colonies in order to amplify the bacterial 16S rRNA gene. Thermal lysis was first carried out to extract DNA from the suspended bacterial colonies. This was achieved by heating the suspended bacteria to 98°C for 7 minutes using a thermocycler. The tubes were then centrifuged for 10 minutes at 8,000xg.

PCR was then performed on the supernatant using oligonucleotide primers designed to amplify the whole 16S rRNA gene (Table 4.8) and a GoTaq Green master mix PCR protocol (Table 4.9). PCR was performed in 25µl reactions containing 12.5µl GoTaq Green master mix, 2.0µl of each forward and reverse Total 16S Amp oligonucleotides (10µM), 6.5µl UV-treated molecular biology grade water, and 2.0µl of suspended bacteria. Gel

electrophoresis was then carried out to confirm successful amplification of the 16S rRNA gene.

**Table 4.8: Molecular properties of the primers used to amplify the total 16S rRNA gene**

Primer	Sequence (5' -> 3')	Concentration [pmol/ $\mu$ l]	Melting temperature ( $^{\circ}$ C)	GC Content (%)
Total 16S rRNA Forward Primer	AGAGTTTGATYMTGGC TCAG (20)	10.0	55.3	45
Total 16S rRNA Reverse Primer	ACGGYTACCTTGTTACG ACCT (21)	10.0	58.3	50

**Table 4.9: PCR cycling parameters used when amplifying the total 16S rRNA gene using the GoTaq Green master mix protocol.**

Cycle Step	Temperature ( $^{\circ}$ C)	Time	Cycles
Initial Denaturation:	95.0	5 minutes	1
Denaturation	95.0	30 seconds	
Annealing	55.0	30 seconds	35
Extension	73.0	45 seconds	
Final Extension:	73.0	5 minutes	1

For some of the selected bacterial colonies, 16S rRNA amplification using the GoTaq Green master mix PCR protocol did not generate sufficient 16S rRNA DNA required for Sanger sequencing. A second protocol using a Phusion Blood Direct PCR protocol, was thus devised to generate 16S rRNA DNA from the bacterial colonies which failed to display successful 16S rRNA amplification using the GoTaq Green master mix PCR protocol. In brief, 1.0 $\mu$ l of extracted bacterial DNA from each of the suspended bacterial colonies was mixed with 10.0 $\mu$ l of 2X Phusion Blood PCR Buffer, 6.6 $\mu$ l of UV-treated molecular biology grade water, 1.0 $\mu$ l of each forward and reverse Total 16S Amp oligonucleotide (10 $\mu$ M), and 0.4 $\mu$ l of



Phusion Blood II DNA Polymerase, and 35 cycles of PCR was carried out (Table 4.10). Gel electrophoresis was then carried out to confirm successful amplification of the 16S rRNA gene.

**Table 4. 10: PCR cycling parameters used when amplifying the total 16S rRNA gene using the Phusion Blood Direct protocol.**

Cycle Step	Temperature (°C)	Time	Cycles
Initial Denaturation:	98.0	5 minutes	1
Denaturation	98.0	16 seconds	
Annealing	55.0	20 seconds	35
Extension	72.0	45 seconds	
Final Extension:	72.0	7 minutes	1

#### 4.2.20. Sanger Sequencing of total 16S rRNA amplicons amplified from Human Plasma Samples

Following confirmation of successful amplification of the 16S rRNA gene from DNA extracted from cultured bacterial colonies, the 16S amplicons were submitted to *Genewiz* for Sanger sequencing. The sequenced data was then analysed for sufficient read coverage and quality using SnapGene Viewer. The most abundant read sequences were then uploaded to the NCBI nucleotide blast server to determine that likely identity of the bacterial colonies the 16S rRNA gene was amplified and sequenced from [Public web access: <https://blast.ncbi.nlm.nih.gov/Blast.cgi>].

### 4.3. Results

#### 4.3.1. Development of a Protocol for Amplifying Regions of the Bacterial 16S rRNA Gene from Human Blood Samples

Characterisation of the microbiome present in human plasma samples was initially performed by amplifying and sequencing the V3-V4 region of the bacterial 16S rRNA gene.

A protocol for amplifying the V3-V4 region of the bacterial 16S rRNA gene from human plasma samples was successfully developed. Gradient PCR was used to determine that the optimum annealing temperature for the V3-V4 primers was 55°C (see Supplementary Materials, Figure S2). End-point PCR and gel electrophoresis revealed that V3-V4 amplification was only successful when PCR was performed directly on the human plasma samples rather than microbial DNA extracted from the plasma samples (see Supplementary Materials, Figures S3 and S4).

Analysis of different plasma concentrations revealed that a 5% plasma concentration was optimum for PCR amplification of the V3-V4 region (see Supplementary Materials, Figure S4). This finding was unsurprising given that human plasma samples are known to contain PCR inhibitors<sup>513,514</sup>, and it highlights the importance of adapting the PCR protocol for the clinical sample under investigation.

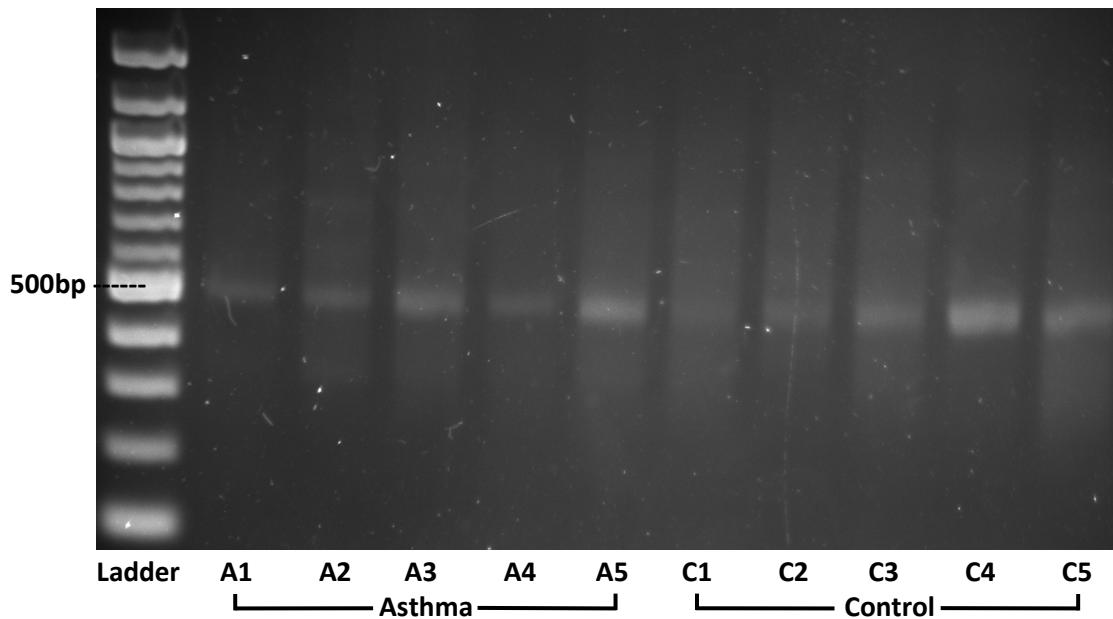
Following successful development of an end-point PCR protocol for amplifying the V3-V4 region of the 16S rRNA gene, the protocol was utilised to generate V3-V4 amplicons that contained ion torrent sequencing motifs. This involved carrying out an end-point PCR protocol using V3-V4 primers that had been modified to contain the ion torrent sequencing motifs. Analysis of the PCR products using gel electrophoresis revealed that V3-V4

amplification using the modified primers and end-point PCR was unsuccessful (see Supplementary Materials, Figure S5).

A nested PCR protocol was, therefore, developed in order to generate V3-V4 amplicons containing the sequencing motifs from the human plasma samples. Using *E.coli* DNA, it was determined that initial amplification of the V3-V4 region using 30 PCR cycles followed by 10 cycles of PCR to attach the sequencing motifs was optimum for the generation of V3-V4 amplicons containing the required sequencing motifs (see Supplementary Materials, Figure S6).

#### 4.3.2. Amplification of the V3-V4 region of the 16S rRNA gene using Nested PCR

Following successful development of a nested PCR protocol, the protocol was applied to the human plasma samples. Analysis of the nested PCR end-product using gel electrophoresis revealed that the ion torrent sequencing motifs had been successfully added to the V3-V4 amplicons as evidenced by the increased size of the V3-V4 amplicon bands (Figure 4.3). Analysis of the experimental negative controls generated from first stage and second stage PCR revealed no V3-V4 amplification present in the negative controls (Supplementary Materials, Figure S7). This demonstrated that the detected bacterial DNA was not the consequence of environmental and/ or reagent contamination and thus supported the presence of a circulatory microbiome.



**Figure 4.3: Generation of V3-V4 amplicons containing the ion torrent sequencing motifs from human plasma samples using nested PCR.** Plasma samples from asthmatic subjects (n = 5, A lanes) and control subjects (n = 5, B lanes) first underwent 35 cycles of end-point PCR using the optimised GoTaq Green master mix PCR protocol and V3-V4 primers in order to amplify the V3-V4 region of the bacterial 16S rRNA gene. The V3-V4 amplicons were then purified using the MinElute protocol and the underwent an additional 7 cycles of end-point PCR using the optimised GoTaq Green master mix PCR protocol and the modified V3-V4 primers in order to attach the ion torrent sequencing motifs to the V3-V4 amplicons. The V3-V4 amplicons were then purified using the SPRI bead protocol.

*Abbreviations: bp, number of nucleotide base pairs*

#### 4.3.3. Quantification of the Ion Torrent V3-V4 amplicons

Following confirmation of successful amplification of V3-V4 amplicons containing the ion torrent sequencing motifs, and removal of primer dimers, the concentration of V3-V4 amplicons was quantified using a Qubit 3.0 HS dsDNA quantification protocol (Table 4.11). Quantification of the V3-V4 amplicons demonstrated low levels of bacterial DNA present in all the plasma samples investigated and enabled accurate dilution of the amplicons to the required 100pM concentration for ion torrent sequencing using the Ion PGM™ Hi-Q™ protocol.

**Table 4.11: Quantification of V3-V4 reads containing the ion torrent sequencing motif generated from human plasma samples.** The V3-V4 region of the bacterial 16S gene was amplified from plasma samples from asthmatic subjects (n = 5) and non-asthmatic control subjects (n = 5) using a nested PCR protocol that enabled attachment of ion torrent sequencing motifs to the amplified V3-V4 amplicons. Following the final purification stage, the V3-V4 amplicons containing the sequencing motifs were quantified using a Qubit 3.0 HS dsDNA quantification protocol.

Sample	DNA Concentration (ng/μl)
Control_1 (C1)	3.28
Control_2 (C2)	4.22
Control_3 (C3)	3.96
Control_4 (C4)	3.90
Control_5 (C5)	4.02
Asthma_1 (A1)	2.06
Asthma_2 (A2)	3.46
Asthma_3 (A3)	4.16
Asthma_4 (A4)	1.68
Asthma_1 (A5)	3.60

#### 4.3.4. Sequencing of the V3-V4 amplicons using Ion Torrent Sequencing Technology

Evaluation of the percentage of V3-V4-positive ISPs revealed that generation and enrichment of V3-V3 positive ISPs had been successful, with 21% of the total ISPs being V3-V4 positive (Table 4.12).

**Table 4.12: Quantification of the number of enriched V3-V4-positive Ion Sphere™ Particles generated from the V3-V4 amplicon library.** V3-V4-Positive Ion Sphere particles (ISPs) were generated from the V3-V4 amplicon library using OneTouch 2 Ion torrent technology. Quality control testing using a Qubit 3.0 Ion sphere assay was performed to determine the percentage of ISPs that were V3-V4 positive. This was achieved by first calibrating the assay using two Alexa Fluor standards (**A**), and then measuring the ISP sample fluorescence of the Alexa Fluor 488 conjugate dye and the Alexa Fluor 647 conjugate dye (**B**).

**A**

Calibration Standard	RFU	Calibration Factor
Alexa Fluor 488 Calibration Standard	33643.9	0.46
Alexa Fluor 488 Calibration Standard	66714.75	

**B**

Sample	Raw RFU Value		Background RFU		Conversion factor	Percent templated ISPs
	AF 488	AF 647	AF 488	AF 647		
V3-V4 ISP library	1264.7	362.7	43.8	10.3	1.58	21.0

Sequencing of the V3-V4 amplicons using ion torrent sequencing technology generated a total of 415,945 V3-V4 reads from the human plasma samples, of which 52% were classed as useable reads. Analysis of the mean length of the V3-V4 reads revealed that the sequenced reads were significantly truncated, with a mean length of just 77bp.

#### 4.3.5. Amplification of the V4 region of the 16S rRNA gene from Human Plasma Samples using Nested PCR

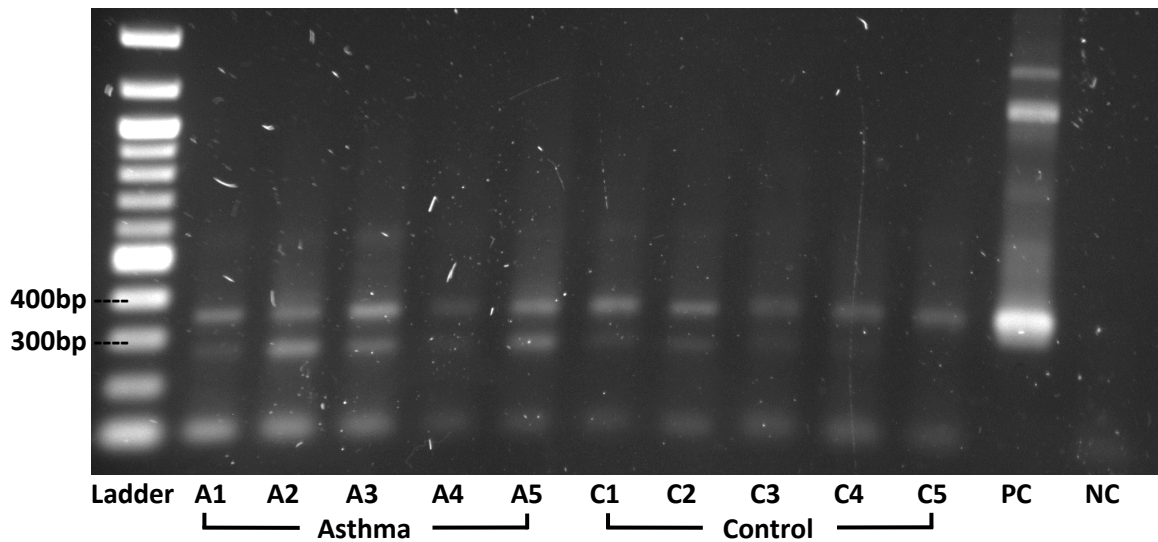
Following sequencing of the V3-V4 amplicons using ion torrent sequencing the generated reads were observed to be significantly truncated. Decreased length of the V3-V4 reads would likely result in decreased accuracy when assigning the reads to known bacterial

OTUs, subsequently reducing the ability to accurately characterise the circulatory microbiome in asthmatic and control subjects.

A nested PCR protocol was therefore designed to amplify the V4 region of the 16S rRNA. Amplification of the V4 region has been demonstrated to be a reliable and accurate means of characterising the human microbiome in previous studies<sup>220, 335, 352,515</sup>, and it was predicted that a reduced amplicon size would reduce the risk of amplicon truncation occurring during ion torrent sequencing .

Gradient PCR was first performed to determine the optimum annealing temperature of the V4 primers. Following confirmation that 55°C was the optimum annealing temperature (see Supplementary Materials, Figure S8), the nested PCR protocol developed using the V3-V4 primers was performed on the human plasma samples using primers designed to amplify just the V4 region of the 16S rRNA gene.

Analysis of the nested PCR end-products using gel electrophoresis demonstrated the generation of V4 amplicons containing the ion torrent sequencing motifs from human plasma samples, as evidenced by the detection of DNA bands approximately 350bp (Figure 4.4). However, with the exception of the Control\_5 plasma sample (Figure 4.4, lane C5), attachment of the sequencing motifs appeared to be only partially successful, as evidenced by the detection of a second DNA band approximately 290bp (Figure 4.4). The V4 amplicons with the sequencing motifs attached are approximately 355bp, with the sequencing motifs amounting to 60bp of the amplicon's total length (A1 adaptor = 26bp, key = 4bp, barcode = 10, TrP1 adaptor = 20). The presence of DNA bands at 290bp, therefore, indicates the presence of V4 amplicons that do not have the sequencing motif attached (355 – 60 = 295bp).



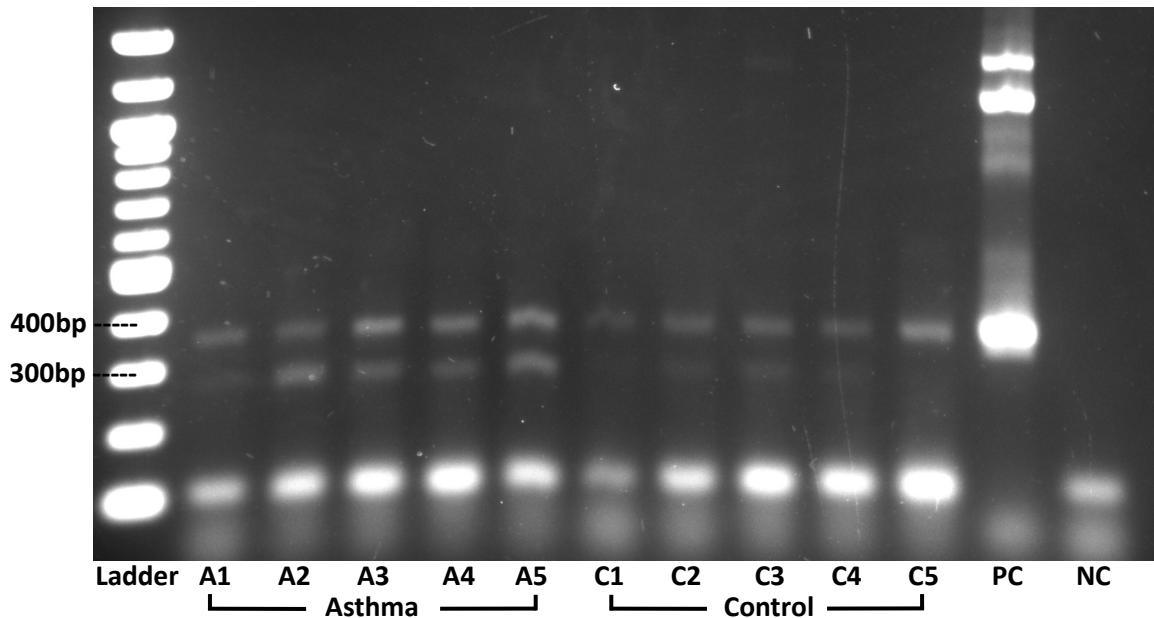
**Figure 4.4: Generation of V4 amplicons containing the ion torrent sequencing motifs from human plasma samples from asthmatic subjects and non-asthmatic control subjects using nested PCR.** Plasma samples from asthmatic subjects (n = 5, A lanes) and control subjects (n = 5, C lanes) first underwent 35 cycles of end-point PCR using the optimised Phusion blood direct PCR protocol and the V4 primers in order to amplify the V4 region of the bacterial 16S rRNA gene. The V4 amplicons were then purified using the MinElute protocol and the underwent an additional 7 cycles of end-point PCR using the Accuprime PCR protocol and the modified V4 primers in order to attach the ion torrent sequencing motifs to the V4 amplicons. The V4 amplicons were then purified using the SPRI bead protocol.

*Abbreviations: PC, positive control; NC, Negative Control*

Nested PCR was also performed on the plasma samples in order to generate a V4 amplicon library suitable for Illumina sequencing. Analysis of the nested PCR end-products using gel electrophoresis demonstrated the generation of V4 amplicons containing the Illumina sequencing motifs from human plasma samples, as evidenced by the detection of DNA bands approximately 350bp (Figure 4.5). However, attachment of the sequencing motifs appeared to be only partially successful, as evidenced by the detection of a second DNA band approximately 290bp (Figure 4.5). The Illumina sequencing motifs account for 67bp of the amplicon's total length (the i7 adaptor = 33bp and the i5 = 34bp). The detection of



DNA bands at 290bp, therefore, indicates the presence of V4 amplicons that do not contain the sequencing motif attached ( $350 - 67 = 283\text{bp}$ ).



**Figure 4.5: Generation of V4 amplicons containing the Illumina sequencing motifs from human plasma samples from asthmatic subjects and non-asthmatic control subjects using nested PCR.** Plasma samples from asthmatic subjects ( $n = 5$ , A lanes) and control subjects ( $n = 5$ , C lanes) first underwent 35 cycles of end-point PCR using the optimised Phusion blood direct PCR protocol and the V4 primers in order to amplify the V4 region of the bacterial 16S rRNA gene. The V4 amplicons were then purified using the MinElute protocol and the underwent an additional 7 cycles of end-point PCR using the Accuprime PCR protocol and the 515F/806R primers in order to attach the Illumina sequencing motifs to the V4 amplicons.

#### 4.3.6. Quantification of the Ion torrent V4 amplicons

Following confirmation of successful amplification of the V4 region containing the ion torrent sequencing motifs, the amplicons were purified, and the primer dimers generated from the PCR reactions were removed using the SPRI beads protocol (Chapter 2, section 2.2.2). The V4 amplicon concentrations were then determined using the Qubit 3.0 HS DNA

quantification protocol. Quantification of the V4 amplicons demonstrated low levels of bacterial DNA present in all the plasma samples investigated (Table 4.13).

Comparison of the V4 amplicons concentrations (Table 4.13) and the V3-V4 amplicon concentrations (Table 4.11) revealed that amplification of the V4 region of the 16S rRNA gene generated significantly more amplicons compared to the number of amplicons generated when the V3-V4 region was amplified ( $P$  value = 0.0259, *Unpaired t test*). Furthermore, comparison of the V4 amplicon concentrations generated for the plasma samples from asthmatic samples was significantly higher compared to the V4 amplicon concentration generated from the control subjects ( $P$  value = 0.0034, *Welch's two sample t test*). This suggested that the asthmatic subjects had increased bacterial load in the blood compared to the control subjects.

**Table 4. 13: Quantification of V4 amplicons containing the Ion torrent sequencing motifs generated from human plasma samples.** The V4 region of the bacterial 16S rRNA gene was amplified from plasma samples from asthmatic subjects ( $n = 5$ ) and non-asthmatic control subjects ( $n = 5$ ) using a nested PCR protocol that enabled attachment of ion torrent sequencing motifs to the amplified V3-V4 amplicons. Following the final purification stage, the V4 amplicons containing the sequencing motifs were quantified using a Qubit 3.0 HS DNA quantification protocol.

Sample	DNA Concentration (ng/ $\mu$ l)
Control_1 (C1)	3.82
Control_2 (C2)	3.60
Control_3 (C3)	3.36
Control_4 (C4)	3.66
Control_5 (C5)	3.50
Asthma_1 (A1)	5.22
Asthma_2 (A2)	6.14
Asthma_3 (A3)	5.48
Asthma_4 (A4)	4.34
Asthma_1 (A5)	5.92
Negative Control	0.98

#### 4.3.7. Quantification of the Illumina V4 amplicons

Following submission of the V4 amplicons for Illumina sequencing (*Earlham Institute*, Illumina MiSeq system) the V4 amplicons were quantified twice during library preparation; once following arrival of the amplicons to the *Earlham Institute* and again following attachment of the Illumina adapters (i7 and i5) using the Nextera DNA library kit (Table 4.14).

Quantification of the V4 amplicon libraries revealed good amplification of the V4 region of the bacterial 16S rRNA gene in all plasma samples analysed (Table 4.14). Comparison of the V4-XT amplicons compared to the V4 amplicons containing the ion torrent sequencing motifs found that the V4-XT primers produced increased amplicon concentrations compared to the modified V4 16S primers used when generating amplicons with the ion torrent sequencing motif.

Comparison of the V4 library concentrations from plasma samples from asthma subjects compared to control subjects revealed no significant difference in library concentration ( $P$  value = 0.8385, *Unpaired t test*). The experimental negative control was found to contain DNA despite gel electrophoresis showing it to be PCR negative. However, following addition of the Illumina adapters the DNA concentration for the negative control significantly decreased, suggesting that the majority of DNA detected in negative control V4-XT amplicon library was not from V4 amplicons, but rather another source of DNA.

**Table 4.14: Quantification of V4 amplicons containing the Illumina sequencing motifs generated from human plasma samples.** The V4 region of the bacterial 16S rRNA gene was amplified from asthma plasma samples (n = 5) and non-asthmatic control plasma samples (n = 5) using a nested PCR protocol that enabled attachment of the Illumina sequencing motifs to the V4 amplicons. Following purification, quantification was carried out after the second stage of PCR, where the XT adapters were attached to the amplicons, and then again following the attachment of the Illumina i5 and i7 adapters using a Qubit HS dsDNA quantification protocol.

Sample	Library Concentration (ng/μl)	
	V4-XT Amplicon library	V4-i7/i5 Amplicon library
Control_1	11.8	1.076
Control_2	15.8	1.480
Control_3	21.2	1.509
Control_4	24.2	1.191
Control_5	30.4	1.571
Asthma_1	14.5	1.416
Asthma_2	21.4	1.725
Asthma_3	24.4	1.620
Asthma_4	26.1	1.827
Asthma_5	21.0	1.843
Negative Control	10.6	0.448

#### 4.3.8. Sequencing of the V4 amplicons using Ion Torrent Sequencing Technology

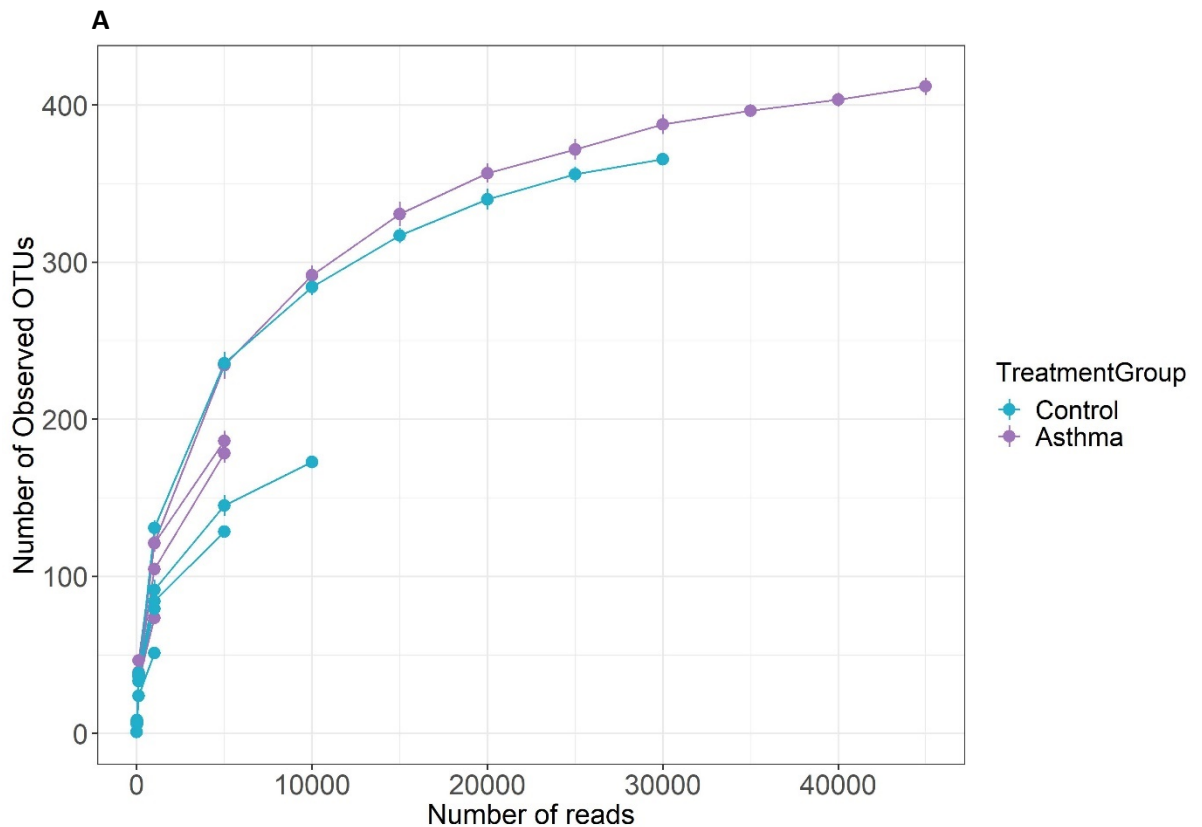
Sequencing of the V4 amplicons using ion torrent sequencing technology generated a total of 1,506,835 reads from the human plasma samples (Figure 4.6). Following removal of the 5' adaptor sequence the total number of reads was reduced to 1,336,137, indicating that 170,698 sequenced reads did not contain the V4 amplicon sequence (Figure 4.6).

A total of 716,589 trimmed reads were generated from the control plasma samples (average = 143,317.80, range = 84,152 – 317,912) and 619,548 trimmed reads were generated from the asthma samples (average = 154,887.00, range = 132,742 – 210,090)

(Figure 4.6). One of the Asthma sequencing files, Asthma\_5, was unable to be trimmed and thus was removed from further downstream analysis.

Following quality control analysis and alignment of the trimmed V4 reads to bacterial OTUs with a 99% similarity threshold, a total of 122,620 V4 reads were aligned to 940 bacterial OTUs. The number trimmed V4 reads that were aligned to bacterial OTUs was just 9.18% of the total number of trimmed V4 reads generated from the plasma samples, and for the majority of plasma samples, less than 10,000 trimmed V4 reads were aligned to bacterial OTUs (Figure 4.6).

Analysis of the number of OTUs detected in the individual plasma samples was highly variable, and in the majority of samples, less than 250 OTUs were detected (Figure 4.6). Statistical analysis of the number of OTU-aligning reads sequenced from each sample and the number of OTUs detected in each sample revealed no significant differences in the asthmatic and control samples (*Wilcoxon rank sum test and Unpaired t test, P value = 0.2857 and 0.5351, respectively*).



**B**

Sample	Number of raw reads	Number of trimmed Reads	Number of OTU-aligned Reads	Number of OTUs detected
Control_1	102,920	101,618	4,276	82
Control_2	120,130	118,523	10,797	205
Control_3	84,152	82,357	1,247	96
Control_4	102,975	101,886	7,849	156
Control_5	317,912	312,205	32,421	408
Asthma_1	142,855	140,020	7,170	221
Asthma_2	138,731	136,696	6,800	225
Asthma_3	212,344	210,090	48,198	445
Asthma_4	133,537	132,742	3,862	105
Asthma_5	151,279	-	-	-

**Figure 4.6: Quantification of bacterial V4 reads sequenced from human plasma samples using ion torrent sequencing.** Ion torrent sequencing was used to sequence bacterial V4 amplicons generated from plasma samples from asthmatic subjects (n = 5) and control subjects (n = 5). Following successful sequencing of the V4 amplicons, *Galaxy* software was used to demultiplex the sequencing data using the barcode splitter tool and remove the 5' adaptor and barcode sequence using the FASTQ Trimmer tool. *Nephel* 2.0 was used to remove low-quality reads and chimeric sequences, and to align the high-quality V4 reads to bacterial operational taxonomic units (OTUs). **(A)** A rarefaction curve showing the level

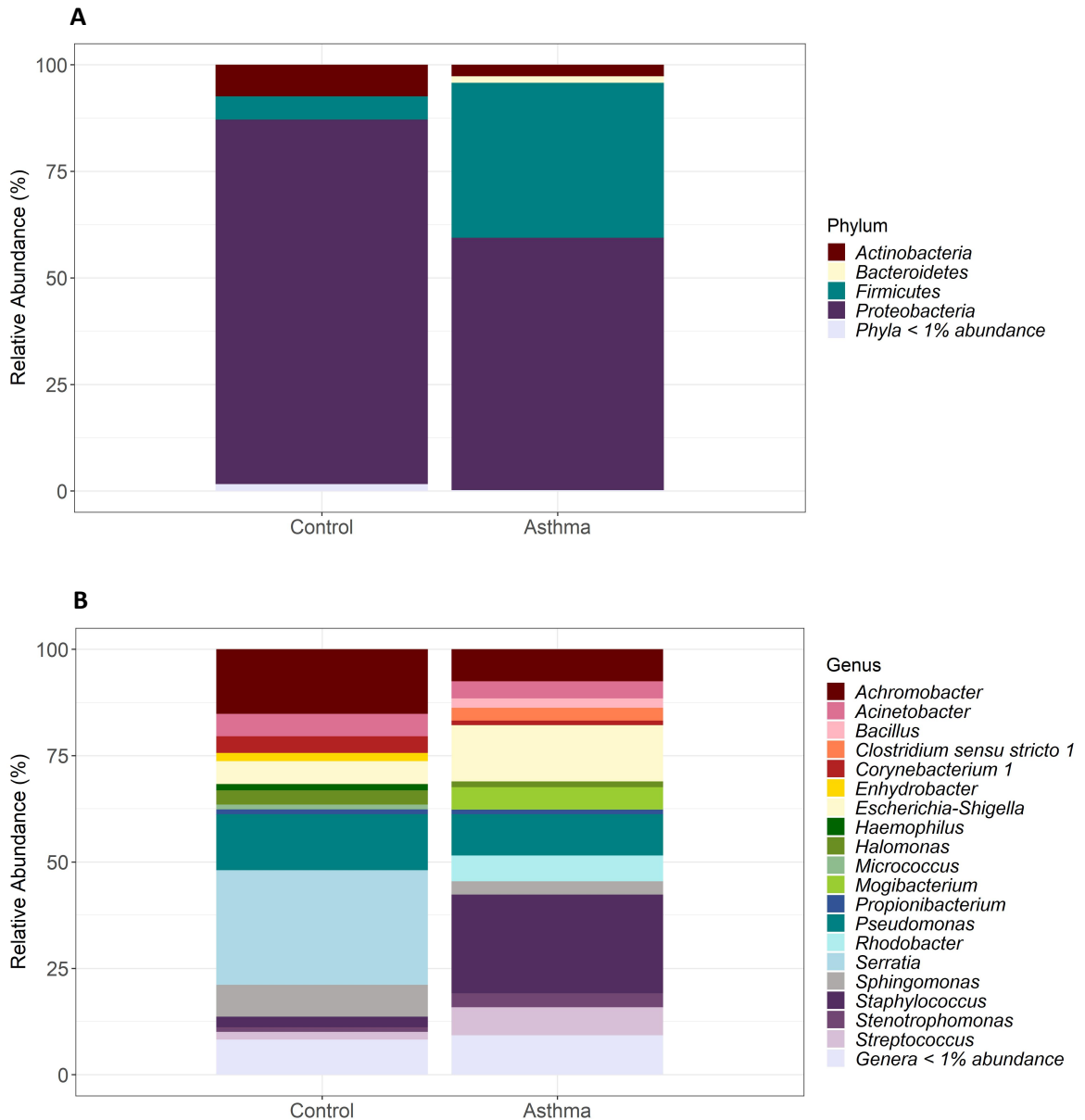
of OTU species richness detected in the plasma samples. **(B)** Quantification of the V4 reads generated from the plasma samples using ion torrent sequencing and the total number of bacterial OTUs the reads align to with a 99% similarity threshold.

#### 4.3.9. Taxonomic Classification of the OTUs detected in the Human Plasma Samples using Ion Torrent Sequencing Technology

The OTUs detected in the human plasma samples using ion torrent sequencing could be classified into 9 bacterial phyla and 103 bacterial genera, the majority of which were detected at low abundance (defined as contributing less than 1% of bacterial DNA generated from the plasma samples). At the phylum level the circulatory microbiome was dominated by the Proteobacteria phylum (85.53% of bacterial DNA sequenced from the control samples, and 59.21% of bacterial DNA sequenced from the asthma samples), and to a lesser extent, the Firmicutes (5.44%, 36.34%), Actinobacteria (7.42%, 2.73%), and Bacteroidetes phyla (0.20%, 1.50%) (Figure 4.7.A).

At the genus level, 19 bacterial genera were detected at high abundant levels (relative abundance greater than 1%). The detected genera were predominately members of the Proteobacteria phylum and included; *Serratia* (26.94%, 0.69%), *Pseudomonas* (13.18%, 9.74%), *Achromobacter* (15.17%, 7.51%), *Escherichia-Shigella* (5.41%, 13.22%), *Sphingomonas* (7.46%, 3.09%), *Acinetobacter* (5.32%, 4.06%), *Rhodobacter* (0.00%, 6.08%), *Halomonas* (3.33%, 1.35%), *Stenotrophomonas* (1.08%, 3.31%), *Enhydrobacter* (1.93%, 0.97%), and *Haemophilus* (1.45%, 0.00%) (Figure 4.7.B). A number of bacterial genera belonging to the Firmicutes and Actinobacteria phyla were also detected at high abundance levels in the plasma samples. These included the Firmicutes *Staphylococcus* (2.52%, 23.19%), *Streptococcus* (1.78%, 6.57%), *Mogibacterium* (0.00%, 5.27%), *Clostridium sensu stricto 1* (0.00%, 1.99%), and *Bacillus* (0.01%, 2.22%); and the Actinobacteria members

*Corynebacterium 1* (3.88%, 1.07%), *Propionibacterium* (1.10%, 1.07%), and *Micrococcus* (1.19%, 0.19%) (Figure 4.7.B).



**Figure 4.7: Relative abundance of bacteria detected in the human circulatory microbiome using Ion torrent sequencing.** Bacterial composition determined using QIIME 16S FASTQ Single end analysis on sequenced V4 reads generated from plasma samples taken from asthmatic subjects (n = 4; mean number of reads = 11,318) and control subjects (n = 5; mean number of reads per sample = 16,508). Taxa with a relative abundance  $\geq 1\%$  were plotted, and low abundance taxa (< 1.0%) were grouped and plotted as Taxa < 1% abundance. **(A)** Relative abundance of bacteria detected at the phylum level. **(B)** Relative abundance of bacteria detected at the genus level.



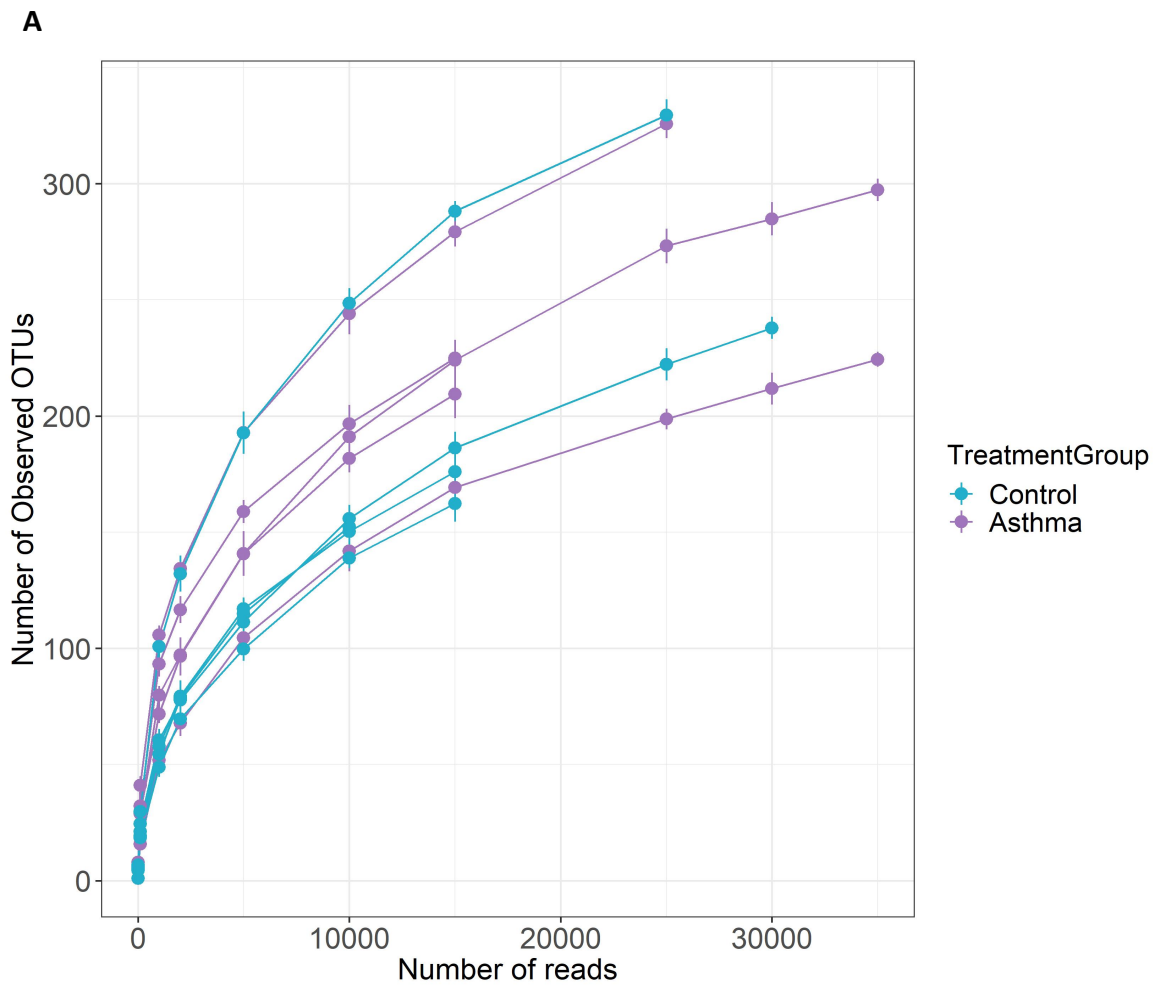
The low level of sequenced V4 reads that could be assigned to bacterial OTUs meant that the characterisation of the circulatory microbiome using ion torrent sequencing techniques was unlikely to be a true representation of the bacterial populations present in the plasma samples. The decision, therefore, was made to do no further downstream statistical analysis using the ion torrent sequencing data.

#### 4.3.10. Sequencing of the V4 amplicons using Illumina Sequencing Technology

A total of 928,569 V4 16S rRNA reads were generated from the human plasma samples using Illumina sequencing. Following removal of low-quality reads and chimeric sequences, 26.61% of the V4 reads (247,064 reads) generated from the plasma samples could be aligned to 1,128 bacterial OTUs with a 99% certainty. This included an average of 22,337.60 high-quality reads generated from the control samples that aligned to 787 OTUs (range = 199 – 395 OTUs per sample), and an average of 27,075.20 reads generated from the asthma samples that aligned to a total of 907 bacterial OTUs (range = 277 – 399 OTUs per sample) (Figure 4.8)(see also Supplementary Materials, Table S10).

Comparison of the OTUs detected in the individual plasma samples revealed a shared core circulatory microbiome composed of 566 OTUs. An additional 221 OTUs were uniquely detected in the control samples, and 341 OTUs were uniquely detected in the asthma samples. Examination of the rarefaction curve revealed potential differences in the number of OTUs detected in the asthma samples compared to the control samples. However, statistical analysis revealed that there were no significant differences between the control and asthmatic samples with regards to number of high-quality V4 reads generated and the number of OTUs detected (*Unpaired t test*, *P* values = 0.4140 and 0.3288, respectively).

With regards to the experimental negative control, a total of 57,239 V4 reads were generated during the amplification and sequencing process. None of the reads, however, passed the stringent quality control and chimeric sequence removal stage of analysis, and thus the detection of bacterial DNA in the negative control is unlikely to impact downstream characterisation and analysis of the human circulatory microbiome.



**B**

Group	Number of Samples	Mean number of raw reads	Mean number of high-quality reads	Total number of bacterial OTUs
Control	5	89,711.40	22,337.60	787
Asthma	5	96,002.40	27,075.20	907
Negative Control	1	57,239.00	0.00	NA

**Figure 4.8: Quantification of bacterial V4 reads sequenced from human plasma samples using Illumina sequencing.** Illumina sequencing was used to sequence bacterial V4 amplicons generated from plasma samples from asthmatic subjects (n = 5) and control subjects (n = 5). Following successful sequencing of the V4 amplicons *Nephele* 2.0 was used to remove low-quality reads and chimeric sequences, and to align the high-quality V4 reads to bacterial operational taxonomic units (OTUs). **(A)** A rarefaction curve showing the level of species richness of OTUs detected in the plasma samples. **(B)** Quantification of the V4 reads generated from asthma plasma samples (n = 5) and control samples (n = 5), and the total number of bacterial OTUs the reads align to with a 99% similarity threshold.

#### 4.3.11. Taxonomic Classification of the OTUs detected in the Human Plasma Samples using Illumina Sequencing Technology

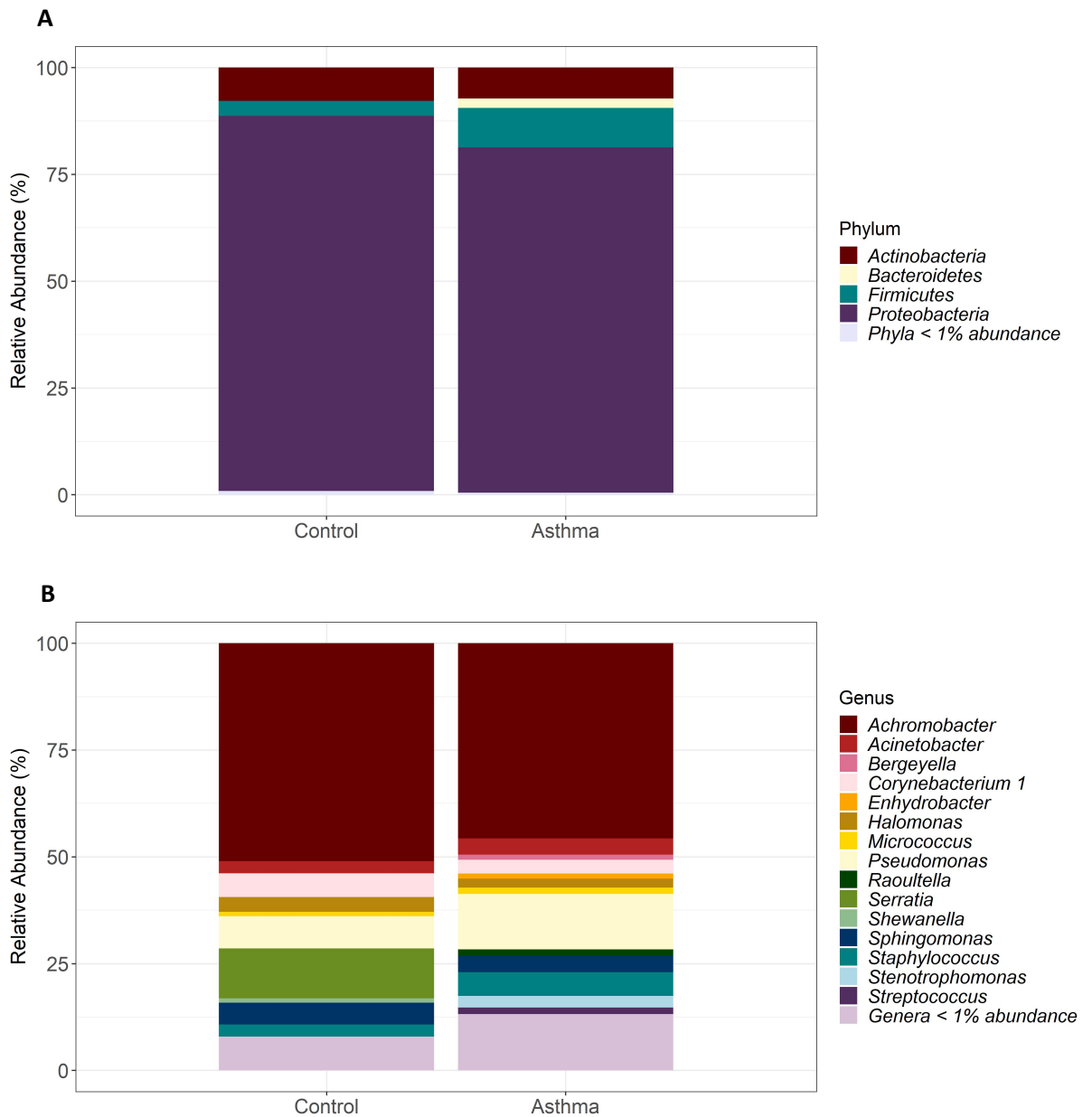
The OTUs detected in the human plasma samples could be classified into 12 phyla and 133 bacterial genera, the majority of which were detected at low abundance (defined as contributing less than 1% of bacterial DNA generated from the plasma samples). At the phylum level the human circulatory microbiome was found to be predominately composed of bacteria belonging to the Proteobacteria phylum (87.79% of bacterial DNA sequenced from the non-asthmatic plasma samples, and 80.79% of bacterial DNA sequenced from the asthma plasma samples), and to a lesser extent Actinobacteria (7.82%, 7.26%), Firmicutes (3.53%, 9.21%), and Bacteroidetes (0.22%, 2.22%) (Figure 4.9.A).

At the genus level the majority of bacterial genera identified were detected at low abundance levels, with 113 genera having a relative abundance score of less than 0.5%. In the control samples 89/133 bacterial genera were detected, of which 14 had a relative abundance greater than 0.5%, whilst in the asthmatic plasma samples 115 bacterial genera were detected, of which 20 had a relative abundance greater than 0.5%.

A total of 11 bacterial genera had a relative abundance score greater than 1.0% and were defined as high-abundant taxa. High-abundant genera were predominately members of the Gammaproteobacteria class of bacteria and included *Achromobacter* (51.05% of bacterial DNA sequenced from the control samples, and 45.71% of bacterial DNA sequenced from the asthma samples), *Pseudomonas* (7.53%, 12.95%), *Serratia* (11.71%, 0.93%), *Acinetobacter* (2.83%, 3.79%), *Halomonas* (3.44%, 2.11%), *Stenotrophomonas* (0.44%, 2.72%), and *Enhydrobacter* (0.89%, 1.20%). (Figure 4.9.B). Additional highly abundant genera that did not belong to the Gammaproteobacteria class included the Alphaproteobacteria member *Sphingomonas* (5.12%, 3.87%), the Firmicutes genus

*Staphylococcus* (2,82%, 5.55%), and the Actinobacteria genera *Corynebacterium 1* (5.54%, 3.20%) and *Micrococcus* (1.05%, 1.47%) (Figure 4.9.B).

There was also a number of high abundant genera detected that were condition specific. These included *Shewanella* (1.00%, 0.58%), which was present at high abundance levels in the control samples, and *Raoultella* (0.11%, 1.49%), *Streptococcus* (0.32%, 1.52%), and *Bergeyella* (0.00%, 1.18%), which were present at high abundance levels in the asthma samples (Figure 4.9.B).

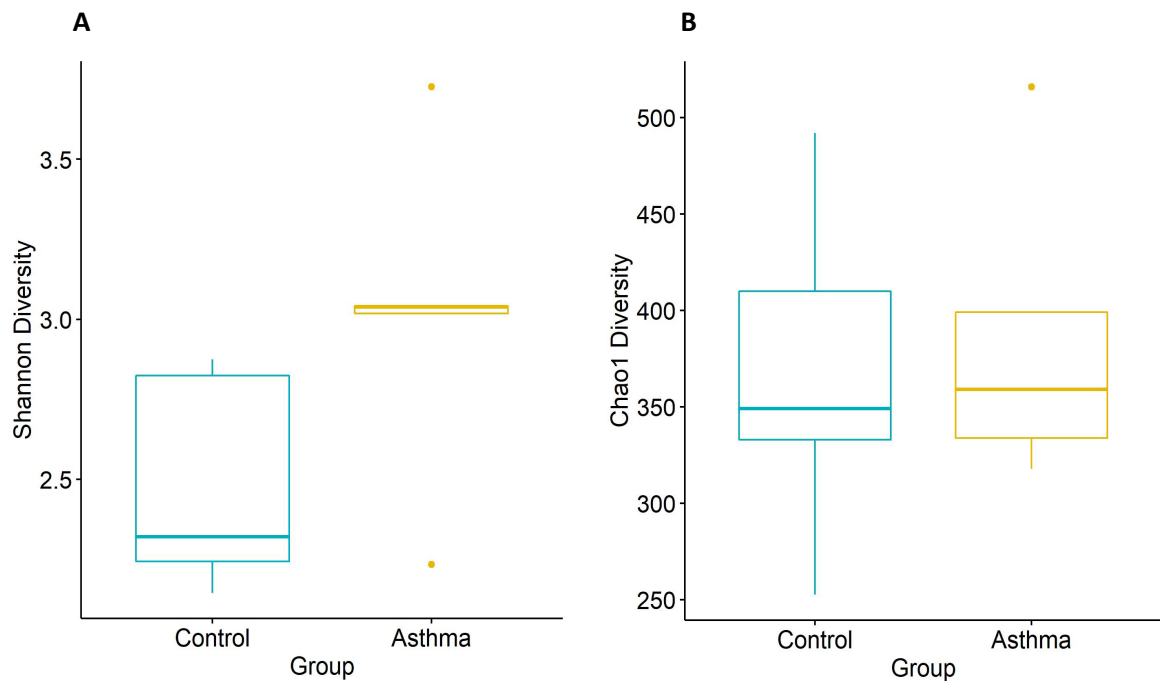


**Figure 4.9: Relative abundance of bacteria detected in the human circulatory microbiome.** Bacterial composition determined using QIIME 16S FASTQ paired end analysis on sequenced V4 reads generated from plasma samples taken from asthmatic subjects (n = 5, mean number of reads = 27,075.20) and control subjects (n = 5; mean number of reads per sample = 22,337.60). Taxa with a relative abundance  $\geq 1\%$  were plotted, and low abundance taxa (< 1.0%) were grouped and plotted as Taxa < 1% abundance. **(A)** Relative abundance of bacteria detected at the phylum level. **(B)** Relative abundance of bacteria detected at the genus level.

#### 4.3.12. Bacterial Alpha Diversity in the Asthmatic Circulatory Microbiome compared to the Control Microbiome

Alpha diversity was determined by calculating the Shannon diversity index and Chao1 diversity index for each plasma sample (see Supplementary Materials, Table S11). The diversity indices generated from the asthma and control samples were then compared to determine whether the asthma circulatory microbiome differed significantly to the control microbiomes with regards to bacterial diversity (Figure 4.10).

Comparison between the asthma and control subjects revealed that overall the asthmatic subjects scored higher Shannon and Chao1 index scores compared to the control subjects, although these values were not statistically significant (Figure 4.10, see also Supplementary Materials, Table S11). This was particularly apparent for Shannon diversity ( $P$  value = 0.0965, *Unpaired t test*)(Figure 4.10. A & C). Intriguingly, one of the asthma subjects, Asthma\_3, displayed a level of Shannon diversity more similar to the level of diversity detected in the control subjects than the remaining asthmatic subjects (see Supplementary Materials. Table S11). This subject was diagnosed with asthma relatively late in childhood (age 12 years, see Supplementary Materials S11), and so it is possible that the age of asthma onset may influence the level of microbial diversity present in the blood. This is further supported by the high levels of alpha diversity detected in the circulatory microbiome of Asthma\_5, an asthmatic subject who was diagnosed with asthma early on in childhood (age 3 years)(see Supplementary Materials, Table S2).



**C**

Alpha Diversity	Control Mean (S.D)	Asthma Mean (S.D)	P Value
Shannon	2.48 (0.31)	3.01 (0.47)	0.0965
Chao1	367.29 (80.07)	385.10 (70.91)	0.7477

**Figure 4.10: Comparison of alpha diversity in the asthmatic circulatory microbiome compared to the control microbiome.** Alpha diversity was measured using rarefied OTU tables generated from 16S rRNA sequencing data generated from plasma samples collected from asthmatic subjects (n = 5) and control subjects (n = 5). Shannon diversity index scores were generated from OTU tables in order to measure the richness and evenness of bacterial taxa present in the plasma samples. Chao1 index scores were measured to determine the predicted number of bacterial taxa present in the plasma samples by extrapolating out the number of rare organisms that may not have been detected due to under-sampling. **(A)**. Shannon diversity in the asthma circulatory microbiome compared to the control circulatory microbiome. **(B)**. Chao1 diversity in the asthma circulatory microbiome compared to the control circulatory microbiome. **(C)**. Statistical analysis of alpha diversity detected in the asthmatic subjects compared to the control subjects using Unpaired t tests.

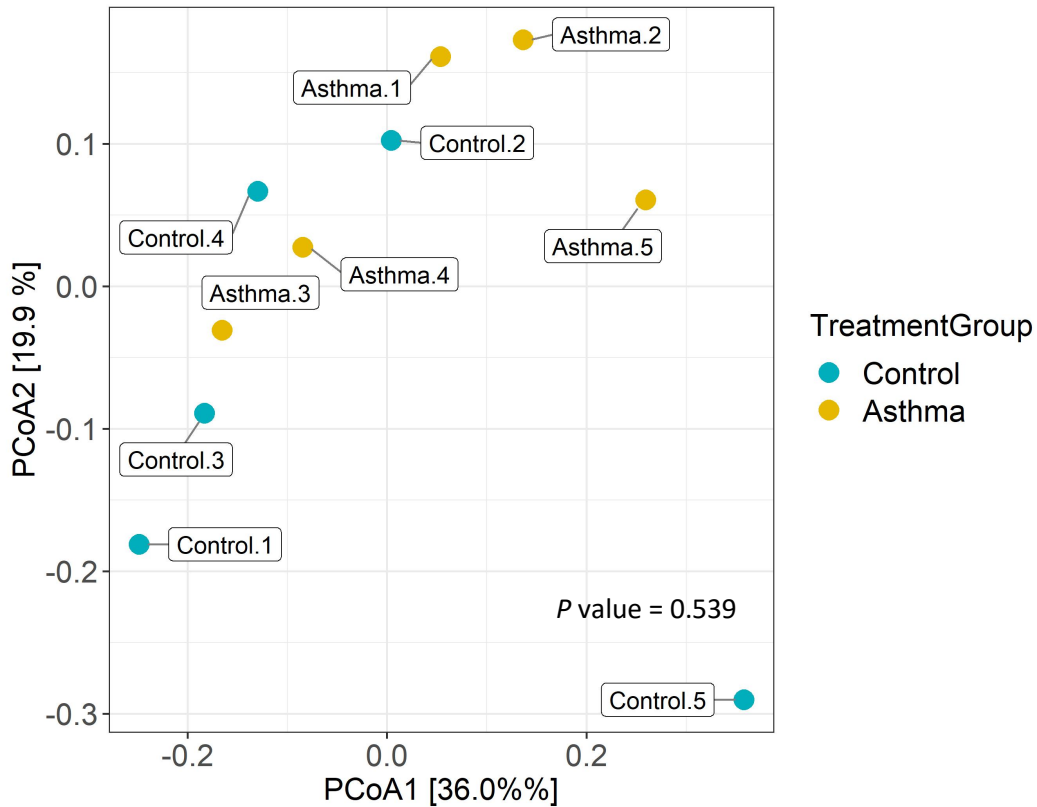


#### 4.3.13. Bacterial Beta Diversity in the Asthmatic Circulatory Microbiome compared to the Control Microbiome

Beta diversity of the circulatory microbiome detected in the asthmatic and non-asthmatic subjects was measured to determine how similar individual circulatory microbiomes were to one another, and whether the presence of a chronic respiratory disorder (asthma) influenced the diversity of bacterial populations present in the circulatory microbiome. Beta diversity was measured by calculating Bray-Curtis dissimilarity to determine compositional dissimilarity between the plasma samples that was based on both the presence/ absence of bacterial OTUs and OTU abundance, and PERMANOVA analysis was carried out to determine if the asthmatic circulatory microbiomes differed significantly to the control circulatory microbiomes in terms of OTU composition.

Plotting of Bray-Curtis dissimilarity using PCoA revealed that the circulatory microbiomes did not cluster on the basis of disease state (Figure 4.11). This was further supported by PERMANOVA analysis which detected no significant differences in the asthmatic circulatory microbiomes compared to the control circulatory microbiomes ( $P$  value = 0.539). However, there did appear to be clustering of the samples on the basis of PCoA1, whereby the circulatory microbiome of subjects Asthma\_1, Asthma\_2, Asthma\_5, and Control\_2 had positive PCoA1 scores and clustered more closely, and the circulatory microbiome from subjects Asthma\_3, Asthma\_4, Control\_1, Control\_3, and Control\_4 had negative PCoA1 scores and clustered more closely (Figure 4.11). This clustering is likely the result of an unknown variable, though it is interesting to note that the majority of subjects with a positive PCoA score were negative for circulatory IgE protein (Asthma\_5, Control\_2, and Control\_5), whilst the majority of subjects with a negative PCoA score were positive for IgE circulatory protein (Asthma\_4, Control\_1, Control\_3, Control\_4)(See Supplementary

Materials, Table S6). However, as this was a small sample group, further investigation would be required to determine the significance of this observation.



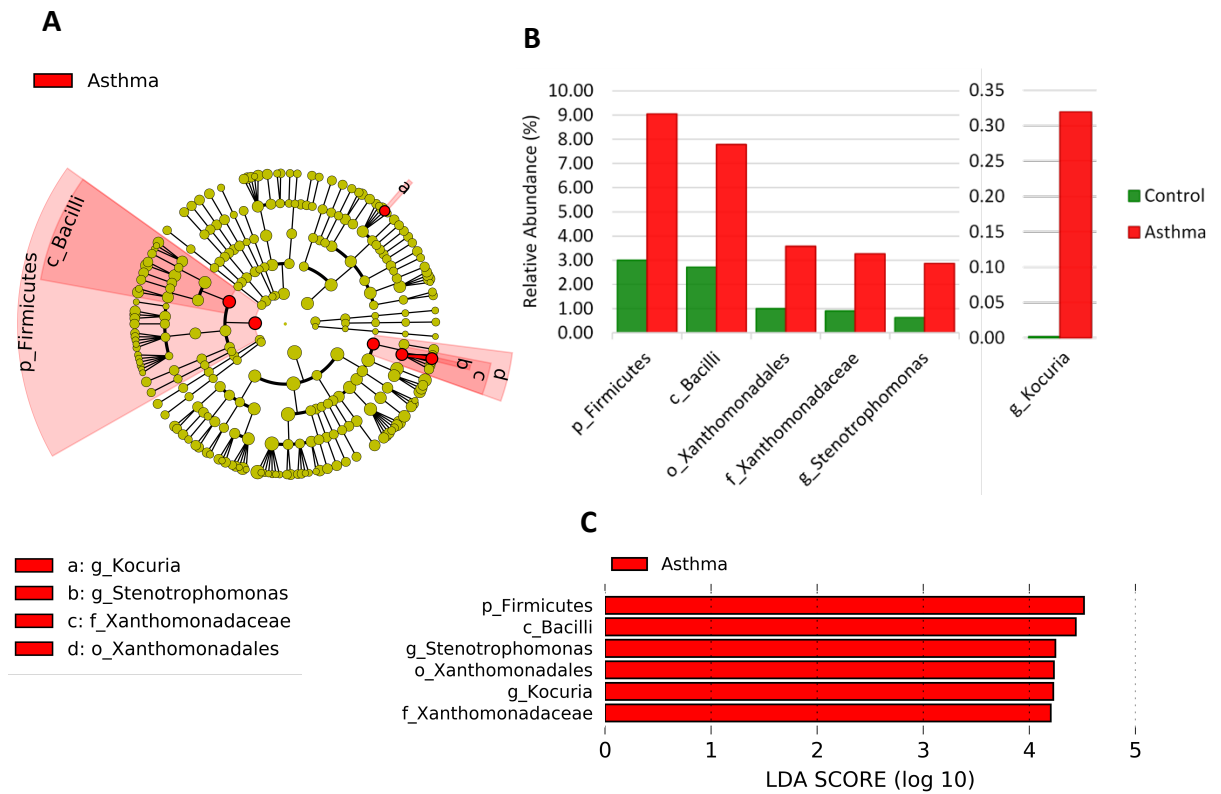
**Figure 4.11: Comparison of beta diversity in the asthmatic circulatory microbiome compared to the control microbiome.** PCoA was performed on OTU tables generated from 16S rRNA sequencing data from the asthma plasma samples (n = 5) and control samples (n = 5). Quantitative compositional dissimilarity between each of the samples was measured using Bray-Curtis dissimilarity, and a PCoA graph was plotted. Each dot represents an individual sample, and the microbiomes of samples that appear more closely together are more similar. Statistical analysis using PERMANOVA revealed no significant differences in the plasma samples.

#### 4.3.14. Differential Bacterial Abundance in the Asthmatic Circulatory Microbiome compared to the Control Microbiome

Statistical analysis of the circulatory microbiome composition at the phylum level revealed atopic asthma was associated with a significant increase in Firmicutes ( $P$  value = 0.0146, *Unpaired t test*), and concomitant decrease in Proteobacteria ( $P$  value = 0.0715, *Unpaired t test*). Additionally, whilst not significantly increased overall in the atopic subjects ( $P$  value = 0.6905, *Wilcoxon rank sum test*), Bacteroidetes were found to be increased in the asthmatic subjects who were not taking anti-inflammatory medication at the time of sample collection (asthma subjects 1, 2, and 5), whilst those on the medication (asthma subjects 3 and 4) displayed similar Bacteroidetes abundance to the control subjects.

LEfSe analysis was performed on the bacterial taxa relative abundance scores to identify biologically significant changes in bacterial composition at all taxonomic levels in the asthmatic subjects compared to the control subjects.

Analysis of the bacterial composition of the circulatory microbiome using LEfSe revealed that 6 bacterial taxa were significantly enriched in the asthmatic subjects compared to the non-asthmatic control subjects. Overall, taxa found to be enriched in the asthmatic circulatory microbiome were high-abundant taxa (had a relative abundance > 1.0%) and included the Firmicutes phylum, the Bacilli and Xanthomonadales classes, the *Xanthomonadaceae* family, and the *Stenotrophomonas* genus (Figure 4.12). Additionally, the low-abundant *Kocuria* genus was also observed to be enriched in the asthmatic subjects compared to the control subjects, and detection of the genus appeared to be condition specific, with detection of the genus observed in just one of the control subjects at low levels (relative abundance = 0.009%) (Figure 4.12).



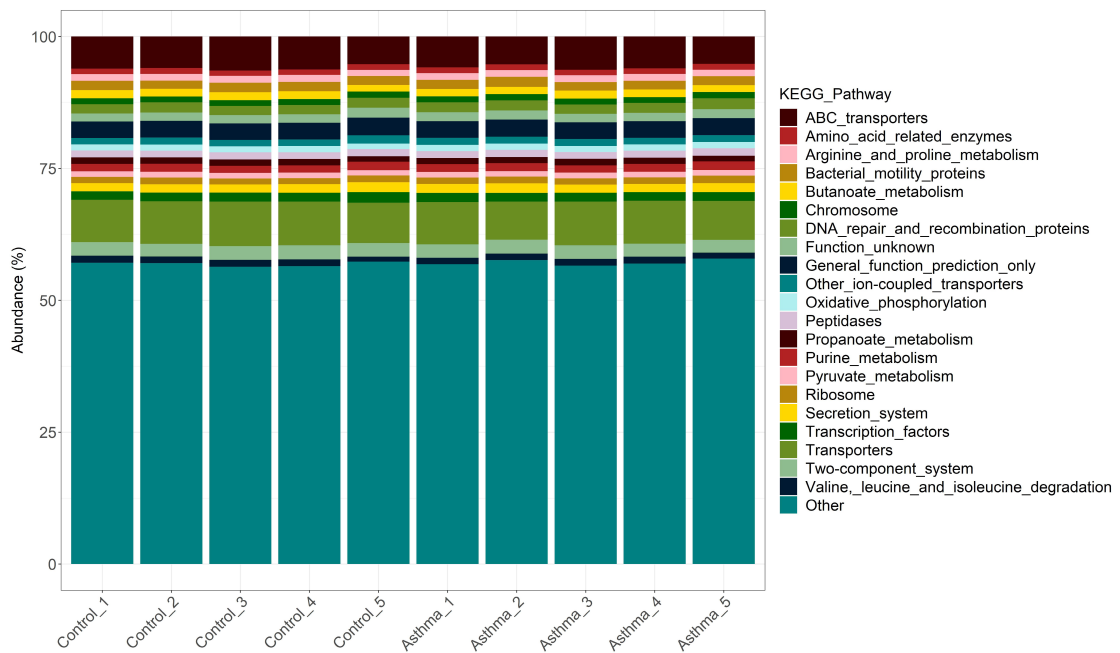
**Figure 4.12: Significant changes in bacterial taxa relative abundance in the circulatory microbiome of atopic asthmatic subjects compared to control subjects.** LEfSe analysis was performed on the bacterial relative abundance data to determine the presence of bacterial taxa with statistically significant changes in taxa abundance in the asthmatic subjects ( $n = 5$ ) compared to the control subjects ( $n = 5$ ) (defined as having a LDA effect size  $> 2.0$  and a  $p$  value  $< 0.05$ ). **(A)** A taxonomic cladogram highlighting the statistically and biologically consistent differences between the asthmatic circulatory microbiome compared to the control circulatory microbiome. Differences are presented in the colour of the most abundant sample group (red represents taxa significantly enriched in the asthmatic subjects, green represents taxa significantly enriched in the non-asthmatic subjects, and yellow representing non-significant taxa). The circle diameter is proportional to the taxon's abundance in the circulatory microbiome. **(B)** Relative abundance of the differentially abundant bacterial taxa. **(C)** Histogram of the LDA scores generated for the differentially abundant taxa present in the asthmatic subjects compared to the control subjects.

*Abbreviations: p\_ = phylum; c\_ = class; o\_ = order; f\_ = family; g\_ = genus*

#### 4.3.14. Prediction of the Plasma Metagenome Function Content

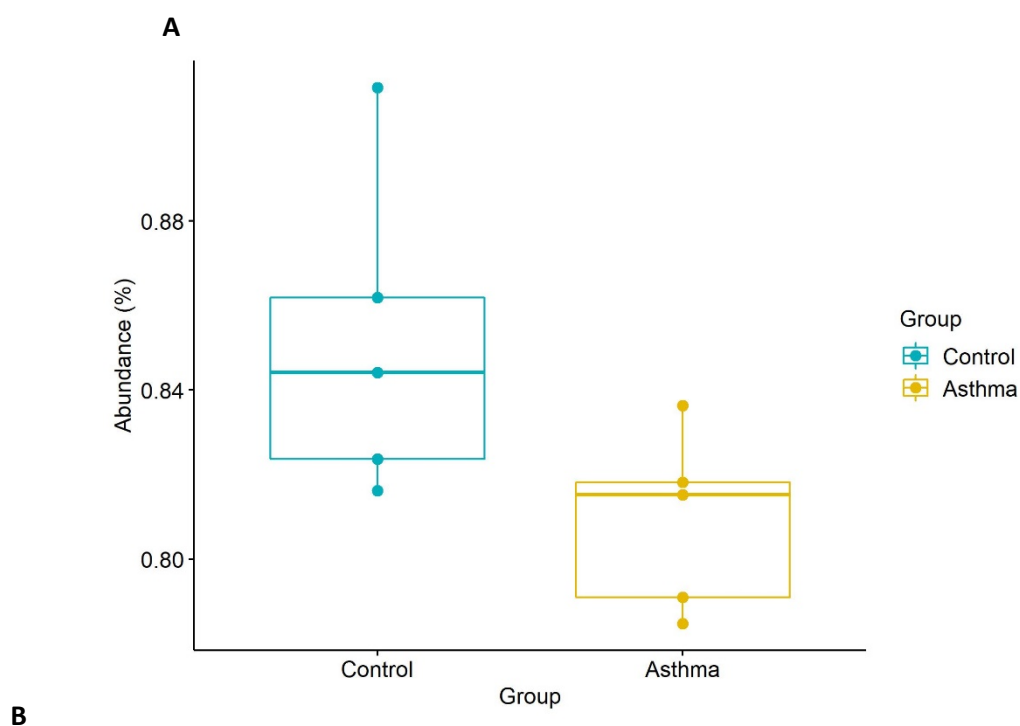
Prediction of the functional capacities of the plasma bacterial community characterised from the V4 16S rRNA sequencing data identified a total of 273 level 3 KEGG pathways belonging to the level 1 KEGG categories *Cellular processes* (total number of KEGG pathways identified = 11), *Environmental information* (13), *Genetic information* (27), *Human diseases* (31), *Metabolism* (142), *Organismal systems* (22), and *Unclassified* (27).

The majority of level 3 KEGG pathways detected scored abundance values of less than 1%. 21 KEGG pathways, however, had total abundance scores greater than 1% (Figure 4.13). These high-abundant KEGG pathways included 1 member of the *Cellular processes* category (Bacterial motility, total abundance = 1.72%), 4 members of the *Environmental information processing* category [ABC transporters (5.85%), Secretion systems (1.66%), Transporters (7.69%), and Two-component system (2.55%)], 4 members of the *Genetic information processing* category [Chromosome (1.14%), DNA repair and recombination proteins (1.86%), Transcription factors (1.69%), and Ribosome (1.22%)], 8 members of the *Metabolism* category [Amino acid related enzymes (1.06%), Arginine and proline metabolism (1.27%), Valine, leucine, and isoleucine degradation (1.21%), Butanoate metabolism (1.43%), Propanoate metabolism (1.18%), Pyruvate metabolism (1.06%), Oxidative phosphorylation (1.15%), Peptidases (1.33%), and Purine metabolism (1.48%)], and 3 members of the *Unclassified* category [Other ion-coupled transporters (1.32%), Function unknown (1.64%), and General function prediction only (3.19%)] (Figure 4.13)



**Figure 4.13: Functional analysis of the plasma circulatory microbiome.** PICRUSt software was used to predict functional content of the plasma metagenome based on the V4 16S rRNA sequencing data generated from control subjects (n = 5) and asthmatic subjects (n = 5). High activity level 3 KEGG pathways (as determined by a predicted abundance of greater than 1% of the total serum sample metagenome) are plotted and KEGG pathways with an abundance less than 1% are grouped together and plotted as other.

Analysis of level 1 and level 2 KEGG pathway orthologs using LEfSe revealed that there were no significant differences in inferred microbial functions of the bacterial populations detected in the asthma plasma samples compared to the control samples at the KEGG levels 1 and 2. Analysis at KEGG level 3, however, revealed that bacterial functional pathways related to energy metabolism were significantly reduced in the asthmatic subjects compared to the control subjects (P value = 0.0472 , LDA effect size = 2.28) (Figure 4.14).



KEGG Pathway	Control Mean Abundance (SD)	Asthma Mean Abundance (SD)	Log2 Fold Change	LDA effect size	P Value
Energy Metabolism	0.85 (0.03)	0.81 (0.02)	- 0.07	2.28	0.0472

**Figure 4.14: Comparison of energy metabolism abundance in the asthma circulatory microbiome compared to the control microbiome.** PICRUSt was used to predict functional potential of the control and asthma circulatory microbiome using the V4 16S rRNA sequencing data. LEfSe analysis was used to identify differential bacterial functions present in the asthma circulatory microbiome (n = 5) compared to the control microbiome (n = 5), and energy metabolism was identified as being significantly decreased in the asthma circulatory microbiome compared to the control microbiome. **(A)** Abundance of energy metabolism detected in the asthma circulatory microbiome compared to the non-atopic control microbiome. **(B)** Statistical analysis of energy abundance detected in the asthma circulatory microbiome compared to the control microbiome (n = 5).

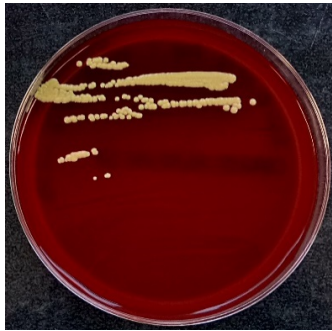
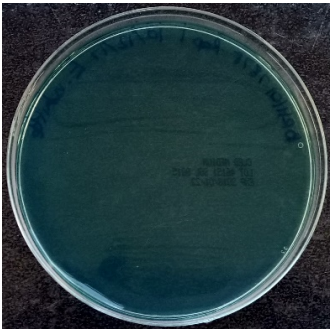
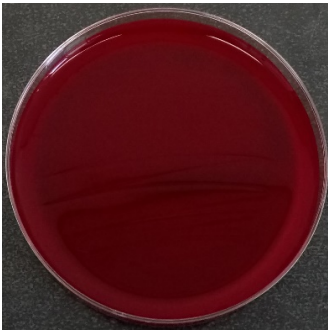

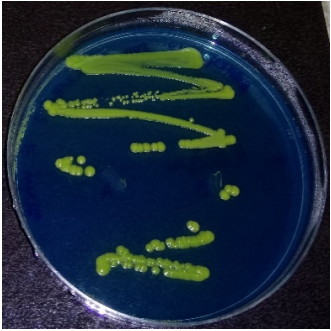
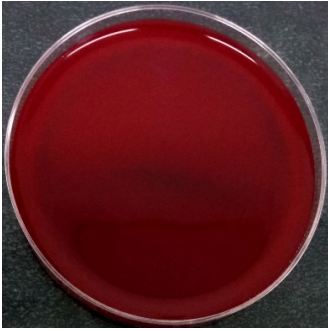

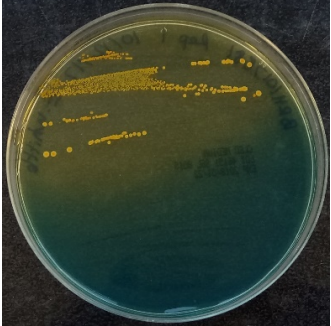
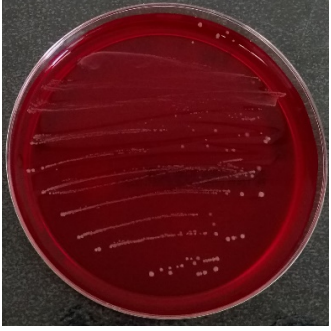
#### 4.3.15. Bacterial Growth Cultures and Identification of Viable Bacteria

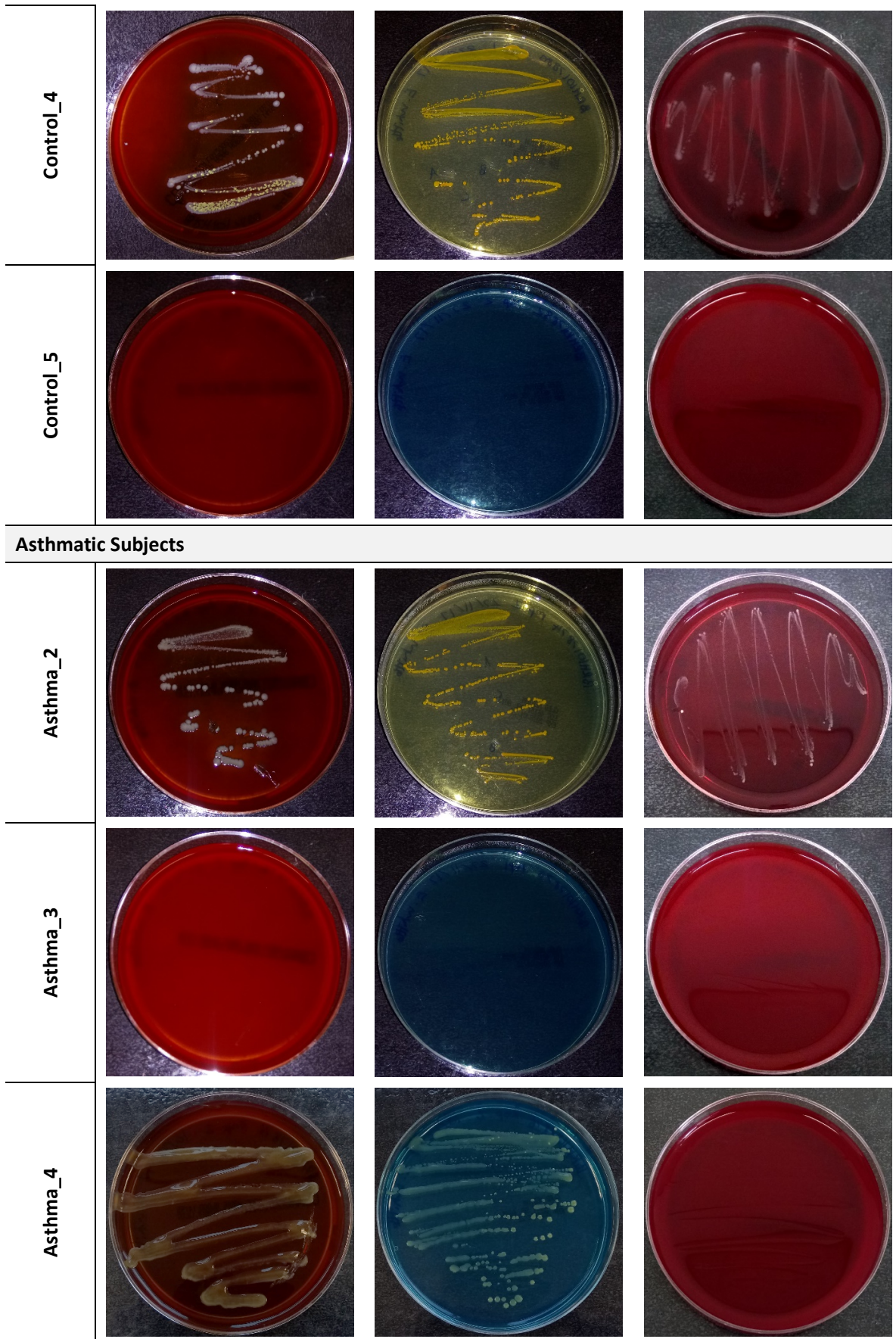
Analysis of the growth agar plates streaked with nutrient broth inoculated with the plasma samples revealed that viable bacteria were present in 78% of plasma samples assayed (7/9 samples; 4 control samples and 3 asthma samples) (Figure 4.15), whilst all negative control plates had no growth as expected (Figure 4.15). Comparison of the growth conditions found that bacterial growth was more successful using aerobic conditions compared to anaerobic conditions (Figure 4.15). Analysis of the two growth agar plates used for aerobic conditions revealed similar success rates with regards to bacterial growth.

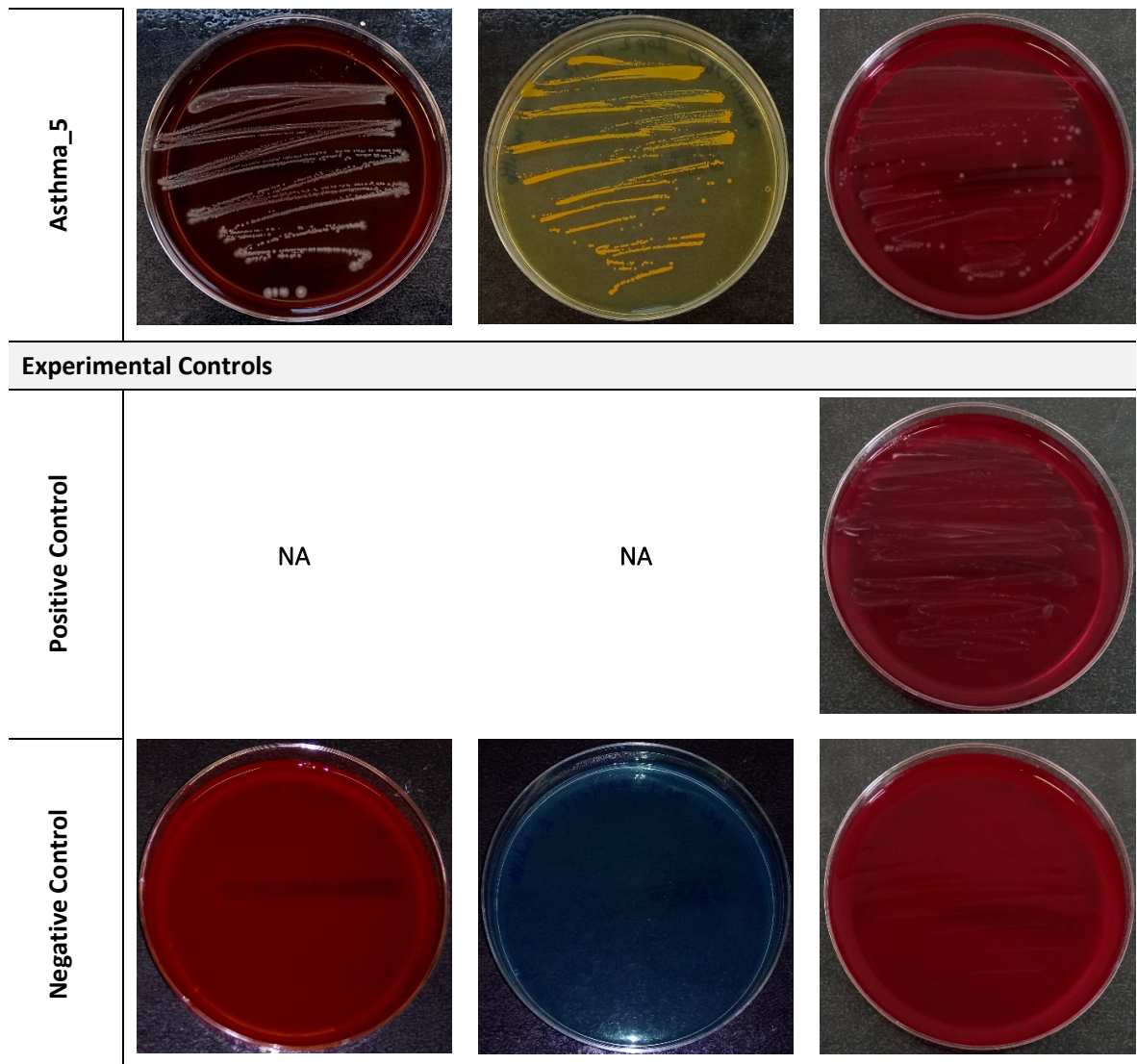
Appearance of the bacterial colonies on the agar plates indicated that the cultures were mono-culture and the lack of over-growth of the bacteria suggested that the viable bacteria were present at low levels in the plasma samples.



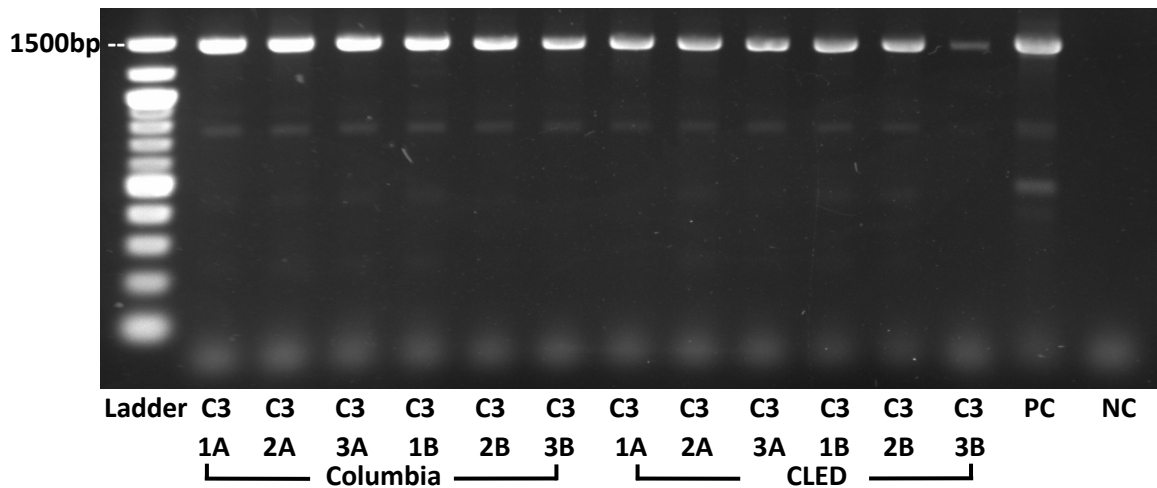
**Figure 4.15: Bacterial growth on selective media streaked with nutrient broth inoculated with human plasma samples.** Viable bacterial cells present in the human plasma samples were revived by inoculating the plasma samples into brain infusion nutrient broth. After a 5 day incubation period, the inoculated broths were streaked onto selective agar media and the streaked plates were incubated for 72 hrs in aerobic conditions (Columbia blood agar, CLED Medium agar) and 120 hrs in anaerobic conditions (A.R.I.A agar).

Sample	Nutrient Growth Culture		
	Columbia Blood Agar	CLED Medium	A.R.I.A
<b>Control Subjects</b>			
Control_1			
Control_2			
Control_3			





Amplification of the total 16S rRNA gene from the cultured bacterial cell was successful for all bacterial colonies, with the exception of the bacterial colonies selected from the Asthma\_2 CLED and A.R.I.A plates and the Asthma\_5 CLED plates (Supplementary Materials, Table S12). A gel representing successful amplification of the total 16S rRNA gene from bacterial DNA extracted from the cultured bacteria is shown below. Samples represented in the gel are DNA extractions from bacterial colonies from Columbia blood agar plates and CLED agar plates streaked with nutrient broth inoculated with plasma from the Control\_3 subject (Figure 4.16).



**Figure 4.16: Amplification of total 16S rRNA gene from DNA extracted from bacterial colonies cultured from human plasma.** 3 bacterial colonies were selected from each growth agar plate positive for bacterial growth. DNA was extracted from the bacterial colonies using thermal lysis and then underwent 35 cycles of end-point PCR using oligonucleotide primers designed to amplify the 16S rRNA gene.

*Abbreviations: C3, Control\_3; A, agar plate replicate 1; B, agar plate replicate 2*

Following successful amplification of the total 16S rRNA gene from DNA extracted from the cultured bacteria colonies, the 16S rRNA amplicons were submitted to *Genewiz* to undergo sanger sequencing.

Analysis of the sequenced 16S rRNA amplicons using NCBI nucleotide blast revealed that bacteria isolated from the anaerobic plates (A.R.I.A) belonged solely to the facultatively anaerobic *Staphylococcus* genus (Table 4.15.A). In contrast, the bacteria isolated from the aerobic plates (Columbia blood agar and CLED plated) were more diverse and belonged to the following genera; *Staphylococcus*, *Micrococcus*, *Kocuria*, *Corynebacterium*, and *Propionibacterium* (Table 4.15.B).

**Table 4.15: Identification of bacterial colonies grown on selective media streaked with nutrient broth inoculated with human plasma samples.** PCR amplification of the total 16S rRNA gene was carried out and the 16S rRNA amplicons were sequenced using Sanger sequencing. The sequencing data was inputted into the NCBI database to determine identification of the bacterial colonies. (A) Identification of bacterial colonies grown in aerobic conditions. (B) Identification of bacterial colonies grown in anaerobic conditions.

Abbreviation used: NA, not applicable – used when colonies were grown but amplification of the whole 16S rRNA gene was unsuccessful; NS, no significance similarity found.

A	Control Samples				Asthma Samples		
	Contol_1	Control_2	Control_3	Control_4	Asthma_3	Asthma_4	Asthma_5
A.R.I.A Agar	NA	NA	<i>Staphylococcus epidermidis</i>	<i>Staphylococcus hominis subsp. novobiosepticus</i>	NA	NA	<i>Staphylococcus epidermidis</i>
	NA	NA	<i>Staphylococcus epidermidis</i>	<i>Staphylococcus hominis strain SubaKolSh24</i>	NA	NA	<i>Staphylococcus epidermidis</i>
	NA	NA	<i>Staphylococcus epidermidis</i>	<i>Staphylococcus hominis</i>	NA	NA	<i>Staphylococcus epidermidis strain L3</i>
	NA	NA	<i>Staphylococcus epidermidis</i>	<i>Staphylococcus hominis</i>	NA	NA	<i>Staphylococcus epidermidis strain BQER2-01</i>
	NA	NA	<i>Staphylococcus epidermidis strain LLP-16</i>	<i>Staphylococcus sp.</i>	NA	NA	<i>Uncultured bacterium clone nbu588e11c1</i>
	NA	NA	<i>Staphylococcus epidermidis</i>	<i>Staphylococcus sp.</i>	NA	NA	<i>Staphylococcus sp. Strain S14</i>

B	Control Samples				Asthma Samples		
	Contol_1	Control_2	Control_3	Control_4	Asthma_2	Asthma_4	Asthma_5
Columbia Blood Agar	<i>Kocuria rhizophilia</i>	<i>Micrococcus luteus</i>	<i>Staphylococcus hominis</i>	<i>Staphylococcus hominis</i>	<i>Staphylococcus hominis</i>	NA	<i>Staphylococcus sp.</i>
	<i>Kocuria rhizophilia</i>	<i>Micrococcus</i>	<i>Staphylococcus hominis</i>	<i>Staphylococcus epidermidis</i>	<i>Staphylococcus hominis</i>	NA	<i>Staphylococcus epidermidis</i>
	<i>Kocuria rhizophilia</i>	<i>Micrococcus yunnanensis</i>	<i>Staphylococcus epidermidis</i>	<i>Staphylococcus sp. CS21</i>	<i>Staphylococcus hominis</i>	NA	<i>Staphylococcus epidermidis</i>
	<i>Kocuria sp.</i>	<i>Micrococcus yunnanensis</i>	<i>Staphylococcus</i>	<i>Staphylococcus sp. CS21</i>	<i>Staphylococcus hominis</i>	NA	Uncultured bacterium clone ncd2456a03c1
	<i>Kocuria rhizophilia</i>	<i>Micrococcus</i>	<i>Staphylococcus sp.</i>	<i>Staphylococcus sp. CS21</i>	<i>Staphylococcus hominis</i>	NA	Uncultured bacterium partial 16S rRNA gene
	<i>Kocuria rhizophilia</i>	<i>Micrococcus</i>	<i>Staphylococcus epidermidis</i>	<i>Staphylococcus hominis</i>	<i>Staphylococcus hominis</i>	NA	<i>Staphylococcus epidermidis</i>
CLED Agar	NA	<i>Micrococcus luteus</i>	<i>Staphylococcus</i>	<i>Staphylococcus hominis</i>	NA	<i>Corynebacterium mucifaciens</i>	NA
	NA	<i>Micrococcus</i>	<i>Staphylococcus hominis</i>	Uncultured bacterium clone ncd539a09c1	NA	<i>Corynebacterium mucifaciens</i>	NA
	NA	<i>Micrococcus</i>	NS	<i>Staphylococcus sp. CS21</i>	NA	<i>Corynebacterium mucifaciens</i>	NA
	NA	<i>Micrococcus</i>	<i>Cutibacterium acnes</i>	<i>Staphylococcus hominis</i>	NA	<i>Corynebacterium mucifaciens</i>	NA
	NA	<i>Micrococcus</i>	NS	<i>Staphylococcus sp. CS21</i>	NA	<i>Corynebacterium mucifaciens</i>	NA
	NA	<i>Micrococcus</i>	NS	<i>Staphylococcus sp.</i>	NA	<i>Corynebacterium mucifaciens</i>	NA

#### 4.3.16. Likely Origins of the Circulatory Microbiome

Whilst evidence of a circulatory microbiome is steadily increasing, it is not yet known whether the detected bacteria are exploiting a viable ecological niche or are simply transient residents of the blood vessels<sup>516</sup>.

Atopobiosis, whereby bacteria translocate into the circulation from their usual place of habitation (classical niches, such as the gastrointestinal tract, the oral tract, and the skin), has been proposed as an explanation for the presence of a circulatory microbiome.

The V4 16S rRNA data generated from the human plasma samples, therefore, was compared to the gastrointestinal tract, oral cavity, and skin microbiome data made available by the Human Microbiome Project (HMP). Comparison was achieved using *Nephele* 1.0 software and involved combining the human plasma 16S rRNA data with the HMP data, calculating weighted UniFrac distances, and performing PCoA.

The circulatory microbiome of the control and asthmatic subjects was found to cluster more closely with the oral cavity and skin HMP data than it did with the gastrointestinal tract HMP data (Figure 4.17). This suggested that if the detected circulatory microbiome was the consequence of atopobiosis, it was more likely to have resulted from translocation of bacteria from the oral and skin niches than due to translocation from the gastrointestinal tract.





**Figure 4.17: Principal coordinate analysis of weighted unifrac distances between the V4 16S rRNA data generated from human plasma samples and the Human Microbiome Project Gut, Oral Cavity, and Skin data.** PCoA was performed on OTU tables generated from V4 16S rRNA sequencing data generated from the human plasma samples and 16S rRNA sequencing data generated from the Human Microbiome Project (HMP) on the human gut, oral cavity, and skin microbiome. Quantitative phylogenetic distances between each of the samples was measured using a weighted UniFrac distance, and the weighted UniFrac distances were plotted as a PCoA graph to show beta diversity with the plasma samples from control subjects (n = 5, data plots = blue) and asthmatic subjects (n = 5, data plots = red) compared to beta diversity present in the HMP gut microbiome, oral cavity microbiome, and skin microbiome. Each data point represents a single sample, and the distance between data points is representative of how similar the sample microbiomes are to one another.

## 4.4. Discussion

### 4.4.1. Development of Research Techniques

The human blood is thought to be sterile and despite increasing evidence of a circulatory microbiome it is still a controversial subject. Recent re-analysis of pleomorphic bacteria detected using electron microscope, for instance, have suggested that the supposed bacterial structures identified in the early circulatory microbiota studies are actually host derived structures <sup>516–518</sup>. This has highlighted the importance of developing stringent experimental procedures and the use of experimental negative controls.

This study aimed to develop a stringent experimental protocol to facilitate characterisation of the circulatory microbiome in asthmatic subjects and non-asthmatic control subjects.

A nested PCR protocol was successfully developed to enable successful generation of 16S rRNA V3-V4 and V4 amplicons containing sequencing adaptors for Ion torrent sequencing and Illumina sequencing. Comparison of sequenced V3-V4 reads and V4 reads generated from Ion torrent sequencing revealed that sequencing the V4 region was optimum over sequencing the V3-V4 region, presumably due to the decreased size of the V4 region compared to the V3-V4 region. When the success rates of sequencing the V4 region using Ion torrent technology and Illumina sequencing were assessed, Illumina sequencing using the MiSeq protocol was found to be optimum over the use of the ion torrent sequencing using the Ion PGM™ Hi-Q™ protocol. This perhaps was not surprising as analysis of previous circulatory microbiome studies found that the majority of the studies that utilised 16S sequencing techniques to characterise the circulatory microbiome used Illumina MiSeq protocols <sup>327, 329, 333–339,365</sup>.

Analysis of the experimental negative control revealed that no high-quality V3-V4/V4 reads were generated from the sample. This demonstrated that the strict sterile conditions maintained during generation of the 16S rRNA reads were sufficient to inhibit bacterial contamination from the immediate environment and/ or laboratory reagents. However, as the blood samples were acquired from a company (*Sera Laboratories Limited*) rather than collected from the subjects directly, it is unknown if sufficient sterile procedures were used during sample collection and handling prior to their delivery.

#### 4.4.2. Detection of a Human Circulatory Microbiome

The circulatory microbiome was successfully characterised for all plasma samples under investigation using *Nephela* 2.0 to align the sequenced V4 reads to bacterial OTUs. Statistical analysis using *R* software and LEfSe analysis was carried out to determine significant differences in bacterial diversity and abundance in the asthmatic circulatory microbiome compared to the control microbiome.

Alignment of the sequenced V4 16S rRNA reads revealed that the human circulatory microbiome was predominately composed of bacterial RNA belonging to the Proteobacteria phylum (total relative abundance = 83.9%, control = 90.0%, and Asthma = 80.3%), and to a lesser extent the Actinobacteria (7.5%, 6.0%, 7.5%), Firmicutes (6.6%, 3.0%, 9.0%), and Bacteroidetes (1.2%, 0.2%, 2.2%) phyla. These findings mirror previous investigations into the circulatory microbiome<sup>323, 327, 332,361</sup>, and thus further support the notion of a core circulatory microbiome predominated by four key phyla.

At the genus level the circulatory microbiome was predominated by the genus *Achromobacter*, which accounted for 51.1% and 45.7% of the total bacteria detected in the control and asthma subjects, respectively. To a lesser extent, the blood samples also

comprised of a number of bacterial genera that have previously been detected in the circulatory microbiome. These included *Pseudomonas*<sup>324,345</sup> (7.5%, 13.0%), *Serratia*<sup>331,339,519</sup> (11.7%, 0.9%), *Sphingomonas*<sup>327,361</sup> (5.1%, 3.9%), *Staphylococcus*<sup>336,338,366</sup> (5.5%, 2.8%), *Corynebacterium*<sup>324,327</sup> (3.2%, 2.8%), *Acinetobacter*<sup>327,331,366</sup> (2.8%, 3.8%), and *Stenotrophomonas*<sup>327,335,339</sup> (0.4%, 2.7%), and the detection of these genera across the different circulatory microbiome studies provides further evidence of a shared circulatory microbiome core.

Whilst the majority of genera detected at high levels have been previously described in the blood, the predominance of *Achromobacter* warrants further consideration. It is interesting to note that the *Achromobacter* genus has been detected at high levels in the lower respiratory tract of healthy mice<sup>520</sup>, humans (HMP airway dataset), and in various respiratory conditions<sup>521,522</sup>. Furthermore, no *Achromobacter* was detected in the experimental negative control, thus indicating that presence of the bacterial genus was not the result of bacterial contamination. It is, therefore, speculated that *Achromobacter* was detected in the circulatory microbiome as a result of translocation from the airways

#### 4.4.3. Comparison of Bacterial diversity in the Asthmatic Circulatory Microbiome compared to the Healthy Controls

To determine whether atopic asthma significantly influences the bacterial composition of the detected circulatory microbiome, alpha diversity, beta diversity, and bacterial taxa relative abundance scores generated from the asthma and control plasma samples were compared.

Alpha diversity was determined by calculating the Shannon and Chao1 indices for each plasma sample. Comparison between the asthma and control cohort revealed that the

asthmatic subjects scored higher Shannon and Chao1 index scores compared to the control subjects, thus suggesting that asthma is associated with increased bacterial diversity. This was particularly apparent for the Shannon diversity scores ( $P$  value = 0.0710, *Unpaired t test*). Intriguingly, one of the asthma samples, belonging to the asthma\_3 subject, displayed a Shannon diversity score more similar to the control subjects than the asthmatic subjects. This subject developed asthma relatively late in childhood (age 12 years), and so it is possible that the age of asthma onset may influence the level of microbial diversity present in the blood. This theory is further supported by the observation of high levels of alpha diversity present in the blood of Asthma\_5, an asthmatic subject who was diagnosed with asthma early on in childhood (3 years of age).

Increased bacterial diversity has also been observed in the asthmatic airways compared to healthy controls <sup>256,281</sup>. This is likely the consequence of the immune dysregulation that typically occurs in the asthmatic lung and suggests that immune activity in the airways influences bacterial diversity in the airways, and subsequent diversity of bacteria capable of translocation into the blood vessels. However, it is also possible that immune dysregulation in the airways and blood as a result of atopic asthma has an adverse effect on the immune system's ability to detect and control colonisation of bacteria in these body habitats. This would explain the increased trend in bacterial diversity in the asthmatic circulatory microbiome compared to the control microbiome.

With regards to beta diversity, PCoA analysis found that beta diversity was principally the consequence of PCoA1 variation (36.0%). Comparison of the control and asthmatic samples revealed no significant clustering of the asthmatic subjects compared to the control subjects, as determined by analysis of the PCoA graph and PERMANOVA analysis. Of interest was the observation of circulatory IgE protein levels appeared to correlate with

PCoA1 score, thus suggesting that this variable may influence the circulatory microbiome of the subjects. However, as this was a preliminary investigation into the circulatory microbiome, only a small sample set was utilised. Further investigations with a larger sample size, therefore, would be required to determine whether circulatory IgE protein levels significantly influences diversity of the circulatory microbiome.

#### 4.4.4. Differential Relative Abundance of Bacterial Populations detected in the Circulatory Microbiome

Microbial characterisation of the circulatory microbiome from asthmatic subjects compared to non-asthmatic healthy controls revealed increased levels of Firmicutes and decreased levels of Proteobacteria in the asthma plasma samples. This finding was associated with the identification of several additional bacterial taxa displaying significantly altered levels in the asthmatic state compared to the control state. Significant changes in relative abundance were predominately detected in high-abundant taxa, and included increased levels of the Firmicutes phylum, the Bacilli class, the Xanthomonadales order, the *Xanthomonadaceae* family, and the *Stenotrophomonas* and *Kocuria* genera.

The observed decrease in circulating Proteobacteria rRNA in the asthmatic state is likely to be indicative of reduced Proteobacteria carriage within the asthmatic state at a distant microbiome niche (e.g. the gastrointestinal tract, airways, and/or oral cavity). This may explain the decreased levels of endotoxin detected in the asthmatic subjects (Chapter 3, section 3.4.8), given that endotoxin-producing Gram negative bacteria dominate the Proteobacteria phylum.

Decreased Proteobacteria have been detected in the gut microbiota of atopic infants <sup>267</sup>, suggesting that Proteobacteria colonisation may confer protective properties against

development of atopic disease. Furthermore, urban living has been found to negatively correlate to the abundance of Proteobacteria present in the skin microbiome <sup>249</sup>, thus suggesting that the positive correlation between increased urbanisation and asthma prevalence may be in part due to decreased Proteobacteria colonisation. In the airways of asthmatics, however, Proteobacteria are typically increased <sup>256,261,262</sup> and have been positively associated with disease severity <sup>259</sup> and corticosteroid resistance <sup>255</sup>. This suggests that members of the phylum can be both protective and harmful with regards to atopic disease, and the protective/ harmful effects of the phylum may be dependent on the microbiome environment.

The observation of increased levels of Firmicutes in the asthmatic subjects was of particular interest as expansion of this phylum has been associated with severe asthma <sup>261</sup>. Furthermore, increased levels of Firmicutes in the asthmatic subjects was found to be primarily due to increased levels of *Staphylococcus* and *Streptococcus* genera, both of which have been associated with the development of asthma during early childhood <sup>260, 280,523,524</sup>. The observation of increased levels of these genera in adults suffering from asthma, therefore, suggests that changes in the circulatory microbiome that occur during childhood, either as precursor of asthma development and/ or due to the development of asthma, persist into adulthood.

The asthmatic subjects were also found to have increased levels of Bacteroidetes, and this appeared to be dependent on medication status, with those taking anti-inflammatory medications having lower levels of circulating Bacteroidetes compared to asthmatic subjects who were not taking anti-inflammatory medications. This finding suggested that asthma medication may influence composition of the circulatory microbiome. However, as this study was a preliminary investigation involving a small cohort of asthmatic subjects,

further research would be required to determine the effects of anti-inflammatory medication on the asthmatic circulatory microbiome.

As the blood circulates the body where it functions as a medium that samples from virtually all body sites <sup>358</sup>, it was not possible to determine the microbial niche from which the detected bacteria originated from. However, this study hypothesises that changes in the circulatory microbiome are reflective of dysbiosis at distant sites with well-characterised microbial communities (e.g. the gut, oral cavity, and skin), and have significant biomarker potential.

In support of this interpretation, studies investigating the asthmatic airway microbiome have observed reduced Firmicutes in the asthmatic airways compared to healthy control subjects <sup>256,525</sup>. It is, therefore, possible that the increased levels of Firmicutes RNA observed in the blood in this study is a consequence of increased translocation of these bacteria and/ or their DNA from the airways into the blood compared to the control subjects.

Additionally, the observed changes to the circulatory microbiome were reflective of a previous study investigating the oral microbiome, whereby Firmicutes, *Stenotrophomonas*, and *Lactobacillus* were found to be increased in asthmatic subjects compared to the control subjects. This suggests that the bacterial DNA detected in the blood may have originated from the oral cavities, and that the changes in the circulatory microbiome in the asthmatic subjects is reflective of microbial dysbiosis occurring in the asthmatic oral cavities.



#### 4.4.5. Predicted Functional Activity of the Circulatory Microbiome

The observed changes in bacterial relative abundance in the circulatory microbiome of the asthmatic subjects compared to the control subjects were predicted to decrease energy metabolism in the asthmatic subjects.

Decreased energy metabolism in the asthmatic subjects was of interest due to the essential role the gut microbiome has in host energy metabolism <sup>161,526–528</sup>. In the human gastrointestinal (GI) tract simple sugars (i.e. glucose) and disaccharides (i.e. lactose) are absorbed into the blood by the host <sup>527,529</sup>. The human GI tract, however, is unable to digest dietary carbohydrates (i.e. fibre), and subsequently dietary carbohydrates pass through the GI tract undigested and are instead fermented by members of the gut microbiota in the cecum and large intestine <sup>527</sup>. Bacterial fermentation is carried out by anaerobic bacteria (primarily members of the Firmicutes and Bacteroidetes phyla, the dominant phyla in the gut microbiome), and results in the production of multiple metabolites, of which short chain fatty acids (SCFAs; a waste product of bacterial fermentation) are the major group <sup>527,530,531</sup>.

The identification of energy metabolism being significantly reduced in the asthmatic subjects is indicative of reduced relative abundance of energy-metabolising bacteria present in the plasma of the asthmatic subjects. This could be reflective of microbial dysbiosis in the gut of the asthmatic subjects that is associated with reduced energy-metabolising potential of the gut microbiome.

Reduced microbial energy metabolism in the asthmatic subjects, could be indicative of reduced fibre consumption and a subsequent decrease in SCFA production. This interpretation is supported by epidemiological studies that have demonstrated that asthmatic subjects consume less fibre and exhibit reduced levels of SCFAs compared to

control subjects <sup>532-534</sup>. Moreover, SCFAs have been demonstrated to inhibit histone deacetylase <sup>535-537</sup>. RNA analysis of the asthmatic subjects in Chapter 3 found that expression of histone deacetylase 9 (HDAC9) was significantly decreased in the asthmatic subjects (See Supplementary Materials, Table S4). The HDACs have been demonstrated to regulate the immune responses <sup>538</sup> and the administration of HDAC inhibitors has been found to suppress inflammation <sup>539-541</sup>. In asthmatic subjects reduced production of SCFAs would likely result in decreased regulation of HDAC activity, subsequently resulting in increased inflammation. This is further supported by the observations that SCFAs are protective against asthma in murine experimental models <sup>542,543</sup>.

Additionally, SCFAs have been demonstrated to be protective against metabolic diseases, such as obesity and diabetes <sup>544-548</sup>. Both these diseases have been found to be comorbid with asthma <sup>549-554</sup>, and thus reduced SCFA production may explain why these diseases often present together.

However, reduced energy metabolism potential in the asthmatic microbiome could suggest altered translocation of bacteria into circulation in the asthmatic subjects compared to the control subjects. For instance, it may be indicative of increased bacterial translocation from other body habitats in the asthmatic subjects, or it may demonstrate reduced bacterial translocation from the gut of the asthmatic subjects compared to the control subjects. Further investigations, therefore, would be required to determine where the microbial populations originated from in order to fully assess the significance of reduced energy metabolism in the asthmatic subjects.

#### 4.4.6. The Detection of Viable Bacteria in Human Plasma Samples

The presence of viable, proliferating bacteria was detected in 78% of plasma samples assayed (7/9 plasma samples, 4 control plasma samples and 3 asthma samples), whilst all negative control plates were negative for bacterial growth as expected. These results were consistent with previous studies investigating the presence of viable organisms present in the blood, whereby 2-100% of blood samples were found to be positive for viable bacterial cells<sup>203, 315, 333, 346,555</sup>. In contrast to previous investigations, however, was that aerobic growth was observed for all culture-positive samples, but anaerobic growth was only observed for four of the culture-positive plasma samples. This was an unexpected finding as previous investigations have demonstrated that bacterial growth from blood cultures is predominately achieved using anaerobic conditions<sup>203,345</sup>.

Following identification of the cultured bacteria using Sanger sequencing, aerobic cultures included the following genera; *Corynebacterium*, *Kocuria*, *Micrococcus*, and *Staphylococcus*. In contrast, bacteria isolated from the anaerobic cultures were less variable and included members of the *Staphylococcus* genus only. The identified bacteria were all represented in the 16S rRNA data, and with the exception of *Kocuria*, all bacteria identified displayed some of the highest total relative abundance scores in the 16S rRNA sequencing results; *Corynebacterium* (4.2%), *Kocuria* (0.2%), *Micrococcus* (1.3%), and *Staphylococcus* (4.3%).

The skin microbiome is dominated by members of the *Corynebacterium*, *Micrococcus*, and *Staphylococcus* genera, the proportions of which vary markedly between individuals<sup>556–558</sup>. Furthermore, several studies have reported the presence of the *Kocuria* genus on the skin of humans and other mammals<sup>559–561</sup>. This, therefore, suggests that the organisms detected through the microbial culture experiments most likely originate from the skin. The

organisms may have translocated into the blood vessels following wounding of the skin prior to sample collection or are the result of bacterial contamination of the blood sample. Whilst transient bacteraemia due to breaching of the skin barrier is an accepted occurrence, it is thought that such organisms would be rapidly targeted and removed from circulation by the immune system <sup>562,563</sup>. It is, therefore, more likely that the viable organisms detected in the plasma samples were the result of venepuncture contamination, whereby organisms from the skin were drawn into the vacutainer during blood collection.

However, it has also been proposed that bacteria exist in the blood in a dormant state that goes undetected by the immune system <sup>326,333</sup>. It is, therefore, also possible that pre-growth in brain heart infusion broth prior to plating revived bacteria present in the dormant state in the plasma samples.

#### 4.4.7. Likely Origins of the Circulatory Microbiome

PCoA analysis was also used to compare the circulatory microbiome to well established Human HMP microbiomes (the gut, oral cavities, and skin) to determine how similar the circulatory microbiome was to other, well-established microbiomes. These particular microbiome environments were selected as it is the gut, oral cavities, and skin that are frequently proposed as the original location of the circulatory microbiome bacteria prior to translocation into the blood vessels.

When PCoA analysis was performed on the circulatory microbiome and various other microbiome niches within the human body, the circulatory microbiome data points were observed to cluster more closely in the PCoA space with the oral cavity and skin HMP microbiome data than it did with the gastrointestinal tract HMP data. This suggested that the circulatory microbiome community was more likely to be the result of translocation

from the oral cavity and/ or skin microbiome than from translocation of organisms that traditionally colonise the gastrointestinal tract.

Translocation from the oral cavity is likely to result as a consequence of daily activities, including chewing, tooth brushing, flossing<sup>311,564–566</sup>, and periodontal procedures<sup>567</sup>. Furthermore, of the different oral environments, the circulatory microbiome most closely resembled the subgingival plaque and supragingival plaque, thus providing further support for the theory that the circulatory microbiome derives from microbial translocation as a result of dental care (tooth brushing).

However, it is also important to take into consideration sources of bacterial contamination that may occur during blood sample collection. Venepuncture, the process by which the majority of blood samples are collected, is recognised as a cause of transient bacteraemia<sup>568,569</sup>, and despite the use of preventative measures, such as alcohol cleansing of the skin prior to breaking the surface, there remains the possibility that organisms may enter the blood sample from the skin via this route. In support of this entry route, was the observation that when the circulatory microbiome was compared to different skin environments, it displayed the highest degree of similarity with the antecubital fossa microbiome, an area on the arm where blood is most commonly drawn from when collecting blood samples.

The observed lack of similarity between the gut microbiome and the circulatory microbiome is supported by two studies by Lelouvier *et al* (2016)<sup>361</sup> and Qian *et al* (2018)<sup>337</sup>, who independently characterised both the faecal and circulatory microbiome of healthy controls and patients suffering from liver fibrosis and Parkinson's, respectively, and found that composition of the circulatory microbiome was largely different to that observed for

the gut microbiome. This suggested that it is unlikely that bacteria detected in the blood originate from the gut as a result of bacterial translocation across the intestinal barrier.

#### 4.4.8. Chapter Summary

In summary a protocol for amplifying and sequencing the V4 region of the bacterial 16S rRNA gene from plasma samples was successfully developed. The bacterial populations present in the plasma samples were found to be predominately Proteobacteria, and to a lesser extent, Actinobacteria, Firmicutes, and Bacteroidetes, and reflected the findings of previous investigations into the circulatory microbiome. Moreover, no high-quality V4 sequences were generated from the experimental negative control, demonstrating that the detected microbial DNA originated from the human plasma samples and not as a result of microbial contamination from the immediate environment and/ or laboratory reagents.

Comparison of the asthma circulatory microbiome to the control microbiome revealed a number of significant differences in the asthma circulatory microbiome. This included increased alpha diversity of the asthmatic microbiome compared to the control microbiome, an increased ratio of Firmicutes to Proteobacteria, the detection of several bacterial taxa displaying differential relative abundance and decreased metabolic potential of the asthmatic microbiome compared to the control microbiome.

Altered circulatory microbiome composition in the asthmatic subjects is likely due to microbial dysbiosis at previously described body sites (airways, gut) influencing microbial translocation into the bloodstream. This is likely due to decreased permeability of the epithelial barrier and immune dysregulation in the asthmatic subjects changing how the asthmatic immune system responds to microbe

## Chapter 5: Characterisation of the Circulatory Microbiome in Different Atopic Populations

### 5.1. Introduction

Atopic asthma is a disease phenotype of atopy, whereby sensitisation to one or more allergen results in production of allergen-specific IgE and Th2-driven inflammation. Other clinical manifestations of atopy include atopic dermatitis (eczema), a skin disease characterised by chronic cutaneous inflammation as a result of hyperreactivity to one or more environmental allergen, and allergic rhinitis (hayfever), an inflammatory disorder of the nasal mucosa due to sensitivity to one more environmental allergen.

Atopic sensitisation typically occurs during the first two years of life in genetically predisposed infants and can persist through a lifetime, with disease typically first presenting as atopic dermatitis (0 – 2 years), followed by the development of asthma (> 5 years) in approximately half of atopic dermatitis patients, and allergic rhinitis (> 8 years) in approximately two thirds of atopic dermatitis patients <sup>33,34</sup>. The pattern of clinical manifestations presenting in atopic individuals is referred to as the atopic march.

This results in atopic individuals frequently presenting with more than one clinical manifestation of atopic disease. A study carried out by Kapoor *et al* (2008), for instance, found that by the age of 3 years 66% of infants diagnosed with atopic dermatitis had developed one or more additional forms of atopic disease <sup>35</sup>.

Asthma and allergic rhinitis are two atopic manifestations that share similar prevalence, pathophysiology, and treatment approaches. Both frequently coexist within the same patient, with approximately 20-50% of allergic rhinitis patients also presenting with asthma <sup>570–572</sup>, and over 80% of asthmatic patients also presenting with allergic rhinitis <sup>570,571,573–575</sup>.

Allergic rhinitis has been associated with the development of asthma<sup>577–581</sup> and asthma severity<sup>582</sup>. Furthermore, bronchial hyperresponsiveness in the absence of asthma is relatively common in subjects with allergic rhinitis<sup>583,584</sup>, whilst in asthmatics eosinophilic infiltration of the nasal mucosa has been observed in the absence of allergic rhinitis<sup>585</sup>, and both diseases are typically treated with corticosteroids.

These similarities and overlap in pathogenesis of asthma and allergic rhinitis has led to the ‘united airway disease hypothesis’ being proposed, whereby it is speculated that the upper and lower airway diseases are both manifestations of a single inflammatory process<sup>586,587</sup>. Prevalence of both diseases has been increasing, and thus it is highly likely that the two diseases share the same environmental factor(s) responsible for the increasing prevalence rates.

#### 5.1.1. Aims of the Chapter

The aim of this study was to expand the knowledge of the circulatory microbiome in atopic disease, by characterising the circulatory microbiome of subjects with asthma, allergic rhinitis, or both asthma and allergic rhinitis (hyper-allergic) compared to non-atopic healthy controls. This was achieved using the V4 rRNA amplification and sequencing techniques developed in Chapter 4, and the study predominately focussed on identifying bacterial taxa that could be used as circulatory biomarkers for asthma, allergic rhinitis, or hyper-allergic.



## 5.2. Methods

### 5.2.1. Sample Collection

To examine the effects of atopic disease on the circulatory microbiome, 25 historic serum samples were acquired as a result of a collaboration with Professor Debbie Jarvis of the *National Lung and Heart Institute*. Professor Jarvis kindly donated serum samples from 4 asthmatic subjects, 7 allergic rhinitis subjects, 3 hyper-allergic subjects (diagnosed with both asthma and allergic rhinitis), and 11 healthy control subjects, as part of a preliminary investigation into whether a circulatory microbiome could be characterised using historic serum samples.

### 5.2.2. Extraction and Amplification of the V4 region of the Bacterial 16S rRNA Gene

Extraction and amplification of the V4 region of the bacterial 16S rRNA gene was performed using the optimised nested PCR protocol developed in Chapter 4.

In brief, direct amplification was performed on the human serum samples using the V4 primers and the Phusion blood direct PCR kit (*Thermo Fisher Scientific*) (Table 5.1). An experimental negative control was generated, whereby serum was replaced with UV-treated molecular biology grade water, and sterile conditions during PCR set-up were maintained (see Chapter 2, section 2.1 for full details).

**Table 5.1: PCR Amplification of the V4 region of the 16S rRNA gene in historic serum samples.** The optimised Phusion blood direct protocol developed in Chapter 4 was utilised to amplify the V4 region of the bacterial 16S rRNA gene in 25% human serum sample. **(A)** The reagents used in the Phusion blood direct end-point PCR protocol. **(B)** The cycling parameters used in the Phusion blood direct end-point PCR protocol.

**A.**

Reagent	Volume ( $\mu$ l)
UV-treated molecular biology grade water	2.6
2X Phusion blood PCR buffer	10.0
V4 Fwd primer (10 $\mu$ M)	1.0
V4 Rev primer (10 $\mu$ M)	1.0
Phusion blood II DNA polymerase	0.4
Serum	5.0

**B.**

Cycle Step	Temperature ( $^{\circ}$ C)	Time	Cycles
Lysis of cells	98	5 minutes	1
Denaturation	98	1 second	
Annealing	53	5 seconds	35
Extension	72	15 seconds	
Final Extension	72	7 minute	1

Gel electrophoresis was then carried out to confirm successful amplification of the V4 region, and the MinElute purification protocol was carried out to purify the V4 amplicons ready for the second nested PCR step. Full descriptions of the two methods can be found in the general methods chapter (sections 2.2 & 2.3.1). Attachment of the Illumina XT adaptor was performed on the purified V4 amplicons using a second PCR step involving the V4 primer pair 515F and 806R and an Accuprime Pfx supermix mastermix (*Thermo Fisher Scientific*) (Table 5.2).

**Table 5.2: Attachment of Illumina sequencing motifs onto V4 16S rRNA amplicons generated from historic serum samples using PCR.** Following confirmation of successful V4 16S rRNA amplification, Accuprime PCR was performed on the V4 amplicons generated from the serum samples to attach Illumina XT adaptors onto the amplicons. **(A)** The reagents used in the Accuprime end-point PCR protocol. **(B)** The cycling parameters used in the Accuprime end-point PCR protocol.

**A.**

Reagent	Volume ( $\mu$ l)
Accuprime master mix	22.5 $\mu$ l
515F primer (10 $\mu$ M)	0.5 $\mu$ l
806R primer (10 $\mu$ M)	0.5 $\mu$ l
Purified V4 amplicons	1.5 $\mu$ l

**B.**

Cycle Step	Temperature ( $^{\circ}$ C)	Time	Cycles
Lysis of cells	95	5 minutes	1
Denaturation	95	15 second	
Annealing	55	30 seconds	7
Extension	68	25 seconds	
Final Extension	68	7 minutes	1

### 5.2.3. Sequencing of the XT-V4 amplicons

Following confirmation of successful attachment of the XT adaptors using gel electrophoresis (Chapter 2, section 2.2). The XT-V4 amplicons were then purified using AMPure XP PCR purification protocol (Chapter 2, section 2.3.2) and then submitted to the *Centre for Genomic Research* at the University of Liverpool to undergo Illumina sequencing. At the centre the XT-V4 amplicons were barcoded using the Nextera DNA library kit, and then multiplexed and sequenced using the Illumina MiSeq system with a 250bp paired-end read metric.

#### 5.2.4. Alignment of the V4 Amplicons to known Bacterial Genomes

Following successful sequencing of the V4 amplicons using Illumina sequencing technology, the trimmed and demultiplexed sequencing data was uploaded to *Nephele* 2.0 [Public web access: <https://nephele.niaid.nih.gov/#cloud>]. The *Nephele* 2.0 QIIME 16S FASTQ paired-end open reference pipeline was used to remove low-quality V4 reads (defined as having a Phred quality score less than 19.0), remove chimeric sequences, and align the V4 reads to bacterial OTUs with a 99% similarity threshold using the Silva database.

#### 5.2.5. Comparison of the Atopic Microbiome compared to the Control Microbiome

The phylogenetic diversity of the bacterial OTUs detected in the serum samples was first analysed by generating a rarefaction curve using *R* software (see Chapter 2, section 2.4.2 for additional detail).

*Nephele* 2.0 software was then used to assign the bacterial OTUs to bacterial taxa, and *R* software was used to measure the relative abundance of the bacterial taxa detected in the serum samples (See Chapter 3, section 2.3.2 for additional detail). The relative abundance values of high-abundant bacterial phyla and genera (taxa with a relative abundance greater than 1%) were plotted (see Chapter 2.4.2).

Alpha diversity of the bacterial populations detected in the serum samples was measured using the *Nephele* 2.0 QIIME 16S FASTQ paired-end open reference pipeline to calculate Shannon and Chao1 diversity indices [Public web access: <https://nephele.niaid.nih.gov/#cloud>]. *R* software was then used to plot alpha diversity as a boxplot and perform the appropriate statistical tests to determine if the atopic

microbiomes differed significantly to the control microbiome in terms of alpha diversity (see Chapter 2, section 2.4.4).

Beta diversity was also measured using the OTU table generated from the *Nephele* 2.0 QIIME 16S FASTQ paired-end open reference pipeline. This involved measuring Bray Curtis dissimilarity and plotting PCoA graphs using *R* software (See Chapter 2, section 2.4.6 for additional information). PERMANOVA analysis was then performed to determine if there were any significant differences between the atopic and control microbiomes.

LEfSe analysis was then applied to the relative abundance data to determine bacterial taxa significantly associated with the atopic microbiomes compared to the control microbiome. This was performed using the default settings of the online *Galaxy* workflow framework<sup>394</sup> on the relative abundance tables of all bacterial taxa detected in the serum samples [Public web access: <http://huttenhower.sph.harvard.edu/galaxy/>] (See Chapter 2, Section 2.4.3. for additional information).

#### 5.2.6. Prediction of the Serum Metagenome Functional Content

To determine how differential bacterial abundance in the atopic subjects altered microbial activity in the atopic microbiome PICRUSt analysis was performed using the online *Galaxy* platform. An OTU table was first generated from the V4 16S rRNA sequencing data using *Nephele* 2.0 software with a closed reference OTU picking strategy and the GreenGenes 99 database. The OTU table was then uploaded to *Galaxy*, normalised, and functional predictions based on the bacterial OTUs detected in the serum samples was performed to determine KEGG ortholog abundance present in the samples (See Chapter 2, section 2.4.5 for additional information).

The level 1 – 3 KEGG ortholog counts were converted into abundance percentage values, and *R* software was used to plot the abundance of high-abundant level 3 KEGG pathways detected in the serum samples (defined as having a predicted total abundance greater than 1% in the serum samples). LEfSe analysis was then performed on the level 1,2, and 3 KEGG orthologs to determine differential KEGG ortholog abundance present in the atopic serum compared to the control serum.

#### 5.2.7. Culturing of Serum Samples on Selective Growth Media

To determine whether there were viable bacterial cells present in the serum samples, the blood sample culture method developed in Chapter 4 was carried out using the serum samples. In brief, 250µl of serum was inoculated into 10ml of brain heart infusion broth. Negative and positive experimental controls were generated by inoculating 10ml of brain heart infusion broth with UV-treated molecular biology grade water and *Pseudomonas* bacterial colonies respectively.

The inoculated broths were incubated at 37°C for 5 days. After the incubation period the inoculated broths were removed from the incubator and immediately streaked onto Columbia Blood agar (*Biomerieux*), CLED medium (*Biomerieux*), and A.R.I.A plates (*Biomerieux*) using sterile 20µl loops. This was performed in duplicate for each sample/control and sterile conditions were maintained throughout. The streaked Columbia Blood agar plates and CLED agar plates were incubated at 37°C for 72 hrs. At 24 hrs, 48 hrs, and 72 hrs, the plates were assessed for bacterial growth.

The A.R.I.A plates were placed in a 2.5L anaerobic chamber (*Sigma-Aldrich*) and incubated at 37°C for 120hrs. After 120hrs the plates were removed from the anaerobic chamber and assessed for bacterial growth.

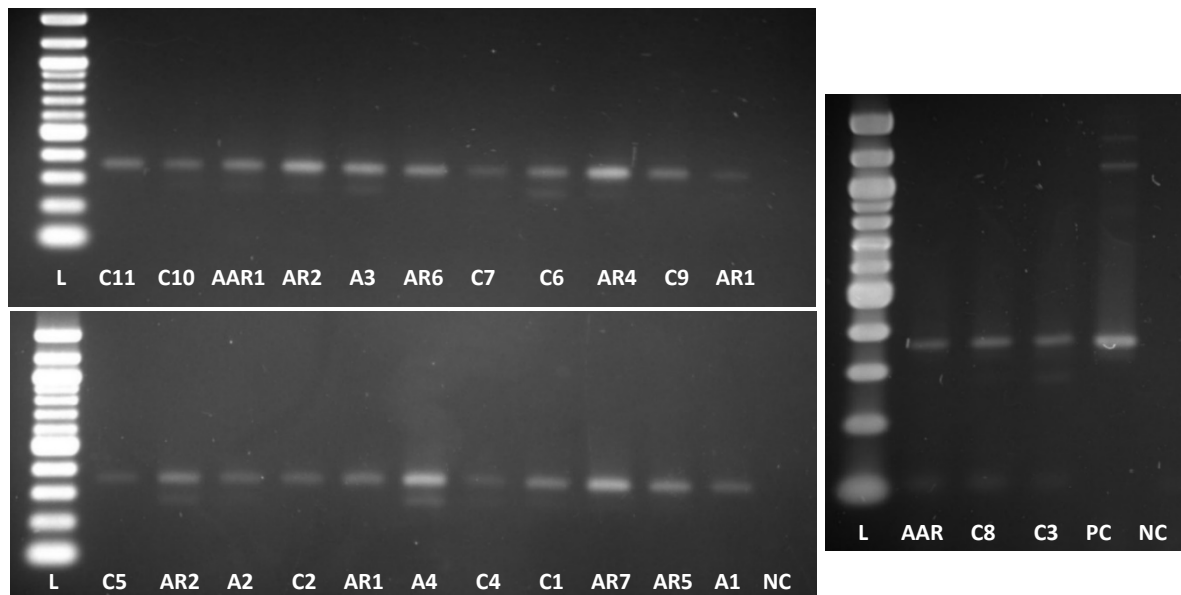
### 5.3. Results

#### 5.3.1. Amplification of the V4 region of the 16S rRNA gene from Bacterial DNA present in Human Serum Samples

Nested PCR was performed on the serum samples to generate a V4 amplicon library suitable for Illumina MiSeq Sequencing.

Analysis of the nested PCR end-products using gel electrophoresis revealed that the protocol had successfully generated V4 amplicons containing the Illumina XT adapters from all serum samples under investigation. This was evident in the observation of a single band of approximately 355bp in length. A number of samples, however, displayed a faint band at approximately 290bp (Figure 5.1). The V4 amplicons alone are approximately 290bp in length, whilst the V4-XT amplicons are approximately 355bp in length (V4 amplicon = 290bp, the forward XT adaptor sequence = 33bp, and the reverse XT adaptor sequence = 34bp). The detection of faint bands representing DNA approximately 290bp long, therefore, indicates the presence of V4 amplicons that do not have the XT adaptor sequences attached.

Analysis of the experimental negative control was as expected, with no amplification of the V4 region observed. This indicated that the sterile conditions utilised had successfully prevented bacterial DNA being introduced to the PCR reactions from the immediate environment and/ or PCR reagents (Figure 5.1, NC).



**Figure 5.1: Direct amplification of the V4 region of the bacterial 16S rRNA gene from human serum samples.** Amplification of the V4 region of the 16S rRNA gene was achieved by performing nested PCR on serum samples from control subjects (n = 11, C lanes), asthmatic subjects (n = 4, A lanes), allergic rhinitis subjects (n = 7, AR lanes), and hyper-allergic subjects (n = 3, AAR lanes). The first stage involved 35 cycles of PCR, the V4 primers and a Phusion blood direct protocol. The V4 amplicons were purified using the MinElute protocol, and second stage PCR was performed using 7 cycles of PCR, the V4 primer pair 515F and 806R, and an Accuprime protocol. The V4-XT amplicons then underwent a final clean-up using SPRI beads at a 0.8X ratio of PCR product to beads.

*Abbreviations: L, 100bp ladder; C, control samples; A, Asthma samples; AR, Allergic Rhinitis samples; AAR, hyper-allergic samples; PC, E.coli positive control; NC, UV dH<sub>2</sub>O negative control.*

### 5.3.2. Sequencing of the V4 16S rRNA reads generated from Human Serum Samples

The total number of V4 16S rRNA reads generated from the serum samples was 2,580,704. Following removal of low quality reads and chimeric sequences, an average of 84,124.09 high-quality reads were generated from the control samples (range = 59,431 – 128,000), 70,735.75 from the asthma samples (range = 58,396 – 94,415), 84,104.86 from the allergic rhinitis samples (range = 61,979 – 112,915), and 90,654.33 from the hyper-allergic samples



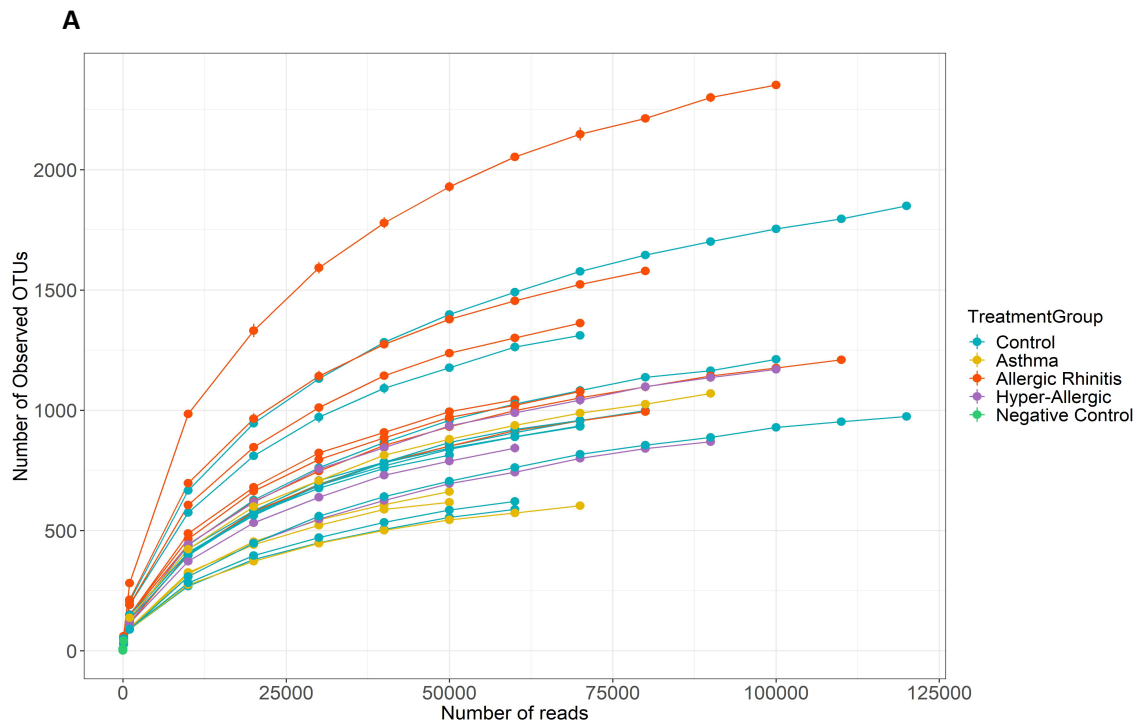
(range = 68,123 – 109,027) (Figure 5.2, see also Supplementary materials, Table S13). Statistical analysis of the number of high-quality V4 16S rRNA reads generated from the different sample groups using a Pairwise t test found no significant differences in the number of V4 reads generated from each group, thus suggesting similar bacterial loads in the different sample groups (data not shown).

A total of 12,098 OTUs with a 99% similarity threshold were detected in the serum samples. This included a total of 7,601 different OTUs detected in the control subjects (range = 738 – 2,206 per sample), 2,878 OTUs detected in the asthmatic subjects (range = 751 – 1,323 per sample), 7,369 OTUs detected in the allergic rhinitis subjects (range = 1,241 – 2,757 per sample), and 2,856 OTUs detected in the hyper-allergic subjects (range = 1,084 – 1,447 per sample)(Figure 5.2 see also Supplementary materials, Table S13).

Comparison of the atopic samples to the control samples revealed a shared core circulatory microbiome composed of 780 OTUs that were present in all four sample groups. An additional 2,719 OTUs were uniquely detected in the control subjects, 441 OTUs were only detected in the asthmatic subjects, 2,723 in the allergic rhinitis subjects, and 449 were unique to the hyper-allergic subjects.

Analysis of the experimental negative control revealed that although the negative control was negative for V4 amplification when examined using gel electrophoresis, a small amount of V4 amplification was achieved. A total of 204 high-quality V4 reads were generated from the negative control, which aligned to 93 OTUs (Figure 5.2 see also Supplementary Materials, Table S23). However, compared to the serum samples, the number of V4 reads generated from the negative control was significantly lower, suggesting that the detection of bacterial DNA in the negative control is unlikely to affect microbiome analysis of the serum samples.

Analysis of the rarefaction curve suggested that the number of OTUs detected in the asthma and allergic rhinitis subjects differed significantly, as demonstrated by noticeably higher numbers of OTUs detected in the allergic rhinitis samples compared to the asthmatic samples (Figure 5.2). Statistical analysis using a Pairwise t test further supported this interpretation, whereby the only close to significant difference in number of OTUs was between the asthmatic and allergic rhinitis subjects ( $P$  value = 0.0600, *Pairwise t test*). Intriguingly, the number of OTUs detected in the hyper-allergic samples was similar to the number detected in the asthma samples (Figure 5.2), suggesting that asthma was associated with decreased numbers of bacterial OTUs present in the blood vessels.



**B**

Group	Number of Samples	Mean number of raw reads	Mean number of high-quality reads	Total number of bacterial OTUs
Control	11	108,294.73	84,124.09	7,601
Asthma	4	90,334.50	70,735.75	2,878
Allergic Rhinitis	7	102,954.14	84,104.86	7,369
Hyper-Allergic	3	116,420.33	90,654.33	2,856
Negative Control	1	402.00	204.00	93

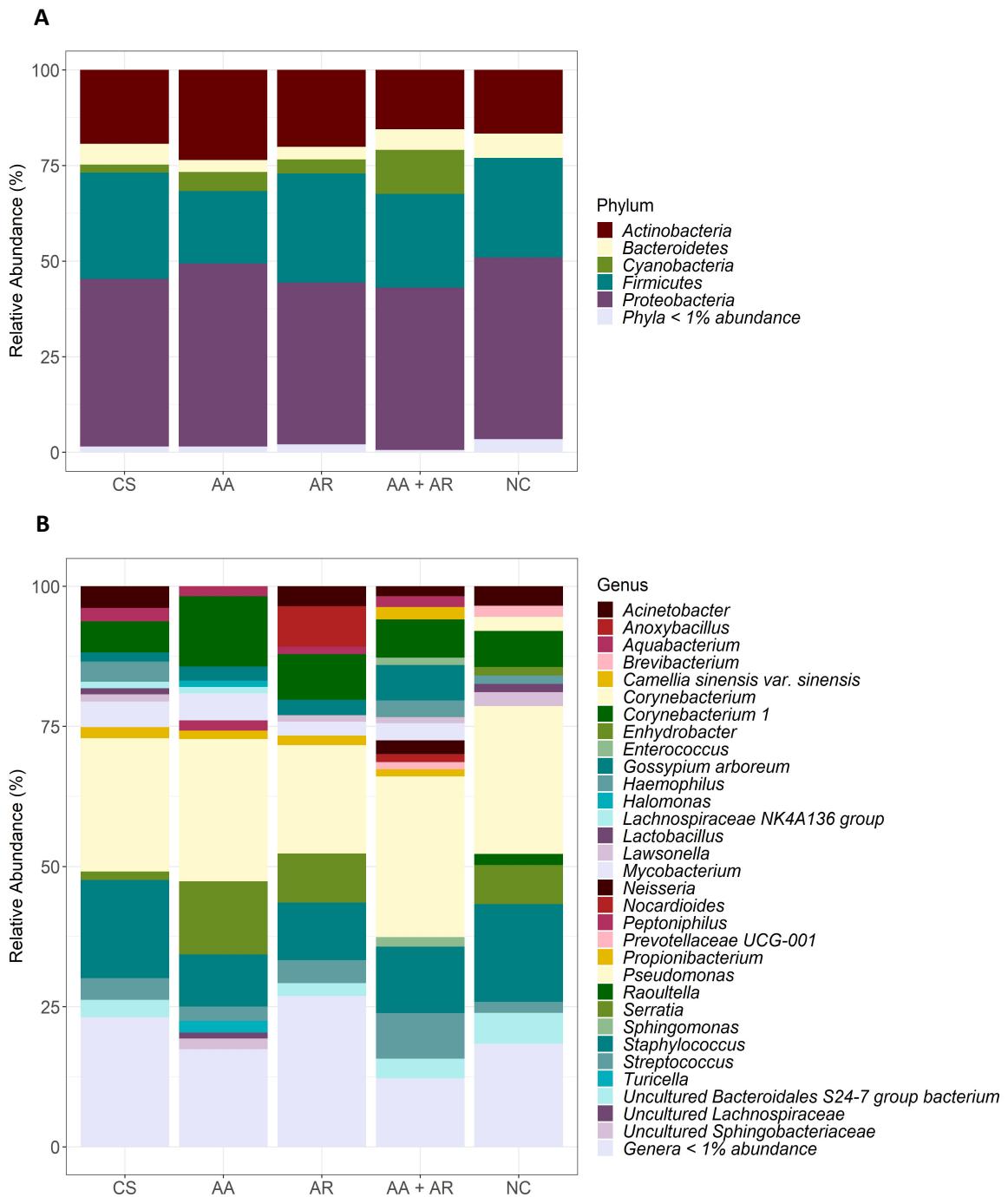
**Figure 5.2: Quantification of bacterial V4 reads sequenced from human serum samples using Illumina sequencing.** Illumina sequencing was used to sequence bacterial V4 amplicons generated from serum samples from control subjects ( $n = 11$ ), asthmatic subjects ( $n = 4$ ), allergic rhinitis subjects ( $n = 7$ ), hyper-allergic rhinitis ( $n = 3$ ). Following successful sequencing of the V4 amplicons *Nephel* 2.0 was used to remove low-quality reads and chimeric sequences, and to align the high-quality V4 reads to bacterial operational taxonomic units (OTUs). **(A)** A rarefaction curve showing the level of phylogenetic diversity of OTUs detected in the serum samples. **(B)** Quantification of the V4 reads generated from the control serum samples, asthmatic serum samples, allergic rhinitis serum samples, and hyper-allergic, and the total number of bacterial OTUs the reads align to with a 99% similarity threshold.

### 5.3.3. Taxonomic Classification of the detected OTUs

The detected OTUs were classified into 19 phyla and 348 genera. At the phylum level, the detected bacterial taxa were predominately Proteobacteria, representing a total of 50.50% of the detected bacteria, and to a lesser extent Firmicutes (23.75%), Actinobacteria (16.11%), Cyanobacteria (4.68%), and Bacteroidetes (3.74%) (Figure 5.3.A).

Analysis at the genus level revealed that the circulatory microbiome was predominately composed of 13 bacterial genera displayed an average relative abundance greater than 1%. These genera included, *Pseudomonas* (total relative abundance = 24.30%), *Staphylococcus* (12.24%), *Corynebacterium 1* (8.25%), *Serratia* (5.83%), *Streptococcus* (4.67%), *Mycobacterium* (3.75%), *Gossypium arboreum* (3.30%), *Acinetobacter* (2.53%), *uncultured Bacteroidales S24-7 group bacterium* (2.34%), *Haemophilus* (1.90%), *Aquabacterium* (1.86%), *Anoxybacterium* (1.86%), and *Propionibacterium* (1.60%) (Figure 5.3.B). An additional 14 genera had a mean relative abundance greater than 1% in one or more of the sample groups but did not have a total relative abundance score greater than 1% overall (Figure 5.3.B).

Analysis of the experimental negative control revealed that the negative control contained a similar bacterial population at both the phylum and genus level to the bacterial populations detected in the serum samples. However, the sample contained significantly less microbial DNA compared to the serum samples, and thus it is unlikely that the detection of low-level bacterial contamination will have a significant impact on downstream analysis of the serum microbiome.



**Figure 5.3: Composition of the bacterial circulatory microbiome in control and atopic subjects.** Bacterial composition was determined using QIIME FASTQ paired-end analysis on sequenced 16S rRNA (V4 region) reads generated from human serum samples taken from control subjects (CS, n = 11, mean number of reads = 88,169), asthmatic subjects (AA, n= 4, mean number of reads = 73,966), allergic rhinitis subjects (AR, n = 7, mean number of reads = 91,502) and hyper-allergic subjects (AA + AR, n = 3, mean number of reads = 99,329), and an experimental negative control (NC, n = 1, number of reads = 204). Taxa with a relative abundance  $\geq 1$  were plotted, and low-abundant taxa ( $< 1.0\%$ ) were grouped and plotted as Taxa < 1% abundance.

#### 5.3.4. Alpha Diversity of the Circulatory Microbiome in Atopic Populations

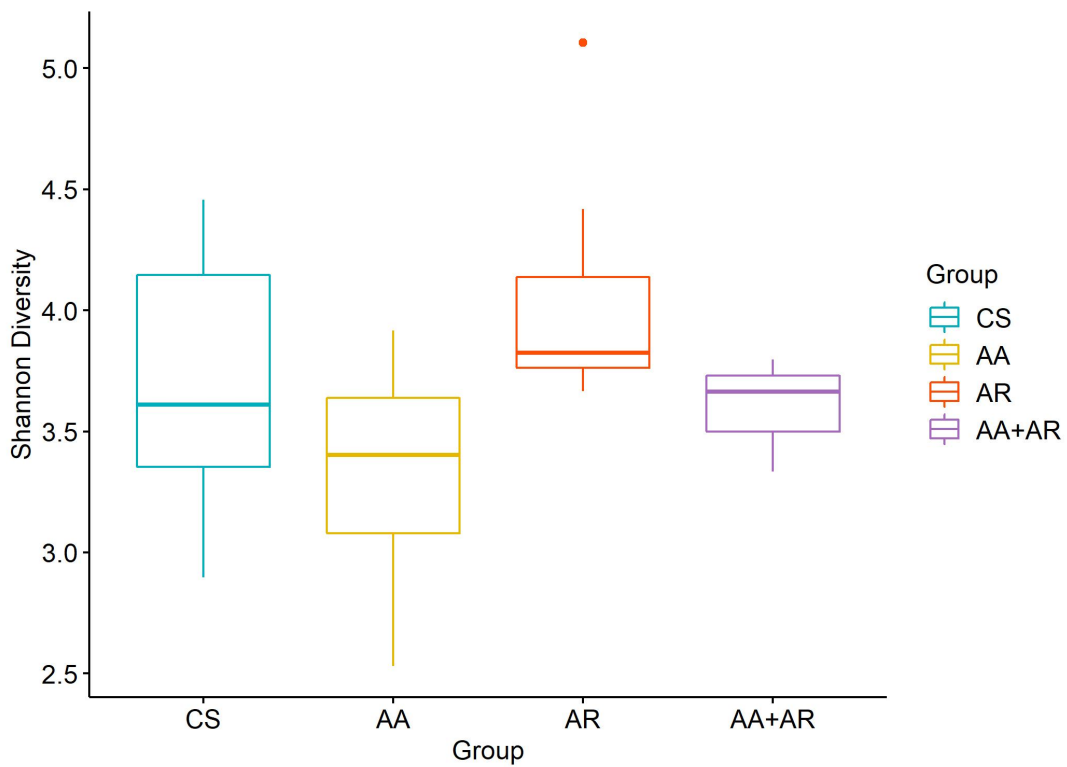
Alpha diversity was calculated to determine whether the mean species diversity present in the circulatory microbiome of atopic subjects was significantly different to the level of diversity present in non-atopic subjects. Alpha diversity was determined by measuring the richness and evenness of bacterial taxa present in the serum samples (Shannon diversity). The predicted number of bacterial taxa present in the serum samples was also calculated by extrapolating out the number of rare organisms that likely went undetected due to under-sampling (Chao1 diversity).

The mean Shannon and Chao1 diversity indices were first calculated for the control and atopic circulatory microbiomes. Statistical analysis was performed and there were no significant differences detected in the alpha diversity of the atopic circulatory microbiome compared to the control microbiome (Shannon diversity,  $P$  value = 0.6150, *Unpaired t test* ; Chao1 diversity,  $P$  value = 0.6475, *Wilcoxon rank sum test*).

The mean Shannon and diversity indices for the different atopic populations (asthma, allergic rhinitis, hyper-allergic) were then determined (Figure 5.4 and 5.5, respectively). Statistical analysis using a one-way ANOVA test revealed that the sample group had no significant impact on Shannon diversity indices ( $P$  value = 0.1520, *ANOVA test*) (Figure 5.4), but did have a significant impact on Chao1 diversity indices ( $P$  value = 0.0218, *ANOVA test*) (Figure 5.5).

Additional statistical analysis on the alpha diversity indices were performed using Pairwise  $t$  tests to determine whether the different atopic sample groups differed significantly. As expected, the pairwise  $t$  test performed on the Shannon diversity scores revealed no significant differences in Shannon diversity, thus confirming the results of the one-way ANOVA test (Figure 5.4)

In contrast, analysis of the Chao1 diversity scores using the Pairwise t test revealed that the asthmatic subjects Chao1 diversity scores were significantly lower compared to Chao1 diversity observed in the allergic rhinitis subjects ( $P$  value = 0.0210, *Pairwise t test*) (Figure 5.5). Additionally, when the allergic rhinitis subjects were compared to the control subjects, the allergic rhinitis subjects displayed a close to significant increase in Chao1 diversity compared to the control subjects ( $P$  value = 0.0950, *Pairwise t test*), whilst the asthmatic subjects displayed a close to significant decrease in Chao1 diversity compared to the control subjects ( $P$  value = 0.1810, *Pairwise t test*) (Figure 5.5). This suggests that allergic rhinitis increases bacterial diversity in the circulatory microbiome, whilst asthma decreases diversity.

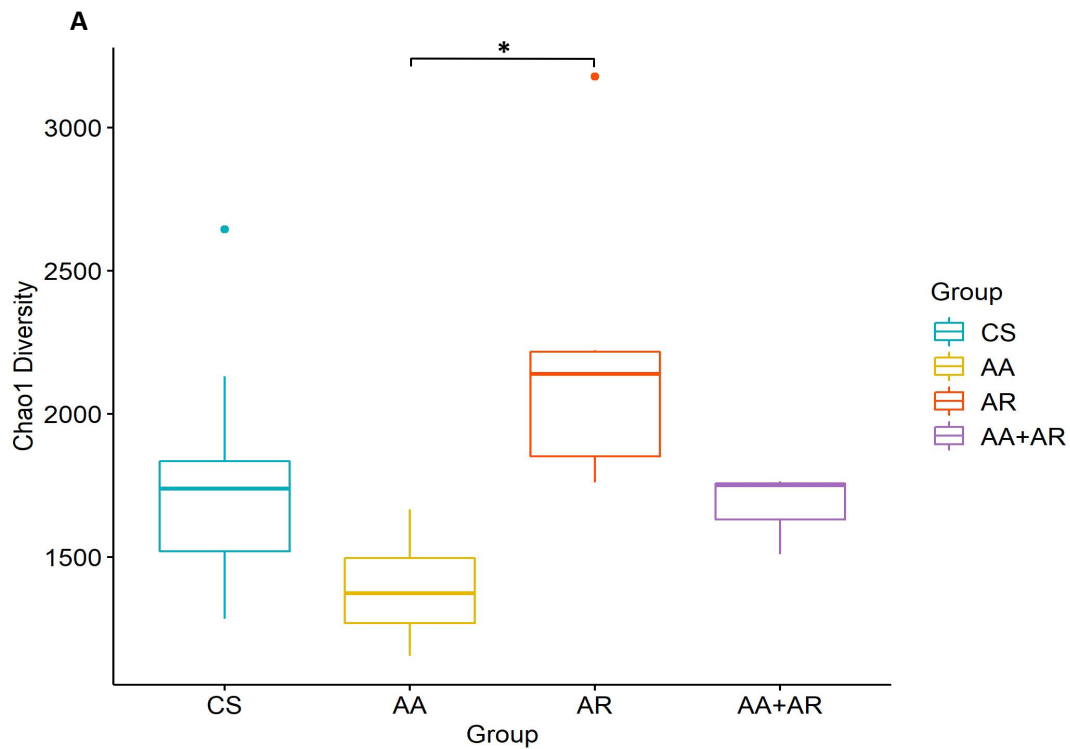


**B**

Group	Pairwise T test		
	Control (CS)	Asthma (AA)	Allergic Rhinitis (AR)
Asthma (AA)	0.31	-	-
Allergic Rhinitis (AR)	0.31	0.17	-
Hyper-allergic (AA + AR)	0.75	0.56	0.31

**Figure 5.4: Comparison of Shannon diversity detected in the circulatory microbiome of atopic subjects compared to control subjects.** Alpha diversity was measured using rarefied OTU tables generated from 16S rRNA sequencing data from serum samples collected from asthmatic subjects (AA, n = 4), allergic rhinitis subjects (AR, n = 7), hyper-allergic subjects (AA + AR, n = 3), and non-atopic control subjects (CS, n = 11). Shannon diversity index scores were generated from the OTU tables in order to measure the richness and evenness of bacterial taxa present in the serum samples. **(A)** Shannon diversity detected in the circulatory microbiome of control subjects compared to the level of diversity detected in different atopic populations. **(B)** Statistical analysis of the Shannon diversity scores detected in the serum samples using a Pairwise t test.





**B**

Group	Pairwise T test		
	Control (CS)	Asthma (AA)	Allergic Rhinitis (AR)
Asthma (AA)	0.181	-	-
Allergic Rhinitis (AR)	0.095	0.021	-
Hyper-allergic (AA + AR)	0.761	0.409	0.141

**Figure 5.5: Comparison of Chao1 diversity detected in the circulatory microbiome of atopic subjects compared to control subjects.** Alpha diversity was measured using rarefied OTU tables generated from 16S rRNA sequencing data from serum samples collected from asthmatic subjects (AA, n = 4), allergic rhinitis subjects (AR, n = 7), hyper-allergic subjects (AA + AR, n = 3), and non-atopic control subjects (CS, n = 11). Chao1 diversity scores were generated from the OTU tables in order to determine the predicted number of bacterial taxa present in the serum samples by extrapolating out the number of rare organisms that may not have been detected in the serum samples due to under-sampling. **(A)** Chao1 diversity detected in the circulatory microbiome of control subjects compared to the level of diversity detected in different atopic populations. **(B)** Statistical analysis of the Chao1 diversity scores detected in the serum samples using a Pairwise t test.

### 5.3.5. Beta Diversity of the Circulatory microbiome in Atopic Populations

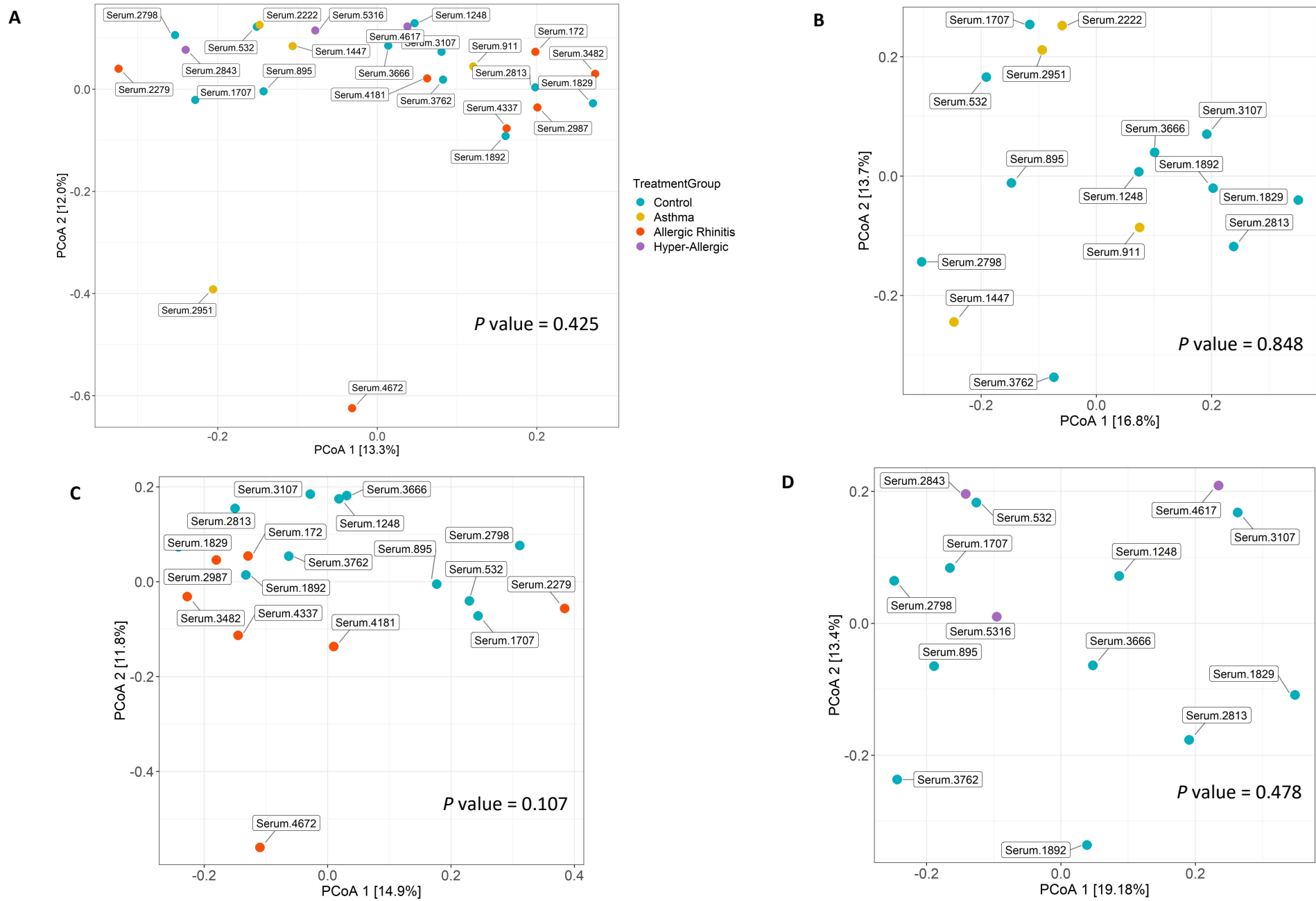
In addition to measuring alpha diversity, beta diversity was also measured to determine how similar the individual circulatory microbiomes were to one another, and whether the presence of atopic disease significantly altered the composition of the circulatory microbiome. This was achieved by measuring Bray Curtis dissimilarity using the V4 16S rRNA sequencing data generated from the serum samples. PCoA analysis was then performed to determine whether the serum samples clustered on the basis of atopic disease, and PERMANOVA was carried out to determine if any observed clustering was statistically significant.

Overall analysis of the PCoA plot revealed no distinct clustering of the circulatory microbiomes (Figure 5.6). Comparison of the different atopic diseases, however, found that of the four subject groups under investigation (Control, Asthma, Allergic rhinitis, Hyper-Allergic), the allergic rhinitis microbiomes appeared more similar to one another compared to the microbiomes of members of the other subject groups (Figure 5.6). This suggests the possibility that the circulatory microbiome of the control subjects, asthma subjects, and hyper-allergic subjects, is due to non-specific bacterial translocation, resulting in a high level of inter-variation, whereas translocation in allergic rhinitis subjects may be more specific, thus reducing the level of variability in the circulatory microbiome of these subjects.

Interpretation of the PCoA plot was supported by PERMANOVA, whereby comparison of all the samples, and comparison of the control serum samples against the different atopic diseases, revealed no statistically significant differences in the circulatory microbiomes (Figure 5.6). Moreover, analysis of the control samples to the allergic rhinitis samples generated the lowest *P* value, thus providing further support that allergic rhinitis had the

greatest effect on composition of the circulatory microbiome (Figure 5.6). However, the allergic rhinitis subject group was the largest group of the three atopic disease groups under investigation, and thus changes in the circulatory microbiome of this subject group may be more apparent compared to the remaining two disease groups due to increased sample numbers.

**Figure 5.6: Comparison of beta diversity of the bacterial populations detected in the circulatory microbiome of atopic subjects compared to a control subjects.** Beta diversity of the bacterial populations detected in serum samples from control subjects (n = 11), asthmatic subjects (n = 4), allergic rhinitis subjects (n = 7), and hyper-allergic subjects (n = 3) was determined by measuring quantitative phylogenetic distances between each of the serum samples. This was achieved by measuring Bray Curtis dissimilarity from a normalised OTU table generated from the 16S rRNA sequencing data obtained from the serum samples. PCoA analysis was performed. Each data point represents an individual serum sample, and the distance between datapoints is representative of the similarity between samples. Statistical analysis using PERMANOVA revealed no significant differences in the serum samples (**A**), in the asthma samples compared to the control samples (**B**), in the allergic rhinitis samples compared to the control samples (**C**), or in the hyper-allergic samples compared to the control samples (**D**).



### 5.3.6. Differential Bacterial Abundance in the Atopic Subjects compared to the Control Subjects

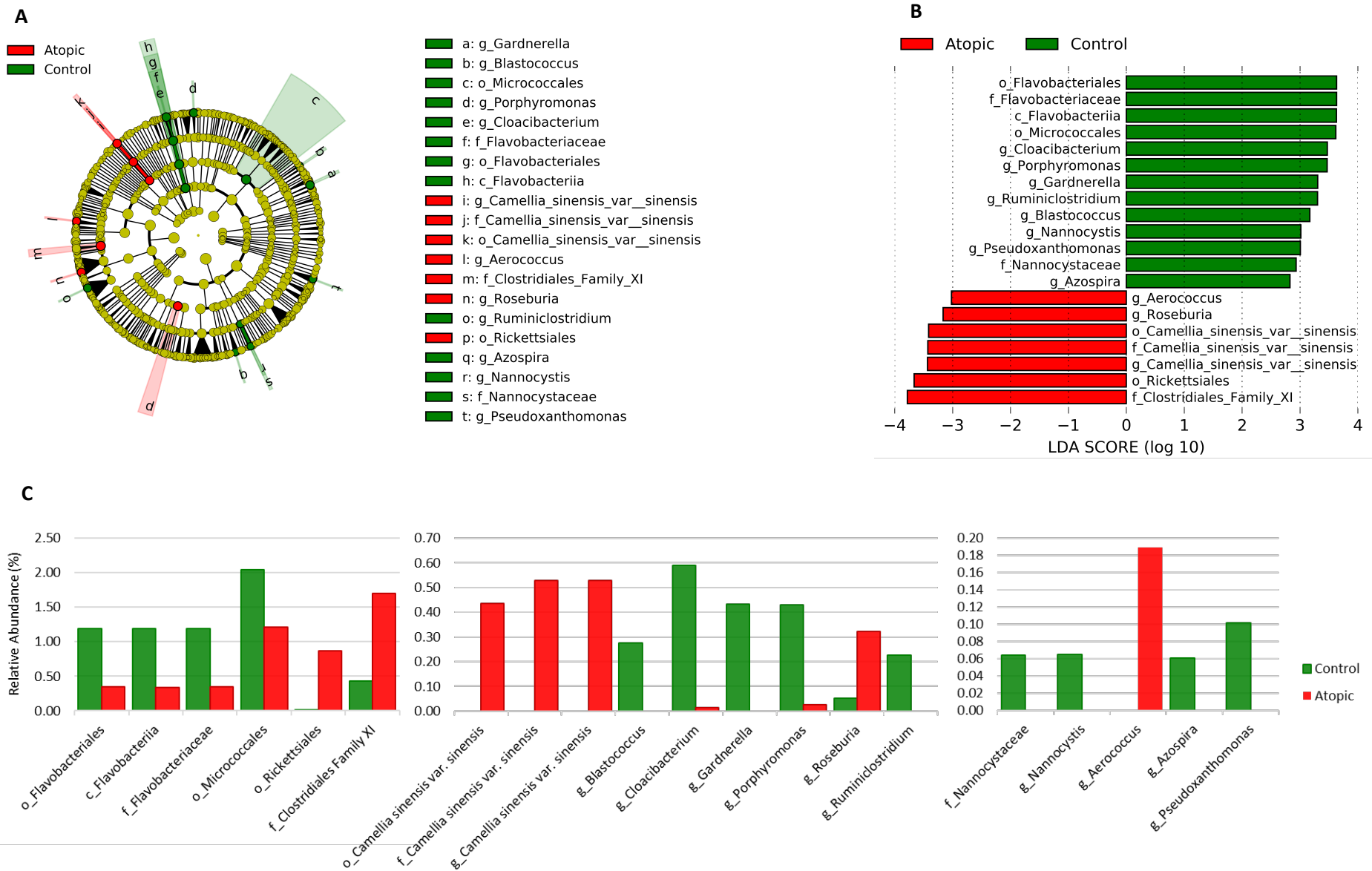
The circulatory microbiome detected in the atopic subjects was first compared to the circulatory microbiome detected in the non-atopic control subjects to determine whether atopic disease was associated with changes in the circulatory microbiome.

Comparison of the control and atopic subjects was achieved by performing LEfSe analysis on the bacterial taxa relative abundance values. A total of 20 bacterial taxa were detected at significantly altered levels in the atopic circulatory microbiome compared to the control circulatory microbiome ( $P$  value < 0.05, LDA effect size > 2.0) (Figure 5.7). The majority of bacterial taxa detected at significantly altered levels were low abundant (relative abundance < 1.0%), and included 7 bacterial taxa that were enriched in the atopic subjects compared to the control subjects, and 13 taxa that were significantly decreased in the atopic subjects compared to the control subjects (Figure 5.7). Of note was the observation that the high-abundant taxa displaying significant differential abundance were typically detected in both the control and atopic subjects, whereas the low-abundant taxa displaying differential abundance were generally condition specific (Figure 5.7.C).

Bacterial taxa significantly increased in the atopic subjects included the Rickettsiales order, the *Clostridiales Family XI*, and the *Aerococcus*, *Camellia sinensis var sinensis*, and *Roseburia* genera (Figure 5.7). Of interest was the observation that, with the exception of the *Clostridiales Family XI* and the *Roseburia* genus, the bacterial taxa significantly increased in the atopic subjects were not detected in the controls subjects (Figure 5.7.C), suggesting that in the absence of atopic disease these bacterial taxa are not typically present in the circulatory microbiome.

Similarly, to the enriched taxa, the majority of bacterial taxa observed to be significantly decreased in the atopic subjects were condition specific, and only detected in the control subjects. These taxa included the Nannocystaceae family, and the *Blastococcus*, *Gardnerella*, *Nannocystis*, *Azospira*, and *Pseudoxanthomonas* genera. Additionally, the Flavobacteriales and Micrococcales orders, the Flavobacteriia class, the *Flavobacteriaceae* family, and the *Cloacibacterium* and *Porphyromonas* genera, were also detected at increased levels in the control subjects, although these taxa were also present in the atopic subjects (Figure 5.7).

Overall, the results revealed the presence of significant changes in the circulatory microbiome in an atopic population compared to a non-atopic control population. The next step, therefore, was to determine whether the different atopic populations were associated with distinct changes to the circulatory microbiome.



**Figure 5.7: Significant changes in bacterial taxa relative abundance in the circulatory microbiome of atopic subjects compared to control subjects.** LEfSe analysis was performed on the bacterial relative abundance data from atopic subjects (n = 14) and non-atopic control subjects (n = 11) to determine the presence of bacterial taxa with statistically significant changes in taxa abundance in the atopic subjects compared to the control subjects (defined as having a LDA effect size > 2.0 and a *P* value < 0.05). (A) A taxonomic cladogram highlighting the statistically and biologically consistent differences between the atopic circulatory microbiome compared to the control circulatory microbiome. Differences are presented in the colour of the most abundant sample group (red represents taxa significantly enriched in the asthmatic subjects, green represents taxa significantly enriched in the control subjects, and yellow representing non-significant taxa). The circle diameter is proportional to the taxon's abundance in the circulatory microbiome. (B) Histogram of the LDA scores generated for the differentially abundant taxa present in the atopic subjects compared to the control subjects. (C) Relative abundance of the differentially abundant bacterial taxa.

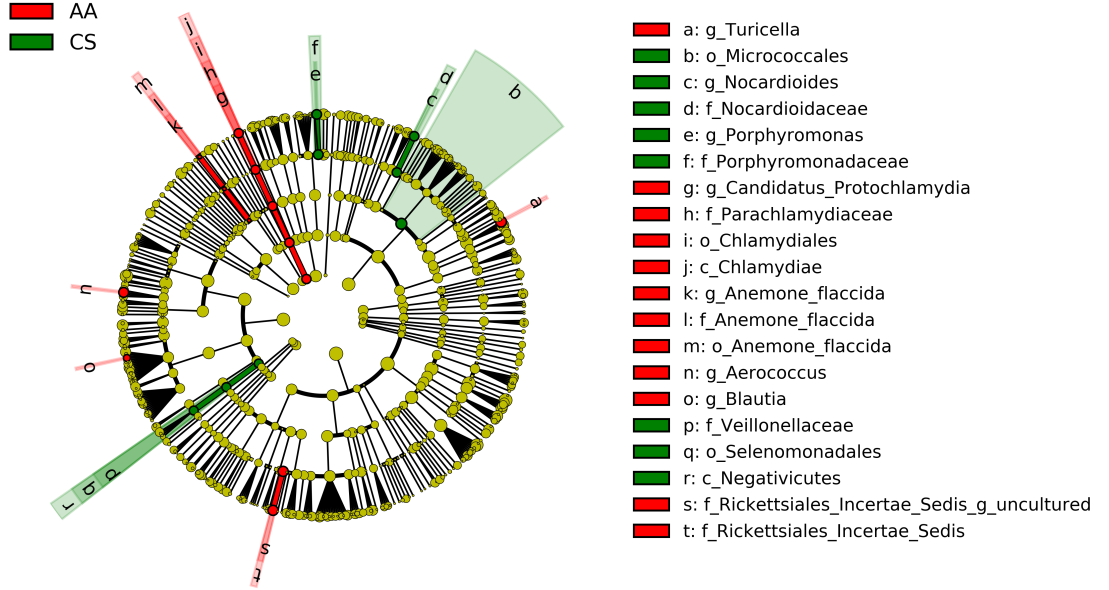
Analysis of the bacterial populations present in the asthmatic circulatory microbiome compared to the non-atopic control circulatory microbiome revealed that 20 bacterial taxa significantly differed in relative abundance in the asthmatic subjects compared to the control subjects (*P* value < 0.05, LDA effect size > 2.0) (Figure 5.8). This included 12 taxa that were had significantly increased abundance in the asthmatic circulatory microbiome, and 8 that had significantly decreased abundance compared to the levels detected in the control subjects.

Bacterial taxa significantly decreased in the asthmatic subjects belonged to the Negativicutes class, the Micrococcales order, and the *Nocardioideaceae* and *Porphyromonadaceae* families. In contrast, the bacterial taxa significantly increased in the asthmatic subjects belonged to the Chlamydiae phylum, the *Anemone flaccida* order, and the *Rickettsiales Incertae Sedis* family. Additionally, there were also a number of bacterial genera significantly increased in the asthmatic subjects, including *Turicella*, *Aerococcus*, and *Blautia* (Figure 5.8).

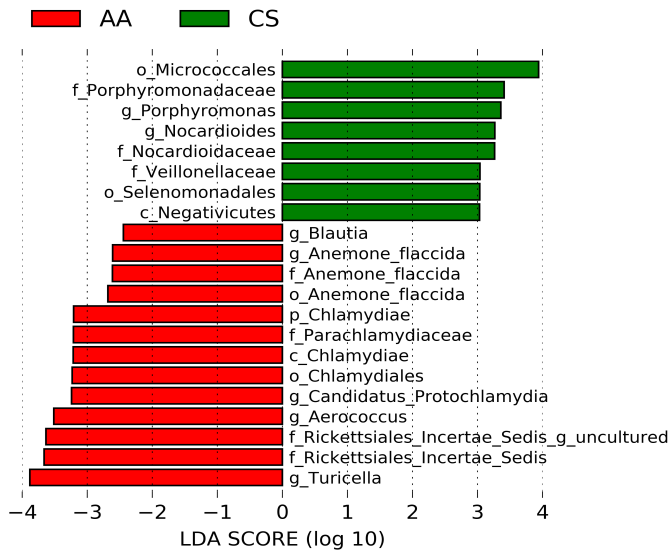


Overall, the majority of taxa that were detected at significantly altered levels in the asthmatic subjects were defined as low-abundant taxa (had a relative abundance < 1.0%), and were condition specific, whereby the bacterial taxa was only present at detectable levels in just the control samples or just the asthmatic samples (Figure 5.8.D). The Micrococcales order and *Turicella* genus were the exception. These bacterial taxa were detected at high abundance levels (relative abundance > 1.0%) and were observed in both the control subjects and the asthmatic subjects (Figure 5.8.C). Micrococcales were significantly decreased in the asthmatic subjects compared to the control subjects, whilst *Turicella* were significantly enriched in the asthmatic subjects (Figure 5.8.C).

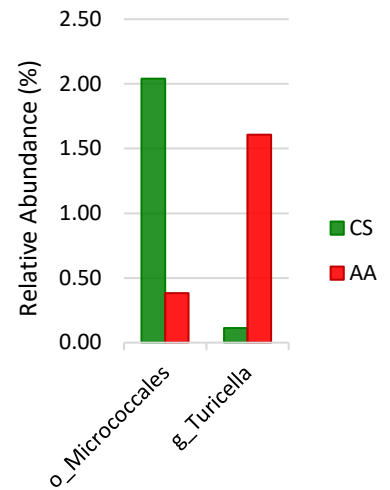
**A**



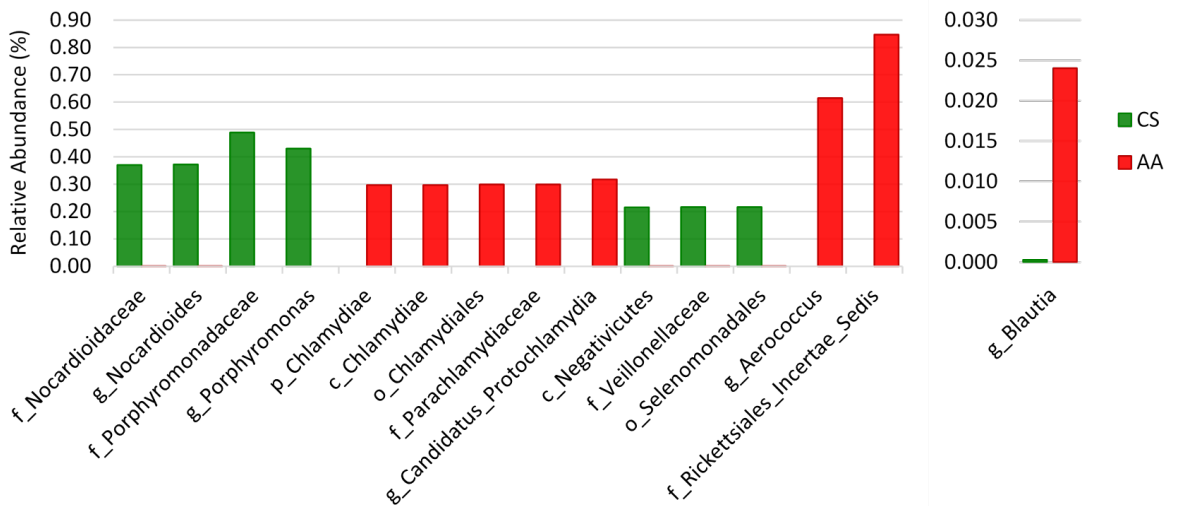
**B**



**C**



**D**



**Figure 5.8: Significant changes in bacterial taxa relative abundance in the circulatory microbiome of asthmatic subjects compared to control subjects.** LEfSe analysis was performed on the bacterial relative abundance data from asthma subjects (AA; N = 4) and control subjects (CS; n = 11) to determine the presence of bacterial taxa with statistically significant changes in taxa abundance in the asthmatic subjects compared to the control subjects (defined as having a LDA effect size > 2.0 and a *P* value < 0.05). **(A)** A taxonomic cladogram highlighting the statistically and biologically consistent differences between the asthmatic circulatory microbiome compared to the control microbiome. Differences are presented in the colour of the most abundant sample group (red represents taxa significantly enriched in the asthmatic subjects, green represents taxa significantly enriched in the control subjects, and yellow representing non-significant taxa). The circle diameter is proportional to the taxon's abundance in the circulatory microbiome. **(B)** Histogram of the LDA scores generated for the differentially abundant taxa present in the asthmatic subjects compared to the non-asthmatic subjects. **(C)** Relative abundance of high-abundant bacterial taxa displaying differential abundance. **(D)** Relative abundance of low-abundant bacterial taxa displaying differential abundance.

Comparison of the circulatory microbiome of allergic rhinitis subjects compared to non-atopic controls using LEfSe analysis identified 29 bacterial taxa that significantly differed between the two groups (defined as having a *P* value < 0.05 and a LDA effect size > 2.0) (Figure 5.9). In total, 28 bacterial taxa were significantly increased in the allergic rhinitis subjects, and one taxon, the *Lachnospiraceae NK4A136 group* genus, was significantly decreased in the allergic rhinitis subjects compared to the controls (Figure 5.9). 5 bacterial taxa had mean relative abundance scores less than 0.004% (range = 0.000516 – 0.003093) and were not included in further evaluation as changes in bacterial populations at such low levels is unlikely to have significant impact on the overall composition of the circulatory microbiome. These taxa included the *Camellia sinesis* var. *sinesis* order, family, and genus, the *Mitochondria* family, and the *Tetrasphaera* genus; and detection of the taxa was only observed in the allergic rhinitis subjects.

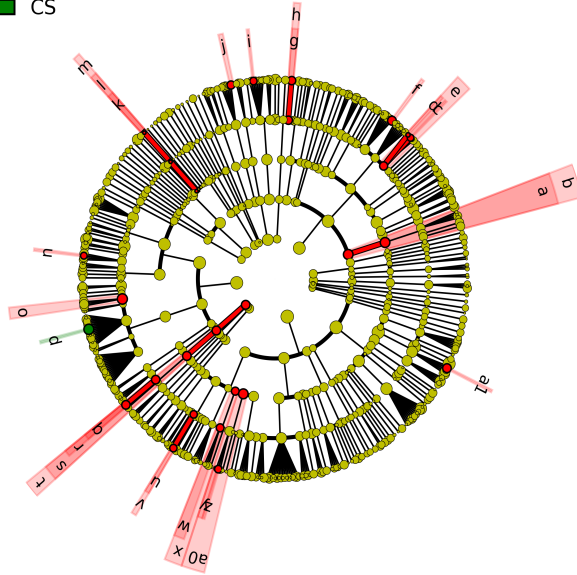
The remaining 23 taxa enriched in the allergic rhinitis circulatory microbiome were predominately members of the Actinobacteria phylum (the Acidimicrobiia class; the

Acidimicrobiales order; the *Intrasporangiaceae* and *Solirubrobacteraceae* families; and the *Arthrobacter*, *Ornithinibacter*, and *Solirubrobacter* genera) and the Proteobacteria phylum (the Rhodospirillales and Rickettsiales orders; the *Acetobacteraceae* and *Hyphomicrobiaceae* families, and the *Devosia*, *Oryza sativa Indica Group*, and *Psychrobacter* genera)(Figure 5.9). Additionally the Fusobacteria phylum and a number of its members (*Fusobacteriia*, *Fusobacteriales*, *Fusobacteriaceae*, and *Fusobacterium*) were enriched in the allergic rhinitis circulatory microbiome along with two genera of the Bacteroidetes phylum (*Bergeyella* and *Prevotella 7*), and two members of the Firmicutes phylum (*Family XI* of the Clostridiales order and the *Aerococcus* genus)(Figure 5.9).

Of the bacterial taxa identified, 2 taxa were classed as high-abundant (the *Family XI* of the Clostridiales order and the *Lachnospiraceae NK4A136 group* genus) (Figure 5.9.C). The remaining 27 taxa were low abundant, with mean relative abundance values less than 0.4% (Figure 5.9.D).

**A**

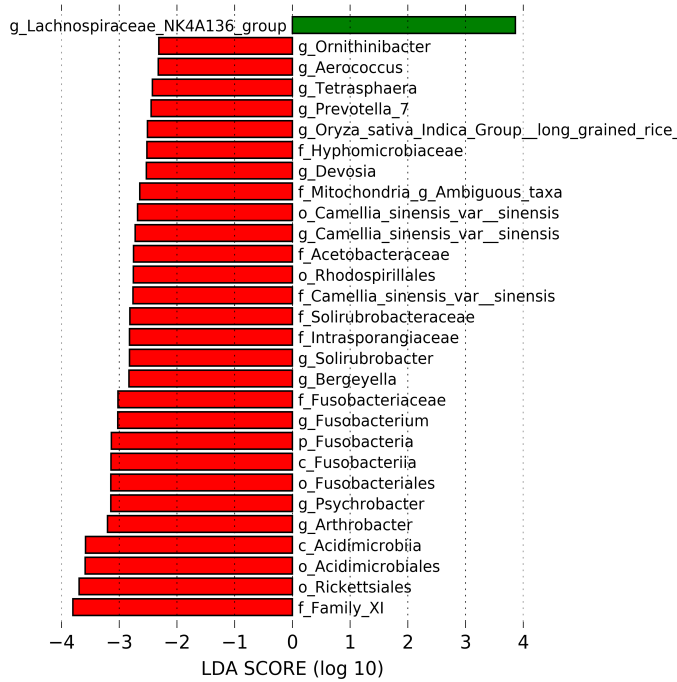
AR  
CS



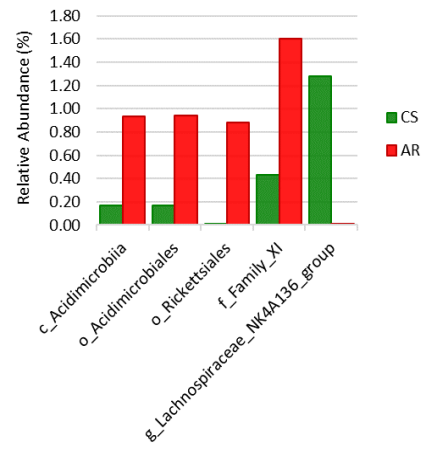
- a: o\_Acidimicrobiales
- b: c\_Acidimicrobiia
- c: g\_Ornithinibacter
- d: g\_Tetrasphaera
- e: f\_Intrasporangiaceae
- f: g\_Arthrobacter
- g: g\_Solirubrobacter
- h: f\_Solirubrobacteraceae
- i: g\_Prevotella\_7
- j: g\_Bergeyella
- k: g\_Camellia\_sinensis\_var\_sinensis
- l: f\_Camellia\_sinensis\_var\_sinensis
- m: o\_Camellia\_sinensis\_var\_sinensis
- n: g\_Aerococcus
- o: f\_Family\_XI
- p: g\_Lachnospiraceae\_NK4A136\_group
- q: g\_Fusobacterium
- r: f\_Fusobacteriaceae
- s: o\_Fusobacteriales
- t: c\_Fusobacteriia
- u: g\_Devosia
- v: f\_Hyphomicrobiaceae
- w: f\_Acetobacteraceae
- x: o\_Rhodospirillales
- y: f\_Mitochondria\_g\_Ambiguous\_taxa
- z: g\_Oryza\_sativa\_Indica\_Group\_long\_grained\_rice
- a0: o\_Rickettsiales
- a1: g\_Psychrobacter

**B**

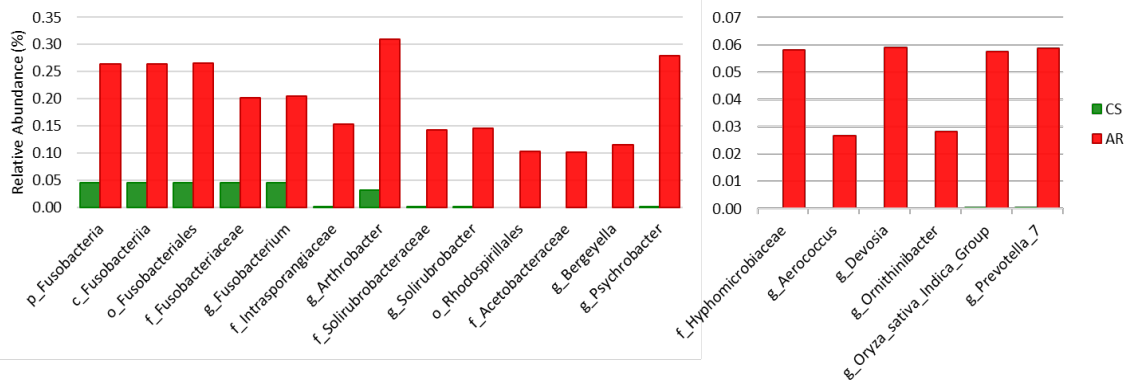
AR CS



**C**



**D**

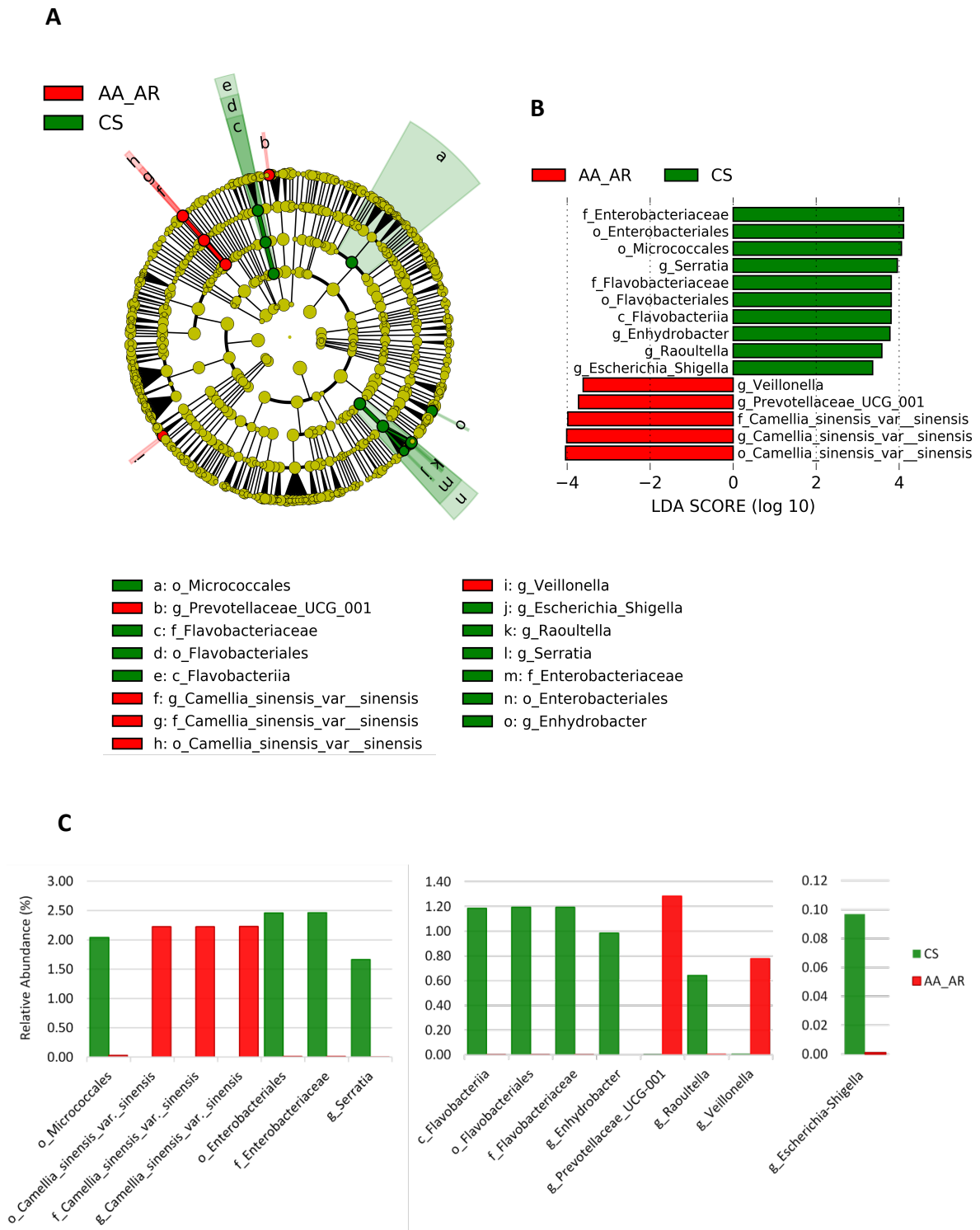


**Figure 5.9: Significant changes in bacterial taxa relative abundance in the circulatory microbiome of allergic rhinitis subjects compared to control subjects.** LEfSe analysis was performed on the bacterial relative abundance data from allergic rhinitis subjects (AR; n = 7) and control subjects (CS; n = 11) to determine the presence of bacterial taxa with statistically significant changes in taxa abundance in the allergic rhinitis subjects compared to the control subjects (defined as having a LDA effect size > 2.0 and a *P* value < 0.05). **(A)** A taxonomic cladogram highlighting the statistically and biologically consistent differences between the allergic rhinitis circulatory microbiome compared to the control circulatory microbiome. Differences are presented in the colour of the most abundant sample group (red represents taxa significantly enriched in the allergic rhinitis subjects, green represents taxa significantly enriched in the control subjects, and yellow representing non-significant taxa). The circle diameter is proportional to the taxon's abundance in the circulatory microbiome. **(B)** Histogram of the LDA scores generated for the differentially abundant taxa present in the allergic rhinitis subjects compared to the non-asthmatic subjects. **(C)** Relative abundance of high-abundant bacterial taxa displaying differential abundance. **(D)** Relative abundance of low-abundant bacterial taxa displaying differential abundance.

Comparison of the bacterial taxa present in the circulatory microbiome of the hyper-allergic subjects compared to non-atopic controls revealed that 15 bacterial taxa were present at significantly different levels between the two subject groups. This included 10 taxa that were decreased in the hyper-allergic subjects, and 5 bacterial taxa that were enriched in the hyper-allergic subjects (Figure 5.10). With the exception of the *Escherichia-Shigella*, the identified bacteria were classed as high-abundant taxa (present in the circulatory microbiome at levels greater than 1%), and were typically condition specific, whereby if the taxa was detected in the hyper-allergic subjects it displayed little to none detection in the control subjects and if it was detected in the control subjects it showed little to none abundance in the hyper-allergic subjects (Figure 5.10.C).

The majority of bacterial taxa detected in the hyper-allergic subjects compared to the control subjects belonged to either the Flavobacteriia class, or the *Camellia sinensis* var *sinensis*, Micrococcales, and Enterobacteriales orders (Figure 5.10). Taxa belonging to the *Camellia sinensis* var *sinensis* order were increased in the hyper-allergic subjects, whilst taxa

belonging the Flavobacteriia class, Micrococcales order, and Enterobacteriales order, were decreased in the hyper-allergic subjects (Figure 5.10). Additionally, the *Prevotellaceae* UCG-001 and *Veillonella* genera were increased in the hyper-allergic subjects, whilst the *Enhydrobacter* genus was decreased in the hyper-allergic subjects (Figure 5.10).



**Figure 5.10: Significant changes in bacterial taxa relative abundance in the circulatory microbiome of hyper-allergic subjects compared to control subjects.** LEfSe analysis was performed on the bacterial relative abundance data from hyper-allergic subjects (AA\_AR; n = 3) and control subjects (CS; n = 11) to determine the presence of bacterial taxa with statistically significant changes in taxa abundance in the hyper-allergic subjects compared to the control subjects (defined as having a LDA effect size > 2.0 and a *P* value < 0.05). **(A)** A taxonomic cladogram highlighting the statistically and biologically consistent differences between the asthmatic and allergic rhinitis circulatory microbiome compared to the control circulatory microbiome. Differences are presented in the colour of the most abundant sample group (red represents taxa significantly enriched in the subjects with asthma and allergic rhinitis, green represents taxa significantly enriched in the control subjects, and yellow representing non-significant taxa). The circle diameter is proportional to the taxon's abundance in the circulatory microbiome. **(B)** Histogram of the LDA scores generated for the differentially abundant taxa present in the hyper-allergic subjects compared to the control subjects. **(C)** Relative abundance of the differentially abundant bacterial taxa.

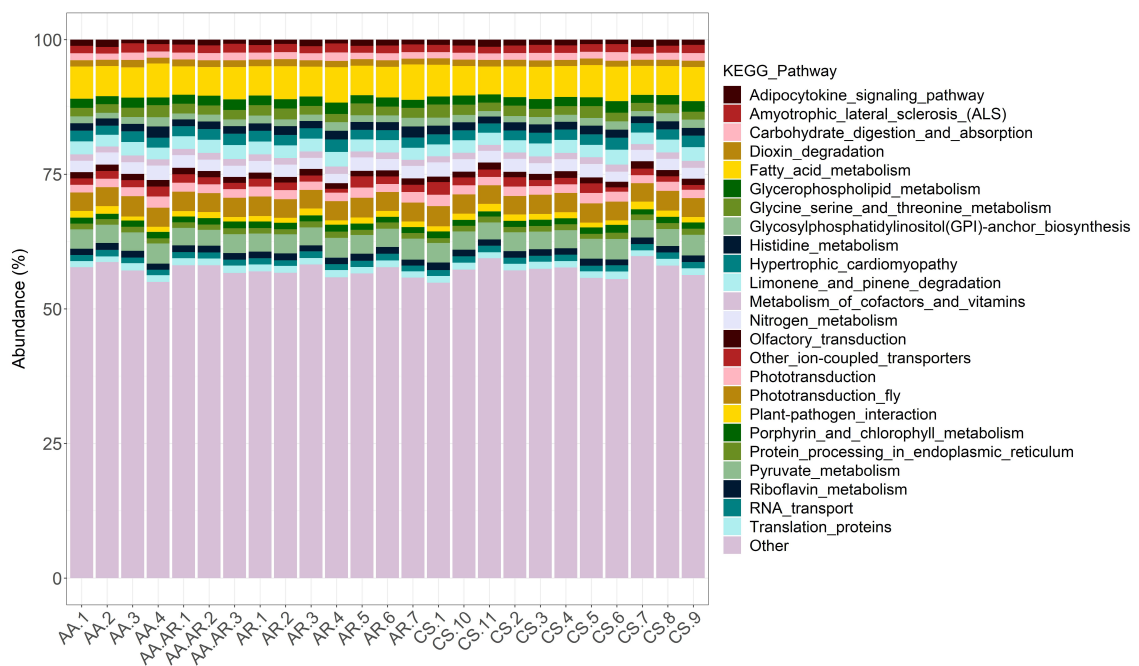
### 5.3.7. Prediction of the Serum Metagenome Functional Content

PICRUSt analysis was performed on the V4 16S rRNA sequencing data generated from the serum samples to determine the functional capacity of the bacterial communities detected in the samples. LEfSe analysis was then carried out on the KEGG pathway 1 – 3 levels identified to establish whether bacterial activities are significantly altered in the atopic subjects compared to the control subjects, as a consequence of differential bacterial abundance.

A total of 301 level 3 KEGG pathways were found to be encoded by the bacterial members detected in the serum samples. This included 18 pathways belonging to the level 1 *Cellular processes* category, 22 *Environmental information processing* pathways, 24 *Genetic information processing* pathways, 35 *Human diseases* pathways, 137 *Metabolism* pathways, 40 *Organismal systems* pathways, and 25 *Unclassified* pathways.



The majority of detected pathways had a total predicted abundance of less than 1%. 24 level 3 KEGG pathways were detected at high abundance in the serum metagenome (as defined by a predicted abundance of greater than 1%), and included 2 *Genetic information processing* members, 2 *Human diseases'* members, 11 *Metabolism* members, 6 *Organismal systems'* members, and 3 *Unclassified* members (Figure 5.11).

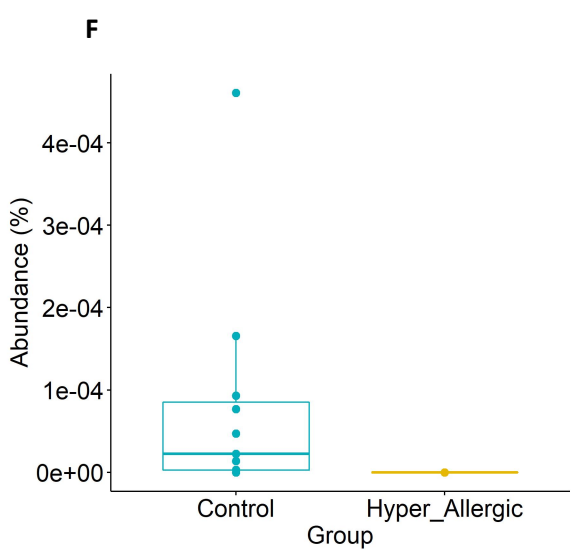
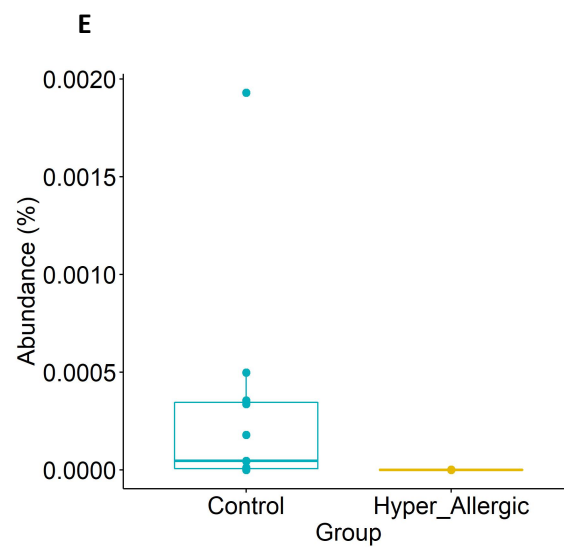
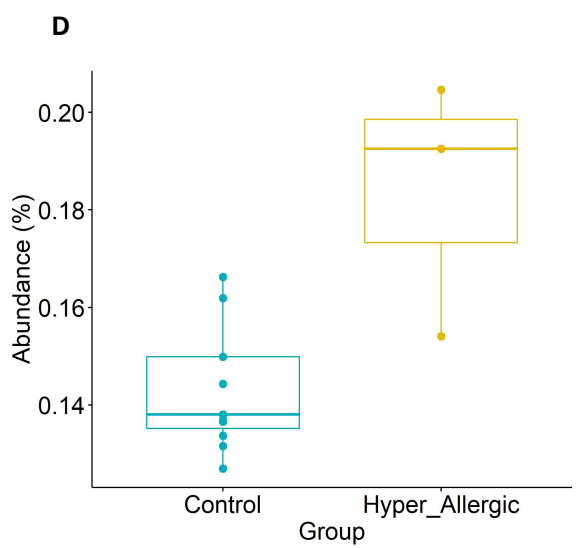
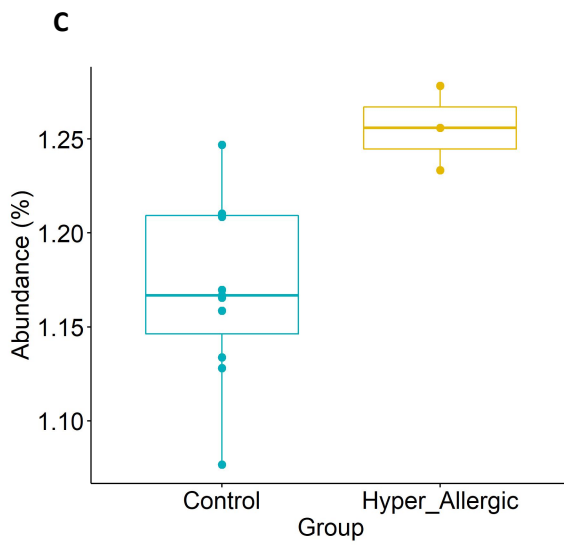
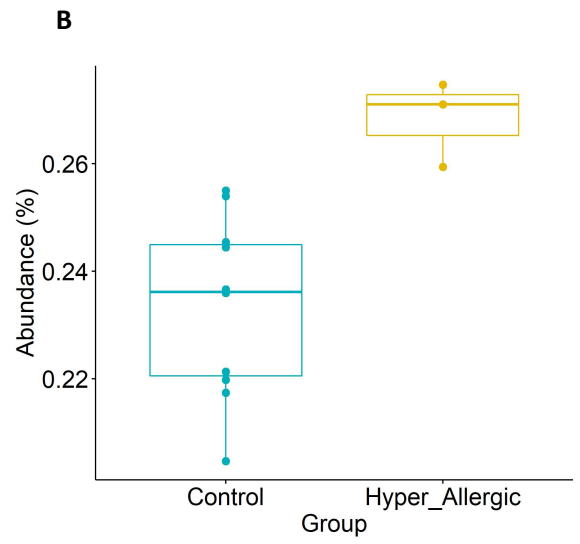
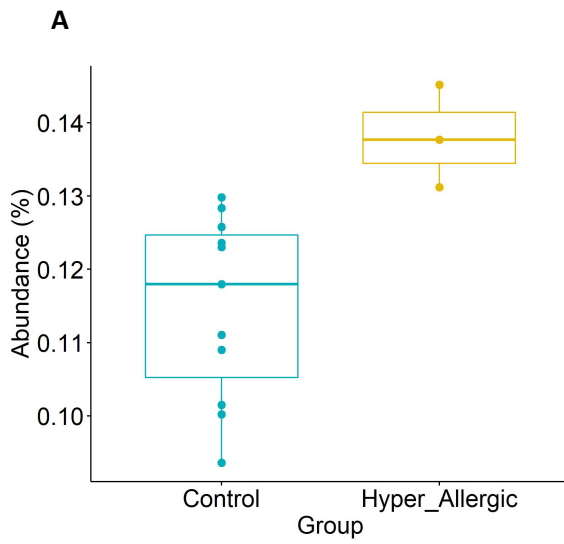


**Figure 5.11: Functional analysis of the serum circulatory microbiome.** PICRUSt software was used to predict functional content of the serum metagenome based on the V4 16S rRNA sequencing data generated from control subjects (CS, n =11), allergic rhinitis subjects (AR, n = 7), asthmatic subjects (AA, n = 3), and hyper-allergic subjects (AA.AR, n = 3). High activity level 3 KEGG pathways (as determined by a predicted abundance of greater than 1% of the total serum sample metagenome) are plotted and KEGG pathways with an abundance less than 1% are grouped together and plotted as other.

Statistical analysis of the KEGG pathways detected in the atopic subjects compared to the control subjects revealed no significant changes in microbial activity in the atopic subjects. Further analysis found that there were also no statistically significant differences in

predicted microbial activity in the asthmatic subjects and allergic rhinitis subjects compared to the control subjects. Analysis of the KEGG pathways detected in the hyper-allergic subjects compared to the control subjects, however, revealed several significant changes to microbial activity in the hyper-allergic subjects compared to the control subjects.

Of the 41 level 2 KEGG functional categories, *Cell growth and Death* was found to be significantly increased in the hyper-allergic subjects compared to the control subjects (0.51% v 0.46%,  $P$  value = 0.0158, LDA effect size = 2.85). With regards to the 301 detected level 3 KEGG pathways detected, 8 were found to display significantly altered abundance in the hyper-allergic subjects compared to the control subjects, as determined by a  $P$  value of less than 0.05% (see Supplementary Materials, Table S14). Of the 8 level 3 KEGG pathways, 6 were predicted to be biologically significant, as defined by an LDA effect size of 2.0 or greater (see Supplementary Materials, Table S14). These included 4 pathways that displayed increased abundance in the hyper-allergic subjects [Flavonoid biosynthesis (0.14% v 0.11%,  $P$  value = 0.0102, LDA effect size = 2.15), Retinol metabolism (0.27% v 0.23%,  $P$  value = 0.0102, LDA effect size = 2.24), Dioxin degradation (1.26% v 1.17%,  $P$  value = 0.01281, LDA effect size = 2.71), and Toluene degradation (0.18% v 0.14%,  $P$  value = 0.0240, LDA effect size = 2.35)] and two pathways that were observed to be decreased in the hyper-allergic subjects compared to the control subjects [Thiamine metabolism ( $3.1E-04$  v  $4.1E-07$ ,  $P$  value = 0.0347, LDA effect size = 2.10) and Peroxisome proliferator-activated receptor (PPAR) signalling ( $0$  v  $8.04E-05$ ,  $P$  value = 0.0316, LDA effect size = 2.17)](Figure 5.12).



**Figure 5.12: Comparison of microbial activity in hyper-allergic subjects compared to healthy controls.** PICRUSt was used to predict functional potential of the bacterial communities detected in hyper-allergic subjects (n = 3) compared to healthy controls (n = 11) using V4 16S rRNA sequencing data. LEfSe analysis was used to identify differential bacterial functions present in the hyper-allergic subjects compared to the control subjects. Flavonoid biosynthesis (A), Retinol metabolism (B), Dioxin degradation (C), Toluene degradation (D) KEGG pathways were observed to be significantly increased in the hyper-allergic subjects compared to the control subjects ( $P$  value < 0.05, LDA effect size > 2.0). Thiamine metabolism (E) and PPAR Signalling (F) were observed to be significantly decreased in the hyper-allergic subjects compared to the healthy controls ( $P$  value < 0.05, LDA effect size < -2.0).

#### 5.3.8. Analysis of Viable Bacterial Cells in the Serum Samples

Bacterial growth was negative for all agar plates streaked with nutrient broth inoculated with human serum, thus indicating a lack of viable bacterial cells present in the human serum samples.

## 5.4. Discussion

Changes to the circulatory microbiome have not previously been studied in relation to atopic disease. In Chapter 4 a circulatory microbiome was successfully characterised using plasma samples from subjects with atopic asthma and healthy control subjects. The detected microbial populations were predicted to have translocated into the blood from other body sites, and changes in the circulatory microbiome of the asthmatic subjects was thought to be the result of microbial dysbiosis at the distant body sites.

Changes in the microbiome of atopic subjects compared to non-atopic control subjects are well described for a number of body sites, including the airways, gastrointestinal tract, and skin. However, what is not known is how microbial dysbiosis at the distant body sites affects translocation into the blood, and whether atopic disease manifesting at different body sites (the lungs and nasal passages for asthma and allergic rhinitis, respectively) influences microbial translocation into the blood.

This study, therefore, aimed to compare the circulatory microbiome of different atopic manifestations (asthma, allergic rhinitis, hyper-allergic) to determine whether allergen-induced inflammatory responses at different body sites influenced composition of the circulatory microbiome differently.

### 5.4.1. Characterisation of the Serum Circulatory Microbiome

Characterisation of the microbial populations present in serum samples from atopic and control subjects revealed that the circulatory microbiome was predominately composed of three key phyla; Proteobacteria, Firmicutes, and Actinobacteria, and to a lesser extent, Bacteroidetes and Cyanobacteria.

With regards to the experimental negative control, at both the phylum and the genus level the negative control displayed similar bacterial composition to the serum samples. The bacterial DNA detected in the negative control, however, was significantly lower compared to the serum samples. This, therefore, suggests that whilst it was likely that there was some contaminating microbial DNA present in the samples prior to sequencing, the contaminating DNA was just a small proportion of the microbial DNA detected in the serum samples and unlikely to affect the overall findings of the study.

The identification of bacterial DNA in the negative control highlights the importance of sequencing and characterising the experimental negative control, regardless of whether the sample is PCR positive or negative.

#### 5.4.2. Comparison of the Serum Circulatory Microbiome compared to the Plasma Circulatory Microbiome

Characterisation of the serum circulatory microbiome at the phylum level revealed similar bacterial populations to that observed in the plasma circulatory microbiome (as described in Chapter 4). The circulatory microbiome detected in the plasma and serum samples was dominated by Proteobacteria, and to a lesser extent, Firmicutes, Actinobacteria, and Bacteroidetes, and a number of bacterial genera were detected at high levels in both sample types (*Acinetobacter*, *Corynebacterium* 1, *Haemophilus*, *Halomonas*, *Propionibacterium*, *Pseudomonas*, *Serratia*, *Sphingomonas*, *Staphylococcus*, and *Streptococcus*). These findings mirror the observations of previous investigations into the circulatory microbiome <sup>323, 327, 332, 339,361</sup>, and thus provides further evidence of a core circulatory microbiome that may be less transient than previously thought. However, it may also be that the bacterial genera are more efficient at translocation into the blood or are

more likely to be blood contaminants, entering the blood sample during the venepuncture procedure at time of sample collection and/ or existing as contaminants of laboratory reagents.

#### 5.4.3. Comparison of the Significant Changes in Different Atopic Diseases

The number of V4 16S rRNA reads generated from the serum samples were similar across the atopic phenotypes, and comparable to the number of reads generated from the healthy controls. Analysis of the diversity of bacterial taxa detected in the samples revealed that allergic rhinitis was associated with increased alpha diversity whilst asthma was associated with decreased alpha diversity present in the circulatory microbiome compared to the control subjects.

This was an unexpected find as characterisation of plasma samples in Chapter 4 had demonstrated increased bacterial diversity in the asthmatic subjects compared to the control subjects. As the two studies varied in geographical location of the atopic subjects, age of sample, type of sample, and sequencing protocol, it is possible that one or more of these factors influenced the level of bacterial diversity detected in the asthma samples. Further investigations, therefore, would be required to determine the effects of asthma on bacterial diversity in the circulatory microbiome.

Statistical analysis of the alpha diversity detected in the serum samples of the atopic subjects revealed that there were significant differences in the level of alpha diversity detected in the asthmatic subjects compared to the allergic rhinitis subjects. This indicates that allergen-induced inflammation in the nasal passages and lungs influences diversity of the circulatory microbiome differently, and thus provides further support for the theory

that the circulatory microbiome is composed of bacterial populations/ microbial DNA that have translocated from distant body sites.

With regards to beta diversity, there were no significant clustering of atopic and control microbiomes. However, of the atopic groups investigated, allergic rhinitis displayed the greatest level of dissimilarity to the control samples. This provided further support to the interpretation that allergic rhinitis had the greatest impact on bacterial diversity in the circulatory microbiome, however, the allergic rhinitis group was the largest of the atopic groups, and so it may be that the increased number of samples in this group makes differences in the atopic population compared to the control population more apparent. Therefore, this preliminary study has demonstrated the possibility of significant differences in the circulatory microbiome compared to the control subjects, but a larger study with a more equal distribution of atopic population sample groups would be required to confirm this.

#### 5.4.4. Microbial dysbiosis associated with Atopic Disease

This study identified several bacterial taxa that exhibited significant differential abundance in the atopic subjects compared to the control subjects. A number of these bacterial taxa have also been detected at significant differential abundance at other body sites in atopic subjects.

Of the bacterial taxa identified as having increased relative abundance in the atopic circulatory microbiome *Clostridiales* have been detected at increased levels in the gut microbiome of asthmatic adults <sup>274</sup>, *Fusobacterium* has been observed to be increased in the airway microbiome of asthmatic subjects <sup>588,589</sup>, *Chlamydiae pneumoniae* has been detected at increased frequency in the asthmatic nasopharynx <sup>590</sup>, *Blautia* has been



observed to be significantly increased in both the asthmatic airways<sup>263</sup> and the gut<sup>270,276</sup>, *Prevotella* has been detected at increased levels in the asthmatic airway microbiome<sup>256</sup> and nasal microbiome of patients with exacerbated asthma<sup>589</sup>, and *Veillonella* has been found to be increased in the gut microbiome of atopic children<sup>271</sup> and asthmatic adults with fixed airway obstruction<sup>274</sup>.

With regards to bacterial taxa detected at significantly reduced levels in the atopic circulatory microbiome *Rothia* (a member of the Micrococcales order) has been observed at decreased levels in the gut microbiome of atopic infants<sup>258</sup> and undetectable in the gut microbiome of asthmatic children<sup>253</sup>, *Porphyromonas* has been detected at significantly decreased levels in the airway microbiome of neutrophilic asthmatics<sup>591</sup>, *Dialister* (a member of the *Veillonaceae* family) have been observed at reduced levels in the gut microbiome of atopic infants<sup>217</sup>, and decreased levels of *Enterobacteriaceae*-derived extracellular vesicle have been detected in urine samples from children diagnosed with asthma or allergic rhinitis<sup>275</sup>.

However, the observed changes in the atopic circulatory microbiome do not always mimic changes in the microbiome at other body sites in the atopic subject, and reports of bacterial taxa associated with atopic disease are variable. Fusobacteria and *Prevotella*, for example, have been detected at both increased and decreased levels in the asthmatic airways<sup>255,256, 261, 277, 588,589,592</sup>, whilst *Clostridiales* spp. and *Veillonella* have been detected at both increased and decreased abundance in the atopic gut microbiome<sup>258, 264, 271,272, 274,593,594</sup>

Variation across the different studies appeared to be due to the temporal nature of bacterial association with atopic disease. *Veillonella*, for example, has been consistently detected at reduced levels in the gut microbiome of infants in the process of developing atopy<sup>258,593,594</sup>, but is detected at increased levels in the gut microbiome of atopic children

<sup>271</sup> and asthmatic adults <sup>274</sup>. Similarly, *Clostridiales* have been detected in at decreased levels in gut microbiome of atopic infants <sup>264</sup> but at increased levels in the gut microbiome of asthmatic children and adults <sup>274</sup>.

#### 5.4.5. Microbial dysbiosis Associated with Disease Phenotype

Several investigations into the atopic microbiome have identified significant differences between subjects suffering from different disease phenotypes. Sverrild *et al* (2017), for example, observed that there was a significant increase in *Rothia* species in the airway microbiome of eosinophil-low asthmatic patients compared to eosinophil-high asthmatic patients and non-atopic control subjects <sup>263</sup>. Additionally, *Blautia* was detected at increased levels in the airway microbiome of eosinophil-high subjects compared to eosinophil-low and control subjects <sup>263</sup>, thus suggesting that the eosinophil-high and eosinophil-low asthma phenotypes had distinct patterns of microbial dysbiosis.

In another study both *Rothia* and *Porphyromonas* were found to be significantly reduced in the airway microbiome in patients with neutrophilic asthma compared to the levels observed in patients with eosinophilic asthma and paucigranulocytic asthma.

*Blautia* was increased in the circulatory microbiome of the asthmatic subjects in this study, whilst *Rothia* and *Porphyromonas* were decreased in the asthmatic circulatory microbiome. This, therefore, suggests that microbial dysbiosis in the blood reflects microbial dysbiosis present in the asthmatic airways, and thus characterisation of these genera may function as microbial biomarkers of asthma that have the potential to aid in asthma diagnosis and in the identification of the different asthma phenotypes.

#### 5.4.6. Microbial dysbiosis associated with Atopic Disease Severity

In addition to the being associated with the development/ occurrence of atopic disease, a number of the bacterial taxa detected at significantly altered levels in the atopic circulatory microbiomes have been associated with disease severity.

*Prevotella*, for example, was detected at significantly increased levels in the circulatory microbiome of the allergic rhinitis and hyper-allergic subjects and has been observed to be decreased in the oropharynx in asthmatic subjects with uncontrolled disease compared to subjects with mild disease <sup>595</sup>. This suggests that the bacteria may have a protective role against the development of severe, treatment-unresponsive, disease, and thus increased translocation of the bacteria into the bloodstream is likely to influence atopic disease severity, potentially making the individual more susceptible to severe, treatment-unresponsive disease. Microbial dysbiosis, however, may also be a consequence of the disease itself, and the different abundance observed in the two disease states may simply be reflective of disease severity.

Several of the bacterial taxa detected at significantly altered levels in the atopic subjects have been associated with acute episodes of asthma (exacerbated asthma). *Prevotella* and *Escherichia-Shigella*, for example, have been observed at significantly increased levels in nasal and gut microbiome, respectively, of patients with exacerbated asthma compared to patients with non-exacerbated asthma, whilst *Dialister* (a member of the *Veillonaceae* family increased in the serum of the asthmatic subjects) has been found to be significantly decreased in the nasal microbiome of non-exacerbated asthma compared to exacerbated asthma <sup>589</sup>.

In another study *Veillonella* and *Escherichia-Shigella* were both observed to be significantly increased in the gut microbiome of asthmatics with irreversible airway

obstruction compared to asthmatic subjects with no airway obstruction detected, and *Lachnospiraceae* was found to be significantly decreased in the gut microbiome of asthmatics with irreversible airway obstruction compared to asthmatic subjects with no airway obstruction detected <sup>274</sup>. This suggests that *Lachnospiraceae* colonisation may be protective against the long-term effects of the chronic airway inflammation associated with asthma. However, it may also suggest that the pathology associated with irreversible airway obstruction results in a gut environment less well suited for *Lachnospiraceae* survival.

Additionally, several of the bacterial taxa detected at significantly differential abundance in the circulatory microbiome of atopic subjects have been associated with IgE responses in asthmatic subjects <sup>274</sup>. *Veillonellaceae*, for example, has been demonstrated to be enriched in the gut microbiome of asthmatic subjects that exhibit high-IgE responses to the HDM allergen <sup>274</sup>, whilst *Clostridiales* and *Lachnospiraceae* are reported to be enriched in the gut microbiome of asthmatics that exhibit low IgE responses to HDM <sup>274</sup>. This suggests that some bacterial taxa may confer protection against allergic disease by suppressing the IgE response to common allergens. In the circulatory microbiome of the atopic subjects, *Clostridiales*, *Lachnospiraceae*, and *Veillonellaceae* were detected at significant differential abundance in the atopic subjects, thus suggesting that the bacterial taxa may function as circulatory microbial biomarkers of IgE responsivity.

Another interesting observation was the observed increase in *Chlamydiae* in the asthmatic circulatory microbiome. Infection with *C. pneumoniae* has been associated by increased rates of lung function decline in asthmatic subjects <sup>596–598</sup>, and persistent and/ or recurrent infection is thought to promote the development of chronic airflow obstruction <sup>598</sup>. The observed increase in *Chlamydiae* in the circulatory microbiome of the asthmatic subjects

suggest that the asthmatic subjects have increased *Chlamydiae* colonisation, and thus may be more susceptible towards developing chronic airway obstruction.

#### 5.4.7. Loss of Beneficial Bacteria and Atopic Pathogenesis

The changes in the circulatory bacterial populations detected in the atopic subjects is likely to be reflective of microbial dysbiosis at other body sites. Changes in the bacterial populations may simply be a passive reflection of the altered immune status in atopic subjects, or they may actively contribute to disease development, severity, or response to treatment.

In support of microbial dysbiosis actively contributing towards atopy is an interesting study carried out by Arrieta *et al* (2015) who demonstrated that transferal of the gut microbiota of an atopic infant to adult GF mice enhanced the atopic response to the OVA allergen following sensitisation<sup>258</sup>. The adult offspring from the mice colonised with the atopic gut microbiota exhibited a severe lung inflammatory response to the OVA allergen that was characterised by increased airway infiltration of neutrophils, eosinophils, macrophages, and lymphocytes<sup>258</sup>. The atopic microbiota was characterised by low levels of *Faecalibacterium spp.*, *Lachnospira spp.*, *Veillonella spp.*, and *Rothia spp.*, and reduced levels of the bacterial species was predicted to actively cause the enhanced lung inflammation observed in the mice as inoculation of the bacteria to the GF mice ameliorated OVA-induced airway inflammation in their adult progeny<sup>258</sup>.

The association with the atopic microbiota and atopic disease was thought to be due to loss of beneficial activities carried out by *Faecalibacterium sp.*, *Lachnospira sp.*, *Veillonella sp.*, and *Rothia sp.* In the infant the atopic microbiota was derived from, the authors

observed reduced LPS biosynthesis and decreased production of acetate (a SCFA) at 3 months of age<sup>258</sup>.

Decreased levels of LPS was thought to be a direct consequence of reduced *Veillonella* colonisation. Furthermore, decreased LPS in the infant gut was predicted to have a significant impact on the maturation of the infant immune system and susceptibility towards atopic disease, as LPS has been demonstrated to promote the Th1 arm of the immune system by inducing the proliferation of IL-12-producing dendritic cells<sup>599</sup>.

This interpretation is supported by the observation that LPS exposure is inversely correlated with the development of asthma and the demonstration that reduced LPS exposure in neonatal mice as the result of caesarean birth inhibited the development of immune tolerance in the neonatal mice<sup>600</sup>.

In the circulatory microbiome, the asthmatic subjects displayed significantly decreased levels of *Veillonellaceae*, suggesting that the asthmatic subjects would display reduced Th1 activity as a result of decreased LPS-induced stimulus.

With regards to the observed decreased levels of acetate, SCFAs have been demonstrated to be anti-inflammatory<sup>601–603</sup>, promote gut homeostasis<sup>604</sup>, maintain the integrity of the epithelial barrier<sup>605,606</sup>, and promote Treg differentiation and proliferation<sup>607–609</sup>. Moreover, SCFAs have been found to be protective against murine atopic disease<sup>542</sup>, and reduced fibre consumption in the diet has been associated with atopic disease<sup>532,533</sup>. Reduced ability of the gut microbiota to produce SCFAs, therefore, likely actively contributes towards disease susceptibility.

In the circulatory microbiome several SCFA-producing bacterial taxa were detected at reduced levels in the atopic subjects compared to the control subjects. These bacterial taxa

included *Lachnospiraceae* and *Veillonella*, and their decreased levels in the atopic circulatory microbiome suggests that the atopic subjects would exhibit reduced SCFA production. This would likely reduce the number of Tregs in the subjects, thus contributing towards the atopic inflammatory responses by removing one of the key immune modulator mechanisms required to maintain Th1/ Th2 immune homeostasis.

The asthmatic subjects in this study also displayed reduced levels of *Porphyromonas*, a bacterial genus that has been demonstrated to be protective against allergen sensitivity and subsequent airway inflammation. In a study carried out by Card and colleagues (2010), establishment of a subcutaneous infection with *Porphyromonas gingivalis* prior to allergen sensitisation in mice resulted in a significant reduction in infiltration of inflammatory cells and production of Th2 cytokines (IL-4, IL-5, and IL-13) in the airways of mice sensitised to the OVA allergen <sup>610</sup>.

Amelioration of the inflammatory response, however, was not observed when subcutaneous infection of the bacterium was induced after allergen sensitisation <sup>610</sup>, thus indicating that colonisation of the bacterium was important in preventing the development of allergen sensitisation, but not in controlling the inflammatory responses once disease had developed. Protection against allergen sensitisation may be due to the ability of the bacterium's ability to degrade pro-inflammatory proteins (IL-1 $\beta$ , IL-4, IL-5, IL-6, IL-8, IL-12) <sup>611-614</sup>, downregulate Th17 differentiation <sup>615</sup>, and upregulate Treg differentiation <sup>615</sup>.

#### 5.4.8. Expansion of Harmful Bacteria and Atopic Pathogenesis

In addition to loss of beneficial bacteria, expansion of harmful bacteria was detected in the circulatory microbiome of the atopic subjects. *Fusobacterium*, for example, was found to be significantly enriched in the serum samples from subjects with allergic rhinitis. This

bacterial genus has been demonstrated to directly induce the production of MUC5AC, a core protein of mucin, by bronchial cells at both the protein and mRNA level <sup>616</sup>. Nasal epithelial cells have been demonstrated to produce MUC5AC upon stimulation by IL-13 <sup>617</sup>, and mucous hypersecretion is a common feature of atopic disease. Increased *Fusobacterium* detected in the allergic rhinitis subjects, therefore, is likely to contribute towards disease by enhancing mucous production in the nasal passages.

*Prevotella* was another bacterial taxon enriched in the atopic subjects that has been demonstrated to display immunomodulation activities relevant to atopic disease. The bacteria have been shown to activate dendritic cells in a TLR2-dependent manner, resulting in the production of Th17-polarising cytokines (IL-1 $\beta$ , IL-6, and IL-23). *Prevotella* have also been demonstrated to stimulate epithelial cells to produce IL-6, IL-8, and CCL20, resulting in neutrophil recruitment (IL-8) and activation of Th17 cells (IL-6).

Whilst a Th1/ Th2 imbalance has been well documented in atopic pathogenesis, there is increasing evidence that Th17 immunity is also a contributing factor in atopic pathogenesis <sup>481,618–621</sup>. Th17 cytokines have also been found to increase production of MUC5AC <sup>622</sup>, stimulate goblet cell metaplasia <sup>623</sup>, and increased proliferation and migration of the airway smooth muscle cells <sup>624,625</sup>. Increased *Prevotella* colonisation, therefore, is likely to actively contribute towards disease pathology in a Th17-dependent manner.

Furthermore, *Blautia*, a bacterial genus typically thought to be a beneficial microbe due to its ability to produce SCFAs, may also contribute towards atopic pathogenesis. The bacterial genus was observed to be increased in the asthmatic circulatory microbiome, and expansion of this bacterial genus in other microbiome sites (airways, gut) has previously been associated with increased risk of asthma development <sup>270</sup>, chronic asthma <sup>263,276</sup>, and asthma severity <sup>263</sup>. This association may be due to the bacteria's ability to induce



proliferation of mucosal invariant T cells<sup>626</sup>, a cell type that has been found to be involved in asthma pathogenesis<sup>627</sup>. Additionally, *Blautia* has been found to suppress the production of IFN $\gamma$  and the Th1 immune response<sup>628</sup>, and thus increased abundance of the bacteria would likely contribute towards a Th2-biased immune system.

#### 5.4.9. Microbial dysbiosis and Treatment Responsivity

In addition to contributing towards immune mechanisms involved in atopic pathogenesis, changes in the microbiome may also contribute towards disease responsiveness to treatment. In a study by Goleva *et al* (2013), for example, resistance to corticosteroid treatment was associated with a significant expansion of the Actinobacteria and Fusobacteria phyla in the airway microbiome of asthmatic subjects<sup>255</sup>. There was a significant increase in Fusobacteria, specifically the *Fusobacterium* genus, observed in the circulatory microbiome of subjects with allergic rhinitis in this study. This, therefore, suggests that possibility that the allergic rhinitis subjects would be resistant to corticosteroid treatment, and that the circulatory microbiome may function as a biomarker of disease responsiveness.

#### 5.4.10. Microbial Dysbiosis a consequence of Atopic Pathogenesis

The development of atopy typically occurs during infancy, the same developmental period that changes in the microbiome are first detected in atopy susceptible individuals. It is, therefore, difficult to determine which comes first; allergen sensitisation or microbial dysbiosis. Although microbial dysbiosis and specific bacterial taxa have been associated with atopy, it is possible that their altered abundance in the atopic microbiota is simply a consequence of altered immune state in the atopic individuals.

In a study carried out by Rivas *et al* (2013), for example, the induction of OVA-sensitisation in mice resulted in a number of significant changes to bacterial taxa detected in the murine gut microbiome, including a decrease in *Lachnospiraceae* and expansion of *Porphyromonadaceae* and *Rikenellaceae* species <sup>629</sup>. Interestingly, the induction of oral tolerance using Treg therapy inhibited microbial dysbiosis, thus suggesting that the observed microbial dysbiosis in allergen-sensitive mice was associated with atopic immune responses.

Microbial dysbiosis in allergen-sensitive individuals may be a consequence of impaired immune responses to bacteria. In a study carried out by Habibzay *et al* (2012), for example, the HDM-exposed lung of mice was found to exhibit impaired immune responses to bacteria, characterised by upregulation of TLR2-negative regulators, impeded recruitment of neutrophils, and subsequent bacterial invasion and bacteraemia <sup>630</sup>. Furthermore, in GF and gnotobiotic mice that exhibited a Th2 biased immune system, global impairment of the immune function has been demonstrated to increase bacterial translocation <sup>231,631</sup>. As enhanced Th2 activity is a key feature of atopic disease, it is likely that atopic subjects would also exhibit increased bacterial translocation, subsequently altering the composition of the circulatory microbiome.

Impaired immune responses to bacteria are also likely present in clinical atopy, as evidenced by increased infection with bacterial pathogens (*Chlamydia pneumoniae*, *Haemophilus influenzae*, *Moraxella catarrhalis*, *Mycoplasma pneumoniae*, *Streptococcus pneumoniae*) <sup>280,632–636</sup> and respiratory viruses <sup>632,637,638</sup> in asthmatic subjects, and the observations that antibiotics can improve clinical presentation <sup>639–641</sup>.

Furthermore, recent work carried out by Dzidic and colleagues (2017), has demonstrated infants with atopic symptoms during the first 7 years of life displayed significantly lower proportions of IgA-coated gut bacteria at 12 months of age<sup>642</sup>.

IgA is the primary mediator of humoral mucosal immunity, and it is thought to be an important neutralising antibody that preserves mucosal barrier integrity<sup>642,643</sup>. IgA is also thought to promote growth of commensal organisms by facilitating adhesion and/ or nutrient utilisation within the mucous layer<sup>644</sup>, and IgA deficiency has been associated with expansion of pro-inflammatory bacterial species in the gut microbiota<sup>645</sup>. Innate receptor signalling in T cells is thought to regulate IgA specificity<sup>646</sup>, and thus it is likely that altered T cell activity in atopic subjects influence IgA specificity. IgA has been detected at significantly reduced levels in atopic children<sup>647</sup>, and thus reduced IgA levels with altered IgA-binding activity is likely to alter the ratio of pro- and anti-inflammatory bacterial species in the atopic microbiota.

Impaired immune responses to bacteria and viruses would likely alter the composition of the human microbiota, enabling the expansion of some microbial members at the cost of others. Moreover, expansion of particular bacterial groups will often alter the environment and/ or result in the production of metabolites that enable optimal growth conditions for other microbes. *Aerococcus viridans*, for example, has been demonstrated to secrete a protease that cleaves hemagglutinin, a pre-requisite for effective Influenzae A viral replication and infectivity<sup>648</sup>. Asthma has frequently been associated with increased risk for respiratory viral infections, and it is interesting to note that *Aerococcus* was significantly increased in the atopic circulatory microbiome. It is, therefore, possible to speculate that microbial dysbiosis in the atopic microbiota could directly enhance susceptibility towards respiratory viral infections by creating a more hospitable environment for viral replication.

In turn increased viral infection could enhance growth and pathogenesis of bacterial pathogens by impairing mucosal clearance, enabling increased bacterial adhesion to epithelial cells, and reducing the integrity of the epithelial layer, thus enabling bacterial translocation <sup>649</sup>.

Furthermore, clinical presentation itself may influence the microbiome. Hypersecretion of mucous, for example, increases the availability of mucin proteins in the airways and nasal passages of atopic individuals, which selectively encourages the growth of mucin-degrading bacteria. In support of this is the observation of increased mucin-degrading bacteria in the circulatory microbiome of atopic subjects in this study (*Prevotella*, *Veillonella*, and *Fusobacterium* <sup>650</sup>).

Additionally, it should also be noted that the use of corticosteroids has been demonstrated to significantly alter the atopic microbiome <sup>588,651</sup>. In a study by Denner *et al* (2016), for example, the relative abundance of Proteobacteria and *Pseudomonas* was significantly increased and the relative abundance of Bacteroidetes, Fusobacteria, *Prevotella*, and *Veillonella* were significantly decreased in the airway microbiome of asthmatics being treated with corticosteroids compared to asthmatic subjects not undergoing corticosteroid treatment <sup>651</sup>. This suggests that possibility that corticosteroids may influence the microbiome, and that some of the observed changes in the circulatory microbiome are reflective of asthma treatment rather than asthma pathogenesis. This interpretation is further supported by more recent work carried out by Durack *et al* (2017), who demonstrated that treatment with inhaled corticosteroids resulted in a significant alterations in the relative abundance of a number of bacterial taxa including a significant decrease in *Dialister* <sup>588</sup>. However, as corticosteroids are typically used to control asthma and reduce the risk of asthma exacerbations, the differences in airway microbiome in

asthmatics who are treated with corticosteroids compared to those who don't require treatment may also be reflective of asthma severity.

#### 5.4.11.Changes in Microbial Activity in the Atopic Circulatory Microbiome

In addition to identifying changes in the relative abundance of bacterial taxa in the atopic circulatory microbiome compared to the control, and how they relate to disease development, severity, and pathogenesis, changes in predicted microbial activity of the atopic circulatory microbiome were also assessed.

Comparison of the bacterial populations detected in the atopic subjects compared to the control subjects using PICRUSt analysis revealed that changes in the circulatory microbiome of hyper-allergic subjects resulted in significant changes in microbial activity in the hyper-allergic subjects compared to the control subjects. Flavonoid synthesis, retinol metabolism, dioxin degradation and toluene degradation activity were predicted to be increased in the hyper-allergic circulatory microbiome, whilst thiamine metabolism and PPAR signalling was predicted to be decreased in the hyper-allergic subjects. As the circulatory microbiome is predicted to be reflective of microbial dysbiosis at other body sites, it is likely that the identified changes in microbial activity are also present elsewhere in the body, most likely the nasal passages and lungs of the atopic subjects.

Increased retinol metabolism was of interest as it suggested that there were increased levels of retinoids in the hyper-allergic subjects, resulting in expansion of bacterial populations capable of metabolising retinoids. This observation supports the 'Hygiene hypothesis', as previous studies have demonstrated that a lack of certain childhood infection causes retinoids to accumulate in the lungs <sup>652,653</sup>. Furthermore, retinol concentrations have been negatively correlated with the development of atopic disease

<sup>654–656</sup> and asthma severity <sup>657</sup>, and epigenetic investigations have demonstrated that B cells from subjects with HDM-associated atopic diseases have increased retinol metabolism activity <sup>658</sup>.

The positive association between increased retinol metabolism and atopic disease is likely due to the biological activities of retinoic acid, a major metabolite of retinol metabolism. The vitamin D receptor/ retinoic acid receptor, for example, has previously been demonstrated to display increased activity in atopic subjects compared to control subjects <sup>658</sup>, and expression of the vitamin D receptor and retinoic acid receptor was found to be increased in the plasma samples of the asthmatic subjects described in Chapter 4.

Increased levels of retinoic acid has been demonstrated to induce eosinophilia, promote the accumulation of mucin <sup>659</sup>, increase IL-4 and IL-5 expression (Th2 cytokines) <sup>660</sup>, decrease expression of IL-2, IL-12, TNF $\alpha$ , and IFN $\gamma$  (a Th1-like cytokine profile)<sup>660,661</sup>, promote the development of Th2 cells <sup>662</sup>, stimulate B cell proliferation and maturation <sup>663–667</sup>, and increase primary and memory antibody responses <sup>668–670</sup>. Additionally, retinoic acid has been found to promote IgA class switch recombination, and thus altered retinol metabolism in atopic subjects may contribute towards to the observed changes in IgA levels and activity in atopic subjects.

However, retinoic acid has also been found to promote Treg differentiation <sup>671–674</sup>, inhibit Th17 differentiation <sup>672,673</sup>, inhibit IL-4-induced IgE class switch recombination <sup>675,676</sup>, inhibit granulocyte development <sup>677,678</sup>, and inhibit the production of GM-CSF <sup>677</sup>. As these activities are typically associated with protection against atopic disease further study is required to resolve the conflicting data regarding the role retinoic acid plays in atopic disease.

The observed increase in toluene and dioxin metabolism in the hyper-allergic subjects was also of interest, as both chemical compounds have been associated with asthma development. Toluene is a leading cause of occupational asthma<sup>679–681</sup>, whilst dioxin is found in cigarette smoke and prenatal exposure to the chemical has been associated with increased risk of atopic disease<sup>682–684</sup>.

In contrast to retinol and its metabolites, toluene, and dioxin, the consumption of flavonoids has been demonstrated to be protective against atopic disease<sup>685–687</sup>. It was, therefore, unexpected to report increased flavonoid synthesis in the hyper-allergic subjects compared to the control subjects. This group of plant secondary metabolites are acquired through diet and have been demonstrated to possess immune-modulating activities and anti-atopic properties. In the OVA-induced murine model of asthma, for example, administration of flavonoids suppressed OVA-induced bronchoconstriction and airway hyperresponsiveness<sup>688–697</sup>; reduced airway inflammation<sup>690–692, 694–696, 698, 699</sup> and airway remodelling<sup>696</sup>, pulmonary oxidative stress<sup>696</sup>, goblet cell hyperplasia and mucous production<sup>691, 692, 694, 697, 698</sup>, eosinophilia<sup>691, 692, 694, 696–698, 700–702</sup>, eosinophil peroxidase activity, IgE levels<sup>688–690, 696–698</sup>, IL-6, IL-17 and IL-33 levels<sup>692, 697, 701</sup>, Th2 cytokine production (IL-4, IL-5, IL-13)<sup>688, 689, 700, 690–695, 697, 699</sup>, and the Th2-predominant transcriptional factor, GATA-3<sup>691, 693, 699</sup>; and caused an increase in IFN $\gamma$  and the Th1 transcription factor T-bet<sup>688, 690, 693, 695, 699</sup>. It is possible that increased flavonoid-synthesising potential in the circulatory system is representative of increased translocation of flavonoid-synthesising bacteria from the airways and gut, and subsequent decreased abundance of these bacteria and the beneficial properties provided by the flavonoids in the airways and gut of the atopic subjects

With regards to the microbial activities predicted to be decreased in the hyper-allergic subjects, daily consumption of thiamine (also known as vitamin B1) has been observed to be significantly decreased in asthmatic subjects compared to non-asthmatic subjects <sup>703</sup>. However, in children increased thiamine consumption has been associated with the development of allergic rhinitis <sup>704</sup>, thus suggesting that the association between thiamine consumption and development of atopic disease may differ between the different atopic diseases. In a murine experimental model of chronic inflammation, administration of thiamine was associated with reduced TNF $\alpha$  and IL-6 in the inflamed tissue, thus demonstrating anti-inflammatory properties of thiamine. Furthermore, treatment with benfotiamine, a lipid-soluble derivative of thiamine, has been shown to suppress endotoxin-induced inflammation, decrease production of nitric oxidise synthase, cyclooxygenase-2 (COX-2), TNF $\alpha$ , and IL-6, and increased production of IL-10 <sup>705,706</sup>.

PPAR $\gamma$  expression is increased in the submucosa, smooth muscle layer, and epithelium of asthmatic subjects, <sup>707</sup>, and OVA-induced asthma has been demonstrated to increase PPAR $\gamma$  levels in the murine airways <sup>708</sup>. In OVA-sensitised mice administration of PPAR $\gamma$  has been observed to decrease allergen-induced eosinophil and lymphocyte influx into the airways <sup>709</sup> and expression of Th2 cytokines (IL-4, IL-5, and IL-13), and in PPAR $\gamma$ -deficient mice, airway hyperresponsiveness, airway inflammation, eosinophilia, IgE production, GATA-3 expression is increased following OVA-sensitisation <sup>710</sup>.

This suggests that PPAR $\gamma$  signalling is protective against asthma pathogenesis, an interpretation supported by *in vitro* studies, whereby induced activation of PPAR $\gamma$  in human airway smooth muscle cells resulted in anti-inflammatory effects similar to those observed with steroid treatment <sup>711</sup>.



The observed decrease in PPAR $\gamma$  signalling in the circulatory microbiome of hyper-allergic subjects suggests decreased PPAR $\gamma$  signalling in these subjects, and subsequent loss of the protective effects PPAR $\gamma$  provides against atopic disease. However, predicted abundance of the downregulated level 3 KEGG pathways (thiamine metabolism and PPAR $\gamma$  signalling) was less than 0.002% of total microbial activity, and thus further investigation would be required to validate the potential role of decreased thiamine metabolism and PPAR $\gamma$  signalling activity in atopic disease pathogenesis.

#### 5.4.12. Chapter Summary

In conclusion the circulatory microbiome was successfully characterised in serum samples from control subjects, asthmatic subjects, allergic rhinitis subjects, and hyper-allergic subjects. Characterisation of the bacterial populations present in the circulatory microbiome revealed that the circulatory microbiome consisted of similar bacterial taxa to that observed in the circulatory microbiome in Chapter 4 and in previous circulatory microbiome studies.

Comparison of the circulatory microbiome in atopic and non-atopic subjects revealed significant differences in the atopic microbiome compared to the control microbiome. Asthma was associated with decreased bacterial diversity, whilst allergic rhinitis was associated with increased bacterial diversity. Furthermore, individual analysis of the different atopic disease groups found that bacterial taxa present in significantly altered levels in the atopic circulatory microbiome was dependent on disease state, and in the hyper-allergic subjects, changes in bacterial relative abundance had a significant impact on the microbiome functional potential.

This indicated that atopic disease present at different body sites (the airways in asthma, the nasal mucosa in allergic rhinitis) influences composition of the circulatory microbiome. This is likely due to loss of epithelial barrier integrity in the airways/ nasal passages altering bacterial translocation from these sites in the circulatory system. Furthermore, it is likely that immune activity as a consequence of atopic disease alters the environment of the airways and nasal passages, subsequently altering bacterial colonisation in these environments. This in turn further alters bacterial translocation into the blood.

Furthermore, several of the bacterial taxa identified as having significant differential abundance in the circulatory microbiome have been previously found to display significant differential abundance in the gut and airways of atopic subjects. This suggests that the observed changes in the circulatory microbiome reflected microbial dysbiosis of the gut and airway microbiota. Characterisation of the circulatory microbiome, therefore, could be used to identify microbial dysbiosis in atopic subjects, and altered abundance of specific bacterial taxa could be used as circulatory biomarkers for atopic disease. However, as this study is the first known study to investigate the circulatory microbiome in different atopic populations, further research would be required to validate the use of the circulatory microbiome as a potential source of microbial biomarkers for atopic disease.

## Chapter 6: Characterisation of the Murine Microbiome following exposure to the House Dust Mite allergen

### 6.1. Introduction

The human microbiota has been demonstrated to be an important determinant in health and disease. The different human body sites have been demonstrated to harbour distinct bacterial populations that are important in maintaining homeostasis of the body site. The factors that influence composition and stability of these microbial populations, however, have yet to be fully elucidated.

In asthma and the other atopic diseases, microbial dysbiosis of the airways, skin, and gastrointestinal tract have been observed <sup>242, 254, 263,255–262</sup>, and various early-life factors have been positively associated with disease development, including mode of delivery <sup>242,246</sup>, increased urbanisation <sup>245,247–250</sup>, and the use of antibiotics <sup>235, 251–253,266</sup>.

Whether early-life microbial dysbiosis triggered by early-life factors causes atopic disease or is simply the consequence of atopic disease in genetically predisposed individuals has yet to be determined.

The development of atopy typically occurs during infancy; the same developmental period that the neonatal immune system matures, and the microbiome is established. Due to this overlap it is difficult to determine which comes first, an impaired immune system which alters microbial colonisation, or altered microbial colonisation which adversely affects maturation of the immune system.

One method of determining whether the inflammatory responses associated with allergen sensitisation adversely affect composition of the microbiota in atopic individuals is to use

*in vivo* experimental models of asthma. Of the available models available, the murine experimental model is the most commonly used. This is in part due to the ease in which mice can be bred, maintained, and handled. Moreover, repeated allergen exposure in mice results in many of the hallmark features of atopic asthma, including Th2-driven inflammation in the airways, eosinophilia, increased infiltration of neutrophils and lymphocytes, increased mucin production, increased muscle cell proliferation, and increased respiratory system resistance and elastance of the airway tissues <sup>41, 381–383,712</sup>.

The HDM allergen is increasingly being used in the murine experimental model of asthma in order to better mimic the uniquely human disease. This is one of the most common human allergens, with an estimated 50-85% of asthmatics being diagnosed with a HDM allergy.

With regards to the effect asthma has on the microbiota, there is increasing evidence supporting the theory that the development of asthma can directly alter composition of the microbiota. This has been shown by a number of studies independently demonstrating that OVA- and HDM-induced experimental asthma results in significant changes to the murine gut microbiome <sup>384–386</sup> and airway microbiome <sup>384,387,388</sup>.

The observation that HDM sensitisation and challenge results in significant changes to the microbiome suggests that possibility that HDM sensitisation may also influence the composition of the human microbiota. This may make the individual more susceptible to immune dysregulation and the development of atopic diseases.

These investigations, however, have typically looked at microbial composition in either the murine gut microbiome or the murine lung microbiome. This, therefore, has prevented analysis on whether HDM-induced inflammatory responses in the lungs can simultaneously affect the microbiota at multiple body sites.

### 6.1.1. Chapter Aims

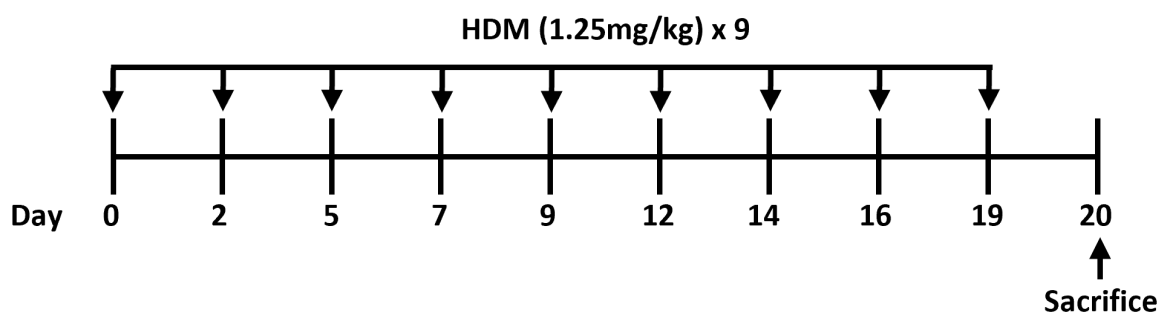
The purpose of this study, therefore, was to examine the effects of pulmonary exposure to the common HDM allergen on microbial populations in the exposed host. This was achieved by examining the bacterial composition of the murine microbiome at various body sites (the airways using BAL samples, the gut using faecal samples, and the circulatory system using plasma samples) in mice exposed to the HDM allergen and HDM-naïve mice.

## 6.2. Methods

### 6.2.1. Murine HDM Exposure Model

The murine HDM exposure model was designed and carried out by Dr Martin Leonard and his team at *Public Health England* as part of a larger study looking into the effects of cerium dioxide nanoparticles on respiratory inflammatory responses in experimental allergic asthma<sup>383</sup>. The experimental procedure Martin and his team used is described below.

Female BALB/c mice aged between 6 and 8 weeks (obtained from *Envigo*, UK) were anaesthetised with 5% isoflurane in oxygen using a precision vaporizer and intranasally instilled with HDM (1.25mg protein/ kg; *Greer Laboratories*, Lenoir, cat # XPB82D3A25), as described in Figure 6.1. Instillation of an equivalent dosing volume of phosphate buffered saline (PBS) was performed as a control procedure. Following the treatment procedure, the mice were euthanized using an overdose of 0.1ml sodium pentobarbital (200µl/ ml) by intraperitoneal injection and exsanguinated by cardiac puncture.



**Figure 6.1: Experimental protocol for intranasal administration of HDM.** 7 BALB/c mice were exposed to HDM over the course of a three-week exposure protocol involving 9 individual instillations of house dust mite (HDM) (1.25mg protein/ kg) on the days indicated. An additional 7 BALB/c mice were exposed to equivalent doses of PBS and functioned as the experiment controls. Sacrifice and collection of tissue samples was carried out on the day indicated following completion of the experimental protocol.

### 6.2.2. Sample Collection

Blood samples were collected into EDTA coated tubes and plasma was isolated by centrifugation at 1500xg for 15 minutes at 4°C. BAL fluid was collected by exposing and cannulating the trachea and then lavaging the lungs with 500µl of ice-cold sterile PBS. The lungs were gently aspirated, and the process repeated a further 2 times to generate 1.5ml of BAL fluid in total. Fresh faecal pellets were collected shortly before mouse sacrifice. The plasma, BAL, and faecal samples were then stored at -80°C prior to DNA extraction.

### 6.2.3. Extraction of Microbial DNA from the Murine BAL and Faecal Samples

Total bacterial genomic DNA was extracted from 40µl of BAL fluid and 8mg of faeces using the PowerSoil® DNA isolation kit (*Mobio*) as per the manufacturers recommended protocol.

The BAL/ faecal samples were added to the kit PowerBead Tubes and mixed by vortexing. Solution C1 (60µl) was added to the tubes and the tubes were vortexed briefly. The tubes were then loaded onto a horizontal vortexer (*MoBio*) and vortexed at maximum speed for 10 minutes. The tubes were then centrifuged for 30 seconds at 10,000xg, and following centrifugation the supernatant was transferred to sterile 2ml collection tubes. Solution C2 (250µl) was added to the collection tubes and the tubes were vortexed for 5 seconds and incubated at 4°C for 5 minutes. Following incubation, the collection tubes were centrifuged for 1 minute at 10,000xg. 750µl of the supernatant was transferred to sterile 2ml collection tubes and 1.2ml of solution C4 was added to the collection tubes. The tubes were vortexed for 5 seconds and then 675µl of the solution was added onto a spin filter and centrifuged for 1 minute at 10,000xg. The flow-through was discarded and an additional 675µl of the solution was added to the spin filter. The spin filters were centrifuged at 10,000xg for 1

minute and the flow-through was discarded. The remaining solution was then added to the spin filter and centrifuged at 10,000xg for 1 minute. Solution C5 (500µl) was added to the spin filters and the filters were then centrifuged for 30 seconds at 10,000xg. The flow-through was discarded and the filters were centrifuged for an additional minute at 10,000xg. The spin filters were then transferred to sterile 2ml collection tubes and solution C6 (100µl) was added to the centre of the filter membrane. The filters were centrifuged for 30 seconds at 10,000xg in order to elute the DNA. The filters were removed, and the eluted DNA samples were placed in storage (-20°C).

All DNA extractions were accompanied by a “kit control”, whereby the BAL/ faecal sample was replaced with UV-treated molecular biology grade water. The “kit control” served to characterise any reagent or environmentally introduced contamination throughout the entire experimental procedure.

#### 6.2.4. Direct amplification of the V4 region of the 16S rRNA gene from Murine Plasma Samples

PCR amplification of the V4 region of the 16S rRNA gene was performed directly on the murine plasma samples using the optimised Phusion blood direct PCR protocol developed in Chapter 4 (Table 6.1).



**Table 6.1: Amplification of the V4 region of the 16S rRNA gene from microbial DNA present in murine plasma samples using an optimised Phusion blood direct protocol.** An optimised Phusion blood direct PCR protocol was used to amplify the V4 region of the 16S rRNA gene from bacterial DNA present in 5% murine plasma samples. **(A)** The reagents used in the Phusion blood direct PCR protocol. **(B)** The cycling parameters used in the Phusion blood direct PCR protocol.

**A.**

Reagent	Volume ( $\mu$ l)
UV-treated molecular biology grade water	6.6
2X Phusion blood PCR buffer	10.0
V4 Fwd primer	1.0
V4 Rev primer	1.0
Phusion blood II DNA polymerase	0.4
Murine Plasma	1.0

**B.**

Cycle Step	Temperature ( $^{\circ}$ C)	Time	Cycles
Lysis of cells	98	5 minutes	1
Denaturation	98	1 second	
Annealing	55	5 seconds	35
Extension	72	15 seconds	
Final Extension	72	1 minute	1

Successful amplification of the V4 region from the murine plasma samples was determined using gel electrophoresis (as described in Chapter 2, section 2.2), and experimental negative controls were generated to monitor possible bacterial contamination. This was achieved by replacing murine plasma with UV-treated molecular biology grade water, and sterile conditions were utilised during PCR set-up to minimise the risk of bacterial contamination (as described in Chapter 2, section 2.1).

Amplification of the V4 region of the 16S rRNA gene using the optimised Phusion blood direct PCR protocol was unsuccessful. Amplification of the V4 region from microbial DNA present in the murine plasma samples were, therefore, attempted using a second kit - a SureDirect blood PCR kit (*Agilent technologies*) following the recommended kit protocol (Table 6.2).

**Table 6.2: Amplification of the V4 region of the 16S rRNA gene from microbial DNA present in murine plasma samples using a SureDirect Blood PCR protocol.** A SureDirect blood PCR protocol was used to amplify the V4 region of the 16S rRNA gene from bacterial DNA present in 20% murine plasma samples. **(A)** The reagents used in the SureDirect blood PCR protocol. **(B)** The cycling parameters used in the SureDirect Blood PCR protocol.

**A.**

Reagent	Volume ( $\mu$ l)
SureDirect blood PCR 2X master mix	12.5
V4 Fwd primer	1.0
V4 Rev primer	1.0
UV-treated molecular biology grade water	5.5
Murine Plasma	5.0

**B.**

Cycle Step	Temperature ( $^{\circ}$ C)	Time	Cycles
Lysis of cells	90	5 minutes	1
Denaturation	95	30 seconds	
Annealing	55	30 seconds	35
Extension	72	1 minute	
Final Extension	72	5 minutes	1

#### 6.2.5. Amplification of the V4 region of the 16S rRNA gene from Microbial DNA isolated from the Murine BAL and Faecal Samples

Amplification of the V4 region from microbial DNA extracted from the murine faecal and BAL samples was performed using an Accuprime Pfx SuperMix (*Thermo fisher Scientific*) protocol and the V4 515F/806R oligonucleotide primers (Table 6.3). The same PCR protocol was performed on microbial DNA extracted from the murine BAL and faecal samples. However, due to reduced levels of microbial DNA present in the BAL samples, 38 PCR cycles were required for successful amplification of the V4 region from DNA extracted from the BAL samples, whereas only 30 PCR cycles were required for successful amplification of microbial DNA extracted from the faecal samples (Table 6.3). Successful amplification of the V4 region of the 16S rRNA gene was confirmed using gel electrophoresis as described in Chapter 2, section 2.2

Sterile conditions (as described in Chapter 2, section 2.1) were maintained throughout the experimental procedure in order to reduce the risk of microbial contamination. Additionally, PCR amplification of the 16S rRNA V4 region was also performed on microbial DNA extracted from the BAL and faecal DNA extraction “kit controls”, and amplification of the “kit controls” served as experimental negative controls for the BAL and faecal samples.

**Table 6.3: PCR Amplification of the V4 region of the 16S rRNA gene from microbial DNA extracted from murine BAL and faecal samples.** An Accuprime PCR protocol was used to amplify the V4 region of the 16S rRNA gene from bacterial DNA extracted from the murine BAL and faecal samples. **(A)** The reagents used in the Accuprime PCR protocol. **(B)** The cycling parameters used in the Accuprime PCR protocol.

**A.**

Reagent	Volume ( $\mu$ l)
Accuprime master mix	22.5
515F (10 $\mu$ M)	0.5
806R (10 $\mu$ M)	0.5
Microbial DNA	1.5

**B.**

Cycle Step	Temperature ( $^{\circ}$ C)	Time	Cycles
Lysis of cells	95	2 minutes	1
Denaturation	95	20 seconds	
Annealing	55	15 seconds	30/38
Extension	68	5 minute	
Final Extension	68	5 minutes	1

#### 6.2.6. Sequencing of the V4 amplicons using Illumina Sequencing Technology

The XT-V4 amplicons generated from the murine BAL and faecal samples were submitted to the *Earlham Institute* to undergo library preparation. In brief, the Nextera DNA library kit was used to tagment the V4 amplicons (cleave the double stranded V4 DNA to generate universal single stranded DNA overhangs) and attach the Illumina i7 and i5 adapters to the V4 amplicons. The V4-adaptor amplicons were then purified, quantified, barcoded, multiplexed (the individual sample V4 libraries were pooled together), and sequenced using the Illumina MiSeq system with a 250 base paired-end read metric.

### 6.2.7. Alignment of the V4 amplicons to known Bacterial Genomes

Following successful sequencing of the V4 amplicons using Illumina sequencing technology, the trimmed and demultiplexed sequencing data was uploaded to *Nephele* 2.0 [Public web access: <https://nephele.niaid.nih.gov/#cloud>]. The *Nephele* 2.0 QIIME 16S FASTQ paired-end open reference pipeline was used to remove low-quality V4 reads (defined as having a Phred quality score less than 19.0), remove chimeric sequences, and align the V4 reads to bacterial OTUs with a 99% similarity threshold using the Silva database (see Chapter 2, section 2.4.1 for additional detail).

### 6.2.8. Comparison of the HDM-exposed Microbiome to the HDM-naïve Microbiome

The phylogenetic diversity of the bacterial populations detected in the murine BAL and faecal samples were first assessed by generating a rarefaction curve using *R* software (see Chapter 2, section 2.4.2 for additional detail).

Alpha diversity indices (Shannon and Chao1) were measured using the *Nephele* 2.0 QIIME 16S FASTQ paired-end open reference pipeline [Public web access: <https://nephele.niaid.nih.gov/#cloud>]. The diversity indices were then uploaded to *R* software where alpha diversity boxplots were generated and statistical analysis was performed (see Chapter 2, section 2.4.5).

Beta diversity was also determined using the OTU tables generated from the *Nephele* 2.0 QIIME 16S FASTQ paired-end open reference pipeline. This involved measuring Bray Curtis dissimilarity and plotting PCoA graphs using *R* software (See Chapter 2, section 2.4.6 for additional information). PERMANOVA analysis using 999 permutations was then performed to determine whether the bacterial populations present in the HDM-exposed

mice differed significantly to the bacterial populations detected in the HDM-naïve mice (see Chapter 2, section 2.4.6).

The bacterial OTUs were then assigned to bacterial taxa and the relative abundance of the bacterial taxa present in the murine samples was determined using *R* software (See Chapter 2, section 2.4.4 for additional detail). *R* was then used to plot the relative abundance of highly abundant bacterial phyla and genera (taxa with a relative abundance greater than 1%) (See Chapter 2.4.4).

LEfSe analysis was applied to the relative abundance data to determine bacterial taxa significantly associated with the HDM-exposed and HDM-naïve microbiome. This was performed on the relative abundance tables of all bacterial taxa detected in the murine samples using the online *Galaxy* workflow framework<sup>394</sup> set to the default settings [Public web access: <http://huttenhower.sph.harvard.edu/galaxy/>](See Chapter 2, Section 2.4.7. for additional information).

#### 6.2.9. Prediction of the Murine Microbiome Metagenome Function Content

To predict the microbial activity of the bacterial populations detected in the murine microbiome PICRUSt analysis was performed using the online *Galaxy* platform. OTU tables were generated from the V4 16S rRNA sequencing data using *Nephele* 2.0 software with a closed reference OTU picking strategy and the GreenGenes 99 database. The OTU tables was uploaded to *Galaxy*, normalised, and functional predictions were performed to determine KEGG ortholog abundances present in the murine samples (See Chapter 2, section 2.4.8 for additional information).

The level 1, 2, and 3 KEGG ortholog counts were converted into abundance percentages, and *R* software was used to plot the abundance of high-abundant level 3 KEGG pathways detected in the murine samples (defined as having a predicted total abundance greater than 1% in the murine samples). LEfSe analysis was then performed on the level 1,2, and 3 KEGG orthologs to determine differential KEGG ortholog abundance present in the HDM-exposed mice compared to the HDM-naïve mice.

Abundance of KEGG orthologs that displayed significant differential abundance were plotted as boxplots using *R* software (see Supplementary Materials S4 for *R* codes used).

## 6.3. Results

### 6.3.1. Amplification of the V4 region of the 16S rRNA gene from Microbial DNA present in Murine Plasma Samples

Direct amplification of the V4 region of the bacterial 16S rRNA gene was unsuccessful in the murine plasma samples using both the optimised Phusion blood direct PCR protocol and the SureDirect blood PCR protocol. Analysis of the positive control was successful for both protocols however, thus indicating that failure to amplify the V4 region was due to insufficient microbial DNA present in the samples. Example gels of both PCR protocols are shown in the Supplementary Materials (Figure S9).

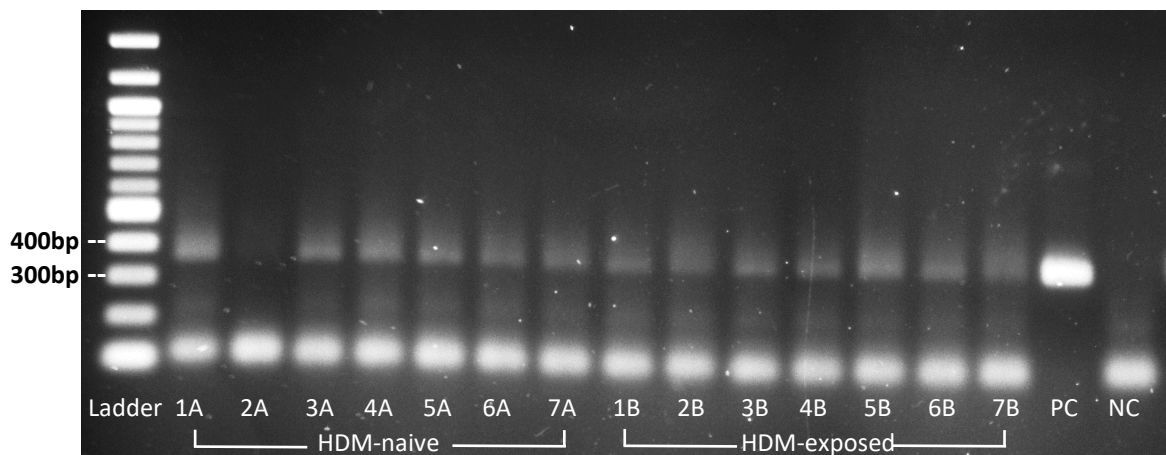
### 6.3.2. Amplification of the V4 region of the 16S rRNA gene from Microbial DNA isolated from Murine BAL Samples

Analysis of the end-point PCR reaction using gel electrophoresis revealed that the V4 region of the bacterial 16S rRNA gene had been successfully amplified from microbial DNA extracted from murine BAL samples, as demonstrated by the detection of DNA bands of approximately 350bp in length (Figure 6.2). Faint banding at approximately 200bp revealed that a small amount of non-specific DNA amplification had occurred.

Amplification of the V4 region from bacterial DNA isolated from HDM-naive sample 2 was observed to be noticeably weaker compared to the other samples (Figure 6.2, 2A lane). However, subsequent attempts to increase V4 amplification from this sample resulted in similar results to the one shown below and thus it was deemed that extraction of bacterial DNA from this sample was not as successful, perhaps due to error during the extraction process or due to an initial lack of bacterial DNA present in the BAL sample.



Analysis of the experimental negative control (Figure 6.2, NC lane) revealed that as expected the sample was PCR negative, and that no amplification of the V4 region of the bacterial 16S rRNA gene had been achieved. This indicated that no environmental and/ or reagent bacterial contamination had been introduced to the samples during the PCR experimental procedure, and that completely sterile conditions had been achieved.



**Figure 6.2: Amplification of the V4 region of the bacterial 16S rRNA gene from microbial DNA extracted from murine BAL samples.** Amplification of the V4 region of the 16S rRNA gene was performed on microbial DNA extracted from BAL samples from control mice (HDM-naïve, n = 7) and mice exposed to the HDM allergen (HDM-exposed, n = 7). Amplification was achieved using 38 cycles of end-point PCR using the XT-tagged 515F/806R primer pair and the Accuprime master mix.

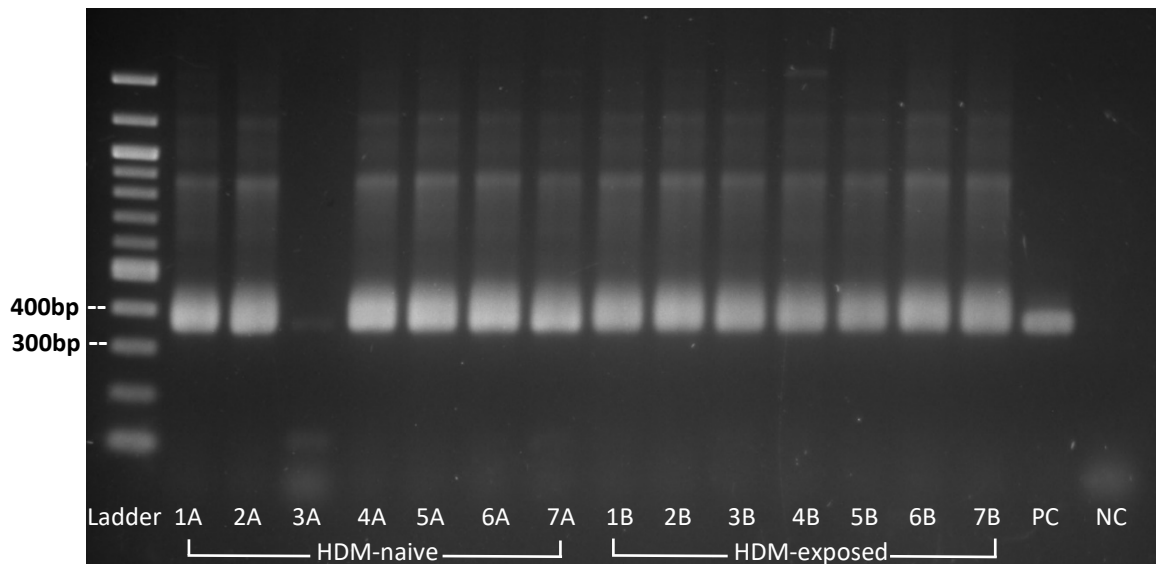
### 6.3.3. Amplification of the V4 region of the 16S rRNA gene from Microbial DNA isolated from Murine Faecal Samples

Amplification of the V4 region of the 16S rRNA gene from microbial DNA isolated from the faecal samples was successful. Initial examination of the V4 bands using gel electrophoresis found that amplified V4 DNA was the expected length, with bands approximately 350bp observed on the gel (290bp for the V4 amplicon, 33bp for the Illumina forward XT adaptor,

and 34bp for the Illumina reverse XT adaptor) (Figure 6.3). The thickness of the V4 bands indicated that a high degree of amplification was achieved, demonstrating that high concentrations of bacterial DNA were present in the samples (Figure 6.3), as you would expect from this sample type.

Amplification of the V4 region from microbial DNA isolated from HDM-naïve sample 3 was observed to be noticeably weaker compared to the other samples (Figure 6.3, 3A lane). However, subsequent attempts to increase V4 amplification from this sample resulted in similar results to the one shown below and thus it was deemed isolation of bacterial DNA from this sample was not as successful, perhaps due to error during the extraction process or due to an initial lack of bacterial DNA present in the faecal sample.

Analysis of the experimental negative control (Figure 6.3, NC lane) found that the sample was PCR negative, and that no amplification of the V4 region of the bacterial 16S rRNA gene had been achieved. This indicated that no environmental and/ or reagent bacterial contamination was introduced to the samples during the PCR experimental procedure, and that completely sterile conditions had been achieved.



**Figure 6.3: Amplification of the V4 region of the bacterial 16S rRNA gene from microbial DNA extracted from murine faecal samples.** Amplification of the V4 region of the 16S rRNA gene was performed on microbial DNA extracted from faecal samples from control mice (HDM-naïve, n = 7) and mice exposed to the HDM allergen (HDM-exposed, n = 7). Amplification was achieved using 30 cycles of end-point PCR using the 515F/806R primer pair and the Accuprime master mix.

#### 6.3.4. Sequencing of the V4 16S rRNA reads generated from Murine BAL Samples

Following removal of low-quality reads (defined as having a Phred quality score < 19) and chimeric sequences, a total of 616,365 high-quality V4 16S rRNA reads were generated from the BAL samples. This included 304,118 high-quality reads generated from the HDM-naïve BAL samples (average per sample = 43,445.43, range = 12,528 – 61,602) and 312,247 high-quality reads generated from the HDM-exposed BAL samples (average per sample = 44,606.71, range = 29,733 – 51,627) (Figure 6.4, see also Supplementary Materials, Table S15).

As predicted from the gel electrophoresis results, Control 2 generated noticeable less V4 16S rRNA reads compared to the remaining samples (Figure 6.4, see also Supplementary

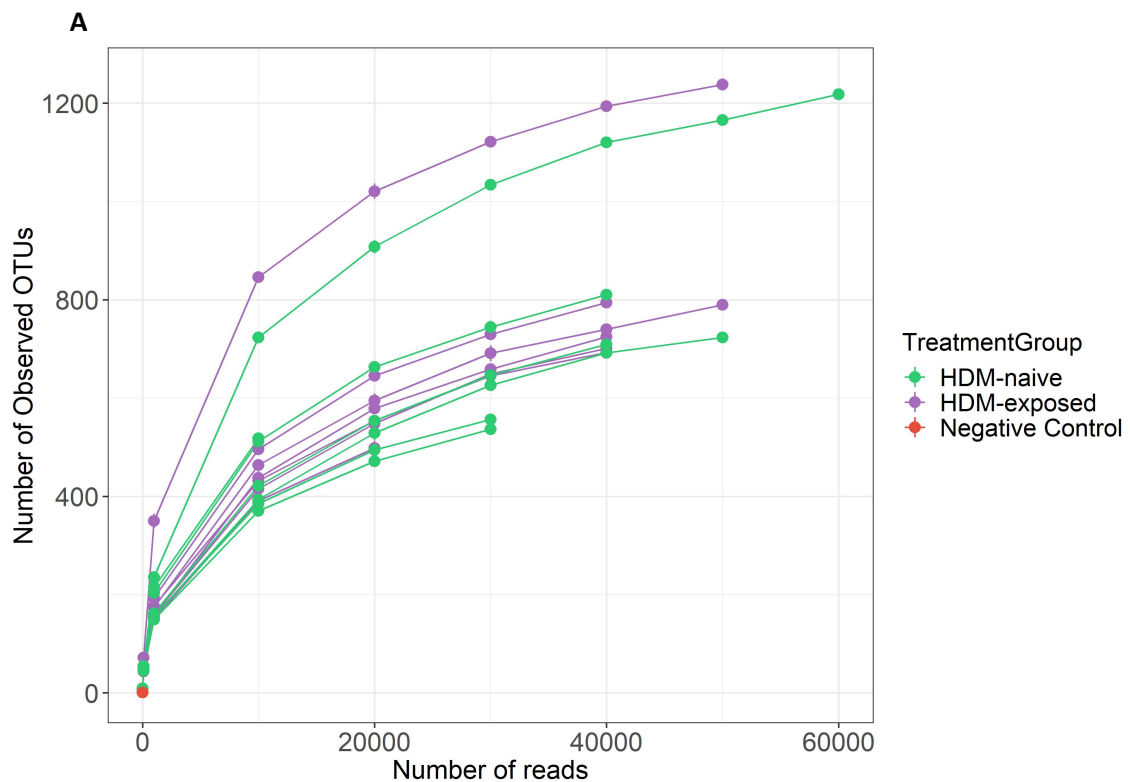
Materials, Table S15). However, the number of V4 16S rRNA reads to pass quality control for the sample (18,220 reads) was sufficient to enable characterisation of the microbial populations present in the sample.

Statistical testing found that there were no significant differences in the number of high-quality reads generated from the HDM-exposed samples compared to the HDM-naïve samples ( $P$  value = 0.8491, *Unpaired t test*).

Following read alignment to the Silva database, a total of 4,227 OTUs with a 99% similarity threshold were detected in the BAL samples. This included a total of 2,805 OTUs detected in the HDM-naïve samples (range = 640 – 1,352 per sample) and 3,310 OTUs detected in the HDM-exposed samples (range = 640 – 1,335)(Figure 6.4)(Supplementary Materials, Table S15). Examination of the rarefaction curve indicated no differences in number of OTUs detected in the HDM-exposed BAL samples compared to the HDM-naïve samples (Figure 6.4); an interpretation which was supported by statistical analysis of the number of OTUs detected in the HDM-exposed samples compared to the HDM-naïve samples ( $P$  value = 0.8981, *Wilcoxon rank sum test with continuity correction*).

Comparison of the OTUs detected in the HDM-exposed BAL samples compared to the HDM-naïve samples revealed a shared core BAL microbiome made up of 1,888 OTUs, an additional 917 OTUs were detected in the HDM-naïve samples alone, and 1,422 OTUs were unique to the HDM-exposed samples.

Analysis of the experimental negative control found that a single high quality V4 16S rRNA read was generated from the sample (Figure 6.5, see also Supplementary Materials, Table S15).



**B**

Group	Number of Samples	Mean number of raw reads	Mean number of high-quality reads	Total number of bacterial OTUs
HDM-naive	7	111,277.00	43,445.43	2,805
HDM-exposed	7	130,752.71	44,606.71	3,310
Negative Control	1	115,138.00	1.000	1

**Figure 6.4: Quantification of bacterial V4 reads sequenced murine BAL samples using Illumina sequencing.** Illumina sequencing was used to sequence bacterial V4 amplicons generated from murine BAL samples from HDM-naïve mice (n = 7) and HDM-exposed mice (n = 7). Following successful sequencing of the V4 amplicons *Nephele* 2.0 was used remove low-quality reads and chimeric sequences, and to align the high-quality V4 reads to bacterial operational taxonomic units (OTUs). **(A)** A rarefaction curve showing the level of phylogenetic diversity of the OTUs detected in the murine BAL samples. **(B)** Quantification of the V4 reads generated from HDM-naïve BAL samples and HDM-exposed BAL samples, and the total number of bacterial OTUs the reads align to with a 99% similarity threshold.

#### 6.3.5. Sequencing of the V4 16S rRNA reads generated from Murine Faecal Samples

Following removal of low-quality reads and chimeric sequences, a total of 1,321,241 high-quality V4 16S rRNA reads were generated from the murine faecal samples. This included

680,103 high-quality reads generated from the HDM-naïve faecal samples (average per sample = 97,157.57, range = 74,906 – 126,585) and 641,138 high-quality reads generated from the HDM-exposed faecal samples (average per sample = 91,591.14, range = 77,140 – 103,248) (Figure 6.5, see also Supplementary Materials, Table S16).

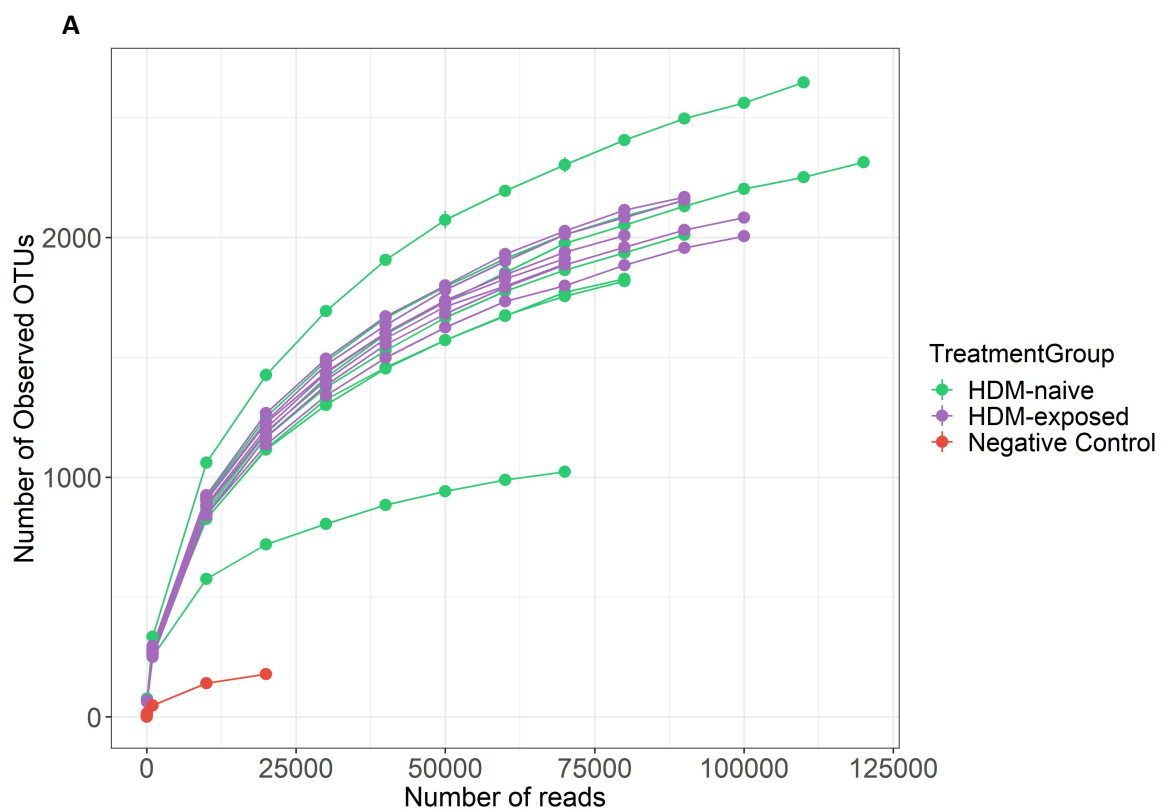
Statistical testing found that there were no significant differences in the number of high-quality V4 reads generated from the HDM-exposed samples compared to the HDM-naïve samples ( $P$  value = 0.5197, *Unpaired t test*).

Following read alignment to the Silva database, a total of 8,068 different OTUs were detected in the faecal samples. This included a total of 6,727 detected in the HDM-naïve samples (range = 1,240 – 3,230) and 6,443 in the HDM-exposed samples (range = 2,382 – 2,692) (Figure 6.5, see also Supplementary Materials, Table S16).

Comparison of the OTUs detected in murine faecal samples revealed a shared core faecal microbiome made up of 5,102 OTUs, an additional 1,341 OTUs were detected in the HDM-naïve samples alone, and 1,625 OTUs were unique to the HDM-exposed samples. Analysis of the number of OTUs detected in the HDM-exposed faecal samples compared to the HDM-naïve samples revealed no statistical difference ( $P$  value = 0.9015, *Wilcoxon rank sum test*). Evaluation of the rarefaction curve found that the lack of statistical differences with regards to the number of OTUs detected was likely due to the increased level of diversity in the number of OTUs detected in the HDM-naïve faecal samples compared to the HDM-exposed faecal samples (Figure 6.5.A).

With regards to the experimental negative control, 28,232 high-quality V4 16S rRNA reads were generated from the experimental negative control (Figure 6.5, see also Supplementary Materials, Table S16). Following read alignment 218 OTUs were detected in the control sample, the majority of which had a read count of less than 10. A total of 140

of the bacterial OTUs detected in the negative control were also detected in the murine faecal samples. However, the majority of OTUs detected in both the experimental negative control and the murine faecal samples were detected in low levels in the negative control, with 89% of OTUs being represented by less than 100 reads in the negative control. With regards to OTUs detected at high levels in the experimental control (represented by > 100 reads), only one OTU was of concern, being detected at similar levels in both the murine faecal samples and experimental negative control. This was OTU HW066314.1.1472, and taxonomic assignment revealed that the OTU represented a member of the *Ruminococcus 1* genus.



**B**

Group	Number of Samples	Mean number of raw reads	Mean number of high-quality reads	Total number of bacterial OTUs
HDM-naive	7	108,945.14	97,157.57	6,727
HDM-exposed	7	100,784.86	91,591.14	6,443
Negative Control	1	36,394	28,232	218

**Figure 6.5: Quantification of bacterial V4 reads sequenced from murine faecal samples using Illumina sequencing.** Illumina sequencing was used to sequence bacterial V4 amplicons generated from faecal samples from HDM-naive (n = 7) and HDM-exposed mice (n = 7). Following successful sequencing of the V4 amplicons *Nephele 2.0* was used to remove low-quality reads and chimeric sequences, and to align the high-quality V4 reads to bacterial operational taxonomic units (OTUs). (A) A rarefaction curve showing the level of phylogenetic diversity of OTUs detected in the faecal samples. (B) Quantification of the V4 reads generated from murine HDM-naïve samples and HDM-exposed faecal samples, and the total number of bacterial OTUs the reads align to with a 99% similarity threshold.

### 6.3.6. Taxonomic Classification of the OTUs detected in the Murine BAL Samples

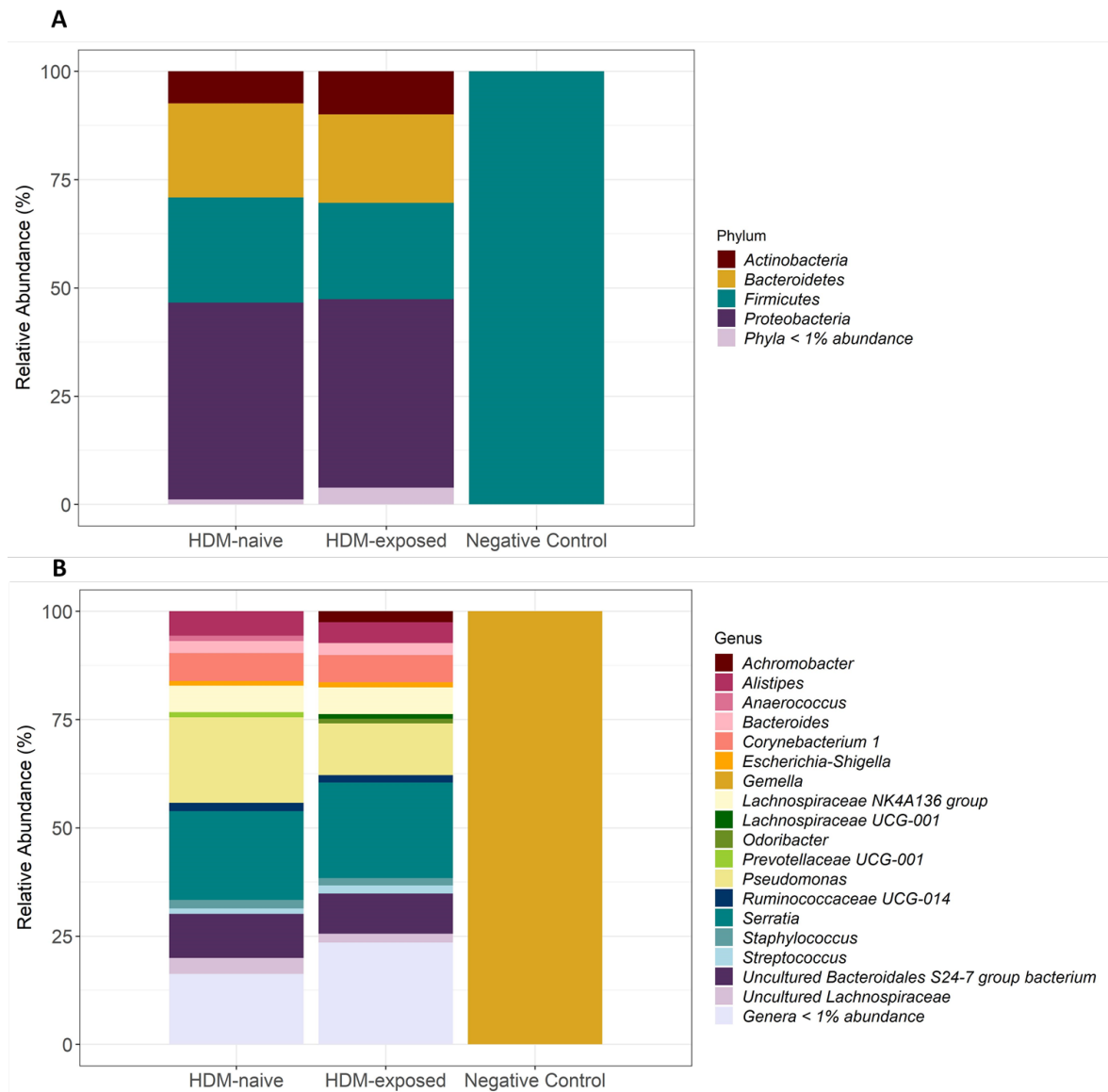
The OTUs identified in the murine BAL samples were classified into 21 phyla and 361 bacterial genera, the majority of which represented less than 1% of bacterial DNA sequenced from the samples (81% of phyla and 96% of genera). At the phylum level the murine BAL microbiome was dominated by four key phyla; Proteobacteria (45.44% of HDM-naïve DNA, and 43.49% of HDM-exposed DNA), Firmicutes (24.29%, 22.27%), Bacteroidetes (21.74%, 20.42%), and Actinobacteria (7.37%, 9.93%) (Figure 6.6.A).

At the genus level 14 genera were detected at high abundance (defined as representing > 1.0% of the total bacterial DNA) in the BAL samples. High-abundant genera included *Serratia* (20.52% of HDM-naïve DNA, and 22.07% of HDM-exposed DNA), *Pseudomonas* (19.75%, 11.95%), *uncultured Bacteroidales S24-7 group bacterium* (10.19%, 9.28%), *Corynebacterium 1* (6.44%, 6.31%), *Lachnospiraceae NK4A136 group* (6.10%, 6.14%),



*Alistipes* (5.63%, 4.81%), *uncultured Lachnospiraceae* (3.67%, 2.03%), *Bacteroides* (2.79%, 2.77%), *Staphylococcus* (1.98%, 1.72%), *Ruminococcaceae UCG-014* (1.89%, 1.65%), *Achromobacter* (0.82%, 2.51%), *Streptococcus* (1.24%, 1.88%), *Escherichia-Shigella* (1.10%, 1.18%), and *Anaerococcus* (1.24%, 0.79%) (Figure 6.6.B). Additionally, *Prevotellaceae UCG-001* was detected at high abundance levels in the HDM-naïve samples (1.21%, 0.17%), and *Lachnospiraceae UCG-001* (0.42%, 1.12%) and *Odoribacter* (0.42%, 1.08%) were detected at high abundance in the HDM-exposed samples (Figure 6.6.B).

The single high-quality V4 read detected in the negative control was classified as belonging to the *Gemella* genus of the Firmicutes phylum, and due to the singular nature of the read it was deemed highly unlikely that detection of bacterial DNA present in the negative control would impact the downstream analysis of the murine BAL microbiome.



**Figure 6.6: Composition of the bacterial gut microbiome in mice exposed to the HDM allergen compared to HDM-naïve mice.** Bacterial composition determined using QIIME FASTQ paired end analysis on sequenced 16S rRNA (V4 region) reads generated from BAL samples taken from HDM-naïve mice (n = 7; mean number of reads = 43,445), HDM-exposed mice (n = 7, mean number of reads = 44,606), and an experimental negative control (n = 1, number of reads = 1). Taxa with a relative abundance  $\geq 1\%$  were plotted, and low-abundant taxa ( $< 1.0\%$ ) were grouped and plotted as Taxa < 1% abundance. **(A)** Relative abundance of bacteria detected at the phylum level, **(B)** Relative abundance of bacteria detected at the genus level.

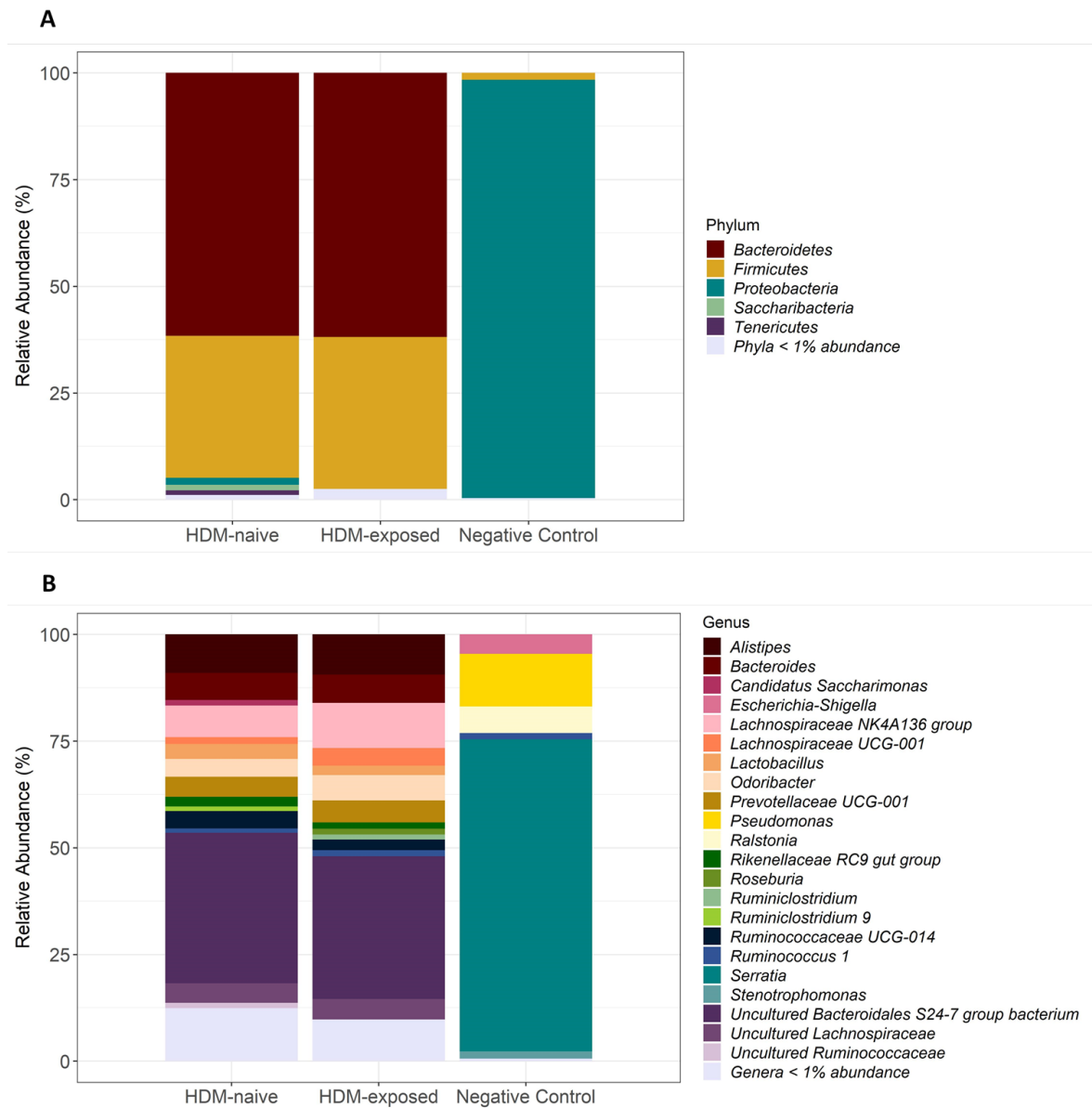
### 6.3.7. Taxonomic Classification of the OTUs detected in the Murine Faecal Samples

The OTUs detected in the murine faecal samples were classified into 12 bacterial phyla and 177 genera, the majority of which represented less than 1% of bacterial DNA amplified from the samples (9/12 phyla and 163/ 177 genera). At the phylum level the detected bacterial taxa were predominately Bacteroidetes (61.59% of HDM-naïve DNA, 61.89% of HDM-exposed DNA) and Firmicutes (33.27%, 35.59%) (Figure 6.7.A). A number of Proteobacteria (1.67%, 0.74%) were also detected (Figure 6.7.A).

Analysis at the genus level found that the faecal microbiome was dominated by *uncultured Bacteroidales S24-7 group bacterium*, which represented 34.35% of total bacterial DNA (35.22% in HDM-naïve samples and 33.48% in HDM-exposed samples) (Figure 6.7.B). Several other bacterial genera were detected at high abundance (defined as having a total relative abundance > 1.0%) in the murine faecal samples. These included *Alistipes* (9.04%, 9.46%), *Lachnospiraceae NK4A136 group* (7.40%, 10.63%), *Bacteroides* (6.33%, 6.57%), *Odoribacter* (4.20%, 5.96%), *Prevotellaceae UCG-001* (4.67%, 5.14%), *uncultured Lachnospiraceae* (4.62%, 4.80%), *Ruminococcaceae UCG-014* (4.08%, 2.46%), *Lachnospiraceae UCG-001* (1.60%, 4.11%), *Lactobacillus* (3.48%, 2.18%), *Rikenellaceae RC9 gut group* (2.26%, 1.47%), *Ruminococcus 1* (1.05%, 1.40%), *Roseburia* (1.00%, 1.39%), and *Ruminiclostridium* (0.91%, 1.21%) (Figure 6.8.B). Additionally, *Candidatus Saccharimonas*, *uncultured Ruminococcaceae* and *Ruminiclostridium 9* were present in the HDM-naïve samples at high abundant levels (1.32%, 1.22%, and 1.08%, respectively) (Figure 6.7.B).

Taxonomic assignment of the OTUs detected in the murine faeces experimental negative control found that the murine faeces experimental negative control OTUs could be classified into 5 phyla and 32 genera. At the phylum level the majority of detected bacterial

taxa belonged to the Proteobacteria phyla (98.01%), and to a lesser extent Firmicutes (1.62%) (Figure 6.7.A). At the genus level, 6 high-abundant bacterial genera were detected, these included *Serratia* (73.15%), *Pseudomonas* (12.35%), *Ralstonia* (6.21%), *Escherichia-Shigella* (4.55%), *Stenotrophomonas* (1.67%), and *Ruminococcus 1* (1.45%) (Figure 6.7.B). With the exception of *Ruminococcus 1*, the bacterial genera detected in the experimental control were detected at low levels in the murine faecal samples (less than 0.3% of total bacterial DNA generated from the faecal samples), and thus the presence of bacteria in the experimental control was unlikely to impact downstream analysis of the murine gut microbiome.

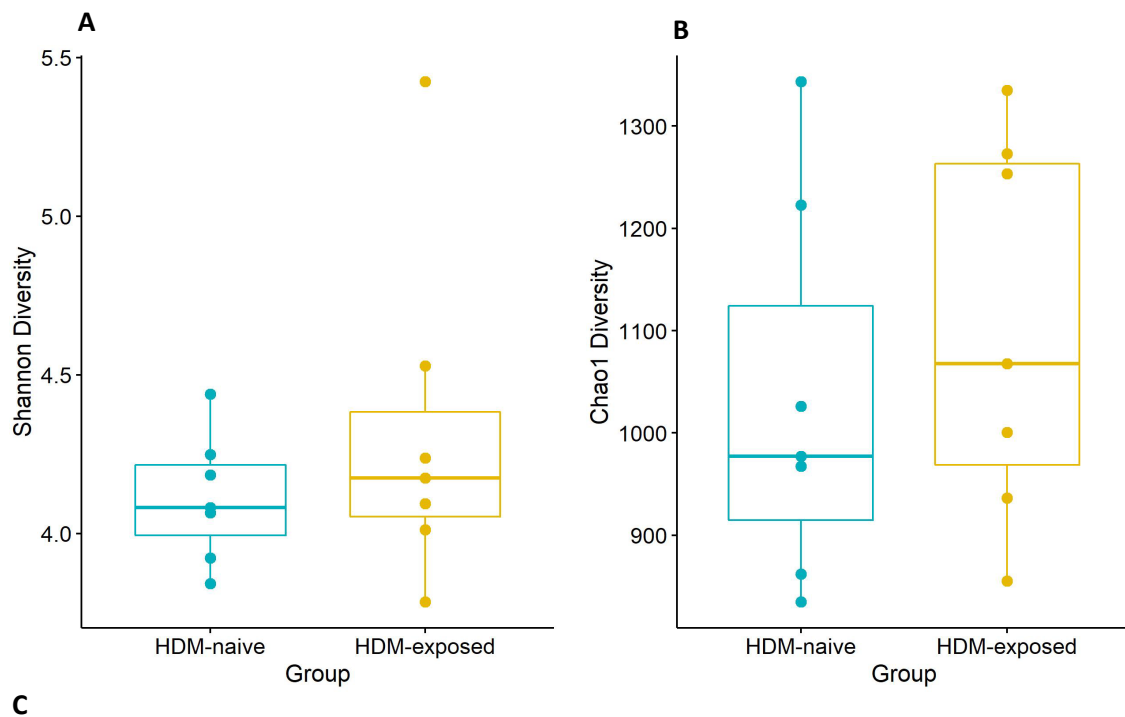


**Figure 6.7: Composition of the bacterial gut microbiome in mice exposed to the HDM allergen compared to HDM-naïve mice.** Bacterial composition determined using QIIME FASTQ paired end analysis on sequenced 16S rRNA (V4 region) samples generated from murine faecal samples taken from HDM-naïve mice (n = 7; mean number of reads = 97,158), HDM-exposed mice (n = 7; mean number of reads = 91,591), and an experimental negative control (n = 1; number of reads = 28,232). Taxa with a relative abundance  $\geq 1$  were plotted, and low-abundant taxa (< 1.0%) were grouped and plotted as Taxa < 1% abundance. **(A)** Relative abundance of bacteria detected at the phylum taxonomic level. **(B)** Relative abundance of bacteria detected at the genus taxonomic level.

#### 6.3.8. Changes in Bacterial Diversity in the Microbiome of mice exposed to the HDM allergen compared to HDM-naïve mice

To determine whether exposure to the HDM allergen had a significant impact on bacterial diversity in the murine airway and gut microbiome, alpha and beta diversity was measured

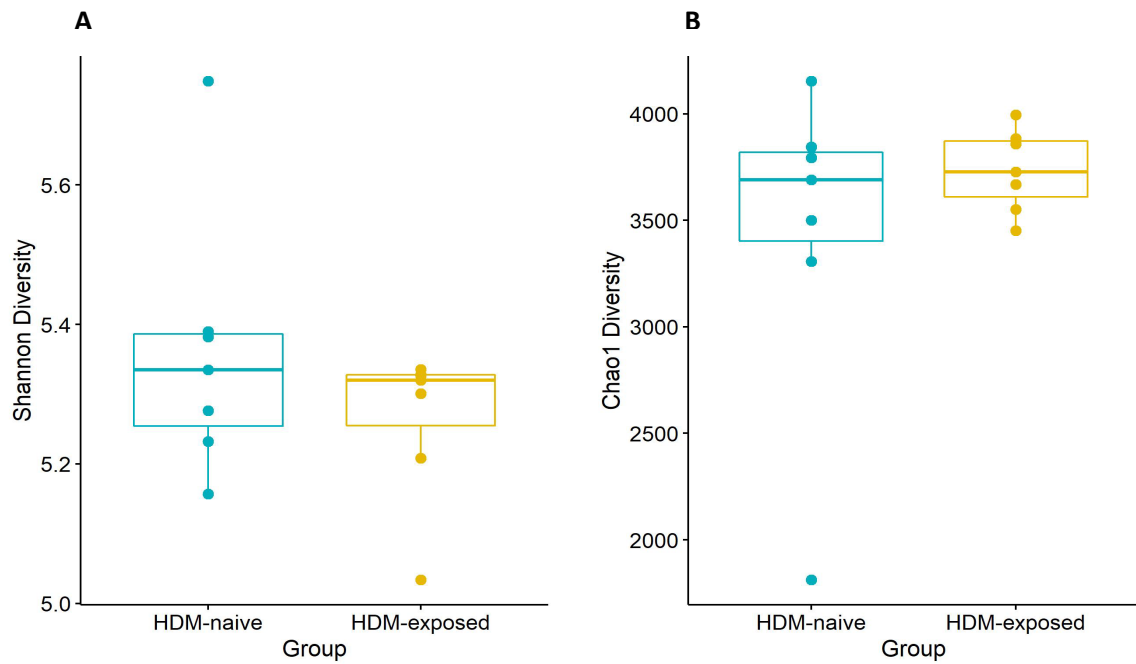
Comparison of alpha diversity of the BAL samples revealed that in mice exposed to HDM there was a slight increase in bacterial diversity when both Shannon and Chao1 diversity was measured (Figure 6.8). However, when statistical tests were applied the observed increase in bacterial diversity in the HDM-exposed mice compared to the HDM-naïve mice was found to be non-significant (Figure 6.8.C).



Alpha Diversity	HDM-naïve Mean (S.D)	HDM-exposed Mean (S.D)	P Value
Shannon	4.11 (0.19)	4.32 (0.50)	0.6200
Chao1	1033.35 (172.43)	1103.05 (171.60)	0.4962

**Figure 6.8: Comparison of alpha diversity in the airway microbiome of HDM-exposed mice compared to HDM-naïve mice.** Alpha diversity was measured using rarefied OTU tables generated from 16S rRNA sequencing data obtained from BAL samples collected from HDM-exposed mice (n = 7) and HDM-naïve mice (n = 7). Shannon diversity index scores were generated from OTU tables in order to measure the richness and evenness of bacterial taxa present in the BAL samples. Chao1 index scores were measured to determine the predicted number of bacterial taxa present in the BAL samples by extrapolating out the number of rare organisms that may not have been detected due to under-sampling. **(A)** Comparison of Shannon index scores generated from HDM-naïve BAL samples and HDM-exposed BAL samples. **(B)** Chao1 index scores generated from HDM-naïve BAL samples and HDM-exposed BAL samples. **(C)** Statistical analysis of alpha diversity detected in the murine airway microbiome of HDM-naïve mice and HDM-exposed mice.

Comparison of the alpha diversity detected in the faecal samples of mice exposed to the HDM allergen compared to the HDM naïve mice revealed no significant changes in alpha diversity (Figure 6.9). This indicated that pulmonary inflammation in the airways as a result of HDM exposure had no significant impact on the diversity of bacteria residing in the murine gut.



**C**

Alpha Diversity	HDM-naïve Mean (S.D)	HDM-exposed Mean (S.D)	P Value
Shannon	5.36 (0.18)	5.26 (0.10)	0.3829
Chao1	3443.26 (710.27)	3781.58 (179.02)	0.5350

**Figure 6.9: Comparison of alpha diversity in the gut microbiome of HDM-exposed mice compared to HDM-naïve mice.** Alpha diversity was measured using rarefied OTU tables generated from 16S rRNA sequencing data from murine faecal samples collected from HDM-naïve mice (n = 7) and HDM-exposed mice (n = 7). Shannon diversity index scores were generated from the OTU tables in order to measure the richness and evenness of bacterial taxa present in the sample. Chao1 index scores were measured to determine the predicted number of bacterial taxa present in the samples by extrapolating out the number of rare organisms that may not have been detected due to under-sampling. **(A)** Comparison of Shannon index scores generated from HDM-naïve faecal samples and HDM-exposed faecal samples. **(B)** Chao1 index scores generated from HDM-naïve faecal samples and

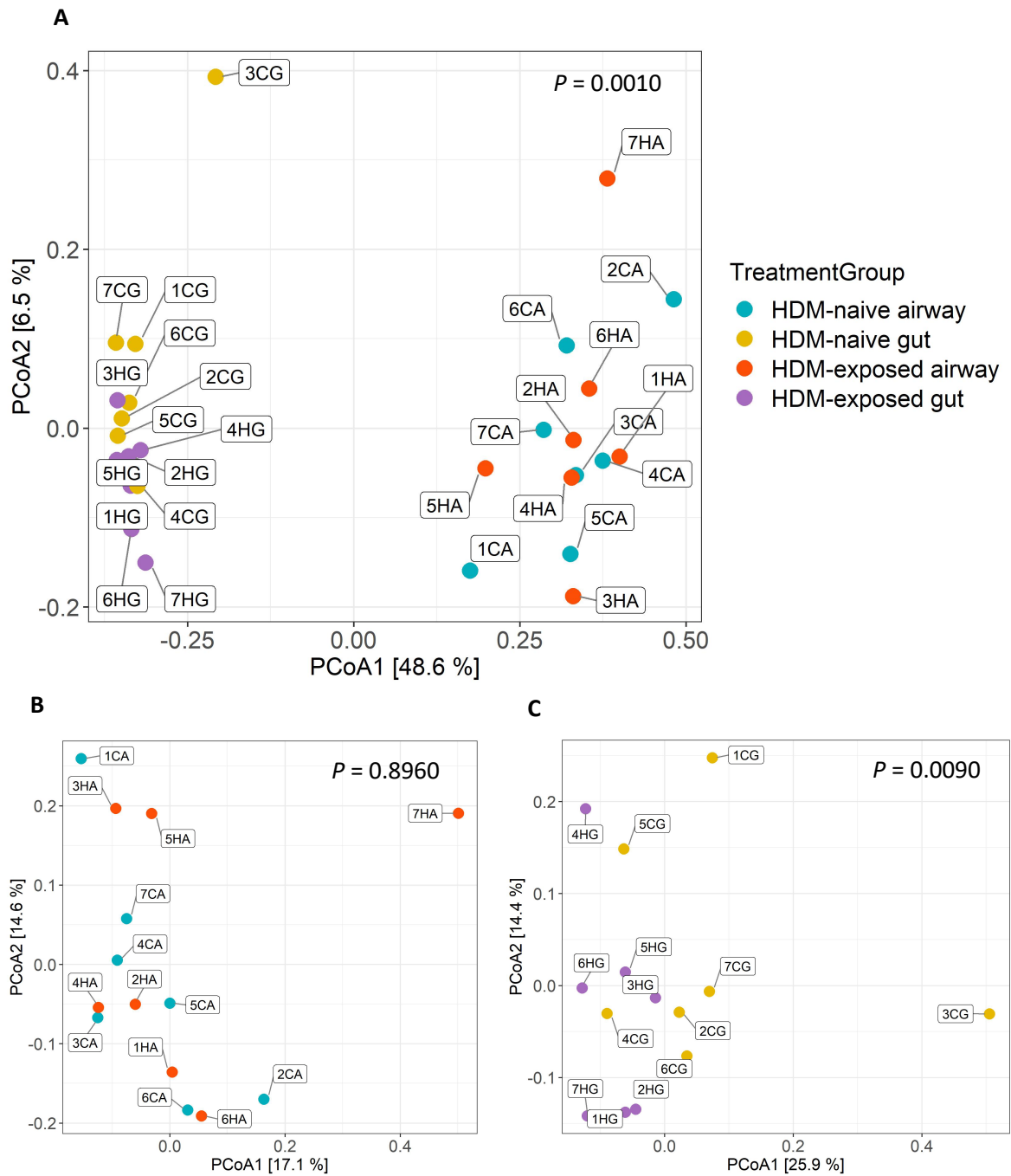


HDM-exposed faecal samples. (C) Statistical analysis of alpha diversity detected in the murine gut microbiome of HDM-naïve mice and HDM-exposed mice.

Beta diversity of the microbial populations detected in the murine BAL and faecal samples was measured to determine how similar the airway and gut microbiomes were to one another. Beta diversity was determined by measuring Bray-Curtis dissimilarity using the 16S rRNA sequencing data generated from the murine BAL and faecal samples. PCoA analysis was then performed to determine how similar the microbial composition of the samples was to one another, and PERMANOVA analysis was carried out to determine whether the observed differences in beta diversity were statistically significant.

Comparison of the murine airway and gut microbiome found that the gut and airway environments have distinct bacterial populations from one another (Figure 6.10). Analysis of the two environments found that the level of inter-variation (variation between samples from the same environment) within the BAL samples was increased compared to the level of inter-variation observed within the faecal samples (Figure 6.10).

Statistical analysis of beta diversity detected in samples taken from the murine airways (BAL samples) and gastrointestinal tract (faecal samples) revealed that body habitat of the microbiome significantly influenced microbial diversity ( $P$  value = 0.0010, *PERMANOVA*). Statistical analysis also revealed that exposure to the HDM allergen had a significant impact on the overall beta diversity of the bacterial populations detected in the murine airways and gastrointestinal tract ( $P$  value = 0.004, *PERMANOVA*). This was primarily due to significant differences in beta diversity of the microbial populations detected in the gut microbiome of mice exposed to the HDM allergen ( $P$  value = 0.0090, *PERMANOVA*) as opposed to changes in the diversity of the microbial populations detected in the airways of the HDM-exposed mice ( $P$  value = 0.896, *PERMANOVA*)(Figure 6.10).

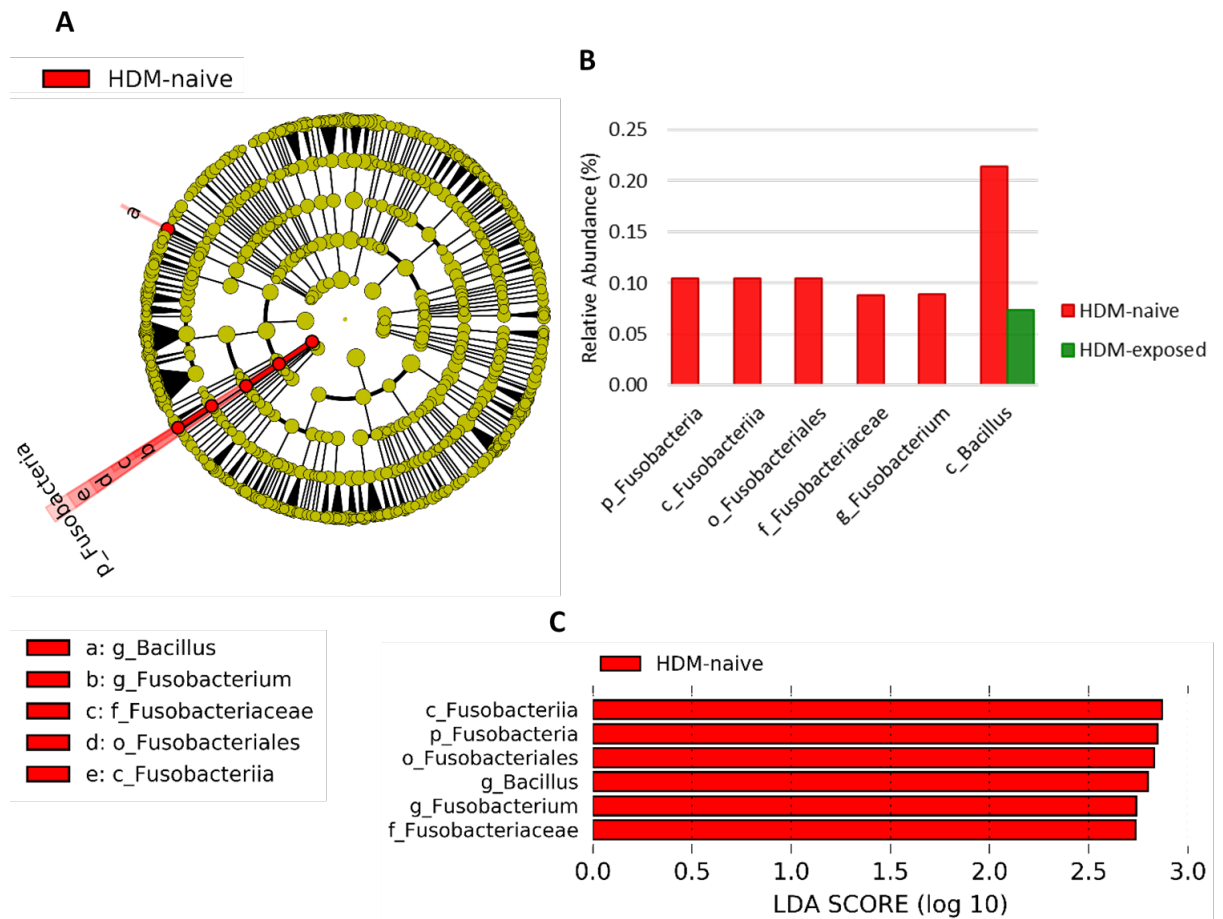


**Figure 6.10: Comparison of beta diversity of the bacterial populations detected in the murine airway and gut microbiomes.** Beta diversity of the bacterial populations detected in murine BAL samples ( $n = 14$ ) and murine faecal samples ( $n = 14$ ) was determined by measuring quantitative phylogenetic distances between each of the murine samples. This was achieved by measuring Bray Curtis dissimilarity from a normalised OTU table generated from the 16S rRNA sequencing data obtained from the murine samples. PCoA analysis was performed, and statistically significant differences in beta diversity was assessed using PERMANOVA. **(A)** Comparison of beta diversity present in the bacterial populations detected in the murine BAL and faecal samples revealed that the murine airway and gastrointestinal tract microbiomes were significantly different ( $P$  value = 0.0010,

PERMANOVA). Comparison of the murine BAL samples revealed that HDM exposure did not influence composition of the airway microbiome ( $P$  value = 0.8960, PERMANOVA) (B), whilst comparison of the murine faecal samples found that HDM exposure significantly altered composition of the murine gut microbiome ( $P$  value = 0.0080, PERMANOVA) (C).

#### 6.3.9. Significant changes to Bacterial Relative Abundance in the Murine Airway Microbiome

Analysis of the bacterial taxa detected in the murine BAL samples detected a number of low-abundant bacterial taxa (relative abundance < 0.5%) that were significantly decreased in the airways of mice exposed to the HDM allergen. These changes included a complete loss of members of the Fusobacteria phylum in the HDM-exposed mice, resulting in a statistically significant reduction in bacteria belonging to the Fusobacteriia class, Fusobacteriales order, *Fusobacteriaceae* family, and *Fusobacterium* genus (Figure 6.11), and a significant reduction in the *Bacillus* genus of the Firmicutes phylum in the airways of HDM-exposed mice (Figure 6.11).



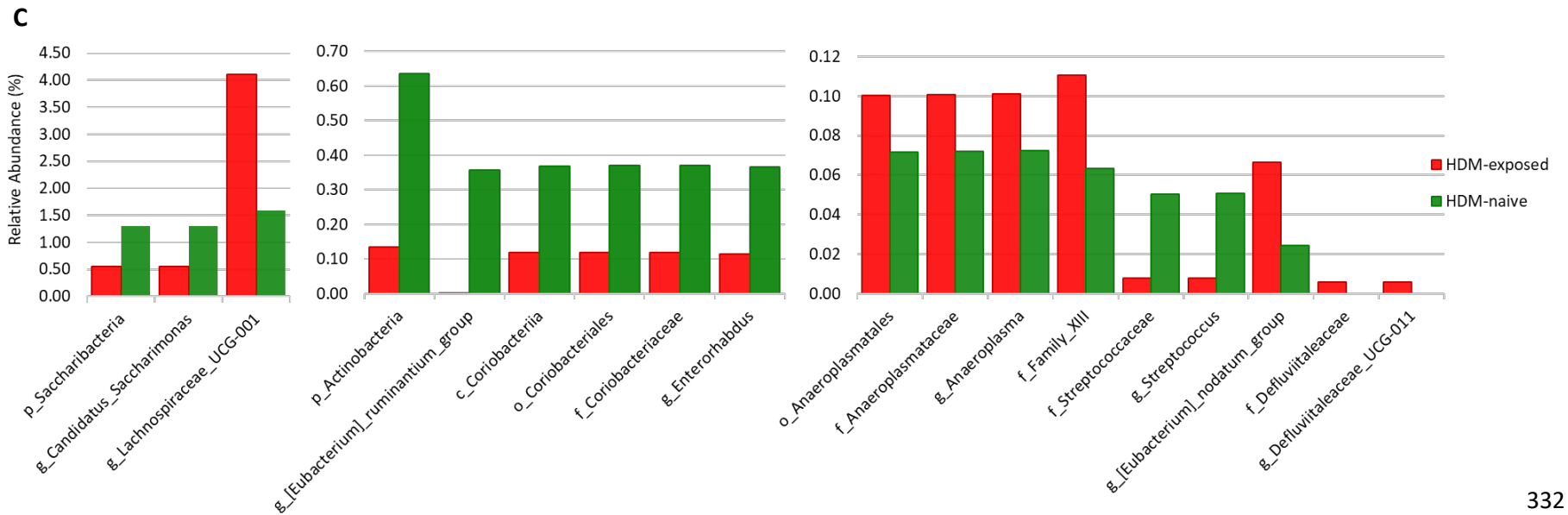
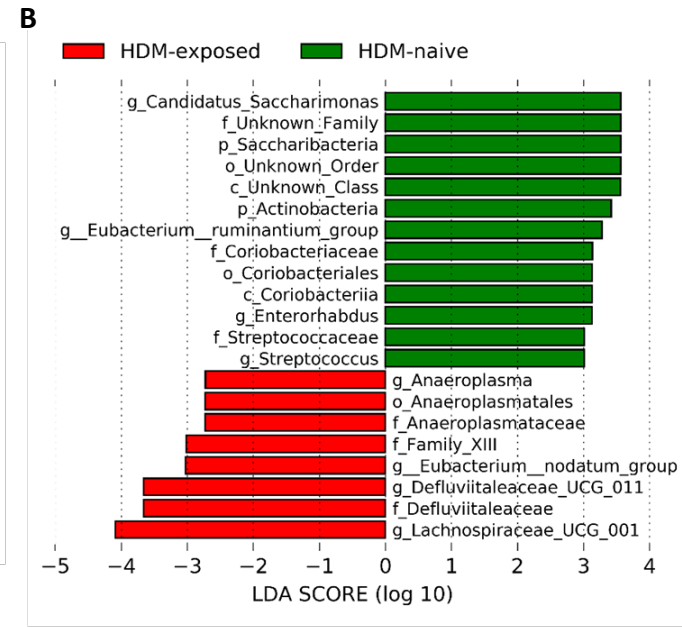
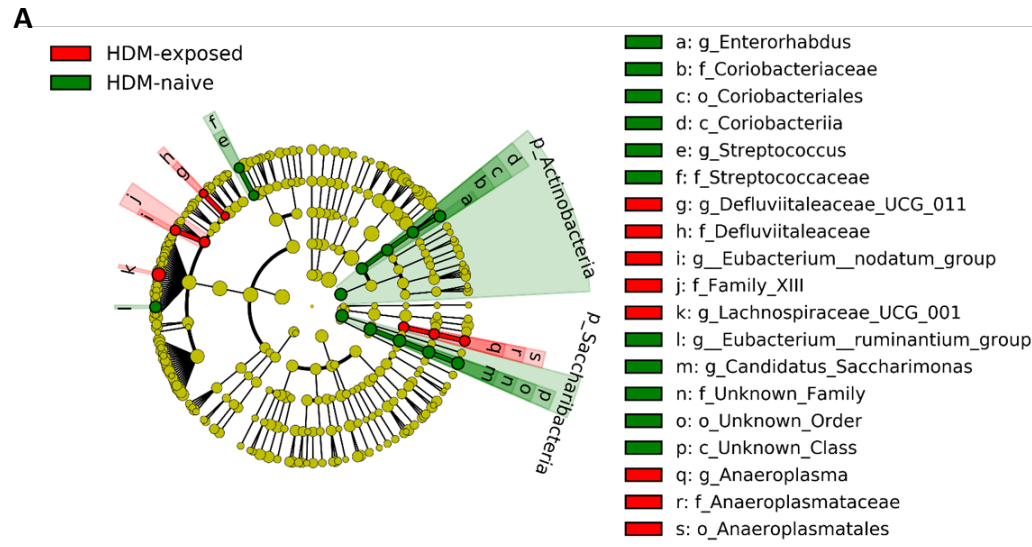
**Figure 6.11: Significant changes in bacterial taxa relative abundance in the murine airway microbiome of mice exposed to the HDM allergen compared to HDM naïve mice.** LEfSe analysis was performed on the bacterial relative abundance data to determine the presence of differentially abundant bacterial taxa in the HDM-exposed mice ( $n = 7$ ) compared to the HDM-naïve mice ( $n = 7$ ) (defined as having a LDA effect size  $> 2.0$  and a  $P$  value  $< 0.05$ ). **(A)** A taxonomic cladogram highlighting the statistically and biologically consistent differences between the HDM-exposed airway microbiome compared to the HDM-naïve microbiome. Differences are presented in the colour of the most abundant sample group (red represents taxa significantly enriched in the HDM-naïve mice and yellow representing non-significant taxa). The circle diameter is proportional to the taxon's abundance in the murine airway microbiome. **(B)** Relative abundance of the differentially abundant bacterial taxa. **(C)** Histogram of the LDA scores generated for the differentially abundant taxa present in the HDM-exposed mice compared to the HDM-naïve mice.

### 6.3.10. Significant Changes to Bacterial Relative Abundance in the Murine Gut Microbiome

Analysis of bacterial composition in the murine gut microbiome using LEfSe analysis found that 18 bacterial taxa were present in significantly altered levels in the HDM-exposed mice compared to the HDM-naïve mice (as defined by a log<sub>10</sub> LDA score > 2.0 and a *P* value < 0.05) (Figure 6.12). In total 13 taxa were significantly decreased in the HDM-exposed mice compared to the HDM-naïve mice, and 5 taxa were significantly increased in the HDM-exposed mice compared to the HDM-naïve mice (Figure 6.12). Bacterial taxa identified as being differentially abundant in the HDM-exposed mice were predominately low-abundant taxa (relative abundance < 0.05%), with the exception being *Lachnospiraceae*, which had a relative abundance of 1.59% in the HDM-naïve mice and a relative abundance of 4.10% in the HDM-exposed mice (Figure 6.12.C). Bacterial taxa significantly increased in the HDM-exposed mice were predominately members of the Clostridiales order (*Defluviitaleaceae*, [*Eubacterium*] *nodatum* group, Family XIII, and *Defluviiraleaceae*), and also included the *Lachnospiraceae* UCG-001 genus. In contrast, bacterial taxa significantly decreased in the HDM-exposed mice were predominately members of the Actinobacteria and Saccharibacteria phylum, and the *Streptococcaceae* family (Figure 6.12).

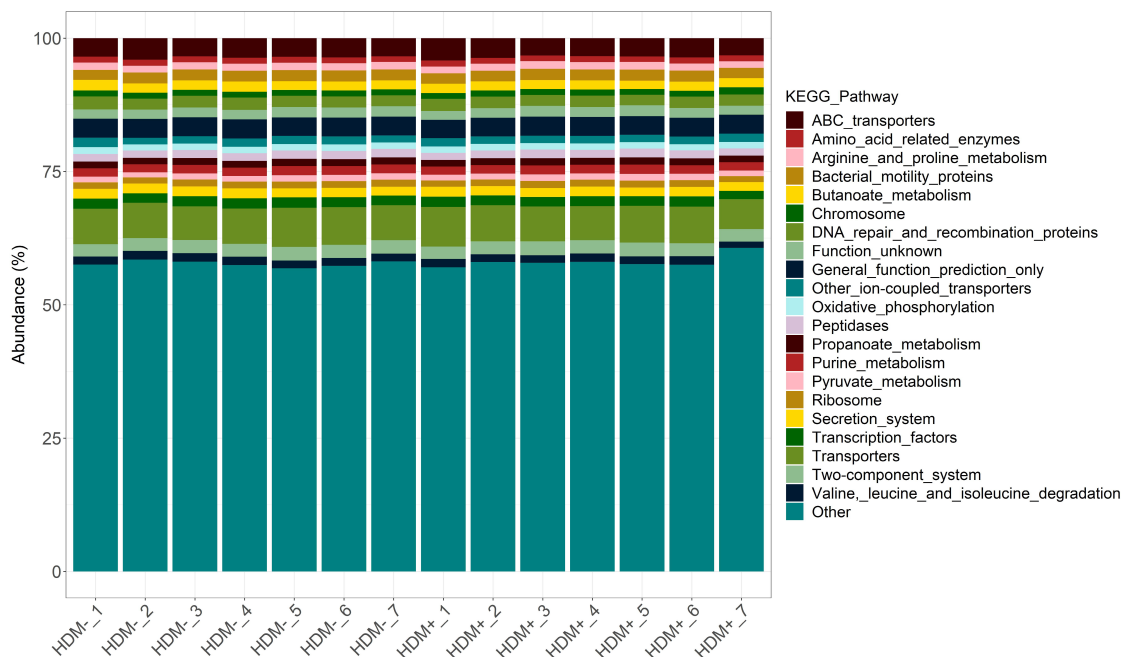
Of particular interest was the expansion of the highly abundant *Lachnospiraceae* UCG-001 genus, and the detection of the *Defluviitaleaceae* family and *Defluviitaleaceae*\_UCG-011 genus, which were absent in the HDM-naïve mice (Figure 6.12).

**Figure 6.12: Significant changes in bacterial taxa relative abundance in the gut microbiome of mice exposed to the HDM allergen compared to HDM naïve mice.** LEfSe analysis was performed on the bacterial relative abundance data to determine the presence of differentially abundant bacterial taxa in the HDM-exposed mice ( $n = 7$ ) compared to the HDM-naïve mice ( $n = 7$ ) (defined as having a LDA effect size  $> 2.0$  and a  $P$  value  $< 0.05$ ). **(A)** A taxonomic cladogram highlighting the statistically and biologically consistent differences between the HDM-exposed gut microbiome compared to the HDM-naïve gut microbiome. Differences are presented in the colour of the most abundant sample group (red represents taxa significantly enriched in the HDM-naïve mice, green represents taxa significantly enriched in the HDM-exposed mice, and yellow representing non-significant taxa). The circle diameter is proportional to the taxon's abundance in the murine gut microbiome. **(B)** Histogram of the LDA scores generated for the differentially abundant taxa present in the HDM-exposed mice compared to the HDM-naïve mice. **(C)** Relative abundance of the differentially abundant bacterial taxa.



### 6.3.11. Prediction of Microbial Activity of the Murine Airway Microbiome

PICRUSt analysis detected a total of 284 level 3 KEGG pathways encoded by the bacterial members of the murine airway microbiome. The majority of detected pathways had a total predicted abundance of less than 1% in the BAL samples (262/ 284 KEGG pathways), and included 19 *Cellular processes*, 16 *Environmental information processing*, 27 *Genetic information processing*, 31 *Human diseases*, 142 *Metabolism*, 22 *Organismal systems*, and 27 *Unclassified* pathways. Microbial functions present at high levels in the airway microbiome (as determined by a predicted KEGG pathway abundance greater than 1%) are shown below (Figure 6.13). Comparison on the detected KEGG pathways at levels 1 – 3 using LEfSe analysis revealed no significant changes in microbial activity in the airways of the mice exposed to the HDM allergen compared to HDM-naïve mice (data not shown).



**Figure 6.13: Microbial functions of the murine airway microbiome.** PICRUSt analysis was used to predict the functional capacity of the V4 16S rRNA metagenome present in BAL samples from HDM-naïve mice (HDM<sup>-</sup> mice, n = 7) and HDM-exposed mice (HDM<sup>+</sup> mice, n = 7). High activity level 3 KEGG pathways (as determined by a predicted total abundance greater than 1%) are plotted and KEGG pathways with an abundance less than 1% are grouped together and plotted as other.



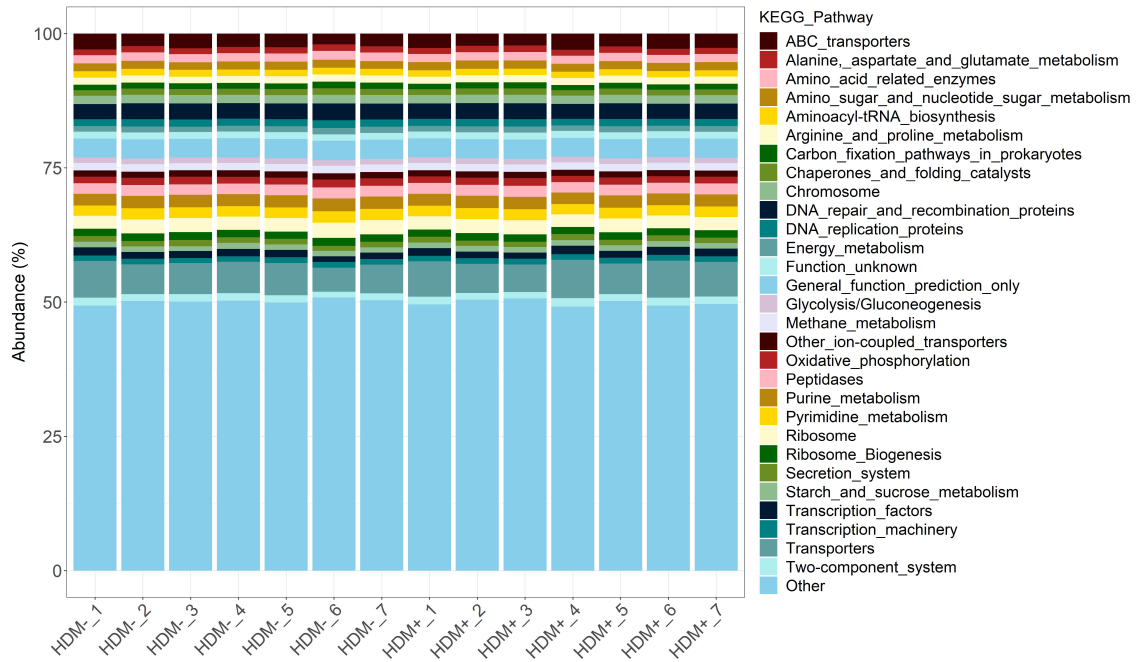
### 6.3.12. Prediction of Microbial Activity of the Murine Gut Microbiome

PICRUSt analysis of the V4 16S rRNA sequencing data generated from the murine faecal samples revealed that the bacterial members of the murine gut microbiome encoded a predicted 268 level 3 KEGG pathways. The majority of these pathways had a total abundance of less than 1%, and included 11 *Cellular processes*, 12 *Environmental information processing*, 26 *Genetic information processing*, 31 *Human diseases*, 141 *Metabolism*, 20 *Organismal systems*, and 27 *Unclassified* pathways.

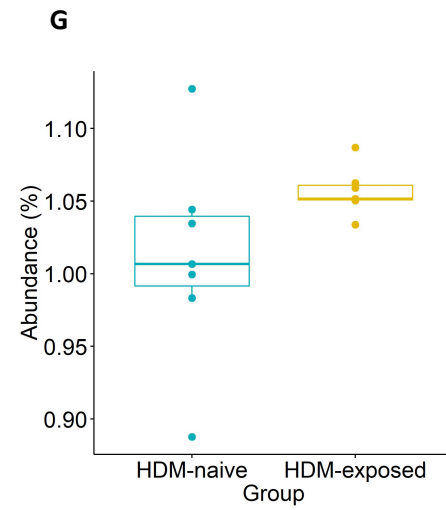
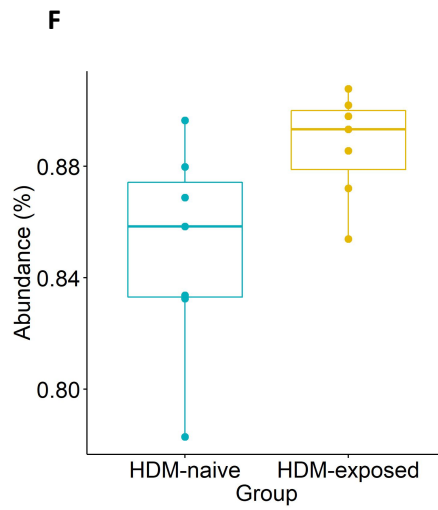
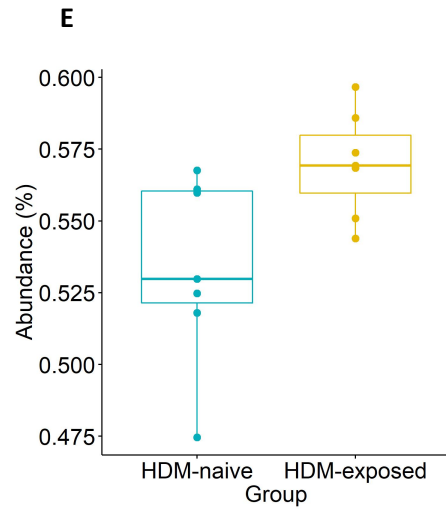
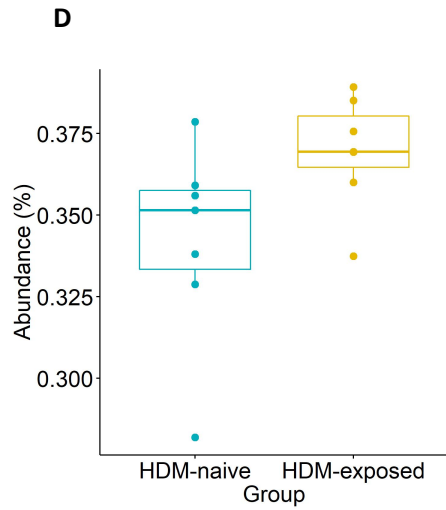
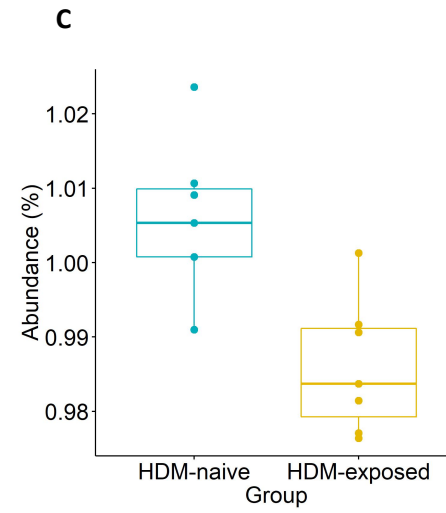
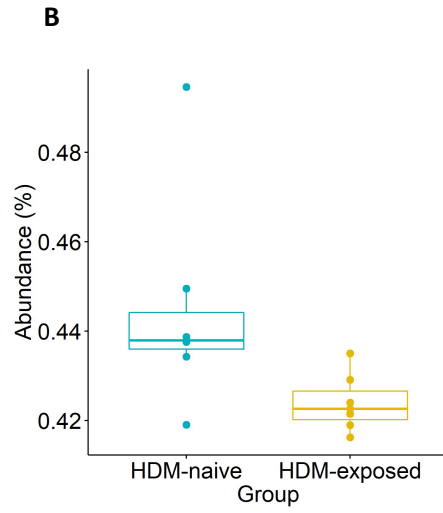
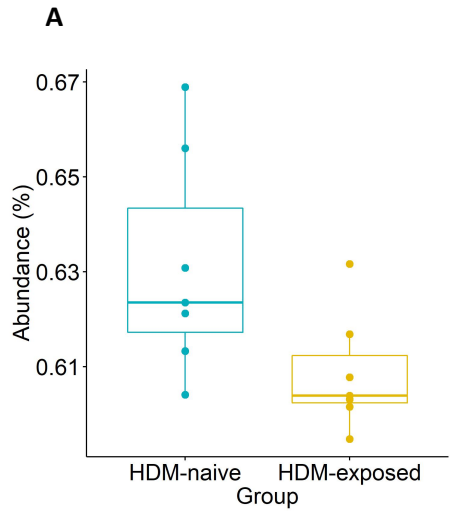
Microbial functions predicted to be present at high levels in the gut microbiome (as determined by a predicted KEGG pathway abundance greater than 1%) are shown below (Figure 6.14). Comparison on the detected KEGG pathways at levels 1 – 3 using LEfSe analysis revealed that two of the 40 detected level 2 KEGG functional categories were significantly altered in the HDM-exposed mice compared to the HDM-naïve mice. These included increased *Enzyme families* (2.30% v 2.28%,  $P$  value = 0.0253, LDA effect size = 2.42) and decreased *Unclassified Genetic Information processing* (2.48% v 2.52%,  $P$  value = 0.0040, LDA effect size = 2.58).

With regards to the 268 level 3 detected KEGG pathways, 28 displayed significant differential abundance, as determined by a  $P$  value of less than 0.05 (see Supplementary Materials, Table S17). Of the 28 pathways, 7 were deemed to be of biological significance, as determined by an LDA effect size of 2.0 or greater. These included 4 pathways that were significantly increased in the HDM-exposed mice [Starch and sucrose metabolism (1.06% v 1.01%,  $P$  value = 0.0476), Galactose metabolism (0.89% v 0.85%,  $P$  value = 0.0350), Pentose and glucuronate interconversions (0.57% v 0.53%,  $P$  value = 0.0181), and Sphingolipid metabolism (0.37% v 0.34%,  $P$  value = 0.0476)] and 3 pathways that were significantly decreased in the HDM-exposed mice [Recombination and repair proteins (0.61% v 0.63%,

*P* value = 0.0350), Propanoate metabolism (0.42% v 0.44%, *P* value = 0.0181), and Pyruvate metabolism (0.99% v 1.01%, *P* value = 0.0088)] (Figure 6.15 A - G).



**Figure 6.14: Microbial functions of the murine gut microbiome.** PICRUSt analysis was used to predict the functional capacity of the V4 16S rRNA metagenome present in faecal samples from HDM-naïve mice (HDM<sup>-</sup> mice, n = 7) and HDM-exposed mice (HDM<sup>+</sup> mice, n = 7). High activity level 3 KEGG pathways (as determined by a predicted total abundance greater than 1%) are plotted and KEGG pathways with an abundance less than 1% are grouped together and plotted as other.



**Figure 6.15: Comparison of microbial activity in the gut microbiome of mice exposed to the HDM allergen compared to HDM naïve mice.** PICRUSt was used to predict functional potential of the gut microbiome in HDM-naïve mice (n = 7) and HDM-exposed mice (n = 7) using V4 16S rRNA sequencing data. LEfSe analysis was used to identify differential bacterial functions present in the HDM-exposed gut microbiome compared to the HDM-naïve gut microbiota. Replication, recombination and repair proteins (**A**), Propanoate metabolism (**B**), and Pyruvate metabolism (**C**), KEGG pathways were observed to be significantly decreased in the HDM-exposed gut microbiota compared to the HDM-naïve gut microbiota. Starch and sugar metabolism (**D**), Galactose metabolism (**E**), Pentose and glucuronate interconversions (**F**), and Sphingolipid metabolism (**G**), were observed to be significantly increased in the gut microbiome of HDM-exposed mice compared to the HDM-naïve mice. Significantly altered activity is defined as the KEGG pathway having a *P* value < 0.05 and an LDA effect size score > 2.0.

## 6.4. Discussion

### 6.4.1. Atopic HDM Sensitisation and Composition of the Murine Microbiome

It has been firmly established that there are significant changes in the gut and airway microbiomes of asthmatic individuals compared to non-asthmatics<sup>242, 254, 263,255–262</sup>. These changes are frequently detected during the microbiota developmental stage of early childhood, and it is thought that reduced exposure to environmental microorganisms during these critical developmental years is having an adverse impact on the maturation of the immune system, thus increasing the risk of atopic sensitisation and childhood asthma.

Atopic asthma is frequently associated with sensitisation to the common HDM allergen<sup>713–717</sup>. Exposure to the HDM allergen in HDM-sensitive individuals results in acute allergic responses within the airways, which are thought to exacerbate asthma.

This study aimed to determine whether pulmonary exposure to the HDM allergen, and the subsequent inflammatory responses associated with HDM-sensitisation, can alter the bacterial composition of the microbiome.

Investigation into the effect of pulmonary HDM-exposure on the microbiome was achieved using a murine experimental model of HDM-sensitisation, whereby female BALB/c mice were exposed and sensitised to the HDM allergen using 9 intranasal instillations of the allergen. Plasma, BAL, and faecal samples were taken, and the circulatory, airway, and gut microbiome was determined using 16S rRNA sequencing techniques. A circulatory microbiome went undetected in the mice, but the murine airway and gut microbiomes were characterised, and significant changes were detected in both microbiomes as a result of HDM exposure.

#### 6.4.2. Characterisation of the Murine Circulatory Microbiome

Analysis of the murine plasma samples using PCR amplification of the V4 region of the bacterial 16S rRNA gene failed to detect microbial DNA in the samples. This was not unexpected as murine blood samples have been previously demonstrated to degrade more rapidly than human blood samples <sup>718</sup>. A study carried out Makley *et al* (2010) found that murine packed red blood cells exhibited increased lactate levels, more severe acidosis, and haemolysed earlier and more rapidly, compared to human packed red blood cells <sup>718</sup>.

Moreover, previous investigations have also shown that foreign DNA is rapidly cleared from the murine circulatory system. Kawabata and colleagues, for example, demonstrated that circular DNA intravenously injected into mice is swiftly degraded, with a half-life of approximately 10 minutes <sup>719</sup>. Furthermore, in addition to efficient degradation mechanisms, the murine circulation system has also been observed to remove the majority of free DNA from circulation and into the liver within 30 minutes of intravenous administration <sup>720</sup>.

A study by Sze *et al* (2014), did however, successfully characterise the murine circulatory microbiome by sequencing the V1-V3 hypervariable region of the bacterial 16S rRNA gene from whole blood samples <sup>341</sup>. As whole blood has been demonstrated to contain more bacterial DNA than plasma samples <sup>327</sup>, it is likely that the success of the study was partly due to the use of whole blood rather than blood fractions. It would, therefore, be beneficial to try repeating this study using whole blood samples and plasma samples taken from mice exposed to the HDM allergen to determine if the lack of successful amplification in this study was due to the use of plasma samples rather than whole blood.

#### 6.4.3. Characterisation of the Murine Airway and Gut Microbiomes

The murine airway microbiome was found to be dominated by four key phyla, Proteobacteria, Firmicutes, Bacteroidetes, and Actinobacteria; whilst the murine gut microbiome was predominately composed of two key phyla; Bacteroidetes and Firmicutes. These results are consistent with previous studies that characterised the murine airway <sup>721,722</sup> and gut microbiomes <sup>723,724</sup>, and suggest that regardless of the murine strain and animal housing facilities, composition of the murine airway and gut microbiomes at the phylum level is relatively consistent. Comparison of the two microbiomes revealed that the airway and gut environments are composed of distinctly different microbial populations, as is evident in other higher organisms <sup>188,725–728</sup>.

At the phylum level the murine airway and gut microbiome shared similar microbial profiles to those previously observed in the human airway microbiome <sup>255,256, 277,278,281</sup> and gut microbiome <sup>192,729–732</sup>. However, at the lower taxonomic levels, such as the genus, the murine airway and gut microbiome bacterial profiles displayed reduced similarity to the human airway and gut microbiome. These results reflect previous investigations into the murine and human microbiome, which demonstrated that at the high taxonomic levels human and mice have similar bacterial profiles within the microbiome, whilst at the lower taxonomic levels there is reduced similarity in bacterial profiles <sup>730,733</sup>. Ley *et al* (2005), for instance, found that examination of the bacterial genera revealed that 85% of bacterial genera detected in the murine gut microbiome are not observed in the human gut microbiome <sup>730</sup>. Differences in microbial communities at the lower taxonomic levels are not unexpected given that laboratory mice are typically housed in clean facilities, are fed a standardised diet of chow, and differ from humans anatomically and genetically <sup>733</sup>.

#### 6.4.4. HDM-induced changes to the Bacterial Composition of the Murine Microbiome

Comparison of the HDM-exposed and HDM-naïve airway and gut microbiomes found that bacterial beta diversity was significantly altered in the gut microbiome of mice exposed to the HDM allergen compared to HDM-naïve mice. Furthermore, in both the gut and airway microbiome there were a number of significant changes in the relative abundance of bacterial populations detected in the HDM-exposed mice compared to the HDM-naïve mice. These included a complete loss of *Fusobacteria* members in the airways, a significant reduction of *Bacillus spp.* in the airways, introduction of novel *Defluviitaleaceae UCG-001 spp.* into the gut, a significant increase in *Lachnospiraceae UCG-001*, *Clostridiales Family XIII*, and *Eubacterium nodatum group* in the gut, a significant reduction in *Enterorhabdus spp.*, *Candidatus Saccharimonas*, and *Streptococcus spp.* in the gut, and a complete loss of *Eubacterium ruminantium spp.* in the gut of mice exposed to the allergen.

The majority of bacterial taxa identified as having significantly altered abundance in the HDM-exposed murine microbiome have been previously identified in the murine gut and airway microbiomes<sup>235, 341, 734–743, 384, 744, 385–387, 520, 629,721,722</sup>. *Fusobacterium spp.* and *Eubacterium ruminantium spp.*, were the exceptions, as these bacteria are more commonly associated with the human microbiome<sup>745–749</sup>.

A number of the identified bacterial taxa been previously associated with atopic disease. *Eubacterium nodatum group spp.* and *Lachnospiraceae spp.*, for example, have been observed to be increased in the gut of mice with induced atopic asthma<sup>385</sup>, whilst *Candidatus Saccharibacteria*, *Streptococcus*, and *Bacillus spp.* have been observed to be protective against allergen sensitisation and atopic disease<sup>385,750,751</sup>.



Furthermore, several of identified bacterial taxa were also detected at significantly differential levels in the human circulatory microbiome in the atopic subjects described in Chapter 5. The *Clostridiales XI* family displayed overall increased abundance in the human atopic subjects, whilst the *Clostridiales XIII* family was observed to be significantly increased in abundance in the gut microbiome of the HDM-exposed mice. Fusobacteria were significantly depleted in the airways of HDM-exposed mice and significantly enriched in the circulatory microbiome of human allergic rhinitis subjects. Furthermore, the *Lachnospiraceae NK4A131* group was found to be significantly decreased in the circulatory microbiome of the allergic rhinitis subjects, and *Lachnospiraceae UCG-001* were increased in the gut microbiome of mice exposed to the HDM allergen.

Intriguingly, all three bacterial taxa detected as displaying significant differential abundance in the circulatory microbiome of human atopic subjects and in the airways and gut of mice exposed to the HDM allergen (*Fusobacteria*, *Clostridiales*, and *Lachnospiraceae*) have been previously associated with atopic disease. This suggests that short-term HDM sensitivity in mice had similar effects on the murine microbiome to that observed in chronic atopic disease in humans, and that the inflammatory responses involved in allergen sensitisation directly alter the microbiome composition. This is likely to result in the loss of beneficial members of the microbiome, and subsequently may lead to the expansion of bacterial taxa harmful to human health.

#### 6.4.5. Loss of beneficial bacterial Taxa as a result of HDM Exposure

In the HDM-exposed murine microbiome, a number of bacterial taxa detected at significantly reduced abundance have been previously associated with protection against

asthma. This suggested that HDM sensitisation in the mice resulted in a loss of bacterial taxa protective against atopic disease.

Protective microbes significantly reduced in the HDM-exposed mice included *Bacillus*, which were significantly reduced in the HDM-exposed murine airways, and *Streptococcus* and *Eubacterium ruminantium group spp.*, which were significantly reduced HDM-exposed murine gut.

Intranasal administration of *Bacillus licheniformis* spores prior to OVA allergen sensitisation and challenge in mice by Vogel *et al* (2008), for example, was demonstrated to decrease eosinophilia and mucous-producing goblet cells in mice sensitised and challenged with the OVA allergen. Moreover, *in vitro* work by the authors revealed that *B. licheniformis* bacteria activated dendritic cells, resulting in a Th1 cytokine expression profile characterised by increased IL-12 production and the upregulation of IFN $\gamma$ <sup>751</sup>. Th1 polarisation was also observed in a *in vivo* model of spore exposure, whereby spore administration resulted in neutrophil infiltration and Th1-inflammation<sup>751</sup>.

Loss of IL-12 signalling has been demonstrated to result in increased Th2 polarisation. Decreased levels of *Bacillus* in the murine airways, therefore, is likely to influence the Th1/Th2 ratio, resulting in increased Th2 polarisation and decreased Th1 polarisation. This would actively contribute towards Th2-driven pulmonary inflammation induced by the HDM allergen by enhancing the number of Th2 cells present in the murine airways.

Furthermore, the ability of *B. licheniformis* to induce Th1 polarisation suggests that exposure to the bacterium would be particularly important during the early years of immune development, when the infant immune system shifts towards a Th1 polarised system, and colonisation by *Bacillus* members is likely to protect against allergen sensitisation and development of atopic disease.

In support of this interpretation is the observation that *B. licheniformis* is commonly found in animal sheds and mattress dust<sup>751</sup>. Exposure to livestock has been demonstrated to be protective against asthma development in young children<sup>248,250</sup>. It is likely that the negative association between farm exposure and asthma development may partly be due to increased *Bacillus* colonisation in young children that have increased contact with livestock. Similarly, exposure to *Streptococcus pneumoniae* (a member of the *Streptococcus* genus that was decreased in the gut microbiome of HDM-exposed mice) in mice has been shown to reduce Th2 cytokine production, goblet cell hyperplasia, eosinophilia, antibody responses, airway hyperresponsiveness, and IgE production following allergen sensitisation and challenge<sup>750,752,753</sup>.

The effects of *S. pneumoniae* on allergic disease appears to be dependent on timing of exposure to the bacterium. Preston and colleagues, for instance, demonstrated that when mice were treated with *S. pneumoniae* before OVA sensitisation and challenge, the bacterium induced a significant increase in the production of the Th1 cytokine IFN $\gamma$ . However, when the bacterium was administered during or after OVA sensitisation and challenge, the mice exhibited a significant reduction in IL-5 and IL-13 production<sup>752</sup>. This suggests that *S. pneumoniae* protects against allergen sensitisation and attenuates allergic disease when administered to allergen-sensitive individuals. Subsequent work by Preston and colleagues demonstrated that the attenuating effects of *S. pneumoniae* on atopic asthma in mice was a result of the bacteria's ability to induce Treg expansion<sup>750</sup>. However, it should be noted that 39% and 91% of class I and II bacteriocins in the HMP metagenomic dataset have been found to match *Streptococcus* genomes<sup>754</sup>. This suggests that *Streptococcus* species encode the majority of bacteriocins in the human microbiome, and as bacteriocins kill or inhibit the growth of other bacteria<sup>755,756</sup>, it is likely that changes in

*Streptococcus* abundance would have a significant impact on microbiome composition and subsequent effects on the immune system.

In this study, *Streptococcus* was decreased following allergen sensitisation and challenge, and thus the research carried out by Preston *et al* suggest that this would actively contribute towards to HDM-induced pulmonary inflammation by increasing IL-5 and IL-13 production. Moreover, it is predicted that reduced *Streptococcus* in the murine gut would lead to reduced levels of bacteriocins in the gut, subsequently resulting in expansion of other bacterial taxa.

In humans, *Streptococcus spp.* have traditionally been associated with respiratory infections, but increasingly the bacterial genus is being recognised as a member of the human gut microbiome <sup>757</sup>, skin microbiome <sup>758</sup>, and oral microbiome <sup>726</sup>. Decreased abundance of *Streptococcus* has been observed in the gut microbiome of asthmatic subjects <sup>274</sup>. Furthermore, *Streptococcal* vaccination of asthmatic children has been demonstrated to reduce the incidence of acute asthma exacerbations <sup>759</sup>, whilst *S. pneumoniae* vaccination in elderly asthmatic patients has been shown to reduce the frequency and severity of asthma exacerbations <sup>760</sup>, thus suggesting colonisation with the bacterial genus is protective against atopic disease.

However, colonisation with *Streptococcus spp.* has also been associated with increased risk of atopic disease <sup>260, 280,761,762</sup> and disease severity <sup>763</sup>. Variances in clinical studies and murine asthma studies, however, may be explained by the effect corticosteroids have on the human microbiota. Zhang *et al* (2013), for example, demonstrated that children who regularly used inhaled corticosteroids to treat their asthma had increased oropharyngeal colonisation of *S. pneumoniae* <sup>764</sup>. As corticosteroid usage is typically increased with

asthma severity, the positive association between *Streptococcus* and severe asthma may simply be due to increased corticosteroid usage.

In addition to reduction of *Bacillus* and *Streptococcus spp.*, mice exposed to the HDM allergen suffered complete loss of the *Eubacterium ruminantium group spp.* in the gut microbiome. Whilst not typically associated with the murine gut microbiome, bacterial members of this genus are likely to protect against atopic asthma due to their ability to produce SCFAs<sup>765,766</sup>.

SCFAs have been observed to induce Treg cell differentiation<sup>608</sup> and homeostasis<sup>767</sup>, and thus are important in the regulation of the immune system. This suggests that airway inflammation as a result of HDM exposure reduces SCFA production in the gut, which subsequently induces further immune dysregulation as a consequence of reduced Treg differentiation and activity.

The association between SCFA production and asthma is further supported by *in vivo* studies. In mice, for example, increased fibre (a dietary nutrient that is fermented into SCFA by anaerobic microbes in the gut) intake is associated with protection against atopic asthma<sup>542,543</sup>. Moreover, in patients with severe asthma, reduced fibre consumption has been associated with reduced lung function and increased airway eosinophilia<sup>533</sup>, thus demonstrating that changes in the gut influences the airway environment.

#### 6.4.6. Expansion of Bacterial Taxa Protective against Atopy in the HDM-exposed Gut Microbiome

Not all of the observed changes in the murine gut microbiome were associated with loss of beneficial taxa. *Clostridiales Family XIII* and *Lachnospiraceae UCG-001*, for example, were both observed to be significantly increased in the gut microbiome of HDM-exposed mice,

and have both been demonstrated to promote expansion of Treg cells (a cell type associated with protection against atopic disease) <sup>768,769</sup>. Furthermore, *Clostridiales* have also been demonstrated to regulate accumulation of iNKT cells <sup>770</sup> (a cell type associated with asthma pathogenesis), and inoculation with the bacterial taxa during early life has been found to confer protection against systemic IgE responses in adult mice <sup>769</sup>. Collectively, this suggests that expansion of *Clostridiales* and *Lachnospiraceae* in the gut of HDM-exposed mice would be beneficial against atopic disease, thus suggesting that HDM-induced changes in the microbiome may not always be harmful to the host.

#### 6.4.7. HDM-induced Changes to the Microbial Activity of the Murine Microbiome

The observed changes in microbiome composition were found to significantly alter the microbial activity of the gut microbiome in mice exposed to the HDM allergen. Of particular interest was the predicted increase in galactose and sphingolipid metabolism and decrease in propanoate metabolism in the HDM-exposed gut microbiome compared to the HDM-naïve gut microbiome.

Galactose has been observed to be decreased in the airways of murine models of experimental asthma <sup>771,772</sup>. Moreover, in an OVA-induced murine model of asthma, galactose levels were negatively associated with macrophage, eosinophil, lymphocyte, and neutrophil recruitment to the airways, and arabinogalactan, a downstream product of galactose and arabinose, is protective against allergen sensitisation, airway inflammation, and airway hyperresponsiveness <sup>773</sup>. Loss of galactose as a result of increased microbial consumption of galactose, therefore, is likely to increase susceptibility towards asthma.

Sphingolipid metabolites, such as ceramide and S1P, have been demonstrated to be potent bioactive messengers involved in cell differentiation, proliferation, apoptosis, activation,

and migration <sup>774</sup>, and there is increasing evidence suggesting a role for S1P in asthma pathogenesis. In asthmatic subjects, S1P has been demonstrated to be significantly increased in the airways and plasma of asthmatic patients following antigen challenge <sup>775,776</sup>, and the metabolite has been demonstrated to trigger airway hyperresponsiveness <sup>776–780</sup>, induce smooth muscle contraction and cell growth <sup>774,775,781,782</sup>, stimulate migration of eosinophils <sup>775,783</sup>, B cells <sup>784,785</sup>, mast cells <sup>774</sup>, neutrophils <sup>786</sup>, and T lymphocytes <sup>785,787</sup>, activate mast cells <sup>774,788,789</sup>, and increase proinflammatory cytokine production (IL-4, IL-6, IL-8, IL-13, IL-17) <sup>775, 779,780, 783,786</sup>, airway mucous production, and IgE levels <sup>780</sup>. Increased abundance of sphingolipid metabolising bacteria in the gut, therefore, would likely contribute to a number of key mechanisms involved in asthma pathology.

Decreased metabolism of propanoate by the HDM-exposed gut microbiome was indicative of reduced levels of SCFA in the HDM-exposed gut. Reduced levels of propionate producers have been detected in children at risk of developing asthma <sup>258</sup>, and propionate has been demonstrated to be protective against atopic disease, primarily due to the compounds ability to induce Treg cell differentiation <sup>542, 607,608,790,791</sup>. The results of this study, therefore, suggest that HDM exposure and the resultant inflammatory responses observed in genetically disposed individuals reduce the levels of propanoate in the gut, resulting in decreased Treg differentiation and increased susceptibility to atopic diseases.

#### 6.4.8. The Lung-Gut Axis influences changes to the Murine Microbiome

The majority of changes to the murine microbiome following pulmonary exposure to the HDM allergen were detected in the gut microbiome rather than the airway microbiome. This suggests that an allergic immune responses localised in the murine airways altered the composition of the bacterial populations present in the murine gut. This interpretation is

supported by a number of studies, whereby induction of airway allergic disease using the HDM or OVA allergen resulted in significant changes to the murine gut microbiome<sup>341,384–386</sup>. Moreover, despite these studies using different allergens, similar changes were observed across the different investigations and in this one. These similarities included the observation of significant increases in the relative abundance of *Eubacterium nodatum*, *Lachnospiraceae spp.*, and members of the Clostridiales order in the gut microbiome of mice exposed to the HDM/ OVA allergen compared to control mice<sup>341,384–386</sup>. This suggests that the inflammatory responses associated with sensitisation to different allergens have similar effects on the murine microbiome.

Moreover, in a murine study examining the influence of food allergy on the murine gut microbiome, it was observed that allergic disease susceptibility could be induced in allergen-naïve mice by reconstituting the gut microbiome in GF mice using faecal samples taken from allergen sensitised mice<sup>629</sup>. This suggests that allergen-induced changes to the gut microbiome can actively contribute towards disease development and pathogenesis.

Microbial changes in the airways may also alter microbial populations present in the gut. A study carried out by Sze *et al* (2014), for instance, demonstrated that instillations of LPS, a bacterial endotoxin protein expressed on the cell-surface of Gram negative bacteria, into the murine lungs caused a number of significant changes to the murine gut and circulatory microbiome<sup>341</sup>. These changes were associated with a significant increase in total bacterial load in the gut and circulatory microbiomes, and a non-significant decrease in total bacterial load was observed in the airway microbiome of mice exposed to LPS<sup>341</sup>. Reduction in total bacterial count in the airways was associated with decreased levels of *Phyllobacteriaceae*; a bacterial taxa that was observed to be increased in the circulatory microbiome following LPS exposure<sup>341</sup>. This suggested that changes in the airway



environment as a result of exposure to LPS resulted in increased translocation of bacteria from the airways and into the circulatory vessels.

LPS induces acute inflammatory responses, and collectively this study provides evidence of a lung-gut axis, whereby airway inflammation alters the bi-directional crosstalk between the lung and gut environment. This is thought to alter the gut environment, resulting in changes in the microbial populations residing in the gut<sup>386</sup>. Changes to the gut microbial population can promote or suppress inflammatory responses depending on which microbes are lost/ gained, and result in a range of diseases affecting various body systems, including the nervous system (depression<sup>792,793</sup>, bipolar<sup>794</sup>), circulatory system (cardiovascular disease<sup>795,796</sup>), and respiratory system (asthma<sup>257</sup>, cystic fibrosis<sup>797</sup>).

Further evidence of a lung-gut axis is in the form of numerous studies which have demonstrated the comorbidity of chronic lung diseases, such as COPD and asthma, and gastrointestinal diseases, such as irritable bowel disease<sup>798-802</sup> and functional dyspepsia<sup>802</sup>, and gastrointestinal symptoms, such as vomiting, diarrhoea, and abdominal pain<sup>803,804</sup>. Moreover, none of the identified bacterial taxa were detected in the experimental negative controls, thus indicating that changes in bacterial composition were due to pulmonary exposure to the HDM allergen rather than as a consequence of experimental error.

#### 6.4.9. Suitability of the Experimental Murine Model in studying Atopic Asthma

Asthma is a human disease, and thus despite the development of experimental asthma in various laboratory animals, including the murine model, there has yet to be an *in vivo* model that perfectly mimics this uniquely human disease.

The murine model of asthma is the most commonly used *in vivo* model of investigating factors that influence the composition of the microbiome, such as the effects of diet, age, antibiotic use, disease state. However, mice differ from humans significantly in terms of anatomy, genetics, and microbiome composition. Moreover, the shortened lifespan and laboratory environment means that mice are exposed to fewer environmental microbes compared to humans. Additionally, the lack of life events that induce microbial dysbiosis in the murine lifespan means that the murine microbiome is less likely to undergo the temporal shifts in composition that the human microbiome may undergo over a lifetime.

However, despite these differences the murine model remains the most advantageous of animal models for microbiome/ microbiota studies . Moreover, it is a well-established model for investigating allergen-induced airway hypersensitivity<sup>380,381,805</sup>, thus making this model the most optimum for investigating how the HDM allergen influences the composition of the microbiome.

#### 6.4.10. Chapter Summary

In summary, this study has demonstrated that exposure to the HDM allergen alters the airway and gut microbiota in mice. It is postulated that in humans, pulmonary HDM exposure and subsequent allergic responses alters the lung environment and composition of the airway microbiota. This then changes the lung-gut signals, resulting in changes to the composition of the gut microbiota. These changes may in turn make the individual more susceptible to developing atopic diseases, such as atopic asthma, and explain the common occurrence gastrointestinal disorders observed in asthmatic individuals.

## Chapter 7: Conclusions and Future Work

### 7.1. Summary of Research Findings

Asthma is one of the most common chronic diseases of the 21<sup>st</sup> century, affecting over 300 million people worldwide <sup>1</sup>, and placing considerable strain on healthcare systems globally. Variations in clinical presentation and pathogenesis has resulted in speculation into whether asthma is a single disease or spectrum of related airway diseases with subtle but distinct differences in aetiology and pathophysiology <sup>22,23</sup>. This had led to the disease being separated into a number of phenotypes which are further subdivided into a number of endotypes <sup>20,22–25</sup>. The different asthma phenotypes and endotypes have been demonstrated to differ in disease presentation, in terms of cause, development, severity, and response to medication.

Standard diagnosis of asthma relies on patient history of symptoms and confirmed expiratory airflow limitation, and diagnosis of the atopic asthma phenotype is determined by the use of skin pricks tests in order to identify allergen sensitisation asthma <sup>102,103</sup>. However, asthma as a disease is highly heterogenous, and thus symptom presentation and lung function measurements may not always reflect the underlying airway inflammation. Furthermore, current methods for diagnosing the asthma endotypes are limited, invasive, and unsuitable for daily clinical practise.

In addition to issues with assessing disease state and identifying the asthma endotypes, the medications currently available for asthma treatment (bronchodilators and anti-inflammatory's) have been developed as universal treatments for asthma, and thus do not take into account the subtle differences in pathology between the different asthma endotypes. This is likely affecting the efficiency of the currently available asthma

treatments, and overall an estimated 5-10% of asthmatics fail to respond to conventional asthma medications. In order to improve asthma diagnostic protocols and treatments, increased understanding of the endotype pathologies, is required.

The first aim of this study, therefore, was to analyse plasma samples from a small, but well-defined cohort of female subjects with poorly controlled atopic asthma associated with HDM sensitivity, in order to improve understanding of the molecular mechanisms behind the asthma endotype and to identify potential biomarkers present in the blood. This was achieved by performing a comprehensive molecular characterisation of circulating mRNA, miRNA, and protein-based markers of the immune response.

#### 7.1.1. Characterisation of Atopic Asthma at the Molecular Level

Overall, the mRNA and miRNA profiles in the asthmatic subjects were found to be significantly altered compared to the control subjects, as determined by cluster analysis and the detection of significant changes in gene expression and miRNA levels. Of note, was the observation that asthma severity appeared to influence gene expression, whilst miRNA expression appeared to be influenced by the presence of additional atopic diseases. Of the 289 genes displaying significant differential expression in the asthmatic subjects, 10 genes have been previously identified as potential asthma biomarkers, whilst many of the 13 miRNAs that displayed significant differential expression in the asthmatic subjects have been previously associated with various features of asthma pathogenesis. This, therefore, validated the identified mRNA and miRNA as potential circulatory biomarkers of the asthma endotype, and suggested the possibility that a blood test aimed at quantifying known asthma biomarkers could be used as a future diagnostic tool for the asthma endotype.

In addition to identifying a number of potential circulatory RNA biomarkers, functional analysis performed on the sequenced RNA detected a number of immune functions with predicted altered activity in the asthmatic subjects compared to the control subjects. This increased understanding of the pathogenic mechanisms of the asthma endotype, subsequently identifying potential novel therapeutic targets for the endotype.

With regards to the protein investigations, there was an overall increase in inflammatory proteins in the asthmatic subjects compared to the control subjects, but no significant differences in the levels of individual proteins detected. However, it was intriguing to note that the asthmatic subjects appeared to cluster into two distinct groups; high-inflammatory protein levels and low-inflammatory protein levels, thus suggesting the possibility that the endotype could be further subcategorised on the basis of circulatory inflammation. The co-occurrence of additional atopic diseases appeared to influence circulatory inflammation, this was particularly apparent for IL-17A, which was observed to be increased in asthmatic subjects diagnosed with additional atopic diseases and the two control subjects who self-identified as having atopic dermatitis. Investigation into circulatory inflammation in asthmatic subjects, therefore, warrants further attention.

Additionally, the proteomic investigation found that the endotoxin microbial protein was decreased in the asthmatic subjects compared to the control subjects. This was of interest as bacterial endotoxin has previously been demonstrated to be protective against asthma development and pathogenesis<sup>250</sup>. Furthermore, several of the observed changes in the asthmatic RNA and inflammatory protein profiles were identified as being antimicrobial, and thus changes in the immune state of the asthmatic subjects was predicted to be influencing the bacterial populations present in the asthmatic circulatory microbiome.

### 7.1.2. Characterisation of the Circulatory Microbiome in Atopic Asthma

Microbial dysbiosis in the asthmatic airways and gut has been well described. Alterations to the human microbiome due to changes to the environment, diet, and microbial exposure that have occurred in the past century are thought to be contributing to increased prevalence of asthma. However, to date there have been no published characterisations of the asthmatic circulatory microbiome, barring the published work of this study. The second aim of this study, therefore, was to characterise the circulatory microbiome in the asthmatic and control subjects.

Using the plasma samples from the 5 atopic asthmatic subjects and 5 healthy control subjects, a 16S rRNA sequencing technique was successfully developed to enable characterisation of the circulatory microbiome in the 10 subjects. Characterisation of the circulatory microbiome was comparable to other studies investigating the circulatory microbiome<sup>323, 327, 332,361</sup>, thus supporting the notion of a core circulatory microbiome dominated by members of the Proteobacteria, and to a lesser extent, the Actinobacteria, Firmicutes, and Bacteroidetes phyla.

Comparison of the asthmatic circulatory microbiome to the control microbiome revealed that atopic asthma did not significantly alter the diversity of bacteria detected in the plasma samples. However, analysis of the relative abundance of detected bacteria demonstrated that atopic asthma was associated with an increased ratio of Firmicutes to Proteobacteria, and significantly increased abundance of the Firmicutes phylum, Bacilli class, the Xanthomonadales order, the *Xanthomonadaceae* family, and the *Stenotrophomonas* and *Kocuria* genera, in the circulatory microbiome compared to the control microbiome.

The reduced abundance of Proteobacteria detected in the asthmatic subjects likely explains the decreased concentration of circulatory endotoxin detected in the asthmatic subjects as

the Proteobacteria phylum is predominately composed of endotoxin-producing Gram negative bacteria. Additionally, the phylum contains a variety of known human pathogens, and thus reduced levels of these bacteria in the asthmatic subjects may be the consequence of increased antimicrobial production in the asthmatic subjects, as evidenced in the RNA and pro-inflammatory data.

It was also interesting to note the observed increase in Firmicutes in the asthmatic subjects, as increased levels of Firmicutes have also been detected in the airways of asthmatic diagnosed with severe asthma <sup>261</sup>. This suggests that severe asthma may be characterised by increased Firmicutes abundance, and that increased circulatory levels of Firmicutes may serve as a microbial biomarker of severe asthma. However, as this study only characterised the circulatory microbiome of subjects with severe asthma, a larger study involving multiple asthma severity levels would be required to investigate this further.

Changes to the bacterial circulatory microbiome was predicted to significantly decrease energy metabolism potential of the asthma microbiome compared to the control microbiome. This suggested the possibility of reduced SCFA production in the asthmatic subjects. However, as SCFA production typically occurs in the cecum and large intestine, and comparison of the circulatory microbiome found no similarity with the HMP gut microbiome, further analysis of the origins of the detected bacteria would be required to determine the significance of these findings.

Analysis of the viability of the bacteria detected found that the plasma samples contained viable bacteria. Identification of these organisms, however, demonstrated that the detected bacteria are known members of the skin microbiome, thus suggesting that the detected organisms were contaminating bacteria from the skin of the study subjects and/or the individuals who handled the blood samples prior to the culture work. This

interpretation was supported by comparison of the samples to the HMP microbiomes, whereby the circulatory microbiomes were found to be most similar to the HMP oral cavity and skin microbiota. However, as no experimental negative control was generated during sample collection it was not possible to identify contaminating bacteria introduced to the samples during sample collection.

Previous investigations into the asthma microbiome have demonstrated that the different asthma endotypes are associated with distinct changes to the bacterial populations making up the airway and gut microbiome <sup>242, 254, 263,255–262</sup>. In the asthmatic cohort, a number of the asthmatic subjects suffered from additional atopic diseases (i.e. allergic rhinitis, atopic dermatitis), and this may have influenced the composition of the circulatory microbiome. The third aim of this study, therefore, was to determine whether different atopic diseases are associated with distinct changes to the circulatory microbiome.

### 7.1.3. Characterisation of the Circulatory Microbiome in different Atopic Disease States

The method of detecting the human circulatory microbiome developed using the human plasma samples was applied to serum samples from 4 asthmatic subjects, 7 allergic rhinitis subjects, 3 hyper-allergic subjects (diagnosed with both asthma and allergic rhinitis), and 11 healthy control subjects, that were kindly donated by Professor Jarvis of the *National Lung and Heart Institute* as part of a preliminary investigation into whether the circulatory microbiome could be characterised from historic serum samples.

A circulatory microbiome was successfully characterised from all the serum samples, and was found to be predominately composed of Proteobacteria, Firmicutes, and Actinobacteria, and to a lesser extent Bacteroidetes and Cyanobacteria. These observations



were similar to the circulatory microbiome characterised from the plasma samples (as described in Chapter 4) and reflect the results of previous investigations into the circulatory microbiome, thus providing further support for the theory of a core circulatory microbiome.

The increasing evidence of a core circulatory microbiome suggests that the microbiome may be less transient than previously thought. However, it may be that the detected bacteria are simply more efficient at translocation into the blood, are better adapted to surviving in the circulatory system, and/ or are more likely to be blood contaminants, entering the blood sample upon sample collection, and/ or existing as laboratory contaminants. Further investigation, therefore, would be required to determine the most likely origins of the bacteria detected in the blood samples.

Comparison of the circulatory microbiome detected in the different sample groups revealed allergic rhinitis was associated with increased bacterial alpha diversity in the circulatory microbiome, whilst asthma was associated with decreased bacterial diversity, and the hyper-allergic state displayed similar diversity to the control subjects. This revealed that the different atopic states influenced diversity of the bacterial populations present in the circulatory system differently. This interpretation was further supported by the detection of differentially abundant bacterial taxa in the atopic subjects, whereby differentially abundant taxa were predominately specific to the atopic disease state. Members of the *Prevotellaceae* family, for example, were only significantly increased in subjects with allergic rhinitis (the allergic rhinitis subjects and the hyper-allergic subjects), whereas the Micrococcales order was only significantly decreased in subjects with asthma (the asthmatic subjects and the hyper-allergic subjects).

A number of the observed changes in bacterial abundance in the atopic subjects have previously been associated with atopic disease state in both the airway and gut microbiome. This suggests that changes in the circulatory microbiome reflect microbial dysbiosis present in the atopic airways and gut. Furthermore, several of the differentially abundant bacterial taxa have been associated with disease development, phenotype, pathogenesis, and treatment sensitivity. The circulatory microbiome could, therefore, represent a reservoir of novel biomarkers that could be used in the identification of at-risk infants, diagnosis of atopic disease, classification of disease phenotype and severity, and determining treatment responsiveness.

Changes in the circulatory microbiome was also predicted to significantly alter microbial activity in the hyper-allergic subjects. This was of interest, as it suggested the co-occurrence of multiple atopic diseases in the individual augmented the effect atopic disease on predicted circulatory microbiome functional activity. This contrasted with the results of alpha diversity analysis, whereby the effects asthma and allergic rhinitis had on bacterial diversity counteracted one another, resulting in the hyper-allergic subjects displaying a bacterial diversity similar to the control subjects.

The results of predicted functional activity of the circulatory microbiome were similar to the results of predicted functional activity in the circulatory microbiome (as described in Chapter 4), whereby the functional activities predicted to be altered in the hyper-allergic subjects were predominately metabolic activities (retinol metabolism, toluene degradation, dioxin degradation, Flavonoid biosynthesis, thiamine metabolism). Additionally, whilst no level 3 KEGG pathways displayed significantly altered abundance in the asthmatic serum samples that were biologically significant (as defined by an LDA score greater than 2.0), 2 metabolic KEGG pathways did display significant *P* values, thus

providing further support that the asthma microbiome is associated with changes in metabolic potential. This was a particularly intriguing find as obesity and diabetes have been previously demonstrated to be comorbidities of asthma. This research suggests the possibility that changes in the microbiome associated with atopic disease may alter metabolic potential of the human microbiome, subsequently making atopic individuals more susceptible to developing metabolic syndromes, such as obesity and diabetes.

The bacterial activities identified as being differentially abundant in the hyper-allergic subjects have been previously associated with atopic disease and pathogenesis. Changes in the circulatory microbiome functional potential, therefore, likely reflects altered bacterial activity present at other body sites within the hyper-allergic subjects. This altered activity may contribute towards atopic pathogenesis, or it may reflect changes in the bacterial abundance as a consequence of changes to the microbiome environment.

In the hyper-allergic subjects, for instance, increased abundance of retinol metabolising bacteria likely actively contributes towards atopic pathogenesis through production of retinoic acid, a retinol metabolite that has been demonstrated to enhance several pathogenic features of atopic disease. In contrast, the observed increase in toluene and dioxin metabolising capabilities of the hyper-allergic microbiome may simply reflect the associated risk between toluene and dioxin environmental exposure and atopic disease. Increased inhalation of these compounds would create internal body habitats where the ability to degrade the compounds serves as a beneficial trait, enabling bacteria capable of metabolising the compounds to out compete other members of the human microbiota, thus explaining their increased abundance in atopic subjects.

However, it can also be argued that changes in the circulatory microbiome functional potential is a reflection of the changes in human lifestyle that have occurred in the past

century. For instance, decreased exposure to respiratory infections as a consequence of increased sanitation and development of antibiotics may cause retinoids to accumulate in the lungs, this in turn would encourage growth of bacteria with retinol metabolising activity. Furthermore, changes in the human diet, moving away from a natural food products high in vitamins and fibres towards a diet containing more processed foods high in sugar and fat <sup>806,807</sup>, are likely to result in reduced consumption of key nutrients and vitamins, such as thiamine, thus removing the beneficial adaptation of thiamine metabolising, and subsequently resulting in decreased growth of thiamine metabolising bacteria.

Analysis of the viability of the bacteria detected in the human serum samples found that there were no viable bacteria present in the samples. The serum samples were donated from a collection of historic serum samples and thus had been stored at -80°C for significantly longer than the plasma samples investigated in Chapter 4. This, therefore, suggests that long-term storage of blood samples may influence viability of bacterial cells present in the samples, subsequently making it more difficult to resuscitate the bacteria from their dormant state <sup>333</sup>. However, it may also support the theory that the detected circulatory microbiome is predominately composed of bacterial DNA that has translocated from other body sites, and that the viable bacteria detected in the human plasma samples were the result of contaminating bacterial cells from the skin microbiota. Further investigations using blood samples stored for different lengths of time, therefore, would be beneficial in order to determine the effects of long-term storage on the circulatory microbiota.

#### 7.1.4. Characterisation of the Murine Microbiome following exposure to the HDM allergen

One theory about the atopic microbiome is that an altered immune system associated with persistent airway inflammation in atopic subjects causes the observed changes in the bacterial populations. The final aim of this study, therefore, was to examine changes in the atopic microbiome following HDM-induced pulmonary inflammation in a murine model. This was achieved by examining the murine airway, gut, and circulatory microbiome of mice with HDM-induced pulmonary inflammation (HDM-exposed mice) and control mice (HDM-naïve mice) using murine BAL, faeces, and plasma samples kindly donated by Dr Martin Leonard from *Public Health England*.

Analysis of the murine plasma samples using the circulatory microbiome detection protocol developed in Chapter 4 was unsuccessful at detecting a murine circulatory microbiome. This demonstrated that the protocol developed for human blood samples was not applicable to murine blood samples. Therefore, in order to assess the effects HDM-induced pulmonary inflammation has on the murine circulatory microbiome a new protocol would need to be developed that is tailored to murine blood.

Analysis of the murine BAL and faecal samples, however, was successful, and provided evidence that HDM-induced pulmonary inflammation significantly alters both the murine airway and gut microbiomes. Characterisation of the airway and gut microbiomes revealed that the two microbiomes shared similar microbial profiles to those previously observed in the human airway <sup>255,256, 277,278,281</sup> and gut microbiomes <sup>192,729–732</sup>, thus providing further support that the murine experimental model is currently the most optimum *in vivo* model for examining allergen induced changes to the microbiome.

Comparison of the HDM-exposed and HDM-naïve microbiomes found that bacterial beta diversity was significantly altered in the gut microbiome of mice following HDM-induced pulmonary exposure compared to HDM-naïve mice. Furthermore, in both the airway and gut microbiome a number of significant changes in bacterial relative abundance were detected in the HDM-exposed mice compared to the HDM-naïve mice. Several of the bacterial taxa displaying significant differential abundance have been previously associated with atopic disease, in particular many of the bacteria displaying significant decreased abundance in the HDM-exposed mice have been demonstrated to be protective against atopic disease.

These observations were further supported by the results of PICRUSt analysis, whereby the HDM-exposed gut microbiome displayed changes in predicted microbial activity that would likely augment atopic pathogenesis. Galactose levels, for example have been negatively associated with macrophage, eosinophil, lymphocyte, and neutrophil recruitment to the airways, and thus the observed increase in galactose metabolism potential in the murine gut microbiome following HDM exposure would likely remove the protective role galactose has in atopic disease. Furthermore, increased sphingolipid metabolism in the murine gut would cause an increase in pro-inflammatory metabolites (S1P), and thus actively contribute to allergen-induced inflammation and atopic disease pathogenesis.

It was also intriguing to note that SCFA (propanoate) metabolism was predicted to be decreased in the gut of HDM-exposed mice as it suggested HDM-induced pulmonary exposure resulted in a decrease of SCFA production in the gut, a known feature of atopic disease.

The majority of changes to the murine microbiome following HDM-induced pulmonary inflammation were detected in the murine gut microbiome. This suggested that allergen-

induced immune responses localised in the airways altered the composition of bacterial populations present in the gut, thus providing additional evidence for a lung-gut axis, whereby airway inflammation alters the bi-directional crosstalk between the lung and gut environment.

## 7.2. Research Limitations associated with the Study

Overall this study achieved the main aims and objectives made at the start of the project. However, there were a number of research limitations associated with the study.

Firstly, with regards to the plasma samples used in Chapter's 3 and 4, two of the control subjects had self-diagnosed atopic dermatitis. Although this was not clinician diagnosed and comparison of the RNA, protein, and microbiome characterisation results found no increased similarity of these two control subjects with the asthmatic subjects, atopic dermatitis is still a member of the atopic triad and so the presence of these two sample may of made differences in the control and asthmatic samples less apparent.

Another research limitation associated with the plasma was the limited sample volume which restricted the amount of analysis that could be performed on the samples. This meant that rather than do individual quantitative ELISAs in order to measure circulatory inflammatory proteins, qualitative ELISAs that required less sample volume were used instead. This likely influenced the accuracy of determining the protein levels in the control and asthmatic samples, and if more sensitive, quantitative kits had been used instead, this may have enabled more significant changes in the asthmatic inflammatory protein profile to be detected. Limited sample volume also resulted in IgE quantification not being performed on the Asthma\_1 sample due to insufficient sample. It's possible that IgE protein would have been present in the sample, and that detection of IgE in the sample would have

resulted in the detection of significantly increased IgE levels in the asthmatic samples compared to the control samples.

With regards to the human circulatory microbiome work, there were several research limitations associated with this aspect of the study. Firstly, the blood samples were collected at a single time point. The circulatory microbiome is predicted to be a highly dynamic, transient population of bacteria that have translocated into the bloodstream from elsewhere in the body. A single time point analysis of the circulatory microbiome is, therefore, unlikely to give an accurate characterisation of the circulatory microbiome. Furthermore, atopic disease exhibits high levels of temporal heterogeneity, and thus a characterisation of the circulatory microbiome at a single time-point is unlikely to demonstrate the full effects that atopic diseases exhibit on the circulatory microbiome.

In addition to limitations associated with sample collection, a number of experimental design limitations were also present in the study. Firstly, the only DNA kit to successfully generate microbial 16S rRNA DNA from the blood samples was the Phusion Blood direct kit. This kit, unlike the traditional DNA extraction kits, requires a significantly smaller volume of blood sample (1 – 5µl). Considering the average human adult has 4.5 – 5.5 litres of blood in circulation, there is a risk that the microbiome characterised was not a true reflection of the circulatory microbiome as a whole. Another possible limitation with the experimental design was the use of just three nutrient agars during the bacteria viability experiments. These experiments were performed at the end of the study, and thus time constraints limited the incubation times and number of different agars that could be used. It is, therefore, possible that viable bacteria went undetected as viable bacteria present in the samples may not have been suited for the growth conditions provided in the



experiment, thus reducing the diversity and/ or amount of bacterial growth detected from the samples.

With regards to the human serum samples, the samples were part of a preliminary investigation to determine whether a circulatory microbiome could be successfully characterised using historic serum samples. This meant that the number of samples kindly donated were limited and did not contain equal numbers of the different atopic diseases. This likely will have influenced statistical analysis of the circulatory microbiome, making differences between the different atopic diseases and control subjects less apparent. Furthermore, the samples had been placed in long-term storage and this may have caused degradation of the microbial DNA present in the samples which would have adversely influenced characterisation of the circulatory microbiome. A recent study carried out by Salzmann *et al* (2019), for example, observed increased RNA degradation and decreased bacterial diversity in clinical samples (blood, menstrual blood, saliva, semen, skin, and vaginal secretion) that had been stored for 2 – 9 months compared to fresh samples <sup>808</sup>.

With respect to the murine experimental study, the major limiting factor was use of the experimental negative control. The negative experimental control was introduced to the study at the DNA extraction stage of the investigations, whereby UV-treated biology grade molecular water was used to replace the murine sample during the extraction process. However, it is possible that bacterial contamination occurred upstream of this process, for instance microbial cells and/ or DNA may have been present in the HDM extract, in the PBS solution used to administer the HDM extract and control procedure, or on the surfaces of the equipment used to administer the HDM-PBS/ PBS treatment to the mice. This may have introduced foreign bacteria to the murine microbiota prior to sample collection, which in turn may have altered the bacterial populations present in the murine microbiota,

subsequently distorting downstream characterisation of the murine microbiome. Additionally, if there were microbes/ microbial DNA in the HDM extracts, this may have resulted in false positives with regards to significant changes in the murine microbiome attributed to the HDM-induced pulmonary inflammation.

Another limitation associated with the murine study was the failure to successfully amplify and characterise microbial DNA from the murine plasma samples. This meant that the effects of HDM-induced pulmonary inflammation on the circulatory microbiome could not be assessed. Moreover, direct comparisons between microbial dysbiosis in the airways and gut and changes in the circulatory microbiome could not be performed, and thus evaluation of the effects of microbial dysbiosis at other body sites on the circulatory microbiome could not be carried out. However, it should be noted that to date only one murine study has successfully characterised a murine circulatory microbiome, and thus this limitation was only a minor concern.

### 7.3. Future Work

This study increased understanding of the inflammatory mechanisms involved in a HDM-associated atopic asthma endotype, and identified a number of RNA, protein, and microbial biomarkers that could be used in the diagnosis of the asthma endotype and other atopic diseases. This knowledge and understanding could be further expanded upon through a series of additional studies.

Firstly, the experimental work presented in Chapters 3-5 could be repeated using a larger cohort of atopic and control subjects to determine whether the RNA biomarkers identified would remain significant in a larger cohort of subjects, thus increasing the validity of the proposed circulatory RNA biomarkers. Furthermore, a number of the inflammatory

proteins investigated in this study were close to be significant, and a repeat examination of the inflammatory proteins in a larger cohort would be valuable in determining whether the observed changes in the atopic asthmatic subjects were significant, and thus increasing their potential as asthma biomarkers.

Repeating the experiment with a large cohort would also enable a number of improvements to be applied to the experimental protocol and procedures. Ideally, this second cohort of subjects would be obtained through a clinical collaborator as this would enable greater control over the procedures used to collect the samples. This would help eliminate the concerns that microbial contamination occurred during sample collection.

Furthermore, there was a concern that long-term storage of the samples had degraded protein and/ or microbial DNA present in the samples, and that had impacted the results of the protein and microbial investigation. As the protocols for analysing the protein and microbial profiles were optimised in this study, analysis of samples from a larger cohort of subjects would be performed more efficiently and timely, and thus eliminate the concerns that long-term storage had influenced the results of the study. Moreover, it would be beneficial to establish whether long-term storage influences RNA, protein, and microbial analysis of blood samples, and thus a long-term aim of this second study could be to investigate the effects of storage on the identification of circulatory biomarkers and the characterisation of the circulatory microbiome. This could be achieved by aliquoting the blood samples and placing them in storage. RNA, protein, and microbial analysis of the blood aliquots could then be carried out every three months over the course of several of years to determine whether increased storage time influences RNA, protein, and microbial analysis of the samples.

Another concern of this study was that characterisation of the single blood donation would not be sufficient to accurately characterised the circulatory microbiome and the effects atopic disease has on the circulatory microbiome. This concern could be resolved by carrying out a long-term study on a group of clearly defined asthmatic subjects and an appropriately matched group of control subjects. This would involve taking blood samples on a monthly basis to determine whether the circulatory microbiome is as temporally divergent as predicted, or whether the microbial populations are more stable than previously thought. Investigations into the circulatory microbiome have typically involved single blood donations and so this study would be of particular benefit to microbiome research.

Additionally, it would also be useful to take blood samples during periods of stable disease, during periods of acute asthma exacerbations, and following an acute exacerbation, to determine whether disease severity influences the composition of the circulatory microbiome.

Moreover, repeating the study using a larger cohort would enable new research questions to be introduced to the study. Firstly, this study specifically characterised a female cohort of asthmatic subjects, and as disease presentation has been observed to differ between the two sexes, it would be of interest to determine if sex of the subjects influenced the identification of RNA, protein, and microbial biomarkers in the asthmatic subjects. Repeating the experiments with a larger cohort containing both males and females, would enable the effects of subject sex on asthma pathogenesis and biomarker identification to be evaluated.

Furthermore, the results of Chapter 5 suggested that the different atopic diseases affect the circulatory microbiome differently, and therefore, it would also be beneficial to include

equal numbers of subjects diagnosed with the different atopic diseases in the larger cohort in order to further assess whether the different atopic diseases are associated with disease specific circulatory biomarkers. Moreover, as this study focussed on examining differences between atopic subjects with asthma and allergic rhinitis, it would be useful to include subjects with atopic dermatitis in future work to enable evaluation of the full atopic triad.

Additionally, the results of RNA analysis suggested that as disease progresses, the asthmatic circulatory RNA profile becomes more divergent to that of non-asthmatic subjects. This was demonstrated by the RNA profile of Asthma\_4, an asthmatic subject that displayed the least divergent RNA profile from the control profile and had been living with the disease for a significantly shorter time period compared to the remaining asthmatic subjects. It would, therefore, be interesting to include different age categories in a future cohort of asthmatic subjects to explore the possibility that over time asthmatics display increasing changes in the circulatory RNA profile compared to control subjects in the same age bracket.

Moreover, a number of lifestyle and environmental factors have been demonstrated to influence composition of the gut and airway microbiomes in human populations. It is likely that these lifestyle and environmental factors also indirectly influence the composition of the circulatory microbiome by altering microbial translocation into the bloodstream. As this study was a preliminary investigation to determine if a circulatory microbiome could be detected and characterised from plasma and serum samples, possible lifestyle and environmental factors were not taken into account. This could be addressed in future investigations by having control and atopic subjects fill out a lifestyle and environment questionnaire involving questions regarding the subjects diet (vegetarian v omnivore,

dietary restrictions, fibre intake), home life (pet ownership, number of co-habitants/ children, exercise), and environment (rural living v urban living, job environment).

Furthermore, it is currently thought that the blood microbiome arises as a consequence of microbial translocation into the blood vessels from other body sites. However, in both human studies presented in this thesis, only blood samples were taken from the donors, and thus direct comparisons of the composition of the microbiome present in the different body sites was not performed. In future studies it would be useful to take samples from different body sites from the same donors in order to do direct comparisons of the microbiome at different body sites in order to better predict the likely origin of the blood microbiome.

Additionally, this study focused on identifying circulatory biomarkers in adults with pre-existing disease. The potential RNA, protein, and microbial biomarkers identified in the blood, therefore, may not be applicable to atopic individuals who have yet to develop atopic disease manifestations. It would, therefore, be useful to repeat the study using blood samples taken from infants who are genetically pre-disposed to atopic disease to determine if circulatory biomarkers could be used to predict the risk of developing disease during early childhood.

Following validation of the identified biomarkers using a larger cohort of asthmatic subjects, the role the potential circulatory biomarkers play in atopic pathogenesis could be explored using *in vivo* models of atopic disease. With regards to possible RNA and protein biomarkers, genetically modified mice designed to exhibit overexpression and/ or suppressed expression of the RNA/ protein of interest could be used to evaluate the effect of increased/ suppressed expression of the RNA/ protein of interest has on HDM-induced asthma.

Similarly, murine models of HDM-induced asthma could be used to further explore the relationship between the microbiome and atopic disease. For instance, in Chapter 6 it was successfully demonstrated that HDM-induced pulmonary inflammation resulted in significant changes to the murine microbiome, in particular the murine gut microbiome. A number of the bacterial taxa found to be decreased in the HDM-exposed mice have been previously identified as being protective against asthma pathogenesis. It would, therefore, be intriguing to investigate how the microbial dysbiosis observed in the HDM-exposed mice could influence development of atopic disease. One method of exploring this would be to repeat the murine study present in Chapter 6, and then inoculate neonatal germ-free mice with faeces from either the HDM-exposed or the HDM-naïve mice. The inoculated germ-free mice could then be used to explore the effects of HDM-induced microbial dysbiosis in two parts. Firstly, in humans initial HDM exposure and development of atopic disease typically occurs during early childhood. It would, therefore, be useful to determine how HDM-induced microbial dysbiosis influences in the developing immune system using the inoculated germ-free mice. For instance, do the germ-free neonatal mice inoculated with faeces from the HDM-exposed mice exhibit a prolonged Th2 bias? Do they display reduced Treg differentiation? Increased susceptibility to respiratory infections?

The second part of the study would be to sensitise and challenge the inoculated mice to the HDM allergen in order to determine whether mice inoculated with the HDM-exposed faeces have increased susceptibility to HDM-induced airway inflammation.

An important question raised by this study and other circulatory microbiome studies relates to the origin of the circulatory microbiome; whether the blood functions as another niche for microbial growth or whether the circulatory microbiome is a characterisation of bacteria and/ or microbial DNA that have translocated from other body sites. Are changes

in the circulatory microbiome a result of microbial dysbiosis in the blood or a reflection of microbial dysbiosis occurring elsewhere in the body, affecting the number and types of bacterial translocation into the circulatory system.

Origins of the circulatory microbiome could be examined by inoculating mice with transgenic microorganisms and characterising the location of the transgenic microorganisms after a set period of time. This could be achieved by transforming bacteria with green fluorescent protein (GFP)<sup>809,810</sup>. This protein is a cell-surface protein, and thus epifluorescence microscopy could be used to detect the presence of microbial cells in the sample<sup>809-811</sup>, whilst microbial DNA extraction of the sample and PCR amplification of the *gfp* gene insert could be used to detect DNA derived from the transformed bacteria<sup>811,812</sup>.

To determine the likely origin of the circulatory microbiota/ microbiome the transformed bacteria could be inoculated into different body sites of the mice, for example, the airways, epidermal tissue, and gut. After a set period of time samples from the different habitats (i.e. blood for the circulation, BAL for the airways, faeces for the gut) could then be examined using epifluorescence microscopy and PCR amplification of the GFP gene in order to identify the location of the transformed microbial cells and their DNA. Tagging of both the microbial cell and the microbial DNA would be of value as examination of blood samples using microscopy would prove that the transformed cells had translocated into the blood, whilst the use of PCR amplification of the GFP gene would prove the transformed DNA had translocated into the blood. Initial inoculation site would then demonstrate where the transformed cells had originated from prior to detection in the blood.

This study would be useful as it would enable identification of the most likely origin of the circulatory microbiome and would also help establish whether the circulatory microbiome is composed of translocating bacterial cells and/ or bacterial DNA. Additionally, the use of



transgenic microbes would mean that the microbes could be inoculated into mice with a pre-existing microbiome, and so better mimic host-microbiome interactions.

Alternatively, translocation of bacteria could be investigated by colonising GF mice with known bacterial cultures and then performing 16S rRNA sequencing on samples taken from different body habitats to determine which environments the known bacteria translocate to following inoculation.

However, in this study the murine circulatory microbiome went undetected, and so a technique would need to be developed to enable successful characterisation of the murine circulatory microbiome. A study carried out by Sze *et al* (2014) successfully characterised the murine circulatory microbiome using whole blood samples and targeting the V1-V3 hypervariable region of the 16S rRNA gene. This study used murine plasma samples and targeted the V4 region of the 16S rRNA gene. This technique, whilst successful at characterising the human circulatory microbiome may not be optimum for characterising the murine circulatory microbiome. Therefore, in order to successfully develop a technique for characterising the murine circulatory microbiome, different blood fractions (whole blood, plasma, serum, and buffy coat) would need to be analysed as the microbial DNA present in murine plasma samples may be too low for successful detection and amplification. Furthermore, it would also be beneficial to use primers targeting different regions of the microbial 16S rRNA gene in order to determine which primer set is best suited for amplifying microbial DNA from murine blood samples.

## Publications arising from Thesis

Whittle, E., Leonard, M. O., Harrison, R., Gant, T. W. & Tonge, D. P. Multi-Method Characterization of the Human Circulating Microbiome. *Front. Microbiol.* **9**, 3266 (2018).

Whittle, E., Leonard, M. O., Gant, T. W. & Tonge, D. P. Multi-Method Molecular Characterisation of Human Dust-Mite-associated Allergic Asthma. *Sci. Rep.* **9**, 8912 (2019).

## Supplementary Materials

### S1: R code utilised to generate a rarefaction curve from OTU tables

```
psdata <- data
sample_sums(psdata)
set.seed(42) # Command used to specify the initial value of R's random number generator

calculate_rarefaction_curves <- function(psdata, measures, depths) {
  require('plyr') # lply
  require('reshape2') # melt

  estimate_rarified_richness <- function(psdata, measures, depth) {
    if(max(sample_sums(psdata)) < depth) return()
    psdata <- prune_samples(sample_sums(psdata) >= depth, psdata)

    rarified_psdata <- rarefy_even_depth(psdata, depth, verbose = FALSE)

    alpha_diversity <- estimate_richness(rarified_psdata, measures = measures)

    # as.matrix forces the use of melt.array, which includes the Sample names (rownames)
    molten_alpha_diversity <- melt(as.matrix(alpha_diversity), varnames = c('Sample', 'Measure'),
    value.name = 'Alpha_diversity')

    molten_alpha_diversity } # Commands estimate expected species richness in random
subsamples of size sample from the community

names(depths) <- depths # this enables automatic addition of the Depth to the output by lply
rarefaction_curve_data <- lply(depths, estimate_rarified_richness, psdata = psdata, measures =
measures, .id = 'Depth', .progress = ifelse(interactive(), 'text', 'none'))

# convert Depth from factor to numeric
```

```

rarefaction_curve_data$Depth <-
as.numeric(levels(rarefaction_curve_data$Depth))[rarefaction_curve_data$Depth]

rarefaction_curve_data}

rarefaction_curve_data <- calculate_rarefaction_curves(psdata, c('Observed'), rep(c(1, 10, 100,
1000,10000,20000,30000,40000,50000,60000,70000,80000,90000,100000,110000,
120000,130000,140000,150000,160000,170000,180000,190000,200000,210000,220000,
230000,240000,250000,260000,270000,280000,290000,300000), each = 10))

summary(rarefaction_curve_data) # Command calculates expected species richness of a given
sample size in terms of read number

rarefaction_curve_data_summary <- dply(rarefaction_curve_data, c('Depth', 'Sample',
'Measure'), summarise, Alpha_diversity_mean = mean(Alpha_diversity), Alpha_diversity_sd =
sd(Alpha_diversity)) # Command calculates mean species richness and standard deviation

rarefaction_curve_data_summary_verbose <- merge(rarefaction_curve_data_summary,
data.frame(sample_data(psdata)), by.x = 'Sample', by.y = 'row.names')

data = rarefaction_curve_data_summary_verbose

write.table(data, file="rarefaction_curve_data_summary_verbose.txt",sep = "\t")
write.table(rarefaction_curve_data, file="rarefaction_curve_data_summary_verbose.txt",sep =
"\t")

jpeg(file = "Rarefraction curve.jpeg")
jpeg("Rarefraction curve.jpeg", height = 8*300, width = 12*300, res = 400, pointsize = 10)

p = ggplot(      # Commands plot rarefaction curve and format the graph
data,
mapping = aes(
x = Depth, # Command assigns X data (read numbers)
y = Alpha_diversity_mean, # Command assigns Y data (estimated species richness)
ymin = Alpha_diversity_mean - Alpha_diversity_sd,

```

```

ymax = Alpha_diversity_mean + Alpha_diversity_sd,
colour = TreatmentGroup,
group = X.SampleID
)
) + geom_line(          # Command assigns graph as a line graph
) + geom_pointrange()
+ facet_wrap(scales = 'free_y')
p
p = p + scale_colour_manual(labels = c("Group1", "Group2", "Negative Control"),
                           values=c("#2ECC71", "#A569BD", "#E74C3C")) # Sets legend order and colour
p = p + scale_y_continuous(expression(paste("Number of Observed OTUs"))) # Sets Y axis label
p = p + scale_x_continuous(expression(paste("Number of reads"))) # Sets X axis label
p = p + theme(axis.text = element_text(size = 15), axis.title=element_text(size = 15))
p = p + theme(legend.text = element_text(size = 14))
p = p + theme(legend.title = element_text(size = 14))
p
dev.off()

```

## **S2: R codes used to perform statistical analysis on data**

```

shapiro.test(data$Chao1) # Shapiro-wilk test
wilcox.test(Chao1 ~ Group, data, paired = F) # Wilcoxon rank sum test
var.test(Variable ~ Group, data, alternative = "two.sided") # F test
t.test(Variable ~ Group, data, var.equal = T, paired = F) # Unpaired T test
t.test(Variable ~ Group, data, var.equal = F, paired = F) # Welch two sample T test
res.aov <- aov(Chao1 ~ Group, data = data) # One-way ANOVA test
summary(res.aov)
pairwise.t.test(data$Chao1, data$Group, p.adjust.method = "BH") # Pairwise T test

```

### S3: R code utilised for calculating relative abundance of the bacterial taxa identified in the samples

```
# Generate a relative abundance table using phyloseq data  
y1 <- tax_glom(data, taxrank = 'Phylum') # agglomerate taxa  
y2 <- transform_sample_counts(y1,function(x) ({x/sum(x)*100})) #get abundance in %  
y3 <- psmelt(y2) # create dataframe from phyloseq object  
write.table(y3, file="Sample-otus-Phylum.txt",sep = "\t")# Command generates relative abundance table  
data <- read.table("Sample-otus-Phylum.txt", header = T)
```

These steps were repeated for each bacterial taxa level (Phylum, class, order, family, genus) and relative abundance of the bacterial taxa present in the different sample groups was determined using the below commands.

```
y1 <- tax_glom(data, taxrank='Phylum') # agglomerate taxa  
(y2 = merge_samples(y1, "TreatmentGroup")) # Command used to merge relative abundance of samples from the sample group together  
y3 <- transform_sample_counts(y2,function(x) ({x/sum(x)*100})) # Command used to generate relative abundance values  
y4 <- psmelt(y3)  
write.table(y4, file="TreatmentGroup-otus-Phylum.txt",sep = "\t") # Command used to generate a txt file of the bacteria taxa relative abundance values for each sample
```

The generated relative abundance tables were then used to produce relative abundance graphs highlighting the highly abundant bacterial taxa (bacterial taxa with relative abundance > 1.0%) and functional activity of the microbiome with a predicted abundance greater than 1%. An example showing how the phylum relative abundance graph was generated for the human plasma samples (Chapter 4, Figure 4.9.A).

```
data <- read.table("TreatmentGroup-otus-Phylum.txt", header = T)
```

```

data$Phylum<- as.character(data$Phylum) #convert to character

data$Phylum[data$Abundance < 1.00 ] <- "Phyla < 1% abundance" # Command used to group
taxa with an abundance of less than 1.0% together

data$Phylum <- factor(data$Phylum, levels =
c("Actinobacteria", "Bacteroidetes", "Cyanobacteria", "Firmicutes", "Proteobacteria", "Phyla < 1%
abundance" # Command used to order the phyla on the figure legend
"

jpeg(file = "Relative Abundance Graph.jpeg")

jpeg("Relative Abundance Graph.jpeg", height = 7*300, width = 15*300, res = 400, pointsize = 10)

p = ggplot(data, aes(x=TreatmentGroup, y=Abundance, fill=Phylum))

p = p + geom_bar(aes(), stat="identity", position="stack") +
scale_fill_manual(values=c("#660000", "LEMONCHIFFON", "#008080", "#512E5F", "LAVENDER")) +
theme(legend.position="right") + scale_x_discrete(limits = c("Group1", "Group2"), labels =
c("Group1", "Group2"), drop=F) # Command used to assign colours and set format of the graph

p = p + scale_y_continuous(expression(paste("Relative Abundance (%)"))) # Command used to
label Y axis

p = p + theme(axis.text = element_text(size = 15), axis.title=element_text(size = 15)) # Commands
used to assign axis label sizes and legend position

p = p + theme(axis.title.x = element_blank())

p = p + theme(legend.text = element_text(size = 14))

p = p + theme(legend.title = element_text(size = 14))

p = p + theme(legend.position="right") + guides(fill=guide_legend(ncol =1))

p = p + theme(legend.text = element_text(face = "italic"))

p

dev.off()

```

#### **S4: R code utilised in the generation of boxplots**

```

jpeg(file = "Boxplot1.jpeg")

jpeg("Boxplot1.jpeg", res = 300, height = 5*300, width = 6*300, pointsize =13)

p = ggboxplot(data, x = "Group", y = "Variable",

color = "Group", palette = c("#00AFBB", "#E7B800", "#FC4E07", "#A569BD", "#2ECC71"),

order = c("Group1", "Group2"),

MARGIN = 5,

ylab = "Variable", xlab = "Group")+

```

```

geom_point(aes(color=Group), size = 2.5) # Commands used to assign colours and set format of
the graph

p = p + theme(legend.position="right")

p = p + theme(axis.text = element_text(size = 12), axis.title=element_text(size = 13))

p = p + theme(legend.text = element_text(size = 12))

p = p + theme(legend.title = element_text(size = 13))

p

dev.off()

```

## S5: R codes used to perform PCoA and PCA Analysis

*## Codes used to perform principal coordination analysis (PCoA) using Bray Curtis dissimilarity*

```

data

tdata <- transform_sample_counts(data, function(x){x/sum(x)}) # Transformation by conversion
into relative abundance

library("ggplot2")

library("vegan")

library("ggrepel")

ordu = ordinate(data, "PCoA", "bray") # Measurement of Bray-Curtis dissimilarity

```

*## Generation of a Bray-Curtis Dissimilarity PCoA graph*

```

jpeg(file = "Bray Curtis PCoA.jpeg")

jpeg("Bray Curtis PCoA.jpeg", height = 10*300, width = 12*300, res = 400, pointsize = 12)

p = plot_ordination(data,ordu, color="TreatmentGroup") # Generation of PCoA graph

p = p + geom_point(size=4) # Command determine size of data point

p = p + geom_label_repel(aes(label = X.SampleID),
                        color = "black",
                        box.padding = 0.35,
                        point.padding = 0.8,
                        segment.color = 'grey50') # Commands add sample labels to the graph

p = p + scale_colour_manual(labels = c("Group1","Group2"),
                            values=c("#00AFBB","#E7B800")) # Commands add group names and colour to the
legend

```



```

p = p + theme(axis.text=element_text(size=14), # Sets the axis label sizes
              axis.title = element_text(size = 14))

p = p + theme(legend.text=element_text(size = 14),legend.title=element_text(size=14)) # Sets the
legend label sizes

p
dev.off()

## Codes used to perform principal component analysis (PCA) using Bray Curtis dissimilarity

library("gplots")
library("ggplot2")
library("RColorBrewer")
library("ggfortify")
library("ggrepel")
library("vegan")

Sig.mRNA <- read.table("LOG2 RNA Read Counts", header = T)
data.env <- read.table("data.env.txt", header = T)
data$Group <- ordered(data$Group, levels = c("Control", "Asthma")) # Command sets order of
legend

df <- data[c(5:14230)] # Command generates a data frame from the data

jpeg(file = "All mRNA log2 FPKM PCA with Group.jpeg")

jpeg("All mRNA log2 FPKM PCA with Group.jpeg", height = 7*300, width = 9*300, res = 400,
pointsize = 10)

theme_set(theme_bw()) # Command sets graph background

p = autoplot(prcomp(df), data = data, colour = "Group", size = 4, key = T, key.size = 14) # Command
generates a PCA graph using bray Curtis dissimilarity

p = p + geom_label_repel(aes(label = ID), # Commands format the graph
                        color = "black",
                        box.padding = 0.35,
                        point.padding = 0.9,
                        segment.color = 'grey50')

p = p + scale_colour_manual(labels = c("< 25", "> 25 "),
                            values=c("#00AFBB", "#E7B800"))

```

```

p = p + theme(axis.text=element_text(size=14), # Sets the axis label sizes
              axis.title = element_text(size = 14))
p = p + theme(legend.text=element_text(size = 14),legend.title=element_text(size=14))
p
dev.off()

## PERMANOVA analysis using the Adonis Function

data_bray <- phyloseq::distance(tdata, method = "bray")

braycurtis=as.matrix(data_bray) # Command used to convert bray Curtis results into matrix

write.table(braycurtis, "BrayCurtis_even.txt",row.names=TRUE,col.names=TRUE,sep="\t",
           quote=FALSE) # Download Bray Curtis matrix as a txt file

sampledf <- data.frame(sample_data(data))

adonis(data_bray ~ TreatmentGroup, data = sampledf) # PERMANOVA analysis

```

**Table S1: Asthma Quality Questionnaire (ACQ) completed by the asthmatic subjects following sample collection**

Question		Score	
1	On average, during the past week, how often were you woken by your asthma during the night	0	Never
		1	Hardly ever
		2	A few times
		3	Several times
		4	Many times
		5	A great many time
		6	Unable to sleep because of asthma
2	On average, during the past week, how bad were your asthma symptoms when you woke in the morning	0	No symptoms
		1	Very mild symptoms
		2	Mild symptoms
		3	Moderate symptoms
		4	Quite severe symptoms
		5	Severe symptoms
		6	Very severe symptoms
3	In general, during the past week, how limited were you in your activities because of your asthma	0	Not limited at all
		1	Very slightly limited
		2	Slightly limited
		3	Moderately limited
		4	Very limited
		5	Extremely limited
		6	Totally limited

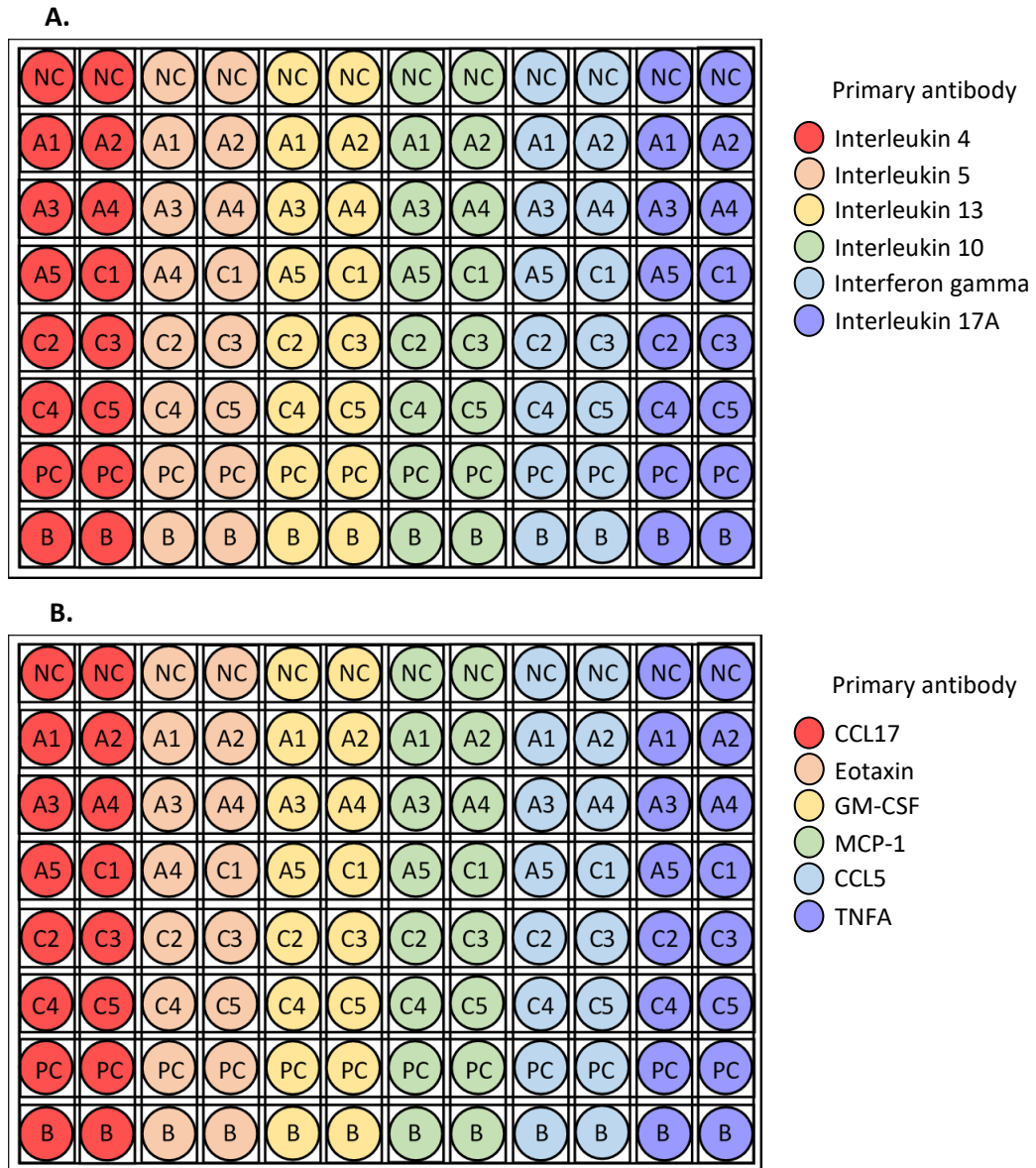
<p>4 In general, during the past week, how much shortness of breath did you experience because of your asthma</p>	<p>0 None  1 A very little  2 A little  3 A moderate amount  4 Quite a lot  5 Great deal  6 A very great deal</p>
<p>5 In general, during the past week, how much of the time did you wheeze</p>	<p>0 Not at all  1 Hardly any of the time  2 A little of the time  3 A moderate amount of the time  4 A lot of the time  5 Most of the time  6 All the time</p>
<p>6 On average, during the past week, how many puffs/ inhalations of short-acting bronchodilator (e.g. Ventolin/ Bricanyl) have you used each day</p>	<p>0 None  1 1-2 puffs/ inhalations most days  2 3-4 puffs/ inhalations most days  3 5-8 puffs/ inhalations most days  4 9-12 puffs/ inhalations most days  5 13-16 puffs/ inhalations most days  6 More than 16 puffs/ inhalations most days</p>

## S6: R code utilised for plotting expression profiles as a heatmap and performing Euclidean cluster analysis

RNA read counts generated from the sequenced RNA data was transformed to a LOG2 scale using the  $\log_2(x) + 1$  formula, and the transformed data was then uploaded to R. RNA expression was plotted as a heatmap and unsupervised clustering analysis was performed using Euclidean distance. The R codes used to generate the RNA heatmaps and perform Euclidean distance are shown below.

```
# Set file directory
setwd("FolderName")
library("gplots")
library("ggplot2")
library("RColorBrewer")
library("ggfortify")
hmcol = colorRampPalette(brewer.pal(9, "GnBu"))(100) # Command used to assign colour palette
data <- read.table("ExpressionData.txt", header = T)
data <- as.matrix(data) Command used to convert data into a matrix
jpeg(file = " ExpressionData Heatmap.jpeg")
jpeg("ExpressionData Heatmap.jpeg", height = 25*300, width = 18*300, res = 400, pointsize = 8)
heatmap.2(data,lhei = c(2,10),cexCol=2.5, cexRow=1.0, srtCol=45,
          col = hmcol, margins=c(10,10), keysize = 1.0, key.par=list(mgp=c(0.5,0.5,0))) # Command
used to generate the heatmap
dev.off()
```

**Figure S1: Plate layout of the multi-analyte sandwich ELISAs used to analysis the inflammatory protein levels present in plasma samples from asthmatic subjects (n = 5) and non-asthmatic subjects (n = 5). (A) = plate 1, (B) = plate 2.**



Abbreviations: NC = Negative control, A = Asthmatic, B = Non-asthmatic, PC = Positive control, B = blank

**Table S2: Characterisation of the Atopic Asthma cohort at the time of sample collection**

Characteristic	Asthma_1	Asthma_2	Asthma_3	Asthma_4	Asthma_5
<b>Current age</b>	52	36	42	19	49
<b>Ethnicity</b>	Hispanic	Hispanic	Caucasian	Caucasian	Hispanic
<b>BMI</b>	27.8	27.3	23.3	21.5	22.3
<b>Age of diagnosis</b>	7	4	12	5	3
<b>Asthma Diagnosis</b>	Allergic Asthma	Allergic Asthma	Allergic Asthma	Allergic Asthma	Allergic Asthma
<b>Years with disease</b>	45	32	30	14	46
<b>ACQ Score</b>					
Total	12	11	11	10	10
Mean	2.0	1.8	1.8	1.7	1.7
<b>Pulmonary test score</b>	65	61	70	78	68
<b>Allergy</b>	House dust mite	House dust mite	House dust mite	House dust mite	House dust mite
<b>Other allergic conditions</b>	Allergic Rhinitis, Nasal Polyps	Allergic Rhinitis, Polycystic Ovary	None	Allergic Rhinitis, Allergic Dermatitis	none
<b>Medications</b>	Dulera, Albuterol	Dulera, Albuterol	Symbicort, Zyrtec, Albuterol	Albuterol, Qvar	Albuterol
<b>Collection Time</b>	9:50am	9:20am	12:10pm	10:30am	10:55am

**Table S3: Results of the ACQ taken at the time of sample collection by the asthmatic subjects.**

<b>Question</b>	<b>Asthma_1</b>	<b>Asthma_2</b>	<b>Asthma_3</b>	<b>Asthma_4</b>	<b>Asthma_5</b>
<b>1</b>	2.00	0.00	1.00	1.00	2.00
<b>2</b>	2.00	2.00	3.00	3.00	1.00
<b>3</b>	3.00	3.00	2.00	2.00	2.00
<b>4</b>	3.00	3.00	2.00	2.00	2.00
<b>5</b>	1.00	1.00	2.00	1.00	2.00
<b>6</b>	1.00	2.00	1.00	1.00	1.00
<b>Total</b>	12.00	11.00	11.00	10.00	10.00
<b>Mean</b>	2.00	1.83	1.83	1.67	1.67



**Table S4: Genes with significant differential expression in asthmatic subjects compared to control subjects.** Analysis was performed by sequencing mRNA isolated from the plasma samples from asthmatic subjects (n = 4) and control subjects (n = 5) and mapping the sequenced mRNA to the hg19 human reference genome using the Tuxedo protocol (*Galaxy* software). Differential expression was carried out using CuffDiff (*Galaxy* software) and genes with a log<sub>2</sub> fold change greater than 2.0 and a Q value < 0.05 were determined to have significant differential expression.

Gene	Control Mean	Asthma Mean	Fold Change (log <sub>2</sub> )	Expression State	P Value	Q Value
HLA-DQA1	0.000	38.842	inf	Upregulated	0.00005	0.00298
IRF2	231.862	1.902	-6.930	Downregulated	0.00185	0.04613
VDR	1.116	24.331	4.447	Upregulated	0.00160	0.04272
ABCF2	14.191	0.361	-5.295	Downregulated	0.00060	0.02165
ACY3	13.545	0.000	-inf	Downregulated	0.00005	0.00298
ADAMTS18	4.844	0.000	-inf	Downregulated	0.00005	0.00298
ADHFE1	0.000	4.406	inf	Upregulated	0.00020	0.00929
AGTPBP1	2641.030	10.935	-7.916	Downregulated	0.00075	0.02582
AIP	170.828	2.390	-6.159	Downregulated	0.00185	0.04613
AKAP12	29.436	0.805	-5.193	Downregulated	0.00170	0.04401
ALX4	9.654	0.000	-inf	Downregulated	0.00005	0.00298
ALYREF	33.614	0.682	-5.623	Downregulated	0.00175	0.04479
ANAPC4	64.985	1.635	-5.313	Downregulated	0.00200	0.04810
ANKHD1,ANKHD1- EIF4EBP3,EIF4EBP3	33.139	0.914	-5.181	Downregulated	0.00020	0.00929
ANKRD11	20.860	0.481	-5.439	Downregulated	0.00015	0.00716

ANKRD62P1-PARP4P3	17.465	0.000	-inf	Downregulated	0.00005	0.00298
ANO2	6.010	0.000	-inf	Downregulated	0.00005	0.00298
ARMC3	0.000	3.276	inf	Upregulated	0.00005	0.00298
ARV1	14.064	0.000	-inf	Downregulated	0.00005	0.00298
ASCC3	9.033	0.512	-4.140	Downregulated	0.00185	0.04613
ASPH	15.551	2.130	-2.868	Downregulated	0.00110	0.03391
B4GALT5	11.155	0.320	-5.122	Downregulated	0.00150	0.04086
BPI	0.000	2.220	inf	Upregulated	0.00005	0.00298
BRI3BP	5.777	0.000	-inf	Downregulated	0.00005	0.00298
C10orf58	1100.390	1.238	-9.796	Downregulated	0.00025	0.01080
C15orf2	9.280	0.000	-inf	Downregulated	0.00005	0.00298
C15orf41	79.198	0.000	-inf	Downregulated	0.00005	0.00298
C16orf96	1.309	0.000	-inf	Downregulated	0.00005	0.00298
C17orf76-AS1, SNORD49B	1093.040	33.304	-5.036	Downregulated	0.00005	0.00298
C19orf12	13.613	0.199	-6.099	Downregulated	0.00175	0.04479
C20orf123	0.000	2.205	inf	Upregulated	0.00010	0.00522
C4orf48	3.294	0.000	-inf	Downregulated	0.00120	0.03585
CABP5	5.295	122.071	4.527	Upregulated	0.00170	0.04401
CAPRIN1	393.033	10.253	-5.261	Downregulated	0.00195	0.04757
CCDC75	5.791	0.000	-inf	Downregulated	0.00010	0.00522
CCDC85A	25.252	0.000	-inf	Downregulated	0.00005	0.00298

CCDC85B	209.821	1.874	-6.807	Downregulated	0.00100	0.03169
CD300A	71.466	0.000	-inf	Downregulated	0.00005	0.00298
CD46	154.097	5.320	-4.856	Downregulated	0.00080	0.02686
CD93	0.000	14.337	inf	Upregulated	0.00025	0.01080
CDCP2	2.395	0.000	-inf	Downregulated	0.00010	0.00522
CDH5	14.345	0.000	-inf	Downregulated	0.00005	0.00298
CEBPA	2.311	0.000	-inf	Downregulated	0.00015	0.00716
CHD1L	363.845	7.689	-5.564	Downregulated	0.00090	0.02935
CHMP1A	898.053	10.776	-6.381	Downregulated	0.00030	0.01256
CKM	0.000	3.703	inf	Upregulated	0.00005	0.00298
CLTB	10.977	241.021	4.457	Upregulated	0.00170	0.04401
CNTNAP3B	68.421	0.000	-inf	Downregulated	0.00005	0.00298
CSF2RB	6.862	0.000	-inf	Downregulated	0.00005	0.00298
CTSG	9.812	0.000	-inf	Downregulated	0.00005	0.00298
CTSL1	69.228	0.578	-6.904	Downregulated	0.00080	0.02686
CUL3	25.084	0.317	-6.306	Downregulated	0.00050	0.01905
CYB5RL	9.320	0.000	-inf	Downregulated	0.00005	0.00298
DCTN1	25.808	1.606	-4.006	Downregulated	0.00105	0.03297
DCUN1D2	6.927	0.000	-inf	Downregulated	0.00005	0.00298
DOHH	972.908	0.000	-inf	Downregulated	0.00005	0.00298
DVL3	3.473	0.166	-4.386	Downregulated	0.00165	0.04354
EBF2	0.000	65.140	inf	Upregulated	0.00030	0.01256

EID2B	0.000	4.005	inf	Upregulated	0.00005	0.00298
EIF4G1	17.787	1.883	-3.240	Downregulated	0.00145	0.04014
ELOF1	806.425	17.862	-5.497	Downregulated	0.00045	0.01795
EMILIN2	0.000	1.118	inf	Upregulated	0.00005	0.00298
ENOPH1	128.094	0.503	-7.992	Downregulated	0.00205	0.04896
F3	136.603	7.235	-4.239	Downregulated	0.00055	0.02038
FAM131C	5.971	0.000	-inf	Downregulated	0.00005	0.00298
FAM183B	9.249	0.000	-inf	Downregulated	0.00005	0.00298
FAM26F	16.122	0.000	-inf	Downregulated	0.00005	0.00298
FAM43A	12.355	0.000	-inf	Downregulated	0.00005	0.00298
FBXL19	87.814	0.891	-6.624	Downregulated	0.00075	0.02582
FBXO40	16.855	0.000	-inf	Downregulated	0.00005	0.00298
FETUB	0.000	11.749	inf	Upregulated	0.00005	0.00298
FGF20	3.360	0.000	-inf	Downregulated	0.00005	0.00298
FGFBP2	5.330	0.000	-inf	Downregulated	0.00005	0.00298
FN1	240.158	33.387	-2.847	Downregulated	0.00005	0.00298
FUS	101.743	5.786	-4.136	Downregulated	0.00110	0.03391
GABPB2	10.661	0.000	-inf	Downregulated	0.00005	0.00298
GBP4	0.000	12.908	inf	Upregulated	0.00005	0.00298
GDF7	1.192	0.000	-inf	Downregulated	0.00005	0.00298
GOLGA6L10	5.225	0.000	-inf	Downregulated	0.00005	0.00298
GOSR2	5.227	97.586	4.223	Upregulated	0.00200	0.04810

GPC2	12.575	0.000	-inf	Downregulated	0.00005	0.00298
GPIHBP1	7.789	0.000	-inf	Downregulated	0.00005	0.00298
GPR108	8.489	0.440	-4.270	Downregulated	0.00140	0.03940
GPR141	915.003	0.000	-inf	Downregulated	0.00015	0.00716
GPR56	1.870	98.538	5.720	Upregulated	0.00030	0.01256
GRB10	1.378	56.460	5.357	Upregulated	0.00050	0.01905
GRK6	107.048	2.212	-5.597	Downregulated	0.00025	0.01080
GSTA1	0.000	25.588	inf	Upregulated	0.00005	0.00298
HBG2	0.000	8.800	inf	Upregulated	0.00010	0.00522
HBM	0.000	7.921	inf	Upregulated	0.00050	0.01905
HDAC9	0.732	52.163	6.156	Upregulated	0.00010	0.00522
HERC2P3	2.274	0.000	-inf	Downregulated	0.00005	0.00298
HINT2	0.000	2.969	inf	Upregulated	0.00015	0.00716
HIST1H2AB	0.000	15.171	inf	Upregulated	0.00025	0.01080
HIST1H2BI	251.282	0.000	-inf	Downregulated	0.00045	0.01795
HIST1H3C	0.000	90.578	inf	Upregulated	0.00005	0.00298
HIST1H3E	40.247	0.000	-inf	Downregulated	0.00005	0.00298
HIST1H3G	1807.630	8.413	-7.747	Downregulated	0.00120	0.03585
HIST1H3I	30.233	0.000	-inf	Downregulated	0.00005	0.00298
HIST1H4D	2636.810	0.000	-inf	Downregulated	0.00005	0.00298
HIST2H2AC	6.239	791.766	6.988	Upregulated	0.00115	0.03482
HIST3H2A	0.000	13.295	inf	Upregulated	0.00005	0.00298

HLA-DRB5	6.090	0.000	-inf	Downregulated	0.00005	0.00298
HOTTIP	0.000	28.228	inf	Upregulated	0.00005	0.00298
HOXB4	6.126	0.000	-inf	Downregulated	0.00005	0.00298
HOXC10	26.492	0.000	-inf	Downregulated	0.00005	0.00298
HRC	7.677	0.000	-inf	Downregulated	0.00005	0.00298
HSH2D	56.243	2.553	-4.461	Downregulated	0.00190	0.04686
HSP90AB3P	169.495	1.844	-6.523	Downregulated	0.00155	0.04172
HUNK	1.107	0.000	-inf	Downregulated	0.00005	0.00298
IBSP	8.864	0.000	-inf	Downregulated	0.00005	0.00298
IDH3B	121.794	0.585	-7.701	Downregulated	0.00070	0.02460
IKBKB	33.299	1.090	-4.933	Downregulated	0.00060	0.02165
IL4I1,NUP62	95.850	0.298	-8.329	Downregulated	0.00130	0.03752
IL7R	95.028	0.000	-inf	Downregulated	0.00005	0.00298
IMPDH1	10.814	212.562	4.297	Upregulated	0.00090	0.02935
INSIG1	136.506	6.802	-4.327	Downregulated	0.00100	0.03169
IPO9	7.624	0.078	-6.603	Downregulated	0.00075	0.02582
ITPKA	0.000	1.834	inf	Upregulated	0.00005	0.00298
JAM2	0.000	21.097	inf	Upregulated	0.00005	0.00298
JMJD7,JMJD7-PLA2G4B,PLA2G4B	44.147	0.457	-6.593	Downregulated	0.00160	0.04272
KDM4DL	0.000	1.543	inf	Upregulated	0.00020	0.00929
KIAA1211	0.000	10.449	inf	Upregulated	0.00005	0.00298
KIF26A	10.373	0.190	-5.772	Downregulated	0.00130	0.03752

KLHL20	4464.310	5.416	-9.687	Downregulated	0.00185	0.04613
KLRF1	0.000	275.313	inf	Upregulated	0.00025	0.01080
KRT9	2.070	0.000	-inf	Downregulated	0.00010	0.00522
LDHA	441.515	18.485	-4.578	Downregulated	0.00165	0.04354
LGALS3	171.195	6.683	-4.679	Downregulated	0.00055	0.02038
LILRA1	11.122	0.000	-inf	Downregulated	0.00005	0.00298
LINC00085	15.023	0.000	-inf	Downregulated	0.00005	0.00298
LMO4	35.311	0.000	-inf	Downregulated	0.00060	0.02165
LOC100128239	2.695	0.000	-inf	Downregulated	0.00005	0.00298
LOC100499405	9.059	0.000	-inf	Downregulated	0.00005	0.00298
LOC100507003	0.000	6.794	inf	Upregulated	0.00005	0.00298
LOC100507632	0.000	2.664	inf	Upregulated	0.00010	0.00522
LOC399829	0.000	0.973	inf	Upregulated	0.00005	0.00298
LOC401127	5.410	0.000	-inf	Downregulated	0.00005	0.00298
LOC653653	0.000	30.071	inf	Upregulated	0.00005	0.00298
LOC730102	10.840	0.000	-inf	Downregulated	0.00005	0.00298
LRRD1	9.763	0.000	-inf	Downregulated	0.00010	0.00522
MAP7	5.385	0.266	-4.337	Downregulated	0.00010	0.00522
MBD1	77.878	0.423	-7.526	Downregulated	0.00005	0.00298
MCM3	30.359	0.287	-6.726	Downregulated	0.00025	0.01080
MEG8	51.071	0.000	-inf	Downregulated	0.00005	0.00298
MIOX	1.539	0.000	-inf	Downregulated	0.00005	0.00298

MPO	0.000	112.127	inf	Upregulated	0.00080	0.02686
MPRIIP	14.371	0.415	-5.113	Downregulated	0.00100	0.03169
MR1	1.076	17.892	4.055	Upregulated	0.00045	0.01795
MRPL54	6482.840	11.728	-9.111	Downregulated	0.00150	0.04086
MSH2	310.346	3.435	-6.498	Downregulated	0.00050	0.01905
MXRA7	9.572	152.388	3.993	Upregulated	0.00055	0.02038
NADSYN1	437.838	4.649	-6.557	Downregulated	0.00060	0.02165
NCAN	12.170	0.000	-inf	Downregulated	0.00010	0.00522
NCF1C	307.061	4.567	-6.071	Downregulated	0.00110	0.03391
NCOA3	0.627	11.227	4.162	Upregulated	0.00165	0.04354
NDUFB6	23.863	0.000	-inf	Downregulated	0.00210	0.04962
NEK9	554.031	6.601	-6.391	Downregulated	0.00210	0.04962
NFXL1	17.842	0.000	-inf	Downregulated	0.00005	0.00298
NHLRC4	0.000	170.224	inf	Upregulated	0.00065	0.02320
NID2	0.000	14.749	inf	Upregulated	0.00005	0.00298
NINJ2	0.000	7.068	inf	Upregulated	0.00005	0.00298
NKAPL	11.110	0.000	-inf	Downregulated	0.00005	0.00298
NLRP6	0.000	0.859	inf	Upregulated	0.00005	0.00298
NPEPL1,STX16	126.825	9.626	-3.720	Downregulated	0.00150	0.04086
NRP1	0.924	18.895	4.354	Upregulated	0.00025	0.01080
NTS	0.000	13.790	inf	Upregulated	0.00010	0.00522
OAS2	391.459	5.096	-6.263	Downregulated	0.00050	0.01905



OLFM2	21.307	0.000	-inf	Downregulated	0.00025	0.01080
PAK4	821.348	1.104	-9.540	Downregulated	0.00140	0.03940
PDE12	47.472	1.767	-4.748	Downregulated	0.00195	0.04757
PDE4A	2.362	0.000	-inf	Downregulated	0.00005	0.00298
PDGFRL	0.000	148.208	inf	Upregulated	0.00055	0.02038
PKD2	200.007	2.440	-6.357	Downregulated	0.00130	0.03752
PDLIM5	5997.300	84.169	-6.155	Downregulated	0.00005	0.00298
PFDN5	4816.400	36.216	-7.055	Downregulated	0.00035	0.01447
PIEZO2	4.184	0.000	-inf	Downregulated	0.00005	0.00298
PKHD1L1	0.000	27.920	inf	Upregulated	0.00015	0.00716
PLEKHG1	175.393	1.897	-6.530	Downregulated	0.00170	0.04401
PLEKHG5,TNFRSF25	13.896	1.553	-3.161	Downregulated	0.00090	0.02935
PML	0.948	178.238	7.554	Upregulated	0.00015	0.00716
PMM2	129.114	2.491	-5.696	Downregulated	0.00150	0.04086
PNMA2	16.276	0.000	-inf	Downregulated	0.00005	0.00298
PNMT	4.372	0.000	-inf	Downregulated	0.00005	0.00298
PNPLA6	35.573	0.369	-6.590	Downregulated	0.00060	0.02165
POLRMT	9.458	0.362	-4.709	Downregulated	0.00180	0.04589
PPEF2	0.000	18.094	inf	Upregulated	0.00005	0.00298
PPM1N	0.000	2.658	inf	Upregulated	0.00005	0.00298
PPP1CA	2049.790	7.976	-8.006	Downregulated	0.00130	0.03752
PPP1R3G	14.955	0.000	-inf	Downregulated	0.00005	0.00298

PPP2R5C	75.785	1.356	-5.805	Downregulated	0.00115	0.03482
PRAM1	0.000	3.057	inf	Upregulated	0.00010	0.00522
PRKAA1	97.106	1.686	-5.848	Downregulated	0.00095	0.03054
PROCA1	7.468	0.000	-inf	Downregulated	0.00005	0.00298
PROL1	27.613	0.000	-inf	Downregulated	0.00005	0.00298
PROSC	3.610	98.071	4.764	Upregulated	0.00140	0.03940
PRR12	213.417	0.500	-8.737	Downregulated	0.00145	0.04014
PSMB11	4.891	0.000	-inf	Downregulated	0.00005	0.00298
PSMD9	192.358	1.203	-7.321	Downregulated	0.00050	0.01905
PTPN23	0.217	6.742	4.957	Upregulated	0.00115	0.03482
PTRH2	87.791	0.000	-inf	Downregulated	0.00005	0.00298
PTS	9.203	0.000	-inf	Downregulated	0.00090	0.02935
QSOX1	7.572	0.559	-3.759	Downregulated	0.00105	0.03297
RAB18	2.691	143.960	5.741	Upregulated	0.00125	0.03718
RAB3IL1	15.123	0.000	-inf	Downregulated	0.00005	0.00298
RAB6B	0.000	8.903	inf	Upregulated	0.00015	0.00716
RAD18	0.000	2.923	inf	Upregulated	0.00010	0.00522
RASGEF1B	0.000	2.803	inf	Upregulated	0.00045	0.01795
RBM10	11.800	0.117	-6.661	Downregulated	0.00015	0.00716
RBM14,RBM14-RBM4,RBM4	3.409	169.880	5.639	Upregulated	0.00120	0.03585
RBM39	8.851	152.169	4.104	Upregulated	0.00185	0.04613
RCSD1	143.939	2.570	-5.808	Downregulated	0.00070	0.02460

RFNG	67.423	0.354	-7.572	Downregulated	0.00155	0.04172
RNF149	138.204	5.887	-4.553	Downregulated	0.00145	0.04014
ROCK1P1	0.000	9.263	inf	Upregulated	0.00020	0.00929
RPL34	1861.930	30.282	-5.942	Downregulated	0.00050	0.01905
RPLP0P2	2.238	0.000	-inf	Downregulated	0.00005	0.00298
RPS5	29863.900	4240.630	-2.816	Downregulated	0.00065	0.02320
RRN3P1	0.000	10.745	inf	Upregulated	0.00010	0.00522
SDF2L1	226.184	8.697	-4.701	Downregulated	0.00210	0.04962
SEMA3G	7.036	0.000	-inf	Downregulated	0.00005	0.00298
SENP1	77.983	0.995	-6.293	Downregulated	0.00200	0.04810
SH2D1B	0.000	2.288	inf	Upregulated	0.00130	0.03752
SHANK3	258.046	1.171	-7.784	Downregulated	0.00200	0.04810
SHC1	303.850	4.551	-6.061	Downregulated	0.00015	0.00716
SKIL	3.563	249.498	6.130	Upregulated	0.00195	0.04757
SLAMF1	0.000	24.432	inf	Upregulated	0.00005	0.00298
SLC2A3	2562.680	4.505	-9.152	Downregulated	0.00145	0.04014
SLC39A13	37.080	0.191	-7.604	Downregulated	0.00135	0.03863
SLC41A2	0.000	5.460	inf	Upregulated	0.00030	0.01256
SLC43A2	599.190	0.988	-9.244	Downregulated	0.00095	0.03054
SLCO4C1	0.000	26.102	inf	Upregulated	0.00005	0.00298
SMTN	1.082	14.755	3.770	Upregulated	0.00130	0.03752
SOX18	0.000	3.099	inf	Upregulated	0.00015	0.00716

SPC24	175.741	0.000	-inf	Downregulated	0.00015	0.00716
SPSB3	223.945	8.420	-4.733	Downregulated	0.00175	0.04479
SSTR1	1.882	0.000	-inf	Downregulated	0.00005	0.00298
ST3GAL4	37.716	0.729	-5.693	Downregulated	0.00055	0.02038
ST8SIA2	1.933	0.000	-inf	Downregulated	0.00005	0.00298
ST8SIA3	7.920	0.000	-inf	Downregulated	0.00005	0.00298
STAG2	1.245	76.678	5.944	Upregulated	0.00090	0.02935
STRN4	1.017	102.211	6.651	Upregulated	0.00070	0.02460
STYX	417.178	5.409	-6.269	Downregulated	0.00080	0.02686
SUV420H2	2.512	0.000	-inf	Downregulated	0.00005	0.00298
SYNDIG1L	0.000	4.403	inf	Upregulated	0.00005	0.00298
TAOK2	15.067	0.143	-6.724	Downregulated	0.00135	0.03863
TARSL2	3.768	0.000	-inf	Downregulated	0.00005	0.00298
TBX15	8.606	0.000	-inf	Downregulated	0.00005	0.00298
TCP11L2	363.919	5.852	-5.959	Downregulated	0.00045	0.01795
TEKT2	2.951	0.000	-inf	Downregulated	0.00005	0.00298
TIGIT	0.000	9.419	inf	Upregulated	0.00005	0.00298
TIMELESS	60.806	0.981	-5.954	Downregulated	0.00085	0.02840
TLR1	0.000	104.195	inf	Upregulated	0.00035	0.01447
TMC1	6.108	0.000	-inf	Downregulated	0.00005	0.00298
TMCC1	15.401	0.239	-6.012	Downregulated	0.00025	0.01080
TMEM151A	0.000	3.256	inf	Upregulated	0.00005	0.00298

TMSB15A	0.000	34.918	inf	Upregulated	0.00015	0.00716
TNFRSF13C	0.000	12.753	inf	Upregulated	0.00010	0.00522
TOMM22	772.966	23.982	-5.010	Downregulated	0.00115	0.03482
TOP1MT	0.345	59.034	7.421	Upregulated	0.00045	0.01795
TPRKB	0.000	29.862	inf	Upregulated	0.00025	0.01080
TRADD	215.120	0.796	-8.078	Downregulated	0.00075	0.02582
TRAPPC6A	12.585	0.000	-inf	Downregulated	0.00005	0.00298
TRIOBP	182.005	1.406	-7.016	Downregulated	0.00140	0.03940
TRNT1	0.000	21.922	inf	Upregulated	0.00005	0.00298
TSPYL5	18.952	0.000	-inf	Downregulated	0.00005	0.00298
TTBK1	1.242	0.000	-inf	Downregulated	0.00005	0.00298
TXK	4.016	0.000	-inf	Downregulated	0.00005	0.00298
UBE2G1	2341.680	15.789	-7.212	Downregulated	0.00130	0.03752
UBE2NL	0.000	4.499	inf	Upregulated	0.00080	0.02686
UBXN10	0.000	17.007	inf	Upregulated	0.00005	0.00298
UNC13C	0.000	3.907	inf	Upregulated	0.00005	0.00298
UQCRB	0.896	104.973	6.873	Upregulated	0.00155	0.04172
VPS13C	9.573	0.383	-4.643	Downregulated	0.00205	0.04896
VPS8	58.873	2.528	-4.542	Downregulated	0.00030	0.01256
WDR87	6.160	0.000	-inf	Downregulated	0.00050	0.01905
YPEL4	0.000	97.024	inf	Upregulated	0.00025	0.01080
ZCCHC12	14.713	0.000	-inf	Downregulated	0.00005	0.00298

ZFAND6	33.113	877.521	4.728	Upregulated	0.00190	0.04686
ZIC1	3.528	0.000	-inf	Downregulated	0.00005	0.00298
ZNF101	0.000	2.617	inf	Upregulated	0.00095	0.03054
ZNF335	18.312	0.105	-7.452	Downregulated	0.00110	0.03391
ZNF584	10.635	0.000	-inf	Downregulated	0.00005	0.00298
ZNF710	132.550	0.805	-7.363	Downregulated	0.00185	0.04613
ZNF876P	0.000	56.823	inf	Upregulated	0.00010	0.00522
ZNRF2	18.166	0.000	-inf	Downregulated	0.00190	0.04686
ZSWIM3	4.348	0.000	-inf	Downregulated	0.00170	0.04401

**Table S5: Levels of circulatory inflammatory proteins in asthmatic and control subjects.** Analysis performed on plasma samples from asthmatic subjects (n = 5) and control subjects (n = 5) using qualitative ELISA. BLD = below level of detection; ALD = above level of detection.

	Protein level (OD at 450 nm)									
	IL-4	IL-5	IL-10	IL-17A	Eotaxin	GM-CSF	IFN $\gamma$	MCP-1	TARC	TNFA
Control_1	0.001	BLD	0.008	0.032	0.210	0.217	BLD	BLD	0.178	0.133
Control_2	0.016	BLD	0.003	0.168	0.146	0.165	0.011	BLD	0.165	0.038
Control_3	0.046	0.075	0.036	0.372	1.142	0.232	0.086	0.143	0.796	0.237
Control_4	0.013	0.003	0.006	0.084	0.270	0.333	BLD	BLD	0.357	0.051
Control_5	0.019	0.004	0.008	0.004	0.215	0.054	BLD	BLD	0.055	0.042
Asthma_1	0.022	0.008	0.009	0.356	0.454	0.187	BLD	BLD	0.268	0.063
Asthma_2	0.202	0.055	0.164	ALD	1.423	ALD	3.877	0.617	2.614	0.619
Asthma_3	0.002	BLD	0.005	0.094	0.137	0.538	0.011	BLD	0.404	0.071
Asthma_4	0.269	0.020	0.043	1.858	0.529	1.582	0.142	0.035	2.516	0.212
Asthma_5	0.019	0.005	0.014	0.068	0.207	0.576	0.019	BLD	0.670	0.085
Control Mean	0.019	0.027	0.012	0.132	0.397	0.200	0.049	0.143	0.310	0.010
Asthma Mean	0.102	0.027	0.047	0.594	0.550	0.720	1.012	0.326	1.294	0.210
Fold Change	5.530	0.988	3.853	4.513	1.387	3.607	20.871	2.280	4.173	2.101
P Value	0.249	0.398	0.209	0.413	0.841	0.111	0.195	0.607	0.095	0.310

**Table S6: Total circulatory IgE concentrations in asthmatic and control subjects.** Total IgE concentrations present in asthma plasma samples (n = 4) and control plasma samples (n = 5) were measured in duplicate using sandwich ELISA (*Genesis Diagnostics Ltd*) and determined using a Sigmoidal 4 parameter curve. Test was repeated for Asthma\_5, and so standard absorbance values for the second test are shown in blue.

	Sample	Absorbance (450nm) Duplicates		Average absorbance (450nm)	Average absorbance - blank	Concentration (IU/ml)	Concentration (ng/ ml)
Standards (IU/ml)	0	0.259/ 0.181	0.254/ 0.256	0.257/0.219	0.000/ 0.000	NA	NA
	50	0.405/ 0.380	0.405/0.382	0.405/ 0.381	0.149/ 0.163	NA	NA
	150	0.810/ 0.682	0.787/ 0.665	0.799/ 0.674	0.542/0.455	NA	NA
	375	1.536/1.317	1.609/ 1.285	1.573/ 1.301	1.316/ 1.083	NA	NA
	1250	2.758/ 1.631	2.819/ 2.534	2.789/ 2.083	2.532/ 1.864	NA	NA
<b>Positive Control</b>		0.538/ 0.526	0.542/ 0.500	0.540/ 0.513	0.284/ 0.295	NA	NA
Plasma Samples	Control_1	0.315	0.324	0.320	0.063	121.275	291.060
	Control_2	0.187	0.198	0.193	-0.064	NA	NA
	Control_3	0.419	0.417	0.418	0.162	267.955	643.092
	Control_4	0.304	0.301	0.303	0.046	91.465	219.516
	Control_5	0.190	0.207	0.199	-0.058	NA	NA
	Asthma_2	1.187	1.176	1.182	0.925	1256.625	3015.900
	Asthma_3	0.162	0.182	0.172	-0.085	NA	NA
	Asthma_4	0.965	1.021	0.993	0.737	999.240	2398.176
Asthma_5	0.244	0.233	0.2385	0.020	NA	NA	



**Table S7: Circulatory endotoxin concentrations present in asthmatic and control subjects.** Endotoxin concentrations present in plasma samples from asthmatic subjects (n = 5) and control subjects (n = 5) were measured in triplicate a Pierce™ Limulus Amebocyte Lysate (LAL) Chromogenic Endotoxin quantitative kit (*Thermo fisher Scientific*) and determined using a Sigmoidal 4 parameter curve.

	Sample	Absorbance (450nm) Triplicates			Average absorbance (450nm)	Average absorbance - blank	Concentration (EU/ml)
Standards (EU/ml)	0.00	0.289	0.273	0.271	0.278	0.000	NA
	0.10	0.529	0.560	0.574	0.554	0.277	NA
	0.25	1.238	1.310	1.360	1.303	1.025	NA
	0.50	1.987	1.827	1.889	1.901	1.623	NA
	1.00	2.099	2.015	1.906	2.007	1.729	NA
Plasma Samples	Control_1	0.324	0.321	0.332	0.326	0.048	3.100
	Control_2	0.335	0.325	0.322	0.327	0.050	3.100
	Control_3	0.315	0.320	0.297	0.311	0.033	3.000
	Control_4	1.034	0.377	0.362	0.370	0.092	3.300
	Control_5	0.363	0.285	0.297	0.315	0.037	3.100
	Asthma_1	0.303	0.315	0.301	0.306	0.029	3.000
	Asthma_2	0.296	0.309	0.307	0.304	0.026	3.000
	Asthma_3	0.320	0.321	0.328	0.323	0.045	3.050
	Asthma_4	0.308	0.279	0.286	0.291	0.013	2.900
	Asthma_5	0.325	0.319	0.321	0.322	0.044	3.050

**Table S8: Molecular properties of the V3-V4 16S Amp oligonucleotide primers with the Ion torrent sequencing motifs incorporated.** The V3-V4 16S Amp oligonucleotide primers were modified to contain the ion torrent sequencing motifs in order to attach the motifs to V3-V4 amplicons generated from human plasma samples. The truncated TrP1 adaptor (green) was attached to the reverse V3-V4 16S primer, and the A1 adaptor (orange), sequencing key (red), and barcode (blue) motifs were attached to the forward V3-V4 16S Amp primer.

Primer	Corresponding plasma sample	Sequence (5' -> 3')	Concentration [pmol/μl]	Melting temperature (°C)	GC Content (%)
mV3-V4 Rev Trp1	NA	CCTCTCTATGGGCAGTCGGTGATGACTACH VGGGTATCTAATCC (44)	10.0	76.0	52.3
mV3-V4 Fwd BC1	Asthma_1	CCATCTCATCCCTGCGTGTCTCCGACTCAGC TAAGGTAACCCTACGGGNGGCWGCAG(57)	10.0	82.7	60.5
mV3-V4 Fwd BC2	Asthma_2	CCATCTCATCCCTGCGTGTCTCCGACTCAGT AAGGAGAACCCTACGGGNGGCWGCAG (57)	10.0	82.7	60.5
mV3-V4 Fwd BC3	Asthma_3	CCATCTCATCCCTGCGTGTCTCCGACTCAGA AGAGGATCCCTACGGGNGGCWGCAG (57)	10.0	82.7	60.5
mV3-V4 Fwd BC4	Asthma_4	CCATCTCATCCCTGCGTGTCTCCGACTCAGT ACCAAGATCCCTACGGGNGGCWGCAG (57)	10.0	82.7	60.5
mV3-V4 Fwd BC5	Asthma_5	CCATCTCATCCCTGCGTGTCTCCGACTCAGC AGAAGGAACCCTACGGGNGGCWGCAG (57)	10.0	83.4	62.3

mV3-V4 Fwd BC6	Control_1	CCATCTCATCCCTGCGTGTCTCCGACTCAGC TGCAAGTTCCTACGGGNGGCWGCAG (57)	10.0	83.4	62.3
mV3-V4 Fwd BC7	Control_2	CCATCTCATCCCTGCGTGTCTCCGACTCAGT TCGTGATTCCTACGGGNGGCWGCAG (57)	10.0	83.4	62.3
mV3-V4 Fwd BC8	Control_3	CCATCTCATCCCTGCGTGTCTCCGACTCAGT TCCGATAACCCTACGGGNGGCWGCAG (57)	10.0	83.4	62.3
mV3-V4 Fwd BC9	Control_4	CCATCTCATCCCTGCGTGTCTCCGACTCAGT GAGCGGAACCCTACGGGNGGCWGCAG (57)	10.0	83.4	62.3
mV3-V4 Fwd BC10	Control_5	CCATCTCATCCCTGCGTGTCTCCGACTCAGC TGACCGAACCCCTACGGGNGGCWGCAG (57)	10.0	84.2	64.0

**Table S9: Molecular properties of the V4 16S Amp oligonucleotide primers with the Ion torrent sequencing motifs incorporated.** The V4 16S oligonucleotide primers were modified to contain the ion torrent sequencing motifs in order to attach the motifs to V4 amplicons generated from human plasma samples. The truncated TrP1 adaptor (green) was attached to the reverse V4 16S Amp primer, and the A1 adaptor (orange), sequencing key (red), and barcode (blue) motifs were attached to the forward V4 16S primer.

Primer	Corresponding plasma sample	Sequence (5' - > 3')	Concentration [pmol/μl]	Melting temperature (°C)	GC Content (%)
mV4 Rev Trp1	NA	CCTCTCTATGGGCAGTCGGTGATGGACT ACHVGGGTWTCTAAT (43)	10.0	75.2	51.2
mV4 Fwd BC1	Asthma_1	CCATCTCATCCCTGCGTGTCTCCGACTCA GCTAAGGTAACGTGCCAGCMGCCGCG GTAA (59)	10.0	83.0	60.2
mV4 Fwd BC2	Asthma_2	CCATCTCATCCCTGCGTGTCTCCGACTCA GTAAGGAGAACGTGCCAGCMGCCGCG GTAA (59)	10.0	83.0	60.2
mV4 Fwd BC3	Asthma_3	CCATCTCATCCCTGCGTGTCTCCGACTCA GAAGAGGATTCGTGCCAGCMGCCGCG GTAA (59)	10.0	83.0	60.2
mV4 Fwd BC4	Asthma_4	CCATCTCATCCCTGCGTGTCTCCGACTCA GTACCAAGATCGTGCCAGCMGCCGCGG TAA (59)	10.0	83.0	60.2
mV4 Fwd BC5	Asthma_5	CCATCTCATCCCTGCGTGTCTCCGACTCA GCAGAAGGAACGTGCCAGCMGCCGCG GTAA (59)	10.0	83.6	61.9

mV4 Fwd BC6	Control_1	CCATCTCATCCCTGCGTGTCTCCGACTCA GCTGCAAGTTCGTGCCAGCMGCCGCGG TAA (59)	10.0	83.6	61.9
mV4 Fwd BC7	Control_2	CCATCTCATCCCTGCGTGTCTCCGACTCA GTTTCGTGATTCGTGCCAGCMGCCGCGG TAA (59)	10.0	83.0	60.2
mV4 Fwd BC8	Control_3	CCATCTCATCCCTGCGTGTCTCCGACTCA GTTCCGATAACGTGCCAGCMGCCGCGG TAA (59)	10.0	83.0	60.2
mV4 Fwd BC9	Control_4	CCATCTCATCCCTGCGTGTCTCCGACTCA GTGAGCGGAACGTGCCAGCMGCCGCG GTAA (59)	10.0	84.3	63.6
mV4 Fwd BC10	Control_5	CCATCTCATCCCTGCGTGTCTCCGACTCA GCTGACCGAACGTGCCAGCMGCCGCG GTAA (59)	10.0	84.3	63.6

## S7: R code utilised to generate a KEGG Orthologue Abundance Graph

```
data <- read.table("KEGG Orthologue Abundance values.txt", header = T)

library("RColorBrewer")

library("ggplot2")

library("vegan")

library("scales")

library("grid")

library("reshape2")

library("dplyr")

theme_set(theme_bw()) # Command used to set graph background colour

data$KEGG_Pathway <- factor(data$KEGG_Pathway, levels = c("KEGG Orthologues")) # Command
used to set order of the legend

# Generate jpeg file

jpeg(file = "KEGG Orthologue Abundance graph.jpeg")

jpeg("KEGG Orthologue Abundance graph.jpeg", height = 15*300, width = 25*300, res = 400,
pointsize = 15)

# Plot

p = ggplot(data, aes(x=Species, y=Count, fill=KEGG_Pathway)) # Commands used to generate and
format a relative abundance graph

p = p + geom_bar(aes(), stat="identity", position="stack")

p = p + scale_fill_manual(values=c("Colours"))

p = p + scale_y_continuous(expression(paste("Abundance (%)"))) # Sets Y axis label

p = p + theme(axis.text = element_text(size = 20), axis.title=element_text(size = 20))

p = p + theme(axis.title.x = element_blank())

p = p + theme(legend.text = element_text(size = 18))

p = p + theme(legend.title = element_text(size = 18))

p = p + theme(axis.text.x=element_text(angle=45,hjust=1))

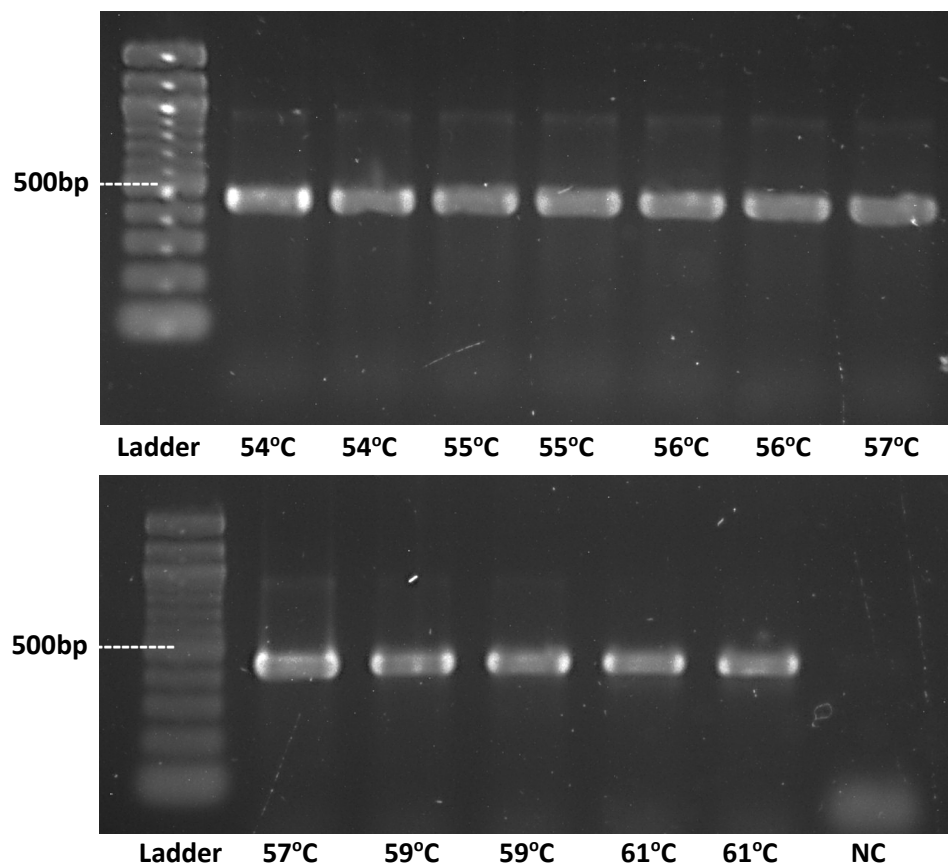
p = p + theme(legend.position="right") + guides(fill=guide_legend(ncol =1)) # Formats legend
position

p = p + theme(plot.margin=unit(c(1,1,1,1),"cm"))

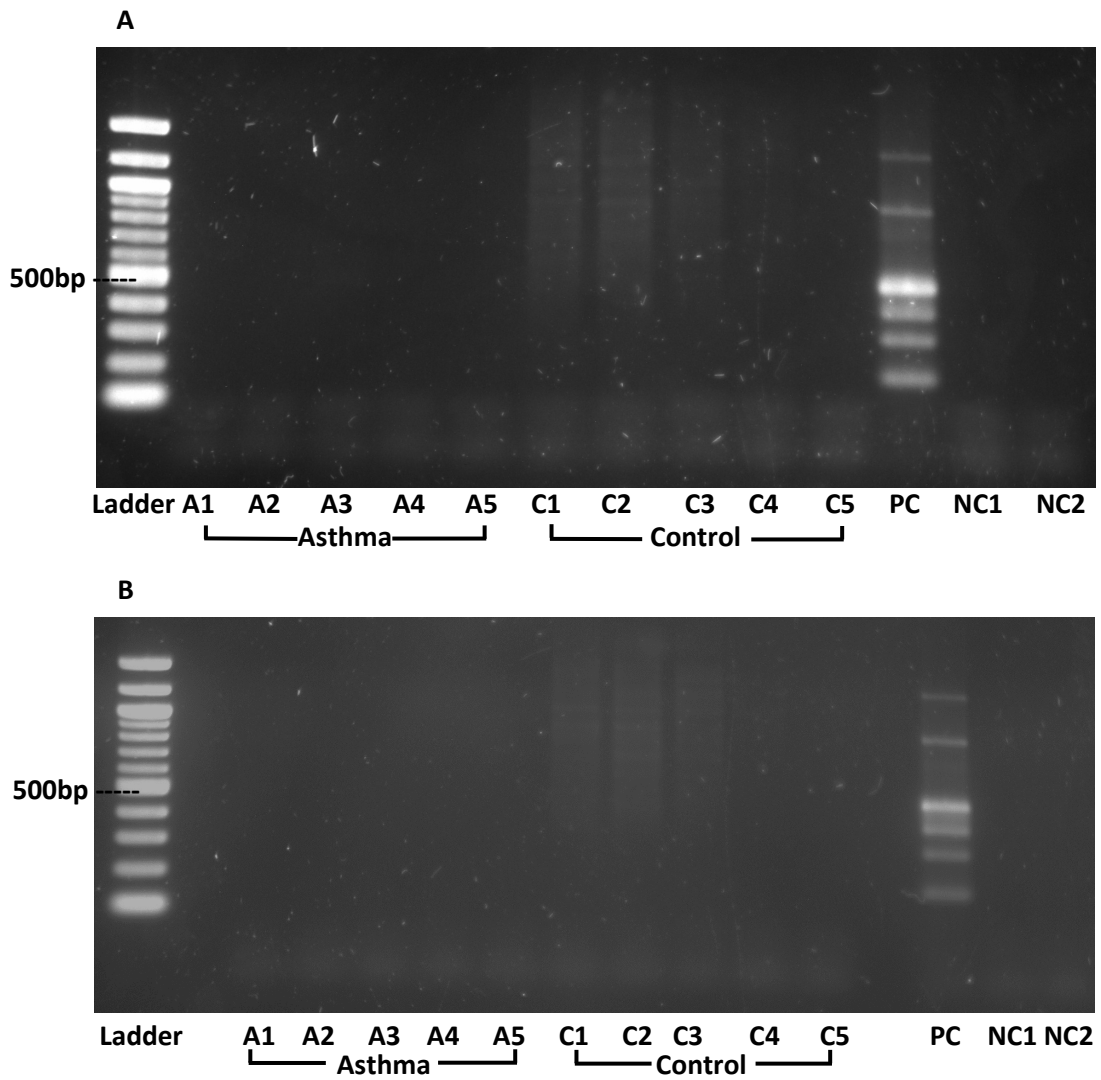
p

dev.off ()
```

**Figure S2: Gradient PCR amplification of the V3-V4 region of the 16S rRNA gene using *Escherichia coli* DNA.** End-point PCR was performed on *Escherichia coli* DNA (25ng/ $\mu$ l) using the optimised GoTaq Green master mix PCR protocol and the V3-V4 oligonucleotide primers. PCR was performed in 35 cycles and utilised a range of annealing temperatures above and below the mean melting temperature of the V3-V4 oligonucleotide primers to determine the optimum primer annealing temperature. 55°C was determined to be the optimum annealing temperature, as demonstrated by the increased thickness and brightness of the DNA band generated by the 55°C PCR products.

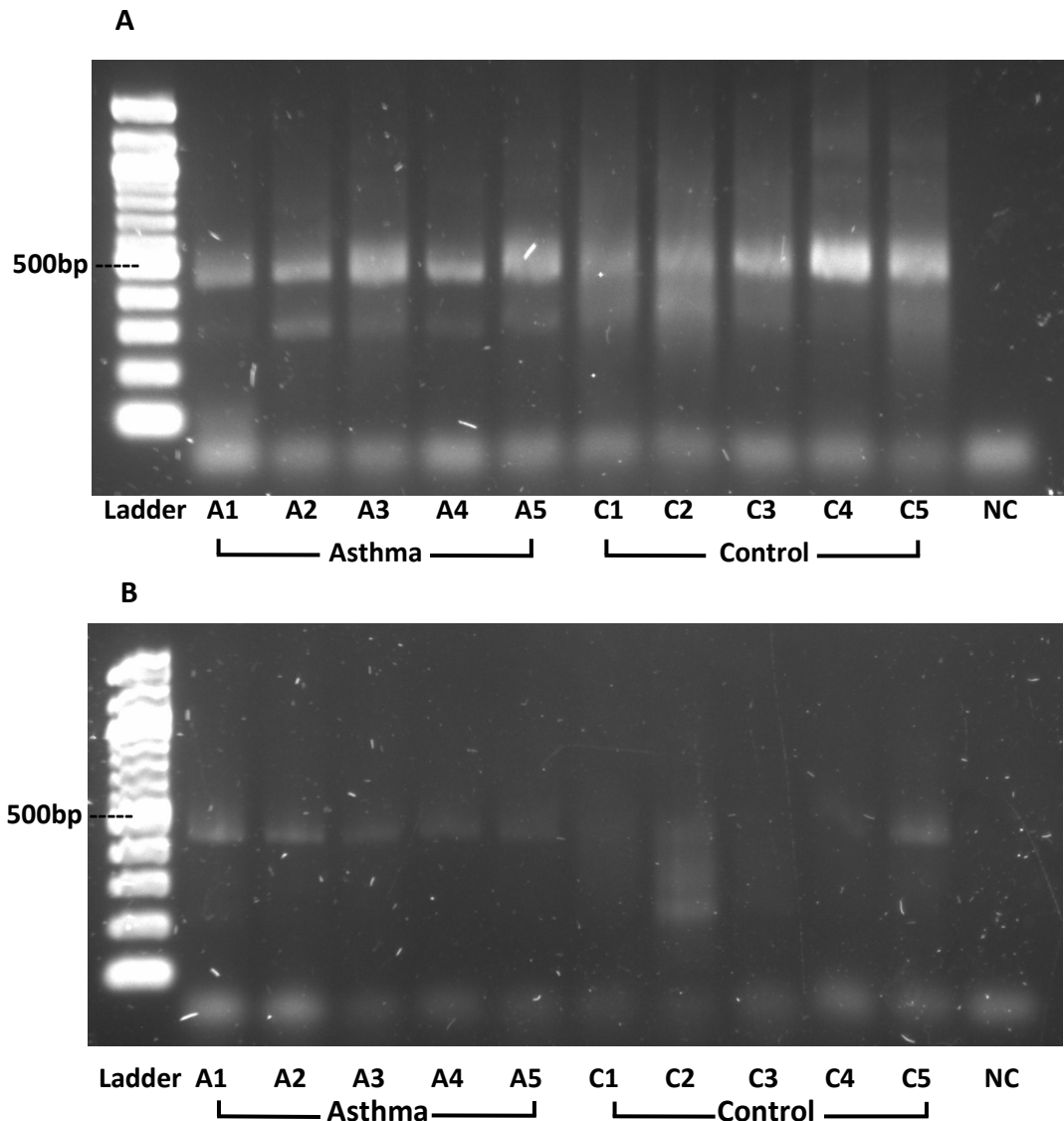


**Figure S3: Amplification of the V3-V4 region of the bacterial 16S rRNA gene from microbial DNA extracted from the human plasma samples.** Microbial DNA was extracted from plasma samples from asthmatic subjects (n = 5, A lanes) and control subjects (n = 5, C lanes) using the QIAamp UCP Mini Pathogen kit. The extracted microbial DNA was purified and the V3-V4 region of the bacterial 16S rRNA gene was amplified using 35 cycles (A) and 38 cycles (B) of end-point PCR using an optimised GoTaq Green master mix PCR protocol.

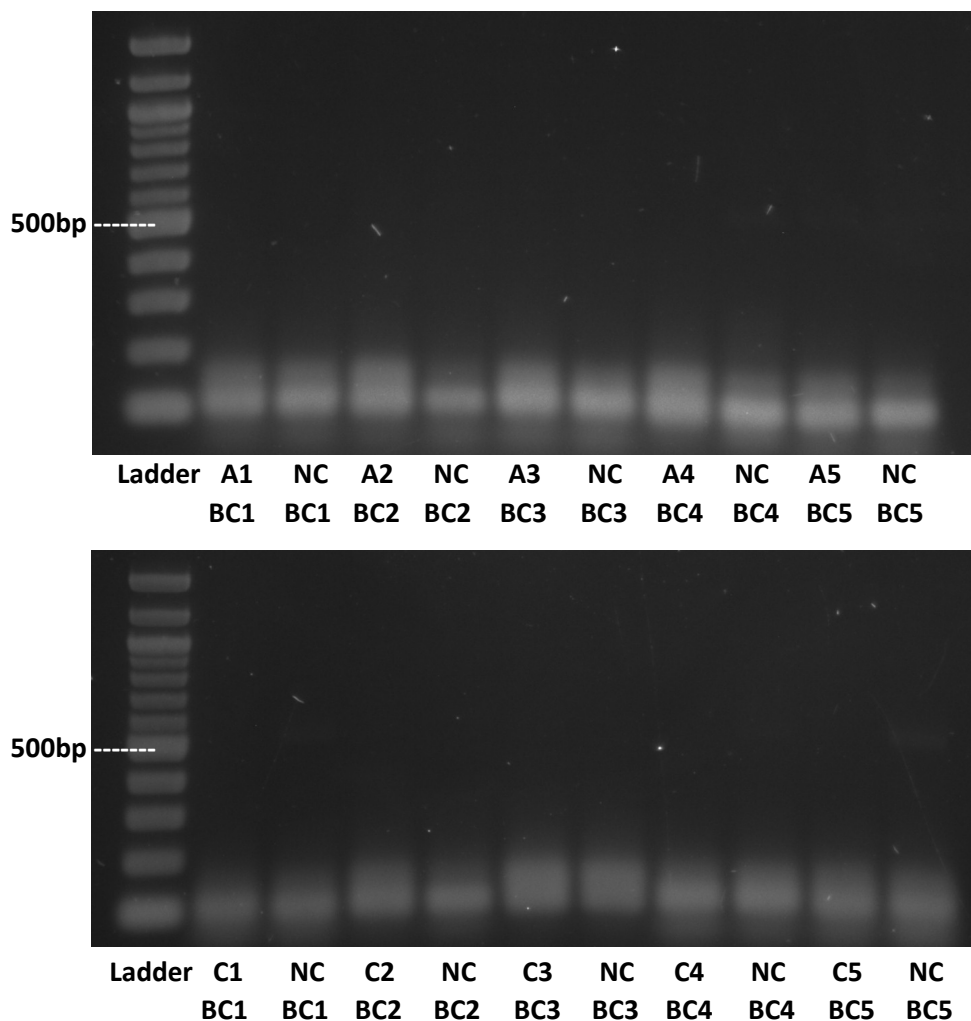




**Figure S4: End-point PCR amplification of the V3-V4 region of the bacterial 16S rRNA gene performed directly on human plasma samples.** 35 cycles of end-point PCR amplification was performed directly on plasma samples from asthmatic subjects (n = 5, A lanes) and control subjects (n = 5, C lanes) in 20 $\mu$ l Phusion blood direct PCR using a 5% plasma concentration (A) and a 20% plasma concentration (B). Comparison of V3-V4 amplification generated using 5% human plasma compared to 20% human plasma revealed that 5% plasma was optimum, as demonstrated by increased band width and brightness of the 5% PCR products compared to the 20% PCR products.

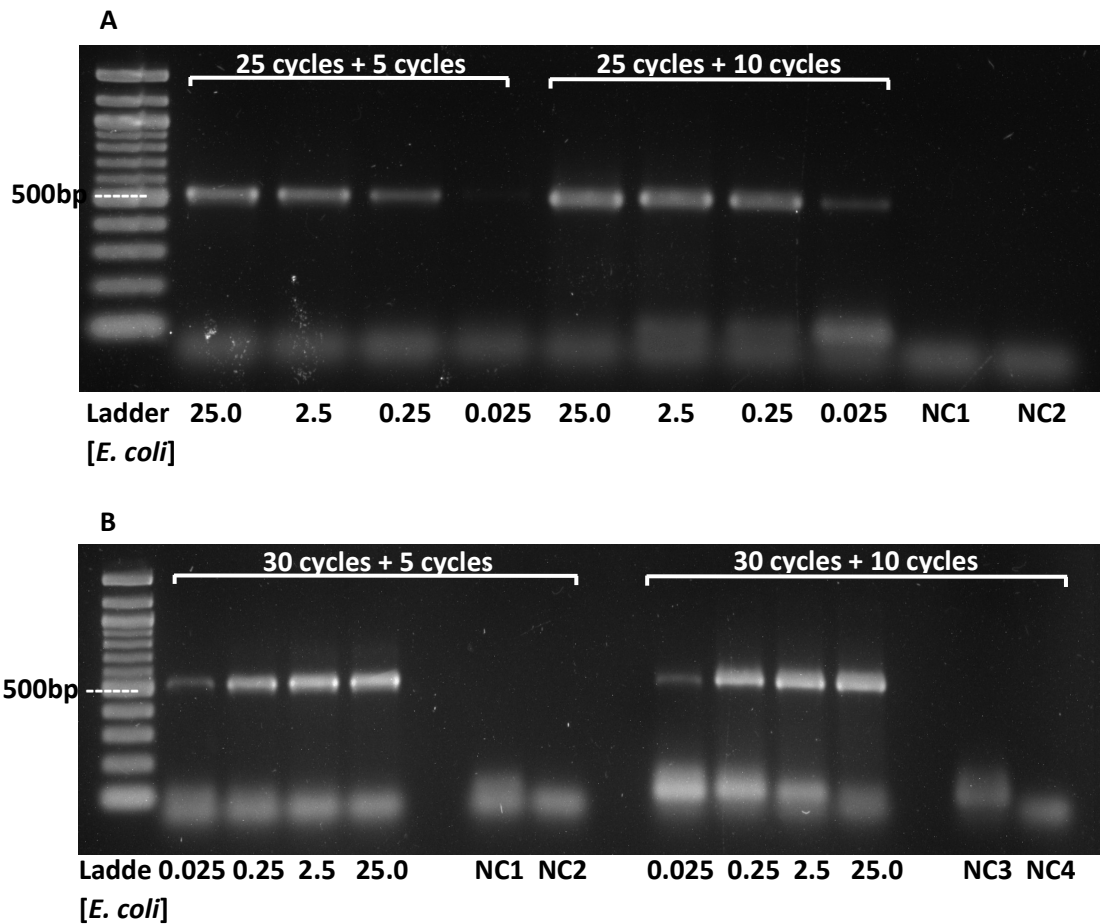


**Figure S5: Generation of V3-V4 16S rRNA amplicons containing the ion torrent sequencing motifs from human plasma samples using end-point PCR.** Amplification of the V3-V4 region of the bacterial 16S rRNA gene was performed directly on plasma samples from asthmatic subjects (n = 5, A lanes) and control subjects (n = 5, C lanes) using 35 cycles of the optimised Phusion blood direct PCR protocol and V3-V4 primers modified to contain Ion torrent sequencing motifs. For each plasma sample, a different V3-V4 forward primer that contained a unique barcode sequence was utilised in the PCR, and a complementary negative control (NC lanes) was generated for each sample to test for environmental and/or reagent bacterial contamination.



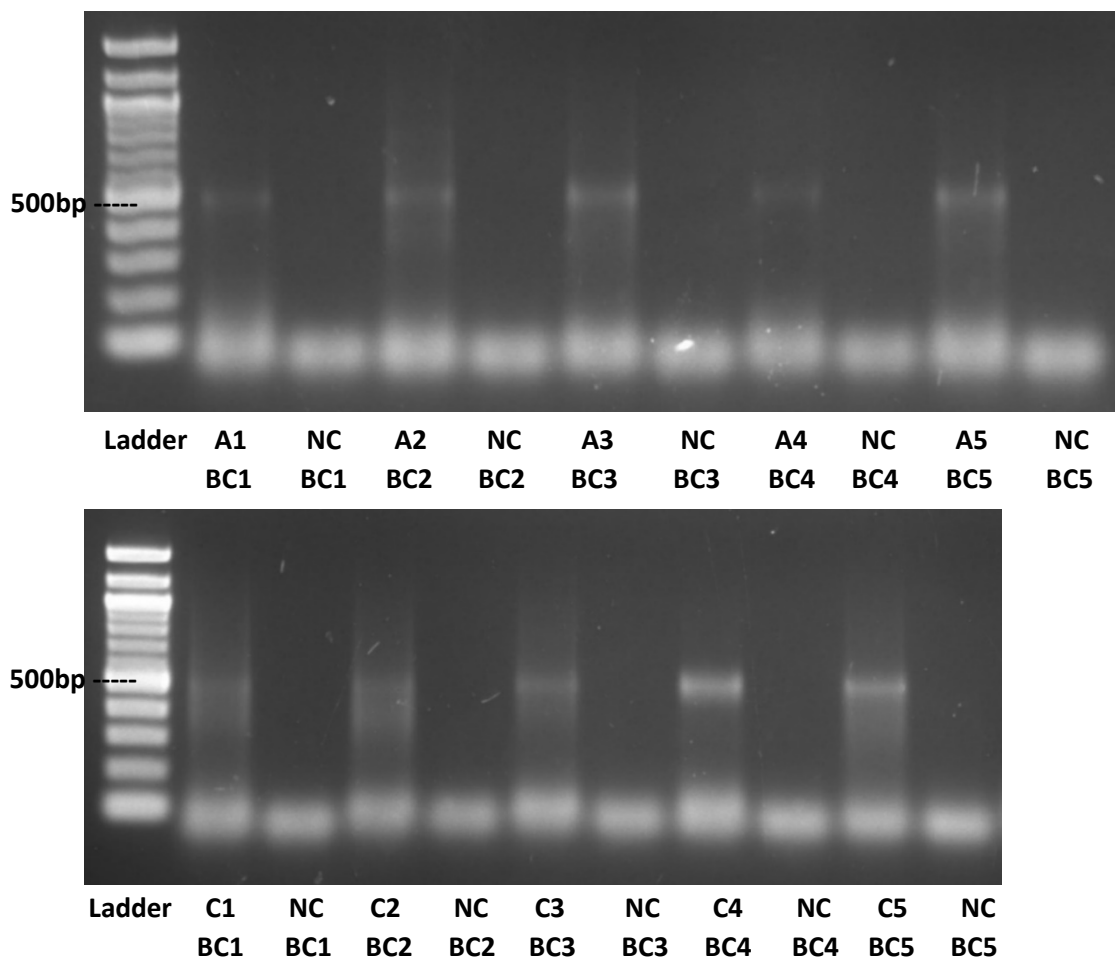
*Abbreviations: BC, barcoded V3-V4 16S oligonucleotide primer used*

**Figure S6: Nested PCR amplification of the V3-V4 region of the bacterial 16S rRNA gene using *Escherichia coli* DNA at varying concentrations.** DNA samples containing varying concentrations of *E. coli* DNA (ranging from 0.025ng/μl – 25.0ng/μl) first underwent 25 (A) or 30 (B) cycles of PCR using the optimised GoTaq Green master mix PCR protocol in order to amplify the V3-V4 region of the 16S rRNA gene. The PCR products were purified and then underwent a further 5 or 10 cycles of PCR (A & B) using the optimised GoTaq Green master mix PCR protocol and the modified V3-V4 primers. The first stage of PCR was designed to amplify the V3-V4 region whilst the second stage was designed to attach the Ion torrent sequencing motifs onto the V3-V4 amplicons.

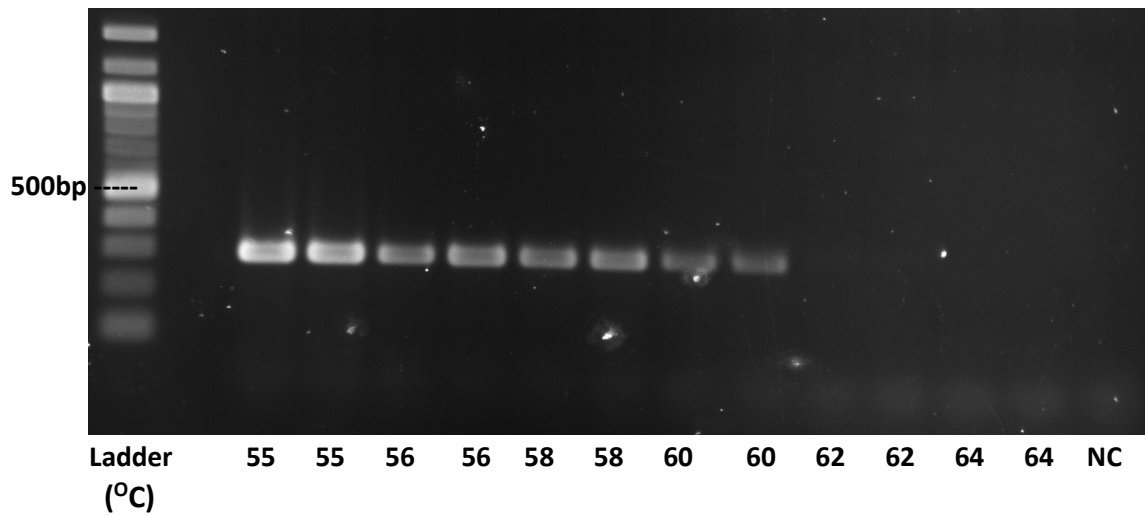


Abbreviations: NC1, negative control generated from 5 cycles of second stage PCR; NC2, negative control generated from 10 cycles of second stage PCR; NC3, negative control generated from first stage PCR; NC4, negative control generated from second stage PCR.

**Figure S7: Generation of V3-V4 amplicons containing the ion torrent sequencing motifs from human plasma samples from asthmatic subjects and non-asthmatic control subjects using nested PCR.** Plasma samples from asthmatic subjects (n = 5, A lanes) and control subjects (n = 5, C lanes) first underwent 35 cycles of end-point PCR using the optimised GoTaq Green master mix PCR protocol and V3-V4 16S Amp oligonucleotides in order to amplify the V3-V4 region of the bacterial 16S rRNA gene. The V3-V4 amplicons were then purified using the MinElute protocol and the underwent an additional 7 cycles of end-point PCR using the optimised GoTaq Green master mix PCR protocol and the modified V3-V4 primers in order to attach the ion torrent sequencing motifs to the V3-V4 amplicons.



**Figure S8: Gradient PCR amplification of the V4 region of the 16S rRNA gene using *Escherichia coli* DNA.** End-point PCR was performed on *E.coli* DNA (25ng/ $\mu$ l) using a GoTaq Green master mix PCR protocol and the V4 16S rRNA primers. PCR was performed in 35 cycles and a range of annealing temperatures above and below the mean annealing temperature of the V4 primers were utilised. 55°C was found to be the optimum annealing temperature for the V4 primers, as demonstrated by increased band thickness and brightness of the 55°C PCR products.



**Table S10: The number of V4 reads generated from human plasma samples following amplification of the V4 region of the 16S rRNA bacterial gene and Illumina sequencing of the V4 amplicons.** Following successful generation of V4 amplicons containing Illumina sequencing motifs from plasma samples from asthmatic subjects (n = 5) and control subjects (n = 5), the V4 amplicons were sequenced using Illumina MiSeq sequencing. Low-quality V4 reads were then removed using *Nephele* 2.0 technology.

<b>Sample</b>	<b>Number of raw V4 reads</b>	<b>Number of high-quality V4 reads</b>	<b>Number of OTUs detected</b>
Control_1	71,007	20,367	221
Control_2	100,419	34,243	311
Control_3	92,603	19,680	243
Control_4	88,650	10,929	199
Control_5	95,878	26,469	395
Asthma_1	94,162	36,136	364
Asthma_2	104,464	19,459	278
Asthma_3	110,121	35,213	277
Asthma_4	72,524	17,155	280
Asthma_5	98,741	27,413	399
Negative Control	57,239	0	-

Table S11: Alpha diversity of the blood microbiome detected in plasma samples from asthma subjects compared to plasma samples from control subjects. Alpha diversity was measured using rarefied OTU tables generated from 16S rRNA sequencing data generated from plasma samples collected from asthmatic subjects (n = 5) and control subjects (n =5). Shannon diversity index scores were generated from OTU tables in order to measure the richness and evenness of bacterial taxa present in the plasma samples. Chao1 index scores were measured to determine the predicted number of bacterial taxa present in the plasma samples by extrapolating out the number of rare organisms that may not have been detected due to under-sampling.

<b>Sample</b>	<b>Shannon Diversity Index</b>	<b>Chao1 Diversity Index</b>
Control_1	2.144	252.577
Control_2	2.874	332.875
Control_3	2.244	492.000
Control_4	2.320	349.000
Control_5	2.824	409.977
Asthma_1	3.042	317.763
Asthma_2	3.018	359.097
Asthma_3	2.233	399.071
Asthma_4	3.038	333.700
Asthma_5	3.727	515.849

**Table S12. End-point PCR amplification of the 16S rRNA gene from bacterial DNA extracted from cultured bacterial colonies generated from human plasma samples.** DNA was extracted from bacterial colonies cultured from asthma plasma samples (n = 4) and control plasma samples (n = 4) using thermal lysis. The 16S rRNA gene was then amplified using oligonucleotide primers that target the 16S rRNA gene and two PCR protocols; the GoTaq Green master mix protocol and the Phusion blood direct protocol.

<b>Sample</b>	<b>GoTaq Green master mix Protocol</b>	<b>Phusion Blood Direct Protocol</b>
<b>Control Subjects</b>		
<b>Control_1</b>		
Columbia Blood agar	Y	Y
CLED Medium	NA*	NA
A.G.I.R agar	NA	NA
<b>Control_2</b>		
Columbia Blood agar	Y	Y
CLED Medium	Y	Y
A.G.I.R agar	NA	NA
<b>Control_3</b>		
Columbia Blood agar	Y	Y
CLED Medium	N	Y
A.G.I.R agar	N	Y
<b>Control_4</b>		
Columbia Blood agar	Y	Y
CLED Medium	N	Y
A.G.I.R agar	N	Y
<b>Control_5</b>		
Columbia Blood agar	NA	NA
CLED Medium	NA	NA
A.G.I.R agar	NA	NA
<b>Asthmatic Subjects</b>		
<b>Asthma_2</b>		
Columbia Blood agar	Y	NA
CLED Medium	N	N
A.G.I.R agar	N	N
<b>Asthma_3</b>		
Columbia Blood agar	NA	NA
CLED Medium	NA	NA



A.G.I.R agar	NA	NA
<b>Asthma_4</b>		
Columbia Blood agar	NA	NA
CLED Medium	Y	NA
A.G.I.R agar	NA	NA
<b>Asthma_5</b>		
Columbia Blood agar	Y	Y
CLED Medium	N	N
A.G.I.R agar	N	Y

*\*NA = when bacterial colonies were not isolated from the agar plates, and thus 16S amplification was not performed, Y = successful amplification of the 16S rRNA gene, N = unsuccessful amplification of the 16S rRNA gene.*

**Table S13: The number of V4 reads generated from human serum samples following amplification of the V4 region of the 16S rRNA bacterial gene and Illumina sequencing of the V4 amplicons.** Following successful generation of V4 amplicons containing Illumina sequencing motifs from serum samples from control subjects (n = 11), asthmatic subjects (n = 4), allergic rhinitis subjects (n = 7) and hyper-allergic subjects (n = 3), the V4 amplicons were sequenced using Illumina MiSeq sequencing. Low-quality reads and chimeric sequences were then removed using *Nephele* 2.0 technology and the remaining reads aligned to bacterial operational taxonomic units at a 99% similarity threshold.

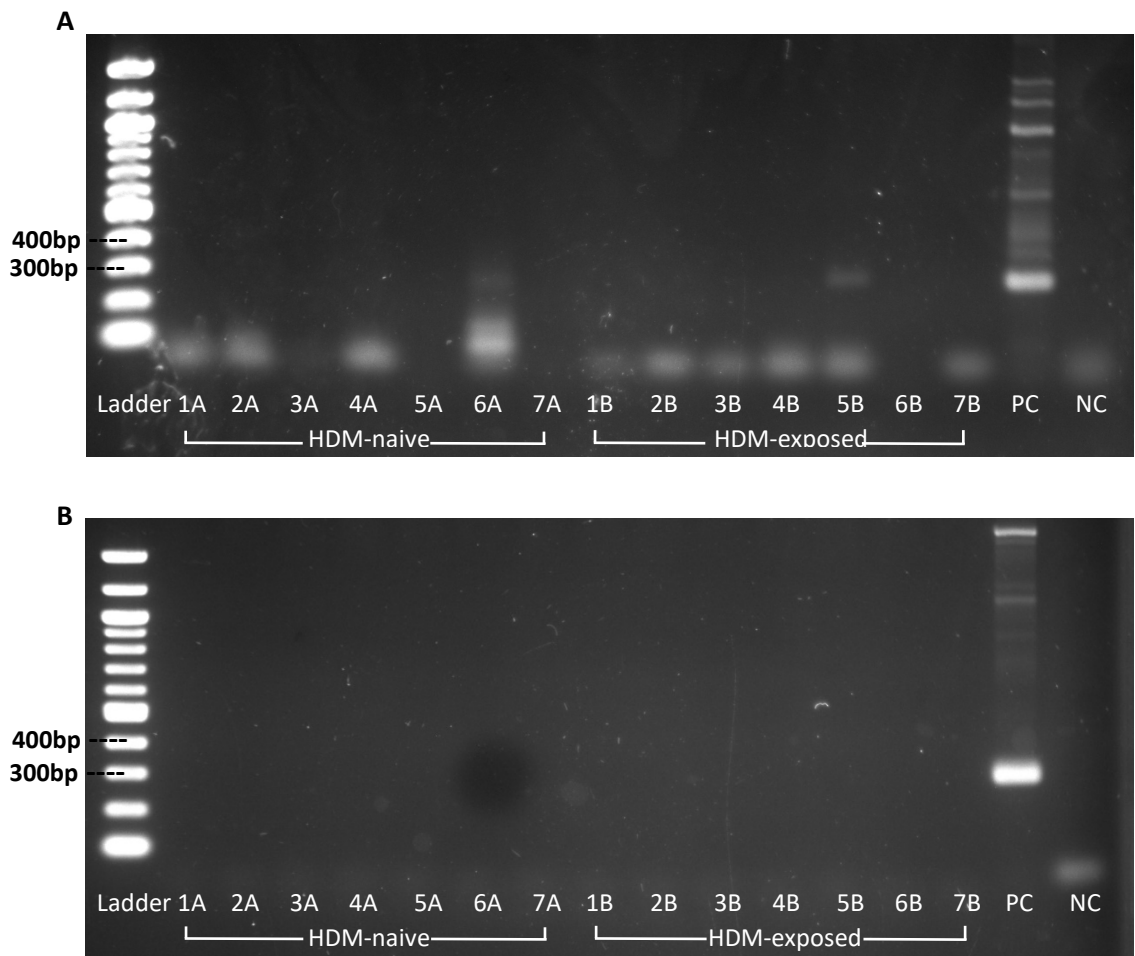
Sample	Number of raw reads	Length of trimmed Reads (bp)	Number of OTU-aligned Reads	Number of detected OTUs
Control_1	81,169	251	64,201	799
Control_2	88,591	251	77,231	1,173
Control_3	124,460	251	87,748	1,270
Control_4	96,530	251	60,310	738
Control_5	145,011	251	124,383	2,206
Control_6	116,807	251	74,420	1,611
Control_7	109,751	251	77,140	1,215
Control_8	120,101	251	101,703	1,487
Control_9	149,188	251	128,000	1,235
Control_10	91,167	251	70,798	1,165
Control_11	68,467	251	59,431	1,064
Asthma_1	106,678	251	94,415	1,323
Asthma_2	76,773	251	58,557	810
Asthma_3	77,430	251	58,396	877
Asthma_4	100,457	251	71,575	751
Allergic rhinitis_1	71,991	251	61,979	1,334
Allergic rhinitis_2	122,505	251	80,559	1,241
Allergic rhinitis_3	85,857	251	71,728	1,665
Allergic rhinitis_4	122,733	251	102,874	2,757
Allergic rhinitis_5	87,148	251	70,729	1,332
Allergic rhinitis_6	129,170	251	112,915	1,478
Allergic rhinitis_7	101,275	251	87,950	1,903
Hyper-Allergic_1	134,085	251	94,813	1,126
Hyper-Allergic_2	89,560	251	68,123	1,084
Hyper-Allergic_3	125,616	251	109,027	1,447
Negative Control	402	251	204	93

**Table S14: Microbial functions predicted to be significantly altered in the circulatory microbiome of hyper-allergic subjects compared to the circulatory microbiome of non-atopic subjects.** PICRUSt analysis was performed on the 16S rRNA sequencing data generated from serum samples taken from hyper-allergic subjects (AA\_AR, N = 3) and control subjects (CS, n = 11) to determine whether changes in the microbial populations present in the atopic circulatory microbiome significantly altered overall functional activity of the microbiome. Abundance of KEGG pathways at levels 1 – 3 was determined, and LEfSe analysis was performed to identify KEGG pathways with significantly altered abundance in the hyper-allergic serum compared to the control circulatory microbiome. Biologically significant altered KEGG abundance is defined as having a *P* value < 0.05 and an LDA effect size > 2.0.

Function	Highest group abundance average (log %)	Group with highest average abundance	LDA Effect Size	<i>P</i> Value
C: Cytoskeleton proteins	0.84	NA	NA	0.0465
M: Thiamine metabolism	0.49	CS	2.10	0.0348
O: PPAR signalling pathway	0.00	CS	2.17	0.0316
M: Toluene degradation	3.26	AA.AR	2.35	0.0240
E: MAPK signaling pathway - yeast	2.19	NA	NA	0.0240
M: Dioxin degradation	4.10	AA.AR	2.71	0.0158
M: Flavonoid biosynthesis	3.14	AA.AR	2.15	0.0102
M: Retinol metabolism	3.43	AA.AR	2.24	0.0102

*Abbreviations: C, Cellular process level 1 KEGG category; M, Metabolism level 1 KEGG category; O, Organismal systems level 1 KEGG category; E, Environmental processing information level 1 KEGG category; NA, defines level 3 KEGG pathways with a significant P value but an LDA effect size < 2.0*

**Figure S9: Direct PCR amplification of the V4 region of the 16S rRNA gene from microbial DNA present in murine plasma samples.** End-point PCR amplification of the V4 region of the 16S rRNA gene was performed directly on plasma samples from control mice (HDM-naïve, n = 7) and mice exposed to the HDM allergen (HDM-exposed, n = 7). PCR was performed using an optimised Phusion blood direct protocol (A) and a SureDirect blood PCR protocol (B).



**Table S15: The number of V4 reads generated from murine BAL samples following amplification of the V4 region of the 16S rRNA bacterial gene and Illumina sequencing of the V4 amplicons.** Following successful generation of V4 amplicons containing Illumina sequencing motifs from BAL samples from HDM-exposed (n = 7) and HDM-naive mice (n = 7), the V4 amplicons were sequenced using Illumina MiSeq sequencing. Low-quality reads and chimeric sequences were then removed using *Nephele* 2.0 technology and the remaining reads aligned to bacterial operational taxonomic units at a 99% similarity threshold.

Sample	Number of raw reads	Length of trimmed Reads (bp)	Number of OTU-aligned Reads	Number of detected OTUs
HDM_naive_1	121,929	251	61,602	1,352
HDM_naive_2	107,247	251	18,220	659
HDM_naive_3	12,528	251	44,324	943
HDM_naive_4	95,756	251	37,165	678
HDM_naive_5	160,559	251	53,504	838
HDM_naive_6	128,582	251	39,652	640
HDM_naive_7	152,338	251	49,651	866
HDM_exposed_1	146,968	251	46,875	838
HDM_exposed_2	159,630	251	50,509	898
HDM_exposed_3	113,019	251	29,733	640
HDM_exposed_4	122,465	251	40,246	924
HDM_exposed_5	119,791	251	46,509	830
HDM_exposed_6	109,828	251	46,748	795
HDM_exposed_7	143,568	251	51,627	1,335
Negative Control	115,138	251	1	1

**Table S16: The number of V4 reads generated from murine faecal samples following amplification of the V4 region of the 16S rRNA bacterial gene and Illumina sequencing of the V4 amplicons.** Following successful generation of V4 amplicons containing Illumina sequencing motifs from faecal samples from HDM-exposed (n = 7) and HDM-naive mice (n = 7), the V4 amplicons were sequenced using Illumina MiSeq sequencing. Low-quality reads and chimeric sequences were then removed using *Nephele* 2.0 technology and the remaining reads aligned to bacterial operational taxonomic units at a 99% similarity threshold.

Sample	Number of raw reads	Length of trimmed Reads (bp)	Number of OTU-aligned Reads	Number of detected OTUs
HDM_naive_1	129,666	251	118,165	3,230
HDM_naive_2	107,196	251	98,296	2,681
HDM_naive_3	101,094	251	74,906	1,240
HDM_naive_4	90,422	251	82,920	2,264
HDM_naive_5	107,400	251	97,882	2,516
HDM_naive_6	137,847	251	126,585	2,831
HDM_naive_7	88,991	251	81,349	2,227
HDM_exposed_1	85,236	251	77,140	2,405
HDM_exposed_2	86,423	251	77,591	2,382
HDM_exposed_3	98,404	251	88,901	2,502
HDM_exposed_4	112,536	251	103,248	2,461
HDM_exposed_5	107,948	251	99,668	2,691
HDM_exposed_6	104,199	251	93,940	2,692
HDM_exposed_7	110,748	251	100,650	2,544
Negative Control	36,394	251	28,232	218

**Table S17: Microbial functions predicted to be significantly altered in the gut microbiome of mice exposed to the HDM allergen compared to HDM-naïve mice.** PICRUSt analysis was performed on the 16S rRNA sequencing data generated from faecal samples taken from HDM-exposed mice (n = 7) and HDM-naïve mice (n = 7) to determine whether changes in the microbial populations present in the gut microbiome of mice exposed to the HDM allergen significantly altered overall functional activity of the microbiome. Abundance of KEGG pathways at levels 1 – 3 was determined, and LEfSe analysis was performed to identify KEGG pathways with significantly altered abundance in the gut microbiome of HDM-exposed mice compared to HDM-naïve mice. Biologically significant altered KEGG abundance is defined as having a *P* value < 0.05 and an LDA effect size > 2.0.

Function	Highest group abundance average (log %)	Group with highest average abundance	LDA Effect Size	<i>P</i> Value
M: Starch and sucrose metabolism	4.02	HDM+	2.41	0.0476
M: Galactose metabolism	3.95	HDM+	2.31	0.0350
M: Pentose and glucuronate interconversions	3.76	HDM+	2.30	0.0181
M: Sphingolipid metabolism	3.57	HDM+	2.18	0.0476
U: Replication, recombination and repair proteins	3.80	HDM-	2.07	0.0350
M: Propanoate metabolism	3.65	HDM-	2.05	0.0181
M: Pyruvate metabolism	4.00	HDM-	2.02	0.0088
M: Geraniol degradation	2.70	NA	NA	0.0476
D: African trypanosomiasis	1.14	NA	NA	0.0350
G: Sulfur relay system	3.22	NA	NA	0.0350
M: Butanoate metabolism	3.80	NA	NA	0.0350
M: Tetracycline biosynthesis	2.91	NA	NA	0.0350
U: Carbohydrate metabolism	3.19	NA	NA	0.0350
G: Non-homologous end joining	1.42	NA	NA	0.0350
M: Gluconeogenesis	4.03	NA	NA	0.0253
C: Meiosis - yeast	1.40	NA	NA	0.0253
M: Biosynthesis of siderophore group non-ribosomal peptides	2.20	NA	NA	0.0253
M: Nitrotoluene degradation	2.54	NA	NA	0.0253
M: Selenocompound metabolism	3.55	NA	NA	0.0253
G: Basal transcription factors	1.05	NA	NA	0.0181
M: Various types of N glycan biosynthesis	1.08	NA	NA	0.0181
M: Fatty acid metabolism	3.32	NA	NA	0.0127

M: Valine, leucine and isoleucine degradation	3.42	NA	NA	0.0127
M: Glycerophospholipid metabolism	3.73	NA	NA	0.0127
U: Nucleotide metabolism	2.73	NA	NA	0.0088
U: Metabolism of cofactors and vitamins	2.86	NA	NA	0.0088
M: Phosphonate and phosphinate metabolism	2.84	NA	NA	0.0060
M: Lysine degradation	3.12	NA	NA	0.0040

*Abbreviations: M, Metabolism level 1 KEGG category; U, Unclassified level 1 KEGG category; D, Human disease level 1 KEGG category; G, Genetic information processing level 1 KEGG category, C, Cellular process level 1 KEGG category; NA, defines level 3 KEGG pathways with a significant P value but an LDA effect size < 2.0.*



## References

1. Pawankar, R., Canonica, G., Holgate, S., Lockey, R. & Blaiss, M. *WAO White Book on Allergy 2013 Update WAO White Book on Allergy WAO White Book on Allergy*.
2. Masoli, M., Fabian, D., Holt, S. & Beasley, R. The global burden of asthma: executive summary of the GINA Dissemination Committee Report. *Allergy* **59**, 469–478 (2004).
3. Braman, S. S. The Global Burden of Asthma. *Chest* **130**, 4S-12S (2006).
4. Asher, I. & Pearce, N. Global burden of asthma among children. *Int. J. Tuberc. Lung Dis.* **18**, 1269–1278 (2014).
5. Pawankar, R. Allergic diseases and asthma: a global public health concern and a call to action. *World Allergy Organ. J.* **7**, 1–3 (2014).
6. Holgate, S. T. Innate and adaptive immune responses in asthma. *Nat. Med.* **18**, 673–683 (2012).
7. Lucini, V., Ciraci, R., Dugnani, S., Pannacci, M., Pisati, F., Caronno, A., Tirone, G. & Scaglione, F. Antibiotics counteract the worsening of airway remodelling induced by infections in asthma. *Int. J. Antimicrob. Agents* **43**, 442–450 (2014).
8. Postma, D. S., Bleeker, E. R., Amelung, P. J., Holroyd, K. J., Xu, J., Panhuysen, C. I. M., Meyers, D. A. & Levitt, R. C. Genetic Susceptibility to Asthma — Bronchial Hyperresponsiveness Coinherited with a Major Gene for Atopy. *N. Engl. J. Med.* **333**, 894–900 (1995).
9. von Hertzen, L. C. Maternal stress and T-cell differentiation of the developing immune system: Possible implications for the development of asthma and atopy. *J. Allergy Clin. Immunol.* **109**, 923–928 (2002).
10. Gilmour, M. I., Jaakkola, M. S., London, S. J., Nel, A. E. & Rogers, C. A. How exposure to environmental tobacco smoke, outdoor air pollutants, and increased pollen burdens influences the incidence of asthma. *Environ. Health Perspect.* **114**, 627–33 (2006).
11. Vercelli, D. Discovering susceptibility genes for asthma and allergy. *Nat. Rev. Immunol.* **8**, 169–182 (2008).
12. Beasley, R., Semprini, A. & Mitchell, E. A. Risk factors for asthma: is prevention possible? *Lancet* **386**, 1075–1085 (2015).
13. Dougherty, R. H. & Fahy, J. V. Acute exacerbations of asthma: epidemiology, biology and the exacerbation-prone phenotype. *Clin. Exp. Allergy* **39**, 193–202 (2009).
14. Hogg, J. C. The pathology of asthma. *APMIS* **105**, 735–45 (1997).
15. Kuyper, L. M., Paré, P. D., Hogg, J. C., Lambert, R. K., Ionescu, D., Woods, R. & Bai, T. R. Characterization of airway plugging in fatal asthma. *Am. J. Med.* **115**, 6–11 (2003).
16. Veith, I. *The Yellow Emperor's classic of internal medicine*. (Univ. of California Press, 1966).
17. Saavedra-Delgado, A. M. & Cohen, S. G. Huang-Ti, the Yellow Emperor and the Nei Ching: antiquity's earliest reference to asthma. *Allergy Proc.* **12**, 197–8 (1991).
18. Walter, M. J. & Holtzman, M. J. A Centennial History of Research on Asthma Pathogenesis. *Am. J. Respir. Cell Mol. Biol.* **32**, 483–489 (2005).
19. Wenzel, S. E. Complex phenotypes in asthma: Current definitions. *Pulm. Pharmacol. Ther.*

- 26, 710–715 (2013).
20. Anderson, G. P. Endotyping asthma: new insights into key pathogenic mechanisms in a complex, heterogeneous disease. *Lancet* **372**, 1107–1119 (2008).
  21. Edwards, M. R., Bartlett, N. W., Hussell, T., Openshaw, P. & Johnston, S. L. The microbiology of asthma. *Nat. Rev. Microbiol.* **10**, 459–471 (2012).
  22. Wenzel, S. E. Asthma: defining of the persistent adult phenotypes. *Lancet* **368**, 804–813 (2006).
  23. Lötvall, J., Akdis, C. A., Bacharier, L. B., Bjermer, L., Casale, T. B., Custovic, A., Lemanske, R. F., Wardlaw, A. J., Wenzel, S. E. & Greenberger, P. A. Asthma endotypes: A new approach to classification of disease entities within the asthma syndrome. *J. Allergy Clin. Immunol.* **127**, 355–360 (2011).
  24. Miranda, C., Busacker, A., Balzar, S., Trudeau, J. & Wenzel, S. E. Distinguishing severe asthma phenotypes: Role of age at onset and eosinophilic inflammation. *J. Allergy Clin. Immunol.* **113**, 101–108 (2004).
  25. Haldar, P., Pavord, I. D., Shaw, D. E., Berry, M. A., Thomas, M., Brightling, C. E., Wardlaw, A. J. & Green, R. H. Cluster Analysis and Clinical Asthma Phenotypes. *Am. J. Respir. Crit. Care Med.* **178**, 218–224 (2008).
  26. Rackemann, F. M. Intrinsic asthma. *J. Allergy* **11**, 147–162 (1940).
  27. Humbert, M., Menz, G., Ying, S., Corrigan, C. J., Robinson, D. S., Durham, S. R. & Kay, A. B. The immunopathology of extrinsic (atopic) and intrinsic (non-atopic) asthma: more similarities than differences. *Immunol. Today* **20**, 528–533 (1999).
  28. Simpson, J. L., Scott, R., Boyle, M. J. & Gibson, P. G. Inflammatory subtypes in asthma: Assessment and identification using induced sputum. *Respirology* **11**, 54–61 (2006).
  29. Woodruff, P. G., Modrek, B., Choy, D. F., Jia, G., Abbas, A. R., Ellwanger, A., Arron, J. R., Koth, L. L. & Fahy, J. V. T-helper Type 2–driven Inflammation Defines Major Subphenotypes of Asthma. *Am. J. Respir. Crit. Care Med.* **180**, 388–395 (2009).
  30. Bosnjak, B., Stelzmueller, B., Erb, K. J. & Epstein, M. M. Treatment of allergic asthma: Modulation of Th2 cells and their responses. *Respir. Res.* **12**, 114 (2011).
  31. Galli, S. J., Tsai, M. & Piliponsky, A. M. The development of allergic inflammation. *Nature* **454**, 445–454 (2008).
  32. Fahy, J. V. Type 2 inflammation in asthma — present in most, absent in many. *Nat. Rev. Immunol.* **15**, 57–65 (2015).
  33. Spergel, J. M. & Paller, A. S. Atopic dermatitis and the atopic march. *J. Allergy Clin. Immunol.* **112**, S118–S127 (2003).
  34. Bull, M. J. & Plummer, N. T. Part 1: The Human Gut Microbiome in Health and Disease. *Integr. Med. (Encinitas)*. **13**, 17–22 (2014).
  35. Kapoor, R., Menon, C., Hoffstad, O., Bilker, W., Leclerc, P. & Margolis, D. J. The prevalence of atopic triad in children with physician-confirmed atopic dermatitis. *J. Am. Acad. Dermatol.* **58**, 68–73 (2008).
  36. Kemeny, D. M., Urbanek, R., Ewan, P., McHugh, S., Richards, D., Patel, S. & Lessof, M. H. The subclass of IgG antibody in allergic disease: II. The IgG subclass of antibodies produced following natural exposure to dust mite and grass pollen in atopic and non-atopic individuals. *Clin. Exp. Allergy* **19**, 545–9 (1989).

37. Ebner, C., Schenk, S., Najafian, N., Siemann, U., Steiner, R., Fischer, G. W., Hoffmann, K., Szépfalusi, Z., Scheiner, O. & Kraft, D. Nonallergic individuals recognize the same T cell epitopes of Bet v 1, the major birch pollen allergen, as atopic patients. *J. Immunol.* **154**, 1932–40 (1995).
38. Gavett, S. H., Chen, X., Finkelman, F. & Wills-Karp, M. Depletion of murine CD4+ T lymphocytes prevents antigen-induced airway hyperreactivity and pulmonary eosinophilia. *Am. J. Respir. Cell Mol. Biol.* **10**, 587–593 (1994).
39. Zhang, D. H., Yang, L., Cohn, L., Parkyn, L., Homer, R., Ray, P. & Ray, A. Inhibition of allergic inflammation in a murine model of asthma by expression of a dominant-negative mutant of GATA-3. *Immunity* **11**, 473–82 (1999).
40. Salazar, F. & Ghaemmaghami, A. M. Allergen Recognition by Innate Immune Cells: Critical Role of Dendritic and Epithelial Cells. *Front. Immunol.* **4**, 356 (2013).
41. Hammad, H., Chieppa, M., Perros, F., Willart, M. A., Germain, R. N. & Lambrecht, B. N. House dust mite allergen induces asthma via Toll-like receptor 4 triggering of airway structural cells. *Nat. Med.* **15**, 410–6 (2009).
42. Janeway, C. A. Approaching the asymptote? Evolution and revolution in immunology. *Cold Spring Harb. Symp. Quant. Biol.* **54 Pt 1**, 1–13 (1989).
43. Takeuchi, O. & Akira, S. Pattern Recognition Receptors and Inflammation. *Cell* **140**, 805–820 (2010).
44. Lei, H.-Y., Yu Chih-Long Chen, C.-K., Lee, C.-T. & Liu, Y.-C. Allergic Sensitization and Inflammation Alveolar Macrophages: Implications for Productions and Accessory Function of Augments Proinflammatory Mediator *Dermatophagoides farinae* House Dust Mite. *J Immunol Ref.* **170**, 528–536 (2003).
45. Yu, C.-K. & Chen, C.-L. Airway Inflammation in Mice-Induced Allergic *Dermatophagoides farinae* Development of House Dust Mite Activation of Mast Cells Is Essential for. *J Immunol Ref.* **171**, 3808–3815 (2003).
46. Akbari, O., Stock, P., Meyer, E., Kronenberg, M., Sidobre, S., Nakayama, T., Taniguchi, M., Grusby, M. J., DeKruyff, R. H. & Umetsu, D. T. Essential role of NKT cells producing IL-4 and IL-13 in the development of allergen-induced airway hyperreactivity. *Nat. Med.* **9**, 582–588 (2003).
47. Banchereau, J. & Steinman, R. M. Dendritic cells and the control of immunity. *Nature* **392**, 245–252 (1998).
48. van Rijjt, L. S., Jung, S., Kleinjan, A., Vos, N., Willart, M., Duez, C., Hoogsteden, H. C. & Lambrecht, B. N. In vivo depletion of lung CD11c+ dendritic cells during allergen challenge abrogates the characteristic features of asthma. *J. Exp. Med.* **201**, 981–91 (2005).
49. Hammad, H. & Lambrecht, B. N. Dendritic cells and epithelial cells: linking innate and adaptive immunity in asthma. *Nat. Rev. Immunol.* **8**, 193–204 (2008).
50. Wan, H., Winton, H. L., Soeller, C., Tovey, E. R., Gruenert, D. C., Thompson, P. J., Stewart, G. A., Taylor, G. W., Garrod, D. R., Cannell, M. B. & Robinson, C. Der p 1 facilitates transepithelial allergen delivery by disruption of tight junctions. *J. Clin. Invest.* **104**, 123–33 (1999).
51. Blum, J. S., Wearsch, P. A. & Cresswell, P. Pathways of antigen processing. *Annu. Rev. Immunol.* **31**, 443–73 (2013).
52. Mantegazza, A. R., Magalhaes, J. G., Amigorena, S. & Marks, M. S. Presentation of

- phagocytosed antigens by MHC class I and II. *Traffic* **14**, 135–52 (2013).
53. McMahon, H. T. & Boucrot, E. Molecular mechanism and physiological functions of clathrin-mediated endocytosis. *Nat. Rev. Mol. Cell Biol.* **12**, 517–533 (2011).
  54. Inaba, K., Turley, S., Yamaide, F., Iyoda, T., Mahnke, K., Inaba, M., Pack, M., Subklewe, M., Sauter, B., Sheff, D., Albert, M., Bhardwaj, N., Mellman, I. & Steinman, R. M. Efficient presentation of phagocytosed cellular fragments on the major histocompatibility complex class II products of dendritic cells. *J. Exp. Med.* **188**, 2163–73 (1998).
  55. Lambrecht, B. N., Pauwels, R. A., Fazekas De St Groth, B., van der Cammen, M. J., Tirion, F., Miltenburg, A. M. & Kraal, G. Induction of rapid T cell activation, division, and recirculation by intratracheal injection of dendritic cells in a TCR transgenic model. *J. Immunol.* **164**, 2937–46 (2000).
  56. Seder, R. A. & Paul, W. E. Acquisition of Lymphokine-Producing Phenotype by CD4+ T Cells. *Annu. Rev. Immunol.* **12**, 635–673 (1994).
  57. Smith, K. M., Brewer, J. M., Mowat, A. M., Ron, Y. & Garside, P. The influence of follicular migration on T-cell differentiation. *Immunology* **111**, 248–51 (2004).
  58. Reinhardt, R. L., Liang, H.-E. & Locksley, R. M. Cytokine-secreting follicular T cells shape the antibody repertoire. *Nat. Immunol.* **10**, 385–93 (2009).
  59. Goenka, R., Barnett, L. G., Silver, J. S., O’Neill, P. J., Hunter, C. A., Cancro, M. P. & Laufer, T. M. Cutting edge: dendritic cell-restricted antigen presentation initiates the follicular helper T cell program but cannot complete ultimate effector differentiation. *J. Immunol.* **187**, 1091–5 (2011).
  60. Andreev, K., Graser, A., Maier, A., Mousset, S. & Finotto, S. Therapeutical Measures to Control Airway Tolerance in Asthma and Lung Cancer. *Front. Immunol.* **3**, 216 (2012).
  61. Crotty, S. Follicular Helper CD4 T Cells (T<sub>FH</sub>). *Annu. Rev. Immunol.* **29**, 621–663 (2011).
  62. Shimoda, K., van Deursent, J., Sangster, M. Y., Sarawar, S. R., Carson, R. T., Tripp, R. A., Chu, C., Quelle, F. W., Nosaka, T., Vignali, D. A. A., Doherty, P. C., Grosveld, G., Paul, W. E. & Ihle, J. N. Lack of IL-4-induced Th2 response and IgE class switching in mice with disrupted State6 gene. *Nature* **380**, 630–633 (1996).
  63. Miller, L., Blank, U., Metzger, H. & Kinet, J. P. Expression of high-affinity binding of human immunoglobulin E by transfected cells. *Science* **244**, 334–7 (1989).
  64. Stone, K. D., Prussin, C. & Metcalfe, D. D. IgE, mast cells, basophils, and eosinophils. *J. Allergy Clin. Immunol.* **125**, S73–S80 (2010).
  65. Bieber, T., de la Salle, H., Wollenberg, A., Hakimi, J., Chizzonite, R., Ring, J., Hanau, D. & de la Salle, C. Human epidermal Langerhans cells express the high affinity receptor for immunoglobulin E (Fc epsilon RI). *J. Exp. Med.* **175**, 1285–90 (1992).
  66. Maurer, D., Fiebiger, E., Reiningner, B., Wolff-Winiski, B., Jouvin, M. H., Kilgus, O., Kinet, J. P. & Stingl, G. Expression of functional high affinity immunoglobulin E receptors (Fc epsilon RI) on monocytes of atopic individuals. *J. Exp. Med.* **179**, 745–50 (1994).
  67. Gould, H. J. & Sutton, B. J. IgE in allergy and asthma today. *Nat. Rev. Immunol.* **8**, 205–217 (2008).
  68. Gomez-Cambronero, J., Horn, J., Paul, C. C. & Baumann, M. A. Granulocyte-macrophage colony-stimulating factor is a chemoattractant cytokine for human neutrophils: involvement of the ribosomal p70 S6 kinase signaling pathway. *J. Immunol.* **171**, 6846–55 (2003).

69. Zhou, B., Comeau, M. R., Smedt, T. De, Liggitt, H. D., Dahl, M. E., Lewis, D. B., Gyarmati, D., Aye, T., Campbell, D. J. & Ziegler, S. F. Thymic stromal lymphopoietin as a key initiator of allergic airway inflammation in mice. *Nat. Immunol.* **6**, 1047–1053 (2005).
70. Ballantyne, S. J., Barlow, J. L., Jolin, H. E., Nath, P., Williams, A. S., Chung, K. F., Sturton, G., Wong, S. H. & McKenzie, A. N. J. Blocking IL-25 prevents airway hyperresponsiveness in allergic asthma. *J. Allergy Clin. Immunol.* **120**, 1324–1331 (2007).
71. Komai-Koma, M., Xu, D., Li, Y., McKenzie, A. N. J., McInnes, I. B. & Liew, F. Y. IL-33 is a chemoattractant for human Th2 cells. *Eur. J. Immunol.* **37**, 2779–2786 (2007).
72. Saba, S., Soong, G., Greenberg, S. & Prince, A. Bacterial Stimulation of Epithelial G-CSF and GM-CSF Expression Promotes PMN Survival in CF Airways. *Am. J. Respir. Cell Mol. Biol.* **27**, 561–567 (2002).
73. Cox, G., Gauldie, J. & Jordana, M. Bronchial Epithelial Cell-derived Cytokines (G-CSF and GM-CSF Promote the Survival of Peripheral Blood Neutrophils *In Vitro*. *Am. J. Respir. Cell Mol. Biol.* **7**, 507–514 (1992).
74. Vancheri, C., Gauldie, J., Bienenstock, J., Cox, G., Scicchitano, R., Stanisiz, A. & Jordana, M. Human Lung Fibroblast-derived Granulocyte-Macrophage Colony Stimulating Factor (GM-CSF) Mediates Eosinophil Survival *In Vitro*. *Am. J. Respir. Cell Mol. Biol.* **1**, 289–295 (1989).
75. Markowicz, S. & Engleman, E. G. Granulocyte-macrophage colony-stimulating factor promotes differentiation and survival of human peripheral blood dendritic cells in vitro. *J. Clin. Invest.* **85**, 955–961 (1990).
76. Soumelis, V., Reche, P. A., Kanzler, H., Yuan, W., Edward, G., Homey, B., Gilliet, M., Ho, S., Antonenko, S., Lauerma, A., Smith, K., Gorman, D., Zurawski, S., Abrams, J., Menon, S., McClanahan, T., Waal-Malefyt, R. de, Bazan, F., Kastelein, R. A. & Liu, Y.-J. Human epithelial cells trigger dendritic cell-mediated allergic inflammation by producing TSLP. *Nat. Immunol.* **3**, 673–680 (2002).
77. Kondo, Y., Yoshimoto, T., Yasuda, K., Futatsugi-Yumikura, S., Morimoto, M., Hayashi, N., Hoshino, T., Fujimoto, J. & Nakanishi, K. Administration of IL-33 induces airway hyperresponsiveness and goblet cell hyperplasia in the lungs in the absence of adaptive immune system. *Int. Immunol.* **20**, 791–800 (2008).
78. Allakhverdi, Z. & Delespesse, G. Cutting Edge: The ST2 Ligand IL-33 Potently Activates and Drives Maturation of Human Mast Cells. *Artic. J. Immunol.* (2007). doi:10.4049/jimmunol.179.4.2051
79. Wang, J.-X., Kaieda, S., Ameri, S., Fishgal, N., Dwyer, D., Dellinger, A., Kepley, C. L., Gurish, M. F. & Nigrovic, P. A. IL-33/ST2 axis promotes mast cell survival via BCLXL. *Proc. Natl. Acad. Sci.* **111**, 10281–10286 (2014).
80. Galli, S. J. & Tsai, M. IgE and mast cells in allergic disease. *Nat. Med.* **18**, 693–704 (2012).
81. Bradding, P., Walls, A. & Holgate, S. The role of the mast cell in the pathophysiology of asthma. *J. Allergy Clin. Immunol.* **117**, 1277–1284 (2006).
82. Galli, S. J., Nakae, S. & Tsai, M. Mast cells in the development of adaptive immune responses. *Nat. Immunol.* **6**, 135–142 (2005).
83. Shim, J. J., Dabbagh, K., Ueki, I. F., Dao-Pick, T., Burgel, P.-R., Takeyama, K., Tam, D. C.-W. & Nadel, J. A. IL-13 induces mucin production by stimulating epidermal growth factor receptors and by activating neutrophils. *Am. J. Physiol. Cell. Mol. Physiol.* **280**, L134–L140 (2001).

84. Kondo, M., Tamaoki, J., Takeyama, K., Nakata, J. & Nagai, A. Interleukin-13 Induces Goblet Cell Differentiation in Primary Cell Culture from Guinea Pig Tracheal Epithelium. *Am. J. Respir. Cell Mol. Biol.* **27**, 536–541 (2002).
85. Atherton, H. C., Jones, G. & Danahay, H. IL-13-induced changes in the goblet cell density of human bronchial epithelial cell cultures: MAP kinase and phosphatidylinositol 3-kinase regulation. *Am. J. Physiol. Cell. Mol. Physiol.* **285**, L730–L739 (2003).
86. Tyner, J. W., Kim, E. Y., Ide, K., Pelletier, M. R., Roswit, W. T., Morton, J. D., Battaile, J. T., Patel, A. C., Patterson, G. A., Castro, M., Spoor, M. S., You, Y., Brody, S. L. & Holtzman, M. J. Blocking airway mucous cell metaplasia by inhibiting EGFR antiapoptosis and IL-13 transdifferentiation signals. *J. Clin. Invest.* **116**, 309–321 (2006).
87. Yamaguchi, Y., Hayashi, Y., Sugama, Y., Miura, Y., Kasahara, T., Kitamura, S., Torisu, M., Mita, S., Tominaga, A. & Takatsu, K. Highly purified murine interleukin 5 (IL-5) stimulates eosinophil function and prolongs in vitro survival. IL-5 as an eosinophil chemotactic factor. *J. Exp. Med.* **167**, 1737–42 (1988).
88. Lopez, A. F., Begley, C. G., Williamson, D. J., Warren, D. J., Vadas, M. A. & Sanderson, C. J. Murine eosinophil differentiation factor. An eosinophil-specific colony-stimulating factor with activity for human cells. *J. Exp. Med.* **163**, 1085–99 (1986).
89. Yamaguchi, Y., Suda, T., Suda, J., Eguchi, M., Miura, Y., Harada, N., Tominaga, A. & Takatsu, K. Purified interleukin 5 supports the terminal differentiation and proliferation of murine eosinophilic precursors. *J. Exp. Med.* **167**, 43–56 (1988).
90. Clutterbuck, E. J., Hirst, E. M. & Sanderson, C. J. Human interleukin-5 (IL-5) regulates the production of eosinophils in human bone marrow cultures: comparison and interaction with IL-1, IL-3, IL-6, and GM-CSF. *Blood* **73**, 1504–12 (1989).
91. Fujisawa, T., Abu-Ghazaleh, R., Kita, H., Sanderson, C. J. & Gleich, G. J. Regulatory effect of cytokines on eosinophil degranulation. *J. Immunol.* **144**, 642–6 (1990).
92. Walsh, G. M., Hartnell, A., Wardlaw, A. J., Kurihara, K., Sanderson, C. J. & Kay, A. B. IL-5 enhances the in vitro adhesion of human eosinophils, but not neutrophils, in a leucocyte integrin (CD11/18)-dependent manner. *Immunology* **71**, 258–65 (1990).
93. Okayama, Y. & Kawakami, T. Development, Migration, and Survival of Mast Cells. *Immunol. Res.* **34**, 97–116 (2006).
94. Grouard, G., Risoan, M. C., Filgueira, L., Durand, I., Banchereau, J. & Liu, Y. J. The enigmatic plasmacytoid T cells develop into dendritic cells with interleukin (IL)-3 and CD40-ligand. *J. Exp. Med.* **185**, 1101–11 (1997).
95. Risoan, M. C., Soumelis, V., Kadowaki, N., Grouard, G., Briere, F., de Waal Malefyt, R. & Liu, Y. J. Reciprocal control of T helper cell and dendritic cell differentiation. *Science* **283**, 1183–6 (1999).
96. Ebner, S., Hofer, S., Nguyen, V. A., Fürhapter, C., Herold, M., Fritsch, P., Heufler, C. & Romani, N. A novel role for IL-3: human monocytes cultured in the presence of IL-3 and IL-4 differentiate into dendritic cells that produce less IL-12 and shift Th cell responses toward a Th2 cytokine pattern. *J. Immunol.* **168**, 6199–207 (2002).
97. Ikebuchi, K., Wong, G. G., Clark, S. C., Ihle, J. N., Hirai, Y. & Ogawa, M. Interleukin 6 enhancement of interleukin 3-dependent proliferation of multipotential hemopoietic progenitors. *Proc. Natl. Acad. Sci. U. S. A.* **84**, 9035–9 (1987).
98. Ikebuchi, K., Clark, S. C., Ihle, J. N., Souza, L. M. & Ogawa, M. Granulocyte colony-stimulating factor enhances interleukin 3-dependent proliferation of multipotential

- hemopoietic progenitors. *Proc. Natl. Acad. Sci. U. S. A.* **85**, 3445–9 (1988).
99. Young, D. A., Lowe, L. D. & Clark, S. C. Comparison of the effects of IL-3, granulocyte-macrophage colony-stimulating factor, and macrophage colony-stimulating factor in supporting monocyte differentiation in culture. Analysis of macrophage antibody-dependent cellular cytotoxicity. *J. Immunol.* **145**, 607–15 (1990).
  100. Ohmori, K., Luo, Y., Jia, Y., Nishida, J., Wang, Z., Bunting, K. D., Wang, D. & Huang, H. IL-3 Induces Basophil Expansion In Vivo by Directing Granulocyte-Monocyte Progenitors to Differentiate into Basophil Lineage-Restricted Progenitors in the Bone Marrow and by Increasing the Number of Basophil/Mast Cell Progenitors in the Spleen. *J. Immunol.* **182**, 2835–2841 (2009).
  101. Bergeron, C., Al-Ramli, W. & Hamid, Q. Remodeling in Asthma. *Proc. Am. Thorac. Soc.* **6**, 301–305 (2009).
  102. Moschino, L., Zanconato, S., Bozzetto, S., Baraldi, E. & Carraro, S. Childhood asthma biomarkers: present knowledge and future steps. *Paediatr. Respir. Rev.* **16**, 205–212 (2015).
  103. Heinzerling, L., Mari, A., Bergmann, K.-C., Bresciani, M., Burbach, G., Darsow, U., Durham, S., Fokkens, W., Gjomarkaj, M., Haahtela, T., Bom, A. T., Wöhrl, S., Maibach, H. & Lockey, R. The skin prick test – European standards. *Clin. Transl. Allergy* **3**, 3 (2013).
  104. Adcock, I. M., Caramori, G. & Chung, K. F. New targets for drug development in asthma. *Lancet* **372**, 1073–1087 (2008).
  105. Dahl, R. Systemic side effects of inhaled corticosteroids in patients with asthma. *Respir. Med.* **100**, 1307–1317 (2006).
  106. Guilbert, T. W., Morgan, W. J., Zeiger, R. S., Mauger, D. T., Boehmer, S. J., Szeffler, S. J., Bacharier, L. B., Lemanske, R. F., Strunk, R. C., Allen, D. B., Bloomberg, G. R., Heldt, G., Krawiec, M., Larsen, G., Liu, A. H., Chinchilli, V. M., Sorkness, C. A., Taussig, L. M. & Martinez, F. D. Long-Term Inhaled Corticosteroids in Preschool Children at High Risk for Asthma. *N. Engl. J. Med.* **354**, 1985–1997 (2006).
  107. Cumming, R. G., Mitchell, P. & Leeder, S. R. Use of Inhaled Corticosteroids and the Risk of Cataracts. *N. Engl. J. Med.* **337**, 8–14 (1997).
  108. Wang, J. J., Rochtchina, E., Tan, A. G., Cumming, R. G., Leeder, S. R. & Mitchell, P. Use of Inhaled and Oral Corticosteroids and the Long-term Risk of Cataract. *Ophthalmology* **116**, 652–657 (2009).
  109. Israel, E., Banerjee, T. R., Fitzmaurice, G. M., Kotlov, T. V., LaHive, K. & LeBoff, M. S. Effects of Inhaled Glucocorticoids on Bone Density in Premenopausal Women. *N. Engl. J. Med.* **345**, 941–947 (2001).
  110. Staa, T. P. van, Staa, T. P. van, Staa, T. P. van, Leufkens, H. G. M. & Cooper, C. The Epidemiology of Corticosteroid-Induced Osteoporosis: a Meta-analysis. *Osteoporos. Int.* **13**, 777–787 (2002).
  111. Salpeter, S. R., Ormiston, T. M. & Salpeter, E. E. Cardiovascular Effects of  $\beta$ -Agonists in Patients With Asthma and COPD: A Meta-Analysis. *Chest* **125**, 2309–2321 (2004).
  112. Sircar, G., Saha, B., Bhattacharya, S. G. & Saha, S. Allergic asthma biomarkers using systems approaches. *Front. Genet.* **4**, 308 (2014).
  113. Strimbu, K. & Tavel, J. A. What are biomarkers? *Curr. Opin. HIV AIDS* **5**, 463–6 (2010).
  114. Vijverberg, S. J., Hilvering, B., Raaijmakers, J. A., Lammers, J.-W. J., Maitland-van der Zee,

- A.-H. & Koenderman, L. Clinical utility of asthma biomarkers: from bench to bedside. *Biologics* **7**, 199–210 (2013).
115. Gemou-Engesaeth, V., Bush, A., Kay, A. B., Hamid, Q. & Corrigan, C. J. Inhaled glucocorticoid therapy of childhood asthma is associated with reduced peripheral blood T cell activation and 'Th2-type' cytokine mRNA expression. *Pediatrics* **99**, 695–703 (1997).
  116. Kuo, C. H. S., Pavlidis, S., Loza, M., Baribaud, F., Rowe, A., Pandis, I., Sousa, A., Corfield, J., Djukanovic, R., Lutter, R., Sterk, P. J., Auffray, C., Guo, Y., Adcock, I. M. & Chung, K. F. T-helper cell type 2 (Th2) and non-Th2 molecular phenotypes of asthma using sputum transcriptomics in U-BIOPRED. *Eur. Respir. J.* **49**, (2017).
  117. Humbert, M., Corrigan, C. J., Kimmitt, P., Till, S. J., Barry Kay, A. & DURHAM, S. R. Relationship between IL-4 and IL-5 mRNA Expression and Disease Severity in Atopic Asthma. *Am. J. Respir. Crit. Care Med.* **156**, 704–708 (1997).
  118. Alyasin, S., Karimi, M. H., Amin, R., Babaei, M. & Darougar, S. Interleukin-17 gene expression and serum levels in children with severe asthma. *Iran. J. Immunol.* **10**, 177–85 (2013).
  119. Tantisira, K. G., Silverman, E. S., Mariani, T. J., Xu, J., Richter, B. G., Klanderma, B. J., Litonjua, A. A., Lazarus, R., Rosenwasser, L. J., Fuhlbrigge, A. L. & Weiss, S. T. FCER2: A pharmacogenetic basis for severe exacerbations in children with asthma. *J. Allergy Clin. Immunol.* **120**, 1285–1291 (2007).
  120. Koster, E. S., Maitland-van der Zee, A.-H., Tavendale, R., Mukhopadhyay, S., Vijverberg, S. J. H., Raaijmakers, J. A. M. & Palmer, C. N. A. FCER2 T2206C variant associated with chronic symptoms and exacerbations in steroid-treated asthmatic children. *Allergy* **66**, 1546–1552 (2011).
  121. Tantisira, K. G., Hwang, E. S., Raby, B. A., Silverman, E. S., Lake, S. L., Richter, B. G., Peng, S. L., Drazen, J. M., Glimcher, L. H. & Weiss, S. T. TBX21: a functional variant predicts improvement in asthma with the use of inhaled corticosteroids. *Proc. Natl. Acad. Sci. U. S. A.* **101**, 18099–104 (2004).
  122. Hawkins, G. A., Lazarus, R., Smith, R. S., Tantisira, K. G., Meyers, D. A., Peters, S. P., Weiss, S. T. & Bleeker, E. R. The glucocorticoid receptor heterocomplex gene STIP1 is associated with improved lung function in asthmatic subjects treated with inhaled corticosteroids. *J. Allergy Clin. Immunol.* **123**, 1376-1383.e7 (2009).
  123. Wang, J., Li, K., Hellermann, G., Lockey, R. F., Mohapatra, S. & Mohapatra, S. Regulating the Regulators: microRNA and Asthma. *World Allergy Organ. J.* **4**, 94–103 (2011).
  124. Pua, H. H. & Ansel, K. M. MicroRNA regulation of allergic inflammation and asthma. *Curr. Opin. Immunol.* **36**, 101–108 (2015).
  125. Sastre, B., Cañas, J. A., Rodrigo-Muñoz, J. M. & del Pozo, V. Novel Modulators of Asthma and Allergy: Exosomes and MicroRNAs. *Front. Immunol.* **8**, 826 (2017).
  126. Huo, X., Zhang, K., Yi, L., Mo, Y., Liang, Y., Zhao, J., Zhang, Z., Xu, Y. & Zhen, G. Decreased epithelial and plasma miR-181b-5p expression associates with airway eosinophilic inflammation in asthma. *Clin. Exp. Allergy* **46**, 1281–90 (2016).
  127. Panganiban, R. P. L., Pinkerton, M. H., Maru, S. Y., Jefferson, S. J., Roff, A. N. & Ishmael, F. T. Differential microRNA expression in asthma and the role of miR-1248 in regulation of IL-5. *Am. J. Clin. Exp. Immunol.* **1**, 154–65 (2012).
  128. Yamamoto, M., Singh, A., Ruan, J., Gauvreau, G. M., O'Byrne, P. M., R Carlsten, C., Fitzgerald, J. M., Boulet, L.-P. & Tebbutt, S. J. Decreased miR-192 expression in peripheral



- blood of asthmatic individuals undergoing an allergen inhalation challenge. *BMC Genomics* **13**, 655 (2012).
129. Fujimoto, K., Kubo, K., Matsuzawa, Y. & Sekiguchi, M. Eosinophil cationic protein levels in induced sputum correlate with the severity of bronchial asthma. *Chest* **112**, 1241–1247 (1997).
  130. Niimi, Amitani, Suzuki, Tanaka, Murayama & Kuze. Serum eosinophil cationic protein as a marker of eosinophilic inflammation in asthma. *Clin. <html\_ent glyph="@amp;" ascii="&"/> Exp. Allergy* **28**, 233–240 (1998).
  131. Leung, T., Wong, C., Chan, I. H. S., Ip, W., Lam, C. W. K. & Wong, G. W. K. Plasma concentration of thymus and activation-regulated chemokine is elevated in childhood asthma. *J. Allergy Clin. Immunol.* **110**, 404–409 (2002).
  132. Jia, G., Erickson, R. W., Choy, D. F., Mosesova, S., Wu, L. C., Solberg, O. D., Shikotra, A., Carter, R., Audusseau, S., Hamid, Q., Bradding, P., Fahy, J. V., Woodruff, P. G., Harris, J. M. & Arron, J. R. Periostin is a systemic biomarker of eosinophilic airway inflammation in asthmatic patients. *J. Allergy Clin. Immunol.* **130**, 647-654.e10 (2012).
  133. Konradsen, J. R., James, A., Nordlund, B., Reinius, L. E., Söderhäll, C., Melén, E., Wheelock, Å., Lödrup Carlsen, K. C., Lidegran, M., Verhoek, M., Boot, R. G., Dahlén, B., Dahlén, S. E. & Hedlin, G. The chitinase-like protein YKL-40: A possible biomarker of inflammation and airway remodeling in severe pediatric asthma. *J. Allergy Clin. Immunol.* **132**, 328-335.e5 (2013).
  134. Lichtenstein, P. & Svartengren, M. Genes, environments, and sex: factors of importance in atopic diseases in 7?9?year-old Swedish twins. *Allergy* **52**, 1079–1086 (1997).
  135. de MARCO, R., LOCATELLI, F., SUNYER, J., BURNEY, P. & Respiratory Health Survey Study Group, the E. C. Differences in Incidence of Reported Asthma Related to Age in Men and Women. *Am. J. Respir. Crit. Care Med.* **162**, 68–74 (2000).
  136. Almqvist, C., Worm, M. & Leynaert, B. Impact of gender on asthma in childhood and adolescence: a GA<sup>2</sup> LEN review. *Allergy* **0**, 070907221144001-??? (2007).
  137. Wijga, A., Tabak, C., Postma, D. S., Kerkhof, M., Wieringa, M. H., Hoekstra, M. O., Brunekreef, B., de Jongste, J. C. & Smit, H. A. Sex differences in asthma during the first 8 years of life: The Prevention and Incidence of Asthma and Mite Allergy (PIAMA) birth cohort study. *J. Allergy Clin. Immunol.* **127**, 275–277 (2011).
  138. Sears, M. R., Greene, J. M., Willan, A. R., Wiecek, E. M., Taylor, D. R., Flannery, E. M., Cowan, J. O., Herbison, G. P., Silva, P. A. & Poulton, R. A Longitudinal, Population-Based, Cohort Study of Childhood Asthma Followed to Adulthood. *N. Engl. J. Med.* **349**, 1414–1422 (2003).
  139. Postma, D. S. Gender Differences in Asthma Development and Progression. *Gend. Med.* **4**, S133–S146 (2007).
  140. Lee, J. H., Haselkorn, T., Chipps, B. E., Miller, D. P., Wenzel, S. E. & For the Tenor Study Group, F. the T. S. Gender Differences in IgE-Mediated Allergic Asthma in the Epidemiology and Natural History of Asthma: Outcomes and Treatment Regimens (TENOR) Study. *J. Asthma* **43**, 179–184 (2006).
  141. Gough, H., Grabenhenrich, L., Reich, A., Eckers, N., Nitsche, O., Schramm, D., Beschorner, J., Hoffmann, U., Schuster, A., Bauer, C.-P., Forster, J., Zepp, F., Lee, Y.-A., Bergmann, R. L., Bergmann, K. E., Wahn, U., Lau, S. & Keil, T. Allergic multimorbidity of asthma, rhinitis and eczema over 20 years in the German birth cohort MAS. *Pediatr. Allergy Immunol.* **26**, 431–437 (2015).

142. TATTERSFIELD, A. E., POSTMA, D. S., BARNES, P. J., SVENSSON, K., BAUER, C.-A., O'BYRNE, P. M., LÖFDAHL, C.-G., PAUWELS, R. A. & ULLMAN, A. Exacerbations of Asthma. *Am. J. Respir. Crit. Care Med.* **160**, 594–599 (1999).
143. O'Connor, R. D., Bleecker, E. R., Long, A., Tashkin, D., Peters, S., Klingman, D. & Gutierrez, B. Subacute Lack of Asthma Control and Acute Asthma Exacerbation History as Predictors of Subsequent Acute Asthma Exacerbations: Evidence From Managed Care Data. *J. Asthma* **47**, 422–428 (2010).
144. Patel, M., Pilcher, J., Reddel, H. K., Qi, V., Mackey, B., Tranquilino, T., Shaw, D., Black, P., Weatherall, M. & Beasley, R. Predictors of Severe Exacerbations, Poor Asthma Control, and  $\beta$ -Agonist Overuse for Patients with Asthma. *J. Allergy Clin. Immunol. Pract.* **2**, 751–758.e1 (2014).
145. Gupta, R. P., Mukherjee, M., Sheikh, A. & Strachan, D. P. Persistent variations in national asthma mortality, hospital admissions and prevalence by socioeconomic status and region in England. *Thorax* **73**, 706–712 (2018).
146. Akinbami, L. J., Moorman, J. E., Bailey, C., Zahran, H. S., King, M., Johnson, C. A. & Liu, X. Trends in asthma prevalence, health care use, and mortality in the United States, 2001–2010. *NCHS Data Brief* 1–8 (2012).
147. Burr, M. L., Butland, B. K., King, S. & Vaughan-Williams, E. Changes in asthma prevalence: two surveys 15 years apart. *Arch. Dis. Child.* **64**, 1452–6 (1989).
148. Asher, M. I., Montefort, S., Björkstén, B., Lai, C. K., Strachan, D. P., Weiland, S. K. & Williams, H. Worldwide time trends in the prevalence of symptoms of asthma, allergic rhinoconjunctivitis, and eczema in childhood: ISAAC Phases One and Three repeat multicountry cross-sectional surveys. *Lancet* **368**, 733–743 (2006).
149. Anderson, H. R., Gupta, R., Strachan, D. P. & Limb, E. S. 50 years of asthma: UK trends from 1955 to 2004. *Thorax* **62**, 85–90 (2007).
150. Lai, C. K. W., Beasley, R., Crane, J., Foliaki, S., Shah, J., Weiland, S. & International Study of Asthma and Allergies in Childhood Phase Three Study Group, the I. P. T. S. Global variation in the prevalence and severity of asthma symptoms: phase three of the International Study of Asthma and Allergies in Childhood (ISAAC). *Thorax* **64**, 476–83 (2009).
151. Lundbäck, B., Umeå, H. B., Lotvall, J., Biosciences, C. & Rönmark, E. Is asthma prevalence still increasing? (2015). doi:10.1586/17476348.2016.1114417
152. Simpson, C. R. & Sheikh, A. Trends in the epidemiology of asthma in England: a national study of 333,294 patients. *J. R. Soc. Med.* **103**, 98–106 (2010).
153. Akinbami, L. J., Simon, A. E. & Rossen, L. M. Changing Trends in Asthma Prevalence Among Children. *Pediatrics* **137**, e20152354 (2016).
154. Kim, B.-K., Kim, J.-Y., Kang, M.-K., Yang, M.-S., Park, H.-W., Min, K.-U., Cho, S.-H. & Kang, H.-R. Allergies are still on the rise? A 6-year nationwide population-based study in Korea. *Allergol. Int.* **65**, 186–191 (2016).
155. Strachan, D. P. Hay fever, hygiene, and household size. *BMJ* **299**, 1259–60 (1989).
156. Matricardi, P. M., Rosmini, F., Ferrigno, L., Nisini, R., Rapicetta, M., Chionne, P., Stroffolini, T., Pasquini, P. & D'Amelio, R. Cross sectional retrospective study of prevalence of atopy among Italian military students with antibodies against hepatitis A virus. *BMJ* **314**, 999–1003 (1997).

157. Matricardi, P. M., Rosmini, F., Riondino, S., Fortini, M., Ferrigno, L., Rapicetta, M. & Bonini, S. Exposure to foodborne and orofecal microbes versus airborne viruses in relation to atopy and allergic asthma: epidemiological study. *BMJ* **320**, 412–7 (2000).
158. Shirakawa, T., Enomoto, T., Shimazu, S. & Hopkin, J. M. The inverse association between tuberculin responses and atopic disorder. *Science* **275**, 77–9 (1997).
159. Hanski, I., von Hertzen, L., Fyhrquist, N., Koskinen, K., Torppa, K., Laatikainen, T., Karisola, P., Auvinen, P., Paulin, L., Mäkelä, M. J., Vartiainen, E., Kosunen, T. U., Alenius, H. & Haahtela, T. Environmental biodiversity, human microbiota, and allergy are interrelated. *Proc. Natl. Acad. Sci. U. S. A.* **109**, 8334–9 (2012).
160. Rook, G. A. W. Hygiene Hypothesis and Autoimmune Diseases. *Clin. Rev. Allergy Immunol.* **42**, 5–15 (2012).
161. Nicholson, J. K., Holmes, E., Kinross, J., Burcelin, R., Gibson, G., Jia, W. & Pettersson, S. Host-gut microbiota metabolic interactions. *Science* **336**, 1262–7 (2012).
162. Rowland, I., Gibson, G., Heinken, A., Scott, K., Swann, J., Thiele, I. & Tuohy, K. Gut microbiota functions: metabolism of nutrients and other food components. *Eur. J. Nutr.* **57**, 1–24 (2018).
163. LeBlanc, J. G., Milani, C., de Giori, G. S., Sesma, F., van Sinderen, D. & Ventura, M. Bacteria as vitamin suppliers to their host: a gut microbiota perspective. *Curr. Opin. Biotechnol.* **24**, 160–168 (2013).
164. Sjögren, Y. M., Tomicic, S., Lundberg, A., Böttcher, M. F., Björkstén, B., Sverremark-Ekström, E. & Jenmalm, M. C. Influence of early gut microbiota on the maturation of childhood mucosal and systemic immune responses. *Clin. Exp. Allergy* **39**, 1842–1851 (2009).
165. Hill, D. A. & Artis, D. Intestinal Bacteria and the Regulation of Immune Cell Homeostasis. *Annu. Rev. Immunol.* **28**, 623–667 (2010).
166. Chung, H., Pamp, S. J., Hill, J. A., Surana, N. K., Edelman, S. M., Troy, E. B., Reading, N. C., Villablanca, E. J., Wang, S., Mora, J. R., Umesaki, Y., Mathis, D., Benoist, C., Relman, D. A. & Kasper, D. L. Gut Immune Maturation Depends on Colonization with a Host-Specific Microbiota. *Cell* **149**, 1578–1593 (2012).
167. Renz, H., Brandtzaeg, P. & Hornef, M. The impact of perinatal immune development on mucosal homeostasis and chronic inflammation. *Nat. Rev. Immunol.* **12**, 9–23 (2012).
168. Sonnenberg, G. F. & Artis, D. Innate Lymphoid Cell Interactions with Microbiota: Implications for Intestinal Health and Disease. *Immunity* **37**, 601–610 (2012).
169. Buffie, C. G. & Pamer, E. G. Microbiota-mediated colonization resistance against intestinal pathogens. *Nat. Rev. Immunol.* **13**, 790–801 (2013).
170. Gensollen, T., Iyer, S. S., Kasper, D. L. & Blumberg, R. S. How colonization by microbiota in early life shapes the immune system. *Science (80-. )*. **352**, 539–544 (2016).
171. Kamada, N., Chen, G. Y., Inohara, N. & Núñez, G. Control of pathogens and pathobionts by the gut microbiota. *Nat. Immunol.* **14**, 685–690 (2013).
172. Lawley, T. D. & Walker, A. W. Intestinal colonization resistance. *Immunology* **138**, 1–11 (2013).
173. Rakoff-Nahoum, S., Paglino, J., Eslami-Varzaneh, F., Edberg, S. & Medzhitov, R. Recognition of Commensal Microflora by Toll-Like Receptors Is Required for Intestinal Homeostasis. *Cell* **118**, 229–241 (2004).

174. Stappenbeck, T. S., Hooper, L. V & Gordon, J. I. Developmental regulation of intestinal angiogenesis by indigenous microbes via Paneth cells. *Proc. Natl. Acad. Sci. U. S. A.* **99**, 15451–5 (2002).
175. Reinhardt, C., Bergentall, M., Greiner, T. U., Schaffner, F., Östergren-Lundén, G., Petersen, L. C., Ruf, W. & Bäckhed, F. Tissue factor and PAR1 promote microbiota-induced intestinal vascular remodelling. *Nature* **483**, 627–631 (2012).
176. Bäckhed, F., Ding, H., Wang, T., Hooper, L. V, Koh, G. Y., Nagy, A., Semenkovich, C. F. & Gordon, J. I. The gut microbiota as an environmental factor that regulates fat storage. *Proc. Natl. Acad. Sci. U. S. A.* **101**, 15718–23 (2004).
177. Hsiao, E. Y., McBride, S. W., Hsien, S., Sharon, G., Hyde, E. R., McCue, T., Codelli, J. A., Chow, J., Reisman, S. E., Petrosino, J. F., Patterson, P. H. & Mazmanian, S. K. Microbiota Modulate Behavioral and Physiological Abnormalities Associated with Neurodevelopmental Disorders. *Cell* **155**, 1451–1463 (2013).
178. Sjögren, K., Engdahl, C., Henning, P., Lerner, U. H., Tremaroli, V., Lagerquist, M. K., Bäckhed, F. & Ohlsson, C. The gut microbiota regulates bone mass in mice. *J. Bone Miner. Res.* **27**, 1357–1367 (2012).
179. Ohlsson, C. & Sjögren, K. Effects of the gut microbiota on bone mass. *Trends Endocrinol. Metab.* **26**, 69–74 (2015).
180. Yan, J., Herzog, J. W., Tsang, K., Brennan, C. A., Bower, M. A., Garrett, W. S., Sartor, B. R., Aliprantis, A. O. & Charles, J. F. Gut microbiota induce IGF-1 and promote bone formation and growth. *Proc. Natl. Acad. Sci. U. S. A.* **113**, E7554–E7563 (2016).
181. Claus, S. P., Ellero, S. L., Berger, B., Krause, L., Bruttin, A., Molina, J., Paris, A., Want, E. J., Waziers, I. de, Cloarec, O., Richards, S. E., Wang, Y., Dumas, M.-E., Ross, A., Rezzi, S., Kochhar, S., Bladeren, P. Van, Lindon, J. C., Holmes, E. & Nicholson, J. K. Colonization-Induced Host-Gut Microbial Metabolic Interaction. *MBio* **2**, e00271-10 (2011).
182. Koppel, N., Maini Rekdal, V. & Balskus, E. P. Chemical transformation of xenobiotics by the human gut microbiota. *Science* **356**, eaag2770 (2017).
183. Laukens, D., Brinkman, B. M., Raes, J., De Vos, M. & Vandenabeele, P. Heterogeneity of the gut microbiome in mice: guidelines for optimizing experimental design. *FEMS Microbiol. Rev.* **40**, 117–132 (2016).
184. Ley, R. E., Lozupone, C. A., Hamady, M., Knight, R. & Gordon, J. I. Worlds within worlds: evolution of the vertebrate gut microbiota. *Nat. Rev. Microbiol.* **6**, 776–788 (2008).
185. Cho, I. & Blaser, M. J. The human microbiome: at the interface of health and disease. *Nat. Rev. Genet.* **13**, 260–70 (2012).
186. Sender, R., Fuchs, S. & Milo, R. Are We Really Vastly Outnumbered? Revisiting the Ratio of Bacterial to Host Cells in Humans. *Cell* **164**, 337–340 (2016).
187. Sender, R., Fuchs, S. & Milo, R. Revised Estimates for the Number of Human and Bacteria Cells in the Body. *PLOS Biol.* **14**, e1002533 (2016).
188. Marsland, B. J. & Gollwitzer, E. S. Host–microorganism interactions in lung diseases. *Nat. Rev. Immunol.* **14**, 827–835 (2014).
189. Backhed, F., Ley, R. E., Sonnenburg, J. L., Peterson, D. A. & Gordon, J. I. Host-Bacterial Mutualism in the Human Intestine. *Science (80- )*. **307**, 1915–1920 (2005).
190. Palmer, C., Bik, E. M., DiGiulio, D. B., Relman, D. A. & Brown, P. O. Development of the Human Infant Intestinal Microbiota. *PLoS Biol.* **5**, e177 (2007).

191. De Filippo, C., Cavalieri, D., Di Paola, M., Ramazzotti, M., Poulet, J. B., Massart, S., Collini, S., Pieraccini, G. & Lionetti, P. Impact of diet in shaping gut microbiota revealed by a comparative study in children from Europe and rural Africa. *Proc. Natl. Acad. Sci. U. S. A.* **107**, 14691–6 (2010).
192. Qin, J., Li, R., Wang, J., *et al.* A human gut microbial gene catalogue established by metagenomic sequencing. *Nature* **464**, 59–65 (2010).
193. Jakobsson, H. E., Abrahamsson, T. R., Jenmalm, M. C., Harris, K., Quince, C., Jernberg, C., Björkstén, B., Engstrand, L. & Andersson, A. F. Decreased gut microbiota diversity, delayed Bacteroidetes colonisation and reduced Th1 responses in infants delivered by caesarean section. *Gut* **63**, 559–66 (2014).
194. Colston, T. J. & Jackson, C. R. Microbiome evolution along divergent branches of the vertebrate tree of life: what is known and unknown. *Mol. Ecol.* **25**, 3776–3800 (2016).
195. Dominguez-Bello, M. G., Costello, E. K., Contreras, M., Magris, M., Hidalgo, G., Fierer, N. & Knight, R. Delivery mode shapes the acquisition and structure of the initial microbiota across multiple body habitats in newborns. *Proc. Natl. Acad. Sci.* **107**, 11971–11975 (2010).
196. Jiménez, E., Marín, M. L., Martín, R., Odriozola, J. M., Olivares, M., Xaus, J., Fernández, L. & Rodríguez, J. M. Is meconium from healthy newborns actually sterile? *Res. Microbiol.* **159**, 187–193 (2008).
197. Gosalbes, M. J., Llop, S., Vallès, Y., Moya, A., Ballester, F. & Francino, M. P. Meconium microbiota types dominated by lactic acid or enteric bacteria are differentially associated with maternal eczema and respiratory problems in infants. *Clin. Exp. Allergy* **43**, 198–211 (2013).
198. Ardissonne, A. N., de la Cruz, D. M., Davis-Richardson, A. G., Rechcigl, K. T., Li, N., Drew, J. C., Murgas-Torrazza, R., Sharma, R., Hudak, M. L., Triplett, E. W. & Neu, J. Meconium Microbiome Analysis Identifies Bacteria Correlated with Premature Birth. *PLoS One* **9**, e90784 (2014).
199. Hitti, J., Riley, D. E., Krohn, M. A., Hillier, S. L., Agnew, K. J., Krieger, J. N. & Eschenbach, D. A. Broad-Spectrum Bacterial rDNA Polymerase Chain Reaction Assay for Detecting Amniotic Fluid Infection Among Women in Premature Labor. *Clin. Infect. Dis.* **24**, 1228–1232 (1997).
200. DiGiulio, D. B., Romero, R., Amogan, H. P., Kusanovic, J. P., Bik, E. M., Gotsch, F., Kim, C. J., Erez, O., Edwin, S. & Relman, D. A. Microbial Prevalence, Diversity and Abundance in Amniotic Fluid During Preterm Labor: A Molecular and Culture-Based Investigation. *PLoS One* **3**, e3056 (2008).
201. Oh, K. J., Lee, S. E., Jung, H., Kim, G., Romero, R. & Yoon, B. H. Detection of ureaplasmas by the polymerase chain reaction in the amniotic fluid of patients with cervical insufficiency. *J. Perinat. Med.* **38**, 261 (2010).
202. Wang, X., Buhimschi, C. S., Temoin, S., Bhandari, V., Han, Y. W. & Buhimschi, I. A. Comparative Microbial Analysis of Paired Amniotic Fluid and Cord Blood from Pregnancies Complicated by Preterm Birth and Early-Onset Neonatal Sepsis. *PLoS One* **8**, e56131 (2013).
203. Jiménez, E., Fernández, L., Marín, M. L., Martín, R., Odriozola, J. M., Nueno-Palop, C., Narbad, A., Olivares, M., Xaus, J. & Rodríguez, J. M. Isolation of Commensal Bacteria from Umbilical Cord Blood of Healthy Neonates Born by Cesarean Section. *Curr. Microbiol.* **51**, 270–274 (2005).
204. Goldenberg, R. L., Andrews, W. W., Goepfert, A. R., Faye-Petersen, O., Cliver, S. P., Carlo,

- W. A. & Hauth, J. C. The Alabama Preterm Birth Study: Umbilical cord blood *Ureaplasma urealyticum* and *Mycoplasma hominis* cultures in very preterm newborn infants. *Am. J. Obstet. Gynecol.* **198**, 43.e1-43.e5 (2008).
205. Satokari, R., Grönroos, T., Laitinen, K., Salminen, S. & Isolauri, E. *Bifidobacterium* and *Lactobacillus* DNA in the human placenta. *Lett. Appl. Microbiol.* **48**, 8–12 (2009).
  206. Stout, M. J., Conlon, B., Landeau, M., Lee, I., Bower, C., Zhao, Q., Roehl, K. A., Nelson, D. M., Macones, G. A. & Mysorekar, I. U. Identification of intracellular bacteria in the basal plate of the human placenta in term and preterm gestations. *Am. J. Obstet. Gynecol.* **208**, 226.e1-226.e7 (2013).
  207. Aagaard, K., Ma, J., Antony, K. M., Ganu, R., Petrosino, J. & Versalovic, J. The placenta harbors a unique microbiome. *Sci. Transl. Med.* **6**, 237ra65 (2014).
  208. Steel, J. H., Malatos, S., Kennea, N., Edwards, A. D., Miles, L., Duggan, P., Reynolds, P. R., Feldman, R. G. & Sullivan, M. H. F. Bacteria and Inflammatory Cells in Fetal Membranes Do Not Always Cause Preterm Labor. *Pediatr. Res.* **57**, 404–411 (2005).
  209. Rotimi, V. O. & Duerden, B. I. The development of the bacterial flora in normal neonates. *J. Med. Microbiol.* **14**, 51–62 (1981).
  210. Solís, G., de los Reyes-Gavilan, C. G., Fernández, N., Margolles, A. & Gueimonde, M. Establishment and development of lactic acid bacteria and bifidobacteria microbiota in breast-milk and the infant gut. *Anaerobe* **16**, 307–310 (2010).
  211. Penders, J., Thijs, C., Vink, C., Stelma, F. F., Snijders, B., Kummeling, I., van den Brandt, P. A. & Stobberingh, E. E. Factors Influencing the Composition of the Intestinal Microbiota in Early Infancy. *Pediatrics* **118**, 511–521 (2006).
  212. Wang, M., Monaco, M. H. & Donovan, S. M. Impact of early gut microbiota on immune and metabolic development and function. *Semin. Fetal Neonatal Med.* **21**, 380–387 (2016).
  213. Fanaro, S., Chierici, R., Guerrini, P. & Vigi, V. Intestinal microflora in early infancy: composition and development. *Acta Paediatr.* **92**, 48–55 (2007).
  214. Grönlund, M.-M., Gueimonde, M., Laitinen, K., Kociubinski, G., Grönroos, T., Salminen, S. & Isolauri, E. Maternal breast-milk and intestinal bifidobacteria guide the compositional development of the *Bifidobacterium* microbiota in infants at risk of allergic disease. *Clin. Exp. Allergy* **37**, 1764–1772 (2007).
  215. Fallani, M., Young, D., Scott, J., Norin, E., Amarri, S., Adam, R., Aguilera, M., Khanna, S., Gil, A., Edwards, C. A. & Doré, J. Intestinal Microbiota of 6-week-old Infants Across Europe: Geographic Influence Beyond Delivery Mode, Breast-feeding, and Antibiotics. *J. Pediatr. Gastroenterol. Nutr.* **51**, 77–84 (2010).
  216. Bezirtzoglou, E., Tsiotsias, A. & Welling, G. W. Microbiota profile in feces of breast- and formula-fed newborns by using fluorescence in situ hybridization (FISH). *Anaerobe* **17**, 478–482 (2011).
  217. Stokholm, J., Blaser, M. J., Thorsen, J., Rasmussen, M. A., Waage, J., Vinding, R. K., Schoos, A.-M. M., Kunøe, A., Fink, N. R., Chawes, B. L., Bønnelykke, K., Brejnrod, A. D., Mortensen, M. S., Al-Soud, W. A., Sørensen, S. J. & Bisgaard, H. Maturation of the gut microbiome and risk of asthma in childhood. *Nat. Commun.* **9**, 141 (2018).
  218. West, C. E., Rydén, P., Lundin, D., Engstrand, L., Tulic, M. K. & Prescott, S. L. Gut microbiome and innate immune response patterns in IgE-associated eczema. *Clin. Exp. Allergy* **45**, 1419–1429 (2015).

219. Koenig, J. E., Spor, A., Scalfone, N., Fricker, A. D., Stombaugh, J., Knight, R., Angenent, L. T. & Ley, R. E. Succession of microbial consortia in the developing infant gut microbiome. *Proc. Natl. Acad. Sci.* **108**, 4578–4585 (2011).
220. Yatsunenکو, T., Rey, F. E., Manary, M. J., Trehan, I., Dominguez-Bello, M. G., Contreras, M., Magris, M., Hidalgo, G., Baldassano, R. N., Anokhin, A. P., Heath, A. C., Warner, B., Reeder, J., Kuczynski, J., Caporaso, J. G., Lozupone, C. A., Lauber, C., Clemente, J. C., Knights, D., Knight, R. & Gordon, J. I. Human gut microbiome viewed across age and geography. *Nature* **486**, 222–227 (2012).
221. Stewart, C. J., Ajami, N. J., O'Brien, J. L., Hutchinson, D. S., Smith, D. P., Wong, M. C., Ross, M. C., Lloyd, R. E., Doddapaneni, H., Metcalf, G. A., Muzny, D., Gibbs, R. A., Vatanen, T., Huttenhower, C., Xavier, R. J., Rewers, M., Hagopian, W., Toppari, J., Ziegler, A.-G., She, J.-X., Akolkar, B., Lernmark, A., Hyoty, H., Vehik, K., Krischer, J. P. & Petrosino, J. F. Temporal development of the gut microbiome in early childhood from the TEDDY study. *Nature* **562**, 583–588 (2018).
222. Guaraldi, F. & Salvatori, G. Effect of Breast and Formula Feeding on Gut Microbiota Shaping in Newborns. *Front. Cell. Infect. Microbiol.* **2**, 94 (2012).
223. Azad, M. B., Konya, T., Maughan, H., Guttman, D. S., Field, C. J., Chari, R. S., Sears, M. R., Becker, A. B., Scott, J. A., Kozyrskyj, A. L. & CHILD Study Investigators. Gut microbiota of healthy Canadian infants: profiles by mode of delivery and infant diet at 4 months. *CMAJ* **185**, 385–94 (2013).
224. Wu, G. D., Chen, J., Hoffmann, C., Bittinger, K., Chen, Y.-Y., Keilbaugh, S. A., Bewtra, M., Knights, D., Walters, W. A., Knight, R., Sinha, R., Gilroy, E., Gupta, K., Baldassano, R., Nessel, L., Li, H., Bushman, F. D. & Lewis, J. D. Linking long-term dietary patterns with gut microbial enterotypes. *Science* **334**, 105–8 (2011).
225. Azad, M. B., Konya, T., Maughan, H., Guttman, D. S., Field, C. J., Sears, M. R., Becker, A. B., Scott, J. A. & Kozyrskyj, A. L. Infant gut microbiota and the hygiene hypothesis of allergic disease: impact of household pets and siblings on microbiota composition and diversity. *Allergy, Asthma Clin. Immunol.* **9**, 15 (2013).
226. Dethlefsen, L., Huse, S., Sogin, M. L. & Relman, D. A. The Pervasive Effects of an Antibiotic on the Human Gut Microbiota, as Revealed by Deep 16S rRNA Sequencing. *PLoS Biol.* **6**, e280 (2008).
227. Fouhy, F., Guinane, C. M., Hussey, S., Wall, R., Ryan, C. A., Dempsey, E. M., Murphy, B., Ross, R. P., Fitzgerald, G. F., Stanton, C. & Cotter, P. D. High-throughput sequencing reveals the incomplete, short-term recovery of infant gut microbiota following parenteral antibiotic treatment with ampicillin and gentamicin. *Antimicrob. Agents Chemother.* **56**, 5811–20 (2012).
228. Holt, P. G. & Jones, C. A. The development of the immune system during pregnancy and early life. *Allergy* **55**, 688–697 (2000).
229. Levy, O. Innate immunity of the newborn: Basic mechanisms and clinical correlates. *Nat. Rev. Immunol.* **7**, 379–390 (2007).
230. Ygberg, S. & Nilsson, A. The developing immune system - from foetus to toddler. *Acta Paediatr.* **101**, 120–127 (2012).
231. Dimmitt, R. A., Staley, E. M., Chuang, G., Tanner, S. M., Soltau, T. D. & Lorenz, R. G. Role of postnatal acquisition of the intestinal microbiome in the early development of immune function. *J. Pediatr. Gastroenterol. Nutr.* **51**, 262–73 (2010).
232. Trowsdale, J. & Betz, A. G. Mother's little helpers: mechanisms of maternal-fetal tolerance.

- Nat. Immunol.* **7**, 241–246 (2006).
233. Nutten, S., Schumann, A., Donnicola, D., Mercenier, A., Rami, S. & Garcia-Rodenas, C. L. Antibiotic administration early in life impairs specific humoral responses to an oral antigen and increases intestinal mast cell numbers and mediator concentrations. *Clin. Vaccine Immunol.* **14**, 190–7 (2007).
  234. Zeissig, S. & Blumberg, R. S. Life at the beginning: perturbation of the microbiota by antibiotics in early life and its role in health and disease. *Nat. Immunol.* **15**, 307–310 (2014).
  235. de Theije, C. G. M., Wopereis, H., Ramadan, M., van Eijndhoven, T., Lambert, J., Knol, J., Garsen, J., Kraneveld, A. D. & Oozeer, R. Altered gut microbiota and activity in a murine model of autism spectrum disorders. *Brain. Behav. Immun.* **37**, 197–206 (2014).
  236. Flohr, C., Pascoe, D. & Williams, H. C. Atopic dermatitis and the ‘hygiene hypothesis’: too clean to be true? *Br. J. Dermatol.* **152**, 202–216 (2005).
  237. Ng, S. C., Bernstein, C. N., Vatn, M. H., Lakatos, P. L., Loftus, E. V., Tysk, C., O’Morain, C., Mow, B., Colombel, J.-F. & Epidemiology and Natural History Task Force of the International Organization of Inflammatory Bowel Disease (IOIBD). Geographical variability and environmental risk factors in inflammatory bowel disease. *Gut* **62**, 630–649 (2013).
  238. Norgaard, M., Nielsen, R. B., Jacobsen, J. B., Gradus, J. L., Stenager, E., Koch-Henriksen, N., Lash, T. L. & Sorensen, H. T. Use of Penicillin and Other Antibiotics and Risk of Multiple Sclerosis: A Population-based Case-Control Study. *Am. J. Epidemiol.* **174**, 945–948 (2011).
  239. Falk, P. G., Hooper, L. V., Midtvedt, T. & Gordon, J. I. Creating and maintaining the gastrointestinal ecosystem: what we know and need to know from gnotobiology. *Microbiol. Mol. Biol. Rev.* **62**, 1157–70 (1998).
  240. Macpherson, A. J. & Uhr, T. Compartmentalization of the Mucosal Immune Responses to Commensal Intestinal Bacteria. *Ann. N. Y. Acad. Sci.* **1029**, 36–43 (2004).
  241. Round, J. L. & Mazmanian, S. K. The gut microbiota shapes intestinal immune responses during health and disease. *Nat. Rev. Immunol.* **9**, 313–23 (2009).
  242. van Nimwegen, F. A., Penders, J., Stobberingh, E. E., Postma, D. S., Koppelman, G. H., Kerkhof, M., Reijmerink, N. E., Dompeling, E., van den Brandt, P. A., Ferreira, I., Mommers, M. & Thijs, C. Mode and place of delivery, gastrointestinal microbiota, and their influence on asthma and atopy. *J. Allergy Clin. Immunol.* **128**, 948-955.e3 (2011).
  243. Dogra, S., Sakwinska, O., Soh, S.-E., Ngom-Bru, C., Brück, W. M., Berger, B., Brüssow, H., Lee, Y. S., Yap, F., Chong, Y.-S., Godfrey, K. M., Holbrook, J. D. & GUSTO Study Group. Dynamics of infant gut microbiota are influenced by delivery mode and gestational duration and are associated with subsequent adiposity. *MBio* **6**, e02419-14 (2015).
  244. Aiello, A. E. & Larson, E. L. What is the evidence for a causal link between hygiene and infections? *Lancet Infect. Dis.* **2**, 103–110 (2002).
  245. Ege, M. J., Mayer, M., Normand, A.-C., Genuneit, J., Cookson, W. O. C. M., Braun-Fahrlander, C., Heederik, D., Piarroux, R. & von Mutius, E. Exposure to Environmental Microorganisms and Childhood Asthma. *N. Engl. J. Med.* **364**, 701–709 (2011).
  246. Salam, M. T., Margolis, H. G., McConnell, R., McGregor, J. A., Avol, E. L. & Gilliland, F. D. Mode of Delivery Is Associated With Asthma and Allergy Occurrences in Children. *Ann. Epidemiol.* **16**, 341–346 (2006).
  247. Viinanen, A., Munhbayarlah, S., Zevgee, T., Narantsetseg, L., Naidansuren, T., Koskenvuo,



- M., Helenius, H. & Terho, E. O. Prevalence of asthma, allergic rhinoconjunctivitis and allergic sensitization in Mongolia. *Allergy* **60**, 1370–1377 (2005).
248. von Mutius, E. & Vercelli, D. Farm living: effects on childhood asthma and allergy. *Nat. Rev. Immunol.* **10**, 861–868 (2010).
249. Ruokolainen, L., von Hertzen, L., Fyhrquist, N., Laatikainen, T., Lehtomäki, J., Auvinen, P., Karvonen, A. M., Hyvärinen, A., Tillmann, V., Niemelä, O., Knip, M., Haahtela, T., Pekkanen, J. & Hanski, I. Green areas around homes reduce atopic sensitization in children. *Allergy* **70**, 195–202 (2015).
250. Schuijs, M. J., Willart, M. A., Vergote, K., Gras, D., Deswarte, K., Ege, M. J., Madeira, F. B., Beyaert, R., Loo, G. van, Bracher, F., Mutius, E. von, Chanez, P., Lambrecht, B. N. & Hammad, H. Farm dust and endotoxin protect against allergy through A20 induction in lung epithelial cells. *Science (80-. )*. **349**, 1106–1110 (2015).
251. Wickens, K., Pearce, N., Crane, J. & Beasley, R. Antibiotic use in early childhood and the development of asthma. *Clin. Exp. Allergy* **29**, 766–71 (1999).
252. Stensballe, L. G., Simonsen, J., Jensen, S. M., Bønnelykke, K. & Bisgaard, H. Use of Antibiotics during Pregnancy Increases the Risk of Asthma in Early Childhood. *J. Pediatr.* **162**, 832-838.e3 (2013).
253. Korpela, K., Salonen, A., Virta, L. J., Kekkonen, R. A., Forslund, K., Bork, P. & de Vos, W. M. Intestinal microbiome is related to lifetime antibiotic use in Finnish pre-school children. *Nat. Commun.* **7**, 10410 (2016).
254. Sjögren, Y. M., Jenmalm, M. C., Böttcher, M. F., Björkstén, B. & Sverremark-Ekström, E. Altered early infant gut microbiota in children developing allergy up to 5 years of age. *Clin. Exp. Allergy* **39**, 518–526 (2009).
255. Goleva, E., Jackson, L. P., Harris, J. K., Robertson, C. E., Sutherland, E. R., Hall, C. F., Good, J. T., Gelfand, E. W., Martin, R. J. & Leung, D. Y. M. The Effects of Airway Microbiome on Corticosteroid Responsiveness in Asthma. *Am. J. Respir. Crit. Care Med.* **188**, 1193–1201 (2013).
256. Marri, P. R., Stern, D. A., Wright, A. L., Billheimer, D. & Martinez, F. D. Asthma-associated differences in microbial composition of induced sputum. *J. Allergy Clin. Immunol.* **131**, 346-352.e3 (2013).
257. Abrahamsson, T. R., Jakobsson, H. E., Andersson, A. F., Björkstén, B., Engstrand, L. & Jenmalm, M. C. Low gut microbiota diversity in early infancy precedes asthma at school age. *Clin. Exp. Allergy* **44**, 842–850 (2014).
258. Arrieta, M. C., Stiemsma, L. T., Dimitriu, P. A., Thorson, L., Russell, S., Yurist-Doutsch, S., Kuzeljevic, B., Gold, M. J., Britton, H. M., Lefebvre, D. L., Subbarao, P., Mandhane, P., Becker, A., McNagny, K. M., Sears, M. R., Kollmann, T., Mohn, W. W., Turvey, S. E. & Finlay, B. B. Early infancy microbial and metabolic alterations affect risk of childhood asthma. *Sci. Transl. Med.* **7**, 307ra152 (2015).
259. Huang, Y. J., Nariya, S., Harris, J. M., Lynch, S. V., Choy, D. F., Arron, J. R. & Boushey, H. The airway microbiome in patients with severe asthma: Associations with disease features and severity. *J. Allergy Clin. Immunol.* **136**, 874–884 (2015).
260. Teo, S. M., Mok, D., Pham, K., Kusel, M., Serralha, M., Troy, N., Holt, B. J., Hales, B. J., Walker, M. L., Hollams, E., Bochkov, Y. A., Grindle, K., Johnston, S. L., Gern, J. E., Sly, P. D., Holt, P. G., Holt, K. E. & Inouye, M. The Infant Nasopharyngeal Microbiome Impacts Severity of Lower Respiratory Infection and Risk of Asthma Development. *Cell Host Microbe* **17**, 704–715 (2015).

261. Zhang, Q., Cox, M., Liang, Z., Brinkmann, F., Cardenas, P. A., Duff, R., Bhavsar, P., Cookson, W., Moffatt, M. & Chung, K. F. Airway Microbiota in Severe Asthma and Relationship to Asthma Severity and Phenotypes. *PLoS One* **11**, e0152724 (2016).
262. Depner, M., Ege, M. J., Cox, M. J., Dwyer, S., Walker, A. W., Birzele, L. T., Genuneit, J., Horak, E., Braun-Fahrländer, C., Danielewicz, H., Maier, R. M., Moffatt, M. F., Cookson, W. O., Heederik, D., von Mutius, E. & Legatzki, A. Bacterial microbiota of the upper respiratory tract and childhood asthma. *J. Allergy Clin. Immunol.* **139**, 826-834.e13 (2017).
263. Sverrild, A., Kiilerich, P., Brejnrod, A., Pedersen, R., Porsbjerg, C., Bergqvist, A., Erjefält, J. S., Kristiansen, K. & Backer, V. Eosinophilic airway inflammation in asthmatic patients is associated with an altered airway microbiome. *J. Allergy Clin. Immunol.* **140**, 407-417.e11 (2017).
264. Kalliomäki, M., Kirjavainen, P., Eerola, E., Kero, P., Salminen, S. & Isolauri, E. Distinct patterns of neonatal gut microflora in infants in whom atopy was and was not developing. *J. Allergy Clin. Immunol.* **107**, 129–134 (2001).
265. Penders, J., Thijs, C., van den Brandt, P. A., Kummeling, I., Snijders, B., Stelma, F., Adams, H., van Ree, R. & Stobberingh, E. E. Gut microbiota composition and development of atopic manifestations in infancy: the KOALA Birth Cohort Study. *Gut* **56**, 661–7 (2007).
266. Verhulst, S. L., Vael, C., Beunckens, C., Nelen, V., Goossens, H. & Desager, K. A Longitudinal Analysis on the Association Between Antibiotic Use, Intestinal Microflora, and Wheezing During the First Year of Life. *J. Asthma* **45**, 828–832 (2008).
267. Abrahamsson, T. R., Jakobsson, H. E., Andersson, A. F., Björkstén, B., Engstrand, L. & Jenmalm, M. C. Low diversity of the gut microbiota in infants with atopic eczema. *J. Allergy Clin. Immunol.* **129**, 434-440.e2 (2012).
268. Fujimura, K. E., Sitarik, A. R., Havstad, S., Lin, D. L., Levan, S., Fadrosch, D., Panzer, A. R., LaMere, B., Rackaityte, E., Lukacs, N. W., Wegienka, G., Boushey, H. A., Ownby, D. R., Zoratti, E. M., Levin, A. M., Johnson, C. C. & Lynch, S. V. Neonatal gut microbiota associates with childhood multisensitized atopy and T cell differentiation. *Nat. Med.* **22**, 1187–1191 (2016).
269. Penders, J., Stobberingh, E. E., Brandt, P. A. van den & Thijs, C. The role of the intestinal microbiota in the development of atopic disorders. *Allergy* **62**, 1223–1236 (2007).
270. Durack, J., Kimes, N. E., Lin, D. L., Rauch, M., McKean, M., McCauley, K., Panzer, A. R., Mar, J. S., Cabana, M. D. & Lynch, S. V. Delayed gut microbiota development in high-risk for asthma infants is temporarily modifiable by Lactobacillus supplementation. *Nat. Commun.* **9**, 707 (2018).
271. Candela, M., Rampelli, S., Turroni, S., Severgnini, M., Consolandi, C., De Bellis, G., Masetti, R., Ricci, G., Pession, A. & Brigidi, P. Unbalance of intestinal microbiota in atopic children. *BMC Microbiol.* **12**, 95 (2012).
272. Hua, X., Goedert, J. J., Pu, A., Yu, G. & Shi, J. Allergy associations with the adult fecal microbiota: Analysis of the American Gut Project. *EBioMedicine* **3**, 172–179 (2016).
273. Begley, L., Madapoosi, S., Opron, K., Ndum, O., Baptist, A., Rysso, K., Erb-Downward, J. R. & Huang, Y. J. Gut microbiota relationships to lung function and adult asthma phenotype: a pilot study. *BMJ Open Respir. Res.* **5**, e000324 (2018).
274. Buendía, E., Zakzuk, J., San-Juan-Vergara, H., Zurek, E., Ajami, N. J. & Caraballo, L. Gut microbiota components are associated with fixed airway obstruction in asthmatic patients living in the tropics. *Sci. Rep.* **8**, 9582 (2018).

275. Samra, M., Donh Hyun, K., Kim, Y.-K. & Hee Kim, J. Urine Bacteria-Derived Extracellular Vesicles and Allergic Airway Diseases in Children Role of Breast-feeding in the Development of Atopic Dermatitis in Early Childhood View project. *Artic. Int. Arch. Allergy Immunol.* (2018). doi:10.1159/000492677
276. Wang, Q., Li, F., Liang, B., Liang, Y., Chen, S., Mo, X., Ju, Y., Zhao, H., Jia, H., Spector, T. D., Xie, H. & Guo, R. A metagenome-wide association study of gut microbiota in asthma in UK adults. *BMC Microbiol.* **18**, 114 (2018).
277. Hilty, M., Burke, C., Pedro, H., Cardenas, P., Bush, A., Bossley, C., Davies, J., Ervine, A., Poulter, L., Pachter, L., Moffatt, M. F. & Cookson, W. O. C. Disordered Microbial Communities in Asthmatic Airways. *PLoS One* **5**, e8578 (2010).
278. Charlson, E. S., Bittinger, K., Haas, A. R., Fitzgerald, A. S., Frank, I., Yadav, A., Bushman, F. D. & Collman, R. G. Topographical Continuity of Bacterial Populations in the Healthy Human Respiratory Tract. *Am. J. Respir. Crit. Care Med.* **184**, 957–963 (2011).
279. Erb-Downward, J. R., Thompson, D. L., Han, M. K., Freeman, C. M., McCloskey, L., Schmidt, L. A., Young, V. B., Toews, G. B., Curtis, J. L., Sundaram, B., Martinez, F. J. & Huffnagle, G. B. Analysis of the Lung Microbiome in the “Healthy” Smoker and in COPD. *PLoS One* **6**, e16384 (2011).
280. Bisgaard, H., Hermansen, M. N., Buchvald, F., Loland, L., Halkjaer, L. B., Bønnelykke, K., Brasholt, M., Heltberg, A., Vissing, N. H., Thorsen, S. V., Stage, M. & Pipper, C. B. Childhood Asthma after Bacterial Colonization of the Airway in Neonates. *N. Engl. J. Med.* **357**, 1487–1495 (2007).
281. Huang, Y. J., Nelson, C. E., Brodie, E. L., DeSantis, T. Z., Baek, M. S., Liu, J., Woyke, T., Allgaier, M., Bristow, J., Wiener-Kronish, J. P., Sutherland, E. R., King, T. S., Icitovic, N., Martin, R. J., Calhoun, W. J., Castro, M., Denlinger, L. C., DiMango, E., Kraft, M., Peters, S. P., Wasserman, S. I., Wechsler, M. E., Boushey, H. A. & Lynch, S. V. Airway microbiota and bronchial hyperresponsiveness in patients with suboptimally controlled asthma. *J. Allergy Clin. Immunol.* **127**, 372–381.e3 (2011).
282. Huang, Y. J., Sethi, S., Murphy, T., Nariya, S., Boushey, H. A. & Lynch, S. V. Airway microbiome dynamics in exacerbations of chronic obstructive pulmonary disease. *J. Clin. Microbiol.* **52**, 2813–23 (2014).
283. Smith, K., McCoy, K. D. & Macpherson, A. J. Use of axenic animals in studying the adaptation of mammals to their commensal intestinal microbiota. *Semin. Immunol.* **19**, 59–69 (2007).
284. Herbst, T., Sichelstiel, A., Schär, C., Yadava, K., Bürki, K., Cahenzli, J., McCoy, K., Marsland, B. J. & Harris, N. L. Dysregulation of Allergic Airway Inflammation in the Absence of Microbial Colonization. *Am. J. Respir. Crit. Care Med.* **184**, 198–205 (2011).
285. Olszak, T., An, D., Zeissig, S., Vera, M. P., Richter, J., Franke, A., Glickman, J. N., Siebert, R., Baron, R. M., Kasper, D. L. & Blumberg, R. S. Microbial exposure during early life has persistent effects on natural killer T cell function. *Science* **336**, 489–93 (2012).
286. Cahenzli, J., Köller, Y., Wyss, M., Geuking, M. B. & McCoy, K. D. Intestinal Microbial Diversity during Early-Life Colonization Shapes Long-Term IgE Levels. *Cell Host Microbe* **14**, 559–570 (2013).
287. McCoy, K. D., Harris, N. L., Diener, P., Hatak, S., Odermatt, B., Hangartner, L., Senn, B. M., Marsland, B. J., Geuking, M. B., Hengartner, H., Macpherson, A. J. S. & Zinkernagel, R. M. Natural IgE Production in the Absence of MHC Class II Cognate Help. *Immunity* **24**, 329–339 (2006).

288. Williams, A. M., Probert, C. S. J., Stepankova, R., Tlaskalova-Hogenova, H., Phillips, A. & Bland, P. W. Effects of microflora on the neonatal development of gut mucosal T cells and myeloid cells in the mouse. *Immunology* **119**, 470–478 (2006).
289. Hansen, C. H. F., Nielsen, D. S., Kverka, M., Zakostelska, Z., Klimesova, K., Hudcovic, T., Tlaskalova-Hogenova, H. & Hansen, A. K. Patterns of Early Gut Colonization Shape Future Immune Responses of the Host. *PLoS One* **7**, e34043 (2012).
290. Russell, S. L., Gold, M. J., Hartmann, M., Willing, B. P., Thorson, L., Wlodarska, M., Gill, N., Blanchet, M.-R., Mohn, W. W., McNagny, K. M. & Finlay, B. B. Early life antibiotic-driven changes in microbiota enhance susceptibility to allergic asthma. *EMBO Rep.* **13**, 440–7 (2012).
291. Lyons, A., O'Mahony, D., O'Brien, F., MacSharry, J., Sheil, B., Ceddia, M., Russell, W. M., Forsythe, P., Bienenstock, J., Kiely, B., Shanahan, F. & O'Mahony, L. Bacterial strain-specific induction of Foxp3<sup>+</sup> T regulatory cells is protective in murine allergy models. *Clin. Exp. Allergy* **40**, 811–819 (2010).
292. Sagar, S., Morgan, M. E., Chen, S., Vos, A. P., Garssen, J., van Bergenhenegouwen, J., Boon, L., Georgiou, N. A., Kraneveld, A. D. & Folkerts, G. Bifidobacterium breve and Lactobacillus rhamnosus treatment is as effective as budesonide at reducing inflammation in a murine model for chronic asthma. *Respir. Res.* **15**, 46 (2014).
293. Forsythe, P., Inman, M. D. & Bienenstock, J. Oral Treatment with Live *Lactobacillus reuteri* Inhibits the Allergic Airway Response in Mice. *Am. J. Respir. Crit. Care Med.* **175**, 561–569 (2007).
294. Díaz-Ropero, M. P., Martín, R., Sierra, S., Lara-Villoslada, F., Rodríguez, J. M., Xaus, J. & Olivares, M. Two Lactobacillus strains, isolated from breast milk, differently modulate the immune response. *J. Appl. Microbiol.* **102**, 337–43 (2007).
295. Mohamadzadeh, M., Olson, S., Kalina, W. V., Ruthel, G., Demmin, G. L., Warfield, K. L., Bavari, S. & Klaenhammer, T. R. Lactobacilli activate human dendritic cells that skew T cells toward T helper 1 polarization. *Proc. Natl. Acad. Sci.* **102**, 2880–2885 (2005).
296. Kinjo, Y., Wu, D., Kim, G., Xing, G.-W., Poles, M. A., Ho, D. D., Tsuji, M., Kawahara, K., Wong, C.-H. & Kronenberg, M. Recognition of bacterial glycosphingolipids by natural killer T cells. *Nature* **434**, 520–525 (2005).
297. Mattner, J., DeBord, K. L., Ismail, N., Goff, R. D., Cantu, C., Zhou, D., Saint-Mezard, P., Wang, V., Gao, Y., Yin, N., Hoebe, K., Schneewind, O., Walker, D., Beutler, B., Teyton, L., Savage, P. B. & Bendelac, A. Exogenous and endogenous glycolipid antigens activate NKT cells during microbial infections. *Nature* **434**, 525–529 (2005).
298. Sriram, V., Du, W., Gervay-Hague, J. & Brutkiewicz, R. R. Cell wall glycosphingolipids of *Sphingomonas paucimobilis* are CD1d-specific ligands for NKT cells. *Eur. J. Immunol.* **35**, 1692–1701 (2005).
299. Hecht, G., Pothoulakis, C., LaMont, J. T. & Madara, J. L. Clostridium difficile toxin A perturbs cytoskeletal structure and tight junction permeability of cultured human intestinal epithelial monolayers. *J. Clin. Invest.* **82**, 1516–1524 (1988).
300. Nusrat, A., von Eichel-Streiber, C., Turner, J. R., Verkade, P., Madara, J. L. & Parkos, C. A. Clostridium difficile toxins disrupt epithelial barrier function by altering membrane microdomain localization of tight junction proteins. *Infect. Immun.* **69**, 1329–36 (2001).
301. Linevsky, J. K., Pothoulakis, C., Keates, S., Warny, M., Keates, A. C., Lamont, J. T. & Kelly, C. P. IL-8 release and neutrophil activation by *Clostridium difficile* toxin-exposed human monocytes. *Am. J. Physiol. Liver Physiol.* **273**, G1333–G1340 (1997).

302. Morinaga, Y., Yanagihara, K., Miyashita, N., Seki, M., Izumikawa, K., Kakeya, H., Yamamoto, Y., Mukae, H., Yamada, Y., Kohno, S. & Kamihira, S. Azithromycin, clarithromycin and telithromycin inhibit MUC5AC induction by *Chlamydia pneumoniae* in airway epithelial cells. *Pulm. Pharmacol. Ther.* **22**, 580–586 (2009).
303. Heinemann, M., Susa, M., Simnacher, U., Marre, R. & Essig, A. Growth of *Chlamydia pneumoniae* induces cytokine production and expression of CD14 in a human monocytic cell line. *Infect. Immun.* **64**, 4872–5 (1996).
304. Netea, M. G., Selzman, C. H., Kullberg, B. J., Galama, J. M. D., Weinberg, A., Stalenhoef, A. F. H., Van der Meer, J. W. M. & Dinarello, C. A. Acellular components of *Chlamydia pneumoniae* stimulate cytokine production in human blood mononuclear cells. *Eur. J. Immunol.* **30**, 541–549 (2000).
305. Rödel, J., Woytas, M., Groh, A., Schmidt, K. H., Hartmann, M., Lehmann, M. & Straube, E. Production of basic fibroblast growth factor and interleukin 6 by human smooth muscle cells following infection with *Chlamydia pneumoniae*. *Infect. Immun.* **68**, 3635–41 (2000).
306. Jupelli, M., Shimada, K., Chiba, N., Slepentin, A., Alsabeh, R., Jones, H. D., Peterson, E., Chen, S., Arditi, M. & Crother, T. R. *Chlamydia pneumoniae* Infection in Mice Induces Chronic Lung Inflammation, iBALT Formation, and Fibrosis. *PLoS One* **8**, e77447 (2013).
307. Coombes, B. K. & Mahony, J. B. *Chlamydia pneumoniae* infection of human endothelial cells induces proliferation of smooth muscle cells via an endothelial cell-derived soluble factor(s). *Infect. Immun.* **67**, 2909–15 (1999).
308. Chen, C.-Z., Yang, B.-C., Lin, T.-M., Lee, C.-H. & Hsiue, T.-R. Chronic and Repeated *Chlamydia pneumoniae* Lung Infection can Result in Increasing IL-4 Gene Expression and Thickness of Airway Subepithelial Basement Membrane in Mice. *J. Formos. Med. Assoc.* **108**, 45–52 (2009).
309. Markova, N. D. L-form bacteria cohabitants in human blood: significance for health and diseases. *Discov. Med.* **23**, 305–313 (2017).
310. Rajendhran, J., Shankar, M., Dinakaran, V., Rathinavel, A. & Gunasekaran, P. Contrasting circulating microbiome in cardiovascular disease patients and healthy individuals. *Int. J. Cardiol.* **168**, 5118–5120 (2013).
311. Parahitiyawa, N. B., Jin, L. J., Leung, W. K., Yam, W. C. & Samaranyake, L. P. Microbiology of Odontogenic Bacteremia: beyond Endocarditis. *Clin. Microbiol. Rev.* **22**, 46–64 (2009).
312. Tedeschi, G. G., Amici, D. & Paparelli, M. Incorporation of nucleosides and amino-acids in human erythrocyte suspensions: possible relation with a diffuse infection of mycoplasmas or bacteria in the L form. *Nature* **222**, 1285–6 (1969).
313. Tedeschi, G. G. & Amici, D. Mycoplasma-like microorganisms probably related to L forms of bacteria in the blood of healthy persons. Cultural, morphological and histochemical data. *Ann. Sclavo.* **14**, 430–42 (1972).
314. Tedeschi, G. G., Amici, D., Sprovieri, G. & Vecchi, A. *Staphylococcus epidermidis* in the circulating blood of normal and thrombocytopenic human subjects: immunological data. *Experientia* **32**, 1600–2 (1976).
315. Domingue, G. J. & Schlegel, J. U. Novel bacterial structures in human blood: cultural isolation. *Infect. Immun.* **15**, 621–7 (1977).
316. Tedeschi, G. G., Bondi, A., Paparelli, M. & Sprovieri, G. Electron microscopical evidence of the evolution of corynebacteria-like microorganisms within human erythrocytes. *Experientia* **34**, 458–460 (1978).

317. Pease, P. E. & Tallack, J. E. A permanent endoparasite of man. 1. The silent zoogloal/sytoplasm/L-form phase. *Microbios* **64**, 173–80 (1990).
318. Kajander, E., Tahvanainen, E., Kuronen, I. & Ciftcioglu, N. Comparison of Staphylococci and Novel Bacteria-Like Particles from Blood. *Zbl Bakt* **26**, 147–149 (1994).
319. McLaughlin, R. W., Vali, H., Lau, P. C. K., Palfree, R. G. E., De Ciccio, A., Sirois, M., Ahmad, D., Villemur, R., Desrosiers, M. & Chan, E. C. S. Are there naturally occurring pleomorphic bacteria in the blood of healthy humans? *J. Clin. Microbiol.* **40**, 4771–5 (2002).
320. Nikkari, S., McLaughlin, I. J., Bi, W., Dodge, D. E. & Relman, D. A. Does Blood of Healthy Subjects Contain Bacterial Ribosomal DNA? *J. Clin. Microbiol.* **39**, 1956–1959 (2001).
321. Lehtiniemi, J., Karhunen, P. J., Goebeler, S., Nikkari, S. & Nikkari, S. T. Identification of different bacterial DNAs in human coronary arteries. *Eur. J. Clin. Invest.* **35**, 13–16 (2005).
322. Amar, J., Serino, M., Lange, C., Chabo, C., Iacovoni, J., Mondot, S., Lepage, P., Klopp, C., Mariette, J., Bouchez, O., Perez, L., Courtney, M., Marre, M., Klopp, P., Lantieri, O., Doré, J., Charles, M. A., Balkau, B., Burcelin, R. & D.E.S.I.R. Study Group. Involvement of tissue bacteria in the onset of diabetes in humans: evidence for a concept. *Diabetologia* **54**, 3055–3061 (2011).
323. Amar, J., Lange, C., Payros, G., Garret, C., Chabo, C., Lantieri, O., Courtney, M., Marre, M., Charles, M. A., Balkau, B. & Burcelin, R. Blood Microbiota Dysbiosis Is Associated with the Onset of Cardiovascular Events in a Large General Population: The D.E.S.I.R. Study. *PLoS One* **8**, e54461 (2013).
324. Dinakaran, V., Rathinavel, A., Pushpanathan, M., Sivakumar, R., Gunasekaran, P. & Rajendhran, J. Elevated Levels of Circulating DNA in Cardiovascular Disease Patients: Metagenomic Profiling of Microbiome in the Circulation. *PLoS One* **9**, e105221 (2014).
325. Kell, D. B. & Pretorius, E. On the translocation of bacteria and their lipopolysaccharides between blood and peripheral locations in chronic, inflammatory diseases: the central roles of LPS and LPS-induced cell death. *Integr. Biol.* **7**, 1339–1377 (2015).
326. Potgieter, M., Bester, J., Kell, D. B. & Pretorius, E. The dormant blood microbiome in chronic, inflammatory diseases. *FEMS Microbiol. Rev.* **39**, 567–591 (2015).
327. Paissé, S., Valle, C., Servant, F., Courtney, M., Burcelin, R., Amar, J. & Lelouvier, B. Comprehensive description of blood microbiome from healthy donors assessed by 16S targeted metagenomic sequencing. *Transfusion* **56**, 1138–1147 (2016).
328. Bhattacharyya, M., Ghosh, T., Shankar, S. & Tomar, N. The conserved phylogeny of blood microbiome. *Mol. Phylogenet. Evol.* **109**, 404–408 (2017).
329. Gosiewski, T., Ludwig-Galezowska, A. H., Huminska, K., Sroka-Oleksiak, A., Radkowski, P., Salamon, D., Wojciechowicz, J., Kus-Slowinska, M., Bulanda, M. & Wolkow, P. P. Comprehensive detection and identification of bacterial DNA in the blood of patients with sepsis and healthy volunteers using next-generation sequencing method - the observation of DNAemia. *Eur. J. Clin. Microbiol. Infect. Dis.* **36**, 329–336 (2017).
330. Huang, Y.-F., Chen, Y.-J., Fan, T.-C., Chang, N.-C., Chen, Y.-J., Midha, M. K., Chen, T.-H., Yang, H.-H., Wang, Y.-T., Yu, A. L. & Chiu, K.-P. Analysis of microbial sequences in plasma cell-free DNA for early-onset breast cancer patients and healthy females. *BMC Med. Genomics* **11**, 16 (2018).
331. Li, Q., Wang, C., Tang, C., Zhao, X., He, Q. & Li, J. Identification and Characterization of Blood and Neutrophil-Associated Microbiomes in Patients with Severe Acute Pancreatitis Using Next-Generation Sequencing. *Front. Cell. Infect. Microbiol.* **8**, 5 (2018).

332. Olde Loohuis, L. M., Mangul, S., Ori, A. P. S., Jospin, G., Koslicki, D., Yang, H. T., Wu, T., Boks, M. P., Lomen-Hoerth, C., Wiedau-Pazos, M., Cantor, R. M., de Vos, W. M., Kahn, R. S., Eskin, E. & Ophoff, R. A. Transcriptome analysis in whole blood reveals increased microbial diversity in schizophrenia. *Transl. Psychiatry* **8**, 96 (2018).
333. Panaiotov, S., Filevski, G., Equestre, M., Nikolova, E. & Kalfin, R. Cultural Isolation and Characteristics of the Blood Microbiome of Healthy Individuals. *Adv. Microbiol.* **08**, 406–421 (2018).
334. Ring, H. C., Thorsen, J., Saunte, D. M., Lilje, B., Bay, L., Theut Riis, P., Larsen, N., O'Brien Andersen, L., Vedel Nielsen, H., Miller, I. M., Bjarnsholt, T., Fuursted, K. & Jemec, G. B. Moderate to severe hidradenitis suppurativa patients do not have an altered bacterial composition in peripheral blood compared to healthy controls. *J. Eur. Acad. Dermatology Venereol.* **32**, 125–128 (2018).
335. Subramaniam, A., Van Der Pol, W. J., Ptacek, T., Lobashevsky, E., Neely, C., Biggio, J. R., Lefkowitz, E. J., Morrow, C. D. & Edwards, R. K. Midtrimester microbial DNA variations in maternal serum of women who experience spontaneous preterm birth. *J. Matern. Neonatal Med.* 1–9 (2018). doi:10.1080/14767058.2018.1490721
336. Xu, W., Luo, Z., Alekseyenko, A. V., Martin, L., Wan, Z., Ling, B., Qin, Z., Heath, S. L., Maas, K., Cong, X. & Jiang, W. Distinct systemic microbiome and microbial translocation are associated with plasma level of anti-CD4 autoantibody in HIV infection. *Sci. Rep.* **8**, 12863 (2018).
337. Qian, Y., Yang, X., Xu, S., Wu, C., Qin, N., Chen, S.-D. & Xiao, Q. Detection of Microbial 16S rRNA Gene in the Blood of Patients With Parkinson's Disease. *Front. Aging Neurosci.* **10**, 156 (2018).
338. Serena, G., Davies, C., Cetinbas, M., Sadreyev, R. I. & Fasano, A. Analysis of blood and fecal microbiome profile in patients with celiac disease. *Hum. Microbiome J.* **11**, 100049 (2019).
339. Shah, N. B., Allegretti, A. S., Nigwekar, S. U., Kalim, S., Zhao, S., Lelouvier, B., Servant, F., Serena, G., Thadhani, R. I., Raj, D. S. & Fasano, A. Blood Microbiome Profile in CKD. *Clin. J. Am. Soc. Nephrol.* **14**, 692–701 (2019).
340. Li, H., Li, T. & Qu, J. Stochastic processes govern bacterial communities from the blood of pikas and from their arthropod vectors. *FEMS Microbiol. Ecol.* **94**, (2018).
341. Sze, M. A., Tsuruta, M., Yang, S.-W. J., Oh, Y., Man, S. F. P., Hogg, J. C. & Sin, D. D. Changes in the Bacterial Microbiota in Gut, Blood, and Lungs following Acute LPS Instillation into Mice Lungs. *PLoS One* **9**, e111228 (2014).
342. Vientós-Plotts, A. I., Ericsson, A. C., Rindt, H., Grobman, M. E., Graham, A., Bishop, K., Cohn, L. A. & Reiner, C. R. Dynamic changes of the respiratory microbiota and its relationship to fecal and blood microbiota in healthy young cats. *PLoS One* **12**, e0173818 (2017).
343. Mandal, R. K., Jiang, T., Al-Rubaye, A. A., Rhoads, D. D., Wideman, R. F., Zhao, J., Pevzner, I. & Kwon, Y. M. An investigation into blood microbiota and its potential association with Bacterial Chondronecrosis with Osteomyelitis (BCO) in Broilers. *Sci. Rep.* **6**, 25882 (2016).
344. Jeon, S. J., Cunha, F., Vieira-Neto, A., Bicalho, R. C., Lima, S., Bicalho, M. L. & Galvão, K. N. Blood as a route of transmission of uterine pathogens from the gut to the uterus in cows. *Microbiome* **5**, 109 (2017).
345. Damgaard, C., Magnussen, K., Enevold, C., Nilsson, M., Tolker-Nielsen, T., Holmstrup, P. & Nielsen, C. H. Viable Bacteria Associated with Red Blood Cells and Plasma in Freshly Drawn Blood Donations. *PLoS One* **10**, e0120826 (2015).

346. Schierwagen, R., Alvarez-Silva, C., Madsen, M. S. A., Kolbe, C. C., Meyer, C., Thomas, D., Uschner, F. E., Magdaleno, F., Jansen, C., Pohlmann, A., Praktiknjo, M., Hischebeth, G. T., Molitor, E., Latz, E., Lelouvier, B., Trebicka, J. & Arumugam, M. Circulating microbiome in blood of different circulatory compartments. *Gut* **68**, 578–580 (2019).
347. Pease, P. Morphological appearances of a bacterial L-form growing in association with the erythrocytes of arthritic subjects. *Ann. Rheum. Dis.* **29**, 439–44 (1970).
348. Consortium, T. H. M. P., Methé, B. A., White, O., *et al.* A framework for human microbiome research. *Nature* **486**, 215–221 (2012).
349. Woese, C. R. & Fox, G. E. Phylogenetic structure of the prokaryotic domain: the primary kingdoms. *Proc. Natl. Acad. Sci. U. S. A.* **74**, 5088–90 (1977).
350. Sogin, M. L., Morrison, H. G., Huber, J. A., Welch, D. M., Huse, S. M., Neal, P. R., Arrieta, J. M. & Herndl, G. J. Microbial diversity in the deep sea and the underexplored “rare biosphere”. *Proc. Natl. Acad. Sci.* **103**, 12115–12120 (2006).
351. Janda, J. M. & Abbott, S. L. 16S rRNA gene sequencing for bacterial identification in the diagnostic laboratory: pluses, perils, and pitfalls. *J. Clin. Microbiol.* **45**, 2761–4 (2007).
352. Tremblay, J., Singh, K., Fern, A., Kirton, E. S., He, S., Woyke, T., Lee, J., Chen, F., Dangl, J. L. & Tringe, S. G. Primer and platform effects on 16S rRNA tag sequencing. *Front. Microbiol.* **6**, 771 (2015).
353. Fukui, H., Brauner, B., Bode, J. C. & Bode, C. Plasma endotoxin concentrations in patients with alcoholic and non-alcoholic liver disease: reevaluation with an improved chromogenic assay. *J. Hepatol.* **12**, 162–169 (1991).
354. Amar, J., Burcelin, R., Ruidavets, J. B., Cani, P. D., Fauvel, J., Alessi, M. C., Chamontin, B. & Ferrières, J. Energy intake is associated with endotoxemia in apparently healthy men. *Am. J. Clin. Nutr.* **87**, 1219–1223 (2008).
355. Aronov, P. A., Luo, F. J.-G., Plummer, N. S., Quan, Z., Holmes, S., Hostetter, T. H. & Meyer, T. W. Colonic contribution to uremic solutes. *J. Am. Soc. Nephrol.* **22**, 1769–76 (2011).
356. Lyte, J. M., Gabler, N. K. & Hollis, J. H. Postprandial serum endotoxin in healthy humans is modulated by dietary fat in a randomized, controlled, cross-over study. *Lipids Health Dis.* **15**, 186 (2016).
357. Andersen, K., Kesper, M. S., Marschner, J. A., Konrad, L., Ryu, M., Kumar Vr, S., Kulkarni, O. P., Mulay, S. R., Romoli, S., Demleitner, J., Schiller, P., Dietrich, A., Müller, S., Gross, O., Ruscheweyh, H.-J., Huson, D. H., Stecher, B. & Anders, H.-J. Intestinal Dysbiosis, Barrier Dysfunction, and Bacterial Translocation Account for CKD-Related Systemic Inflammation. *J. Am. Soc. Nephrol.* **28**, 76–83 (2017).
358. Kowarsky, M., Camunas-Soler, J., Kertesz, M., De Vlaminc, I., Koh, W., Pan, W., Martin, L., Neff, N. F., Okamoto, J., Wong, R. J., Kharbanda, S., El-Sayed, Y., Blumenfeld, Y., Stevenson, D. K., Shaw, G. M., Wolfe, N. D. & Quake, S. R. Numerous uncharacterized and highly divergent microbes which colonize humans are revealed by circulating cell-free DNA. *Proc. Natl. Acad. Sci. U. S. A.* **114**, 9623–9628 (2017).
359. Ono, S., Tsujimoto, H., Yamauchi, A., Hiraki, S., Takayama, E. & Mochizuki, H. Detection of Microbial DNA in the Blood of Surgical Patients for Diagnosing Bacterial Translocation. *World J. Surg.* **29**, 535–539 (2005).
360. Sato, J., Kanazawa, A., Ikeda, F., Yoshihara, T., Goto, H., Abe, H., Komiya, K., Kawaguchi, M., Shimizu, T., Ogihara, T., Tamura, Y., Sakurai, Y., Yamamoto, R., Mita, T., Fujitani, Y., Fukuda, H., Nomoto, K., Takahashi, T., Asahara, T., Hirose, T., Nagata, S., Yamashiro, Y. & Watada,



- H. Gut Dysbiosis and Detection of “Live Gut Bacteria” in Blood of Japanese Patients With Type 2 Diabetes. *Diabetes Care* **37**, 2343–2350 (2014).
361. Lelouvier, B., Servant, F., Païssé, S., Brunet, A.-C., Benyahya, S., Serino, M., Valle, C., Ortiz, M. R., Puig, J., Courtney, M., Federici, M., Fernández-Real, J.-M., Burcelin, R. & Amar, J. Changes in blood microbiota profiles associated with liver fibrosis in obese patients: A pilot analysis. *Hepatology* **64**, 2015–2027 (2016).
  362. Li, S.-K., Leung, R. K.-K., Guo, H.-X., Wei, J.-F., Wang, J.-H., Kwong, K.-T., Lee, S.-S., Zhang, C. & Tsui, S. K.-W. Detection and identification of plasma bacterial and viral elements in HIV/AIDS patients in comparison to healthy adults. *Clin. Microbiol. Infect.* **18**, 1126–1133 (2012).
  363. Santiago, A., Pozuelo, M., Poca, M., Gely, C., Nieto, J. C., Torras, X., Román, E., Campos, D., Sarrabayrouse, G., Vidal, S., Alvarado-Tapias, E., Guarner, F., Soriano, G., Manichanh, C. & Guarner, C. Alteration of the serum microbiome composition in cirrhotic patients with ascites. *Sci. Rep.* **6**, 25001 (2016).
  364. Traykova, D., Schneider, B., Chojkier, M. & Buck, M. Blood Microbiome Quantity and the Hyperdynamic Circulation in Decompensated Cirrhotic Patients. *PLoS One* **12**, e0169310 (2017).
  365. Qiu, J., Zhou, H., Jing, Y. & Dong, C. Association between blood microbiome and type 2 diabetes mellitus: A nested case-control study. *J. Clin. Lab. Anal.* e22842 (2019). doi:10.1002/jcla.22842
  366. Cho, E. J., Leem, S., Kim, S. A., Yang, J., Lee, Y. Bin, Kim, S. S., Cheong, J. Y., Cho, S. W., Kim, J. W., Kim, S.-M., Yoon, J.-H. & Park, T. Circulating Microbiota-Based Metagenomic Signature for Detection of Hepatocellular Carcinoma. *Sci. Rep.* **9**, 7536 (2019).
  367. Whittle, E., Leonard, M. O., Harrison, R., Gant, T. W. & Tonge, D. P. Multi-Method Characterization of the Human Circulating Microbiome. *Front. Microbiol.* **9**, 3266 (2018).
  368. Whittle, E., Leonard, M. O., Gant, T. W. & Tonge, D. P. Multi-Method Molecular Characterisation of Human Dust-Mite-associated Allergic Asthma. *Sci. Rep.* **9**, 8912 (2019).
  369. Glassing, A., Dowd, S. E., Galandiuk, S., Davis, B. & Chiodini, R. J. Inherent bacterial DNA contamination of extraction and sequencing reagents may affect interpretation of microbiota in low bacterial biomass samples. *Gut Pathog.* **8**, 24 (2016).
  370. Stinson, L. F., Keelan, J. A. & Payne, M. S. Identification and removal of contaminating microbial DNA from PCR reagents: impact on low-biomass microbiome analyses. *Lett. Appl. Microbiol.* **68**, 2–8 (2019).
  371. Salter, S. J., Cox, M. J., Turek, E. M., Calus, S. T., Cookson, W. O., Moffatt, M. F., Turner, P., Parkhill, J., Loman, N. J. & Walker, A. W. Reagent and laboratory contamination can critically impact sequence-based microbiome analyses. *BMC Biol.* **12**, 87 (2014).
  372. McFeters, G. A., Broadaway, S. C., Pyle, B. H. & Egozy, Y. Distribution of bacteria within operating laboratory water purification systems. *Appl. Environ. Microbiol.* **59**, 1410–5 (1993).
  373. Kulakov, L. A., Mcalister, M. B., Ogden, K. L., Larkin, M. J. & O’hanlon, J. F. Analysis of Bacteria Contaminating Ultrapure Water in Industrial Systems. *Appl. Environ. Microbiol.* **68**, 1548–1555 (2002).
  374. Shen, H., Rogelj, S. & Kieft, T. L. Sensitive, real-time PCR detects low-levels of contamination by *Legionella pneumophila* in commercial reagents. *Mol. Cell. Probes* **20**, 147–153 (2006).

375. Laurence, M., Hatzis, C. & Brash, D. E. Common Contaminants in Next-Generation Sequencing That Hinder Discovery of Low-Abundance Microbes. *PLoS One* **9**, 97876 (2014).
376. Corless, C. E., Guiver, M., Borrow, R., Edwards-Jones, V., Kaczmarek, E. B. & Fox, A. J. Contamination and Sensitivity Issues with a Real-Time Universal 16S rRNA PCR. *Journal of Clinical Microbiology* **38**, (2000).
377. Hornung, B. V. H., Zwittink, R. D. & Kuijper, E. J. Issues and current standards of controls in microbiome research. *FEMS Microbiol. Ecol.* **95**, (2019).
378. Schierwagen, R., Alvarez-Silva, C., Servant, F., Trebicka, J., Lelouvier, B. & Arumugam, M. Trust is good, control is better: technical considerations in blood microbiome analysis. *Gut* [gutjnl-2019-319123](https://doi.org/10.1136/gutjnl-2019-319123) (2019). doi:10.1136/gutjnl-2019-319123
379. Holmes, A. M., Solari, R. & Holgate, S. T. Animal models of asthma: value, limitations and opportunities for alternative approaches. *Drug Discov. Today* **16**, (2011).
380. Aun, M. V., Bonamichi-Santos, R., Magalhães Arantes-Costa, F., Kalil, J. & Giavina-Bianchi, P. Animal models of asthma: utility and limitations. *J. Asthma Allergy* 10–293 (2017). doi:10.2147/JAA.S121092
381. Zosky, G. R. & Sly, P. D. Animal models of asthma. *Clin. Exp. Allergy* **37**, 973–988 (2007).
382. Sagar, S., Akbarshahi, H. & Uller, L. Translational value of animal models of asthma: Challenges and promises. *Eur. J. Pharmacol.* **759**, 272–277 (2015).
383. Meldrum, K., Robertson, S. B., Römer, I., Marczylo, T., Dean, L. S. N., Rogers, A., Gant, T. W., Smith, R., Tetley, T. D. & Leonard, M. O. Cerium dioxide nanoparticles exacerbate house dust mite induced type II airway inflammation. *Part. Fibre Toxicol.* **15**, 24 (2018).
384. Barfod, K. K., Roggenbuck, M., Al-Shuweli, S., Fakhri, D., Sørensen, S. J. & Sørensen, G. L. Alterations of the murine gut microbiome in allergic airway disease are independent of surfactant protein D. *Heliyon* **3**, e00262 (2017).
385. Tsang, M., Cheng, S.-W., Zhu, J., Atli, K., Chan, B., Liu, D., Chan, H., Sun, X., Chu, I., Hon, K.-L., Lam, C., Shaw, P.-C., Leung, P.-C., Wong, C.-K., Tsang, M. S.-M., Cheng, S.-W., Zhu, J., Atli, K., Chan, B. C.-L., Liu, D., Chan, H. Y.-T., Sun, X., Chu, I. M.-T., Hon, K.-L., Lam, C. W.-K., Shaw, P.-C., Leung, P.-C. & Wong, C.-K. Anti-Inflammatory Activities of Pentaherbs formula and Its Influence on Gut Microbiota in Allergic Asthma. *Molecules* **23**, 2776 (2018).
386. Vital, M., Harkema, J. R., Rizzo, M., Tiedje, J. & Brandenberger, C. Alterations of the Murine Gut Microbiome with Age and Allergic Airway Disease. *J. Immunol. Res.* **2015**, 892568 (2015).
387. Roggenbuck, M., Anderson, D., Barfod, K. K., Feelisch, M., Geldenhuys, S., Sørensen, S. J., Weeden, C. E., Hart, P. H. & Gorman, S. Vitamin D and allergic airway disease shape the murine lung microbiome in a sex-specific manner. *Respir. Res.* **17**, 116 (2016).
388. Remot, A., Descamps, D., Noordine, M.-L., Boukadiri, A., Mathieu, E., Robert, V., Riffault, S., Lambrecht, B., Langella, P., Hammad, H. & Thomas, M. Bacteria isolated from lung modulate asthma susceptibility in mice. *ISME J.* **11**, 1061–1074 (2017).
389. Quast, C., Pruesse, E., Yilmaz, P., Gerken, J., Schweer, T., Yarza, P., Peplies, J. & Glöckner, F. O. The SILVA ribosomal RNA gene database project: improved data processing and web-based tools. *Nucleic Acids Res.* **41**, D590 (2013).
390. Demircan, T., Ovezmyradov, G., Yıldırım, B., Keskin, İ., İlhan, A. E., Fesçioğlu, E. C., Öztürk, G. & Yıldırım, S. Experimentally induced metamorphosis in highly regenerative axolotl (ambystoma mexicanum) under constant diet restructures microbiota. *Sci. Rep.* **8**, 10974

- (2018).
391. Gotelli, N. J. & Colwell, R. K. Estimating species richness. *Biol. Divers. Front. Meas. Assess.* **12**, 39-54. (2011).
  392. Nipperess, D. A. The Rarefaction of Phylogenetic Diversity: Formulation, Extension and Application. in 197–217 (Springer, Cham, 2016). doi:10.1007/978-3-319-22461-9\_10
  393. Langille, M. G. I., Zaneveld, J., Caporaso, J. G., McDonald, D., Knights, D., Reyes, J. A., Clemente, J. C., Burkepile, D. E., Vega Thurber, R. L., Knight, R., Beiko, R. G. & Huttenhower, C. Predictive functional profiling of microbial communities using 16S rRNA marker gene sequences. *Nat. Biotechnol.* **31**, 814–21 (2013).
  394. Segata, N., Izard, J., Waldron, L., Gevers, D., Miropolsky, L., Garrett, W. S. & Huttenhower, C. Metagenomic biomarker discovery and explanation. *Genome Biol.* **12**, R60 (2011).
  395. Juniper, E. F., O'byrne, P. M., Guyatt, G. ., Ferrie, P. . & King, D. . Development and validation of a questionnaire to measure asthma control. *Eur. Respir. J.* **14**, 902 (1999).
  396. Juniper, E. F., Bousquet, J., Abetz, L. & Bateman, E. D. Identifying 'well-controlled' and 'not well-controlled' asthma using the Asthma Control Questionnaire. *Respir. Med.* **100**, 616–621 (2006).
  397. Trapnell, C., Roberts, A., Goff, L., Pertea, G., Kim, D., Kelley, D. R., Pimentel, H., Salzberg, S. L., Rinn, J. L. & Pachter, L. Differential gene and transcript expression analysis of RNA-seq experiments with TopHat and Cufflinks. (2012). doi:10.1038/nprot.2012.016
  398. Rueda, A., Barturen, G., Lebrón, R., Gómez-Martín, C., Alganza, Á., Oliver, J. L. & Hackenberg, M. sRNAtoolbox: an integrated collection of small RNA research tools. *Nucleic Acids Res.* **43**, W467-73 (2015).
  399. Kozomara, A., Birgaoanu, M. & Griffiths-Jones, S. miRBase: from microRNA sequences to function. *Nucleic Acids Res.* **47**, 155–162 (2018).
  400. Robinson, M. D., McCarthy, D. J. & Smyth, G. K. edgeR: a Bioconductor package for differential expression analysis of digital gene expression data. *Bioinformatics* **26**, 139–140 (2010).
  401. Liu, J., Liu, Y., Wang, D., He, M., Diao, L., Liu, Z., Li, Y., Tang, L., He, F., Li, D. & Guo, S. AllerGAtlas 1.0: a human allergy-related genes database. *Database* **2018**, (2018).
  402. Vlachos, I. S., Zagganas, K., Paraskevopoulou, M. D., Georgakilas, G., Karagkouni, D., Vergoulis, T., Dalamagas, T. & Hatzigeorgiou, A. G. DIANA-miRPath v3.0: deciphering microRNA function with experimental support. *Nucleic Acids Res.* **43**, W460-6 (2015).
  403. Krämer, A., Green, J., Pollard, J. & Tugendreich, S. Causal analysis approaches in Ingenuity Pathway Analysis. *Bioinformatics* **30**, 523–530 (2014).
  404. Juniper, E. F., Gruffydd-Jones, K., Ward, S. & Svensson, K. Asthma Control Questionnaire in children: validation, measurement properties, interpretation. *Eur. Respir. J.* **36**, 1410–6 (2010).
  405. Muñoz-Culla, M., Irizar, H., Castillo-Triviño, T., Sáenz-Cuesta, M., Sepúlveda, L., Lopetegi, I., de Munain, A. L., Olascoaga, J., Baranzini, S. & Otaegui, D. Blood miRNA expression pattern is a possible risk marker for natalizumab-associated progressive multifocal leukoencephalopathy in multiple sclerosis patients. *Mult. Scler. J.* **20**, 1851–1859 (2014).
  406. Nielsen, S., Åkerström, T., Rinnov, A., Yfanti, C., Scheele, C., Pedersen, B. K. & Laye, M. J. The miRNA Plasma Signature in Response to Acute Aerobic Exercise and Endurance Training. *PLoS One* **9**, e87308 (2014).

407. Pirola, C. J., Fernández Gianotti, T., Castaño, G. O., Mallardi, P., San Martino, J., Mora Gonzalez Lopez Ledesma, M., Flichman, D., Mirshahi, F., Sanyal, A. J. & Sookoian, S. Circulating microRNA signature in non-alcoholic fatty liver disease: from serum non-coding RNAs to liver histology and disease pathogenesis. *Gut* **64**, 800–12 (2015).
408. Panganiban, R. P., Wang, Y., Howrylak, J., Chinchilli, V. M., Craig, T. J., August, A. & Ishmael, F. T. Circulating microRNAs as biomarkers in patients with allergic rhinitis and asthma. *J. Allergy Clin. Immunol.* **137**, 1423–1432 (2016).
409. Tonge, D. P. & Gant, T. W. What is normal? Next generation sequencing-driven analysis of the human circulating miRNAome. *BMC Mol. Biol.* **17**, 4 (2016).
410. Kemper, C., Chan, A. C., Green, J. M., Brett, K. A., Murphy, K. M. & Atkinson, J. P. Activation of human CD4+ cells with CD3 and CD46 induces a T-regulatory cell 1 phenotype. *Nature* **421**, 388–392 (2003).
411. Xu, Y.-Q., Gao, Y.-D., Yang, J. & Guo, W. A defect of CD4+CD25+ regulatory T cells in inducing interleukin-10 production from CD4+ T cells under CD46 costimulation in asthma patients. *J. Asthma* **47**, 367–73 (2010).
412. Cardone, J., Le Friec, G., Vantourout, P., Roberts, A., Fuchs, A., Jackson, I., Suddason, T., Lord, G., Atkinson, J. P., Cope, A., Hayday, A. & Kemper, C. Complement regulator CD46 temporally regulates cytokine production by conventional and unconventional T cells. *Nat. Immunol.* **11**, 862–871 (2010).
413. Le Friec, G., Sheppard, D., Whiteman, P., Karsten, C. M., Shamoun, S. A.-T., Laing, A., Bugeon, L., Dallman, M. J., Melchionna, T., Chillakuri, C., Smith, R. A., Drouet, C., Couzi, L., Fremeaux-Bacchi, V., Köhl, J., Waddington, S. N., McDonnell, J. M., Baker, A., Handford, P. A., Lea, S. M. & Kemper, C. The CD46-Jagged1 interaction is critical for human TH1 immunity. *Nat. Immunol.* **13**, 1213–1221 (2012).
414. Tsai, Y.-G., Niu, D.-M., Yang, K. D., Hung, C.-H., Yeh, Y.-J., Lee, C.-Y. & Lin, C.-Y. Functional defects of CD46-induced regulatory T cells to suppress airway inflammation in mite allergic asthma. *Lab. Invest.* **92**, 1260–1269 (2012).
415. Rennard, S. I., Hunninghake, G. W., Bitterman, P. B. & Crystal, R. G. Production of fibronectin by the human alveolar macrophage: mechanism for the recruitment of fibroblasts to sites of tissue injury in interstitial lung diseases. *Proc. Natl. Acad. Sci. U. S. A.* **78**, 7147–51 (1981).
416. Muro, A. F., Moretti, F. A., Moore, B. B., Yan, M., Atrasz, R. G., Wilke, C. A., Flaherty, K. R., Martinez, F. J., Tsui, J. L., Sheppard, D., Baralle, F. E., Toews, G. B. & White, E. S. An Essential Role for Fibronectin Extra Type III Domain A in Pulmonary Fibrosis. *Am. J. Respir. Crit. Care Med.* **177**, 638–645 (2008).
417. Hirst, S. J., Twort, C. H. C. & Lee, T. H. Differential Effects of Extracellular Matrix Proteins on Human Airway Smooth Muscle Cell Proliferation and Phenotype. *Am. J. Respir. Cell Mol. Biol.* **23**, 335–344 (2000).
418. Freyer, A. M., Johnson, S. R. & Hall, I. P. Effects of Growth Factors and Extracellular Matrix on Survival of Human Airway Smooth Muscle Cells. *Am. J. Respir. Cell Mol. Biol.* **25**, 569–576 (2001).
419. Sundaram, A., Chen, C., Khalifeh-Soltani, A., Atakilit, A., Ren, X., Qiu, W., Jo, H., DeGrado, W., Huang, X. & Sheppard, D. Targeting integrin  $\alpha 5\beta 1$  ameliorates severe airway hyperresponsiveness in experimental asthma. *J. Clin. Invest.* **127**, 365–374 (2017).
420. Zhao, T., Singhal, S. S., Piper, J. T., Cheng, J., Pandya, U., Clark-Wronski, J., Awasthi, S. & Awasthi, Y. C. The Role of Human Glutathione S-Transferases hGSTA1-1 and hGSTA2-2 in

- Protection against Oxidative Stress. *Arch. Biochem. Biophys.* **367**, 216–224 (1999).
421. Kumar, M., Ahmad, T., Sharma, A., Mabalirajan, U., Kulshreshtha, A., Agrawal, A. & Ghosh, B. Let-7 microRNA-mediated regulation of IL-13 and allergic airway inflammation. *J. Allergy Clin. Immunol.* **128**, 1077–85.e1–10 (2011).
  422. Simonetta, F., Chiali, A., Cordier, C., Urrutia, A., Girault, I., Bloquet, S., Tanchot, C. & Bourgeois, C. Increased CD127 expression on activated FOXP3<sup>+</sup> CD4<sup>+</sup> regulatory T cells. doi:10.1002/eji.201040531
  423. von Freeden-Jeffry, U., Vieira, P., Lucian, L. A., McNeil, T., Burdach, S. E. & Murray, R. Lymphopenia in interleukin (IL)-7 gene-deleted mice identifies IL-7 as a nonredundant cytokine. *J. Exp. Med.* **181**, 1519–26 (1995).
  424. Moore, T. A., von Freeden-Jeffry, U., Murray, R. & Zlotnik, A. Inhibition of gamma delta T cell development and early thymocyte maturation in IL-7<sup>-/-</sup> mice. *J. Immunol.* **157**, 2366–73 (1996).
  425. Tan, J. T., Dudl, E., LeRoy, E., Murray, R., Sprent, J., Weinberg, K. I. & Surh, C. D. IL-7 is critical for homeostatic proliferation and survival of naive T cells. *Proc. Natl. Acad. Sci.* **98**, 8732–8737 (2001).
  426. Vang, K. B., Yang, J., Mahmud, S. A., Burchill, M. A., Vegoe, A. L. & Farrar, M. A. IL-2, -7, and -15, but not thymic stromal lymphopoietin, redundantly govern CD4<sup>+</sup>Foxp3<sup>+</sup> regulatory T cell development. *J. Immunol.* **181**, 3285–90 (2008).
  427. Unsinger, J., McGlynn, M., Kasten, K. R., Hoekzema, A. S., Watanabe, E., Muenzer, J. T., McDonough, J. S., Tschoep, J., Ferguson, T. A., McDunn, J. E., Morre, M., Hildeman, D. A., Caldwell, C. C. & Hotchkiss, R. S. IL-7 promotes T cell viability, trafficking, and functionality and improves survival in sepsis. *J. Immunol.* **184**, 3768–79 (2010).
  428. Kikuchi, K., Lai, A. Y., Hsu, C.-L. & Kondo, M. IL-7 receptor signaling is necessary for stage transition in adult B cell development through up-regulation of EBF. *J. Exp. Med.* **201**, 1197–203 (2005).
  429. Kelly, E. A. B., Koziol-White, C. J., Clay, K. J., Liu, L. Y., Bates, M. E., Bertics, P. J. & Jarjour, N. N. Potential contribution of IL-7 to allergen-induced eosinophilic airway inflammation in asthma. *J. Immunol.* **182**, 1404–10 (2009).
  430. del Pozo, V., Rojo, M., Rubio, M. L., Cortegano, I., Cárđaba, B., Gallardo, S., Ortega, M., Civantos, E., López, E., Martín-Mosquero, C., Peces-Barba, G., Palomino, P., González-Mangado, N. & Lahoz, C. Gene Therapy with Galectin-3 Inhibits Bronchial Obstruction and Inflammation in Antigen-challenged Rats through Interleukin-5 Gene Downregulation. *Am. J. Respir. Crit. Care Med.* **166**, 732–737 (2002).
  431. Fermin Lee, A., Chen, H.-Y., Wan, L., Wu, S.-Y., Yu, J.-S., Huang, A. C., Miaw, S.-C., Hsu, D. K., Wu-Hsieh, B. A. & Liu, F.-T. Galectin-3 Modulates Th17 Responses by Regulating Dendritic Cell Cytokines. *Am. J. Pathol.* **183**, 1209–1222 (2013).
  432. Zhang, R., Brennan, M. L., Shen, Z., Macpherson, J. C., Schmitt, D., Molenda, C. & Hazen, S. L. *Myeloperoxidase Functions as a Major Enzymatic Catalyst for Initiation of Lipid Peroxidation at Sites of Inflammation Downloaded from.* **1**, (JBC Papers in Press, 2002).
  433. Carraway, R., Cochrane, D. E., Lansman, J. B., Leeman, S. E., Paterson, B. M. & Welch, H. J. Neurotensin stimulates exocytotic histamine secretion from rat mast cells and elevates plasma histamine levels. *J. Physiol.* **323**, 403–414 (1982).
  434. Singh, L. K., Pang, X., Alexacos, N., Letourneau, R. & Theoharides, T. C. Acute Immobilization Stress Triggers Skin Mast Cell Degranulation via Corticotropin Releasing

- Hormone, Neurotensin, and Substance P: A Link to Neurogenic Skin Disorders. *Brain Behav. Immun.* **13**, 225–239 (1999).
435. Hatzelmann, A. & Schudt, C. *Anti-Inflammatory and Immunomodulatory Potential of the Novel PDE4 Inhibitor Roflumilast in Vitro.* (2001).
  436. Tang, H.-F., Song, Y.-H., Chen, J.-C., Chen, J.-Q. & Wang, P. Upregulation of Phosphodiesterase-4 in the Lung of Allergic Rats. *Am. J. Respir. Crit. Care Med.* **171**, 823–828 (2005).
  437. Sun, J., Deng, Y., Wu, X., Tang, H., Deng, J., Chen, J., Yang, S. & Xie, Q. Inhibition of phosphodiesterase activity, airway inflammation and hyperresponsiveness by PDE4 inhibitor and glucocorticoid in a murine model of allergic asthma. *Life Sci.* **79**, 2077–2085 (2006).
  438. Wylie, D. H., Kiss-Toth, E., Visintin, A., Smith, S. C., Boussouf, S., Segal, D. M., Duff, G. W. & Dower, S. K. Evidence for an accessory protein function for Toll-like receptor 1 in anti-bacterial responses. *J. Immunol.* **165**, 7125–32 (2000).
  439. Takeuchi, O., Sato, S., Horiuchi, T., Hoshino, K., Takeda, K., Dong, Z., Modlin, R. L. & Akira, S. Cutting edge: role of Toll-like receptor 1 in mediating immune response to microbial lipoproteins. *J. Immunol.* **169**, 10–4 (2002).
  440. Liu, P. T., Stenger, S., Li, H., Wenzel, L., Tan, B. H., Krutzik, S. R., Ochoa, M. T., Schaubert, J., Wu, K., Meinken, C., Kamen, D. L., Wagner, M., Bals, R., Steinmeyer, A., Zügel, U., Gallo, R. L., Eisenberg, D., Hewison, M., Hollis, B. W., Adams, J. S., Bloom, B. R. & Modlin, R. L. Toll-like receptor triggering of a vitamin D-mediated human antimicrobial response. *Science* **311**, 1770–3 (2006).
  441. Wittke, A., Weaver, V., Mahon, B. D., August, A. & Cantorna, M. T. Vitamin D receptor-deficient mice fail to develop experimental allergic asthma. *J. Immunol.* **173**, 3432–6 (2004).
  442. Hartmann, B., Heine, G., Babina, M., Steinmeyer, A., Zügel, U., Radbruch, A. & Worm, M. Targeting the vitamin D receptor inhibits the B cell-dependent allergic immune response. *Allergy* **66**, 540–548 (2011).
  443. He, L. & Hannon, G. J. MicroRNAs: small RNAs with a big role in gene regulation. *Nat. Rev. Genet.* **5**, 522–531 (2004).
  444. Lim, L. P., Lau, N. C., Garrett-Engele, P., Grimson, A., Schelter, J. M., Castle, J., Bartel, D. P., Linsley, P. S. & Johnson, J. M. Microarray analysis shows that some microRNAs downregulate large numbers of target mRNAs. *Nature* **433**, 769–773 (2005).
  445. Eulalio, A., Huntzinger, E. & Izaurralde, E. Getting to the Root of miRNA-Mediated Gene Silencing. *Cell* **132**, 9–14 (2008).
  446. Pietrusinska, M., Pajak, A., Gorski, P., Kuna, P., Szemraj, J., Gozdzińska-Nielepkowicz, A. & Pietras, T. Preliminary studies: differences in microRNA expression in asthma and chronic obstructive pulmonary disease. *Postep. dermatologii i Alergol.* **33**, 276–280 (2016).
  447. Sheu, C.-C., Tsai, M.-J., Chen, F.-W., Chang, K.-F., Chang, W.-A., Chong, I.-W., Kuo, P.-L. & Hsu, Y.-L. Identification of novel genetic regulations associated with airway epithelial homeostasis using next-generation sequencing data and bioinformatics approaches. *Oncotarget* **8**, 82674–82688 (2017).
  448. Garbacki, N., Di Valentin, E., Huynh-Thu, V. A., Geurts, P., Irrthum, A., Crahay, C., Arnould, T., Deroanne, C., Piette, J., Cataldo, D. & Colige, A. MicroRNAs Profiling in Murine Models of Acute and Chronic Asthma: A Relationship with mRNAs Targets. *PLoS One* **6**, e16509

- (2011).
449. Chen, X.-F., Zhang, L.-J., Zhang, J., Dou, X., Shao, Y., Jia, X.-J., Zhang, W. & Yu, B. MiR-151a is involved in the pathogenesis of atopic dermatitis by regulating interleukin-12 receptor beta2. *Exp. Dermatol.* **27**, 427–432 (2018).
  450. Pua, H. H., Steiner, D. F., Patel, S., Gonzalez, J. R., Ortiz-Carpena, J. F., Kageyama, R., Chiou, N.-T., Gallman, A., de Kouchkovsky, D., Jeker, L. T., McManus, M. T., Erle, D. J. & Ansel, K. M. MicroRNAs 24 and 27 Suppress Allergic Inflammation and Target a Network of Regulators of T Helper 2 Cell-Associated Cytokine Production. *Immunity* **44**, 821–832 (2016).
  451. Das, S., Kumar, M., Negi, V., Pattnaik, B., Prakash, Y. S., Agrawal, A. & Ghosh, B. MicroRNA-326 regulates profibrotic functions of transforming growth factor-beta in pulmonary fibrosis. *Am. J. Respir. Cell Mol. Biol.* **50**, 882–892 (2014).
  452. Spooner, C. J., Lesch, J., Yan, D., Khan, A. A., Abbas, A., Ramirez-Carrozzi, V., Zhou, M., Soriano, R., Eastham-Anderson, J., Diehl, L., Lee, W. P., Modrusan, Z., Pappu, R., Xu, M., DeVoss, J. & Singh, H. Specification of type 2 innate lymphocytes by the transcriptional determinant Gfi1. *Nat. Immunol.* **14**, 1229–1236 (2013).
  453. Chang, Y.-J., Kim, H. Y., Albacker, L. A., Baumgarth, N., McKenzie, A. N. J., Smith, D. E., DeKruyff, R. H. & Umetsu, D. T. Innate lymphoid cells mediate influenza-induced airway hyper-reactivity independently of adaptive immunity. *Nat. Immunol.* **12**, 631–638 (2011).
  454. Barlow, J. L., Bellosi, A., Hardman, C. S., Drynan, L. F., Wong, S. H., Cruickshank, J. P. & McKenzie, A. N. J. Innate IL-13–producing nuocytes arise during allergic lung inflammation and contribute to airways hyperreactivity. *J. Allergy Clin. Immunol.* **129**, 191-198.e4 (2012).
  455. Bartemes, K. R., Iijima, K., Kobayashi, T., Kephart, G. M., McKenzie, A. N. & Kita, H. IL-33-responsive lineage- CD25+ CD44(hi) lymphoid cells mediate innate type 2 immunity and allergic inflammation in the lungs. *J. Immunol.* **188**, 1503–13 (2012).
  456. Halim, T. Y. F., Krauß, R. H., Sun, A. C. & Takei, F. Lung Natural Helper Cells Are a Critical Source of Th2 Cell-Type Cytokines in Protease Allergen-Induced Airway Inflammation. *Immunity* **36**, 451–463 (2012).
  457. Wolterink, R. G. J. K., KleinJan, A., van Nimwegen, M., Bergen, I., de Bruijn, M., Levani, Y. & Hendriks, R. W. Pulmonary innate lymphoid cells are major producers of IL-5 and IL-13 in murine models of allergic asthma. *Eur. J. Immunol.* **42**, 1106–1116 (2012).
  458. Barlow, J. L., Peel, S., Fox, J., Panova, V., Hardman, C. S., Camelo, A., Bucks, C., Wu, X., Kane, C. M., Neill, D. R., Flynn, R. J., Sayers, I., Hall, I. P. & McKenzie, A. N. J. IL-33 is more potent than IL-25 in provoking IL-13–producing nuocytes (type 2 innate lymphoid cells) and airway contraction. *J. Allergy Clin. Immunol.* **132**, 933–941 (2013).
  459. Christianson, C. A., Goplen, N. P., Zafar, I., Irvin, C., Good, J. T., Rollins, D. R., Gorentla, B., Liu, W., Gorska, M. M., Chu, H., Martin, R. J. & Alam, R. Persistence of asthma requires multiple feedback circuits involving type 2 innate lymphoid cells and IL-33. *J. Allergy Clin. Immunol.* **136**, 59-68.e14 (2015).
  460. Barnig, C., Cernadas, M., Dutile, S., Liu, X., Perrella, M. A., Kazani, S., Wechsler, M. E., Israel, E. & Levy, B. D. Lipoxin A4 regulates natural killer cell and type 2 innate lymphoid cell activation in asthma. *Sci. Transl. Med.* **5**, 174ra26 (2013).
  461. Bartemes, K. R., Kephart, G. M., Fox, S. J. & Kita, H. Enhanced innate type 2 immune response in peripheral blood from patients with asthma. *J. Allergy Clin. Immunol.* **134**, 671-678.e4 (2014).

462. Liu, T., Wu, J., Zhao, J., Wang, J., Zhang, Y., Liu, L., Cao, L., Liu, Y. & Dong, L. Type 2 innate lymphoid cells: A novel biomarker of eosinophilic airway inflammation in patients with mild to moderate asthma. *Respir. Med.* **109**, 1391–1396 (2015).
463. Jia, Y., Fang, X., Zhu, X., Bai, C., Zhu, L., Jin, M., Wang, X., Hu, M., Tang, R. & Chen, Z. IL-13<sup>+</sup> Type 2 Innate Lymphoid Cells Correlate with Asthma Control Status and Treatment Response. *Am. J. Respir. Cell Mol. Biol.* **55**, 675–683 (2016).
464. Smith, S. G., Chen, R., Kjarsgaard, M., Huang, C., Oliveria, J.-P., O’Byrne, P. M., Gauvreau, G. M., Boulet, L.-P., Lemiere, C., Martin, J., Nair, P. & Sehmi, R. Increased numbers of activated group 2 innate lymphoid cells in the airways of patients with severe asthma and persistent airway eosinophilia. *J. Allergy Clin. Immunol.* **137**, 75-86.e8 (2016).
465. Zhu, J., Jankovic, D., Grinberg, A., Guo, L. & Paul, W. E. Gfi-1 plays an important role in IL-2-mediated Th2 cell expansion. *Proc. Natl. Acad. Sci.* **103**, 18214–18219 (2006).
466. Kuwahara, M., Yamashita, M., Shinoda, K., Tofukuji, S., Onodera, A., Shinnakasu, R., Motohashi, S., Hosokawa, H., Tumes, D., Iwamura, C., Lefebvre, V. & Nakayama, T. The transcription factor Sox4 is a downstream target of signaling by the cytokine TGF- $\beta$  and suppresses TH2 differentiation. *Nat. Immunol.* **13**, 778–786 (2012).
467. Shen, T.-C., Lin, C.-L., Wei, C.-C., Tu, C.-Y. & Li, Y.-F. The risk of asthma in rheumatoid arthritis: a population-based cohort study. *QJM* **107**, 435–442 (2014).
468. Seiskari, T., Viskari, H., Kondrashova, A., Haapala, A.-M., Ilonen, J., Knip, M. & Hyöty, H. Co-occurrence of allergic sensitization and type 1 diabetes. *Ann. Med.* **42**, 352–359 (2010).
469. Biron, C. A., Nguyen, K. B., Pien, G. C., Cousens, L. P. & Salazar-Mather, T. P. NATURAL KILLER CELLS IN ANTIVIRAL DEFENSE: Function and Regulation by Innate Cytokines. *Annu. Rev. Immunol.* **17**, 189–220 (1999).
470. French, A. R. & Yokoyama, W. M. Natural killer cells and viral infections. *Curr. Opin. Immunol.* **15**, 45–51 (2003).
471. Tupin, E., Kinjo, Y. & Kronenberg, M. The unique role of natural killer T cells in the response to microorganisms. *Nat. Rev. Microbiol.* **5**, 405–417 (2007).
472. Vivier, E., Tomasello, E., Baratin, M., Walzer, T. & Ugolini, S. Functions of natural killer cells. (2008). doi:10.1038/ni1582
473. Nicholson, K. G., Kent, J. & Ireland, D. C. Respiratory viruses and exacerbations of asthma in adults. *BMJ* **307**, 982–6 (1993).
474. Johnston, S. L., Pattemore, P. K., Sanderson, G., Smith, S., Lampe, F., Josephs, L., Symington, P., O’Toole, S., Myint, S. H., Tyrrell, D. A. & Holgate, S. T. Community study of role of viral infections in exacerbations of asthma in 9-11 year old children. *BMJ* **310**, 1225–9 (1995).
475. Murray, C. S., Poletti, G., Kebabdz, T., Morris, J., Woodcock, A., Johnston, S. L. & Custovic, A. Study of modifiable risk factors for asthma exacerbations: virus infection and allergen exposure increase the risk of asthma hospital admissions in children. *Thorax* **61**, 376–82 (2006).
476. Busse, W. W., Lemanske, R. F. & Gern, J. E. Role of viral respiratory infections in asthma and asthma exacerbations. *Lancet* **376**, 826–834 (2010).
477. Papadopoulos, N. G., Stanciu, L. A., Papi, A., Holgate, S. T. & Johnston, S. L. A defective type 1 response to rhinovirus in atopic asthma. *Thorax* **57**, 328–32 (2002).
478. Wark, P. A. B., Johnston, S. L., Bucchieri, F., Powell, R., Puddicombe, S., Laza-Stanca, V.,



- Holgate, S. T. & Davies, D. E. Asthmatic bronchial epithelial cells have a deficient innate immune response to infection with rhinovirus. *J. Exp. Med.* **201**, 937–47 (2005).
479. Sykes, A., Edwards, M. R., Macintyre, J., del Rosario, A., Bakhsoliani, E., Trujillo-Torralbo, M.-B., Kon, O. M., Mallia, P., McHale, M. & Johnston, S. L. Rhinovirus 16–induced IFN- $\alpha$  and IFN- $\beta$  are deficient in bronchoalveolar lavage cells in asthmatic patients. *J. Allergy Clin. Immunol.* **129**, 1506-1514.e6 (2012).
480. Openshaw, P. J. & Hussell, T. Intracellular IFN-gamma expression in natural killer cells precedes lung CD8+ T cell recruitment during respiratory syncytial virus infection. *J. Gen. Virol.* **79**, 2593–2601 (1998).
481. Bullens, D. M., Truyen, E., Coteur, L., Dilissen, E., Hellings, P. W., Dupont, L. J. & Ceuppens, J. L. IL-17 mRNA in sputum of asthmatic patients: linking T cell driven inflammation and granulocytic influx? *Respir. Res.* **7**, 135 (2006).
482. Al-Ramli, W., Préfontaine, D., Chouiali, F., Martin, J. G., Olivenstein, R., Lemièrre, C. & Hamid, Q. T(H)17-associated cytokines (IL-17A and IL-17F) in severe asthma. *J. Allergy Clin. Immunol.* **123**, 1185–7 (2009).
483. Doe, C., Bafadhel, M., Siddiqui, S., Desai, D., Mistry, V., Rugman, P., McCormick, M., Woods, J., May, R., Sleeman, M. A., Anderson, I. K. & Brightling, C. E. Expression of the T Helper 17-Associated Cytokines IL-17A and IL-17F in Asthma and COPD. *Chest* **138**, 1140–1147 (2010).
484. Nanzer, A. M., Chambers, E. S., Ryanna, K., Richards, D. F., Black, C., Timms, P. M., Martineau, A. R., Griffiths, C. J., Corrigan, C. J. & Hawrylowicz, C. M. Enhanced production of IL-17A in patients with severe asthma is inhibited by 1 $\alpha$ ,25-dihydroxyvitamin D3 in a glucocorticoid-independent fashion. *J. Allergy Clin. Immunol.* **132**, 297-304.e3 (2013).
485. Irvin, C., Zafar, I., Good, J., Rollins, D., Christianson, C., Gorska, M. M., Martin, R. J. & Alam, R. Increased frequency of dual-positive TH2/TH17 cells in bronchoalveolar lavage fluid characterizes a population of patients with severe asthma. *J. Allergy Clin. Immunol.* **134**, 1175-1186.e7 (2014).
486. Nakae, S., Komiyama, Y., Nambu, A., Sudo, K., Iwase, M., Homma, I., Sekikawa, K., Asano, M. & Iwakura, Y. Antigen-Specific T Cell Sensitization Is Impaired in IL-17-Deficient Mice, Causing Suppression of Allergic Cellular and Humoral Responses. *Immunity* **17**, 375–387 (2002).
487. Nakajima, S., Kitoh, A., Egawa, G., Natsuaki, Y., Nakamizo, S., Moniaga, C. S., Otsuka, A., Honda, T., Hanakawa, S., Amano, W., Iwakura, Y., Nakae, S., Kubo, M., Miyachi, Y. & Kabashima, K. IL-17A as an Inducer for Th2 Immune Responses in Murine Atopic Dermatitis Models. *J. Invest. Dermatol.* **134**, 2122–2130 (2014).
488. Koga, C., Kabashima, K., Shiraishi, N., Kobayashi, M. & Tokura, Y. Possible Pathogenic Role of Th17 Cells for Atopic Dermatitis. *J. Invest. Dermatol.* **128**, 2625–2630 (2008).
489. Gereda, J., Leung, D., Thatayatikom, A., Streib, J., Price, M., Klinnert, M. & Liu, A. Relation between house-dust endotoxin exposure, type 1 T-cell development, and allergen sensitisation in infants at high risk of asthma. *Lancet* **355**, 1680–1683 (2000).
490. Braun-Fahrlander, C., Riedler, J., Herz, U., Eder, W., Waser, M., Grize, L., Maisch, S., Carr, D., Gerlach, F., Bufe, A., Lauener, R. P., Schierl, R., Renz, H., Nowak, D. & von Mutius, E. Environmental Exposure to Endotoxin and Its Relation to Asthma in School-Age Children. *N. Engl. J. Med.* **347**, 869–877 (2002).
491. Douwes, J., van Strien, R., Doekes, G., Smit, J., Kerkhof, M., Gerritsen, J., Postma, D., de Jongste, J., Travier, N. & Brunekreef, B. Does early indoor microbial exposure reduce the

- risk of asthma? The Prevention and Incidence of Asthma and Mite Allergy birth cohort study. *J. Allergy Clin. Immunol.* **117**, 1067–1073 (2006).
492. Gehring, U., Strikwold, M., Schram-Bijkerk, D., Weinmayr, G., Genuneit, J., Nagel, G., Wickens, K., Siebers, R., Crane, J., Doekes, G., Di Domenicantonio, R., Nilsson, L., Priftanji, A., Sandin, A., El-Sharif, N., Strachan, D., van Hage, M., von Mutius, E. & Brunekreef, B. Asthma and allergic symptoms in relation to house dust endotoxin: Phase Two of the International Study on Asthma and Allergies in Childhood (ISAAC II). *Clin. Exp. Allergy* **38**, 1911–1920 (2008).
  493. Tischer, C., Gehring, U., Chen, C.-M., Kerkhof, M., Koppelman, G., Sausenthaler, S., Herbarth, O., Schaaf, B., Lehmann, I., Krämer, U., Berdel, D., von Berg, A., Bauer, C. P., Koletzko, S., Wichmann, H.-E., Brunekreef, B. & Heinrich, J. Respiratory health in children, and indoor exposure to (1,3)- $\beta$ -D-glucan, EPS mould components and endotoxin. *Eur. Respir. J.* **37**, 1050–9 (2011).
  494. Tulić Meri K., Wale Janet L., Holt, P. G. & Sly, P. D. Modification of the Inflammatory Response to Allergen Challenge after Exposure to Bacterial Lipopolysaccharide. *Am. J. Respir. Cell Mol. Biol.* **22**, 604–612 (2000).
  495. Le, J., Lin, J. X., Henriksen-DeStefano, D. & Vilcek, J. Bacterial lipopolysaccharide-induced interferon-gamma production: roles of interleukin 1 and interleukin 2. *J. Immunol.* **136**, 4525–30 (1986).
  496. D'andrea, A., Rengaraju, M., Valiante, N. M., Chehimij, J., Kubin, M., Aste, M., Chan, S. H., Kobayashi, M., Young, D., Nickbarg, E., Chizzonite, R., Wolf, S. F. & Trinchieri, G. Production of Natural Killer Cell Stimulatory Factor (Interleukin 12) by Peripheral Blood Mononuclear Cells. doi:10.1084/jem.176.5.1387
  497. Manetti, R., Parronchi, P., Giudizi, M. G., Piccinni, M. P., Maggi, E., Trinchieri, G. & Romagnani, S. Natural killer cell stimulatory factor (interleukin 12 [IL-12]) induces T helper type 1 (Th1)-specific immune responses and inhibits the development of IL-4-producing Th cells. *J. Exp. Med.* **177**, 1199–204 (1993).
  498. Kaplan, M. H., Sun, Y.-L., Hoey, T. & Grusby, M. J. Impaired IL-12 responses and enhanced development of Th2 cells in Stat4-deficient mice. *Nature* **382**, 174–177 (1996).
  499. Huber, J. P., Ramos, H. J., Gill, M. A. & Farrar, J. D. Cutting edge: Type I IFN reverses human Th2 commitment and stability by suppressing GATA3. *J. Immunol.* **185**, 813–7 (2010).
  500. Liang, S. C., Tan, X.-Y., Luxenberg, D. P., Karim, R., Dunussi-Joannopoulos, K., Collins, M. & Fouser, L. A. Interleukin (IL)-22 and IL-17 are coexpressed by Th17 cells and cooperatively enhance expression of antimicrobial peptides. *J. Exp. Med.* **203**, 2271–2279 (2006).
  501. Peric, M., Koglin, S., Kim, S.-M., Morizane, S., Besch, R., Prinz, J. C., Ruzicka, T., Gallo, R. L. & Schaubert, J. IL-17A Enhances Vitamin D3-Induced Expression of Cathelicidin Antimicrobial Peptide in Human Keratinocytes. *J. Immunol.* **181**, 8504–8512 (2008).
  502. Sigari, N., Jalili, A., Mahdawi, L., Ghaderi, E. & Shilan, M. Soluble CD93 as a Novel Biomarker in Asthma Exacerbation. *Allergy. Asthma Immunol. Res.* **8**, 461 (2016).
  503. Park, H. J., Han, H., Lee, S. C., Son, Y. W., Sim, D. W., Park, K. H., Park, Y. H., Jeong, K. Y., Park, J.-W. & Lee, J.-H. Soluble CD93 in Serum as a Marker of Allergic Inflammation. *Yonsei Med. J.* **58**, 598 (2017).
  504. Lecky, D. M., Hawking, M. K. D., McNulty, C. A. M. & ESBL steering group. Patients' perspectives on providing a stool sample to their GP: a qualitative study. *Br. J. Gen. Pract.* **64**, e684-93 (2014).

505. SHIELDS, M. D. & RIEDLER, J. Bronchoalveolar Lavage and Tracheal Aspirate for Assessing Airway Inflammation in Children. *Am. J. Respir. Crit. Care Med.* **162**, S15–S17 (2000).
506. Shukla, S. K., Cook, D., Meyer, J., Vernon, S. D., Le, T., Clevidence, D., Robertson, C. E., Schrodi, S. J., Yale, S. & Frank, D. N. Changes in Gut and Plasma Microbiome following Exercise Challenge in Myalgic Encephalomyelitis/Chronic Fatigue Syndrome (ME/CFS). *PLoS One* **10**, e0145453 (2015).
507. Buford, T. W., Carter, C. S., VanDerPol, W. J., Chen, D., Lefkowitz, E. J., Eipers, P., Morrow, C. D. & Bamman, M. M. Composition and richness of the serum microbiome differ by age and link to systemic inflammation. *GeroScience* **40**, 257–268 (2018).
508. Herlemann, D. P., Labrenz, M., Jürgens, K., Bertilsson, S., Waniek, J. J. & Andersson, A. F. Transitions in bacterial communities along the 2000 km salinity gradient of the Baltic Sea. *ISME J.* **5**, 1571–1579 (2011).
509. Klindworth, A., Pruesse, E., Schweer, T., Peplies, J., Quast, C., Horn, M. & Glöckner, F. O. Evaluation of general 16S ribosomal RNA gene PCR primers for classical and next-generation sequencing-based diversity studies. *Nucleic Acids Res.* **41**, e1–e1 (2013).
510. Stasik, S., Schuster, C., Ortlepp, C., Platzbecker, U., Bornhäuser, M., Schetelig, J., Ehninger, G., Folprecht, G. & Thiede, C. An optimized targeted Next-Generation Sequencing approach for sensitive detection of single nucleotide variants. *Biomol. Detect. Quantif.* **15**, 6–12 (2018).
511. Caporaso, J. G., Lauber, C. L., Walters, W. A., Berg-Lyons, D., Lozupone, C. A., Turnbaugh, P. J., Fierer, N. & Knight, R. Global patterns of 16S rRNA diversity at a depth of millions of sequences per sample. *Proc. Natl. Acad. Sci. U. S. A.* **108 Suppl 1**, 4516–22 (2011).
512. Parada, A. E., Needham, D. M. & Fuhrman, J. A. Every base matters: assessing small subunit rRNA primers for marine microbiomes with mock communities, time series and global field samples. *Environ. Microbiol.* **18**, 1403–1414 (2016).
513. Al-Soud, W. A., Jönsson, L. J. & Rådström, P. Identification and characterization of immunoglobulin G in blood as a major inhibitor of diagnostic PCR. *J. Clin. Microbiol.* **38**, 345–50 (2000).
514. Schrader, C., Schielke, A., Ellerbroek, L. & Johne, R. PCR inhibitors - occurrence, properties and removal. *J. Appl. Microbiol.* **113**, 1014–1026 (2012).
515. Kuczynski, J., Lauber, C. L., Walters, W. A., Parfrey, L. W., Clemente, J. C., Gevers, D. & Knight, R. Experimental and analytical tools for studying the human microbiome. *Nat. Rev. Genet.* **13**, 47–58 (2011).
516. Castillo, D. J., Rifkin, R. F., Cowan, D. A. & Potgieter, M. The Healthy Human Blood Microbiome: Fact or Fiction? *Front. Cell. Infect. Microbiol.* **9**, 148 (2019).
517. Mitchell, A. J., Gray, W. D., Schroeder, M., Yi, H., Taylor, J. V., Dillard, R. S., Ke, Z., Wright, E. R., Stephens, D., Roback, J. D. & Searles, C. D. Pleomorphic Structures in Human Blood Are Red Blood Cell-Derived Microparticles, Not Bacteria. *PLoS One* **11**, e0163582 (2016).
518. Martel, J., Wu, C.-Y., Huang, P.-R., Cheng, W.-Y. & Young, J. D. Pleomorphic bacteria-like structures in human blood represent non-living membrane vesicles and protein particles. *Sci. Rep.* **7**, 10650 (2017).
519. Moriyama, K., Ando, C., Tashiro, K., Kuhara, S., Okamura, S., Nakano, S., Takagi, Y., Miki, T., Nakashima, Y. & Hirakawa, H. Polymerase chain reaction detection of bacterial 16S rRNA gene in human blood. *Microbiol. Immunol.* **52**, 375–382 (2008).

520. Singh, N., Vats, A., Sharma, A., Arora, A. & Kumar, A. The development of lower respiratory tract microbiome in mice. *Microbiome* **5**, 61 (2017).
521. Segal, L. N., Rom, W. N. & Weiden, M. D. Lung Microbiome for Clinicians. New Discoveries about Bugs in Healthy and Diseased Lungs. *Ann. Am. Thorac. Soc.* **11**, 108–116 (2014).
522. Hogan, D. A., Willger, S. D., Dolben, E. L., Hampton, T. H., Stanton, B. A., Morrison, H. G., Sogin, M. L., Czum, J. & Ashare, A. Analysis of Lung Microbiota in Bronchoalveolar Lavage, Protected Brush and Sputum Samples from Subjects with Mild-To-Moderate Cystic Fibrosis Lung Disease. (2016). doi:10.1371/journal.pone.0149998
523. Sears, M. R., Greene, J. M., Willan, A. R., Taylor, D. R., Flannery, E. M., Cowan, J. O., Herbison, G. P. & Poulton, R. Long-term relation between breastfeeding and development of atopy and asthma in children and young adults: a longitudinal study. *Lancet* **360**, 901–907 (2002).
524. Davis, M. F., Peng, R. D., McCormack, M. C. & Matsui, E. C. Staphylococcus aureus colonization is associated with wheeze and asthma among US children and young adults. *J. Allergy Clin. Immunol.* **135**, 811–3.e5 (2015).
525. Park, H., Shin, J. W., Park, S.-G. & Kim, W. Microbial Communities in the Upper Respiratory Tract of Patients with Asthma and Chronic Obstructive Pulmonary Disease. *PLoS One* **9**, e109710 (2014).
526. Cani, P. & Delzenne, N. The Role of the Gut Microbiota in Energy Metabolism and Metabolic Disease. *Curr. Pharm. Des.* **15**, 1546–1558 (2009).
527. Morowitz, M. J., Carlisle, E. & Alverdy, J. C. Contributions of Intestinal Bacteria to Nutrition and Metabolism in the Critically Ill. *Surg. Clin. North Am.* **91**, 771 (2011).
528. Rooks, M. G. & Garrett, W. S. Gut microbiota, metabolites and host immunity. *Nat. Rev. Immunol.* **16**, 341–52 (2016).
529. Hooper, L. V, Midtvedt, T. & Gordon, J. I. How host-microbial interactions shape the nutrient environment of the mammalian intestine. *Annu. Rev. Nutr.* **22**, 283–307 (2002).
530. Macfarlane, S. & Macfarlane, G. T. Regulation of short-chain fatty acid production. *Proc. Nutr. Soc.* **62**, 67–72 (2003).
531. den Besten, G., van Eunen, K., Groen, A. K., Venema, K., Reijngoud, D.-J. & Bakker, B. M. The role of short-chain fatty acids in the interplay between diet, gut microbiota, and host energy metabolism. *J. Lipid Res.* **54**, 2325–40 (2013).
532. Ellwood, P., Asher, M. I., Björkstén, B., Burr, M., Pearce, N. & Robertson, C. F. Diet and asthma, allergic rhinoconjunctivitis and atopic eczema symptom prevalence: an ecological analysis of the International Study of Asthma and Allergies in Childhood (ISAAC) data. ISAAC Phase One Study Group. *Eur. Respir. J.* **17**, 436–43 (2001).
533. Berthon, B. S., Macdonald-Wicks, L. K., Gibson, P. G. & Wood, L. G. Investigation of the association between dietary intake, disease severity and airway inflammation in asthma. *Respirology* **18**, 447–454 (2013).
534. Roduit, C., Frei, R., Ferstl, R., Loeliger, S., Westermann, P., Rhyner, C., Schiavi, E., Barcik, W., Rodriguez-Perez, N., Wawrzyniak, M., Chassard, C., Lacroix, C., Schmausser-Hechfellner, E., Depner, M., Mutius, E., Braun-Fahrlander, C., Karvonen, A. M., Kirjavainen, P. V., Pekkanen, J., Dalphin, J., Riedler, J., Akdis, C., Lauener, R., O'Mahony, L., Hyvärinen, A., Remes, S., Roponen, M., Chauveau, A., Dalphin, M., Kaulek, V., Ege, M., Genuneit, J., Illi, S., Kabesch, M., Schaub, B., Pfefferle, P. & Doekes, G. High levels of butyrate and propionate in early life are associated with protection against atopy. *Allergy* **74**, 799–809

- (2019).
535. Park, J., Kim, M., Kang, S. G., Jannasch, A. H., Cooper, B., Patterson, J. & Kim, C. H. Short-chain fatty acids induce both effector and regulatory T cells by suppression of histone deacetylases and regulation of the mTOR–S6K pathway. *Mucosal Immunol.* **8**, 80–93 (2015).
  536. Koh, A., De Vadder, F., Kovatcheva-Datchary, P. & Bäckhed, F. From Dietary Fiber to Host Physiology: Short-Chain Fatty Acids as Key Bacterial Metabolites. *Cell* **165**, 1332–1345 (2016).
  537. Kaisar, M. M. M., Pelgrom, L. R., van der Ham, A. J., Yazdanbakhsh, M. & Everts, B. Butyrate Conditions Human Dendritic Cells to Prime Type 1 Regulatory T Cells via both Histone Deacetylase Inhibition and G Protein-Coupled Receptor 109A Signaling. *Front. Immunol.* **8**, 1429 (2017).
  538. Shakespear, M. R., Halili, M. A., Irvine, K. M., Fairlie, D. P. & Sweet, M. J. Histone deacetylases as regulators of inflammation and immunity. *Trends Immunol.* **32**, 335–343 (2011).
  539. Blanchard, F. & Chipoy, C. Histone deacetylase inhibitors: new drugs for the treatment of inflammatory diseases? *Drug Discov. Today* **10**, 197–204 (2005).
  540. Adcock, I. M. HDAC inhibitors as anti-inflammatory agents. *Br. J. Pharmacol.* **150**, 829–831 (2007).
  541. Kim, H. J., Rowe, M., Ren, M., Hong, J.-S., Chen, P.-S. & Chuang, D.-M. Histone deacetylase inhibitors exhibit anti-inflammatory and neuroprotective effects in a rat permanent ischemic model of stroke: multiple mechanisms of action. *J. Pharmacol. Exp. Ther.* **321**, 892–901 (2007).
  542. Trompette, A., Gollwitzer, E. S., Yadava, K., Sichelstiel, A. K., Sprenger, N., Ngom-Bru, C., Blanchard, C., Junt, T., Nicod, L. P., Harris, N. L. & Marsland, B. J. Gut microbiota metabolism of dietary fiber influences allergic airway disease and hematopoiesis. *Nat. Med.* **20**, 159–166 (2014).
  543. Thorburn, A. N., McKenzie, C. I., Shen, S., Stanley, D., Macia, L., Mason, L. J., Roberts, L. K., Wong, C. H. Y., Shim, R., Robert, R., Chevalier, N., Tan, J. K., Mariño, E., Moore, R. J., Wong, L., McConville, M. J., Tull, D. L., Wood, L. G., Murphy, V. E., Mattes, J., Gibson, P. G. & Mackay, C. R. Evidence that asthma is a developmental origin disease influenced by maternal diet and bacterial metabolites. *Nat. Commun.* **6**, 7320 (2015).
  544. Yamashita, H., Fujisawa, K., Ito, E., Idei, S., Kawaguchi, N., Kimoto, M., Hiemori, M. & Tsuji, H. Improvement of obesity and glucose tolerance by acetate in Type 2 diabetic Otsuka Long-Evans Tokushima Fatty (OLETF) rats. *Biosci. Biotechnol. Biochem.* **71**, 1236–43 (2007).
  545. Lin, H. V., Frassetto, A., Kowalik Jr, E. J., Nawrocki, A. R., Lu, M. M., Kosinski, J. R., Hubert, J. A., Szeto, D., Yao, X., Forrest, G. & Marsh, D. J. Butyrate and Propionate Protect against Diet-Induced Obesity and Regulate Gut Hormones via Free Fatty Acid Receptor 3-Independent Mechanisms. *PLoS One* **7**, e35240 (2012).
  546. den Besten, G., Bleeker, A., Gerding, A., van Eunen, K., Havinga, R., van Dijk, T. H., Oosterveer, M. H., Jonker, J. W., Groen, A. K., Reijngoud, D.-J. & Bakker, B. M. Short-Chain Fatty Acids Protect Against High-Fat Diet-Induced Obesity via a PPAR $\gamma$ -Dependent Switch From Lipogenesis to Fat Oxidation. *Diabetes* **64**, 2398–408 (2015).
  547. Lu, Y., Fan, C., Li, P., Lu, Y., Chang, X. & Qi, K. Short Chain Fatty Acids Prevent High-fat-diet-induced Obesity in Mice by Regulating G Protein-coupled Receptors and Gut Microbiota. *Sci. Rep.* **6**, 37589 (2016).

548. Mariño, E., Richards, J. L., McLeod, K. H., Stanley, D., Yap, Y. A., Knight, J., McKenzie, C., Kranich, J., Oliveira, A. C., Rossello, F. J., Krishnamurthy, B., Nefzger, C. M., Macia, L., Thorburn, A., Baxter, A. G., Morahan, G., Wong, L. H., Polo, J. M., Moore, R. J., Lockett, T. J., Clarke, J. M., Topping, D. L., Harrison, L. C. & Mackay, C. R. Gut microbial metabolites limit the frequency of autoimmune T cells and protect against type 1 diabetes. *Nat. Immunol.* **18**, 552–562 (2017).
549. Stene, L. C. & Nafstad, P. Relation between occurrence of type 1 diabetes and asthma. *Lancet* **357**, 607–608 (2001).
550. Ford, E. S. The epidemiology of obesity and asthma. *J. Allergy Clin. Immunol.* **115**, 897–909 (2005).
551. Adams, R. J., Wilson, D. H., Taylor, A. W., Daly, A., Tursan d’Espaignet, E., Dal Grande, E. & Ruffin, R. E. Coexistent Chronic Conditions and Asthma Quality of Life: A Population-Based Study. *Chest* **129**, 285–291 (2006).
552. Beuther, D. A. & Sutherland, E. R. Overweight, Obesity, and Incident Asthma. *Am. J. Respir. Crit. Care Med.* **175**, 661–666 (2007).
553. Caughey, G. E., Vitry, A. I., Gilbert, A. L. & Roughead, E. E. Prevalence of comorbidity of chronic diseases in Australia. *BMC Public Health* **8**, 221 (2008).
554. Cazzola, M., Calzetta, L., Bettoncelli, G., Novelli, L., Cricelli, C. & Rogliani, P. Asthma and comorbid medical illness. *Eur. Respir. J.* **38**, 42–9 (2011).
555. Wilson, W. R., Van Scoy, R. E., Washington, J. A. & II. Incidence of bacteremia in adults without infection. *J. Clin. Microbiol.* **2**, 94–5 (1976).
556. Grice, E. A. & Segre, J. A. The skin microbiome. *Nat. Rev. Microbiol.* **9**, 244–53 (2011).
557. Tett, A., Pasolli, E., Farina, S., Truong, D. T., Asnicar, F., Zolfo, M., Beghini, F., Armanini, F., Jousson, O., De Sanctis, V., Bertorelli, R., Girolomoni, G., Cristofolini, M. & Segata, N. Unexplored diversity and strain-level structure of the skin microbiome associated with psoriasis. *npj Biofilms Microbiomes* **3**, 14 (2017).
558. Byrd, A. L., Belkaid, Y. & Segre, J. A. The human skin microbiome. *Nat. Rev. Microbiol.* **16**, 143–155 (2018).
559. Grice, E. A., Kong, H. H., Renaud, G., Young, A. C., Bouffard, G. G., Blakesley, R. W., Wolfsberg, T. G., Turner, M. L., Segre, J. A. & Segre, J. A. A diversity profile of the human skin microbiota. *Genome Res.* **18**, 1043–1050 (2008).
560. Cosseau, C., Romano-Bertrand, S., Duplan, H., Lucas, O., Ingrassia, I., Pigasse, C., Roques, C. & Jumas-Bilak, E. Proteobacteria from the human skin microbiota: Species-level diversity and hypotheses. *One Heal.* **2**, 33–41 (2016).
561. McIntyre, M. K., Peacock, T. J., Akers, K. S. & Burmeister, D. M. Initial Characterization of the Pig Skin Bacteriome and Its Effect on In Vitro Models of Wound Healing. *PLoS One* **11**, e0166176 (2016).
562. Christaki, E. & Giamarellos-Bourboulis, E. J. The complex pathogenesis of bacteremia. *Virulence* **5**, 57–65 (2014).
563. Broadley, S. P., Plaumann, A., Coletti, R., Lehmann, C., Wanisch, A., Seidlmeier, A., Esser, K., Luo, S., Rämer, P. C., Massberg, S., Busch, D. H., van Lookeren Campagne, M. & Verschoor, A. Dual-Track Clearance of Circulating Bacteria Balances Rapid Restoration of Blood Sterility with Induction of Adaptive Immunity. *Cell Host Microbe* **20**, 36–48 (2016).
564. Forner, L., Larsen, T., Kilian, M. & Holmstrup, P. Incidence of bacteremia after chewing,

- tooth brushing and scaling in individuals with periodontal inflammation. *J. Clin. Periodontol.* **33**, 401–407 (2006).
565. Lockhart, P. B., Brennan, M. T., Sasser, H. C., Fox, P. C., Paster, B. J. & Bahrani-Mougeot, F. K. Bacteremia Associated With Toothbrushing and Dental Extraction. *Circulation* **117**, 3118–3125 (2008).
  566. Horliana, A. C. R. T., Chambrone, L., Foz, A. M., Artese, H. P. C., Rabelo, M. de S., Pannuti, C. M. & Romito, G. A. Dissemination of periodontal pathogens in the bloodstream after periodontal procedures: a systematic review. *PLoS One* **9**, e98271 (2014).
  567. Bahrani-Mougeot, F. K., Paster, B. J., Coleman, S., Ashar, J., Barbuto, S. & Lockhart, P. B. Diverse and novel oral bacterial species in blood following dental procedures. *J. Clin. Microbiol.* **46**, 2129–32 (2008).
  568. Depcik-Smith, N. D., Hay, S. N. & Brecher, M. E. Bacterial contamination of blood products: Factors, options, and insights. *J. Clin. Apher.* **16**, 192–201 (2001).
  569. Hillyer, C. D., Josephson, C. D., Blajchman, M. A., Vostal, J. G., Epstein, J. S. & Goodman, J. L. Bacterial contamination of blood components: risks, strategies, and regulation: joint ASH and AABB educational session in transfusion medicine. *Hematol. Am. Soc. Hematol. Educ. Progr.* **2003**, 575–89 (2003).
  570. Bousquet, J., Van Cauwenberge, P., Khaltaev, N., Aria Workshop Group & World Health Organization. Allergic rhinitis and its impact on asthma. *J. Allergy Clin. Immunol.* **108**, S147–334 (2001).
  571. Vinuya, R. Z. Upper airway disorders and asthma: a syndrome of airway inflammation. *Ann. Allergy, Asthma Immunol.* **88**, 8–15 (2002).
  572. Demoly, P. & Bousquet, J. The relation between asthma and allergic rhinitis. *Lancet (London, England)* **368**, 711–3 (2006).
  573. Yawn, B. P., Yunginger, J. W., Wollan, P. C., Reed, C. E., Silverstein, M. D. & Harris, A. G. Allergic rhinitis in Rochester, Minnesota residents with asthma: Frequency and impact on health care charges. *J. Allergy Clin. Immunol.* **103**, 54–59 (1999).
  574. Leynaert, B., Neukirch, F., Demoly, P. & Bousquet, J. Epidemiologic evidence for asthma and rhinitis comorbidity. *J. Allergy Clin. Immunol.* **106**, S201–S205 (2000).
  575. Togias, A. G. Systemic immunologic and inflammatory aspects of allergic rhinitis. *J. Allergy Clin. Immunol.* **106**, S247–S250 (2000).
  576. Jeffery, P. K. & Haahtela, T. Allergic rhinitis and asthma: inflammation in a one-airway condition. *BMC Pulm. Med.* **6**, S5 (2006).
  577. Settupane, R. J., Hagy, G. W. & Settupane, G. A. Long-term risk factors for developing asthma and allergic rhinitis: a 23-year follow-up study of college students. *Allergy Proc.* **15**, 21–5
  578. Huovinen, E., Kaprio, J., Laitinen, L. A. & Koskenvuo, M. Incidence and Prevalence of Asthma Among Adult Finnish Men and Women of the Finnish Twin Cohort From 1975 to 1990, and Their Relation to Hay Fever and Chronic Bronchitis. *Chest* **115**, 928–936 (1999).
  579. Leynaert, B., Bousquet, J., Neukirch, C., Liard, R. & Neukirch, F. Perennial rhinitis: An independent risk factor for asthma in nonatopic subjects: Results from the European Community Respiratory Health Survey. *J. Allergy Clin. Immunol.* **104**, 301–304 (1999).
  580. Guerra, S., Sherrill, D. L., Martinez, F. D. & Barbee, R. A. Rhinitis as an independent risk factor for adult-onset asthma. *J. Allergy Clin. Immunol.* **109**, 419–425 (2002).

581. Shaaban, R., Zureik, M., Soussan, D., Neukirch, C., Heinrich, J., Sunyer, J., Wjst, M., Cerveri, I., Pin, I., Bousquet, J., Jarvis, D., Burney, P. G., Neukirch, F. & Leynaert, B. Rhinitis and onset of asthma: a longitudinal population-based study. *Lancet* **372**, 1049–1057 (2008).
582. Sazonov Kocevar, V., Thomas, J., Jonsson, L., Valovirta, E., Kristensen, F., Yin, D. D. & Bisgaard, H. Association between allergic rhinitis and hospital resource use among asthmatic children in Norway. *Allergy* **60**, 338–342 (2005).
583. Foresi, A., Leone, C., Pelucchi, A., Mastropasqua, B., Chetta, A., D'Ippolito, R., Marazzini, L. & Olivieri, D. Eosinophils, mast cells, and basophils in induced sputum from patients with seasonal allergic rhinitis and perennial asthma: Relationship to methacholine responsiveness. *J. Allergy Clin. Immunol.* **100**, 58–64 (1997).
584. Bonay, M., Neukirch, C., Grandsaigne, M., Leçon-Malas, V., Ravaud, P., Dehoux, M. & Aubier, M. Changes in airway inflammation following nasal allergic challenge in patients with seasonal rhinitis. *Allergy* **61**, 111–118 (2006).
585. Gaga, M., Lambrou, P., Papageorgiou, N., Koulouris, N. G., Kosmas, E., Fragakis, S., Sofios, C., Rasidakis, A. & Jordanoglou, J. Eosinophils are a feature of upper and lower airway pathology in non-atopic asthma, irrespective of the presence of rhinitis. *Clin. Exp. Allergy* **30**, 663–9 (2000).
586. Togias, A. Rhinitis and asthma: Evidence for respiratory system integration. *J. Allergy Clin. Immunol.* **111**, 1171–1183 (2003).
587. Bourdin, A., Gras, D., Vachier, I. & Chanez, P. Upper airway x 1: allergic rhinitis and asthma: united disease through epithelial cells. *Thorax* **64**, 999–1004 (2009).
588. Durack, J., Lynch, S. V., Nariya, S., Bhakta, N. R., Beigelman, A., Castro, M., Dyer, A.-M., Israel, E., Kraft, M., Martin, R. J., Mauger, D. T., Rosenberg, S. R., Sharp-King, T., White, S. R., Woodruff, P. G., Avila, P. C., Denlinger, L. C., Holguin, F., Lazarus, S. C., Lugogo, N., Moore, W. C., Peters, S. P., Que, L., Smith, L. J., Sorkness, C. A., Wechsler, M. E., Wenzel, S. E., Boushey, H. A. & Huang, Y. J. Features of the bronchial bacterial microbiome associated with atopy, asthma, and responsiveness to inhaled corticosteroid treatment. *J. Allergy Clin. Immunol.* **140**, 63–75 (2017).
589. Fazlollahi, M., Lee, T. D., Andrade, J., Oguntuyo, K., Chun, Y., Grishina, G., Grishin, A. & Bunyavanich, S. The nasal microbiome in asthma. *J. Allergy Clin. Immunol.* **142**, 834-843.e2 (2018).
590. Emre, U., Roblin, P. M., Gelling, M., Dumornay, W., Rao, M., Hammerschlag, M. R. & Schachter, J. The Association of Chlamydia pneumoniae Infection and Reactive Airway Disease in Children. *Arch. Pediatr. Adolesc. Med.* **148**, 727 (1994).
591. Taylor, S. L., Leong, L. E. X., Choo, J. M., Wesselingh, S., Yang, I. A., Upham, J. W., Reynolds, P. N., Hodge, S., James, A. L., Jenkins, C., Peters, M. J., Baraket, M., Marks, G. B., Gibson, P. G., Simpson, J. L. & Rogers, G. B. Inflammatory phenotypes in patients with severe asthma are associated with distinct airway microbiology. *J. Allergy Clin. Immunol.* **141**, 94-103.e15 (2018).
592. Larsen, J. M. The immune response to *Prevotella* bacteria in chronic inflammatory disease. *Immunology* **151**, 363–374 (2017).
593. Arrieta, M.-C., Arévalo, A., Stiemsma, L., Dimitriu, P., Chico, M. E., Loor, S., Vaca, M., Boutin, R. C. T., Morien, E., Jin, M., Turvey, S. E., Walter, J., Parfrey, L. W., Cooper, P. J. & Finlay, B. Associations between infant fungal and bacterial dysbiosis and childhood atopic wheeze in a nonindustrialized setting. *J. Allergy Clin. Immunol.* **142**, 424-434.e10 (2018).
594. Tanaka, M., Korenori, Y., Washio, M., Kobayashi, T., Momoda, R., Kiyohara, C., Kuroda, A.,



- Saito, Y., Sonomoto, K. & Nakayama, J. Signatures in the gut microbiota of Japanese infants who developed food allergies in early childhood. *FEMS Microbiol. Ecol.* **93**, (2017).
595. Ogorodova, L. M., Fedosenko, S. V., Popenko, A. S., Petrov, V. A., Tyakht, A. V., Saltykova, I. V., Deev, I. A., Kulikov, E. S., Kirillova, N. A., Govorun, V. M. & Kostryukova, E. S. [Comparison Study of Oropharyngeal Microbiota in Case of Bronchial Asthma and Chronic Obstructive Pulmonary Disease in Different Severity Levels]. *Vestn. Ross. Akad. meditsinskikh Nauk* 669–78 (2015).
596. Black, P. N., Scicchitano, R., Jenkins, C. R., Blasi, F., Allegra, L., Wlodarczyk, J. & Cooper, B. C. Serological evidence of infection with *Chlamydia pneumoniae* is related to the severity of asthma. *Eur. Respir. J.* **15**, 254–9 (2000).
597. Pasternack, R., Huhtala, H. & Karjalainen, J. *Chlamydia* pneumoniae serology and asthma in adults: A longitudinal analysis. *J. Allergy Clin. Immunol.* **116**, 1123–1128 (2005).
598. Brinke, A. ten, van Dissel, J. T., Sterk, P. J., Zwinderman, A. H., Rabe, K. F. & Bel, E. H. Persistent airflow limitation in adult-onset nonatopic asthma is associated with serologic evidence of *Chlamydia pneumoniae* infection. *J. Allergy Clin. Immunol.* **107**, 449–454 (2001).
599. De Smedt, T., Pajak, B., Muraille, E., Lespagnard, L., Heinen, E., De Baetselier, P., Urbain, J., Leo, O. & Moser, M. Regulation of dendritic cell numbers and maturation by lipopolysaccharide in vivo. *J. Exp. Med.* **184**, 1413–1424 (1996).
600. Chassin, C., Kocur, M., Pott, J., Duerr, C. U., Gütle, D., Lotz, M. & Hornef, M. W. miR-146a Mediates Protective Innate Immune Tolerance in the Neonate Intestine. *Cell Host Microbe* **8**, 358–368 (2010).
601. Segain, J. P., Raingeard de la Blétière, D., Bourreille, A., Leray, V., Gervois, N., Rosales, C., Ferrier, L., Bonnet, C., Blottière, H. M. & Galmiche, J. P. Butyrate inhibits inflammatory responses through NFκB inhibition: implications for Crohn's disease. *Gut* **47**, 397–403 (2000).
602. Cavaglieri, C. R., Nishiyama, A., Fernandes, L. C., Curi, R., Miles, E. A. & Calder, P. C. Differential effects of short-chain fatty acids on proliferation and production of pro- and anti-inflammatory cytokines by cultured lymphocytes. *Life Sci.* **73**, 1683–90 (2003).
603. Tedelind, S., Westberg, F., Kjerrulf, M. & Vidal, A. Anti-inflammatory properties of the short-chain fatty acids acetate and propionate: a study with relevance to inflammatory bowel disease. *World J. Gastroenterol.* **13**, 2826–32 (2007).
604. Macia, L., Tan, J., Vieira, A. T., Leach, K., Stanley, D., Luong, S., Maruya, M., Ian McKenzie, C., Hijikata, A., Wong, C., Binge, L., Thorburn, A. N., Chevalier, N., Ang, C., Marino, E., Robert, R., Offermanns, S., Teixeira, M. M., Moore, R. J., Flavell, R. A., Fagarasan, S. & Mackay, C. R. Metabolite-sensing receptors GPR43 and GPR109A facilitate dietary fibre-induced gut homeostasis through regulation of the inflammasome. *Nat. Commun.* **6**, 6734 (2015).
605. Suzuki, T., Yoshida, S. & Hara, H. Physiological concentrations of short-chain fatty acids immediately suppress colonic epithelial permeability. *Br. J. Nutr.* **100**, 297–305 (2008).
606. Kelly, C. J., Zheng, L., Campbell, E. L., Saeedi, B., Scholz, C. C., Bayless, A. J., Wilson, K. E., Glover, L. E., Kominsky, D. J., Magnuson, A., Weir, T. L., Ehrentauf, S. F., Pickel, C., Kuhn, K. A., Lanis, J. M., Nguyen, V., Taylor, C. T. & Colgan, S. P. Crosstalk between Microbiota-Derived Short-Chain Fatty Acids and Intestinal Epithelial HIF Augments Tissue Barrier Function. *Cell Host Microbe* **17**, 662–671 (2015).

607. Arpaia, N., Campbell, C., Fan, X., Dikiy, S., van der Veecken, J., deRoos, P., Liu, H., Cross, J. R., Pfeffer, K., Coffey, P. J. & Rudenski, A. Y. Metabolites produced by commensal bacteria promote peripheral regulatory T-cell generation. *Nature* **504**, 451–455 (2013).
608. Furusawa, Y., Obata, Y., Fukuda, S., Endo, T. A., Nakato, G., Takahashi, D., Nakanishi, Y., Uetake, C., Kato, K., Kato, T., Takahashi, M., Fukuda, N. N., Murakami, S., Miyauchi, E., Hino, S., Atarashi, K., Onawa, S., Fujimura, Y., Lockett, T., Clarke, J. M., Topping, D. L., Tomita, M., Hori, S., Ohara, O., Morita, T., Koseki, H., Kikuchi, J., Honda, K., Hase, K. & Ohno, H. Commensal microbe-derived butyrate induces the differentiation of colonic regulatory T cells. *Nature* **504**, 446–450 (2013).
609. Smith, P. M., Howitt, M. R., Panikov, N., Michaud, M., Gallini, C. A., Bohlooly-Y, M., Glickman, J. N. & Garrett, W. S. The Microbial Metabolites, Short-Chain Fatty Acids, Regulate Colonic Treg Cell Homeostasis. *Science (80-. )*. **341**, 569–573 (2013).
610. Card, J. W., Carey, M. A., Voltz, J. W., Bradbury, J. A., Ferguson, C. D., Cohen, E. A., Schwartz, S., Flake, G. P., Morgan, D. L., Arbes, S. J., Barrow, D. A., Barros, S. P., Offenbacher, S. & Zeldin, D. C. Modulation of Allergic Airway Inflammation by the Oral Pathogen *Porphyromonas gingivalis*. *Infect. Immun.* **78**, 2488–2496 (2010).
611. Banbula, A., Bugno, M., Kuster, A., Heinrich, P. C., Travis, J. & Potempa, J. Rapid and Efficient Inactivation of IL-6 Gingipains, Lysine- and Arginine-Specific Proteinases from *Porphyromonas gingivalis*. *Biochem. Biophys. Res. Commun.* **261**, 598–602 (1999).
612. Stathopoulou, P. G., Benakanakere, M. R., Galicia, J. C. & Kinane, D. F. The host cytokine response to *Porphyromonas gingivalis* is modified by gingipains. *Oral Microbiol. Immunol.* **24**, 11–17 (2009).
613. Tam, V., O'Brien-Simpson, N. M., Chen, Y.-Y., Sanderson, C. J., Kinnear, B. & Reynolds, E. C. The RgpA-Kgp Proteinase-Adhesin Complexes of *Porphyromonas gingivalis* Inactivate the Th2 Cytokines Interleukin-4 and Interleukin-5. *Infect. Immun.* **77**, 1451–1458 (2009).
614. Moutsopoulos, N. M., Kling, H. M., Angelov, N., Jin, W., Palmer, R. J., Nares, S., Osorio, M. & Wahl, S. M. *Porphyromonas gingivalis* promotes Th17 inducing pathways in chronic periodontitis. *J. Autoimmun.* **39**, 294–303 (2012).
615. Wang, L., Guan, N., Jin, Y., Lin, X. & Gao, H. Subcutaneous vaccination with *Porphyromonas gingivalis* ameliorates periodontitis by modulating Th17/Treg imbalance in a murine model. *Int. Immunopharmacol.* **25**, 65–73 (2015).
616. Nagaoka, K., Yanagihara, K., Harada, Y., Yamada, K., Migiyama, Y., Morinaga, Y., Hasegawa, H., Izumikawa, K., Kakeya, H., Nishimura, M. & Kohno, S. Macrolides Inhibit *Fusobacterium nucleatum*-Induced MUC5AC Production in Human Airway Epithelial Cells. (2013). doi:10.1128/AAC.02466-12
617. Teng, Y., Zhang, R., Liu, C., Zhou, L., Wang, H., Zhuang, W., Huang, Y. & Hong, Z. miR-143 inhibits interleukin-13-induced inflammatory cytokine and mucus production in nasal epithelial cells from allergic rhinitis patients by targeting IL13R $\alpha$ 1. *Biochem. Biophys. Res. Commun.* **457**, 58–64 (2015).
618. Molet, S., Hamid, Q., Davoineb, F., Nutku, E., Tahaa, R., Pagé, N., Olivenstein, R., Elias, J. & Chakir, J. IL-17 is increased in asthmatic airways and induces human bronchial fibroblasts to produce cytokines. *J. Allergy Clin. Immunol.* **108**, 430–438 (2001).
619. Wong, C. K., Ho, C. Y., Ko, F. W. S., Chan, C. H. S., Ho, A. S. S., Hui, D. S. C. & Lam, C. W. K. Proinflammatory cytokines (IL-17, IL-6, IL-18 and IL-12) and Th cytokines (IFN- $\gamma$ , IL-4, IL-10 and IL-13) in patients with allergic asthma. *Clin. Exp. Immunol.* **125**, 177–183 (2001).
620. Matsunaga, K., Yanagisawa, S., Ichikawa, T., Ueshima, K., Akamatsu, K., Hirano, T.,

- Nakanishi, M., Yamagata, T., Minakata, Y. & Ichinose, M. Airway cytokine expression measured by means of protein array in exhaled breath condensate: Correlation with physiologic properties in asthmatic patients. *J. Allergy Clin. Immunol.* **118**, 84–90 (2006).
621. Zhao, Y., Yang, J., Gao, Y. & Guo, W. Th17 Immunity in Patients with Allergic Asthma. *Int. Arch. Allergy Immunol.* **151**, 297–307 (2010).
622. Chen, Y., Thai, P., Zhao, Y.-H., Ho, Y.-S., DeSouza, M. M. & Wu, R. Stimulation of airway mucin gene expression by interleukin (IL)-17 through IL-6 paracrine/autocrine loop. *J. Biol. Chem.* **278**, 17036–43 (2003).
623. Newcomb, D. C., Boswell, M. G., Sherrill, T. P., Polosukhin, V. V., Boyd, K. L., Goleniewska, K., Brody, S. L., Kolls, J. K., Adler, K. B. & Peebles, R. S. IL-17A Induces Signal Transducers and Activators of Transcription–6–Independent Airway Mucous Cell Metaplasia. *Am. J. Respir. Cell Mol. Biol.* **48**, 711–716 (2013).
624. Chang, Y., Al-Alwan, L., Risse, P.-A., Halayko, A. J., Martin, J. G., Bagloli, C. J., Eidelman, D. H. & Hamid, Q. Th17-associated cytokines promote human airway smooth muscle cell proliferation. *FASEB J.* **26**, 5152–5160 (2012).
625. Chang, Y., Al-Alwan, L., Risse, P.-A., Roussel, L., Rousseau, S., Halayko, A. J., Martin, J. G., Hamid, Q. & Eidelman, D. H. TH17 cytokines induce human airway smooth muscle cell migration. *J. Allergy Clin. Immunol.* **127**, 1046-1053.e2 (2011).
626. Bhattacharyya, A., Hanafi, L.-A., Sheih, A., Golob, J. L., Srinivasan, S., Boeckh, M. J., Pergam, S. A., Mahmood, S., Baker, K. K., Gooley, T. A., Milano, F., Fredricks, D. N., Riddell, S. R. & Turtle, C. J. Graft-Derived Reconstitution of Mucosal-Associated Invariant T Cells after Allogeneic Hematopoietic Cell Transplantation. *Biol. Blood Marrow Transplant.* **24**, 242–251 (2018).
627. Ishimori, A., Harada, N., Chiba, A., Harada, S., Matsuno, K., Makino, F., Ito, J., Ohta, S., Ono, J., Atsuta, R., Izuhara, K., Takahashi, K. & Miyake, S. Circulating activated innate lymphoid cells and mucosal-associated invariant T cells are associated with airflow limitation in patients with asthma. *Allergol. Int.* **66**, 302–309 (2017).
628. Miyazaki, Y., Miyake, S., Chiba, A., Lantz, O. & Yamamura, T. Mucosal-associated invariant T cells regulate Th1 response in multiple sclerosis. *Int. Immunol.* **23**, 529–535 (2011).
629. Noval Rivas, M., Burton, O. T., Wise, P., Zhang, Y., Hobson, S. A., Garcia Lloret, M., Chehoud, C., Kuczynski, J., DeSantis, T., Warrington, J., Hyde, E. R., Petrosino, J. F., Gerber, G. K., Bry, L., Oettgen, H. C., Mazmanian, S. K. & Chatila, T. A. A microbiota signature associated with experimental food allergy promotes allergic sensitization and anaphylaxis. *J. Allergy Clin. Immunol.* **131**, 201–12 (2013).
630. Habibzay, M., Saldana, J. I., Goulding, J., Lloyd, C. M. & Hussell, T. Altered regulation of Toll-like receptor responses impairs antibacterial immunity in the allergic lung. *Mucosal Immunol.* **5**, 524–534 (2012).
631. Berg, R. D. & Garlington, A. W. Translocation of certain indigenous bacteria from the gastrointestinal tract to the mesenteric lymph nodes and other organs in a gnotobiotic mouse model. *Infect. Immun.* **23**, 403–11 (1979).
632. Hudgel, D. W., Langston, L., Selner, J. C. & McIntosh, K. Viral and bacterial infections in adults with chronic asthma. *Am. Rev. Respir. Dis.* **120**, 393–7 (1979).
633. KRAFT, M., CASSELL, G. H., HENSON, J. E., WATSON, H., WILLIAMSON, J., MARMION, B. P., GAYDOS, C. A. & MARTIN, R. J. Detection of *Mycoplasma pneumoniae* in the Airways of Adults with Chronic Asthma. *Am. J. Respir. Crit. Care Med.* **158**, 998–1001 (1998).

634. De Schutter, I., Dreesman, A., Soetens, O., De Waele, M., Crokaert, F., Verhaegen, J., Piérard, D. & Malfroot, A. In young children, persistent wheezing is associated with bronchial bacterial infection: a retrospective analysis. *BMC Pediatr.* **12**, 83 (2012).
635. Zhang, Q., Illing, R., Hui, C. K., Downey, K., Carr, D., Stearn, M., Alshafi, K., Menzies-Gow, A., Zhong, N. & Fan Chung, K. Bacteria in sputum of stable severe asthma and increased airway wall thickness. *Respir. Res.* **13**, 35 (2012).
636. Wood, P. R., Hill, V. L., Burks, M. L., Peters, J. I., Singh, H., Kannan, T. R., Vale, S., Cagle, M. P., Principe, M. F. R., Baseman, J. B. & Brooks, E. G. Mycoplasma pneumoniae in children with acute and refractory asthma. *Ann. Allergy, Asthma Immunol.* **110**, 328-334.e1 (2013).
637. Illi, S., von Mutius, E., Lau, S., Bergmann, R., Niggemann, B., Sommerfeld, C., Wahn, U. & MAS Group. Early childhood infectious diseases and the development of asthma up to school age: a birth cohort study. *BMJ* **322**, 390–5 (2001).
638. Walton, R. P. & Johnston, S. L. Role of respiratory viral infections in the development of atopic conditions. *Curr. Opin. Allergy Clin. Immunol.* **8**, 150–153 (2008).
639. Kostadima, E., Tsiodras, S., Alexopoulos, E. I., Kaditis, A. G., Mavrou, I., Georgatou, N. & Papamichalopoulos, A. Clarithromycin reduces the severity of bronchial hyperresponsiveness in patients with asthma. *Eur. Respir. J.* **23**, 714–7 (2004).
640. Hahn, D. L., Plane, M. B., Mahdi, O. S. & Byrne, G. I. Secondary Outcomes of a Pilot Randomized Trial of Azithromycin Treatment for Asthma. *PLoS Clin. Trials* **1**, e11 (2006).
641. Tong, X., Guo, T., Liu, S., Peng, S., Yan, Z., Yang, X., Zhang, Y. & Fan, H. Macrolide antibiotics for treatment of asthma in adults: A meta-analysis of 18 randomized controlled clinical studies. *Pulm. Pharmacol. Ther.* **31**, 99–108 (2015).
642. Dzidic, M., Abrahamsson, T. R., Artacho, A., Björkstén, B., Collado, M. C., Mira, A. & Jenmalm, M. C. Aberrant IgA responses to the gut microbiota during infancy precede asthma and allergy development. *J. Allergy Clin. Immunol.* **139**, 1017-1025.e14 (2017).
643. Stokes, C. R., Soothill, J. F. & Turner, M. W. Immune exclusion is a function of IgA. *Nature* **255**, 745–746 (1975).
644. Nakajima, A., Vogelzang, A., Maruya, M., Miyajima, M., Murata, M., Son, A., Kuwahara, T., Tsuruyama, T., Yamada, S., Matsuura, M., Nakase, H., Peterson, D. A., Fagarasan, S. & Suzuki, K. IgA regulates the composition and metabolic function of gut microbiota by promoting symbiosis between bacteria. *J. Exp. Med.* **215**, 2019–2034 (2018).
645. Fadlallah, J., Kafsi, H. El, Sterlin, D., Juste, C., Parizot, C., Dorgham, K., Autaa, G., Gouas, D., Almeida, M., Lepage, P., Pons, N., Chatelier, E. Le, Levenez, F., Kennedy, S., Galleron, N., Barros, J.-P. P. de, Malphettes, M., Galicier, L., Boutboul, D., Mathian, A., Miyara, M., Oksenhendler, E., Amoura, Z., Doré, J., Fieschi, C., Ehrlich, S. D., Larsen, M. & Gorochov, G. Microbial ecology perturbation in human IgA deficiency. *Sci. Transl. Med.* **10**, ean1217 (2018).
646. Kubinak, J. L., Petersen, C., Stephens, W. Z., Soto, R., Bake, E., O'Connell, R. M. & Round, J. L. MyD88 Signaling in T Cells Directs IgA-Mediated Control of the Microbiota to Promote Health. *Cell Host Microbe* **17**, 153–163 (2015).
647. Böttcher, M. F., Häggström, P., Björkstén, B. & Jenmalm, M. C. Total and allergen-specific immunoglobulin A levels in saliva in relation to the development of allergy in infants up to 2 years of age. *Clin. Exp. Allergy* **32**, 1293–8 (2002).
648. Scheiblaue, H., Reinacher, M., Tashiro, M. & Rott, R. Interactions between Bacteria and Influenza A Virus in the Development of Influenza Pneumonia. *J. Infect. Dis.* **166**, 783–791

(1992).

649. Lynch, S. V. Viruses and Microbiome Alterations. *Ann. Am. Thorac. Soc.* **11**, S57–S60 (2014).
650. Flynn, J. M., Niccum, D., Dunitz, J. M. & Hunter, R. C. Evidence and Role for Bacterial Mucin Degradation in Cystic Fibrosis Airway Disease. *PLOS Pathog.* **12**, e1005846 (2016).
651. Denner, D. R., Sangwan, N., Becker, J. B., Hogarth, D. K., Oldham, J., Castillo, J., Sperling, A. I., Solway, J., Naureckas, E. T., Gilbert, J. A. & White, S. R. Corticosteroid therapy and airflow obstruction influence the bronchial microbiome, which is distinct from that of bronchoalveolar lavage in asthmatic airways. *J. Allergy Clin. Immunol.* **137**, 1398-1405.e3 (2016).
652. Stephensen, C. B., Alvarez, J. O., Kohatsu, J., Hardmeier, R., Kennedy, J. I. & Gammon, R. B. Vitamin A is excreted in the urine during acute infection. *Am. J. Clin. Nutr.* **60**, 388–392 (1994).
653. Mawson, A. R. *Could bronchial asthma be an endogenous, pulmonary expression of retinoid intoxication?* *Frontiers in Bioscience* **6**, (2001).
654. Pesonen, M., Kallio, M. J. T., Siimes, M. A. & Ranki, A. Retinol concentrations after birth are inversely associated with atopic manifestations in children and young adults. *Clin. Exp. Allergy* **37**, 54–61 (2007).
655. Al Senaidy, A. M. Serum Vitamin A and  $\beta$ -Carotene Levels in Children with Asthma. *J. Asthma* **46**, 699–702 (2009).
656. Mihály, J., Gamlieli, A., Worm, M. & Rühl, R. Decreased retinoid concentration and retinoid signalling pathways in human atopic dermatitis. *Exp. Dermatol.* **20**, 326–330 (2011).
657. Arora, P., Kumar, V. & Batra, S. Vitamin A status in children with asthma. *Pediatr. Allergy Immunol.* **13**, 223–226 (2002).
658. Pascual, M., Suzuki, M., Isidoro-Garcia, M., Padrón, J., Turner, T., Lorente, F., Dávila, I. & Grealley, J. M. Epigenetic changes in B lymphocytes associated with house dust mite allergic asthma View supplementary material. (2011). doi:10.4161/epi.6.9.16061
659. Manna, B., Ashbaugh, P. & Bhattacharyya, S. N. Retinoic acid-regulated cellular differentiation and mucin gene expression in isolated rabbit tracheal epithelial cells in culture. *Inflammation* **19**, 489–502 (1995).
660. Racke, M. K., Burnett, D., Pak, S. H., Albert, P. S., Cannella, B., Raine, C. S., McFarlin, D. E. & Scott, D. E. Retinoid treatment of experimental allergic encephalomyelitis. IL-4 production correlates with improved disease course. *J. Immunol.* **154**, 450–8 (1995).
661. Wang, X., Allen, C. & Ballow, M. Retinoic Acid Enhances the Production of IL-10 While Reducing the Synthesis of IL-12 and TNF- $\alpha$  from LPS-Stimulated Monocytes/Macrophages. *J. Clin. Immunol.* **27**, 193–200 (2007).
662. Hoag, K. A., Nashold, F. E., Goverman, J. & Hayes, C. E. Retinoic Acid Enhances the T Helper 2 Cell Development That Is Essential for Robust Antibody Responses through Its Action on Antigen-Presenting Cells. *J. Nutr.* **132**, 3736–3739 (2002).
663. Levin, S. D., Koelling, R. M., Friend, S. L., Isaksen, D. E., Ziegler, S. F., Perlmutter, R. M. & Farr, A. G. Thymic stromal lymphopoietin: a cytokine that promotes the development of IgM+ B cells in vitro and signals via a novel mechanism. *J. Immunol.* **162**, 677–83 (1999).
664. Morikawa, K. & Nonaka, M. All-trans-retinoic acid accelerates the differentiation of human B lymphocytes maturing into plasma cells. *Int. Immunopharmacol.* **5**, 1830–1838 (2005).

665. Chen, Q. & Ross, A. C. Retinoic acid promotes mouse splenic B cell surface IgG expression and maturation stimulated by CD40 and IL-4. *Cell. Immunol.* **249**, 37–45 (2007).
666. Ertesvag, A., Aasheim, H.-C., Naderi, S. & Blomhoff, H. K. Vitamin A potentiates CpG-mediated memory B-cell proliferation and differentiation: involvement of early activation of p38MAPK. *Blood* **109**, 3865–72 (2007).
667. Wei, D., Yang, Y. & Wang, W. The Expression of Retinoic Acid Receptors in Lymph Nodes of Young Children and the Effect of All-trans-Retinoic Acid on the B Cells from Lymph Nodes. *J. Clin. Immunol.* **27**, 88–94 (2007).
668. DeCicco, K. L. & Ross, A. C. All- *trans* -retinoic acid and polyriboinosinic : polyribocytidylic acid cooperate to elevate anti-tetanus immunoglobulin G and immunoglobulin M responses in vitamin A-deficient Lewis rats and Balb/c mice. *Proc. Nutr. Soc.* **59**, 519–529 (2000).
669. DeCicco, K. L., Zolfaghari, R., Li, N. & Ross, A. C. Retinoic Acid and Polyriboinosinic Acid Act Synergistically to Enhance the Antibody Response to Tetanus Toxoid during Vitamin A Deficiency: Possible Involvement of Interleukin-2 Receptor- $\beta$ , Signal Transducer and Activator of Transcription-1, and Interferon Regulatory Factor-1. *J. Infect. Dis.* **182**, S29–S36 (2000).
670. Ma, Y., Chen, Q. & Ross, A. C. Retinoic Acid and Polyriboinosinic:Polyribocytidylic Acid Stimulate Robust Anti-Tetanus Antibody Production while Differentially Regulating Type 1/Type 2 Cytokines and Lymphocyte Populations. *J. Immunol.* **174**, 7961–7969 (2005).
671. Benson, M. J., Pino-Lagos, K., Roseblatt, M. & Noelle, R. J. All-trans retinoic acid mediates enhanced T reg cell growth, differentiation, and gut homing in the face of high levels of co-stimulation. *J. Exp. Med.* **204**, 1765–74 (2007).
672. Mucida, D., Park, Y., Kim, G., Turovskaya, O., Scott, I., Kronenberg, M. & Cheroutre, H. Reciprocal TH17 and regulatory T cell differentiation mediated by retinoic acid. *Science* **317**, 256–60 (2007).
673. Schambach, F., Schupp, M., Lazar, M. A. & Reiner, S. L. Activation of retinoic acid receptor- $\alpha$  favours regulatory T cell induction at the expense of IL-17-secreting T helper cell differentiation. *Eur. J. Immunol.* **37**, 2396–2399 (2007).
674. Bakdash, G., Vogelpoel, L. T., van Capel, T. M., Kapsenberg, M. L. & de Jong, E. C. Retinoic acid primes human dendritic cells to induce gut-homing, IL-10-producing regulatory T cells. *Mucosal Immunol.* **8**, 265–278 (2015).
675. Worm, M., Krah, J. M., Manz, R. A. & Henz, B. M. Retinoic acid inhibits CD40 + interleukin-4-mediated IgE production in vitro. *Blood* **92**, 1713–20 (1998).
676. Scheffel, F., Heine, G., Henz, B. M. & Worm, M. Retinoic acid inhibits CD40 plus IL-4 mediated IgE production through alterations of sCD23, sCD54 and IL-6 production. *Inflamm. Res.* **54**, 113–118 (2005).
677. Smeland, E., Rusten, L., Jacobsen, S., Skrede, B., Blomhoff, R., Wang, M., Funderud, S., Kvalheim, G. & Blomhoff, H. All-trans retinoic acid directly inhibits granulocyte colony-stimulating factor-induced proliferation of CD34+ human hematopoietic progenitor cells. *Blood* **84**, (1994).
678. Upham, J. W., Sehmi, R., Hayes, L. M., Howie, K., Lundahl, J. & Denburg, J. A. Retinoic acid modulates IL-5 receptor expression and selectively inhibits eosinophil-basophil differentiation of hemopoietic progenitor cells. *J. Allergy Clin. Immunol.* **109**, 307–313 (2002).

679. Chan-Yeung, M. Occupational asthma. *Chest* **98**, 148S-161S (1990).
680. Park, H. S. & Nahm, D. H. Isocyanate-induced occupational asthma: challenge and immunologic studies. *J. Korean Med. Sci.* **11**, 314 (1996).
681. Tarlo, S. M. & Lemiere, C. Occupational Asthma. *N. Engl. J. Med.* **370**, 640–649 (2014).
682. Miyashita, C., Sasaki, S., Saijo, Y., Washino, N., Okada, E., Kobayashi, S., Konishi, K., Kajiwara, J., Todaka, T. & Kishi, R. Effects of prenatal exposure to dioxin-like compounds on allergies and infections during infancy. *Environ. Res.* **111**, 551–558 (2011).
683. Hansen, S., Strøm, M., Olsen, S. F., Maslova, E., Rantakokko, P., Kiviranta, H., Rytter, D., Bech, B. H., Hansen, L. V. & Halldorsson, T. I. Maternal Concentrations of Persistent Organochlorine Pollutants and the Risk of Asthma in Offspring: Results from a Prospective Cohort with 20 Years of Follow-up. *Environ. Health Perspect.* **122**, 93–99 (2014).
684. Miyashita, C., Bamai, Y. A., Araki, A., Itoh, S., Minatoya, M., Kobayashi, S., Kajiwara, J., Hori, T. & Kishi, R. Prenatal exposure to dioxin-like compounds is associated with decreased cord blood IgE and increased risk of wheezing in children aged up to 7 years: The Hokkaido study. *Sci. Total Environ.* **610–611**, 191–199 (2018).
685. Shaheen, S. O., C., S. J. A., Thompson, R. L., Songhurst, C. E., Margetts, B. M. & Burney, P. G. J. Dietary Antioxidants and Asthma in Adults. *Am. J. Respir. Crit. Care Med.* **164**, 1823–1828 (2001).
686. Knekt, P., Kumpulainen, J., Järvinen, R., Rissanen, H., Heliövaara, M., Reunanen, A., Hakulinen, T. & Aromaa, A. Flavonoid intake and risk of chronic diseases. *Am. J. Clin. Nutr.* **76**, 560–568 (2002).
687. Tanaka, T., Higa, S., Hirano, T., Kotani, M., Matsumoto, M., Fujita, A. & Kawase, I. Flavonoids as Potential Anti-Allergic Substances. *Curr. Med. Chem. - Anti-inflamm. Anti-Allergy Agents* **2**, 57–65 (2003).
688. Ram, A., Ghosh, B. & Das, M. Luteolin alleviates bronchoconstriction and airway hyperreactivity in ovalbumin sensitized mice. *Inflamm. Res.* **52**, 101–106 (2003).
689. Choi, J.-R., Lee, C.-M., Jung, I. D., Lee, J. S., Jeong, Y.-I., Chang, J. H., Park, H., Choi, I.-W., Kim, J.-S., Shin, Y. K., Park, S. N. & Park, Y.-M. Apigenin protects ovalbumin-induced asthma through the regulation of GATA-3 gene. *Int. Immunopharmacol.* **9**, 918–924 (2009).
690. Li, R.-R., Pang, L.-L., Du, Q., Shi, Y., Dai, W.-J. & Yin, K.-S. Apigenin inhibits allergen-induced airway inflammation and switches immune response in a murine model of asthma. *Immunopharmacol. Immunotoxicol.* **32**, 364–370 (2010).
691. Wu, M.-Y., Hung, S.-K. & Fu, S.-L. Immunosuppressive Effects of Fisetin in Ovalbumin-Induced Asthma through Inhibition of NF-κB Activity. *J. Agric. Food Chem.* **59**, 10496–10504 (2011).
692. Goh, F. Y., Upton, N., Guan, S., Cheng, C., Shanmugam, M. K., Sethi, G., Leung, B. P. & Wong, W. S. F. Fisetin, a bioactive flavonol, attenuates allergic airway inflammation through negative regulation of NF-κB. *Eur. J. Pharmacol.* **679**, 109–116 (2012).
693. Park, H., Lee, C.-M., Jung, I. D., Lee, J. S., Jeong, Y., Chang, J. H., Chun, S.-H., Kim, M.-J., Choi, I.-W., Ahn, S.-C., Shin, Y. K., Yeom, S.-R. & Park, Y.-M. Quercetin regulates Th1/Th2 balance in a murine model of asthma. *Int. Immunopharmacol.* **9**, 261–267 (2009).
694. Song, M.-Y., Jeong, G.-S., Lee, H.-S., Kwon, K.-S., Lee, S.-M., Park, J.-W., Kim, Y.-C. & Park, B.-H. Sulfuretin attenuates allergic airway inflammation in mice. *Biochem. Biophys. Res. Commun.* **400**, 83–88 (2010).

695. Choi, Y. H., Jin, G. Y., Guo, H. S., Piao, H. M., Li, L. Chang, Li, G. Z., Lin, Z. H. & Yan, G. H. Silibinin attenuates allergic airway inflammation in mice. *Biochem. Biophys. Res. Commun.* **427**, 450–455 (2012).
696. Toledo, A., Sakoda, C., Perini, A., Pinheiro, N., Magalhães, R., Grecco, S., Tibério, I., Câmara, N., Martins, M., Lago, J. & Prado, C. Flavonone treatment reverses airway inflammation and remodelling in an asthma murine model. *Br. J. Pharmacol.* **168**, 1736–1749 (2013).
697. Kim, S.-H., Kim, B.-K. & Lee, Y.-C. Antiasthmatic effects of hesperidin, a potential Th2 cytokine antagonist, in a mouse model of allergic asthma. *Mediators Inflamm.* **2011**, 485402 (2011).
698. Su, M., Gu, X., Cai, J., Huang, M. & Su, M. Chrysin attenuates allergic airway inflammation by modulating the transcription factors T-bet and GATA-3 in mice. *Mol. Med. Rep.* **6**, 100–104 (2012).
699. Gao, F., Wei, D., Bian, T., Xie, P., Zou, J., Mu, H., Zhang, B. & Zhou, X. Genistein Attenuated Allergic Airway Inflammation by Modulating the Transcription Factors T-bet, GATA-3 and STAT-6 in a Murine Model of Asthma. *Pharmacology* **89**, 229–236 (2012).
700. Rogerio, A. P., Kanashiro, A., Fontanari, C., da Silva, E. V. G., Lucisano-Valim, Y. M., Soares, E. G. & Faccioli, L. H. Anti-inflammatory activity of quercetin and isoquercitrin in experimental murine allergic asthma. *Inflamm. Res.* **56**, 402–408 (2007).
701. Li, J. & Zhang, B. Apigenin protects ovalbumin-induced asthma through the regulation of Th17 cells. *Fitoterapia* **91**, 298–304 (2013).
702. Gong, J.-H., Shin, D., Han, S.-Y., Kim, J.-L. & Kang, Y.-H. Kaempferol Suppresses Eosinophil Infiltration and Airway Inflammation in Airway Epithelial Cells and in Mice with Allergic Asthma. *J. Nutr.* **142**, 47–56 (2012).
703. Jain, P., Kant, S. & Mishra, R. Assessment of Nutritional Status of Patients Suffering from Asthma. *J Clin Nutr Diet* **3**, (2017).
704. Kim, S. Y., Sim, S., Park, B., Kim, J.-H. & Choi, H. G. High-Fat and Low-Carbohydrate Diets Are Associated with Allergic Rhinitis But Not Asthma or Atopic Dermatitis in Children. *PLoS One* **11**, e0150202 (2016).
705. Yadav, U. C. S., Kalariya, N. M., Srivastava, S. K. & Ramana, K. V. Protective role of benfotiamine, a fat-soluble vitamin B1 analogue, in lipopolysaccharide-induced cytotoxic signals in murine macrophages. *Free Radic. Biol. Med.* **48**, 1423–1434 (2010).
706. Bozic, I., Savic, D., Laketa, D., Bjelobaba, I., Milenkovic, I., Pekovic, S., Nedeljkovic, N. & Lavrnja, I. Benfotiamine Attenuates Inflammatory Response in LPS Stimulated BV-2 Microglia. *PLoS One* **10**, e0118372 (2015).
707. Benayoun, L., Letuve, S., Druilhe, A., Boczkowski, J., Dombret, M.-C., Mechighel, P., Megret, J., Leseche, G., Aubier, M. & Pretolani, M. Regulation of Peroxisome Proliferator-activated Receptor  $\gamma$  Expression in Human Asthmatic Airways. *Am. J. Respir. Crit. Care Med.* **164**, 1487–1494 (2001).
708. Lee, K. S., Park, S. J., Hwang, P. H., Yi, H. K., Song, C. H., Chai, O. H., Kim, J.-S., Lee, M. K. & Lee, Y. C. PPAR- $\gamma$  modulates allergic inflammation through up-regulation of PTEN. *FASEB J.* **19**, 1033–1035 (2005).
709. Trifilieff, A., Bench, A., Hanley, M., Bayley, D., Campbell, E. & Whittaker, P. PPAR- $\alpha$  and - $\gamma$  but not - $\delta$  agonists inhibit airway inflammation in a murine model of asthma: *in vitro* evidence for an NF- $\kappa$ B-independent effect. *Br. J. Pharmacol.* **139**, 163–171 (2003).



710. Woerly, G., Honda, K., Loyens, M., Papin, J.-P., Auwerx, J., Staels, B., Capron, M. & Dombrowicz, D. Peroxisome Proliferator-activated Receptors and Down-regulate Allergic Inflammation and Eosinophil Activation. *J. Exp. Med.* **198**, 411–421 (2003).
711. Yacoub, M. H., Mitchell, J. A., Patel, H. J., Belvisi, M. G. & Bishop-Bailey, D. Pulmonary Disease Therapy Relevance for Chronic Obstructive Corticosteroids: Anti-inflammatory Profile to Airway Smooth Muscle Cells Has a Superior Proliferator-Activated Receptors in Human Activation of Peroxisome. *J Immunol Ref.* **170**, 2663–2669 (2003).
712. Lund, J., Bartel, S., Chung, J., Orinska, Z., Kull, S., Jappe, U., Baines, J. & Krauss-Etschmann, S. House dust mite (HDM)-induced “asthma” phenotypes differ in 4 mouse strains - link to the microbiome? *ERJ Open Res.* **5**, PP106 (2019).
713. Sears, M. R., Herbison, G. P., Holdaway, M. D., Hewitt, C. J., Flannery, E. M. & Silva, P. A. The relative risks of sensitivity to grass pollen, house dust mite and cat dander in the development of childhood asthma. *Clin. Exp. Allergy* **19**, 419–24 (1989).
714. Lau, S., Illi, S., Sommerfeld, C., Niggemann, B., Bergmann, R., von Mutius, E. & Wahn, U. Early exposure to house-dust mite and cat allergens and development of childhood asthma: a cohort study. *Lancet* **356**, 1392–1397 (2000).
715. Illi, S., von Mutius, E., Lau, S., Nickel, R., Niggemann, B., Sommerfeld, C. & Wahn, U. The pattern of atopic sensitization is associated with the development of asthma in childhood. *J. Allergy Clin. Immunol.* **108**, 709–714 (2001).
716. Miraglia del Giudice, M., Pedullà, M., Piacentini, G. L., Capristo, C., Brunese, F. P., Decimo, F., Maiello, N. & Capristo, A. F. Atopy and house dust mite sensitization as risk factors for asthma in children. *Allergy* **57**, 169–172 (2002).
717. Celedón, J. C., Milton, D. K., Ramsey, C. D., Litonjua, A. A., Ryan, L., Platts-Mills, T. A. E. & Gold, D. R. Exposure to dust mite allergen and endotoxin in early life and asthma and atopy in childhood. *J. Allergy Clin. Immunol.* **120**, 144–149 (2007).
718. Makley, A. T., Goodman, M. D., Friend, L. A. W., Johannigman, J. A., Dorlac, W. C., Lentsch, A. B. & Pritts, T. A. Murine blood banking: characterization and comparisons to human blood. *Shock* **34**, 40–45 (2010).
719. Kawabata, K., Takakura, Y. & Hashida, M. The Fate of Plasmid DNA After Intravenous Injection in Mice: Involvement of Scavenger Receptors in Its Hepatic Uptake. *Pharm. Res.* **12**, 825–830 (1995).
720. Ward, C. M., Read, M. L. & Seymour, L. W. Systemic circulation of poly(L-lysine)/DNA vectors is influenced by polycation molecular weight and type of DNA: differential circulation in mice and rats and the implications for human gene therapy. *Blood* **97**, 2221–9 (2001).
721. Barfod, K., Roggenbuck, M., Hansen, L., Schjørring, S., Larsen, S., Sørensen, S. & Krogfelt, K. The murine lung microbiome in relation to the intestinal and vaginal bacterial communities. *BMC Microbiol.* **13**, 303 (2013).
722. Yun, Y., Srinivas, G., Kuenzel, S., Linnenbrink, M., Alnahas, S., Bruce, K. D., Steinhoff, U., Baines, J. F. & Schaible, U. E. Environmentally Determined Differences in the Murine Lung Microbiota and Their Relation to Alveolar Architecture. *PLoS One* **9**, e113466 (2014).
723. Schloss, P. D., Schubert, A. M., Zackular, J. P., Iverson, K. D., Young, V. B. & Petrosino, J. F. Stabilization of the murine gut microbiome following weaning. *Gut Microbes* **3**, 383–93 (2012).
724. Carmody, R. N., Gerber, G. K., Luevano, J. M., Gatti, D. M., Somes, L., Svenson, K. L. &

- Turnbaugh, P. J. Diet Dominates Host Genotype in Shaping the Murine Gut Microbiota. *Cell Host Microbe* **17**, 72–84 (2015).
725. Costello, E. K., Lauber, C. L., Hamady, M., Fierer, N., Gordon, J. I. & Knight, R. Bacterial Community Variation in Human Body Habitats Across Space and Time. *Science* **326**, 1694 (2009).
726. Consortium, T. H. M. P., Huttenhower, C., White, O., *et al.* Structure, function and diversity of the healthy human microbiome. *Nature* **486**, 207–214 (2012).
727. Ursell, L. K., Clemente, J. C., Rideout, J. R., Gevers, D., Caporaso, J. G. & Knight, R. The interpersonal and intrapersonal diversity of human-associated microbiota in key body sites. *J. Allergy Clin. Immunol.* **129**, 1204–1208 (2012).
728. Chu, D. M., Ma, J., Prince, A. L., Antony, K. M., Seferovic, M. D. & Aagaard, K. M. Maturation of the infant microbiome community structure and function across multiple body sites and in relation to mode of delivery. *Nat. Med.* **23**, 314–326 (2017).
729. Eckburg, P. B., Bik, E. M., Bernstein, C. N., Purdom, E., Dethlefsen, L., Sargent, M., Gill, S. R., Nelson, K. E. & Relman, D. A. Diversity of the human intestinal microbial flora. *Science* **308**, 1635–8 (2005).
730. Ley, R. E., Bäckhed, F., Turnbaugh, P., Lozupone, C. A., Knight, R. D. & Gordon, J. I. Obesity alters gut microbial ecology. *Proc. Natl. Acad. Sci. U. S. A.* **102**, 11070–5 (2005).
731. Gill, S. R., Pop, M., Deboy, R. T., Eckburg, P. B., Turnbaugh, P. J., Samuel, B. S., Gordon, J. I., Relman, D. A., Fraser-Liggett, C. M. & Nelson, K. E. Metagenomic analysis of the human distal gut microbiome. *Science* **312**, 1355–9 (2006).
732. Krych, L., Hansen, C. H. F., Hansen, A. K., van den Berg, F. W. J. & Nielsen, D. S. Quantitatively Different, yet Qualitatively Alike: A Meta-Analysis of the Mouse Core Gut Microbiome with a View towards the Human Gut Microbiome. *PLoS One* **8**, e62578 (2013).
733. Nguyen, T. L. A., Vieira-Silva, S., Liston, A. & Raes, J. How informative is the mouse for human gut microbiota research? *Dis. Model. Mech.* **8**, 1–16 (2015).
734. Clavel, T., Charrier, C., Braune, A., Wenning, M., Blaut, M. & Haller, D. Isolation of bacteria from the ileal mucosa of TNFdeltaARE mice and description of *Enterorhabdus mucosicola* gen. nov., sp. nov. *Int. J. Syst. Evol. Microbiol.* **59**, 1805–1812 (2009).
735. Hildebrand, F., Nguyen, T. L. A., Brinkman, B., Yunta, R., Cauwe, B., Vandenabeele, P., Liston, A. & Raes, J. Inflammation-associated enterotypes, host genotype, cage and inter-individual effects drive gut microbiota variation in common laboratory mice. *Genome Biol.* **14**, R4 (2013).
736. Fujimura, K. E., Demoor, T., Rauch, M., Faruqi, A. A., Jang, S., Johnson, C. C., Boushey, H. A., Zoratti, E., Ownby, D., Lukacs, N. W. & Lynch, S. V. House dust exposure mediates gut microbiome Lactobacillus enrichment and airway immune defense against allergens and virus infection. *Proc. Natl. Acad. Sci.* **111**, 805–810 (2014).
737. Langille, M. G., Meehan, C. J., Koenig, J. E., Dhanani, A. S., Rose, R. A., Howlett, S. E. & Beiko, R. G. Microbial shifts in the aging mouse gut. *Microbiome* **2**, 50 (2014).
738. Lu, K., Abo, R. P., Schlieper, K. A., Graffam, M. E., Levine, S., Wishnok, J. S., Swenberg, J. A., Tannenbaum, S. R. & Fox, J. G. Arsenic Exposure Perturbs the Gut Microbiome and Its Metabolic Profile in Mice: An Integrated Metagenomics and Metabolomics Analysis. *Environ. Health Perspect.* **122**, 284–291 (2014).
739. Yang, Y.-W., Chen, M.-K., Yang, B.-Y., Huang, X.-J., Zhang, X.-R., He, L.-Q., Zhang, J. & Hua,

- Z.-C. Use of 16S rRNA Gene-Targeted Group-Specific Primers for Real-Time PCR Analysis of Predominant Bacteria in Mouse Feces. (2015). doi:10.1128/AEM.01906-15
740. Rabot, S., Membrez, M., Blancher, F., Berger, B., Moine, D., Krause, L., Bibiloni, R., Bruneau, A., Gérard, P., Siddharth, J., Lauber, C. L. & Chou, C. J. High fat diet drives obesity regardless the composition of gut microbiota in mice. *Sci. Rep.* **6**, 32484 (2016).
  741. Yu, H., Guo, Z., Shen, S. & Shan, W. Effects of taurine on gut microbiota and metabolism in mice. *Amino Acids* **48**, 1601–1617 (2016).
  742. Wang, Q., Jiao, L., He, C., Sun, H., Cai, Q., Han, T. & Hu, H. Alteration of gut microbiota in association with cholesterol gallstone formation in mice. *BMC Gastroenterol.* **17**, 74 (2017).
  743. Xiao, X., Nakatsu, G., Jin, Y., Wong, S., Yu, J. & Lau, J. Y. W. Gut Microbiota Mediates Protection Against Enteropathy Induced by Indomethacin. *Sci. Rep.* **7**, 40317 (2017).
  744. Kostic, M., Milger, K., Krauss-Etschmann, S., Engel, M., Vestergaard, G., Schloter, M. & Schöler, A. Development of a Stable Lung Microbiome in Healthy Neonatal Mice. *Microb. Ecol.* **75**, 529–542 (2018).
  745. Zaura, E., Keijser, B. J., Huse, S. M. & Crielaard, W. Defining the healthy &quot;core microbiome&quot; of oral microbial communities. *BMC Microbiol.* **9**, 259 (2009).
  746. Kostic, A. D., Gevers, D., Pedamallu, C. S., Michaud, M., Duke, F., Earl, A. M., Ojesina, A. I., Jung, J., Bass, A. J., Taberner, J., Baselga, J., Liu, C., Shivdasani, R. A., Ogino, S., Birren, B. W., Huttenhower, C., Garrett, W. S. & Meyerson, M. Genomic analysis identifies association of *Fusobacterium* with colorectal carcinoma. *Genome Res.* **22**, 292–8 (2012).
  747. Ahn, J., Sinha, R., Pei, Z., Dominianni, C., Wu, J., Shi, J., Goedert, J. J., Hayes, R. B. & Yang, L. Human Gut Microbiome and Risk for Colorectal Cancer. *JNCI J. Natl. Cancer Inst.* **105**, 1907–1911 (2013).
  748. Korpela, K., Flint, H. J., Johnstone, A. M., Lappi, J., Poutanen, K., Dewulf, E., Delzenne, N., de Vos, W. M. & Salonen, A. Gut Microbiota Signatures Predict Host and Microbiota Responses to Dietary Interventions in Obese Individuals. *PLoS One* **9**, e90702 (2014).
  749. Chen, L., Xu, W., Lee, A., He, J., Huang, B., Zheng, W., Su, T., Lai, S., Long, Y., Chu, H., Chen, Y., Wang, L., Wang, K., Si, J. & Chen, S. The impact of *Helicobacter pylori* infection, eradication therapy and probiotic supplementation on gut microenvironment homeostasis: An open-label, randomized clinical trial. *EBioMedicine* **35**, 87–96 (2018).
  750. Preston, J. A., Thorburn, A. N., Starkey, M. R., Beckett, E. L., Horvat, J. C., Wade, M. A., O’Sullivan, B. J., Thomas, R., Beagley, K. W., Gibson, P. G., Foster, P. S. & Hansbro, P. M. *Streptococcus pneumoniae* infection suppresses allergic airways disease by inducing regulatory T-cells. *Eur. Respir. J.* **37**, 53–64 (2011).
  751. Vogel, K., Blümer, N., Korthals, M., Mittelstädt, J., Garn, H., Ege, M., von Mutius, E., Gatermann, S., Bufe, A., Goldmann, T., Schwaiger, K., Renz, H., Brandau, S., Bauer, J., Heine, H. & Holst, O. Animal shed *Bacillus licheniformis* spores possess allergy-protective as well as inflammatory properties. *J. Allergy Clin. Immunol.* **122**, 307–312.e8 (2008).
  752. Preston, J. A., Essilfie, A.-T., Horvat, J. C., Wade, M. A., Beagley, K. W., Gibson, P. G., Foster, P. S. & Hansbro, P. M. Inhibition of allergic airways disease by immunomodulatory therapy with whole killed *Streptococcus pneumoniae*. *Vaccine* **25**, 8154–8162 (2007).
  753. Patel, P. S. & Kearney, J. F. Neonatal Exposure to Pneumococcal Phosphorylcholine Modulates the Development of House Dust Mite Allergy during Adult Life. *J. Immunol.* **194**, 5838–5850 (2015).

754. Zheng, J., Gänzle, M. G., Lin, X. B., Ruan, L. & Sun, M. Diversity and dynamics of bacteriocins from human microbiome. *Environ. Microbiol.* **17**, 2133–2143 (2015).
755. Piard, J. C. & Desmazeaud, M. Inhibiting factors produced by lactic acid bacteria. 2. Bacteriocins and other antibacterial substances. *Lait* **72**, 113–142 (1992).
756. Yang, S.-C., Lin, C.-H., Sung, C. T. & Fang, J.-Y. Antibacterial activities of bacteriocins: application in foods and pharmaceuticals. *Front. Microbiol.* **5**, 241 (2014).
757. Qin, N., Yang, F., Li, A., Prifti, E., Chen, Y., Shao, L., Guo, J., Le Chatelier, E., Yao, J., Wu, L., Zhou, J., Ni, S., Liu, L., Pons, N., Batto, J. M., Kennedy, S. P., Leonard, P., Yuan, C., Ding, W., Chen, Y., Hu, X., Zheng, B., Qian, G., Xu, W., Ehrlich, S. D., Zheng, S. & Li, L. Alterations of the human gut microbiome in liver cirrhosis. *Nature* **513**, 59–64 (2014).
758. Capone, K. A., Dowd, S. E., Stamatas, G. N. & Nikolovski, J. Diversity of the Human Skin Microbiome Early in Life. *J. Invest. Dermatol.* **131**, 2026–2032 (2011).
759. Schuller, D. E. Prophylaxis of otitis media in asthmatic children. *Pediatr. Infect. Dis.* **2**, 280–3 (1983).
760. Ansaldi, F., Turello, V., Lai, P., Bastone, G., De Luca, S., Rosselli, R., Durando, P., Sticchi, L., Gasparini, R., Delfino, E. & Icardi, G. Effectiveness of a 23-valent Polysaccharide Vaccine in Preventing Pneumonia and Non-invasive Pneumococcal Infection in Elderly People: a Large-scale Retrospective Cohort Study. *The Journal of International Medical Research* **33**, (2005).
761. Pauwels, R., Verschraegen, G. & Straeten, M. IgE Antibodies to Bacteria in Patients with Bronchial Asthma. *Allergy* **35**, 665–669 (1980).
762. Esposito, S., Terranova, L., Patria, M. F., Marseglia, G. L., Miraglia del Giudice, M., Bodini, A., Martelli, A., Baraldi, E., Mazzina, O., Tagliabue, C., Licari, A., Ierardi, V., Lelii, M. & Principi, N. Streptococcus pneumoniae colonisation in children and adolescents with asthma: impact of the heptavalent pneumococcal conjugate vaccine and evaluation of potential effect of thirteen-valent pneumococcal conjugate vaccine. *BMC Infect. Dis.* **16**, 12 (2015).
763. Green, B. J., Wiriyaichaiorn, S., Grainge, C., Rogers, G. B., Kehagia, V., Lau, L., Carroll, M. P., Bruce, K. D. & Howarth, P. H. Potentially Pathogenic Airway Bacteria and Neutrophilic Inflammation in Treatment Resistant Severe Asthma. *PLoS One* **9**, e100645 (2014).
764. Zhang, L., Prietsch, S. O. M., Mendes, A. P., Von Groll, A., Rocha, G. P., Carrion, L. & Da Silva, P. E. A. Inhaled corticosteroids increase the risk of oropharyngeal colonization by Streptococcus pneumoniae in children with asthma. *Respirology* **18**, 272–277 (2013).
765. Barcenilla, A., Pryde, S. E., Martin, J. C., Duncan, S. H., Stewart, C. S., Henderson, C. & Flint, H. J. Phylogenetic relationships of butyrate-producing bacteria from the human gut. *Appl. Environ. Microbiol.* **66**, 1654–61 (2000).
766. Schwiertz, A., Lehmann, U., Jacobasch, G. & Blaut, M. Influence of resistant starch on the SCFA production and cell counts of butyrate-producing *Eubacterium* spp. in the human intestine. *J. Appl. Microbiol.* **93**, 157–162 (2002).
767. Smith, P. M., Howitt, M. R., Panikov, N., Michaud, M., Gallini, C. A., Bohlooly-Y, M., Glickman, J. N. & Garrett, W. S. The microbial metabolites, short-chain fatty acids, regulate colonic Treg cell homeostasis. *Science* **341**, 569–73 (2013).
768. Atarashi, K., Tanoue, T., Oshima, K., Suda, W., Nagano, Y., Nishikawa, H., Fukuda, S., Saito, T., Narushima, S., Hase, K., Kim, S., Fritz, J. V., Wilmes, P., Ueha, S., Matsushima, K., Ohno, H., Olle, B., Sakaguchi, S., Taniguchi, T., Morita, H., Hattori, M. & Honda, K. Treg induction by a rationally selected mixture of Clostridia strains from the human microbiota. *Nature*

500, 232–236 (2013).

769. Atarashi, K., Tanoue, T., Shima, T., Imaoka, A., Kuwahara, T., Momose, Y., Cheng, G., Yamasaki, S., Saito, T., Ohba, Y., Taniguchi, T., Takeda, K., Hori, S., Ivanov, I. I., Umesaki, Y., Itoh, K. & Honda, K. Induction of colonic regulatory T cells by indigenous *Clostridium* species. *Science* **331**, 337–41 (2011).
770. De Giorgi, L., Sorini, C., Cosorich, I., Ferrarese, R., Canducci, F. & Falcone, M. Increased iNKT17 Cell Frequency in the Intestine of Non-Obese Diabetic Mice Correlates With High Bacteroidales and Low Clostridiales Abundance. *Front. Immunol.* **9**, 1752 (2018).
771. Ho, W. E., Xu, Y.-J., Xu, F., Cheng, C., Peh, H. Y., Tannenbaum, S. R., Wong, W. S. F. & Ong, C. N. Metabolomics Reveals Altered Metabolic Pathways in Experimental Asthma. *Am. J. Respir. Cell Mol. Biol.* **48**, 204–211 (2013).
772. Ho, W. E., Xu, Y.-J., Cheng, C., Peh, H. Y., Tannenbaum, S. R., Wong, W. S. F. & Ong, C. N. Metabolomics Reveals Inflammatory-Linked Pulmonary Metabolic Alterations in a Murine Model of House Dust Mite-Induced Allergic Asthma. *J. Proteome Res.* **13**, 3771–3782 (2014).
773. Peters, M., Kauth, M., Scherner, O., Gehlhar, K., Steffen, I., Wentker, P., von Mutius, E., Holst, O. & Bufe, A. Arabinogalactan isolated from cowshed dust extract protects mice from allergic airway inflammation and sensitization. *J. Allergy Clin. Immunol.* **126**, 648-656.e4 (2010).
774. Jolly, P. S., Rosenfeldt, H. M., Milstien, S. & Spiegel, S. The roles of sphingosine-1-phosphate in asthma. *Mol. Immunol.* **38**, 1239–1245 (2002).
775. Ammit, A. J., Hastie, A. T., Edsall, L. C., Hoffman, R. K., Amrani, Y., Krymskaya, V. P., Kane, S. A., Peters, S. P., Penn, R. B., Spiegel, S. & Panettieri JR, R. A. Sphingosine 1-phosphate modulates human airway smooth muscle cell functions that promote inflammation and airway remodeling in asthma. *FASEB J.* **15**, 1212–1214 (2001).
776. Kowal, K., Żebrowska, E. & Chabowski, A. Altered Sphingolipid Metabolism Is Associated With Asthma Phenotype in House Dust Mite-Allergic Patients. *Allergy. Asthma Immunol. Res.* **11**, 330 (2019).
777. Kume, H., Takeda, N., Oguma, T., Ito, S., Kondo, M., Ito, Y. & Shimokata, K. Sphingosine 1-phosphate causes airway hyper-reactivity by rho-mediated myosin phosphatase inactivation. *J. Pharmacol. Exp. Ther.* **320**, 766–73 (2007).
778. Roviezzo, F., Di Lorenzo, A., Bucci, M., Brancaleone, V., Vellecco, V., De Nardo, M., Orloff, D., De Palma, R., Rossi, F., D’Agostino, B. & Cirino, G. Sphingosine-1-Phosphate/Sphingosine Kinase Pathway Is Involved in Mouse Airway Hyperresponsiveness. *Am. J. Respir. Cell Mol. Biol.* **36**, 757–762 (2007).
779. Roviezzo, F., D’Agostino, B., Brancaleone, V., De Gruttola, L., Bucci, M., De Dominicis, G., Orloff, D., D’Aiuto, E., De Palma, R., Rossi, F., Sorrentino, R. & Cirino, G. Systemic Administration of Sphingosine-1-Phosphate Increases Bronchial Hyperresponsiveness in the Mouse. *Am. J. Respir. Cell Mol. Biol.* **42**, 572–577 (2010).
780. Roviezzo, F., Sorrentino, R., Bertolino, A., De Gruttola, L., Terlizzi, M., Pinto, A., Napolitano, M., Castello, G., D’Agostino, B., Ianaro, A., Sorrentino, R. & Cirino, G. S1P-induced airway smooth muscle hyperresponsiveness and lung inflammation *in vivo* : molecular and cellular mechanisms. *Br. J. Pharmacol.* **172**, 1882–1893 (2015).
781. Rosenfeldt O, H. M., Amrani, Y., Watterson, K. R., Murthy, K. S., Panettieri, R. A. & Spiegel, S. Sphingosine-1-phosphate stimulates contraction of human airway smooth muscle cells. *FASEB J.* **17**, 1789–1799 (2003).

782. Lockman, K., Hinson, J. S., Medlin, M. D., Morris, D., Taylor, J. M. & Mack, C. P. Sphingosine 1-phosphate stimulates smooth muscle cell differentiation and proliferation by activating separate serum response factor co-factors. *J. Biol. Chem.* **279**, 42422–30 (2004).
783. Roviezzo, F., Del Galdo, F., Abbate, G., Bucci, M., D'Agostino, B., Antunes, E., De Dominicis, G., Parente, L., Rossi, F., Cirino, G. & De Palma, R. Human eosinophil chemotaxis and selective in vivo recruitment by sphingosine 1-phosphate. *Proc. Natl. Acad. Sci.* **101**, 11170–11175 (2004).
784. Cinamon, G., Matloubian, M., Lesneski, M. J., Xu, Y., Low, C., Lu, T., Proia, R. L. & Cyster, J. G. Sphingosine 1-phosphate receptor 1 promotes B cell localization in the splenic marginal zone. *Nat. Immunol.* **5**, 713–720 (2004).
785. Pappu, R., Schwab, S. R., Cornelissen, I., Pereira, J. P., Regard, J. B., Xu, Y., Camerer, E., Zheng, Y.-W., Huang, Y., Cyster, J. G. & Coughlin, S. R. Promotion of lymphocyte egress into blood and lymph by distinct sources of sphingosine-1-phosphate. *Science* **316**, 295–8 (2007).
786. Milara, J., Mata, M., Mauricio, M. D., Donet, E., Morcillo, E. J. & Cortijo, J. Sphingosine-1-phosphate increases human alveolar epithelial IL-8 secretion, proliferation and neutrophil chemotaxis. *Eur. J. Pharmacol.* **609**, 132–139 (2009).
787. Matloubian, M., Lo, C. G., Cinamon, G., Lesneski, M. J., Xu, Y., Brinkmann, V., Allende, M. L., Proia, R. L. & Cyster, J. G. Lymphocyte egress from thymus and peripheral lymphoid organs is dependent on S1P receptor 1. *Nature* **427**, 355–360 (2004).
788. Hong Choi, O., Kim, J.-H. & Kinet, J.-P. Calcium mobilization via sphingosine kinase in signalling by the FcεRI antigen receptor. *Nature* **380**, 634–636 (1996).
789. Prieschl, E. E., Csonga, R., Novotny, V., Kikuchi, G. E. & Baumruker, T. The balance between sphingosine and sphingosine-1-phosphate is decisive for mast cell activation after Fc epsilon receptor I triggering. *J. Exp. Med.* **190**, 1–8 (1999).
790. Louis, P., Hold, G. L. & Flint, H. J. The gut microbiota, bacterial metabolites and colorectal cancer. *Nat. Rev. Microbiol.* **12**, 661–672 (2014).
791. Julia, V., Macia, L. & Dombrowicz, D. The impact of diet on asthma and allergic diseases. *Nat. Rev. Immunol.* **15**, 308–322 (2015).
792. Foster, J. A. & McVey Neufeld, K.-A. Gut–brain axis: how the microbiome influences anxiety and depression. *Trends Neurosci.* **36**, 305–312 (2013).
793. Zheng, P., Zeng, B., Zhou, C., Liu, M., Fang, Z., Xu, X., Zeng, L., Chen, J., Fan, S., Du, X., Zhang, X., Yang, D., Yang, Y., Meng, H., Li, W., Melgiri, N. D., Licinio, J., Wei, H. & Xie, P. Gut microbiome remodeling induces depressive-like behaviors through a pathway mediated by the host's metabolism. *Mol. Psychiatry* **21**, 786–796 (2016).
794. Evans, S. J., Bassis, C. M., Hein, R., Assari, S., Flowers, S. A., Kelly, M. B., Young, V. B., Ellingrod, V. E. & McInnis, M. G. The gut microbiome composition associates with bipolar disorder and illness severity. *J. Psychiatr. Res.* **87**, 23–29 (2017).
795. Wang, Z., Klipfell, E., Bennett, B. J., Koeth, R., Levison, B. S., DuGar, B., Feldstein, A. E., Britt, E. B., Fu, X., Chung, Y.-M., Wu, Y., Schauer, P., Smith, J. D., Allayee, H., Tang, W. H. W., DiDonato, J. A., Lusis, A. J. & Hazen, S. L. Gut flora metabolism of phosphatidylcholine promotes cardiovascular disease. *Nature* **472**, 57–63 (2011).
796. Kelly, T. N., Bazzano, L. A., Ajami, N. J., He, H., Zhao, J., Petrosino, J. F., Correa, A. & He, J. Gut Microbiome Associates With Lifetime Cardiovascular Disease Risk Profile Among Bogalusa Heart Study Participants. *Circ. Res.* **119**, 956–964 (2016).

797. Schippa, S., Iebba, V., Santangelo, F., Gagliardi, A., De Biase, R. V., Stamato, A., Bertasi, S., Lucarelli, M., Conte, M. P. & Quattrucci, S. Cystic Fibrosis Transmembrane Conductance Regulator (CFTR) Allelic Variants Relate to Shifts in Faecal Microbiota of Cystic Fibrosis Patients. *PLoS One* **8**, e61176 (2013).
798. Yazar, A., Atis, S., Konca, K., Pata, C., Akbay, E., Calikoglu, M. & Hafta, A. Respiratory symptoms and pulmonary functional changes in patients with irritable bowel syndrome. *Am. J. Gastroenterol.* **96**, 1511–1516 (2001).
799. Roussos, A., Koursarakos, P., Patsopoulos, D., Gerogianni, I. & Philippou, N. Increased prevalence of irritable bowel syndrome in patients with bronchial asthma. *Respir. Med.* **97**, 75–9 (2003).
800. Powell, N., Huntley, B., Beech, T., Knight, W., Knight, H. & Corrigan, C. J. Increased prevalence of gastrointestinal symptoms in patients with allergic disease. *Postgrad. Med. J.* **83**, 182–6 (2007).
801. Tobin, M. C., Moparty, B., Farhadi, A., DeMeo, M. T., Bansal, P. J. & Keshavarzian, A. Atopic irritable bowel syndrome: a novel subgroup of irritable bowel syndrome with allergic manifestations. *Ann. Allergy, Asthma Immunol.* **100**, 49–53 (2008).
802. Jones, M. P., Walker, M. M., Ford, A. C. & Talley, N. J. The overlap of atopy and functional gastrointestinal disorders among 23 471 patients in primary care. *Aliment. Pharmacol. Ther.* **40**, 382–391 (2014).
803. Caffarelli, C., Deriu, F. M., Terzi, V., Perrone, F., De Angelis, G. & Atherton, D. J. Gastrointestinal symptoms in patients with asthma. *Arch. Dis. Child.* **82**, 131–5 (2000).
804. Ojha, U. C., Singh, D. P., Choudhari, O. K., Gothi, D. & Singh, S. Correlation of Severity of Functional Gastrointestinal Disease Symptoms with that of Asthma and Chronic Obstructive Pulmonary Disease: A Multicenter Study. *Int. J. Appl. basic Med. Res.* **8**, 83–88 (2018).
805. Bates, J. H. T., Rincon, M. & Irvin, C. G. Animal models of asthma. *Am J Physiol Lung Cell Mol Physiol* **297**, 401–410 (2009).
806. Kearney, J. Food consumption trends and drivers. *Philos. Trans. R. Soc. B Biol. Sci.* **365**, 2793–2807 (2010).
807. Tilman, D. & Clark, M. Global diets link environmental sustainability and human health. *Nature* **515**, 518–522 (2014).
808. Salzmann, A. P., Russo, G., Aluri, S. & Haas, C. Transcription and microbial profiling of body fluids using a massively parallel sequencing approach. *Forensic Sci. Int. Genet.* **43**, 102149 (2019).
809. Xie, L., Lim, T. M., Ling, S. H. M., Wang, X. H. & Leung, K. Y. Use of green fluorescent protein (GFP) to study the invasion pathways of *Edwardsiella tarda* in in vivo and in vitro fish models. *Microbiology* **146**, 7–19 (2000).
810. Ma, L., Zhang, G. & Doyle, M. P. Green Fluorescent Protein Labeling of *Listeria*, *Salmonella*, and *Escherichia coli* O157:H7 for Safety-Related Studies. *PLoS One* **6**, e18083 (2011).
811. Scott, K. P., Mercer, D. K., Glover, L. A. & Flint, H. J. The green fluorescent protein as a visible marker for lactic acid bacteria in complex ecosystems. *FEMS Microbiol. Ecol.* **26**, 219–230 (1998).
812. Wang, G. Real-time PCR quantification of a green fluorescent protein-labeled, genetically engineered *Pseudomonas putida* strain during 2-chlorobenzoate degradation in soil. *FEMS*

*Microbiol. Lett.* **233**, 307–314 (2004).